LEVEL III

AFAPL-TR-78-77

AD A067549

20000726151

# AIRCRAFT HYDRAULIC SYSTEMS DYNAMIC ANALYSIS

MCDONNELL AIRCRAFT COMPANY
MCDONNELL DOUGLAS CORPORATION
ST. LOUIS, MISSOURI 63166

DDC FILE COPY

OCTOBER 1978

D D C
APR 19 1979
B

TECHNICAL REPORT AFAPL-TR-78-77
Final Report - February 1977 - September 1978

Approved for public release; distribution unlimited.

AIR FORCE AERO PROPULSION LABORATORY
AIR FORCE WRIGHT AERONAUTICAL LABORATORIES
AIR FORCE SYSTEMS COMMAND
WRIGHT-PATTERSON AIR FORCE BASE, OH 45433

# NOTICE

When Government drawings, specifications, or other data are used for any purpose other than in connection with a definitely related Government procurement operation, the United States Government thereby incurs no responsibility nor any obligation whatsoever; and the fact that the government may have formulated, furnished, or in any way supplied the said drawings, specifications, or other data, is not to be regarded by implication or otherwise as in any manner licensing the holder or any other person or corporation, or conveying any rights or permission to manufacture, use, or sell any patented invention that may in any way be related thereto.

This report has been reviewed by the Information Office (OI) and is releasable to the National Technical Information Service (NTIS). At NTIS, it will be available to the general public, including foreign nations.

This technical report has been reviewed and is approved for publication.

Paul D. Lindquist

PAUL D. LINDQUIST
Project Engineer

Kenneth E. Binns

KENNETH E. BINNS
Group Leader

FOR THE COMMANDER

William F. Bailey

WILLIAM F. BAILEY, Major, USAF
Chief, Vehicle Power Branch

"If your address has changed, if you wish to be removed from our mailing list, or if the addressee is no longer employed by your organization please notify [illegible],W-PAFB, OH 45433 to help us maintain a current mailing list".

Copies of this report should not be returned unless return is required by security considerations, contractual obligations, or notice on a specific document.

UNCLASSIFIED

SECURITY CLASSIFICATION OF THIS PAGE (When Data Entered)

# REPORT DOCUMENTATION PAGE

READ INSTRUCTIONS BEFORE COMPLETING FORM

| | | |
|---|---|---|
| 1. REPORT NUMBER<br>AFAPL-TR-78-77 | 2. GOVT ACCESSION NO. | 3. RECIPIENT'S CATALOG NUMBER |
| 4. TITLE (and Subtitle)<br>AIRCRAFT HYDRAULIC SYSTEMS DYNAMIC ANALYSIS<br>FINAL REPORT | | 5. TYPE OF REPORT & PERIOD COVERED<br>Final Report<br>February 1977-September 1978 |
| | | 6. PERFORMING ORG. REPORT NUMBER |
| 7. AUTHOR(s)<br>H. DeGarcia, N. J. Pierce<br>J. B. Greene<br>R. J. Levek | | 8. CONTRACT OR GRANT NUMBER(s)<br>F33615-74-C-2016 |
| 9. PERFORMING ORGANIZATION NAME AND ADDRESS<br>McDonnell Douglas Corporation<br>P O Box 516<br>St. Louis, Missouri 63166 | | 10. PROGRAM ELEMENT, PROJECT, TASK AREA & WORK UNIT NUMBERS<br>3145-30-18 |
| 11. CONTROLLING OFFICE NAME AND ADDRESS<br>Air Force Aero Propulsion Laboratory (POP)<br>Air Force Systems Command<br>Wright-Patterson Air Force Base, Ohio 45433 | | 12. REPORT DATE<br>October 1978 |
| | | 13. NUMBER OF PAGES<br>337 |
| 14. MONITORING AGENCY NAME & ADDRESS (if different from Controlling Office)<br>354 p. | | 15. SECURITY CLASS. (of this report)<br>Unclassified |
| | | 15a. DECLASSIFICATION/DOWNGRADING SCHEDULE |

16. DISTRIBUTION STATEMENT (of this Report)

Approved for public release, distribution unlimited.

17. DISTRIBUTION STATEMENT (of the abstract entered in Block 20, if different from Report)

18. SUPPLEMENTARY NOTES

19. KEY WORDS (Continue on reverse side if necessary and identify by block number)

Hydraulic System, Transient Response, Frequency Response, Steady State, Final Report, Computer Program Verification, Test Results

20. ABSTRACT (Continue on reverse side if necessary and identify by block number)

This report describes the continued development and test verification of digital computer models used to simulate hydraulic systems under dynamic conditions. Frequency and transient models of a variable delivery vane pump and a fixed displacement piston-type hydraulic motor are included. Additional verification and development of the transient model for the piston-type hydraulic pump was accomplished. Verification and development of a computer program to describe the mechanical response of a hydraulic line to internal

DD FORM 1 JAN 73 1473 EDITION OF 1 NOV 65 IS OBSOLETE

i

403111

UNCLASSIFIED

SECURITY CLASSIFICATION OF THIS PAGE (When Data Entered)

20. ABSTRACT (Cont'd)

excitations from a hydraulic pump was begun. This

The work was conducted by McDonnell Aircraft Company (McDonnell Douglas Corp.) under contract with the Air Force. The effort was a continuation of the basic contract wherein four computer programs for hydraulic system dynamic analysis were developed. The basic contract results were reported in AFAPL-TR-77-63, October 1977.

## PREFACE

This final report was prepared by the McDonnell Aircraft Company, Design Engineering Power and Fluid System Department, McDonnell Douglas Corporation under contract F33615-74-C-2016, Supplemental Agreement P00007.

The effort was sponsored by the Air Force Aero Propulsion Laboratory, Air Force Systems Command, Wright-Patterson AFB, Ohio under Project No. 3145-30-18 with AFAPL/POP , and was under the direction of Paul Lindquist and William Kinzig.

The final report covers work conducted during the contract extension period from 18 February 1977 through 30 September 1978. At McDonnell, Neil Pierce directed the program and J. B. Greene was the principal investigator. Special ackowledgement is also given to R. J. Levek, H. deGarcia, and L. E. Clements.

## TABLE OF CONTENTS

TABLE OF CONTENTS (Cont'd)

## TABLE OF CONTENTS (Cont'd)

## LIST OF ILLUSTRATIONS

## LIST OF ILLUSTRATIONS

LIST OF ILLUSTRATIONS

## LIST OF ILLUSTRATIONS

LIST OF ILLUSTRATIONS

## LIST OF ILLUSTRATIONS

LIST OF ILLUSTRATIONS

| FIGURE | | PAGE |
|---|---|---|

| FIGURE | | PAGE |
|---|---|---|

FIGURE PAGE

## LIST OF TABLES

## SECTION I
## INTRODUCTION

This report describes work performed under the extension (Supplemental Agreement P00007) of the Aircraft Hydraulic System Performance Analysis contract. This effort was a continuation of the basic contract, the results of which were reported in Reference (1).

The task involved the development and verification by test of digital computer models and/or programs in four areas.

1. HYDRAULIC LINE MECHANICAL RESPONSE (HLMR)

A test program was conducted to determine the mechanical resonances and mode shapes of hydraulic lines due to internal excitation by flow/pressure pulsations from a typical piston-type hydraulic pump. The objective was to develop and verify a computer program for predicting line mechanical response based on pump flow/pressure pulsations predicted by the Hydraulic System Frequency Response (HSFR) program, which was developed during the basic contract. Basic data for the design of central hydraulic piping systems was obtained as well as the effects of an intermediate elastomeric pipe support.

2. F-15 PISTON PUMP MODEL VERIFICATION

An F-15 instrumented hydraulic pump (Abex) was used during the basic contract to verify the pump Hydraulic Transient Analysis (HYTRAN) model. A direct case pressure pickup was added to the pump and certain tests were repeated. Direct case pressure data was utilized along with additional analysis of original verification data to further improve the pump model.

3. VANE PUMP MODEL DEVELOPMENT AND VERIFICATION

HSFR and HYTRAN models were developed and verified by test for a variable volume vane pump. The unit modeled and tested was the vane stage of the main fuel pump (MFP-330) on the F-100 turbojet engine. It was designed and is supplied by Chandler Evans Inc., Control Systems Division. The pump was tested using MIL-H-5606B hydraulic oil consistent with previous model development work and the established Hydraulic Performance Analysis Test Facility (HPAF).

4. HYDRAULIC MOTOR MODEL DEVELOPMENT AND VERIFICATION

HSFR and HYTRAN models were developed and verified by test for a constant displacement, piston-type hydraulic motor. The unit modeled and tested was designed and supplied by Aero-Hydraulics, Inc. (The Garrett Corporation). The test motor is used in the F-18 leading edge manuevering flap system, and similar units are used in F-15, F-14, and B-1 applications.

Test methods and instrumentation were the same as described in Reference (1) for test work during the basic program. Special test setups required for the vane pump and hydraulic motor are described in subsequent sections of this report. Computer models developed during the supplemental contract are in the same format as those developed during the original contract, and are compatible, "building block" additions to the HSFR and HYTRAN computer programs documented in References (2) through (5).

## SECTION II

## HYDRAULIC LINE MECHANICAL RESPONSE (HLMR) PROGRAM

Hydraulic line vibrations due to pulsations from axial piston-type pumps can create serious problems in aircraft. These internal forcing functions cause the hydraulic system lines to vibrate and transmit loads into supporting structure. The importance of developing analytical tools coupled with experimental tests was recognized by AFAPL and funds were allocated in the program extension to pursue this development.

The objectives of the HLMR program effort were to:

- o Develop and verify a computer program for prediciting line mechanical response due to predicted pump pulsations.
- o Provide basic data for the design of piping systems.
- o Provide information regarding intermediate supports.

The test program included determining the mechanical resonances and mode shapes due to pump excitation of three configurations: a straight pipe, a pipe with a 90-deg. bend, and a pipe with two 90-deg. bends (dogleg). In addition, the effect of an intermediate elastomeric support was evaluated.

### 1. BACKGROUND

#### a. Previous MCAIR Effort

An initial effort to evaluate the mechanical response of a hydraulic installation due to internal forcing functions was reported in Reference (6). This preliminary investigation used forcing functions from the pressure and flow transmitted by the pump, as provided by the HSFR computer program. The results indicated that the hydraulic line normalized amplitudes varied directly with the intensity of the forcing function. Although the program's predictions indicated the amplitude trend, it did not duplicate the mechanical resonances.

#### b. Literature Survey

A review of published literature was conducted to determine the extent of work performed on fluid-line coupling analyses. Appendix A presents an annotated bibliography of the literature surveyed.

It was determined that much effort has been devoted to analyzing large piping systems transporting oil through the Arabian fields, water within Navy shipboard piping, and academic stylized systems. Except for the Navy studies, all analyses concentrated on straight pipes with different support conditions and variations in internal fluid velocity. None studied the coupling between hydraulic pump pulsations and line mechanical response.

2. TEST SET-UP AND PROCEDURES

Three different pipe configurations of equal length, Figure 1, were installed in MCAIR's HPAF test fixture. The specimens consisted of one-inch outside diameter, with .051-in. wall thickness, 3AL-2.5V titanium tubes; a straight pipe, a pipe with a single 90-deg. bend, and one with two 90-deg bends (dogleg). In each case the pipe was rigidly mounted at each end using Dynatube fittings between brackets, Figure 2, attached to a steel plate. In the test set-up, the pipe specimens were part of the pressure system between the pump and the flow control valve, and isolated from extraneous mechanical vibration inputs in order to determine only the effect of the pump pulsations. The test circuit included a trombone tube section to permit adjustment of the standing wave location in the test specimen. The test fluid was MIL-H-5606B hydraulic oil.

Tests with an intermediate support placed at the locations shown in Figure 1 were conducted to determine the effect of an elastomeric clamp on line responses.

Six single axis accelerometers were installed on each specimen at the same location with respect to the pipe centerline. Triaxial accelerometers to record data simultaneously along three orthogonal axis were not employed, since their weight would have affected the line response. Lightweight single axis accelerometers were used to minimize this effect. Tests had to be repeated for each axis thereby increasing test time for each configuration.

Pressure transducers and thermocouples were installed in the test set-up. The standing pressure wave in the test line was determined as a function of pump speed, by means of a roving transducer.

All the test data was run with a pump outlet flow of 2.0 gpm and a nominal pump inlet temperature of 130°F. Each test specimen was run unclamped and clamped before moving the accelerometers to a different axis. A pump speed sweep from 1000 to 5000 rpm was made while recording analog data on tape. Data plots of acceleration as a function of pump speed were made from the tapes. These plots were used to identify the pump speeds at each mechanical resonance. Then, for each significant mechanical resonance condition, spectrum analyses were obtained while dwelling the pump at the resonant speed. In addition, the phase relationship was obtained between a reference accelerometer and all other accelerometers.

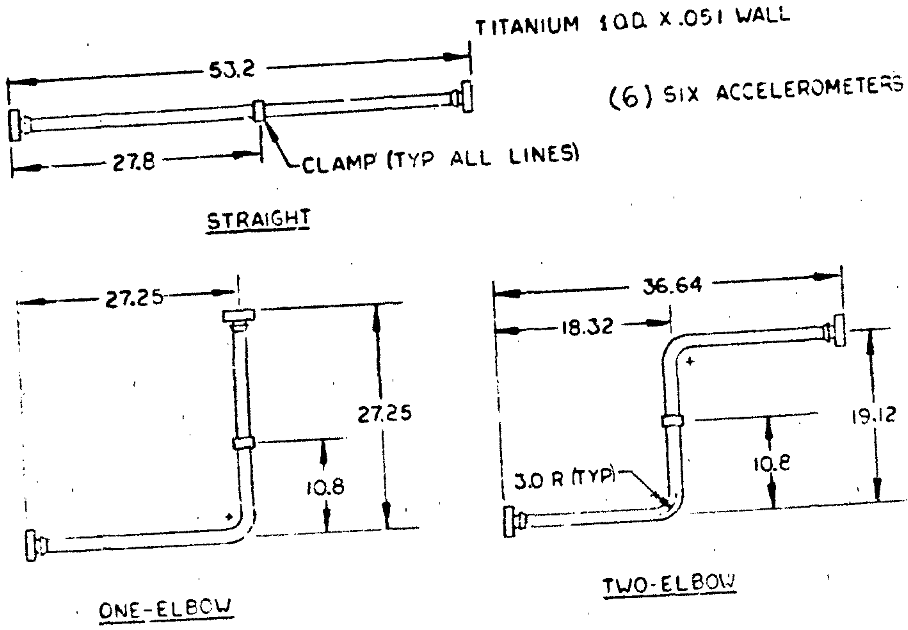


FIGURE 1. TEST CONFIGURATIONS

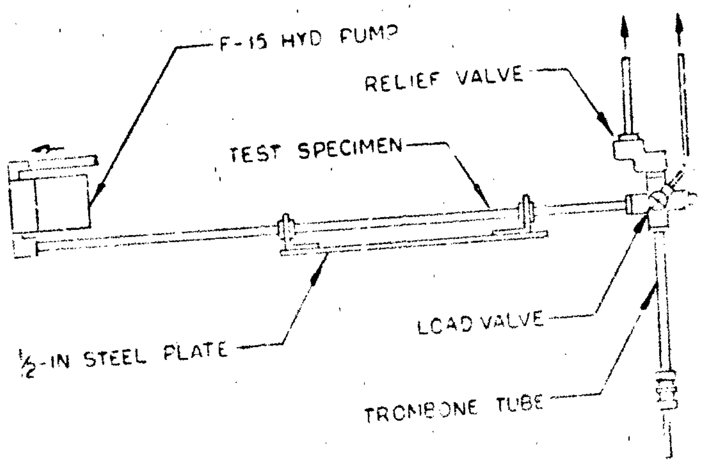


FIGURE 2. TEST SET-UP SCHEMATIC

## 3. TEST RESULTS

### a. Pump Pressure Pulsations

The standing pressure wave was determined from the graphical data of fundamental pressure peaks versus pump speed at a number of pre-set locations using a roving transducer. As previously mentioned, all test data was obtained with a pump outlet flow of 2 gpm and a pump inlet temperature of 130°F.

The results summarized in Figure 3, indicate three resonance speeds.

Pump speeds above and below those shown have lower peak values and have waves with translational nodes as seen in Figures 4 through 8.

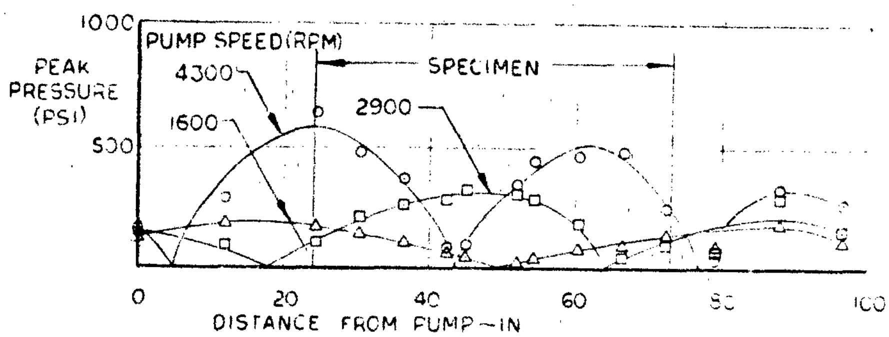


FIGURE 3. HYDRAULIC RESONANCES

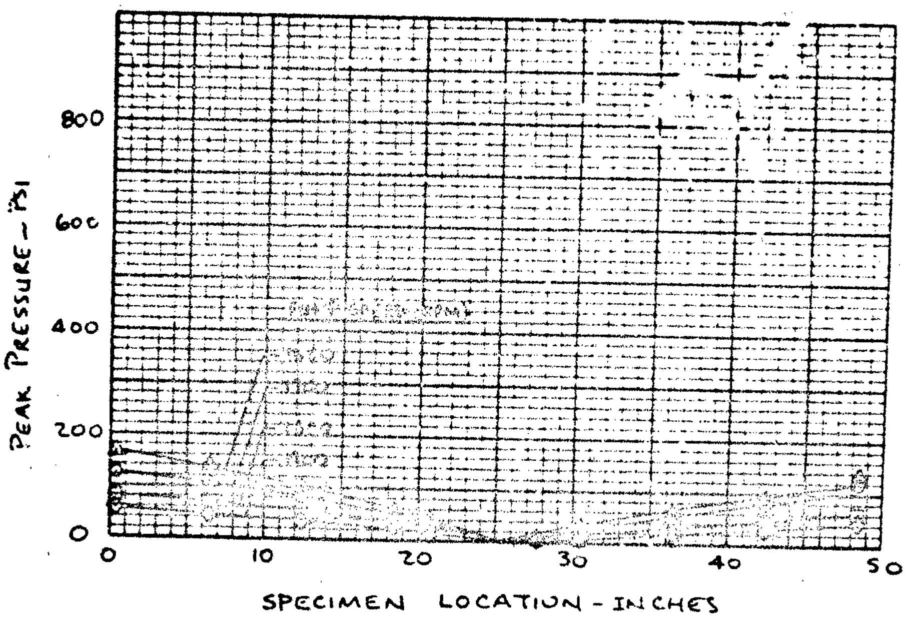


FIGURE 4. PEAK PRESSURES
1600-1900 R.P.M.

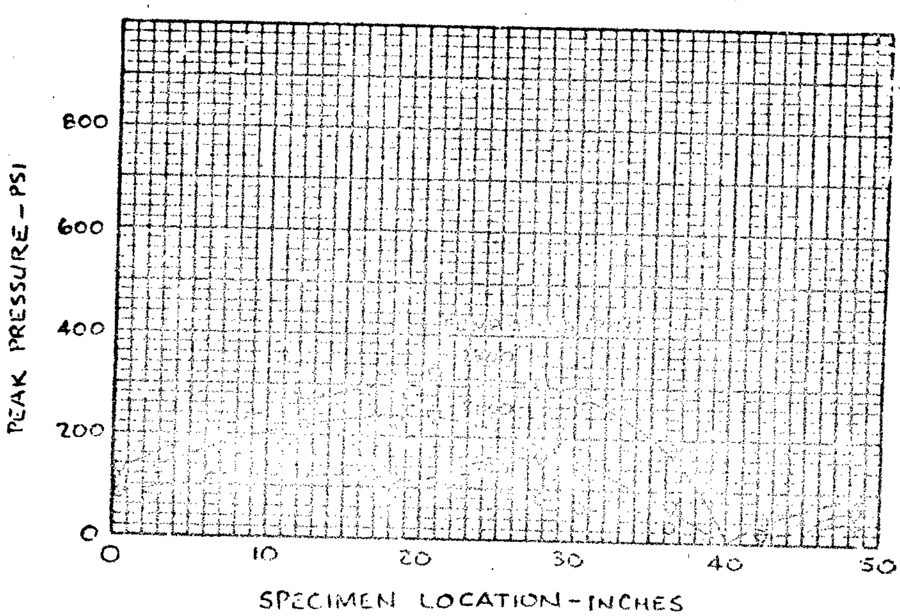


FIGURE 5. PEAK PRESSURES
2700-2900 R.P.M.

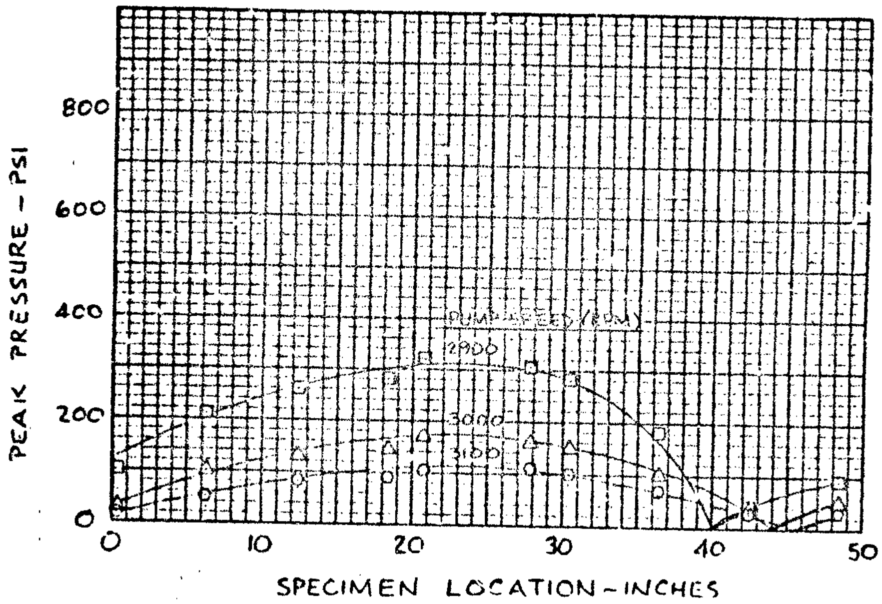


FIGURE 6. PEAK PRESSURES
2900-3100 R.P.M.

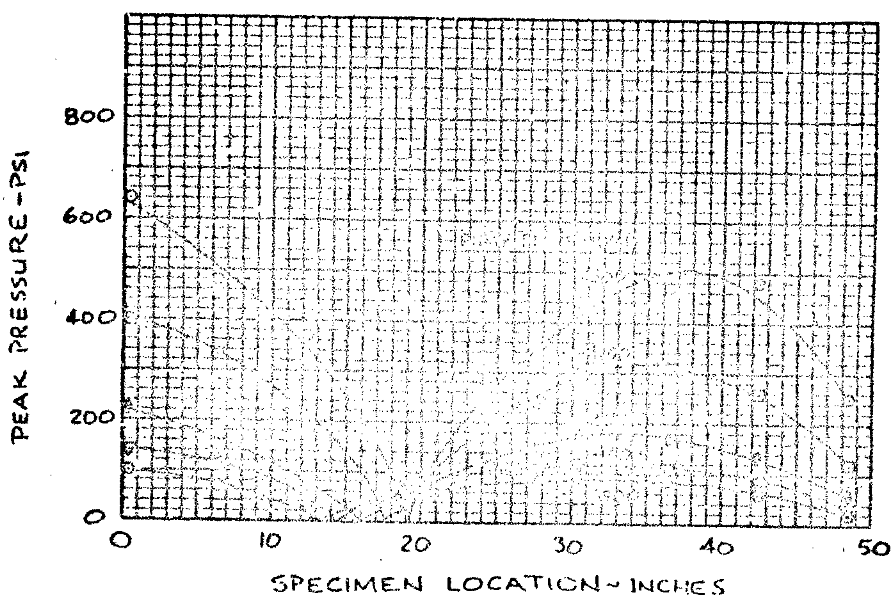


FIGURE 7. PEAK PRESSURES
3900-4300 R.P.M.

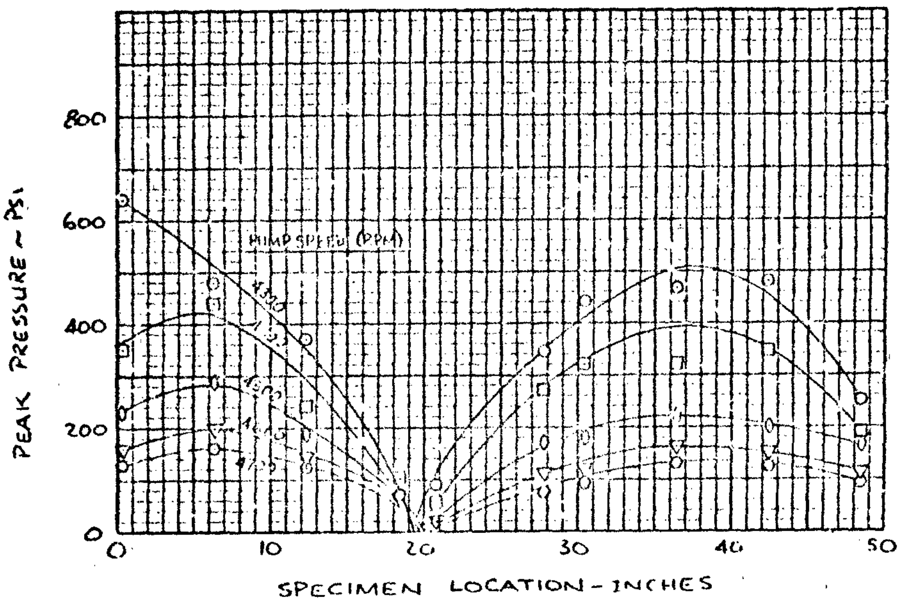


FIGURE 8. PEAK PRESSURES
4300-4700 R.P.M.

b. Line Response

Line response data reduction was made in terms of mode shapes for the three configurations. The graphical presentation made herein shows the normalized deflection, base on maximum amplitude/acceleration, as a function of pipe length for each resonance speed. In addition the reference acceleration previously mentioned is shown for each case. For specimens with bends, the inplane and out-of-plane modes are shown for a visualization of the motions involved. It is seen that the cushioned elastomeric clamp had no effect on restraining the line (almost identical mode shapes) but slightly lowered the acceleration.

(1) Straight Pipe

Both unclamped and clamped configurations exhibit almost identical mode shapes, Figures 9 and 11, equivalent to the third harmonic at the same excitation level. Note that the line resonance condition coincides with the second resonance of the standing pressure wave.

The clamped set-up had a slightly higher acceleration with the clamp providing no physical effect on the mode shape. However, it did produce another distinct resonance, Figure 10, characterized by a longitudinal acceleration which was the highest for the straight line configuration.

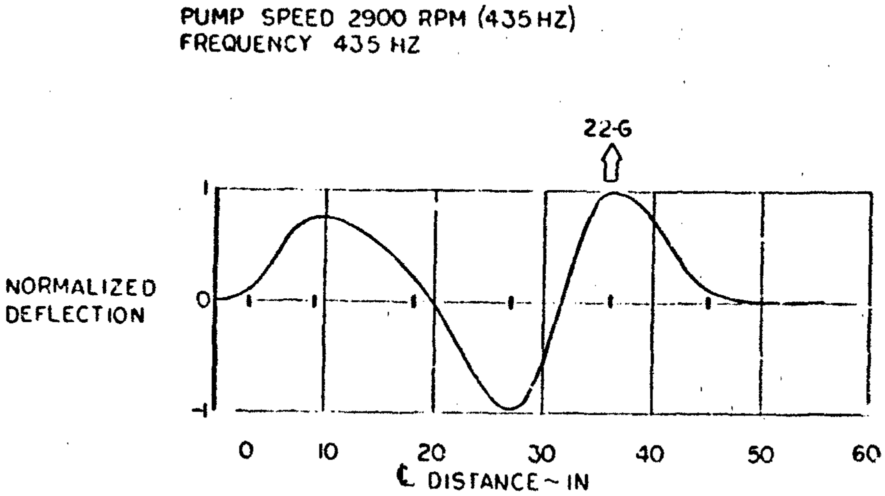


FIGURE 9. HYDRAULIC SYSTEM LINE RESPONSE STRAIGHT PIPE UNCLAMPED MODE SHAPE DATA

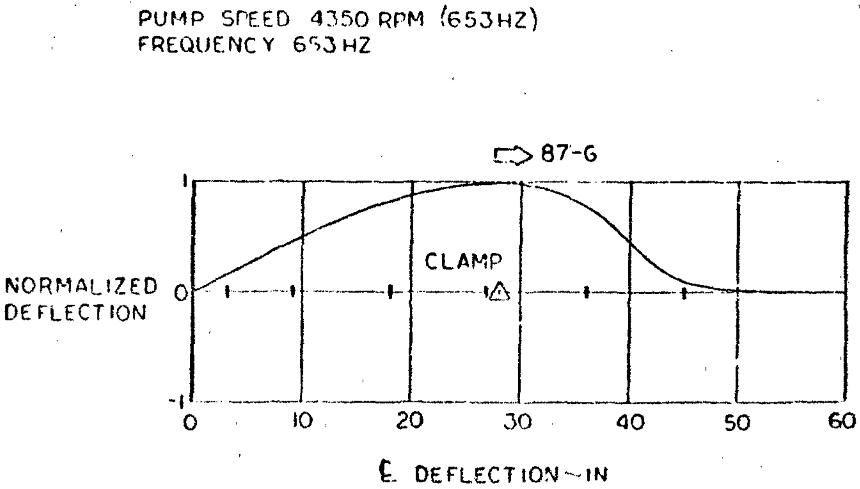


FIGURE 10. HYDRAULIC SYSTEM LINE RESPONSE STRAIGHT PIPE CLAMPED MODE SHAPE DATA

PUMP SPEED 2900 RPM (435 HZ)
FREQUENCY 435 HZ

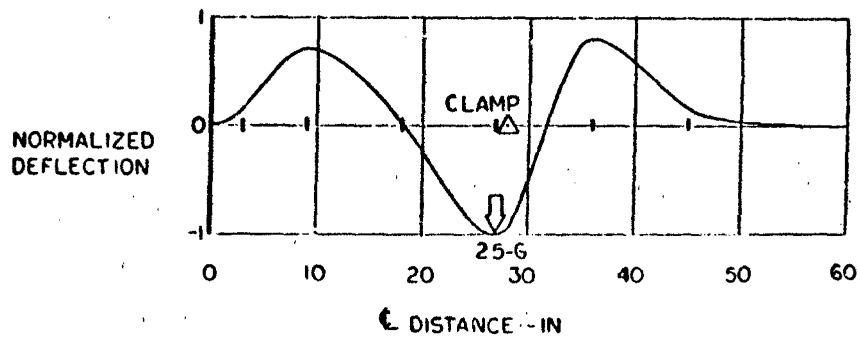


FIGURE 11. HYDRAULIC SYSTEM LINE RESPONSE STRAIGHT PIPE CLAMPED MODE SHAPE DATA

(2) <u>One-Elbow Pipe</u>

Unclamped and clamped configurations had identical resonances, similar mode shapes and accelerations slightly lower for the latter case. Both set-ups had a recurring frequency at 1030-1035 Hz corresponding to higher harmonics of the pump speeds shown on Figures 12 and 15. The basic mode shape for these cases have two nodes such that the inplane normalized deflections show the characteristics of the third mode of a cantilever or fixed-pinned beam for the first leg, and the first mode for the second leg. The out-of-plane deflections compare with those of the third mode for a fixed-fixed beam.

Peak accelerations for this configuration occurred at the elbow in the inplane direction. Interestingly, the second standing pressure wave resonance at 2900 RPM also excited a mode shape similar to the previously discussed inplane deflections for 1035 Hz. However, there was little motion in the out-of-plane direction although only the clamped version was measured as seen in Figures 13 and 16.

The only frequency occurring on the first harmonic of the pump speed is at 653 Hz (4350 RPM) and produced the maximum accelerations for both the unclamped and clamped configurations with the latter having a slightly (ten percent) lower accelerations. The inplane mode shapes, seen in Figures 14 and 17, are basically the first leg motion coupled to that of the second leg with the maximum acceleration measurement at the station after the elbow, away from the pump.

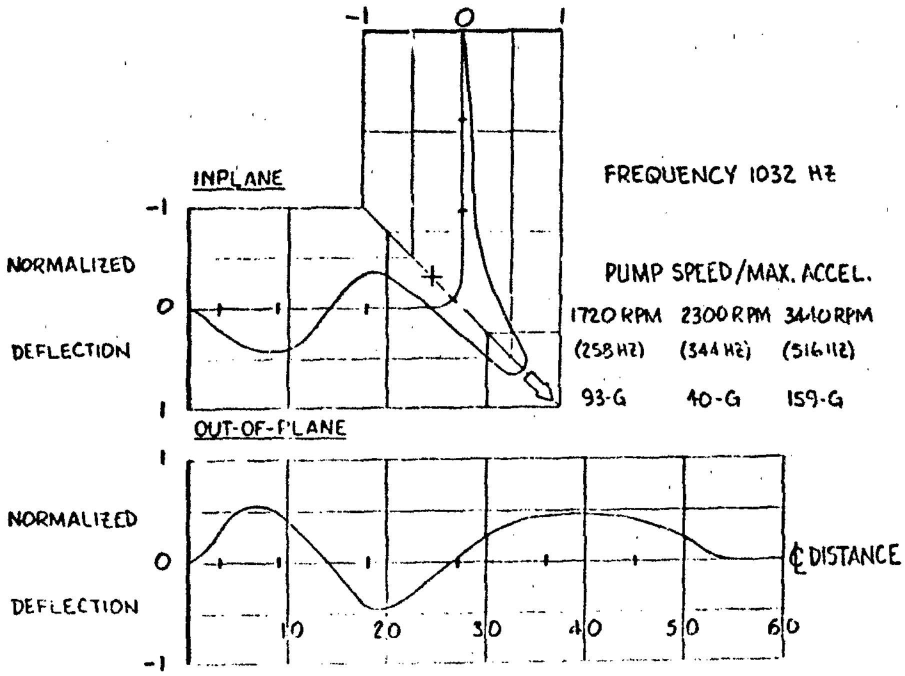


FIGURE 12. HYDRAULIC SYSTEM LINE RESPONSE
ONE-ELBOW PIPE UNCLAMPED MODE SHAPE DATA

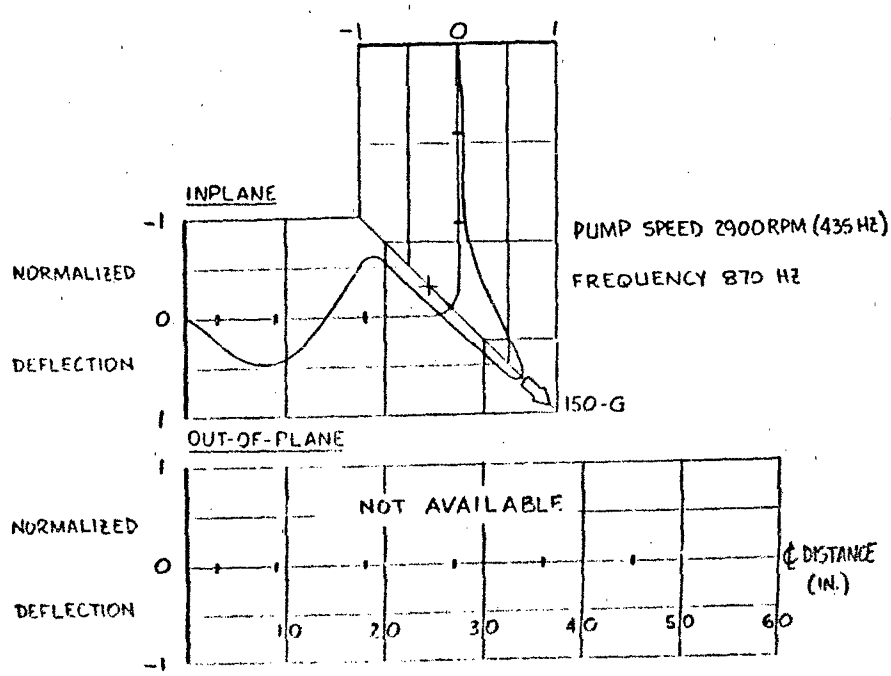


FIGURE 13. HYDRAULIC SYSTEM LINE RESPONSE
ONE-ELBOW PIPE UNCLAMPED MODE SHAPE DATA

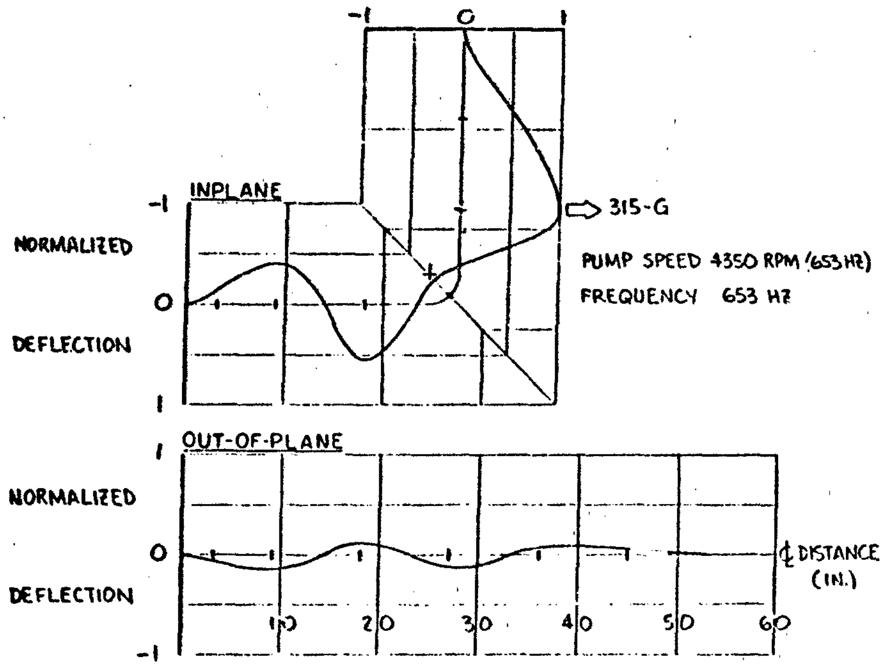


FIGURE 14. HYDRAULIC SYSTEM LINE RESPONSE
ONE-ELBOW PIPE UNCLAMPED MODE SHAPE DATA

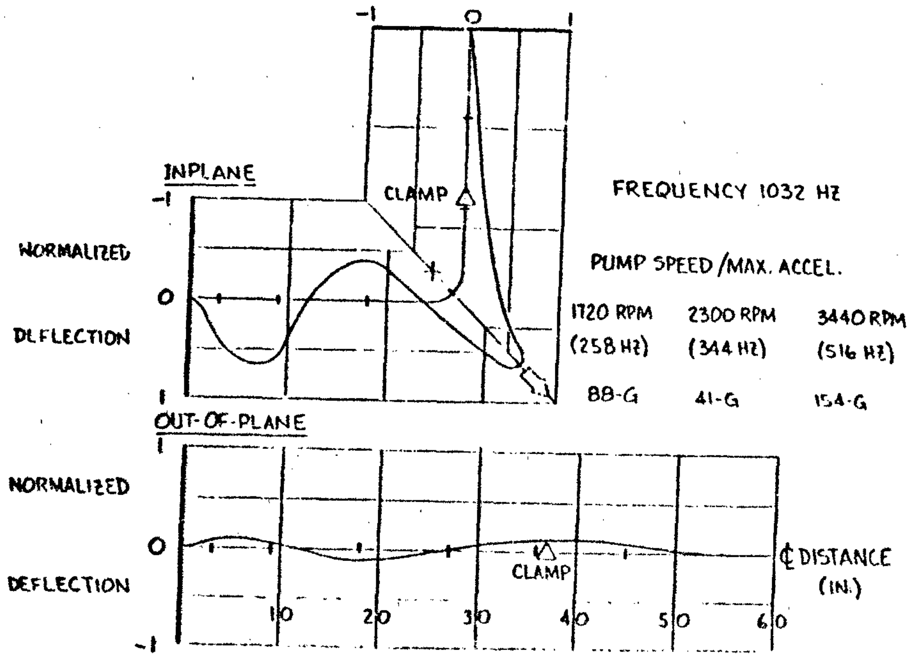


FIGURE 15. HYDRAULIC SYSTEM LINE RESPONSE
ONE-ELBOW PIPE CLAMPED MODE SHAPE DATA

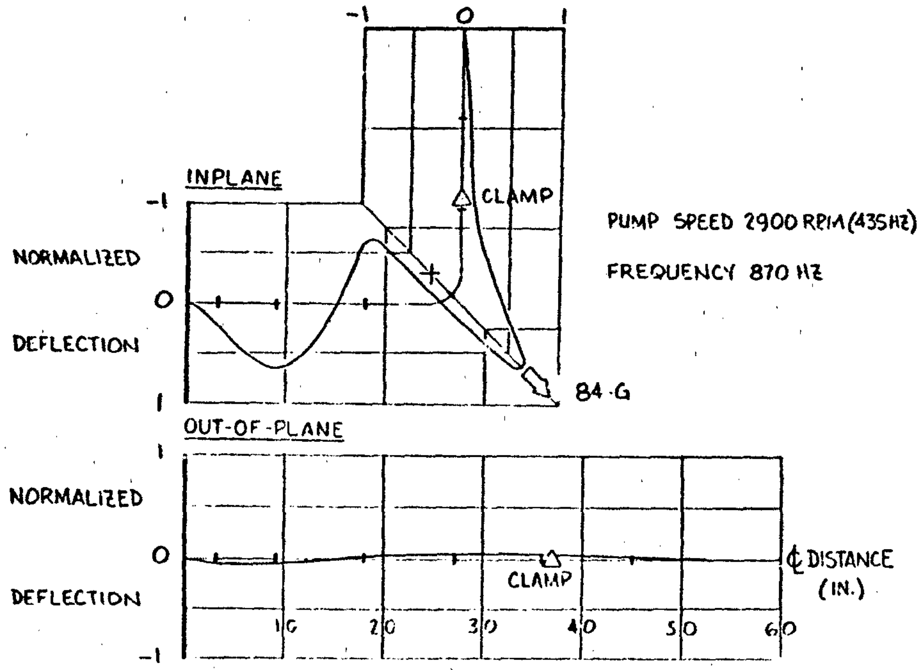


FIGURE 16. HYDRAULIC SYSTEM LINE RESPONSE
ONE-ELBOW PIPE CLAMPED MODE SHAPE DATA

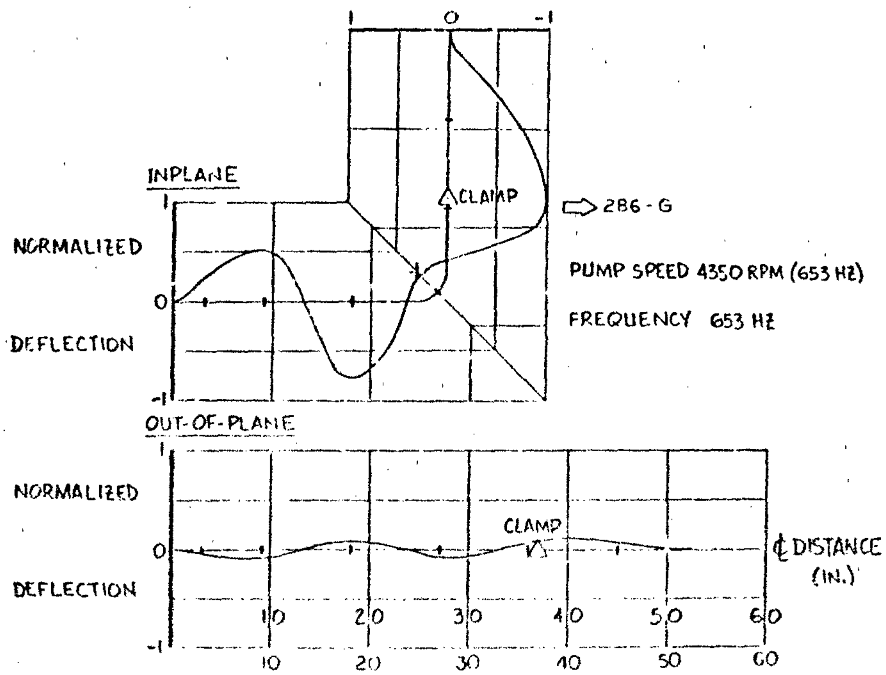


FIGURE 17. HYDRAULIC SYSTEM LINE RESPONSE
ONE-ELBOW PIPE CLAMPED MODE SHAPE DATA

(3) Two-Elbow Pipe

Two fundamental resonances were encountered in this configuration for the unclamped and clamped set-ups. Both sets have similar mode shapes. The out-of-plane peak response occurs at 2900 RPM, the second standing wave resonance, with the maximum deflection midway of the first leg as seen in Figures 18 and 20. In addition, the measured accelerations are close to each other. However, the maximum accelerations occur in the inplane direction with lateral cross-tube motions as shown in Figures 19 and 21. Peak accelerations in the clamped set-up were 15 percent lower than the unclamped version.

(4) Comparison Between Internal and External Data

Graphical superposition of the peak pressures and accelerations are shown in Figures 22 through 28 for the three test configurations. The general trend for the straight and two-elbow lines is for the peak acceleration to occur in the vicinity of zero peak pressure, and for the one-elbow line to have the pressure and acceleration to peak almost simultaneously. A possible explanation to this disparity could be the number of section or legs in a line. Thus, a straight and a two-elbow pipe consist of "odd" sections, and the one-elbow has "even" (two legs) sections.

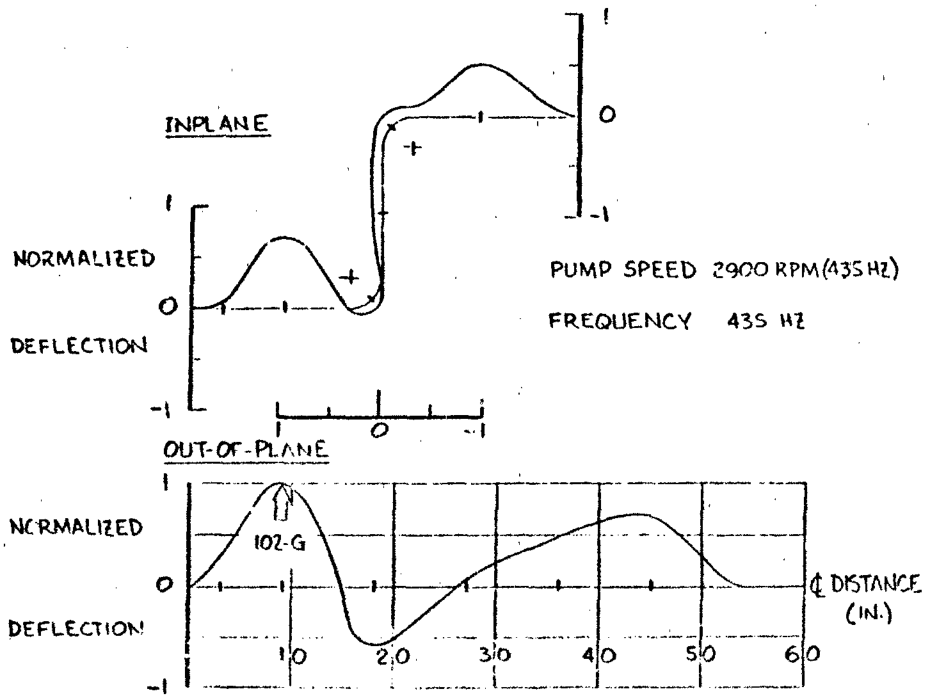


FIGURE 18. HYDRAULIC SYSTEM LINE RESPONSE
TWO-ELBOW PIPE UNCLAMPED MODE SHAPE DATA

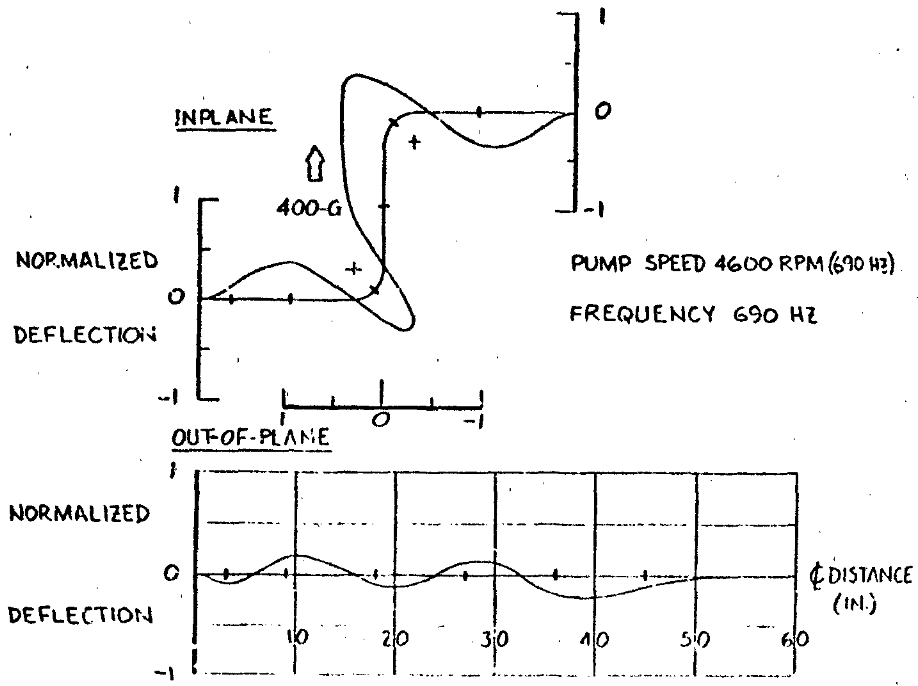


FIGURE 19. HYDRAULIC SYSTEM LINE RESPONSE
TWO-ELBOW PIPE UNCLAMPED MODE SHAPE DATA

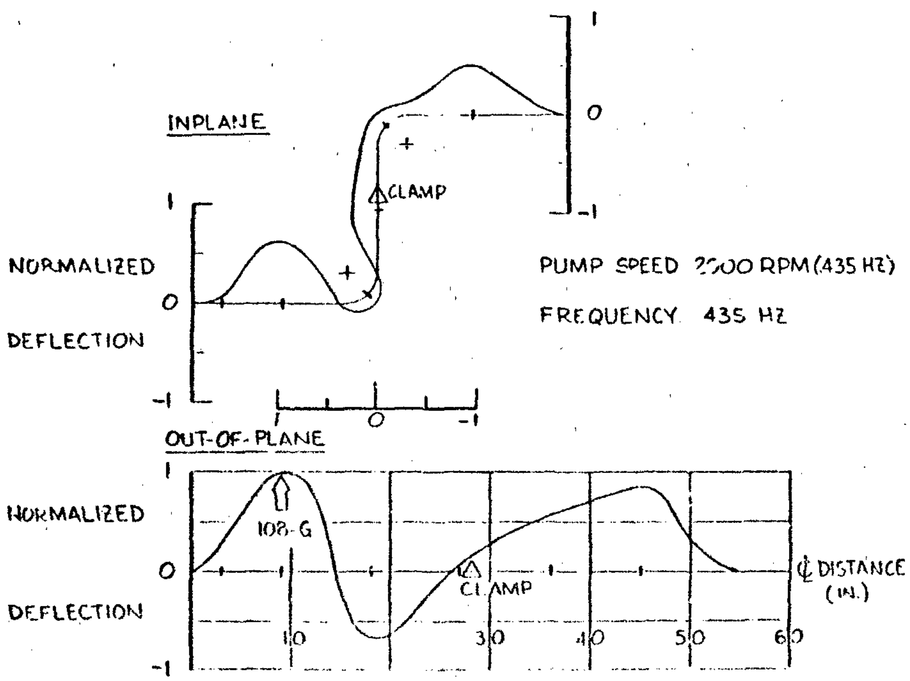


FIGURE 20. HYDRAULIC SYSTEM LINE RESPONSE
TWO-ELBOW PIPE CLAMPED MODE SHAPE DATA

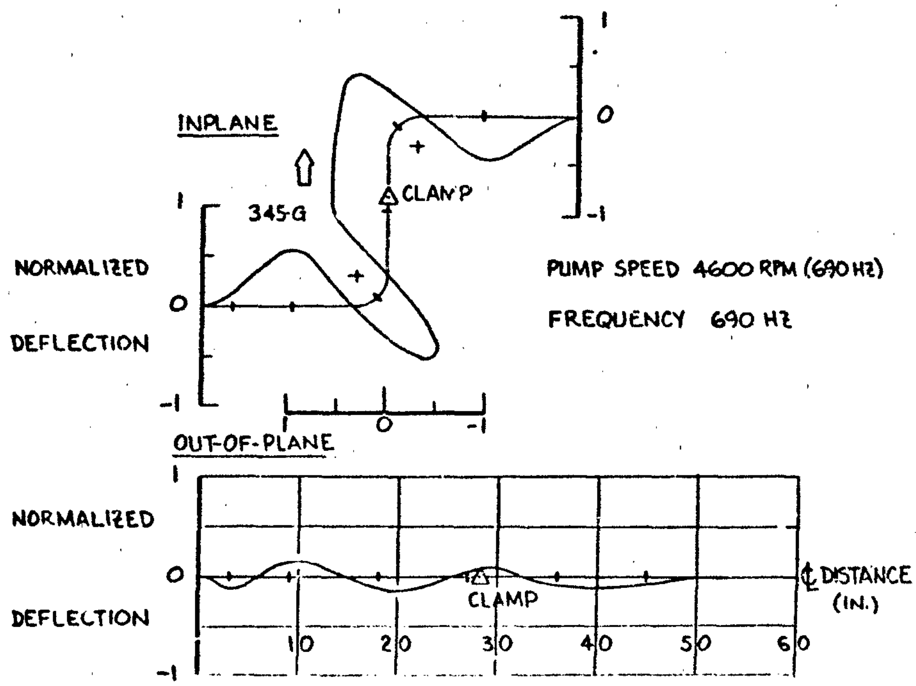


FIGURE 21. HYDRAULIC SYSTEM LINE RESPONSE
TWO-ELBOW PIPE CLAMPED MODE SHAPE DATA

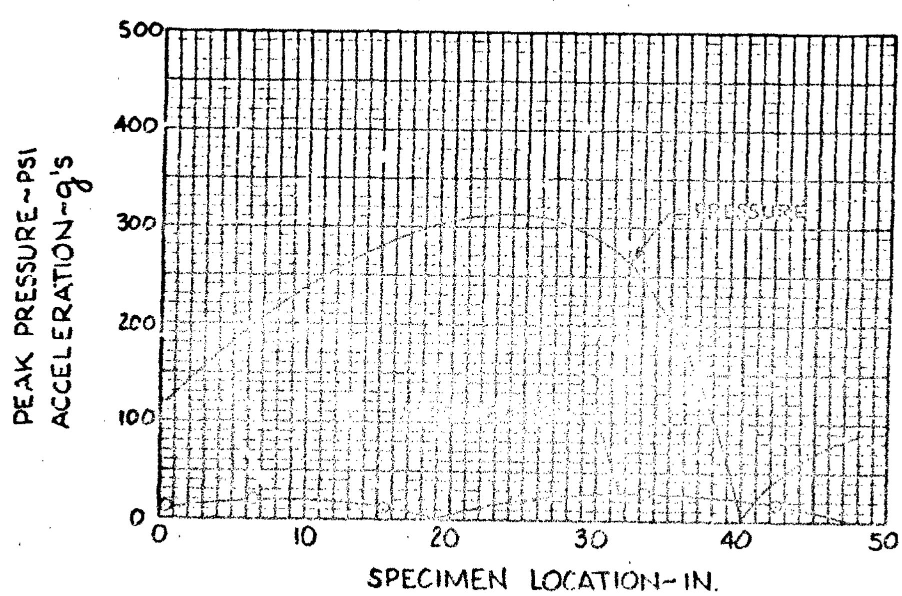


FIGURE 22. STRAIGHT PIPE UNCLAMPED 2900 RPM 435 HZ

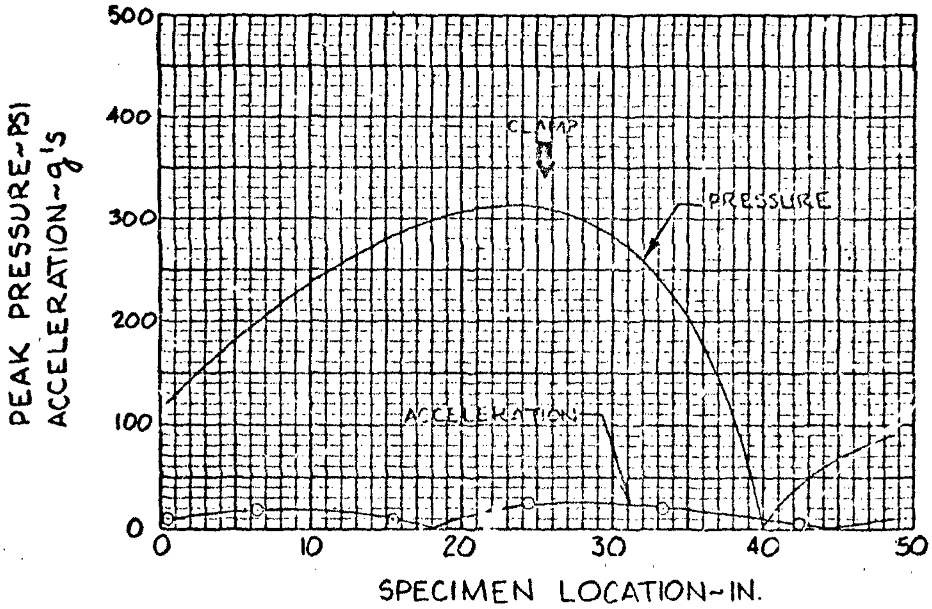


FIGURE 23. STRAIGHT PIPE CLAMPED 2900 RPM 435 HZ

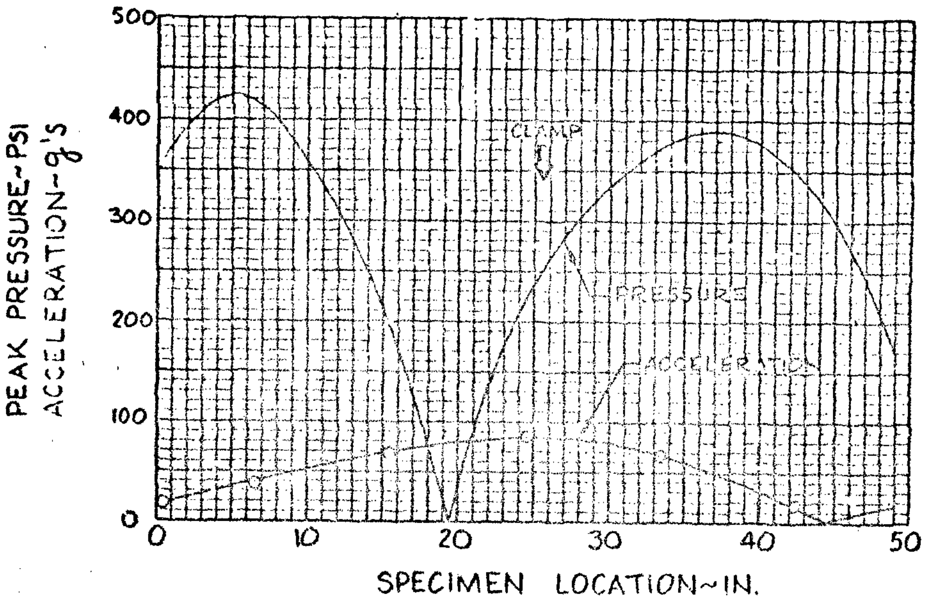


FIGURE 24. STRAIGHT PIPE CLAMPED 4350 RPM 653 HZ

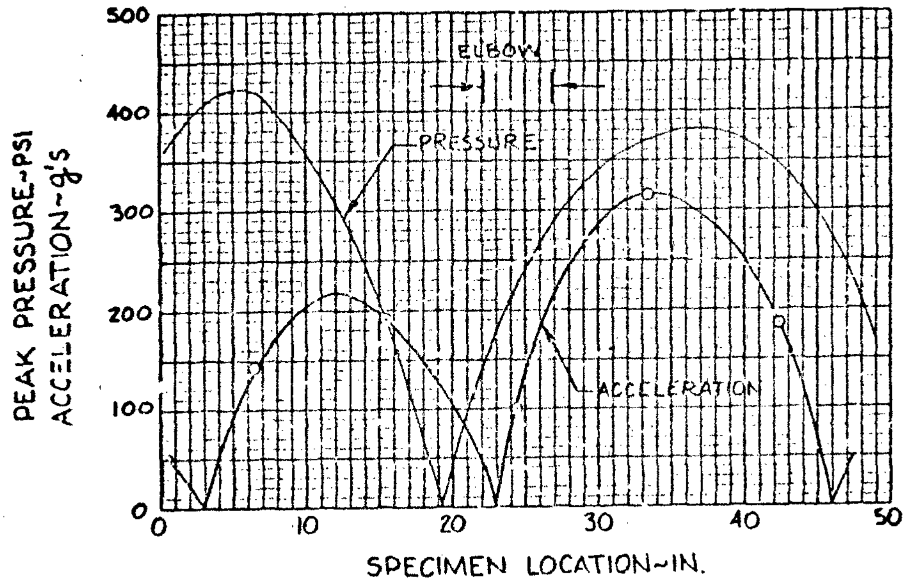


FIGURE 25. ONE-ELBOW PIPE UNCLAMPED 4350 RPM 653 HZ

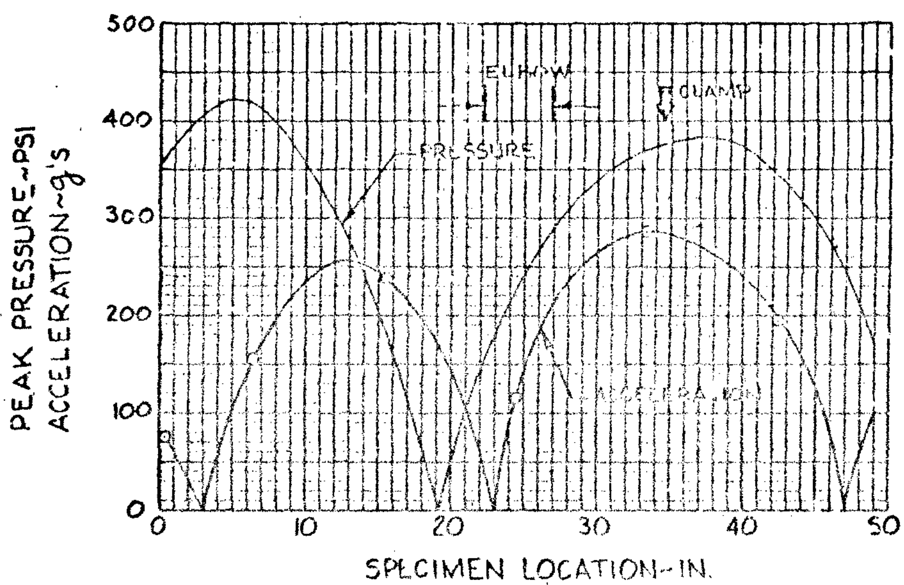


FIGURE 26. ONE-ELBOW PIPE CLAMPED 4350 RPM 653 HZ

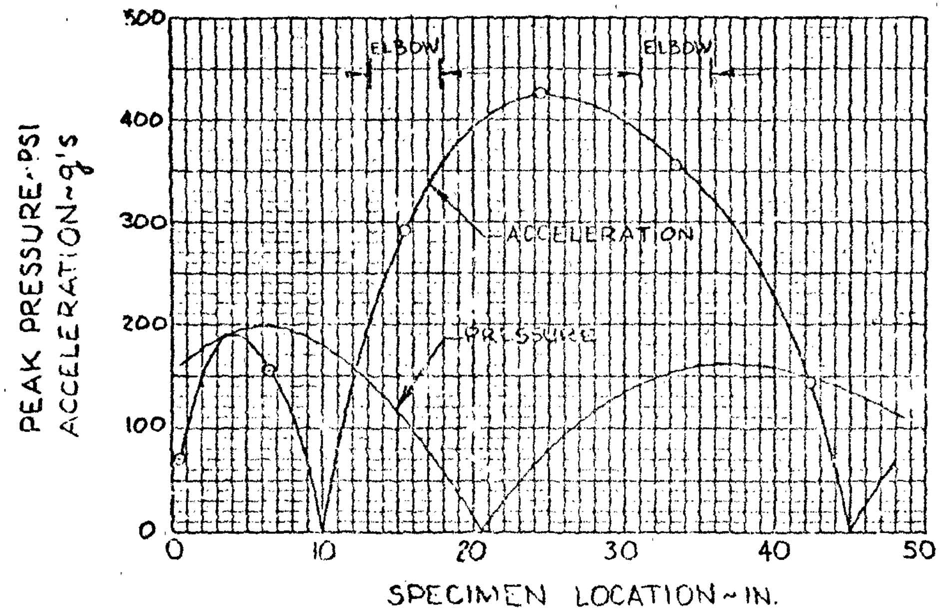


FIGURE 27. TWO-ELBOW PIPE UNCLAMPED 4600 RPM 690 HZ

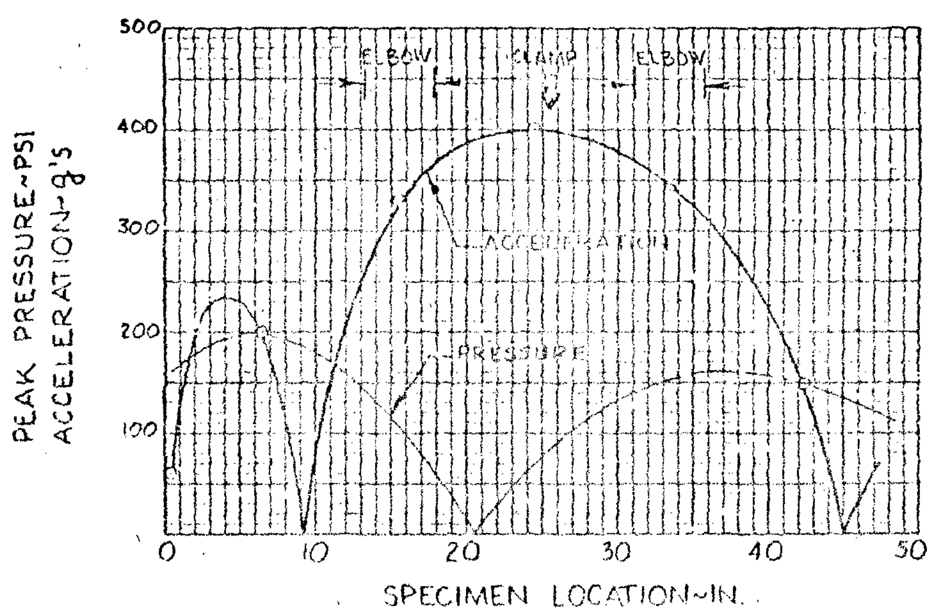


FIGURE 28. TWO-ELBOW PIPE CLAMPED 4600 RPM 690 HZ

(5) Elastomer Flexibility

The clamp elastomer was subjected to successive weights in the test set-up shown in Figure 29. Also shown is a cross-sectional view of the wedge-shaped yellow nitrile clamp elastomer. The results shown in Figure 30, indicate that with increases of one-pound or five-pound weights produce equal slopes or a flexibility (spring rate) of 1290 lb/in. This value can be used in future support flexibility studies.

(6) Strain Measurements

Strain measurements were made on the one-elbow (L-shaped) pipe in the unclamped and clamped configurations to evaluate pump effects. This was beyond the scope of the program. Two gages were placed 3/8-inch from the line specimen edge closest to the pump. One gage was installed to register the longitudinal strain and the other for the circumferential strain. The two gages were attached to the tubing 90-degrees apart with the circumferential strain on the bottom pipe surface and the longitudinal strain on the pipe surface towards the inside of the pipe bend (horizontal plane).

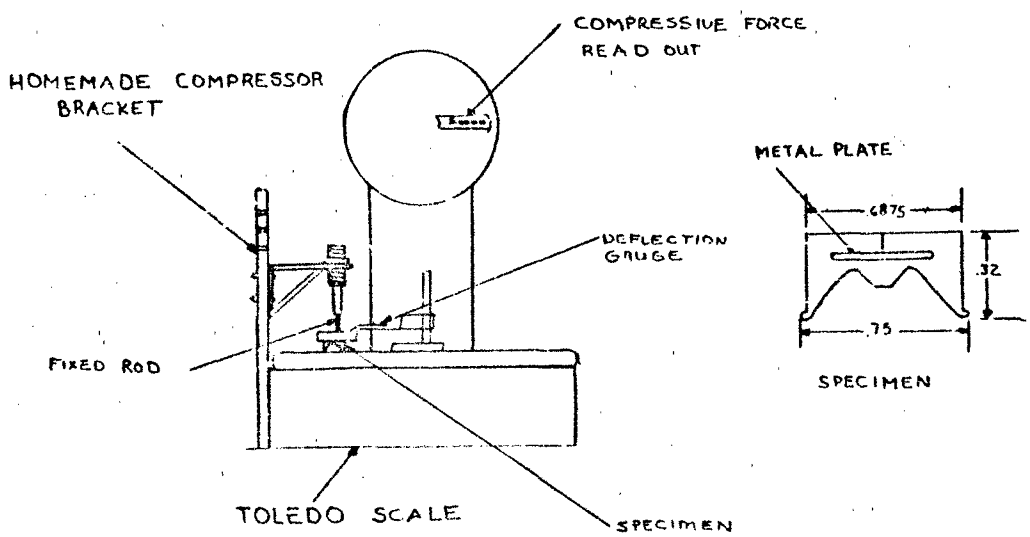


FIGURE 29. ELASTOMER FLEXIBILITY TEST SET-UP

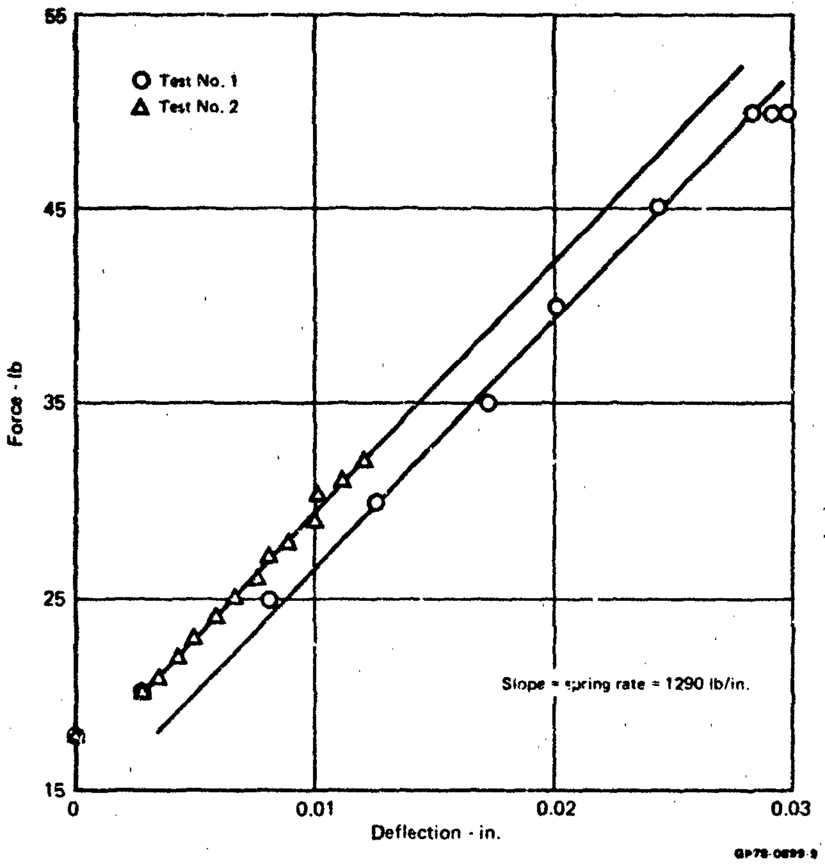


**FIGURE 30 ELASTOMER FLEXIBILITY TEST**
Yellow Nitrile

The measured strains were approximately equal for all resonance conditions encountered and are summarized as follows:

| Test Set-Up | Direction | Strain (Microinches/Inch) |
|---|---|---|
| Unclamped | Longitudinal | 250 |
| | Circumferential | 1080 |
| Clamped | Longitudinal | 300 |
| | Circumferential | 1130 |

The calculated longitudinal and circumferential stresses from the measured strains were about 20 percent and 10 percent lower for the unclamped and clamped configurations, respectively, than those stresses calculated from pressure and geometric considerations.

The results are inconclusive and additional testing is needed, since F-15 Iron Bird has shown the expected variation in stress as a function of motion.

4. ANALYTICAL PROCEDURES

a. Terminology

As previously shown the frequency response data can be used to characterize the shape of deformation of a line associated with each natural frequency or resonance. These unique deformation distributions along the pipe are herein referred to as mode shapes. These mode shapes provide visual means of analyzing the dynamical behavior of a hydraulic line.

A brief review of fundamental considerations in pipe vibrations is appropriate.

(1) Degrees-of-Freedom

This refers to the number of independent quantities defining the position of a system. This means that a system consisting of a mass attached to a massless spring and constrained to a unidirectional motion has one degree of freedom because the system is defined by the deflection of the spring. On the other hand, a simply supported (pinned-pinned) beam or pipe has an infinite number of degrees of freedom. This is due to the flexibility of each element relative to adjoining ones which require an infinite number of element deflections to describe the position completely.

(2) Vibration Modes

The number of principal modes is equal to the number of degrees of freedom. Frequencies of the principal modes of oscillation are called natural frequencies. The lowest natural frequency is called the first or fundamental mode of vibration. A pipe, or beam, has an infinite number of principal modes.

(3) Resonance

Resonance is a phenomenon which occurs when a system is excited periodically (such as by pump pulsations) with a frequency at or very near the natural frequency of the system. At this condition, if the damping of the system is small the system will respond with large amplitudes which have undesirable structural effects.

Between supports or clamps, a pipe is a beam with uniform mass distribution. Each restrained length possesses an infinite number of degrees of freedom, consequently vibration may occur in an infinite number of modes singly or in combination. Table 1 gives an overview of vibration modes as a function of various supports. The frequency factor (multiplier) given in the right hand column is an indication of how the higher model frequencies vary under basic conditions. For example, comparing the factors, the first and second natural frequencies of a fixed-fixed pipe will be the same as the second and third natural frequencies of a cantilever pipe with the same geometric characteristics.

**TABLE 1. PIPE FREQUENCY OVERVIEW**

| SUPPORT | MODES OF VIBRATION | FACTOR |
|---|---|---|
| CANTILEVER | FIRST | 3.52 |
| | SECOND | 22.4 |
| | THIRD | 61.7 |
| PINNED-PINNED | FIRST | 9.87 |
| | SECOND | 39.5 |
| | THIRD | 88.9 |
| FIXED-PINNED | FIRST | 15.4 |
| | SECOND | 50.0 |
| | THIRD | 104 |
| FIXED-FIXED | FIRST | 22.4 |
| | SECOND | 61.7 |
| | THIRD | 121 |

b. Straight Pipe: Transverse and Longitudinal Vibrations

For a straight pipe or beam, the transverse and longitudinal frequencies have been studied by a number of authors such as those in References 7 and 8.

A short computer program including the effects of a fluid in the pipe has been accomplished (Appendix B) and provided the inputs for Figure 31, which shows the effects of varying pipe length between fixed supports. Reducing the length by one-half causes a four-fold increase in the fundamental frequency and a potentially destructive effect if it falls within the pump operating regime. Note that the frequency is approximately the same for aluminum, steel, and titanium tubes. This is because the ratios of modulus of elasticity to density for these materials are nearly equal. The factors shown indicate the effect of fluid on frequencies. Reducing the pipe diameter or increasing the wall thickness lowers the frequency since for a given length the modifying parameter is the square root of the inertia-area ratio as shown in Figure 32. Although the computer program presented in Appendix B is for a pipe with fixed or built-in ends, the fundamental and higher order frequencies for a straight pipe of any length between various types of non-flexible supports can be determined by means of the frequency factors provided in Table 1.

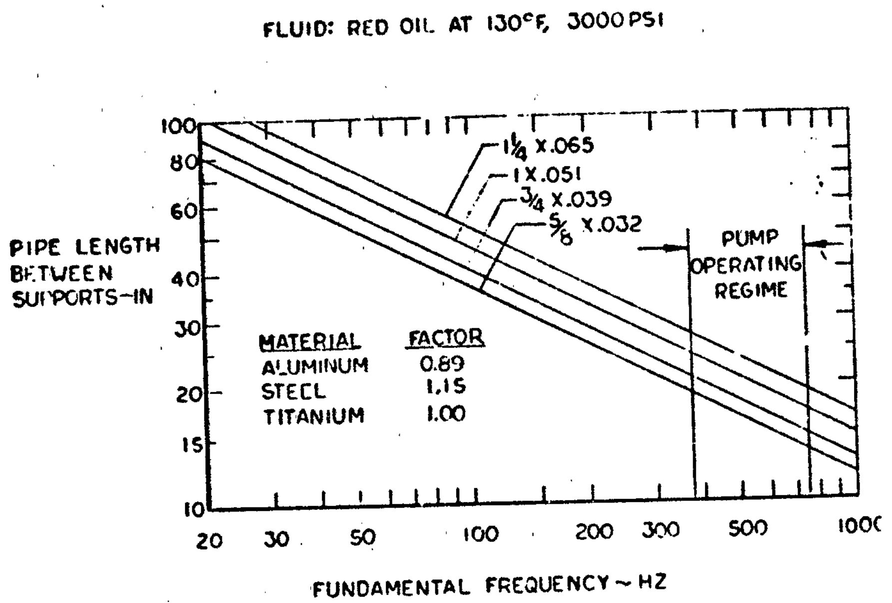


FIGURE 31. STRAIGHT PIPE BENDING VIBRATIONS
FIXED-FIXED SUPPORTS

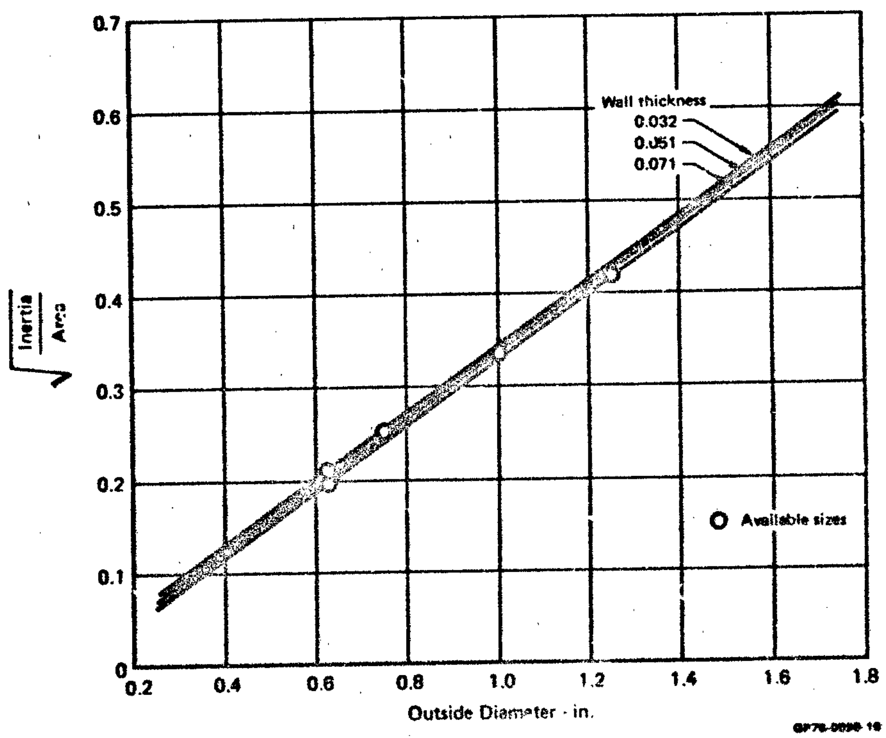


FIGURE 32 INERTIA AREA RATIO EFFECTS ON VIBRATIONS
Equal Pipe Lengths

A brief investigation was made into the effect of clamp elastomer flexibility, Figure 33, which indicates that for midspan clamp tiffnesses below 300 lb/in. (test elastomer 1290 lb/in.), the critical speed is only dependent on pipe length. As the spring rate/stiffness is substantially increased, there is the danger of having the critical speed within the pump operating regime.

c. One-Elbow Pipe Vibrations

Programs were developed for the in-plane and out-of-plane vibrations and are included in Appendix B. For the inplane vibrations, the analysis is based on simplified analysis using frequency factors shown in Table 1 for the appropriate end conditions and modes. In addition, Dunkerley's method was used to find the coupling frequencies. The method is used to find the approximate value of the frequencies of shafting systems. The formula is as follows:

$$\frac{1}{f^2} = \frac{1}{f1^2} + \frac{1}{f2^2} + \frac{1}{f3^2} + \text{---} + \frac{1}{fn^2}$$

where f is the approximate fundamental natural frequency of the system, and f1, f2, f3, --- fn are the natural frequencies of a single mass of a multi-degree of freedom system. The limitations imposed on the program is its applicability to pipes with 90-deg bend angles.

The results are shown in Figures 34 and 35 for the test pipe size (1.00-O.D. x .051 wall) and indicates the effect of material type and leg length on frequency. The numbered modes have been detailed in Table 1. It is seen that for a titanium pipe of equal leg lengths of 23 inches, there are no inplane vibrations of significance within the pump operating regime.

For the out-of-plane vibrations, the analytical development is shown in Appendix C and the computer program incorporated in Appendix B. Computer runs were performed for two different pipe sizes and the results are shown in Figure 36. Variation of leg lengths and type of material are not as important as the pipe length between supports. Thus, undesirable out-of-plane vibrations are encountered in the operating regime if the distance between supports are in the vicinity of 20 inches or less.

d. Two-Elbow Pipe Vibrations

The inplane and out-of-plane vibration analysis were developed using similar techniques as the one-elbow inplane analysis. The derivation of the equations of motion for the crosspipe (middle leg) translational and torsional modes are shown in Appendix C.

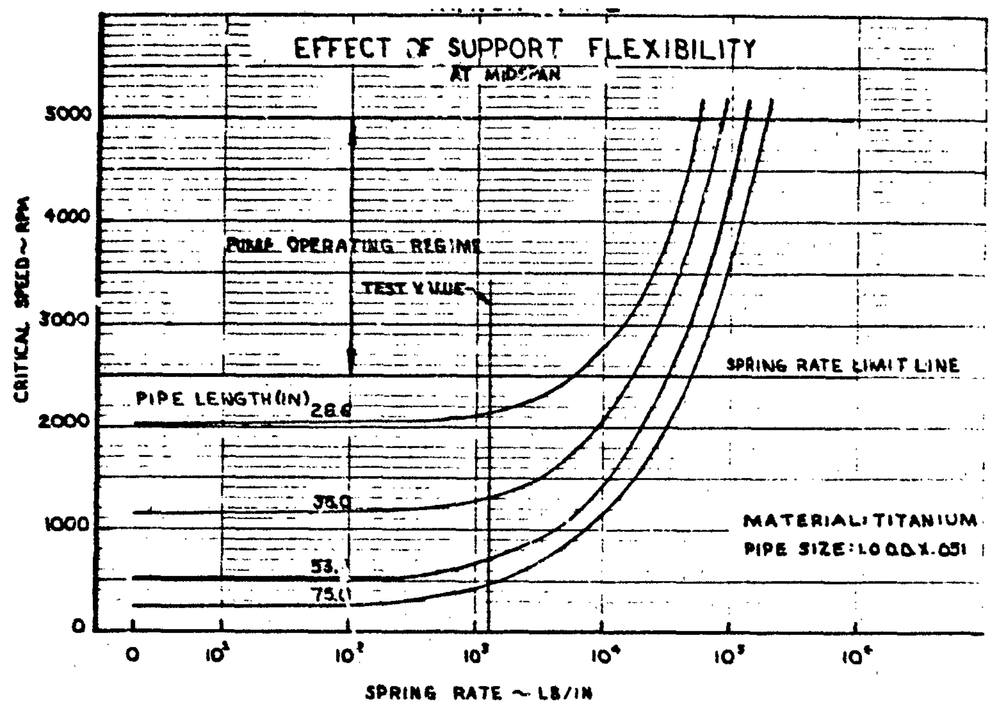


FIGURE 33. CLAMP ELASTOMER FLEXIBILITY, STRAIGHT PIPE

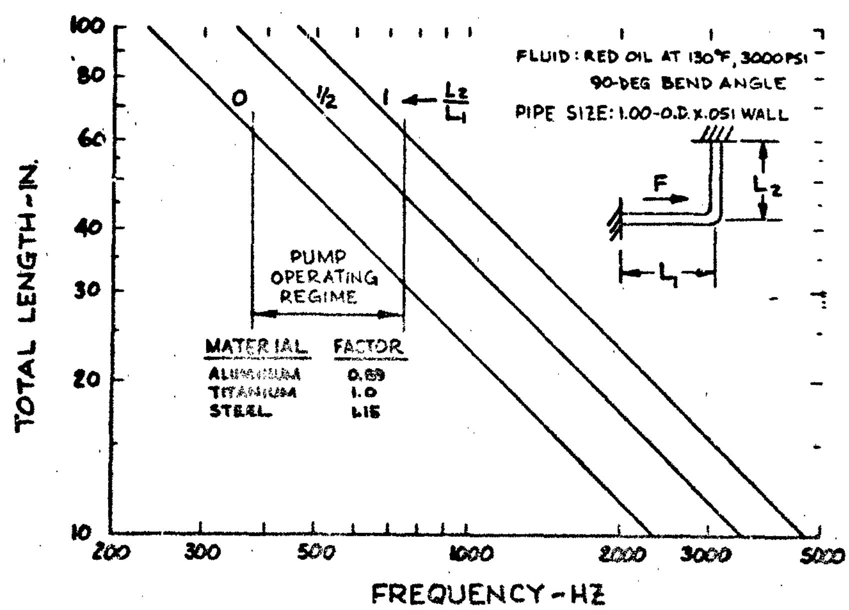


FIGURE 34. ONE-ELBOW PIPE INPLANE VIBRATIONS AXIAL FREQUENCY

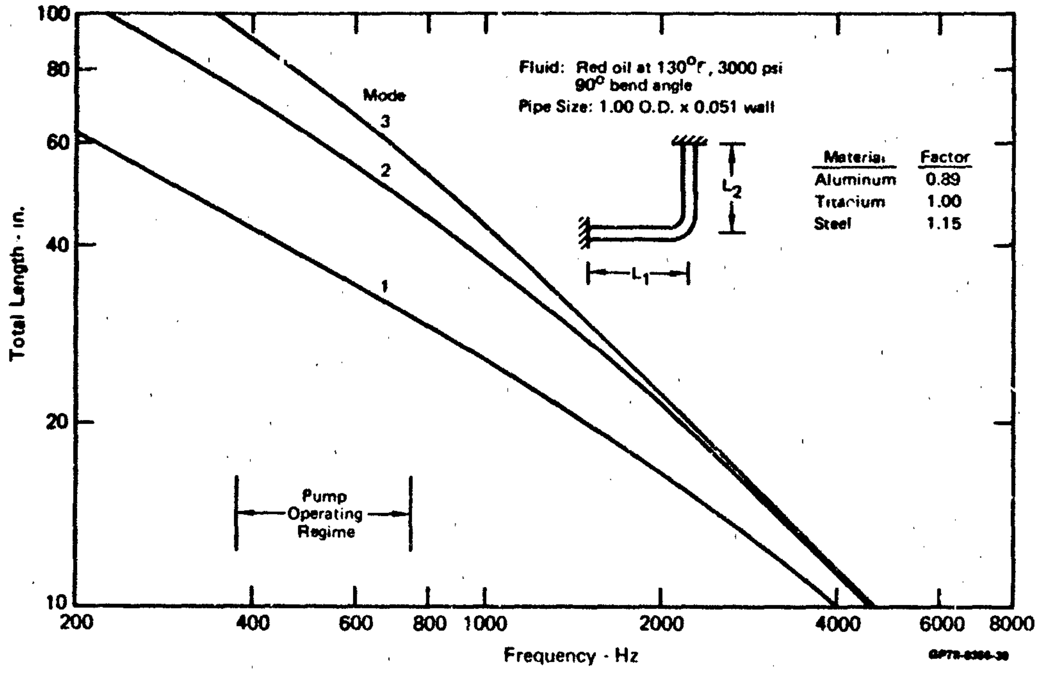


FIGURE 35. **ONE-ELBOW PIPE INPLANE VIBRATIONS COUPLED AXIAL-BENDING FREQUENCY**

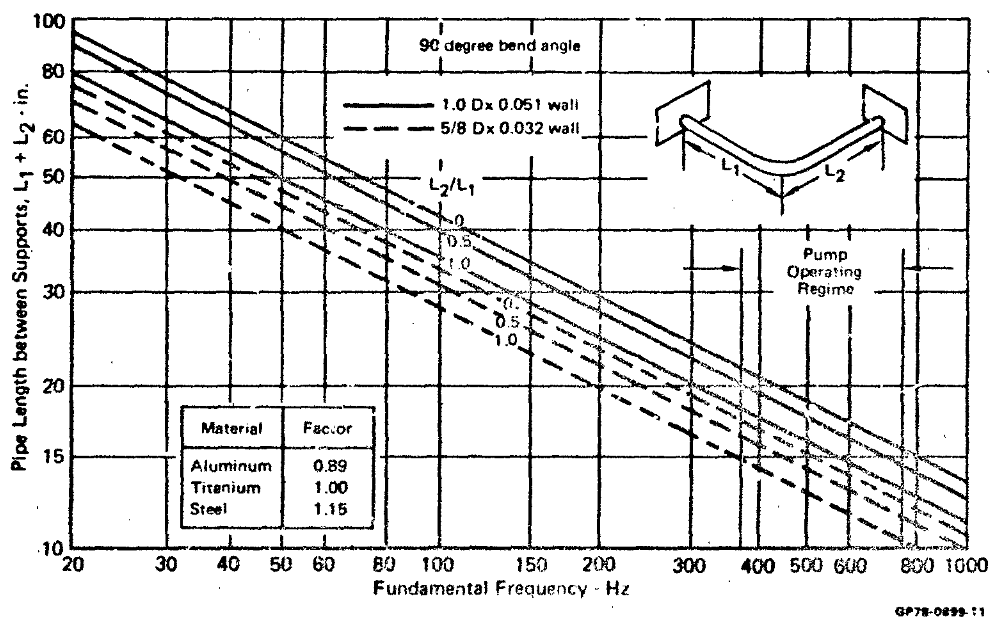


**FIGURE 36 ONE-ELBOW PIPE OUT-OF-PLANE VIBRATIONS**
Fluid: Red Oil at 130°F 3000 psi

5. MODEL VERIFICATION

a. Test Data Summary

Pictorial representations of the relationship between resonances and pump speed, for the data previously reported, are summarized in Figures 37 through 39 for the straight pipe, one-elbow pipe, and two-elbow pipe, respectively. There are two basic sets of data in each figure. The first set are the horizontal lines which indicate the natural frequencies measured on the test set-up. The second set is the radial arrangement of straight lines, with a common point at the origin of the rectangular coordinate system, which depicts the relationship between the exciting frequency and the pump speed. These radial lines have slopes equal to the harmonics of the pump, which is the number of oscillations per revolution. The intersections of these radial lines (hydraulic exciting frequencies) with the horizontal lines (natural mechanical frequencies) indicate conditions of resonance.

Although tests indicated three hydraulic resonances at pump speeds of 1600 rpm, 2900 rpm, and 4300 rpm, none excited a fundamental mechanical resonance. At 1600 rpm no significant mechanical responses were measured in any of the three test configurations. The other two pump speeds produced the larger responses in terms of measured accelerations.

(1) Straight Pipe

The test data summary is shown in Figure 37. At 2900 rpm, the pipe is responding similarly to the third mode of a beam with built-in ends. The measured frequency at this mode was 435 Hz. This is close to the computed value of 409.3 Hz.

At 4350 rpm, a longitudinal excitation was measured at 653 Hz. This value is almost half the calculated frequency of 1370 Hz indicating possible interaction with pipe overhang just outside the supporting brackets or the brackets themselves when a clamp is used.

(2) One-Elbow Pipe

The hydraulic resonances at 2900 rpm and 4300 rpm resulted in predominantly inplane motions. As seen in Figure 38, the peak accelerations were measured at the first harmonic of the pump speed, with 315-G for the unclamped case reduced to 286-G for the clamped version, on the accelerometer located after the elbow, away from the pump. Higher order mechanical responses were measured at 1030-1035 Hz which excited both inplane and out-of-plane motions. The calculated out-of-plane fundamental frequency is 43.8 Hz which is so low with respect to the pump operating regime that it precludes any coupling with mechanical or hydraulic resonances for the system tested.

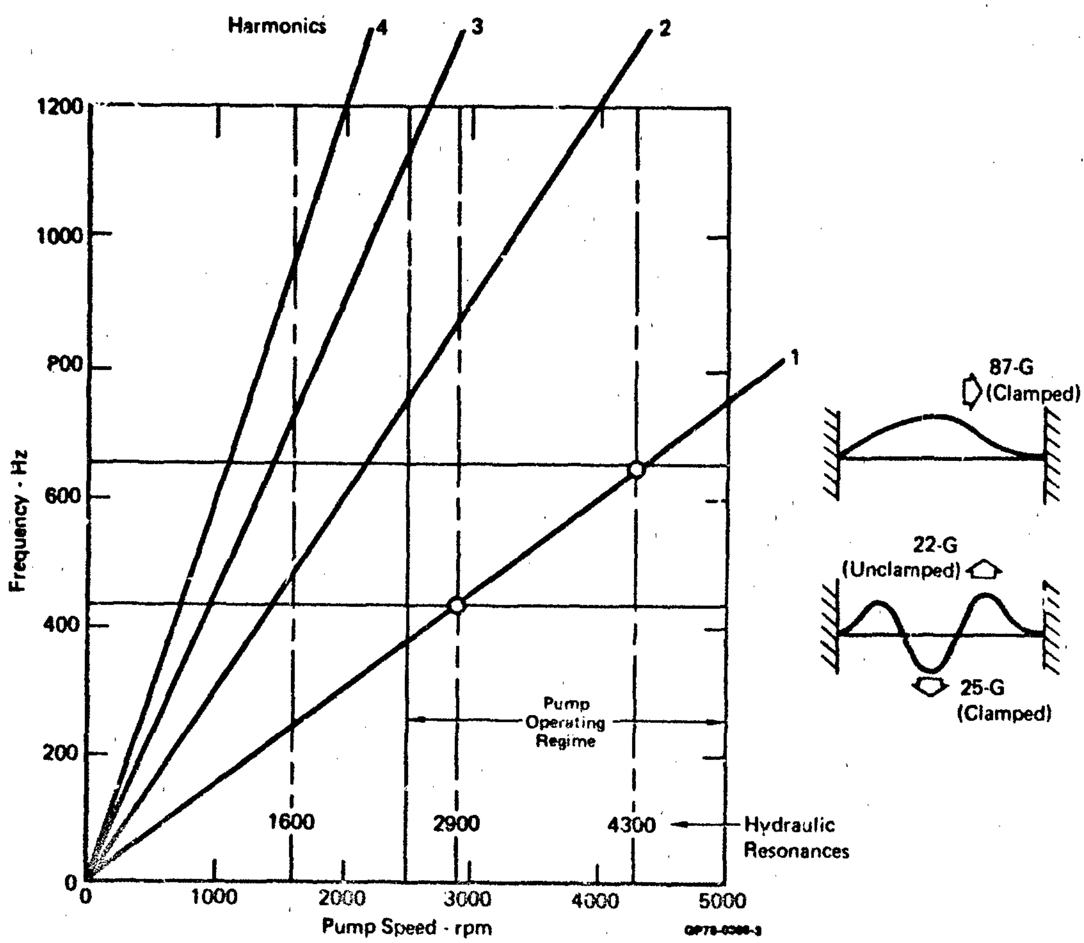


FIGURE 37. HLMR TEST DATA SUMMARY
Straight Pipe

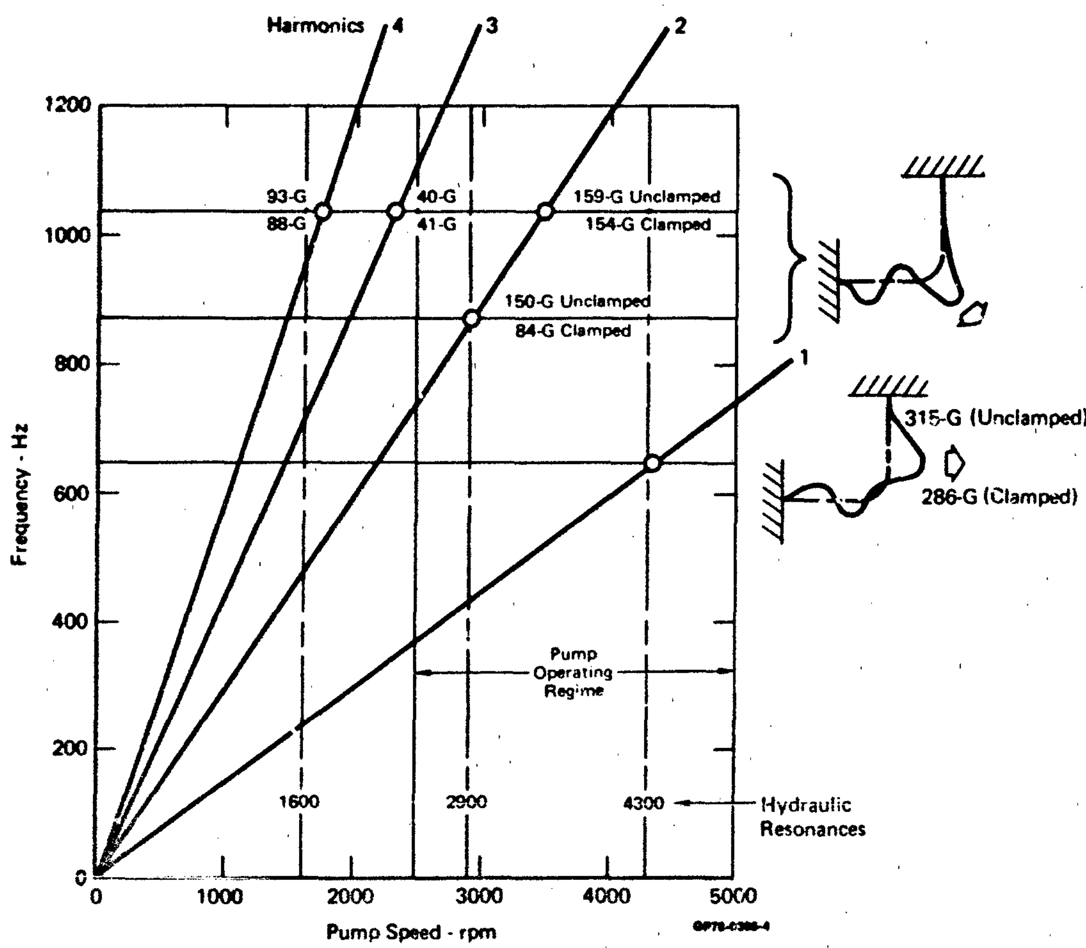


FIGURE 38. **HLMR TEST DATA SUMMARY**
One-Elbow Pipe

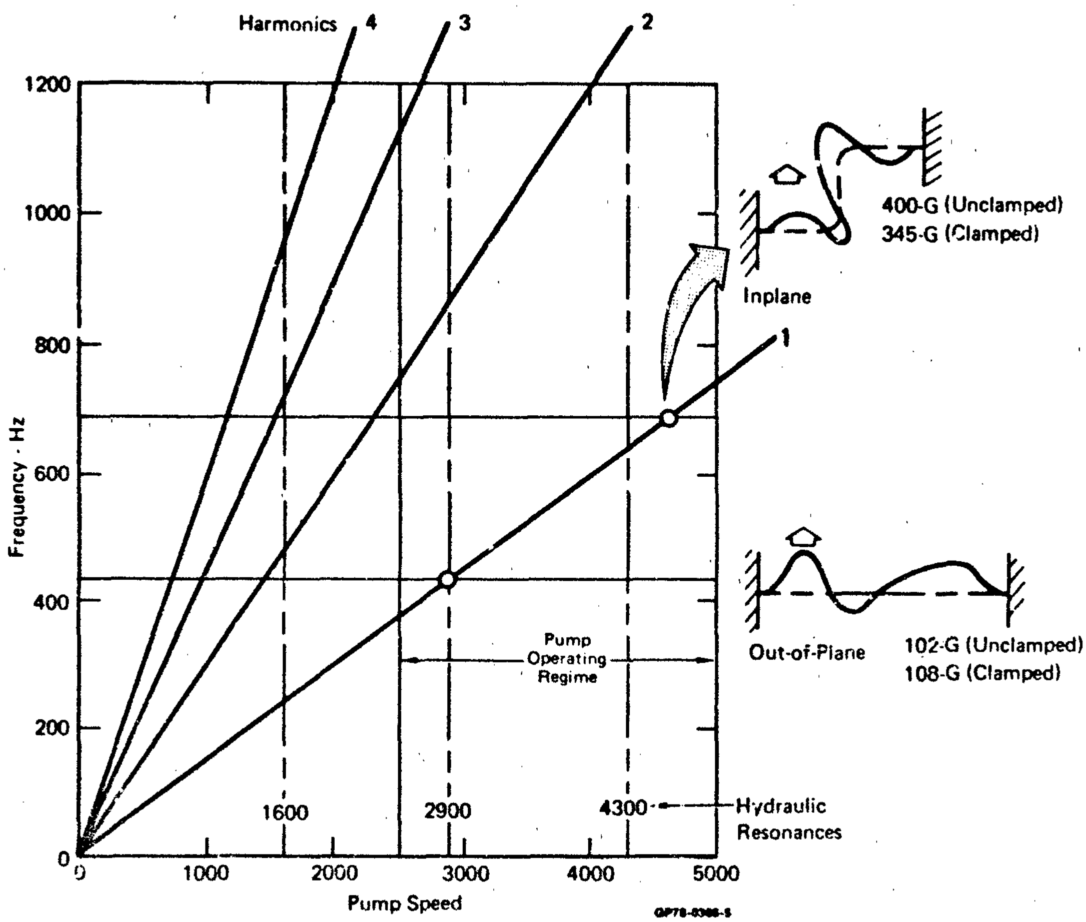


FIGURE 39. **HLMR TEST DATA SUMMARY**
Two-Elbow Pipe

(3) Two-Elbow Pipe

Similarly, the measured data is summarized in Figure 39. The two resonances shown, with insets providing visual representation of the mode shapes, were excited by the first harmonic of the pump speeds at 2900 rpm (out-of-plane) and 4600 rpm (in-plane). The latter pump speed is slightly higher than the hydraulic resonance measured at 4300 rpm.

b. Comparison of Analytical and Test Results

The straight pipe vibration modes and frequencies are predictable, while the one-elbow pipe out-of-plane fundamental frequency was calculated to be far below the pump operating regime and consequently of little relevance. The one-elbow pipe inplane vibrations indicate that for the test configuration, the calculated axial and coupled axial-bending frequencies are within the expected accuracy limits of the analysis but lower than the measured value. In the determination of the axial frequency, the entire fluid weight was considered to be contributing to the total component weight. The contribution of fluid weight to the overall solution has not been studied as extensively as mechanical systems. The results of a brief study into the variation of fluid weight on the axial frequency is shown in Figure 40.

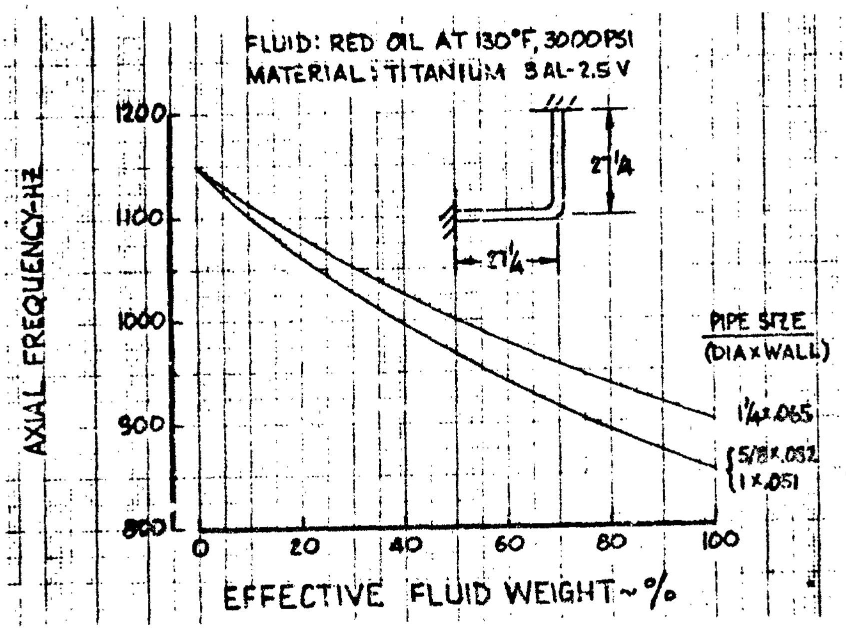


FIGURE 40. ONE-ELBOW PIPE INPLANE VIBRATIONS
EFFECT OF FLUID ON AXIAL FREQUENCY

A 33% effective fluid weight results in an accurate prediction of the axial frequency. Pipe sizes with ratios of flow area to cross-section area which are very close to each other results in similar axial frequencies. It is interesting to note that Reference 8 suggests that in a spring-mass system the determination of frequencies should take into account one-third of the spring weight. The test results and analysis are summarized as follows:

Table 2 - One-Elbow Pipe Data Correlation

| Pump Speed (RPM) | Frequency (Hz) Measured | Calculated | Mode Identification |
|---|---|---|---|
| 1720 | | 851 | Axial (100% fluid) |
| 2300 | 1030-1035 | 1035 | Axial (33% fluid) |
| 3440 | | | |
| 2900 | 870 | 860 | Second bending |
| 4350 | 653 | 605 | Second axial-bending |

The two-elbow pipe computer output data were extracted for comparison with the measured data and the results are summarized as follows:

Table 3 - Two-Elbow Pipe Data Correlation

| Pump Speed (RPM) | Frequency (Hz) Measured | Calculated | Mode Identification |
|---|---|---|---|
| 2900 | 435 | 431 | Coupled axial-bending |
| 4600 | 590 | 634 | Axial |

## SECTION III

## F-15 PISTON PUMP MODEL VERIFICATION

Further testing and computer program model development work was accomplished on the instrumented F-15 hydraulic pump (S/N 038). The HYTRAN pump computer model was enhanced.

The instrumented pump used in the original AFAPL three year contract was refurbished by Abex. The wiped port plate and cylinder barrel were replaced, a case drain pressure tap was installed, and new O'rings were installed.

Steady state tests were run to recheck the case pressure/flow and the heat rejection characteristics.

The HYTRAN pump model calculation of case pressure was to be verified with the case pressure transducer, and tests were repeated for low and high flow demands at several test conditions identical to those for the original pump model verification.

In addition tests were repeated at 4400 psi pump outlet pressure to verify the F-15 pump transient model at the higher pressure. Frequency response data was also taken to determine pressure pulsations at the 4400 psi test pressure with the pump valve plate still timed for 3000 psi outlet pressure.

### 1. FREQUENCY RESPONSE TESTS

The refurbished F-15 instrumented pump was used for the extended frequency response testing. Outlet circuit pressure pulsations at 4400 psi were mapped in the same line locations as in the original 3000 psi frequency response verification tests. Total pressure pulsations and fundamental frequency pulsations were measured at each location during the pump speed sweeps.

a. Test Circuit Description and Computer Model

A load valve was added to the transient test stand and test runs were made on the system configuration shown in Figure 41 with MIL-H-5606B hydraulic fluid. Figure 42 shows the 9 ft. frequency response test section which terminates at the load valve. The figure details the locations of the measured data points used for the frequency mapping. A roving clamp-on transducer was used to collect data at the indicated points between locations P3 and P2, which were permanent transducer locations. For each test point a plot of the fundamental frequency and a oscilloscope trace of the total peak to peak pressure pulsations were made as the pump swept from 1000 to 4300 rpm. The steady state flow rate of 12.9gpm was somewhat higher than desired, but it was necessary to keep the pump operating in a stable mode. HSFR input data for the high pressure verification circuit is shown in Table 4.

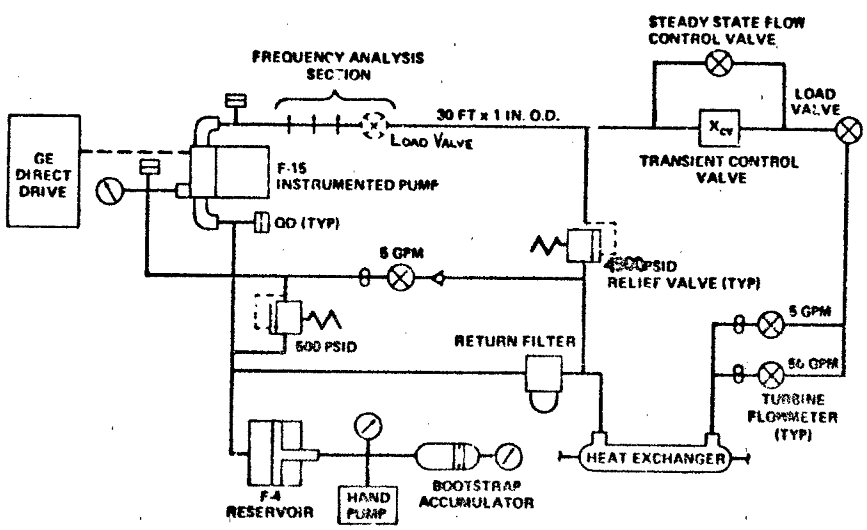


FIGURE 41. HYDRAULIC PUMP VERIFICATION TEST SETUP

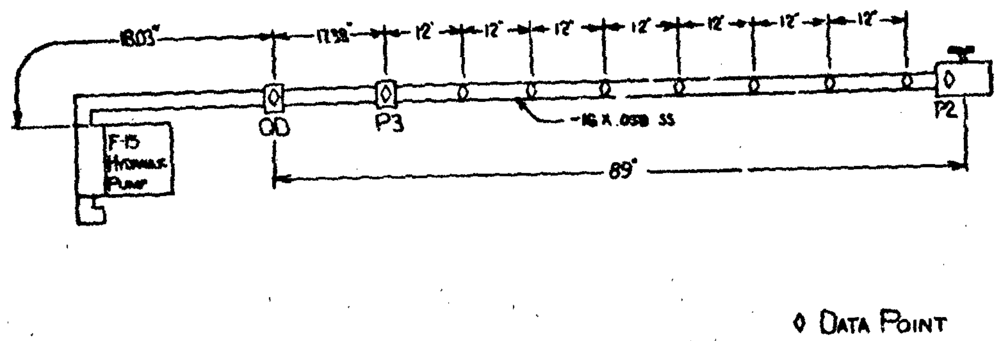


FIGURE 42. 9 FT. FREQUENCY RESPONSE TEST SECTION

TABLE 4. HSFR PROGRAM INPUT DATA HIGH PRESSURE TEST - SHORT LINE

```
FREQUENCY RESPONSE - F-15 PUMP HIGH PRESSURE TEST - SHORT LINE
  18     1    113.0      4250.
                                          1.           9.
   1000.      5000.        50.          1.12        1.172        .698        .57        .18
   9    22      .19       .666         3.375        28.75       26.25        26.       21.75
        .2     19.5       3.60          2.07       .00042         55.       150.         .69
       50.      .06        .78
   1            8.0      1.200          .100       3.0E07
   1            3.5      1.200          .100       3.0E07
   1           3.75      1.000          .058       3.0E07
   1           2.87      1.000          .058       3.0E07
   6     1
  13            .15
   1          17.38      1.000          .058       3.0E07
   1          12.00      1.000          .058       3.0E07
   1          12.00      1.000          .058       3.0E07
   1          12.00      1.000          .058       3.0E07
   1          12.00      1.000          .058       3.0E07
   1          12.00      1.000          .058       3.0E07
   1          12.00      1.000          .058       3.0E07
   1          12.00      1.000          .058       3.0E07
   1          12.00      1.000          .058       3.0E07
   1           1.13      1.000          .058       3.0E07
   1           3.87      1.000          .053       3.0E07
  14          120.0       50.0
   8     1      4      6      9     37     38     39     40
  17     1      4      6      9     10     11     12     13     14     15     16     17     18     37     38
  39    40
   9     1      4      6      9     18
```

b. <u>Test Results and Comparison to HSFR Program Predictions</u>

The test data was manually overplotted on a reduced computer output plot. Manual plotting and reproduction distortion will introduce some error in the correlation process.

Oscilloscope traces of the peak to peak pressure pulsations indicated resonant frequencies at 1500, 2650 and 4000 rpm. These frequencies of course were identical to those seen at the 3000 psi operating pressures. The highest pulsation recorded was located at 83.41 inches from the pump outlet. At approximately 4000 RPM they were 1300 psi peak to peak as indicated in Figure 43.

The fundamental peak pressure pulsation measured in the lab is presented in Figure 44. At 4000 rpm there is a 300 psi peak to peak pulsation. This indicates that the remainder of the pulsation energy is found at the higher harmonics.

The HSFR computer generated pressures at the mapping locations are presented in Figures 45 through 54. The test data has been overplotted on the computer output for comparison. The plots show excellent frequency correlation of 0-3% (0 to 75 rpm) for the second and third resonant speeds of 2650 and 4000 rpm.

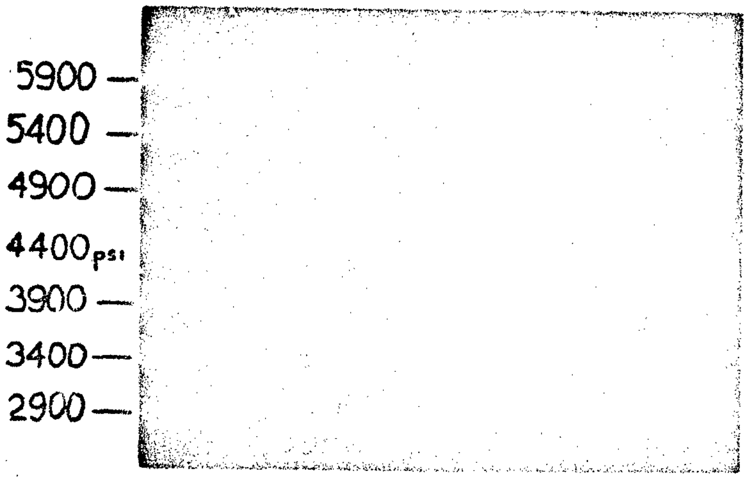


FIGURE 43. PEAK TO PEAK PRESSURE PULSATIONS 83.41 INCHES FROM PUMP OUTLET

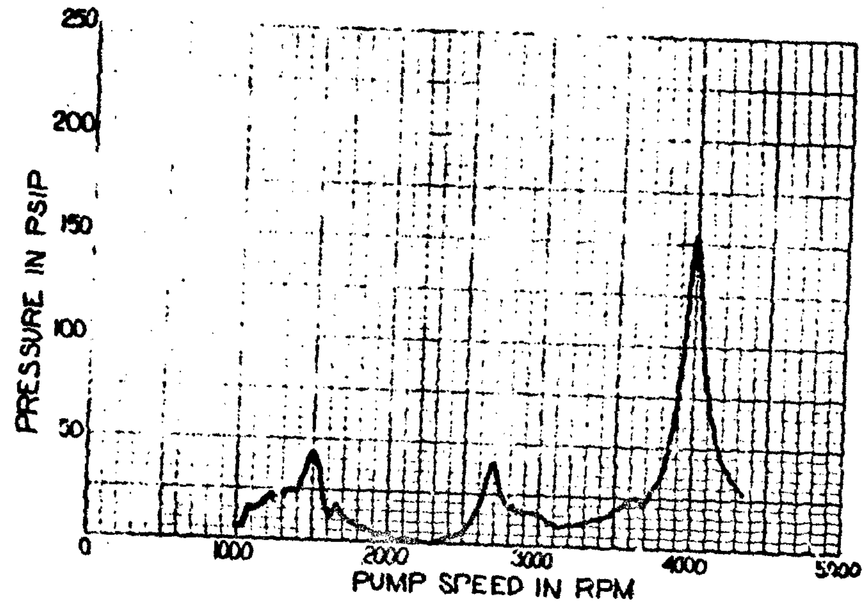


FIGURE 44. 48" FROM P3: FUNDAMENTAL 113°F 12.9GPM

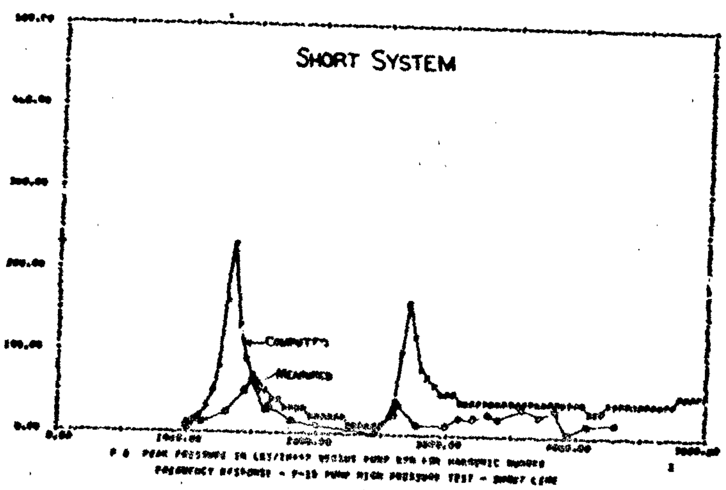


FIGURE 45. FREQUENCY RESPONSE EXTENDED F-15 PUMP VERIFICATION TEST
MIL-H-5606B 4400PSI 130°F 12.9 GPM
18.03 INCHES FROM PUMP OUTLET

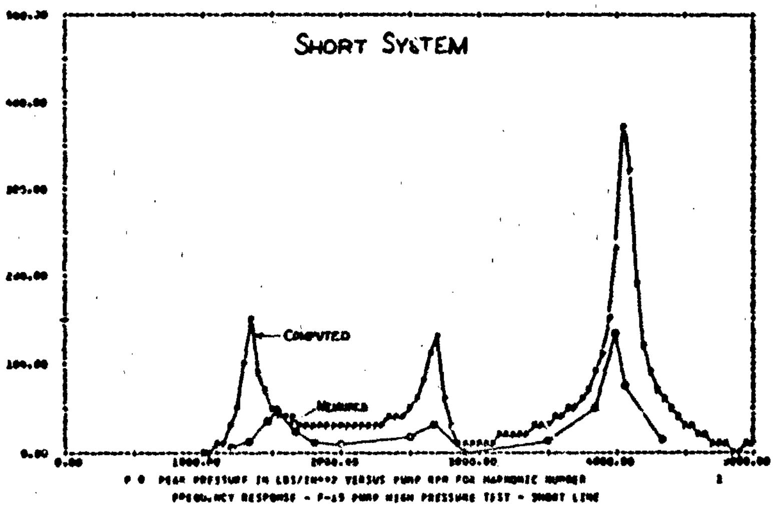


FIGURE 46. FREQUENCY RESPONSE EXTENDED F-15 PUMP VERIFICATION TEST
MIL-H-5606B 4400 PSI 112°F 12.9 GPM
35.41 INCHES FROM PUMP OUTLET

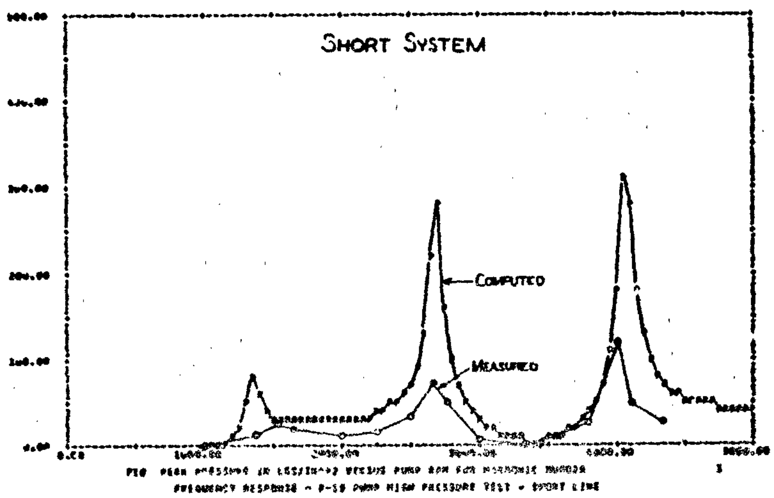


FIGURE 47. FREQUENCY RESPONSE EXTENDED F-15 PUMP VERIFICATION TEST
MIL-H-5606B 4400 PSI 113°F 12.9 GPM
47.41 INCHES FROM PUMP OUTLET

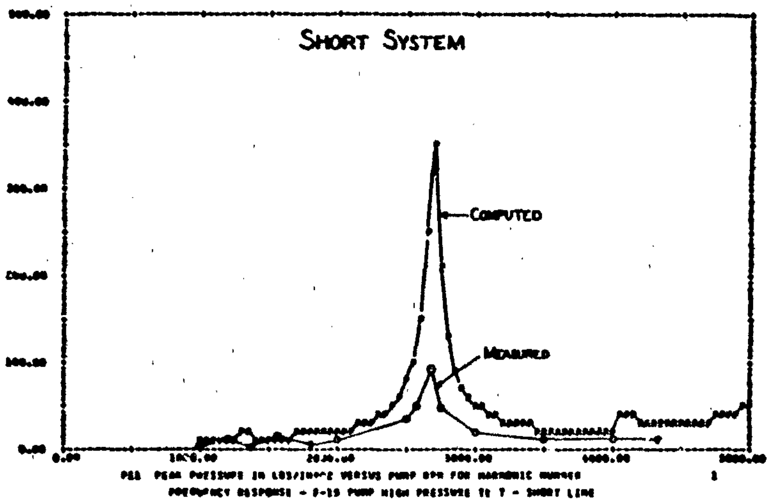


**FIGURE 48.** FREQUENCY RESPONSE EXTENDED F-15 PUMP VERIFICATION TEST
MIL-H-5606B 4400 PSI 113°F 12.9 GPM
59.41 INCHES FROM PUMP OUTLET

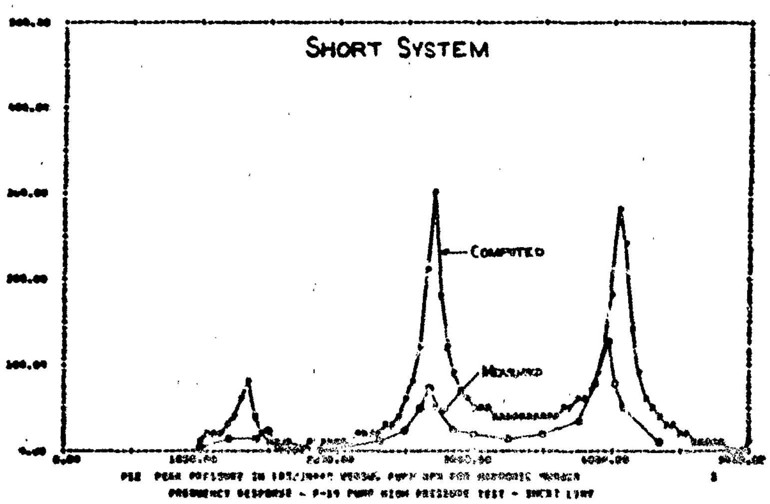


**FIGURE 49.** FREQUENCY RESPONSE EXTENDED F-15 PUMP VERIFICATION TEST
MIL-H-5606B 4400 PSI 113°F 12.9 GPM
71.41 INCHES FROM PUMP OUTLET

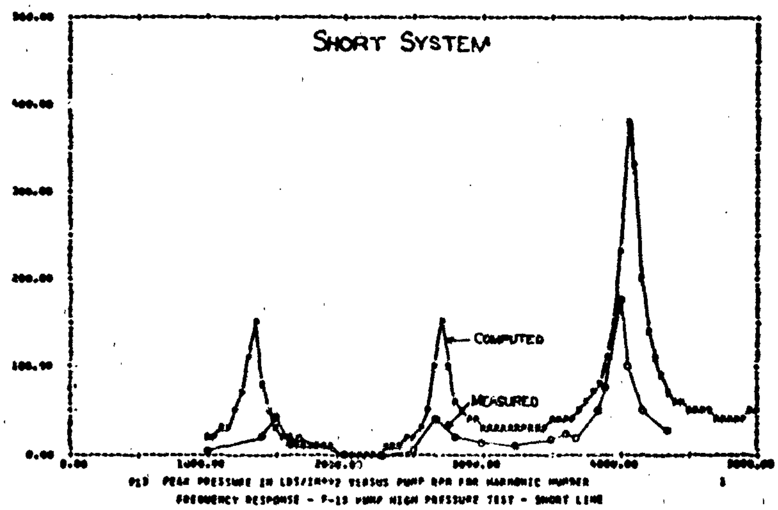


**FIGURE 50.** FREQUENCY RESPONSE EXTENDED F-15 PUMP VERIFICATION TEST
MIL-H-5606B 4400 PSI 113°F 12.9 GPM
83.41 INCHES FROM PUMP OUTLET

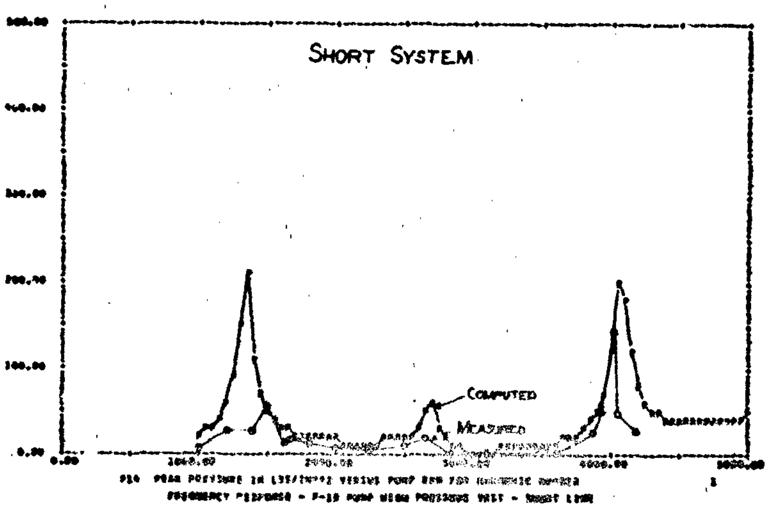


**FIGURE 51.** FREQUENCY RESPONSE EXTENDED F-15 PUMP VERIFICATION TEST
MIL-H-5606B 4400 PSI 113°F 12.9 GPM
95.41 INCHES FROM PUMP OUTLET

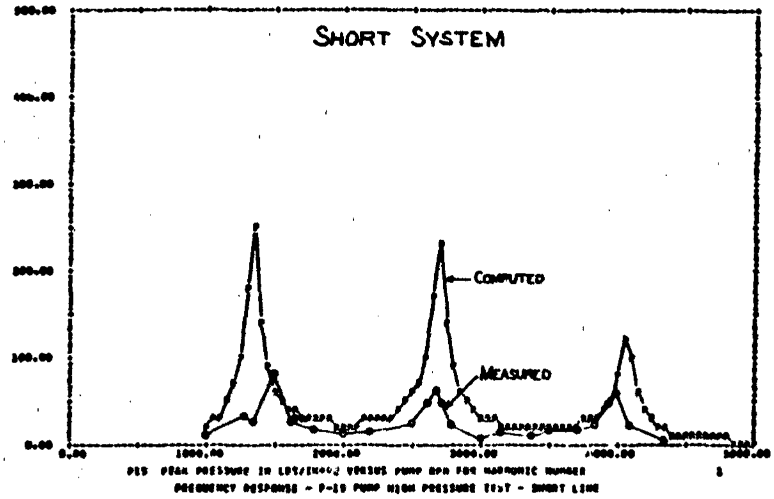


**FIGURE 52.** FREQUENCY RESPONSE EXTENDED F-15 PUMP VERIFICATION TEST
MIL-H-5606B 4400 PSI 113°F 12.9 GPM
107.41 INCHES FROM PUMP OUTLET

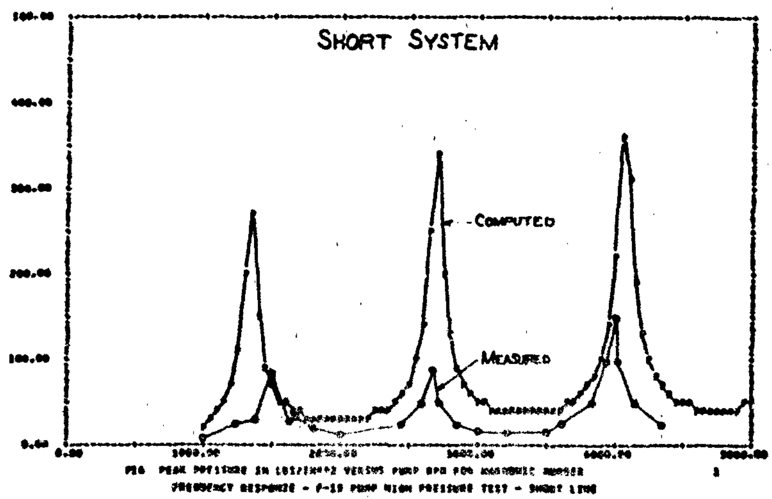


**FIGURE 53.** FREQUENCY RESPONSE EXTENDED F-15 PUMP VERIFICATION TEST
MIL-H-5606B 4400 PSI 113°F 12.9 GPM
119.41 INCHES FROM PUMP OUTLET

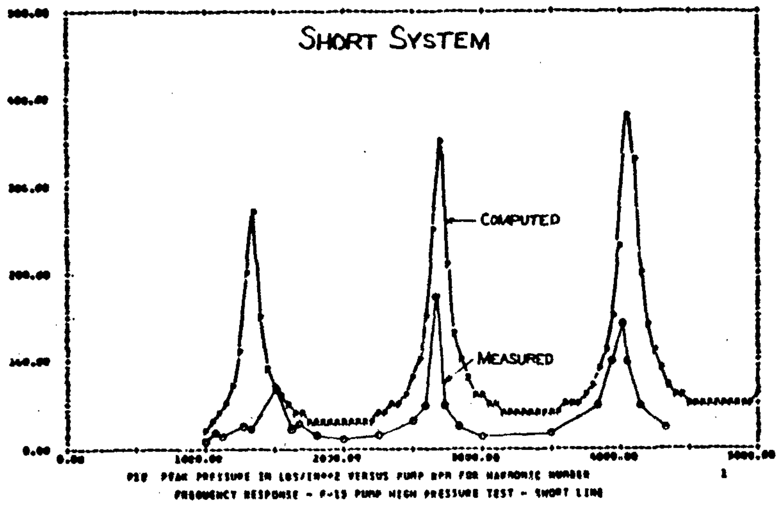


FIGURE 54. FREQUENCY RESPONSE EXTENDED F-15 PUMP VERIFICATION TEST
MIL-H-5606B 4400 PSI 113°F 12.9 GPM
124.41 INCHES FROM PUMP OUTLET

Instrumentation error and temperature drift during testing could account for errors of this magnitude. However, HSFR predicts a first resonant speed that is about 200 rpm too low (1330 vs 1500 rpm). The predicted resonant point is below the compensator valve's natural frequency of 1500 rpm. The predicted point does not appear because it is washed out by the compensator valve whose dynamic behavior is not modeled.

Figures 55 and 56 compare the computed and measured standing pressure waves at 2650 rpm and 4000 rpm. The period of the wave shows excellent correlation between computed and measured results, but the measured amplitudes are much lower than the HSFR program predicts. At 4000 rpm, the predicted amplitude is off by a factor of about 2.5 while the 2650 rpm values disagree by a factor of about 3.7.

Data is not available from the 3000 psi testing at the 12.9 gpm flow rate for direct comparison to the data taken at 4400 psi. However, as expected pulsations were higher with the 4400 psi outlet pressure because the pump valve plate remained timed for a 3000 psi outlet pressure.

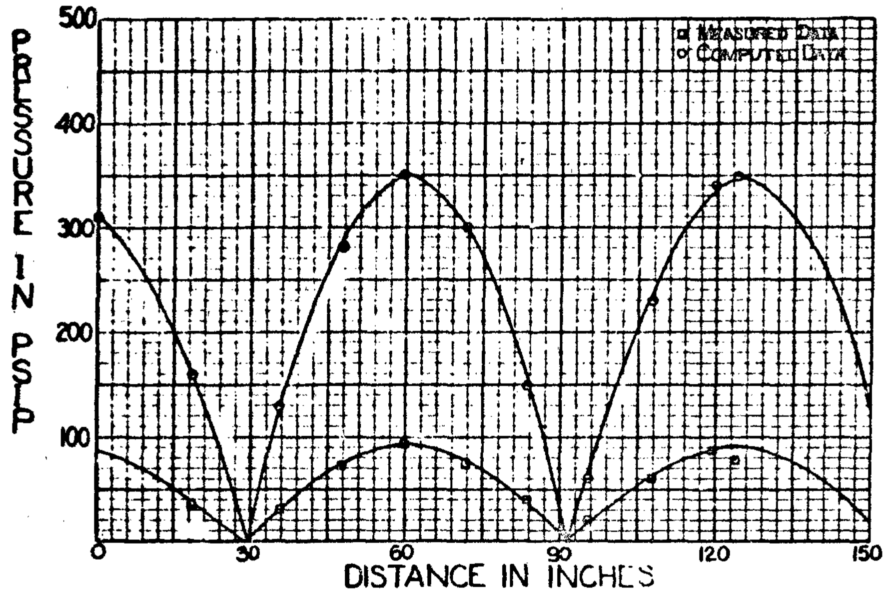


**FIGURE 55. STANDING WAVE PATTERN MEASURED AND COMPUTED DATA 2650 RPM**

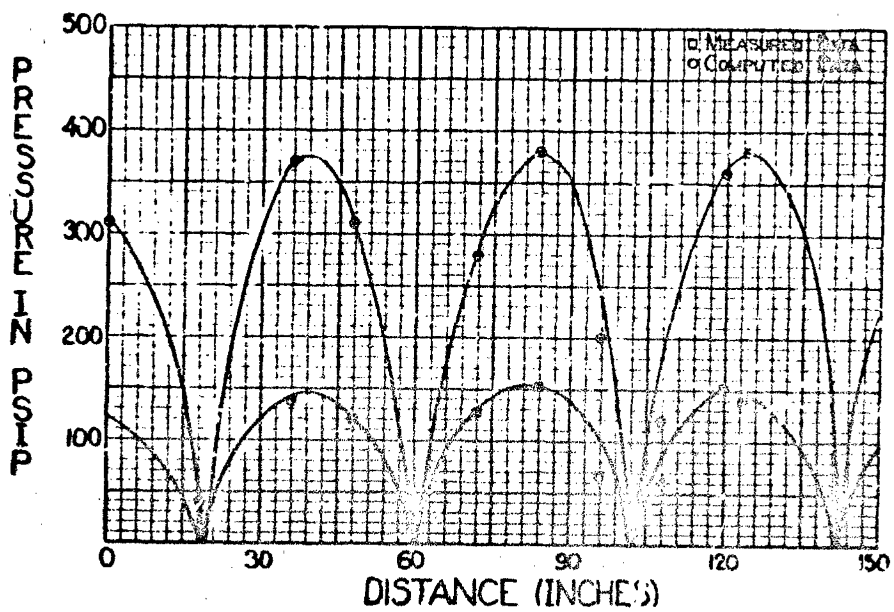


**FIGURE 56. STANDING WAVE PATTERN MEASURED AND COMPUTED DATA 4000 RPM**

## 2. TRANSIENT TEST DESCRIPTION

Transient testing of the F-15 instrumented pump, with MIL-H-5606B hydraulic fluid, investigated load level, speed, temperature and case pressure effects at 3000 psi and 4400 psi pump outlet pressures. A schematic of the test stand is presented in Figure 57. Thirteen data parameters listed in Table 5 were recorded during the testing. The analog signals from the transducers were digitized by waveform recorders and transferred to cassette tapes through the Wang programmable calculator.

A summary of the 3000 psi pump outlet pressure transient test runs appear in Table 6. When checking out the reworked F-15 pump it was found that turn-off transients took longer to stabilize at the same test conditions established during the previous pump testing. It was noticed that the pump actuator pressure during a turn-off transient peaked between 3000 and 3500 psi, and that the hanger hit its stop about three times before stabilizing out. Before the instrumented pump was sent back to Abex, the actuator pressure would peak at approximately 2400 psi. The compensator setting was readjusted to see if this would decrease the actuator pressure. This had very little effect. The compensator spool valve was removed and inspected but nothing was found that could cause the unexplained increased in actuator pressure. The turn-on transients generated similar data as the previous tests, although the pump case drain pressures were now higher.

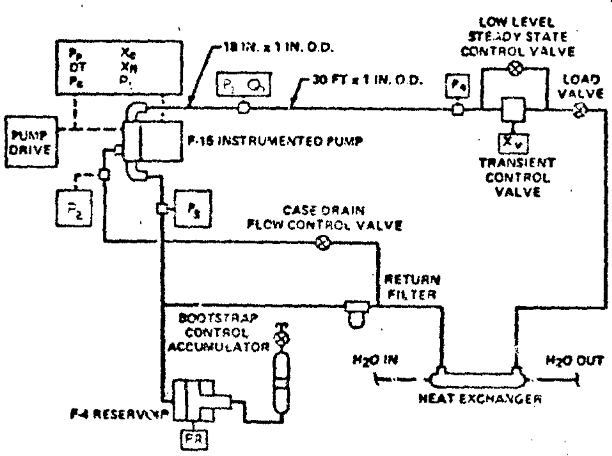


FIGURE 57. HYTRAN PUMP MODEL VERIFICATION TEST SETUP

## TABLE 5 TRANSIENT TESTING DATA RUN PARAMETERS

PC . . . . . . . Pump Control Pressure (Actuator Pressure)
P1 . . . . . . . Pump Case Drain Pressure: Internal
P2 . . . . . . . Case Drain Line Pressure: External
P3 . . . . . . . Pump Outlet Pressure
PS . . . . . . . Suction Pressure
PR . . . . . . . Reservoir Pressure
P4 . . . . . . . Pressure 378 Inches from Pump Outlet
XV . . . . . . . Transient Control Valve Position
XH . . . . . . . Pump Hanger Position
XC . . . . . . . Pump Compensator Spool Position
DT . . . . . . . Drive Torque
PP . . . . . . . Pressure at Port Plate
Q3 . . . . . . . Outlet Flow

## TABLE 6 F-15 PUMP TRANSIENT TESTS AT 3000 PSIG OUTLET PRESSURE

| RUN NUMBER | TYPE OF TRANSIENT | STEADY STATE FLOW LEVEL (CIS) INITIAL | FINAL | INLET TEMP(°F) | DRIVE SPEED(RPM) | APPROX STEADY STATE CASE PRESSURE (PSIG) | RESERVOIR PRESSURE(PSIG) |
|---|---|---|---|---|---|---|---|
| LOAD LEVEL EFFECTS | | | | | | | |
| 94-01+XX | Turn-On | 2 | 19.25 | 133 | 4000 | 70 | 56 |
| 94-01-XX | Turn-Off | 19.25 | 2 | 133 | 4000 | 70 | 38 |
| 94-[illegible]+XX | Turn-On | 2 | 38.5 | 130 | 4000 | 70 | 53 |
| [illegible]-XX | Turn-Off | 38.5 | 2 | 131 | 4000 | 70 | 36 |
| 94-A4+XX | Turn-On | 2 | 77 | 130 | 4000 | 70 | 49-55 |
| 94-A4-XX | Turn-Off | 77 | 2 | 129 | 4000 | 70 | 54-50 |
| 94-A6+XX | Turn-On | 2 | 154 | 130 | 4000 | 70 | 46.5 |
| 94-A6-XX | Turn-Off | 154 | 2 | 130 | 4000 | 70 | 54.5 |
| SPEED EFFECTS | | | | | | | |
| 94-07+XX | Turn-On | 2 | 77 | 131 | 3000 | 70 | 52 |
| 94-07-XX | Turn-Off | 77 | 2 | 129 | 3000 | 70 | 55 |
| 94-08+XX | Turn-On | 2 | 77 | 129 | 5000 | 70 | 50 |
| 94-08-XX | Turn-Off | 77 | 2 | 130 | 5000 | 70 | 55.5 |
| TEMP EFFECT | | | | | | | |
| 94-A5+XX | Turn-On | 2 | 77 | 211 | 4000 | 70 | 55 |
| 94-A5-XX | Turn-Off | 77 | 2 | 215 | 4000 | 70 | 59 |
| CASE PRESSURE EFFECTS | | | | | | | |
| 94-03+XX | Turn-On | 2 | 77 | 130 | 4000 | 100 | 52 |
| 94-03-XX | Turn-Off | 77 | 2 | 130 | 4000 | 100 | 55 |

When the instrumented pump was shipped to Abex for refurbishment, they found that the port plate was wiped. A wiped port plate provides a modified leakage path to inlet from case. The increased leakage flow to inlet results in lower case pressures (58 psig typical). With the modified pump this leakage path was eliminated and consequently the case pressures were higher (80 psig typical). With higher case pressures, the ability for the actuator to dump fluid while destroking on a turn-off transient is lessened. Thus it might take slightly longer for the pump to destroke, and the increased oscillations may be due to this coupled with higher case pressures causing the compensator to take longer to reach a steady state (force balance) condition.

The pump compensator was adjusted to give a 4400 psig pump outlet pressure. Some of the transient tests were repeated at the higher pressure and they are summarized in Table 7. Although the pump was capable of attaining higher outlet pressures, it was necessary to limit the pressure to 4400 psi to avoid excessive outlet transients due to the limited compensator stroke, and the necessity to measure this movement at the higher pressures.

TABLE 7 F-15 PUMP TRANSIENT TESTS AT 4400 PSIG OUTLET PRESSURE

| RUN NUMBER | TYPE OF TRANSIENT | STEADY STATE FLOW LEVEL (CIS) INITIAL | FINAL | INLET TEMP (°F) | DRIVE SPEED (RPM) | APPROX CASE DRAIN PRESSURE (PSIG) | RESERVOIR PRESSURE (PSIG) |
|---|---|---|---|---|---|---|---|
| LOAD LEVEL EFFECTS | | | | | | | |
| 96-01+XX | Turn-On | 17.25 | 77 | 99 | 3000 | 70 | 52 |
| 96-01-XX | Turn-Off | 77 | 17.25 | 100 | 3000 | 70 | 54 |
| 96-03+XX | Turn-On | 17.25 | 38.5 | 100 | 3000 | 70 | 52 |
| 96-03-XX | Turn-Off | 38.5 | 17.25 | 100 | 3000 | 70 | 53 |
| TEMPERATURE EFFECTS | | | | | | | |
| 96-04+XX | Turn-On | 17.25 | 77 | 201 | 3000 | 70 | 53 |
| 96-04-XX | Turn-Off | 77 | 17.25 | 201 | 3000 | 70 | 53 |
| CASE PRESSURE EFFECTS | | | | | | | |
| 96-02+XX | Turn-On | 17.25 | 77 | 100 | 3000 | 100 | 50 |
| 96-02-XX | Turn-Off | 77 | 17.25 | 100 | 3000 | 100 | 52 |

During the testing it was found that the pump compensator was very unstable at steady state flows less than 17.25 CIS and fluid temperatures much greater than 100°F. The transient test also had to be run at 3000 RPM instead of 4000 to stabilize the compensator. Figure 58 shows the pressure upstream of the transient control valve for a turn-on transient from 2 - 19.25 CIS at 130°F. The transient control valve was not activated until 0.02 seconds into the test run. Between 0.0 and 0.02 seconds the pressure varies 400 psi due to the compensator instability. Increasing the steady state flow helped to alleviate the problem.

## 3. PROGRAM CHANGES AND HYTRAN PUMP MODEL VERIFICATION

The objective of the extended testing was further verification of the HYTRAN F-15 pump model. The HYTRAN program schematic of the test system is shown in Figure 59. The recorded inlet pressure and external case drain pressure were chosen as the boundary conditions for the simulation. The suction pressure transducer was located 55.75 inches from the pump inlet, and the case transducer was 18.0 inches from the case drain port.

A HYTRAN component model (TEST91) was written to input the test data as boundary conditions in the simulation. The subroutine TEST91 uses the input pressure data to compute the flow at time t in the simulation using the equation:

$$Q = \frac{C - P(t)}{Z}$$

where

C = line characteristic (PSI)

Z = line impedance (PSI/CIS)

P(t) = P data pressure value at time t (PSI)

The input test data was filtered to eliminate excessive noise and reduce computation error in the simulation. This was accomplished by using a 100 Hz filter on the pressure signals when they were played back from the analog tape into the waveform analyzer. Use of the filtered test data also reduced the same error that might be introduced by imperfections in other component models. The remainder of the system in Figure 59 is the HYTRAN model of the actual test set-up from the pump outlet to the load valve. Component Type 23 is the transient control valve and the two Type 41's are restrictors used to control the maximum and bypass steady state flow rates. The dimensions were taken from the test stand. Table 8 presents the typical HYTRAN input data used to describe the test schematic in Figure 59.

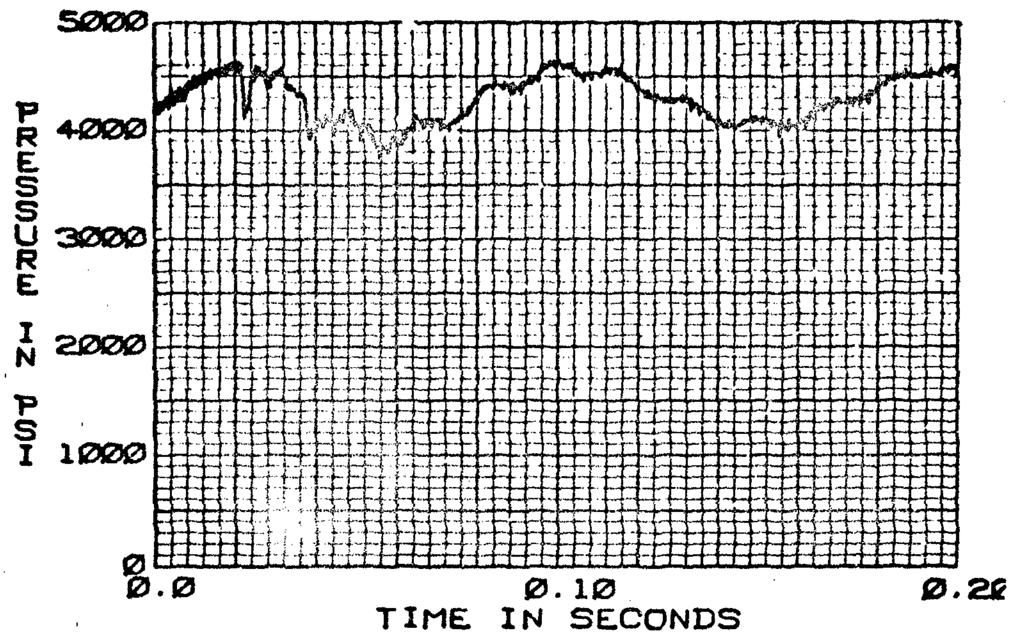


FIGURE 58. F-15 HYDRAULIC PUMP 95-01+P4 TURN-ON TRANSIENT
19.25 CIS 130°F

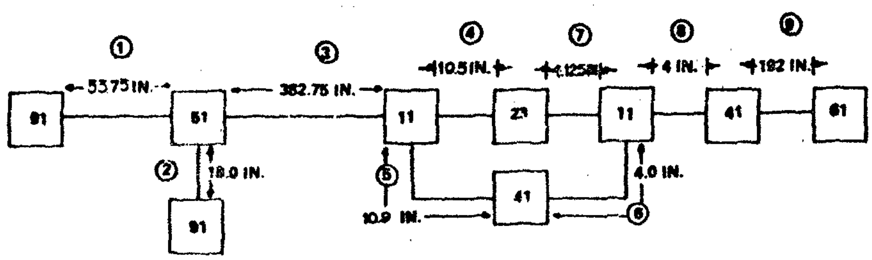


FIGURE 59. HYTRAN SCHEMATIC DIAGRAM FOR PUMP VERIFICATION

**TABLE 8. BASIC HYTRAN INPUT 3000 PSI HYDRAULIC SYSTEM 2-77 CIS TURN-ON TRANSIENT**

```
****DATA RUN NO. 94-A4*PS AND *P2  F-15 PUMP****(OPTSTZ#)
   .0002        .2       .092      130.
 9    9    1
 1    0    3    0    0    0    0          55.75      1.0      .049     3.067
 2    0    3    0    0    0    0          10.00      .375     .020     3.067
 3    0    1    0    0    0    3         302.75      1.0      .054     3.067
 4    0    2    0    0    0    0          10.5       1.0      .058     3.067
 5    0    2    0    2    0    2          10.9       .50      .020     3.067
 6    0    2    0    0    0    0           4.0       .50      .020     3.067
 7    0    2    0    0    0    0           4.125     1.0      .049     3.067
 8    0    2    0    0    0    0           4.0       1.0      .049     3.067
 9    0    2    0    0    0    0         192.        1.0      .049     3.067
 3   91    0   -1    1
 2   51    4    1   -3   -2
  2070.      2000.        .15     .25         0.       .016      .65       .65
   .387       400.        70.    130.       470.       215.      .035      45.
     3.         .75      -.25    .002       .001       .003     .1097      40.
     5.       4000.      .016     .05         0.      .0035        1.        0.
 3   91    0    2    1
 4   11    0    3   -4   -5
 5   23    3    6   -7                                            6
   .022         .65
     0.       .0190     .0210      .2
     0.          0.     4.005   4.005
 6   41    1    5   -6
   .021        .65
 7   11    0    6    7   -8
 8   41    1    8   -9
   .136         .65
 9   61    1    9
    50.
 6    6
 1    1    2    3        00.
 1    1    0    1    2    1
 2    2    3    3         5.
 2    1    0    2    3    1
 3    2    4    3        00.
 2    2    0    3    4    1
 4    4    5    5        00.
 4    2    0    4    5    1    0    7    7    1
 5    4    5    5         5.
 4    3    0    5    6    1    0    0    7    2
 6    5    6    5        00.
 7    1    0    8    0    1    0    9    7    1
 3   15         0                   1
 3    4       10.        -10.
 2    4    2    5    2    6    2    7    2    8    2    9    2   10    2   14
 2   15    2   16    2   25    2   20    2   10    4   11    7   12
```

a. <u>F-15 Pump Model Changes</u>

During the original AFAPL contract, extensive testing was done on the F-15 instrumented pump. The HYTRAN model adequately predicted the initial transients and general operating characteristics of the actual instrumented pump. However the transient decay was not accurately computed. The follow-on contract work has emphasized improving the damping of the pump model. Not adequately defining the damping characteristics of the actuator, hanger and compensator are some of the areas that would cause this problem. The original HYTRAN pump model computed the actuator leakage coefficient as a linear relationship between the leakage coefficient at maximum pump displacement and actuator position plus the leakage coefficient at zero pump displacement. This flow along with case pressure plays a significant part in determining the damping characteristics of the hanger. The computation for actuator leakage was updated using an equation for fully developed laminar steady flow between stationary flat plates. (Eqn 1)

$$Q = \frac{wb^3}{12\mu L} \Delta P \qquad (1)$$

where

$\mu$ = fluid viscosity (lb-sec/in$^2$)

Q = flow rate (cis)

$\Delta P$ = pressure drop (psi)

b = passage height (in)

w = passage width (in)

L = passage length (in)

The user inputs the depth of the flat cut on the actuator and the minimum actuator engagement which occurs when the pump is at minimum outlet flow. The new computation method has slightly improved the pump model. The effects of adding a velocity term due to the motion of the actuator were small for the pressure drops (1000 psi) and actuator rates (50-60in/sec max) of the pump, so it was not included in the computation.

Another area of investigation was the flow forces on the compensator valve. The original HYTRAN model contained a simple computation describing these forces. Efforts to improve the computation did not prove fruitful. Removal of the flow force term did adversely alter the simulation, thus it was not changed.

A paramet . study was performed on the F-15 pump model to determine the sensitivity of the input data in the computer simulation. Four input data parameters were investigated for turn-off and turn-on transients at a pump speed of 4000 rpm, 3000 psi pump outlet pressure, steady state flows of 77 CIS and 2 CIS, 130°F system operating temperature and a control valve operating time of 4 milliseconds. The parameters investigated were hanger damping, actuator displacement, coefficient of pump leakage and case volume.

The hanger damping term had the most significant effect on the damping frequency of the pump model. The hanger damping term accounts for velocity dependent friction factors which include the effects on the changes in precompression and decompression when the hanger is in motion.

Initial attempts to alter this term did not prove successful because of the limited knowledge about the case pressures which affected the dynamics of the hanger. With the addition of the internal case drain transducer, it was possible to significantly vary the damping term and monitor the computed case pressure, the hanger position, actuator, outlet and inlet pressures to assure that these values were not deviating from the measured values. The term was varied until a value was reached that would give good correlation between the computed results and the measured test data. Figure 60 shows the pump outlet pressure for a turn-off transient at 77 CIS and 130°F with the hanger damping term at 25 lbs/in/sec. Although the initial peak pressure correlation is good the subsequent decay of the computed waveform is at a higher frequency. This was the best correlation obtained under the original contract. The value of hanger damping was varied and Figure 61 presents the computed results at 45 and 125 lbs/in/sec. The 125 value significantly slowed down the simulation and the 45 value appears to be the optimum. Increasing the hanger damping in an attempt to obtain good period correlation for the turn-off transient leads to an undesirable increase in the amplitudes of the computed data. This amplitude behavior necessitates stopping short of the value that might give the best period correlation.

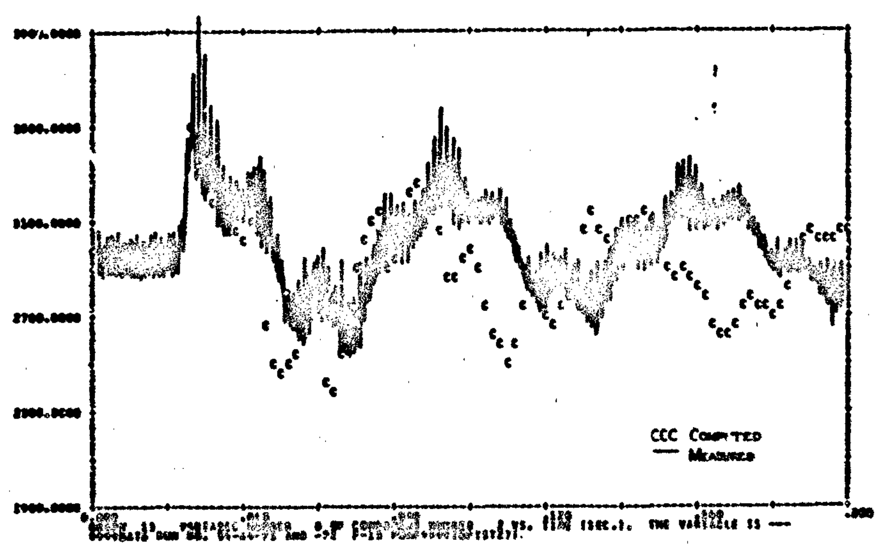


FIGURE 60. OUTLET PRESSURE WITH HANGER DAMPING TERM AT 25
77-2 CIS TURN-OFF TRANSIENT TEST 3000 PSI 130°F

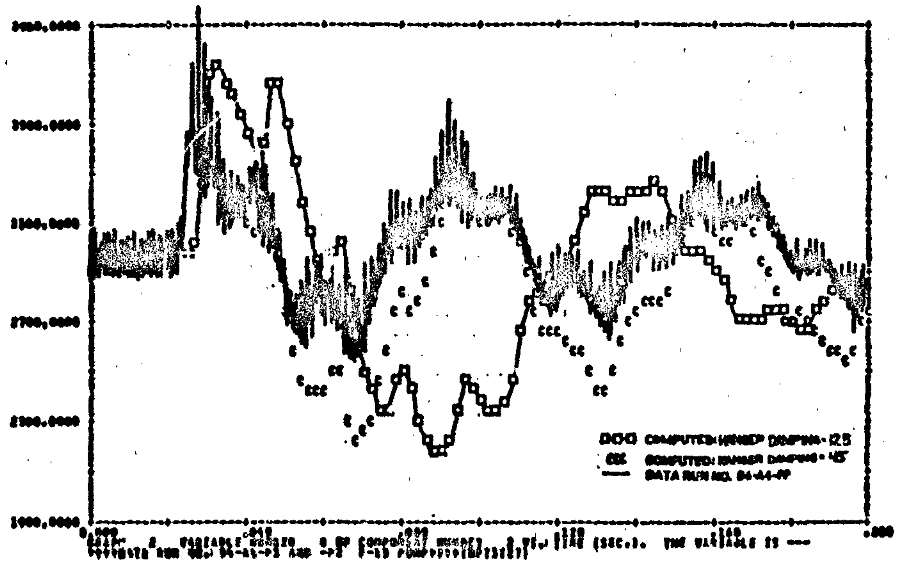

FIGURE 61. HANGER DAMPING TERM AT 45 AND 125
77-2 CIS TURN-OFF TRANSIENT 130°F 4000 RPM

A value of 45.0 lbs/in/sec yielded the best correlation for the simulated conditions. The pump outlet pressure from a turn-on transient run at 77 CIS and 130°F is shown in Figure 62. The hanger damping term was 45 lbs/in/sec for this run. In general the turn-off simulation required a slightly larger hanger damping term than the turn-on case.

The pump model was then run at 38.5 CIS. A value of 70 lbs/in/sec was used to obtain the correlation shown for the pump outlet pressure in the turn-on transient of Figure 63. However the same value for hanger damping did not significantly improve the computer simulation of the 38 CIS turn-off transient shown in Figure 64.

Time has not allowed investigation to determine an algorithm for the hanger damping term for all the cases recorded in the laboratory. It is desirable to develop a method that could be incorporated into HYTRAN to choose the best term based on system conditions. Further work in this area is needed.

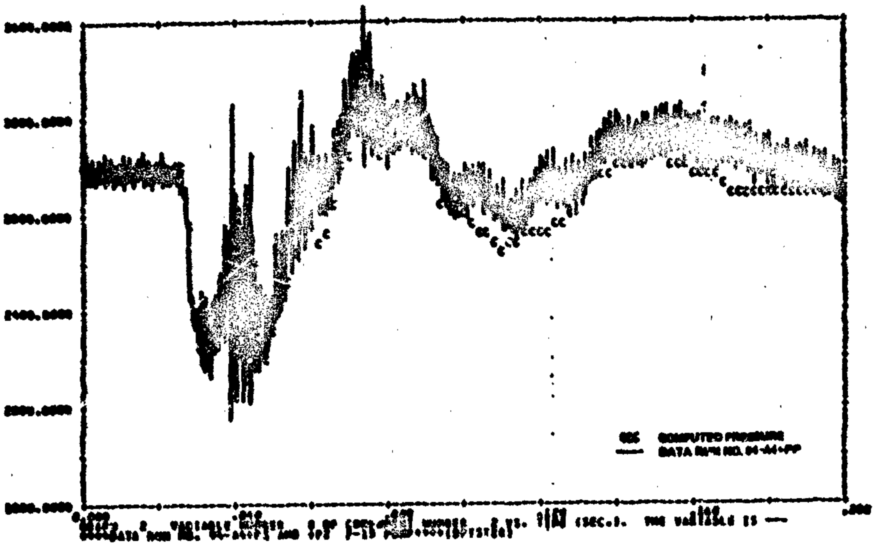

FIGURE 62. OUTLET PRESSURE 2-77 CIS TURN-ON TRANSIENT
130°F 4000 RPM

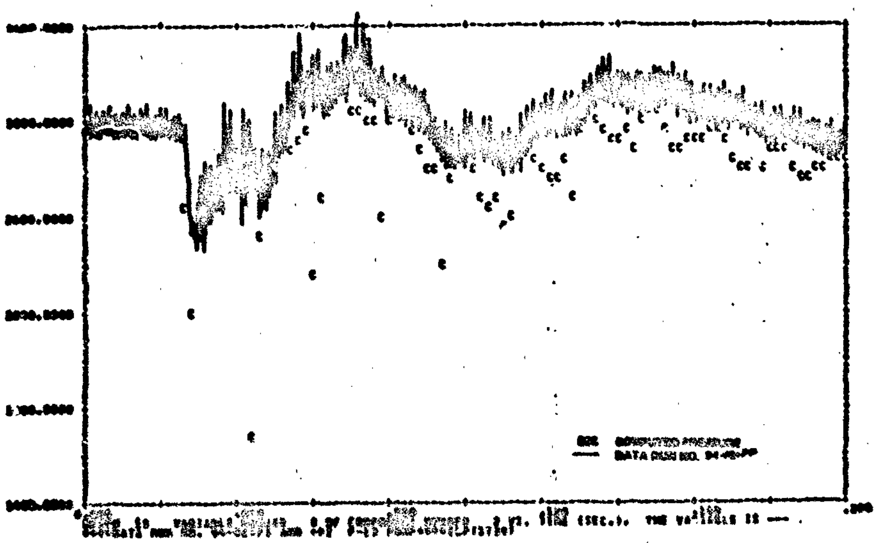

FIGURE 63. OUTLET PRESSURE 2-38.5 CIS TURN-ON TRANSIENT
130°F 4000 RPM

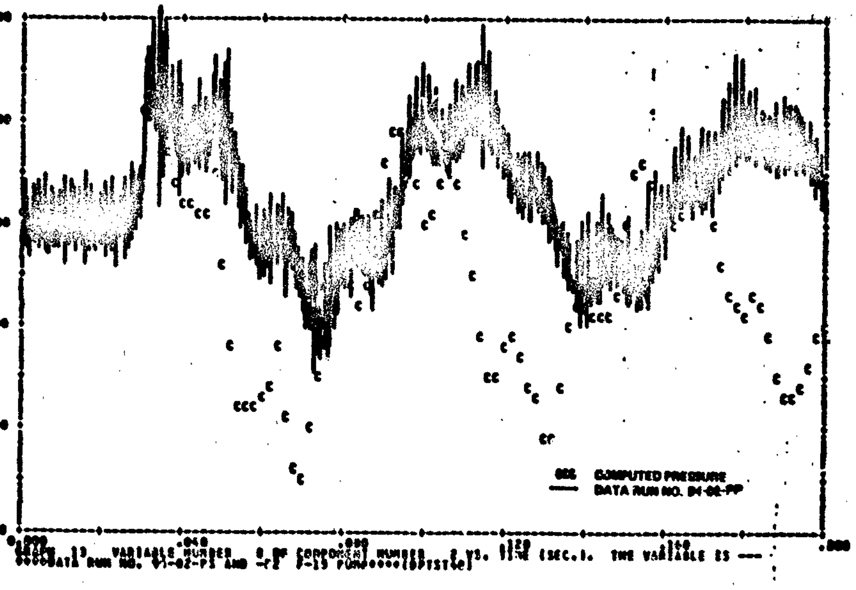


FIGURE 64. OUTLET PRESSURE 38.5-2 CIS TURN-OFF TRANSIENT 130°F 4000 RPM

The coefficient of pump leakage was varied for various turn-on and turn-off transient runs. This term had very little effect on the simulations and appears to be a good candidate for removal.

Varying the actuator displacement had an adverse effect on both turn-on and turn-off transient simulations. The present maximum and minimum value are optimum.

The case volume was changed from 250 $in^3$ to 48 $in^3$ (which is the correct value) with only a minor change in pump outlet pressure amplitudes.

Appendix D presents the revisions to the pump input data and the PUMP51 subroutine listing.

b. Pump Model Verification for 3000 psi Transient Tests

Using the input data in Table 8 for the system shown in Figure 59, a turn-off transient at 77 CIS and 130°F was run. Figure 65 shows the input data boundary conditions for this simulation. The results of the simulation are presented in Figures 66 through 69. The computed pump outlet pressure in Figure 66 compares well with the test data both in magnitude and phase. The computed results are conservative after the initial transient response at approximately 50 milliseconds into the simulation. The computed peak actuator pressure in Figure 67 is 3300 psi while the measured value is only 3000 psi, (about a 10 percent error), but the subsequent response is very good. The computed internal case pressure matches the test data exceedingly well. The case pressure transducer was located in the area of the compensator valve. There is a 1/8" dia hole x 1 3/4" long path between the transducer and the actual case. Statically, the effect of the long orifice is to reduce the pressure. Dynamic effects could result in peak pressure attenuation and misphasing between the two internal case prssures, however, this does not appear to be the case. The hanger position is plotted in Figure 69. The measured data cuts off at -.18 inches but the computed value reaches -.24 inches. There is a similar discrepancy for the overshoot at 80 milliseconds in the simulation. The phasing between the measured and computed position is adequate. The amplitude correlation is relatively poor, although the transient flow does settle to the proper steady state value. The computer printout data is the actuator position. The hanger acts as a lever arm between the actuator and the restoring spring where the measurement of hanger position was taken. The computer actuator velocity term is integrated to obtain the resultant displacement. A simplified Euler integration is used. Perhaps a more sophisticated technique would work better, but at the expense or increased computation time and operating costs. Improving these results may prove to be unattractive.

The next computer simulation was for a turn-on transient run using the same conditions as the previous run with the input boundary conditions of Figure 70. The computed pump outlet pressure in Figure 71 almost matches the data trace. The computed actuator pressure (Figure 72 ) and internal case pressure (Figure 73 ) also follow the measured data. The computed hanger position in Figure 74 is about 0.12 inches below the measure data. The final predicted value however is very close to the test results.

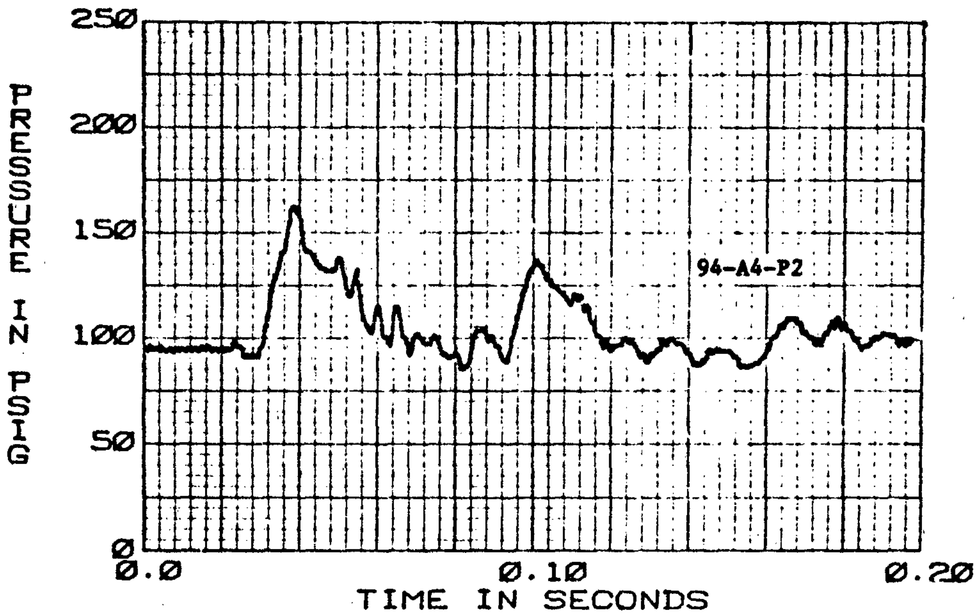


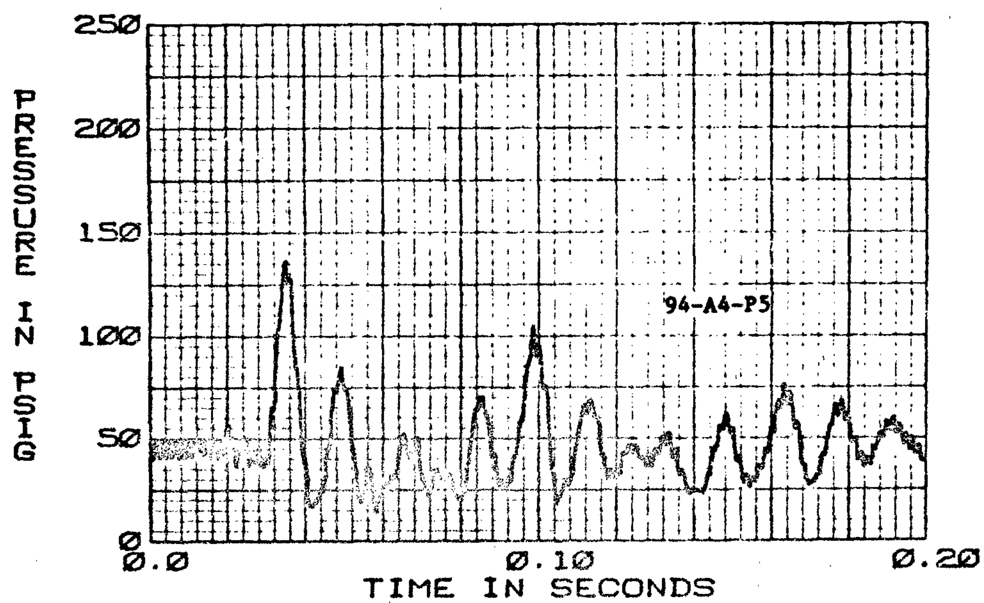


FIGURE 65. F-15 HYDRAULIC PUMP TURN-OFF TRANSIENT
77 CIS 130°F

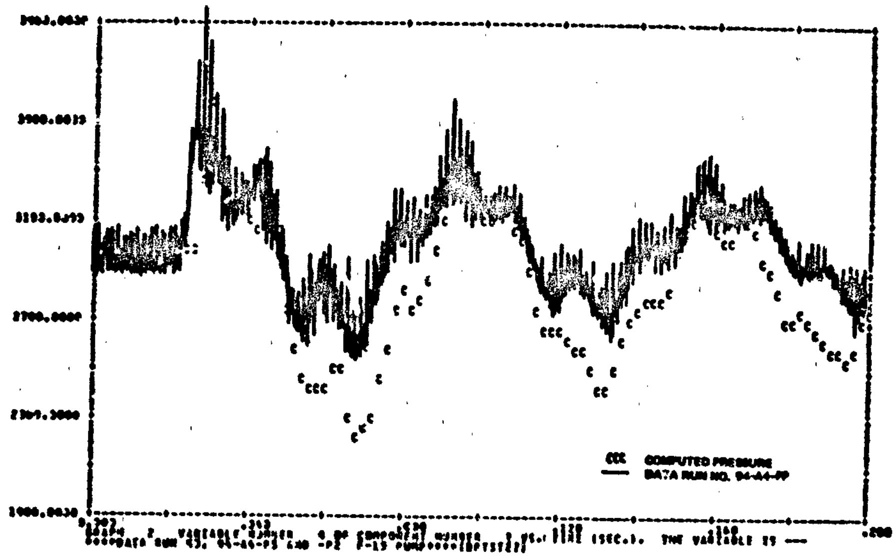


FIGURE 66. OUTLET PRESSURE 77-2 CIS TURN-OFF TRANSIENT
130°F 4000 RPM

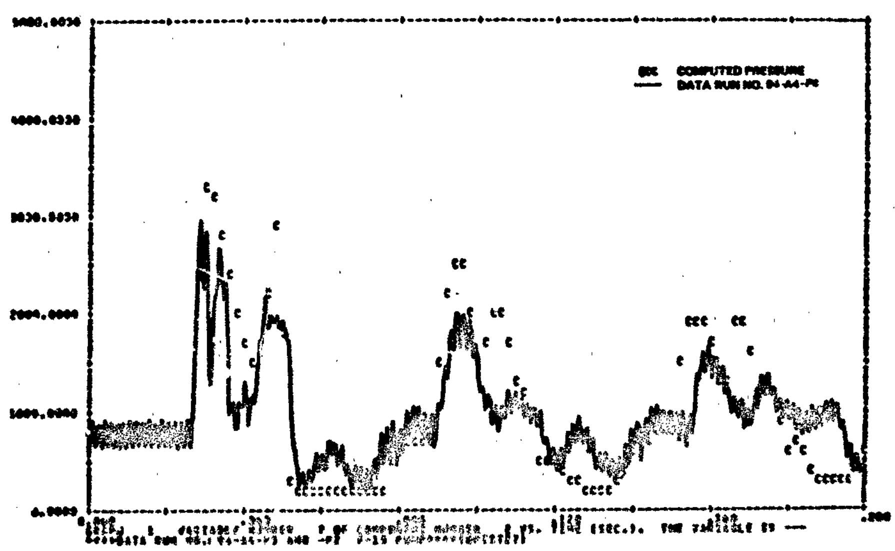


FIGURE 67. CONTROL PRESSURE 77-2 CIS TURN-OFF TRANSIENT
130°F 4000 RPM

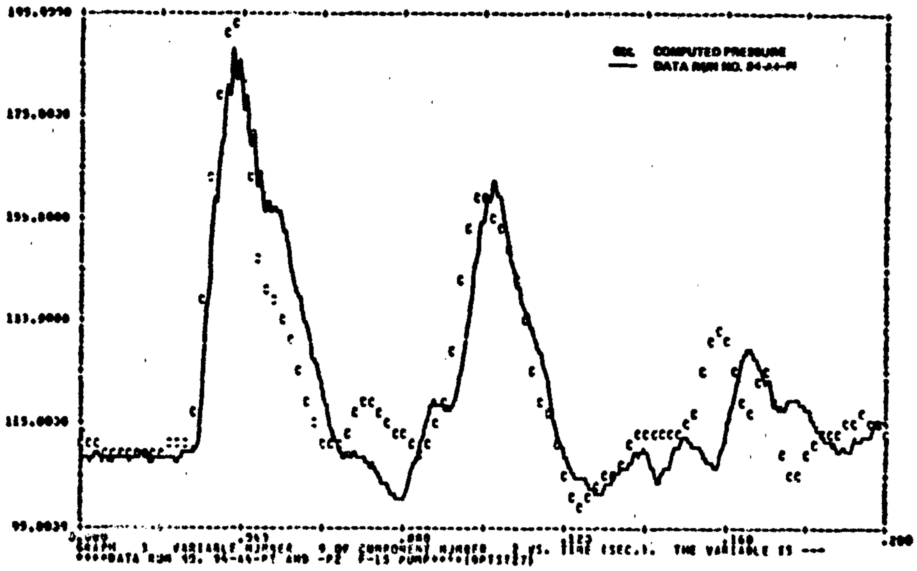


FIGURE 68. INTERNAL CASE PRESSURE 77-2 CIS TURN-OFF TRANSIENT 130°F 4000 RPM

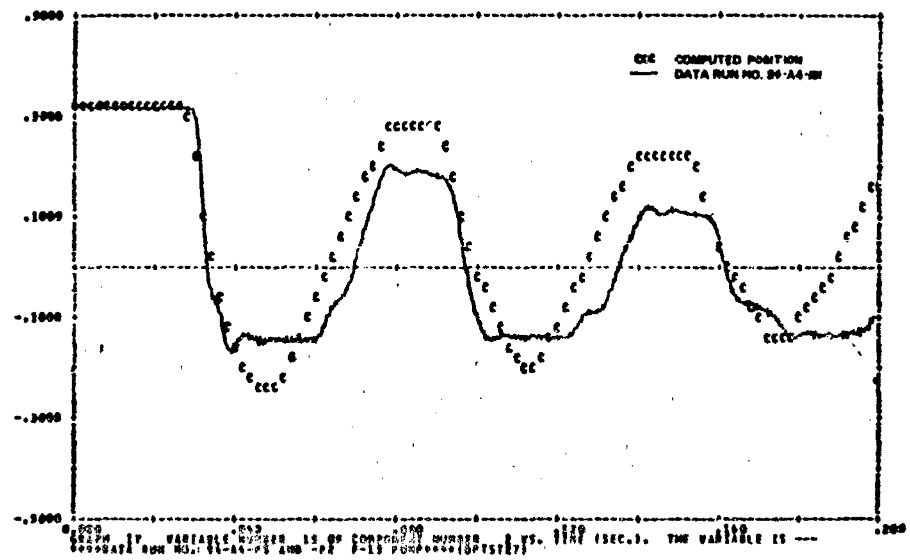


FIGURE 69. HANGER POSITION 77-2 CIS TURN-OFF TRANSIENT 130°F 4000 RPM

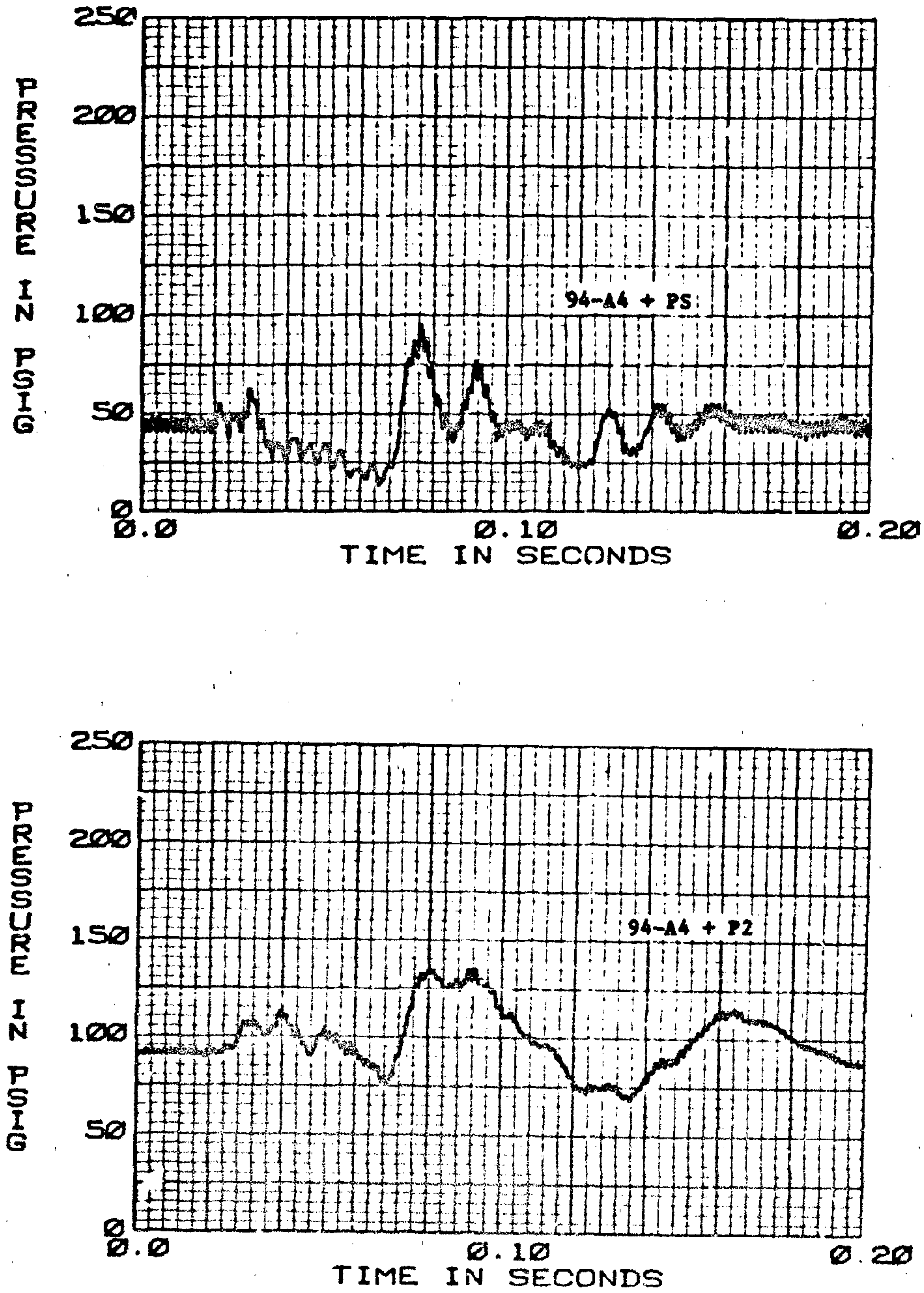


FIGURE 70. F-15 HYDRAULIC PUMP TURN-ON TRANSIENT
77 CIS 130°F

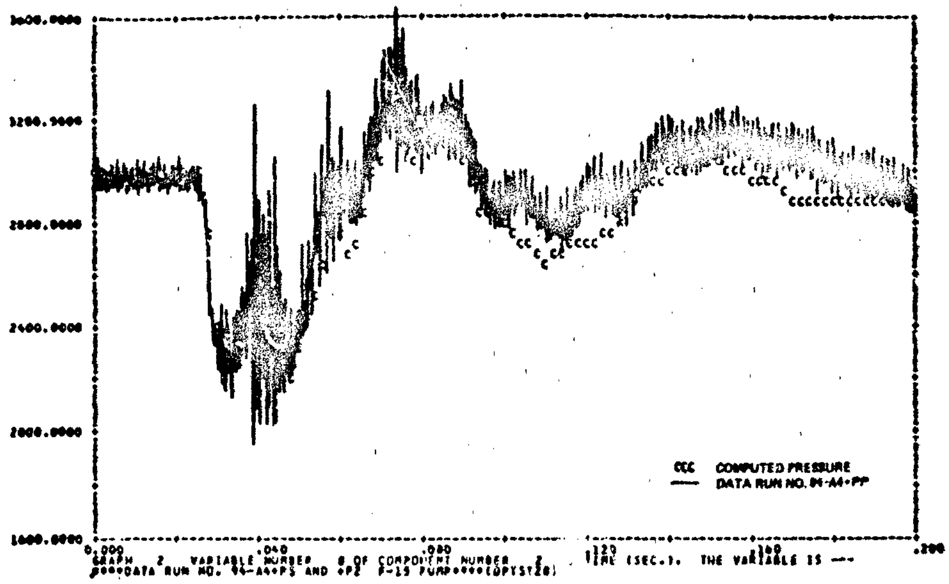


FIGURE 71. OUTLET PRESSURE 2-77 CIS TURN-ON TRANSIENT
130°F 4000 RPM

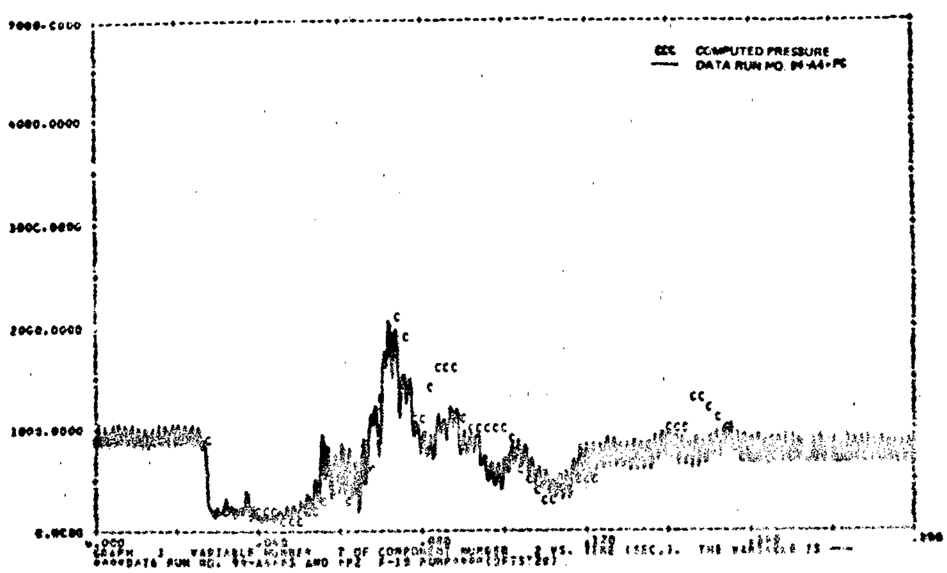


FIGURE 72. CONTROL PRESSURE 2-77 CIS TURN-ON TRANSIENT
130°F 4000 RPM

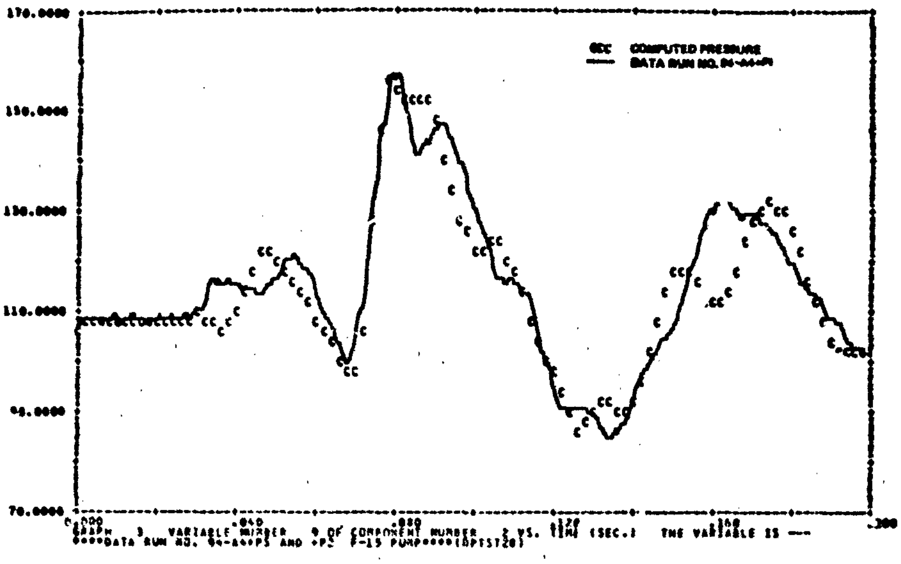


FIGURE 73. INTERNAL CASE PRESSURE 2-77 CIS TURN-ON TRANSIENT 130°F 4000 RPM

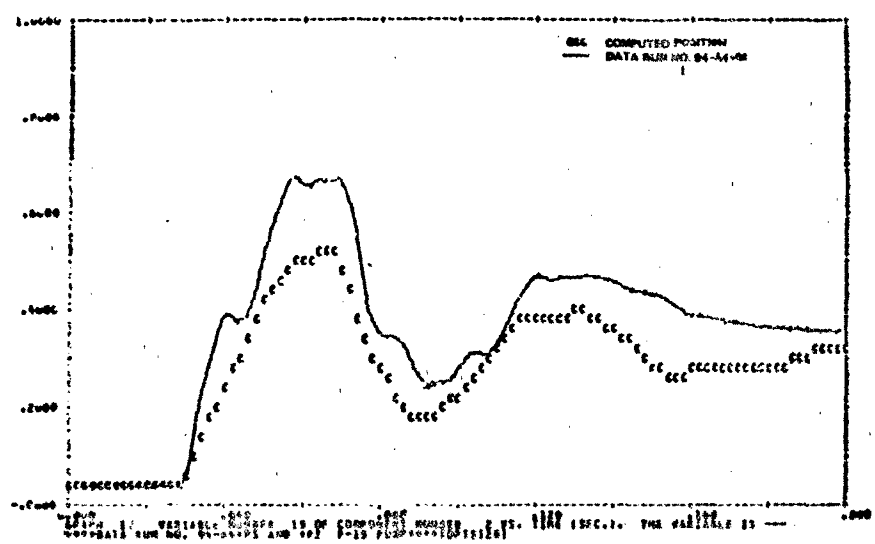


FIGURE 74. HANGER POSITION 2-77 CIS TURN-ON TRANSIENT 130°F 4000 RPM

Turn-on and turn-off simulation were made at a steady state flow of 38.5 CIS. The input data file for the turn-on transient is shown in Table 9 and the boundary conditions in Figure 75. This computer output data for outlet pressure, actuator pressure,case drain pressure and hanger position are shown in Figure 76 through 79.

This boundary conditions for the turn-off transient at 38.5 CIS and 130°F is shown in Figure 80. The output data is presented in Figures 81, 82, 83, and 84.

The general computed vs measured data correlation is better for the turn-on transients. Both amplitude and period characteristics of the data fit much better than for the turn-off case. This is also true for the 77.0 CIS runs.

TABLE 9. HYTRAN INPUT DATA 3000 PSI SYSTEM 2-38.5 CIS TURN-ON TRANSIENT

```
***DATA RUN NO. 94-02+PS AND +P2  F-15 PUMP****(DPTST39)
   .0002        .2        .002       130.
 9    9    1
 1    0    3    0    0    0    0            55.75       1.0       .049      3.0E7
 2    0    3    0    0    0    0            18.00       .375      .028      3.0E7
 3    0    3    0    0    0    3           382.75       1.0       .058      3.0E7
 4    0    2    0    0    0    0            10.5        1.0       .058      3.0E7
 5    0    2    0    2    0    2            10.9        .50       .028      3.0E7
 6    0    2    0    0    0    0             4.0        .50       .028      3.0E7
 7    0    2    0    0    0    0             4.125      1.0       .049      3.0E7
 8    0    2    0    0    0    0             4.0        1.0       .049      3.0E7
 9    0    2    0    0    0    0           192.         1.0       .049      3.0E7
 1   91    0   -1    1
 2   51    4    1   -3   -2
  2870.      2000.       .15        .25        0.        .016       .65       .65
   .307       400.       70.       130.      470.       215.       .035       70.
     3.        .75      -.25       .002      .001       .003      .1097       48.
     5.      4000.      .036        .05        0.       .0035       1.         8.
 3   91    0    2    1
 4   11    0    3   -4   -5
 5   23    3    4   -7                                               4
   .022        .65
     0.      .0180      .0200        .2
     .0         .0       .374      .374
 6   41    1    5   -6
   .021       .65
 7   11    0    6    7   -8
 8   41    1    8   -9
  .1231        .65
 9   61    1    9
    50.
 6    6
 1    1    2    3         80.
 1    1    0    1    2     1
 2    2    3    3          5.
 2    3    0    2    3     1
 3    2    4    3         80.
 2    2    0    3    4     1
 4    4    5    5         80.
 4    2    0    4    5     1    0    7    7    1
 5    4    5    5          5.
 4    3    0    5    6     1    0    6    7    2
 6    5    6    5         80.
 7    3    0    8    8     1    0    9    9    1
 3   15         0                   1
 1    2         1.        -1.
 2    2        13.       -13.
 3    4        18.       -18.      380.      -380.
 2    4    2    5    2     6    2    7    2    8    2    9    2   10    2   14
 2   15    2   16    2    25    2   26    2   30    2   31    2   32
```

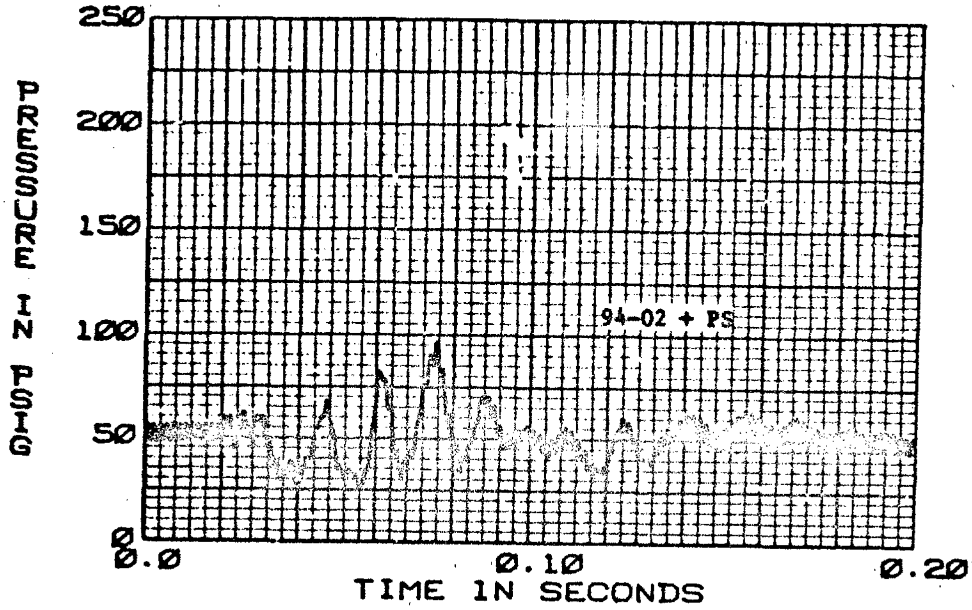


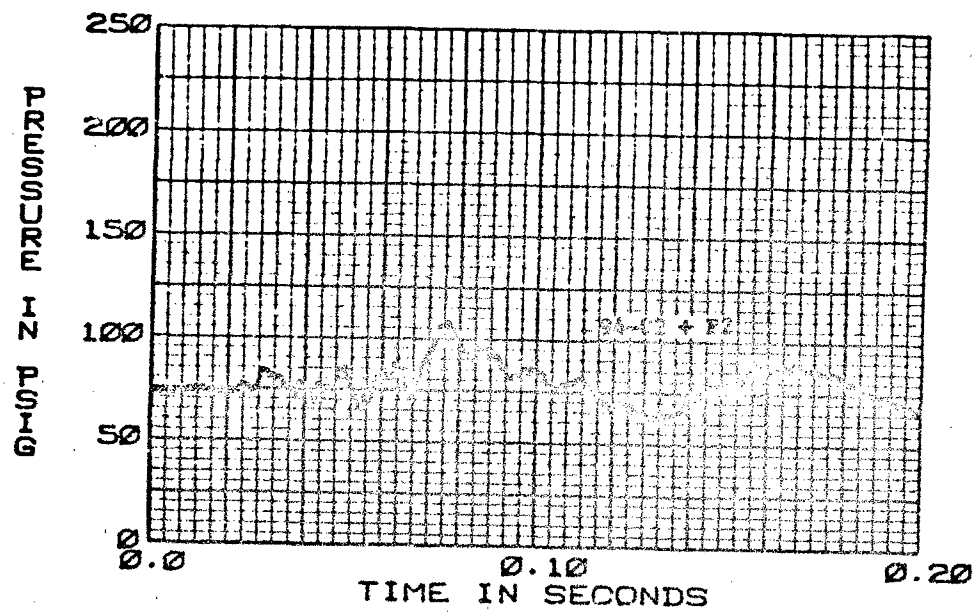


FIGURE 75. F-15 HYDRAULIC PUMP TURN-ON TRANSIENT
38.5 CIS 130°F

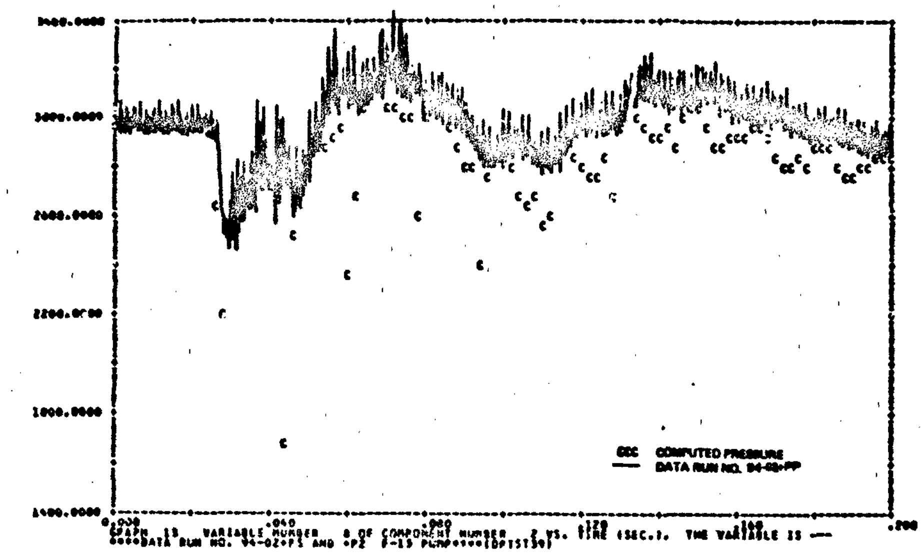


FIGURE 76. OUTLET PRESSURE 2-38.5 CIS TURN-ON TRANSIENT
130°F 4000 RPM

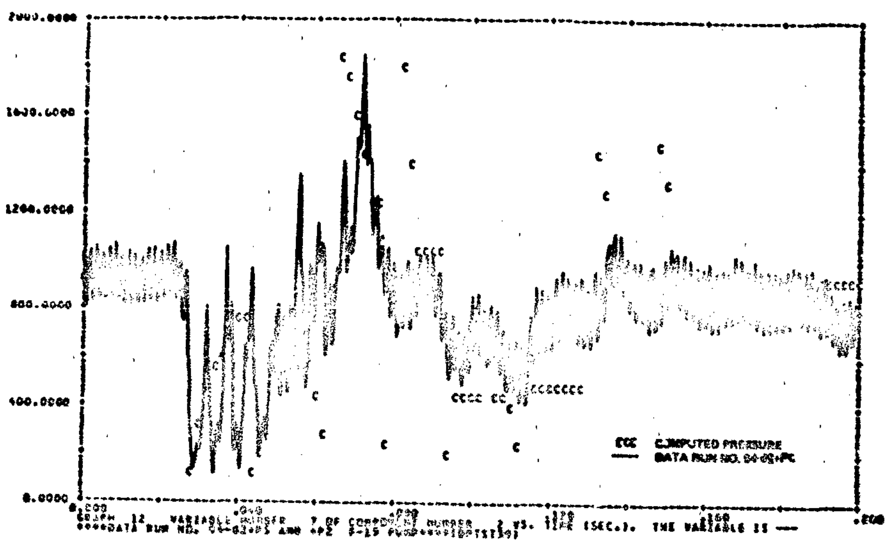


FIGURE 77. CONTROL PRESSURE 2-38.5 CIS TURN-ON TRANSIENT
130°F 4000 RPM

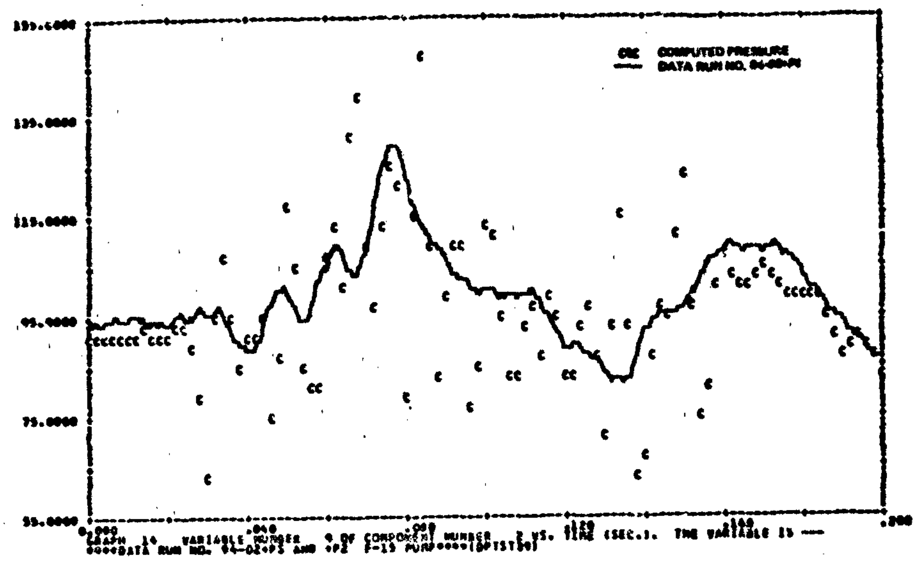


FIGURE 78. INTERNAL CASE PRESSURE 2-38.5 CIS TURN-ON TRANSIENT 130°F 4000 RPM

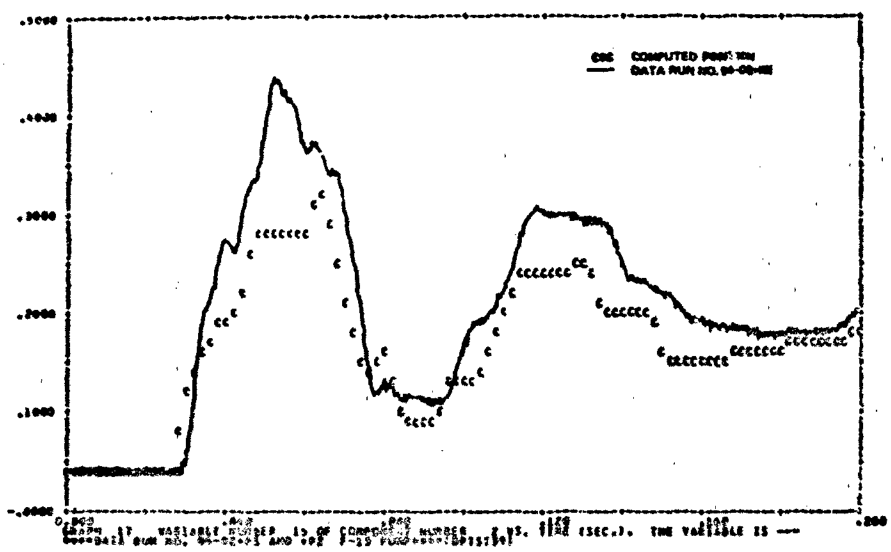


FIGURE 79. HANGER POSITION 2-38.5 CIS TURN-ON TRANSIENT 130°F 4000 RPM

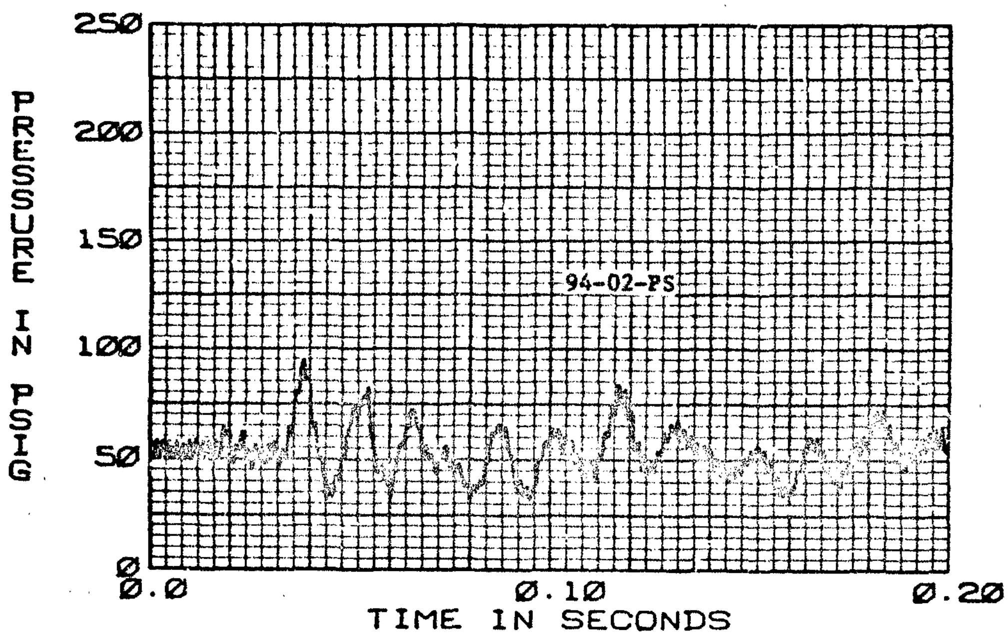


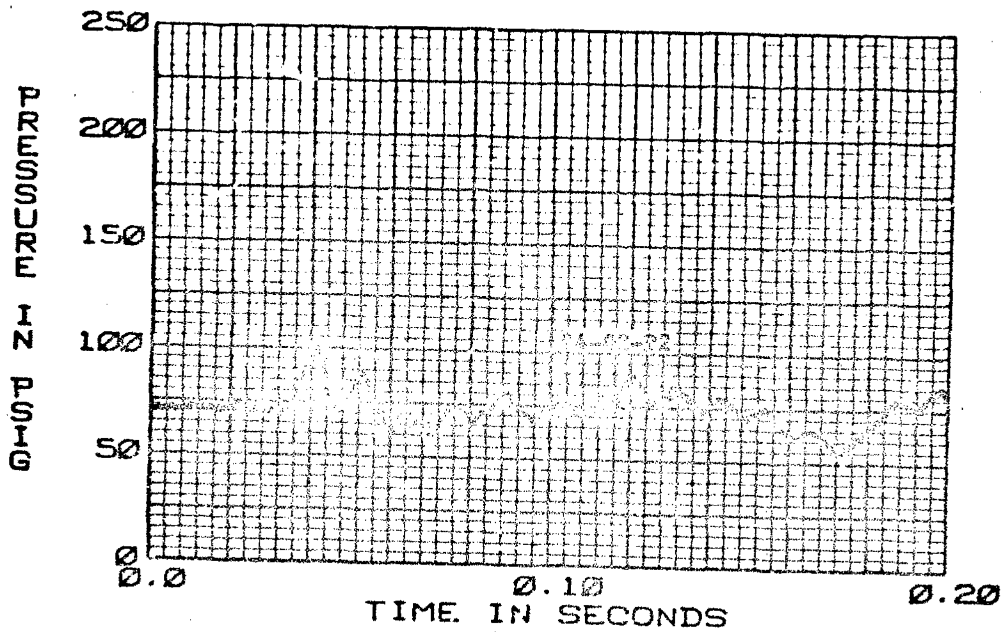


FIGURE 80. F-15 HYDRAULIC PUMP TURN-OFF TRANSIENT
38.5 CIS 130°F

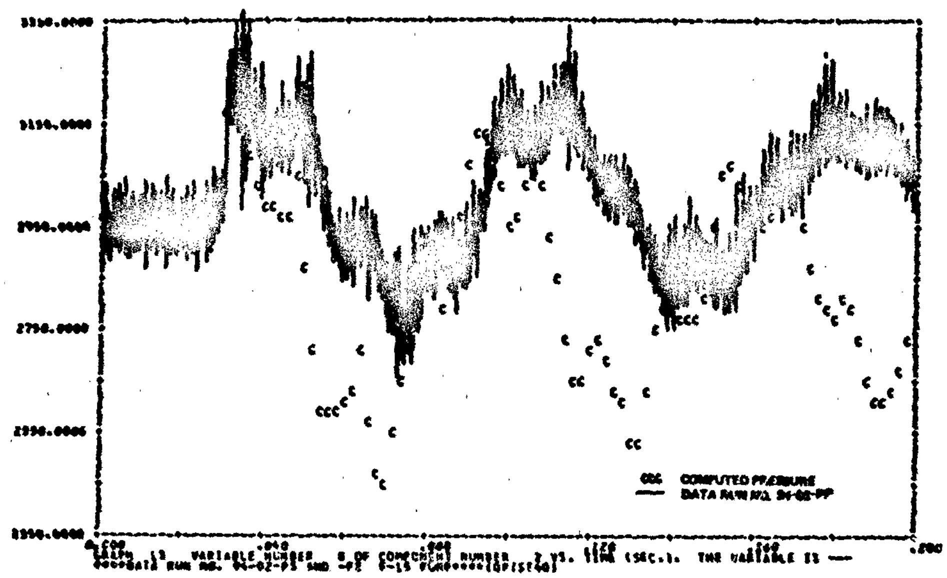


FIGURE 81. OUTLET PRESSURE 38.5-2 CIS TURN-OFF TRANSIENT 130°F 4000 RPM

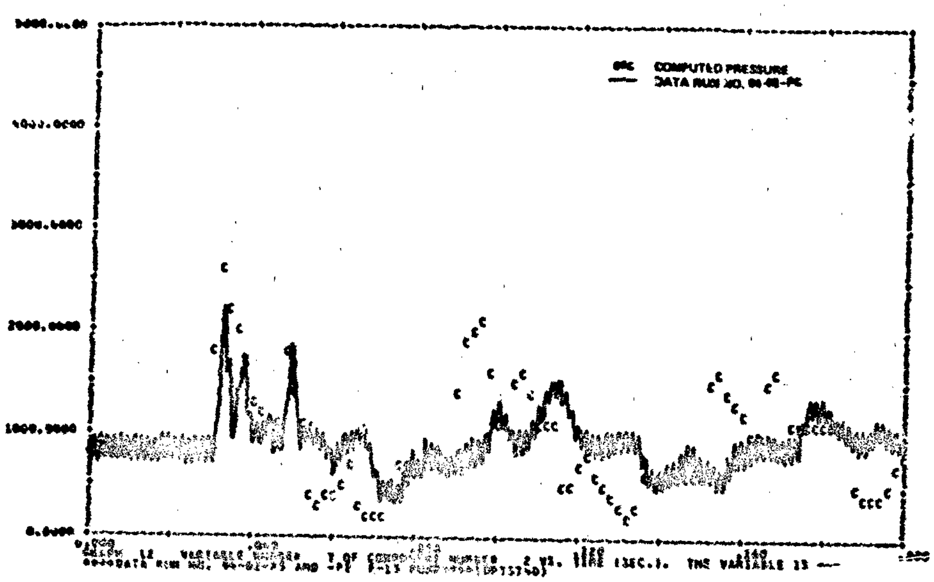


FIGURE 82. CONTROL PRESSURE 38.5-2 CIS TURN-OFF TRANSIENT 130°F 4000 RPM

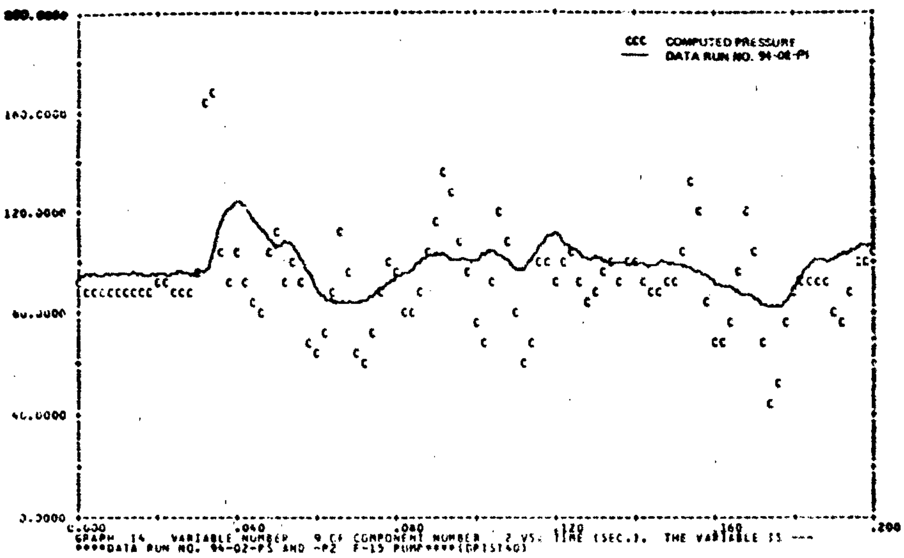


FIGURE 83. INTERNAL CASE PRESSURE 38.5-2CIS TURN-OFF TRANSIENT 130°F 4000 RPM

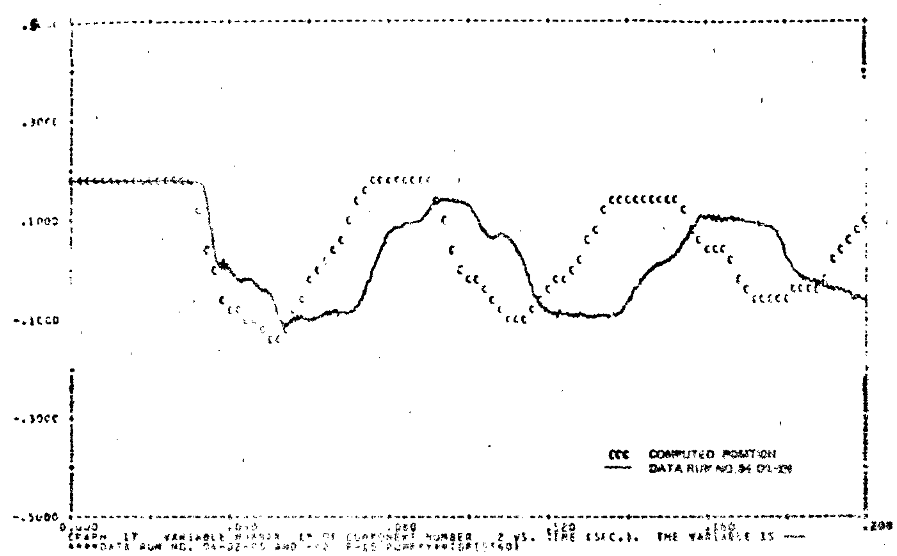


FIGURE 84. HANGER POSITION 38.5-2 CIS TURN-OFF TRANSIENT 130°F 4000 RPM

c. **Pump Model Verification for 4400 psi Transient Tests**

A HYTRAN simulation was made of a turn-on transient from 17.25 CIS to 77.0 CIS at 99°F and 4400 psi pump outlet pressure. The input data is presented in Table 10 and the boundary conditions are shown in Figure 85. The orifice and valve opening were computed to obtain the correct starting and ending flows. The output graphs of pump outlet flow, actuator pressure, internal case pressure and hanger position were overplotted with test data as shown in Figures 86, 87, 88 and 89. The correlation of computed outlet pressure and actuator pressure to test data is good at the higher pump operating pressure. The computed case pressure show a little instability but follow the general wave shape of the test data. The computed hanger position lags the measured data but it looks quite good.

The input boundary conditions for the turn-off transient at the same test conditions is in Figure 90. The results of the HYTRAN simulation are shown in Figures 91 through 94. The initial pump outlet pressure prediction is good but the computed actuator pressures are high.

As with the 3000 psi data the correlation is better both in amplitude and period for the turn-on transient case. The turn-off transient generally requires a larger hanger damping term than the turn-on case. But a value of 60 lbs/in/sec was used in both simulations.

TABLE 10. HYTRAN INPUT DATA 4400 PSI SYSTEM
TURN-ON TRANSIENT RUN

****[illegible] RUN NO. [illegible] AND [illegible] F-15 PUMP****(OPT=T36)

| | | | | | | | | | | | | | | | |
|---|---|---|---|---|---|---|---|---|---|---|---|---|---|---|---|
| | .0002 | | .7 | | .002 | | 99. | | | | | | | | |
| 4 | 9 | 1 | | | | | | | | | | | | | |
| 1 | 0 | 3 | 0 | 0 | 0 | 0 | | | 55.75 | | 1.0 | | .049 | | 3.067 |
| 2 | 0 | 3 | 0 | 0 | 0 | 0 | | | 20.00 | | .375 | | .028 | | 3.067 |
| 3 | 0 | 3 | 0 | 0 | 0 | 2 | | | 302.75 | | 1.0 | | .058 | | 3.067 |
| 4 | 0 | 2 | 0 | 0 | 0 | 0 | | | 8.5 | | 1.0 | | .058 | | 3.067 |
| 5 | 0 | 2 | 0 | 2 | 0 | 2 | | | 30.5 | | .50 | | .028 | | 3.067 |
| 6 | 0 | 2 | 0 | 0 | 0 | 0 | | | 4.0 | | .50 | | .028 | | 3.067 |
| 7 | 0 | 2 | 0 | 0 | 0 | 0 | | | 4.125 | | 1.0 | | .049 | | 3.067 |
| 8 | 0 | 2 | 0 | 0 | 0 | 0 | | | 4.0 | | 1.0 | | .049 | | 3.067 |
| 9 | 0 | 2 | 0 | 0 | 0 | 0 | | | 197. | | 1.0 | | .049 | | 3.067 |
| 1 | 41 | 0 | -1 | 1 | | | | | | | | | | | |
| 2 | 51 | 4 | 1 | -3 | -3 | | | | | | | | | | |
| | 4170. | | 3000. | | .15 | | .25 | | 0. | | .016 | | .65 | | .65 |
| | .307 | | 400. | | 70. | | 130. | | 470. | | 315. | | .035 | | 70. |
| | 3. | | .75 | | -.3 | | .002 | | .001 | | .003 | | .7595 | | 60. |
| | 5. | | 3008. | | .036 | | .95 | | 0. | | .0015 | | 3. | | 0. |
| 3 | 41 | 0. | 3 | 1 | | | | | | | | | | | |
| 4 | 11 | 0 | 3 | -8 | -5 | | | | | | | | | | |
| 5 | 21 | 3 | 4 | -7 | | | | | | | | | 0 | | |
| | .023 | | .65 | | | | | | | | | | | | |
| | 0. | | .020 | | .022 | | .2 | | | | | | | | |
| | 0. | | 0. | | .305 | | .505 | | | | | | | | |
| 6 | 41 | 1 | 3 | -6 | | | | | | | | | | | |
| | .05812 | | .63 | | | | | | | | | | | | |
| 7 | 11 | 0 | 4 | 7 | -8 | | | | | | | | | | |
| 8 | 61 | 1 | 8 | -3 | | | | | | | | | | | |
| | .1100 | | .65 | | | | | | | | | | | | |
| 9 | 61 | 1 | 9 | | | | | | | | | | | | |
| | 70. | | | | | | | | | | | | | | |
| 6 | 6 | | | | | | | | | | | | | | |
| 1 | 1 | 2 | 3 | | 60. | | | | | | | | | | |
| 2 | 1 | 8 | 2 | 2 | 3 | | | | | | | | | | |
| 2 | 2 | 1 | 2 | | 5. | | | | | | | | | | |
| 2 | 3 | 0 | 2 | 3 | 1 | | | | | | | | | | |
| 3 | 2 | 4 | 3 | | 60. | | | | | | | | | | |
| 3 | 2 | 8 | 3 | 4 | 5 | | | | | | | | | | |
| 4 | 4 | 4 | 3 | | 80. | | | | | | | | | | |
| 4 | 2 | 8 | 4 | 5 | 3 | 0 | 7 | 7 | 3 | | | | | | |
| 5 | 4 | 5 | 5 | | 5. | | | | | | | | | | |
| 4 | 3 | 8 | 5 | 6 | 3 | 8 | 6 | 2 | 2 | | | | | | |
| 4 | 4 | 6 | 5 | | 58. | | | | | | | | | | |
| 7 | 3 | 0 | 8 | 8 | 1 | 0 | 4 | 3 | 1 | | | | | | |
| 3 | 14 | | 5 | | | | 1 | | | | | | | | |
| 3 | 2 | | 70.47 | | -20.54 | | | | | | | | | | |
| 2 | 1 | 2 | 4 | 2 | 5 | 2 | 7 | 2 | 8 | 2 | 9 | 2 | 14 | 2 | 15 |
| 2 | 26 | 2 | 19 | 2 | 25 | 2 | 6 | 2 | 30 | 2 | 31 | | | | |

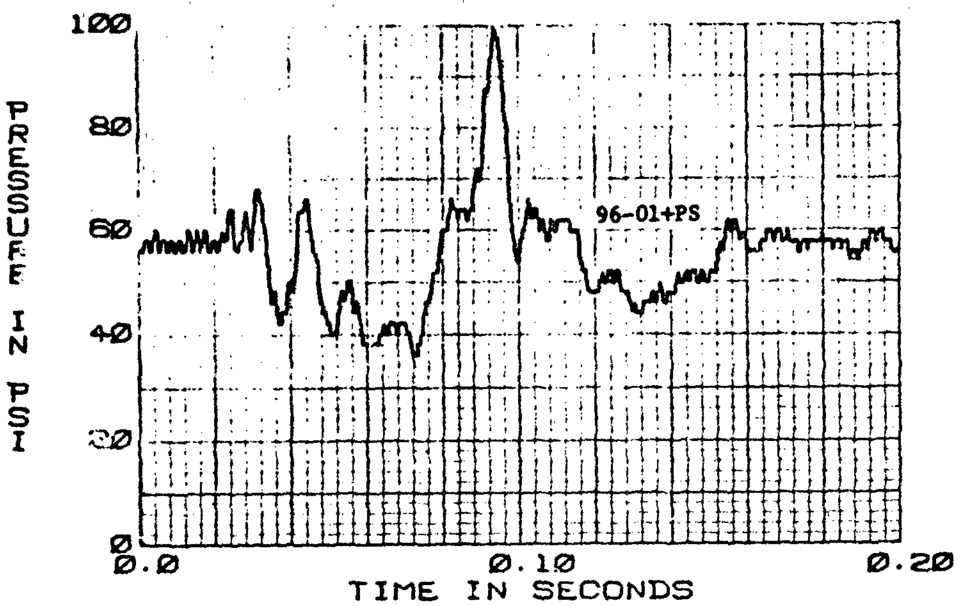


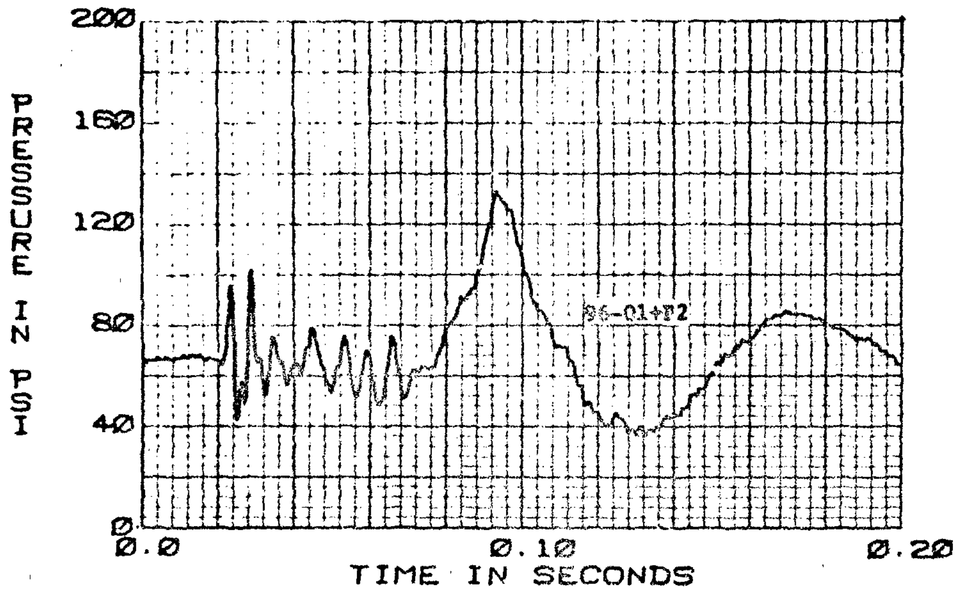


FIGURE 85. F-15 HYDRAULIC PUMP TURN-ON TRANSIENT
17 CIS 100°F

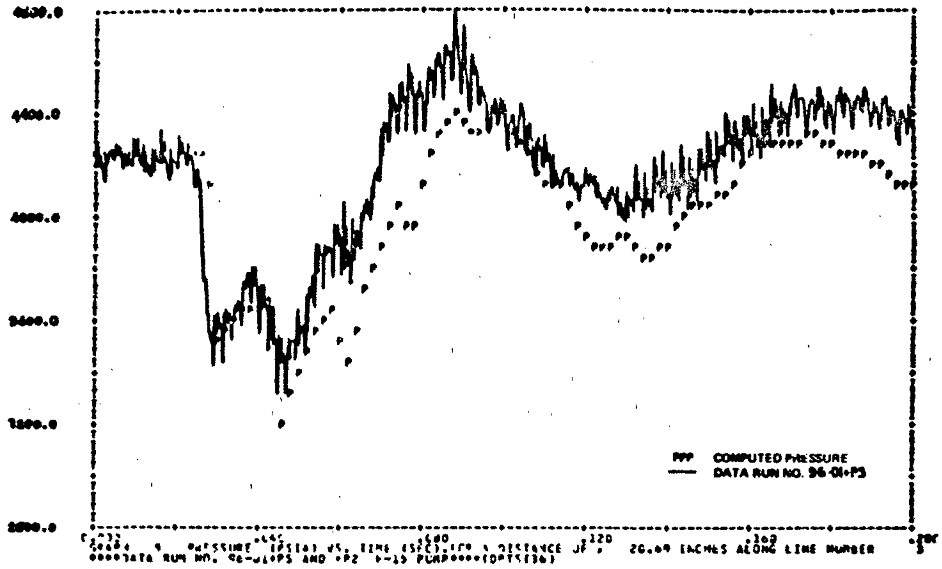


FIGURE 86. OUTLET PRESSURE 17.25 - 77 CIS TURN-ON TRANSIENT
100°F 3000 RPM

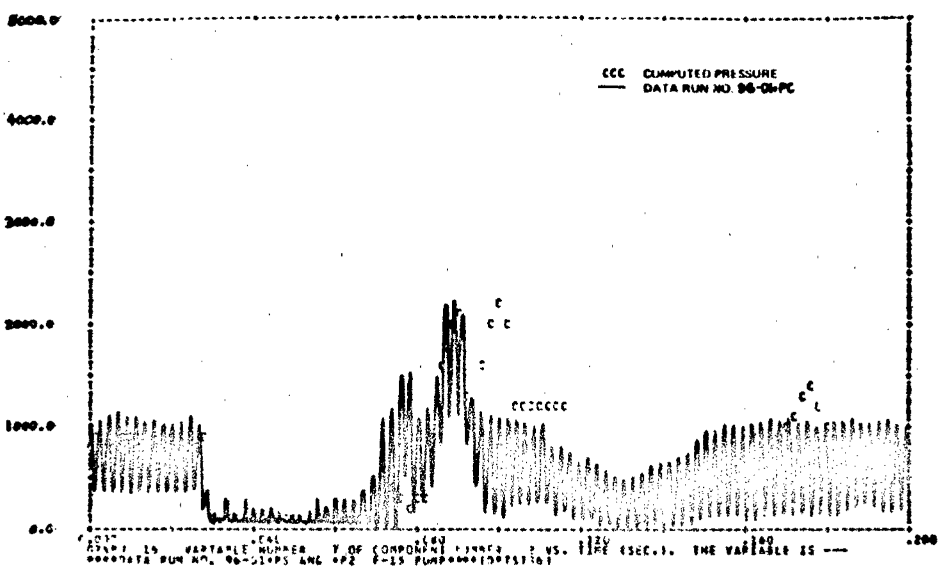


FIGURE 87. CONTROL PRESSURE 17.25 - 77 CIS TURN-ON TRANSIENT
100°F 3000 RPM

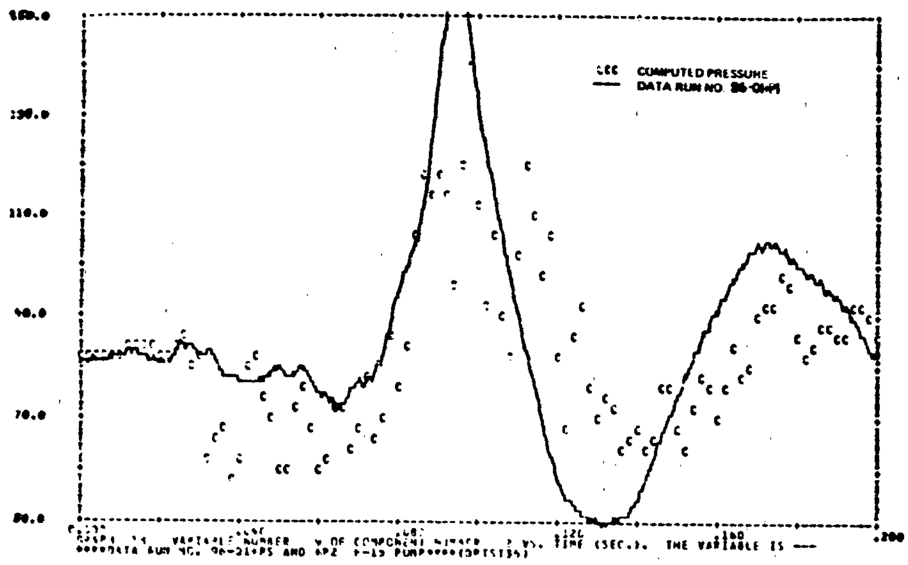


FIGURE 88. INTERNAL CASE PRESSURE 17.25 -77 CIS TURN-ON TRANSIENT
100°F 3000 RPM

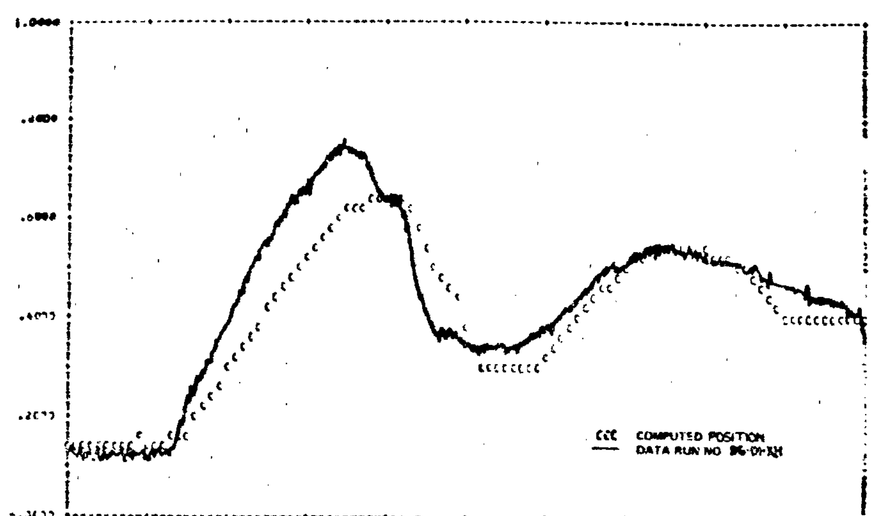


FIGURE 89. HANGER POSITION 17.25 - 77 CIS TURN-ON TRANSIENT
100°F 3000 RPM

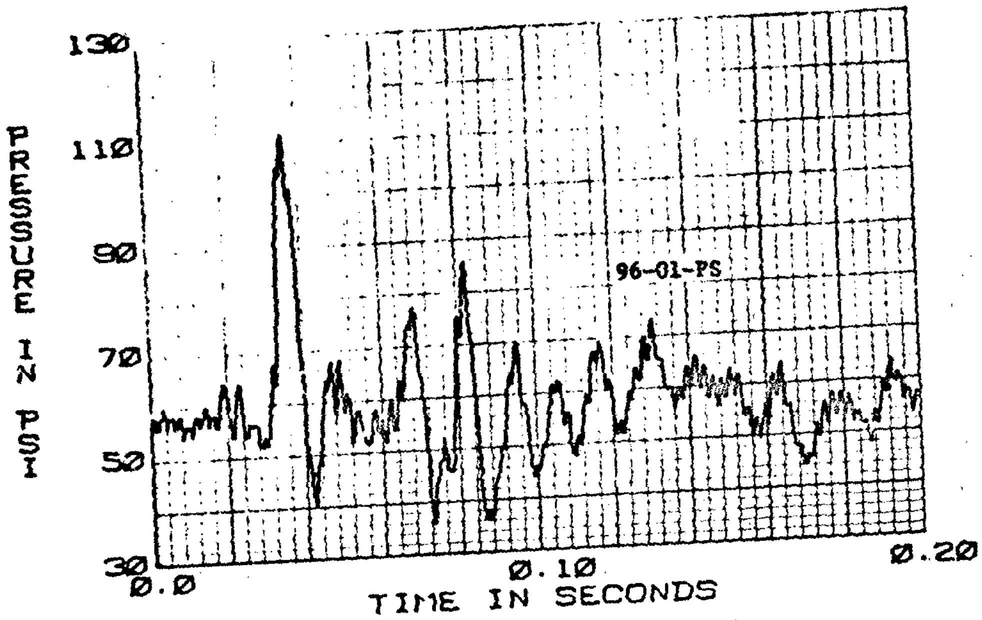


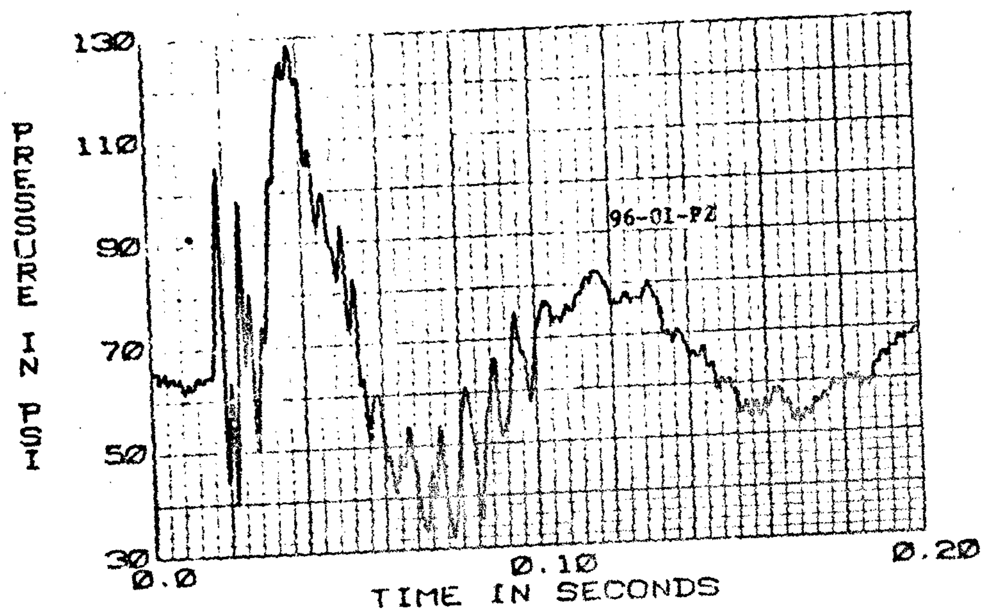


FIGURE 90. F-15 HYDRAULIC PUMP TURN-OFF TRANSIENT
77-17.25 CIS 100°F

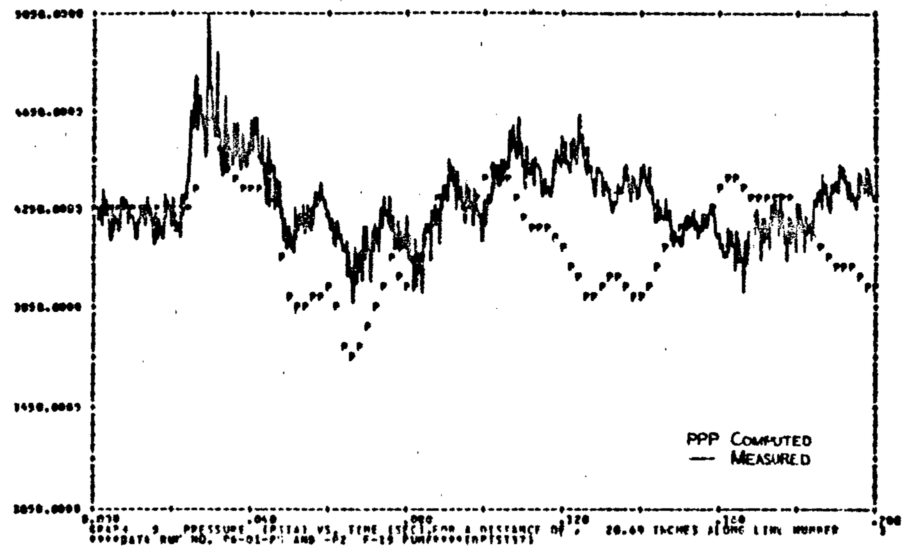


FIGURE 91. OUTLET PRESSURE HIGH PRESSURE SYSTEM
77-17.25 CIS TURN-OFF TRANSIENT
4400 PSI 100°F

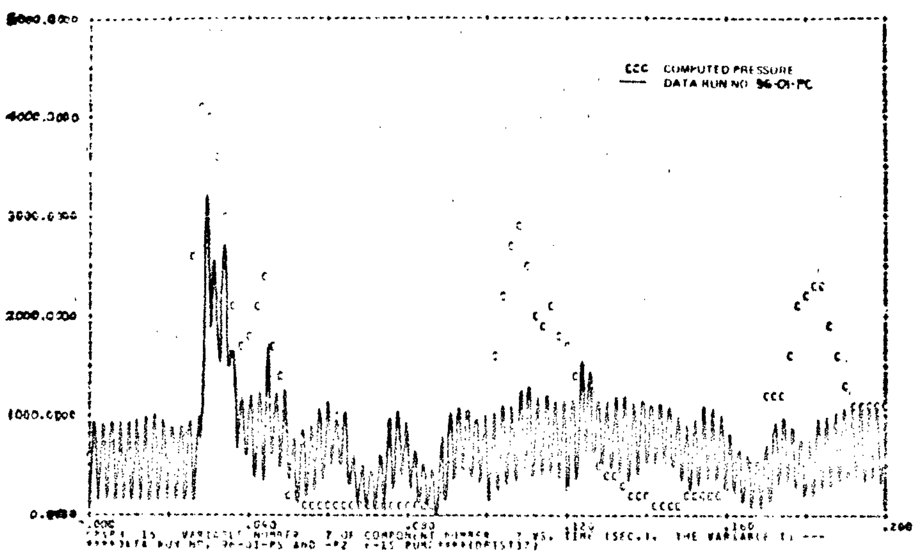


FIGURE 92. CONTROL PRESSURE 77.-17.25 CIS TURN-OFF TRANSIENT
100°F 3000 RPM

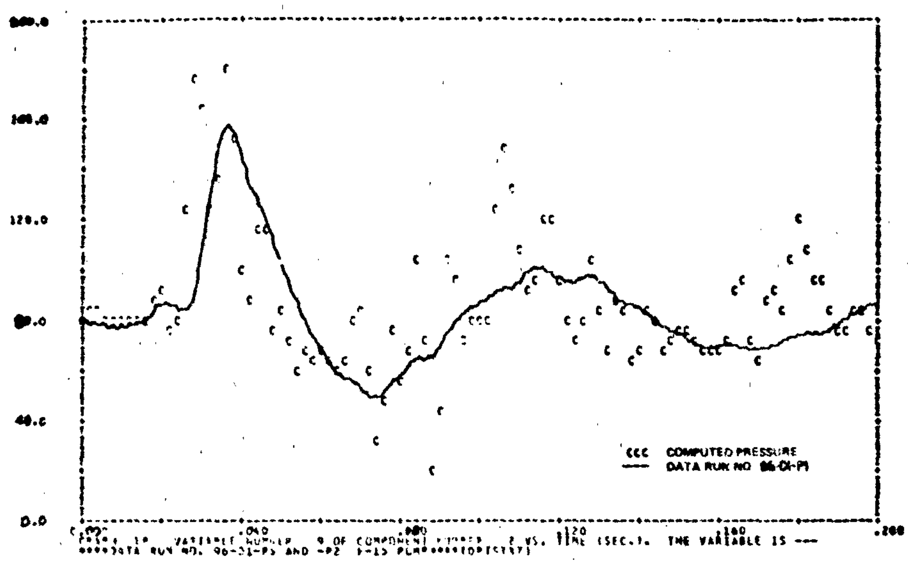


FIGURE 93. INTERNAL CASE PRESSURE 77-17.25 CIS TURN-OFF TRANSIENT
100°F 3000 RPM

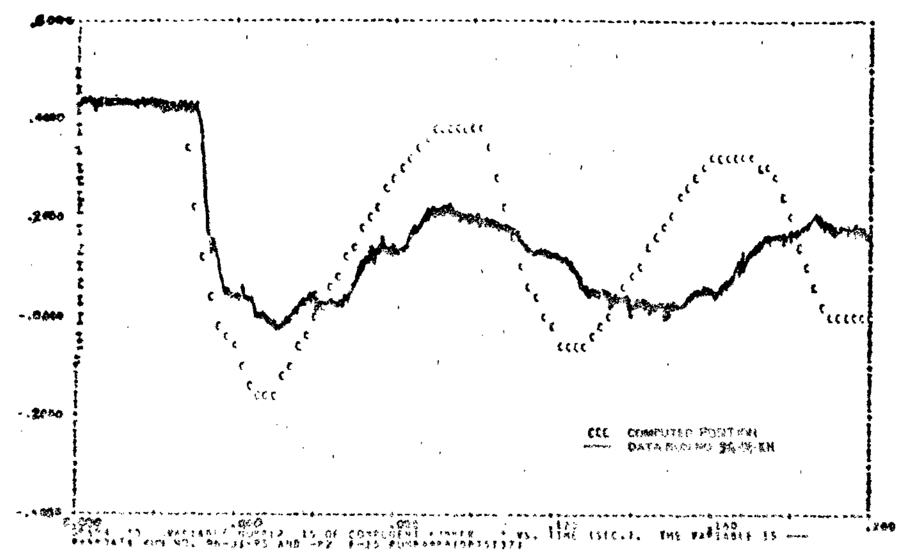

FIGURE 94. HANGER POSITION 77-17.25 CIS TURN-OFF TRANSIENT
100°F 3000 RPM

d. F-15 Pump Model Verification Using The Complete Test Stand Model

The entire F-15 instrumented pump test stand was modeled with the HYTRAN program. The HYTRAN block diagram of the test system is shown in Figure 95 The elements which make up the system are split into lines and components. The lines are numbered sequentially and have upstream and downstream ends. The components are also numbered in a separate sequence. Node numbers are assigned to the points at which the flow divides or combines under steady state flow conditions and leg numbers are labeled between two nodes. The simulation consisted of running the HYTRAN program under the same lab test conditions. The first simulation was of a turn-on transient at 130°F and from 2-77 CIS steady state flows. The reservoir test data in Figure 96 was input as a boundary condition. The results of the computer simulation are shown overplotted with the test data in Figures 97, 98, 99 and 100. The plots of outlet pressure, actuator pressure and hanger position correlate well with the test data. The computed internal case pressure in Figure 99 however does not match the measured results. The calculated pressure values are about 60 psi higher than the data, and the phasing between the two is incorrect. With the external case pressure as a boundary condition this misphasing did not occur.

The next simulation was for a turn-off transient at 130°F and 77.0 CIS. The input reservoir pressure is shown in Figure 101. The computed outlet pressure in Figure 102 is able to predict the maximum amplitude of the first pressure spike but this model undershoots on the subsequent response between 0.050 and 0.090 seconds in the simulation. This undershoot also misphases the measured and computed results. This undershoot characteristic did exist for the turn-off run with the inputted case drain and suction pressures as boundary conditions, but it was not as prevalent. Further work in the area of amplitude damping should correct the modeling discrepancy. The actuator pressure and hanger positions are overplotted with test data in Figures 103 and 104. The internal case pressure plot in Figure 105 shows adequate phase correlation but the amplitude predictions are off.

The next attempt at total system simulation was not to use input data as boundary conditions. This was done to test the basic accuracy of the HYTRAN program without any external forcing factors.

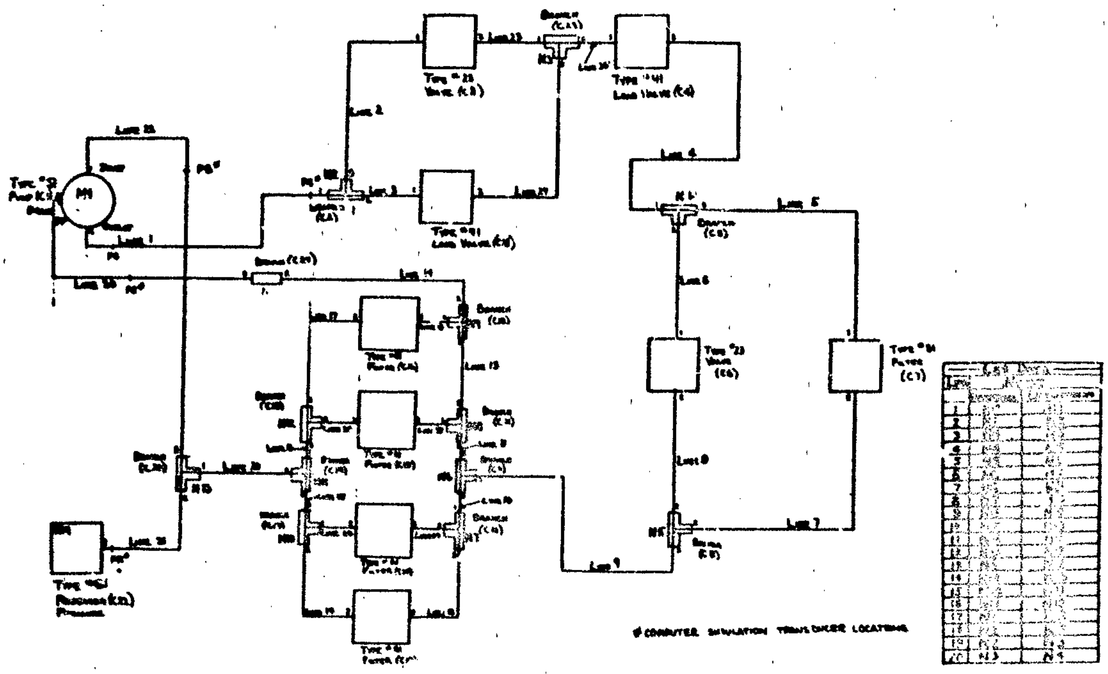

FIGURE 95. SINGLE F-15 PUMP SYSTEM

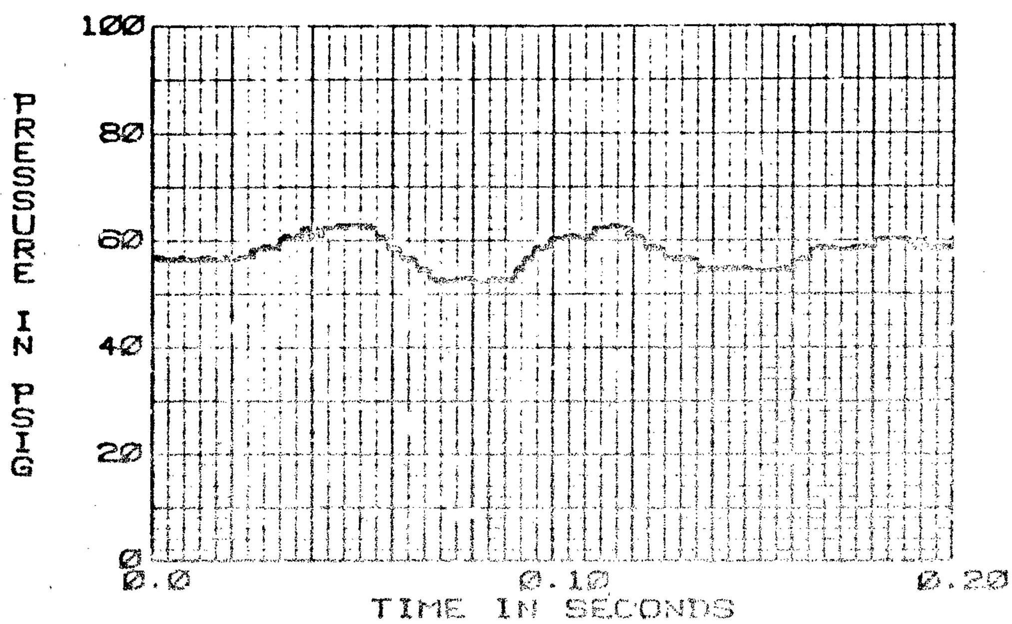


FIGURE 96. F-15 HYDRAULIC PUMP 94-A4+PR TURN-ON TRANSIENT
77 CIS 130°F

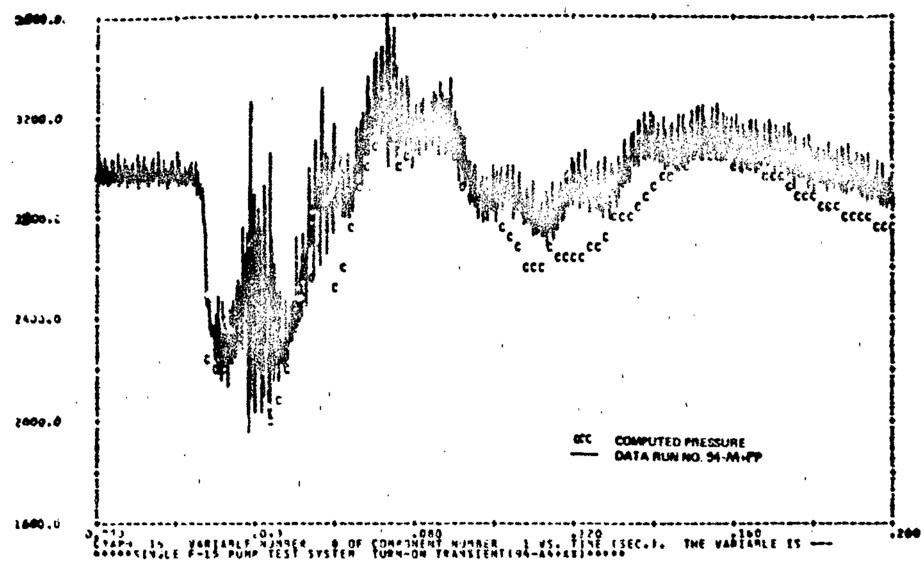


FIGURE 97. OUTLET PRESSURE 2-77 CIS TURN-ON TRANSIENT
130°F 4000 RPM

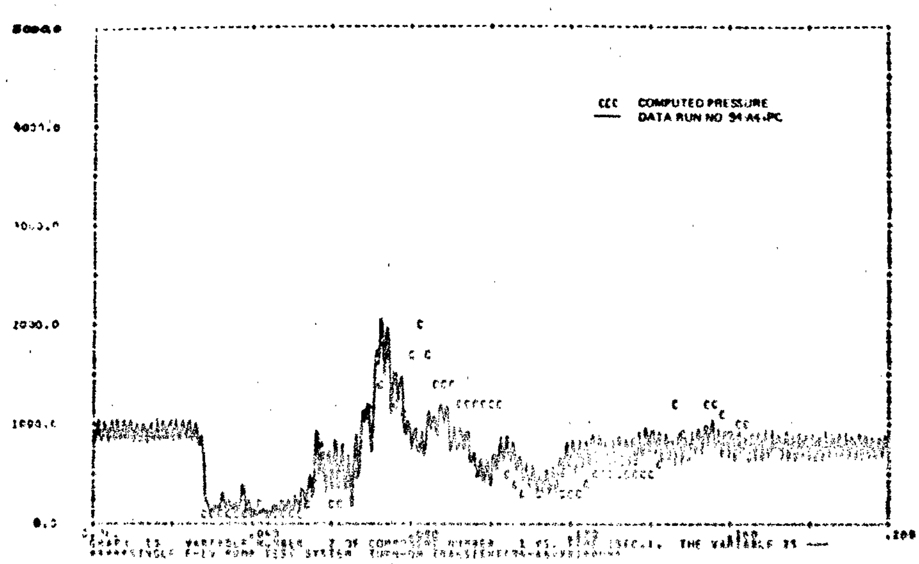


FIGURE 98. CONTROL PRESSURE 2-77 CIS TURN-ON TRANSIENT
130°F 4000 RPM

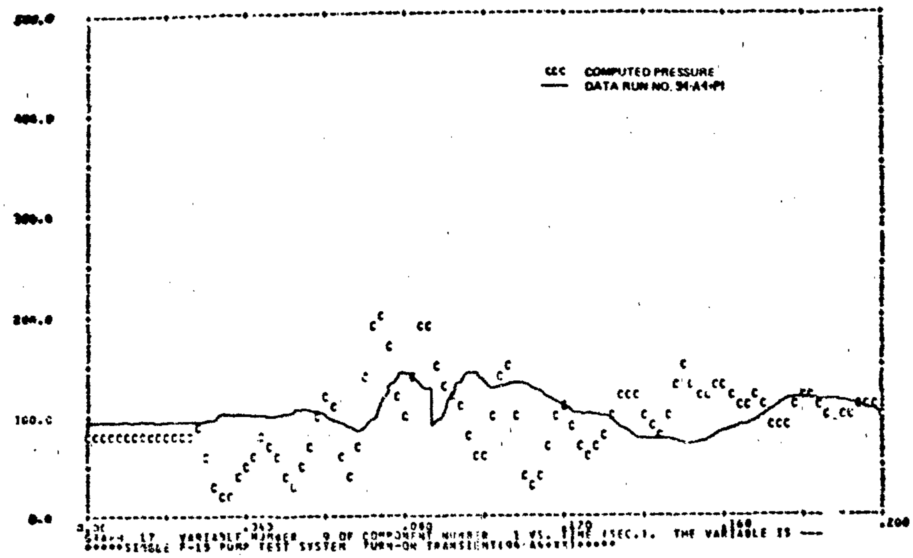


FIGURE 99. INTERNAL CASE PRESSURE 2-77 CIS TURN-ON TRANSIENT
130°F 4000 RPM

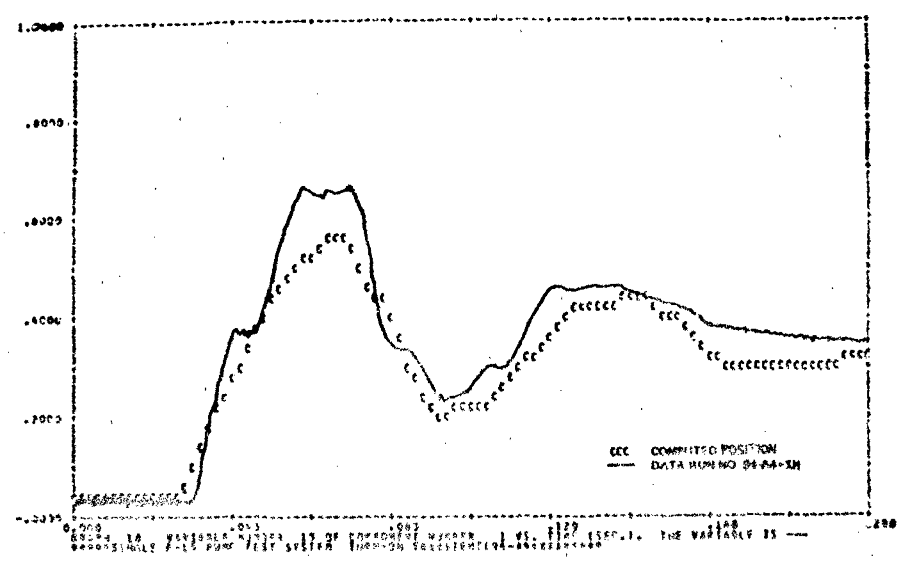


FIGURE 100. HANGER POSITION 2-77 CIS TURN-ON TRANSIENT
130°F 4000 RPM

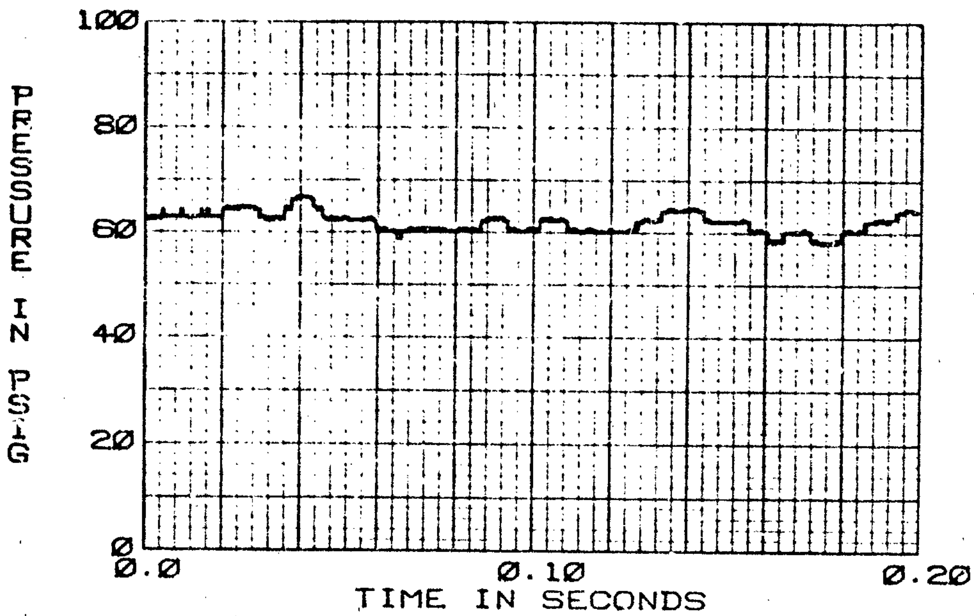


FIGURE 101. F-15 HYDRAULIC PUMP 94-A4-PR TURN-OFF TRANSIENT
77 CIS 130°F

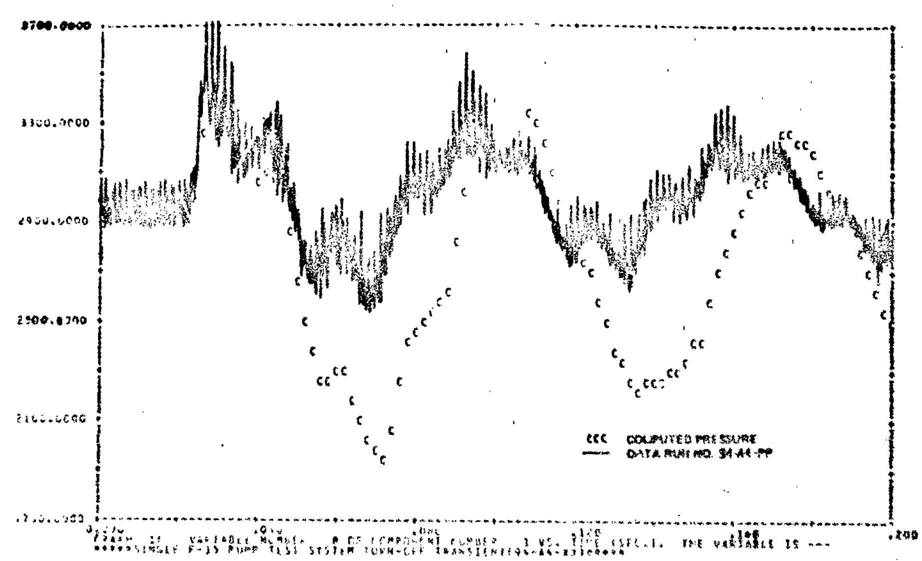


FIGURE 102. OUTLET PRESSURE 77-2 CIS TURN-OFF TRANSIENT
130°F 4000 RPM

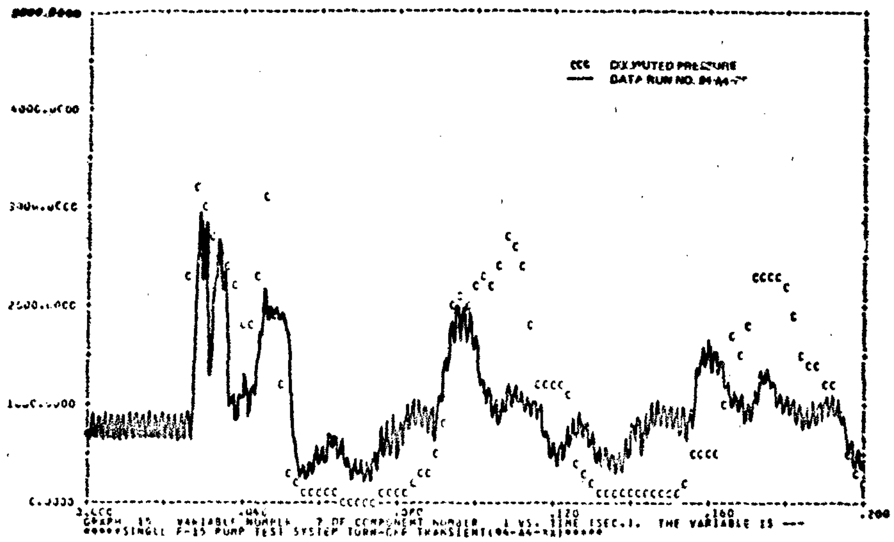

FIGURE 103. CONTROL PRESSURE 77-2 CIS TURN-OFF TRANSIENT
130°F 4000 RPM

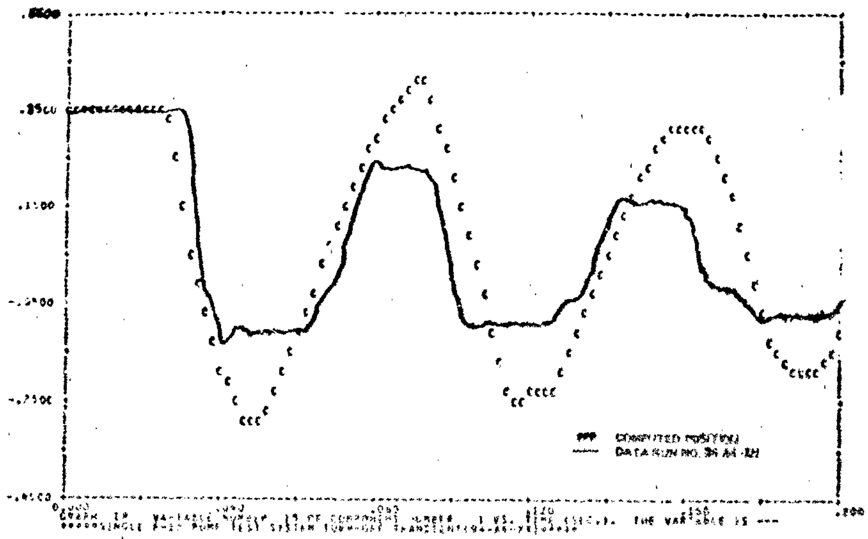

FIGURE 104. HANGER POSITION 77-2 CIS TURN-OFF TRANSIENT
130°F 4000 RPM

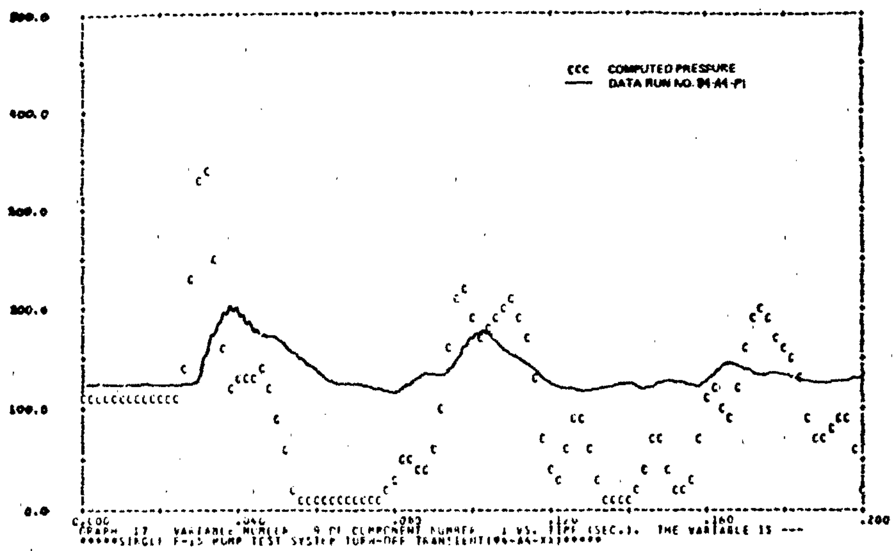


FIGURE 105. INTERNAL CASE PRESSURE 77-2 CIS TURN-OFF TRANSIENT 130°F 4000 RPM

The turn-on transient was made with the test conditions of run number 94-0C-XX. For the turn-on transient simulation, the load valve was sized to drop 3000 psi at 154.0 CIS. The reservoir pressure was 80 psia. A listing of the HYTRAN input data for the turn-on simulation at 130°F is shown in Table 11. Figures 106 and 107 show computed pressures at two locations along the pump outlet line. Corresponding test data has been overplotted for comparison. The initial and final steady state pressure levels are correct for the simulation.

For a turn-on transient the pump destrokes to supply the demanded flow. In the HYTRAN simulation the pump model is able to adequately do this. The subsequent response to the operating steady state pressure however is slightly faster than the measured data as shown in Figures 106 and 107 at 80 milliseconds into the simulation. A lag could be programmed into the compensator circuit to delay the build-up in pressure but the benefits of such a fix may not be applicable for all the test cases. Computed actuator pressure (Figure 108) shows good correlation when compared to the test data. The computed pressures in the case drain circuit in Figures 109 and 110 fail to reach the actual peak pressures. Similarly the inlet pressure plot in Figure 111 shows a peak prediction about 50 psi higher than the measured data.

**TABLE 11. HYTRAN INPUT DATA 154. CIS TURN-ON TRANSIENT 130°F 3000 PSI LINE DATA**

*****SINGLE F-15 PUMP TEST SYSTEM TURN-ON TRANSIENT(04-06+XX)*****

THE TRANSIENT RESPONSE IS FROM T=0.0 TO T= .200 SECONDS AT TIME INTERVALS OF DELT= .00020
WITH OUTPUT POINTS PLOTTED AT INTERVALS OF , .00200 SECONDS

FLUID DATA FOR MIL-H-5606 AT 3000.0 PSIG. - 50.0 PSIG AND 130.0 DEG F IN 10.0 DEG F STEPS
VISCOSITY - .186E-01 .148E-01IN**2/SEC
DENSITY - .813E-04 .803E-04(LB-SEC**2)/IN**4
BULK MODULUS - .223E+06 .187E+06PSI
VAPOUR PRESS.- .200E+01 AT 130.0 DEG F
FIX-UP TAKEN AT LINE 18,VEL OF SOUND IN LINE 23 IS 58.4PER CENT IN ERROR
FIX-UP TAKEN AT LINE 18,VEL OF SOUND IN LINE 24 IS 59.6PER CENT IN ERROR
FIX-UP TAKEN AT LINE 18,VEL OF SOUND IN LINE 25 IS 59.6PER CENT IN ERROR

| LINE DATA LINE NO. | LENGTH | INTERNAL DIA | WALL THICKNESS | MODULUS OF ELASTICITY | DELX | CHARACTERISTIC IMPEDANCE | VELOCITY OF SOUND |
|---|---|---|---|---|---|---|---|
| 1 | 392.7500 | .8840 | .0580 | .300E+08 | 10.0724 | 6.5615 | 49551.4538 |
| 2 | 10.5000 | .8840 | .0580 | .300E+08 | 10.5000 | 6.5615 | 49551.4538 |
| 3 | 10.9000 | .4440 | .0280 | .300E+08 | 10.9000 | 25.9624 | 44460.3746 |
| 4 | 50.6300 | .8840 | .0580 | .300E+08 | 10.1260 | 6.5615 | 49551.4538 |
| 5 | 65.0000 | .8840 | .0580 | .300E+08 | 13.0000 | 6.5615 | 49551.4538 |
| 6 | 33.0000 | .8840 | .0580 | .300E+08 | 11.0000 | 6.5615 | 49551.4538 |
| 7 | 26.0000 | .8840 | .0580 | .300E+08 | 13.0000 | 6.5615 | 49551.4538 |
| 8 | 26.0000 | .8840 | .0580 | .300E+08 | 13.0000 | 6.5615 | 49551.4538 |
| 9 | 33.5000 | .8840 | .0580 | .300E+08 | 11.1667 | 6.5615 | 49551.4538 |
| 10 | 25.0000 | .6940 | .0280 | .300E+08 | 12.5000 | 10.3544 | 48193.7367 |
| 11 | 25.0000 | .6940 | .0280 | .300E+08 | 12.5000 | 10.3544 | 48193.7367 |
| 12 | 25.1900 | .6940 | .0280 | .300E+08 | 12.5950 | 10.3544 | 48193.7367 |
| 13 | 25.0000 | .6940 | .0280 | .300E+08 | 12.5000 | 10.3544 | 48193.7367 |
| 14 | 25.0000 | .6940 | .0280 | .300E+08 | 12.5000 | 10.3544 | 48193.7367 |
| 15 | 25.0000 | .6940 | .0280 | .300E+08 | 12.5000 | 10.3544 | 48193.7367 |
| 16 | 25.0000 | .6940 | .0280 | .300E+08 | 12.5000 | 10.3544 | 48193.7367 |
| 17 | 25.0000 | .6940 | .0280 | .300E+08 | 12.5000 | 10.3544 | 48193.7367 |
| 18 | 25.0000 | .6940 | .0280 | .300E+08 | 12.5000 | 10.3544 | 48193.7367 |
| 19 | 25.0000 | .6940 | .0280 | .300E+08 | 12.5000 | 10.3544 | 48193.7367 |
| 20 | 40.2500 | .8840 | .0580 | .300E+08 | 10.0625 | 6.5615 | 49551.4538 |
| 21 | 26.0000 | .8840 | .0580 | .300E+08 | 13.0000 | 6.5615 | 49551.4538 |
| 22 | 78.1300 | .8840 | .0580 | .300E+08 | 11.1614 | 6.5615 | 49551.4538 |
| 23 | 4.1250 | .8840 | .0580 | .300E+08 | 4.1250 | 6.5615 | 20625.0000 |
| 24 | 4.0000 | .4440 | .0280 | .300E+08 | 4.0000 | 25.9624 | 20000.0000 |
| 25 | 4.0000 | .8840 | .0580 | .300E+08 | 4.0000 | 6.5615 | 20000.0000 |
| 26 | 25.0000 | .6940 | .0280 | .300E+08 | 12.5000 | 10.3544 | 48193.7367 |
| 27 | 25.0000 | .6940 | .0280 | .300E+08 | 12.5000 | 10.3544 | 48193.7367 |
| 28 | 25.0000 | .6940 | .0280 | .300E+08 | 12.5000 | 10.3544 | 48193.7367 |
| 29 | 25.0000 | .6940 | .0280 | .300E+08 | 12.5000 | 10.3544 | 48193.7367 |
| 30 | 98.5000 | .3190 | .0280 | .300E+08 | 10.9444 | 50.9788 | 50132.3294 |

TABLE 11. (CONTINUED) HYTRAN INPUT DATA TURN-ON TRANSIENT
COMPONENT DATA

```
 COMP#.   1  INTEGER DATA     1  51   4  22   -1  -30   0   0   0   0   0   0   0   0   0   0
REAL DATA CARD #   1   .2870E+04   .2000E+04   .1500E+00   .2500E+00  0.          .1600E-01   .6500E+00   .6500E+00
REAL DATA CARD #   2   .3070E+00   .4000E+03   .7000E+02   .1300E+03   .4700E+03   .7150E+03   .3500E-01   .4500E+02
REAL DATA CARD #   3   .1000E+01   .7500E+00  -.3000E+00   .5000E-02   .2100E+01   .3000E-02   .5000E-01   .4800E+02
REAL DATA CARD #   4   .2000E+01   .4000E+04   .3600E-01   .5000E-01  0.          .3500E-02   .1000E+01   .8000E+01
 COMP#.   2  INTEGER DATA     2  11   0   1   -3   -2   0   0   0   0   0   0   0   0   0   0
 COMP#.   3  INTEGER DATA     3  23   3   2  -22    0   0   0   0   0   0   0   0   4   0   0
REAL DATA CARD #   1   .2200E-01   .6500E+00  0.          0.          0.          0.          0.          0.
REAL DATA CARD #   2  0.           .2000E-01   .2400E-01   .2000E+00  0.          0.          0.          0.
REAL DATA CARD #   3  0.          0.           .1270E+01   .1270E+01  0.          0.          0.          0.
 COMP#.   4  INTEGER DATA     4  41   1  25   -4    0   0   0   0   0   0   0   0   0   0   0
REAL DATA CARD #   1   .8840E+00   .4500E+00  0.          0.          0.          0.          0.          0.
 COMP#.   5  INTEGER DATA     5  11   0   4   -6   -5   0   0   0   0   0   0   0   0   0   0
 COMP#.   6  INTEGER DATA     6  23   3   6   -8    0   0   0   0   0   0   0   0   4   0   0
REAL DATA CARD #   1   .1000E+01   .6500E+00  0.          0.          0.          0.          0.          0.
REAL DATA CARD #   2  0.           .1800E-01   .2000E-01   .2000E+00  0.          0.          0.          0.
REAL DATA CARD #   3  0.          0.          0.          0.          0.          0.          0.          0.
 COMP#.   7  INTEGER DATA     7  51   1   5   -7    0   0   0   0   0   0   0   0   0   0   0
REAL DATA CARD #   1   .1000E+04   .1000E+05   .7421E-01   .1000E-03  0.          0.          0.          0.
 COMP#.   8  INTEGER DATA     8  11   0   8    7   -9   0   0   0   0   0   0   0   0   0   0
 COMP#.   9  INTEGER DATA     9  11   0   9  -11  -10   0   0   0   0   0   0   0   0   0   0
 COMP#.  10  INTEGER DATA    10  11   0  10  -29  -12   0   0   0   0   0   0   0   0   0   0
 COMP#.  11  INTEGER DATA    11  11   0  11  -27  -13   0   0   0   0   0   0   0   0   0   0
 COMP#.  12  INTEGER DATA    12  11   0  13  -18   19   0   0   0   0   0   0   0   0   0   0
 COMP#.  13  INTEGER DATA    13  41   1  12  -14    0   0   0   0   0   0   0   0   0   0   0
REAL DATA CARD #   1   .4028E+01   .4028E+01   .1855E+00   .4050E-02  0.          0.          0.          0.
 COMP#.  14  INTEGER DATA    14  41   1  29  -28    0   0   0   0   0   0   0   0   0   0   0
REAL DATA CARD #   1   .4028E+01   .4028E+01   .1855E+00   .4050E-02  0.          0.          0.          0.
 COMP#.  15  INTEGER DATA    15  51   1  27  -26    0   0   0   0   0   0   0   0   0   0   0
REAL DATA CARD #   1   .4028E+01   .4028E+01   .1855E+00   .4050E-02  0.          0.          0.          0.
 COMP#.  16  INTEGER DATA    16  51   1  19  -17    0   0   0   0   0   0   0   0   0   0   0
REAL DATA CARD #   1   .4028E+01   .4028E+01   .1855E+00   .4050E-02  0.          0.          0.          0.
 COMP#.  17  INTEGER DATA    17  11   0  28   14  -15   0   0   0   0   0   0   0   0   0   0
 COMP#.  18  INTEGER DATA    18  11   0  17   26  -16   0   0   0   0   0   0   0   0   0   0
 COMP#.  19  INTEGER DATA    19  11   0  16   15  -20   0   0   0   0   0   0   0   0   0   0
 COMP#.  20  INTEGER DATA    20  11   0  20   21  -22   0   0   0   0   0   0   0   0   0   0
 COMP#.  21  INTEGER DATA    21  41   1   3  -24    0   0   0   0   0   0   0   0   0   0   0
REAL DATA CARD #   1   .2100E-01   .6500E+00  0.          0.          0.          0.          0.          0.
 COMP#.  22  INTEGER DATA    22  61   1 -21    0    0   0   0   0   0   0   0   0   0   0   0
REAL DATA CARD #   1   .8000E+02  0.          0.          0.          0.          0.          0.          0.
 COMP#.  23  INTEGER DATA    23  11   0  23  -25   24   0   0   0   0   0   0   0   0   0   0
 COMP#.  24  INTEGER DATA    24  11   0  30  -19    0   0   0   0   0   0   0   0   0   0   0
     CPU TIME IN SECONDS =   3.299
```

TABLE 11. (CONTINUED) HYTRAN INPUT DATA TURN-ON TRANSIENT STEADY STATE INPUT DATA

NUMBER OF NODES = 14  NUMBER OF LEGS = 20  NUMBER OF CONSTANT PRESSURE NODES = 0

LEG CONNECTION INPUT DATA

| LEG NO | UPST NODE NO | DWST NODE NO | NO OF ELEMENTS | FLOW GUESS | UPST PRESS | DWST PRESS |
|---|---|---|---|---|---|---|
| 1 | 13 | 1 | 3 | 90.00000 | 0.00000 | 0.00000 |
| 2 | 1 | 2 | 3 | 90.00000 | 0.00000 | 0.00000 |
| 3 | 4 | 5 | 5 | 10.00000 | 0.00000 | 0.00000 |
| 4 | 4 | 5 | 5 | 90.00000 | 0.00000 | 0.00000 |
| 5 | 5 | 6 | 3 | 90.00000 | 0.00000 | 0.00000 |
| 6 | 5 | 7 | 3 | 50.00000 | 0.00000 | 0.00000 |
| 7 | 6 | 4 | 3 | 50.00000 | 0.00000 | 0.00000 |
| 8 | 7 | 10 | 5 | 50.00000 | 0.00000 | 0.00000 |
| 9 | 8 | 9 | 3 | 50.00000 | 0.00000 | 0.00000 |
| 10 | 7 | 10 | 5 | 50.00000 | 0.00000 | 0.00000 |
| 11 | 12 | 11 | 3 | 10.00000 | 0.00000 | 0.00000 |
| 12 | 4 | 12 | 5 | 10.00000 | 0.00000 | 0.00000 |
| 13 | 9 | 12 | 5 | 10.00000 | 0.00000 | 0.00000 |
| 14 | 14 | 13 | 3 | .01200 | 0.00000 | 0.00000 |
| 15 | 10 | 11 | 3 | 50.00000 | 0.00000 | 0.00000 |
| 16 | 11 | 13 | 3 | 50.00000 | 0.00000 | 0.00000 |
| 17 | 1 | 9 | 5 | [illegible]0.00000 | 0.00000 | 0.00000 |
| 18 | 2 | 3 | 5 | 5.00000 | 0.00000 | 0.00000 |
| 19 | 2 | 3 | 5 | 90.00000 | 0.00000 | 0.00000 |
| 20 | 3 | 4 | 5 | 90.00000 | 0.00000 | 0.00000 |

| LEG NO | ELEMENTS IN LEG---- | | | | |
|---|---|---|---|---|---|
| 1 | 20 -- 3, | 0 -- 22, | 1 -- 1, | | |
| 2 | 1 -- 7, | 0 -- 1, | 2 -- 1, | | |
| 3 | 5 -- 2, | 0 -- 6, | 6 -- 1, | 0 -- 8, | 8 -- 1, |
| 4 | 8 -- 3, | 0 -- 5, | 7 -- 1, | 0 -- 7, | 8 -- 2, |
| 5 | 8 -- 3, | 0 -- 9, | 9 -- 1, | | |
| 6 | 9 -- 3, | 0 -- 10, | 10 -- 1, | | |
| 7 | 9 -- 2, | 0 -- 11, | 11 -- 1, | | |
| 8 | 10 -- 3, | 0 -- 12, | 13 -- 1, | 0 -- 14, | 17 -- 2, |
| 9 | 11 -- 3, | 0 -- 13, | 12 -- 1, | | |
| 10 | 10 -- 2, | 0 -- 29, | 14 -- 1, | 0 -- 28, | 17 -- 1, |
| 11 | 19 -- 3, | 0 -- 16, | 19 -- 1, | | |
| 12 | 11 -- 2, | 0 -- 27, | 15 -- 1, | 0 -- 26, | 18 -- 2, |
| 13 | 12 -- 2, | 0 -- 18, | 16 -- 1, | 0 -- 17, | 18 -- 1, |
| 14 | 22 -- 1, | 0 -- 21, | 20 -- 2, | | |
| 15 | 17 -- 3, | 0 -- 15, | 19 -- 2, | | |
| 16 | 19 -- 3, | 0 -- 25, | 22 -- 1, | | |
| 17 | 1 -- 3, | 0 -- 30, | 24 -- 1, | 0 -- 19, | 12 -- 3, |
| 18 | 2 -- 2, | 0 -- 3, | 31 -- 1, | 0 -- 24, | 23 -- 3, |
| 19 | 2 -- 3, | 0 -- 2, | 3 -- 1, | 0 -- 23, | 23 -- 1, |
| 20 | 23 -- 2, | 0 -- 2[illegible], | 4 -- 1, | 0 -- 4, | 5 -- 1, |

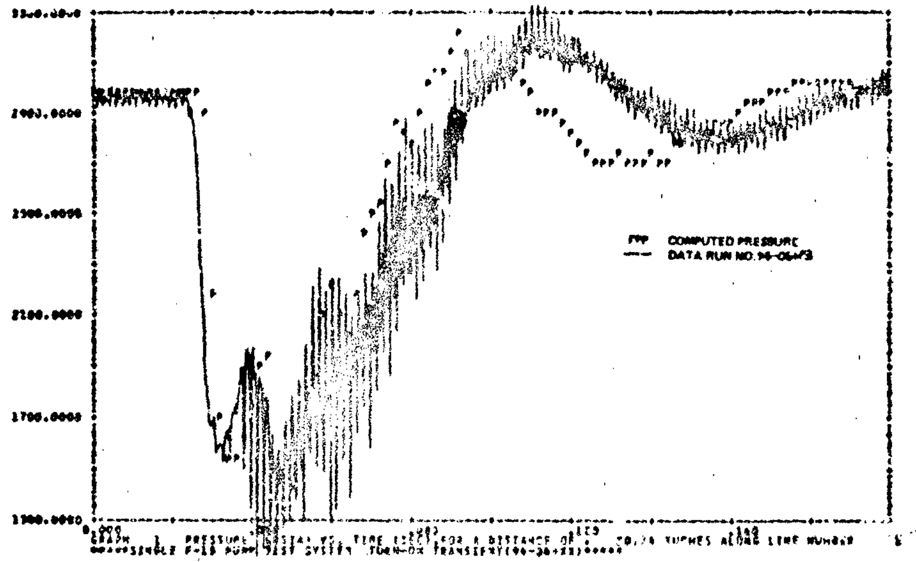

FIGURE 106. OUTLET PRESSURE 2-154 CIS TURN-ON TRANSIENT
130°F 4000 RPM

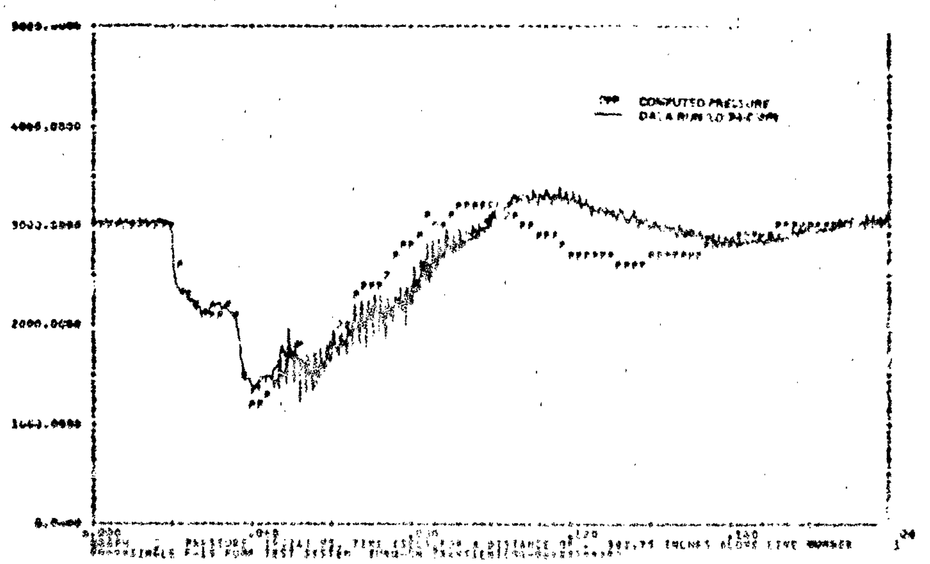

FIGURE 107. PRESSURE 378 INCHES FROM FIRST OUTLET 2-154 CIS
TURN-ON TRANSIENT 130°F 4000 RPM

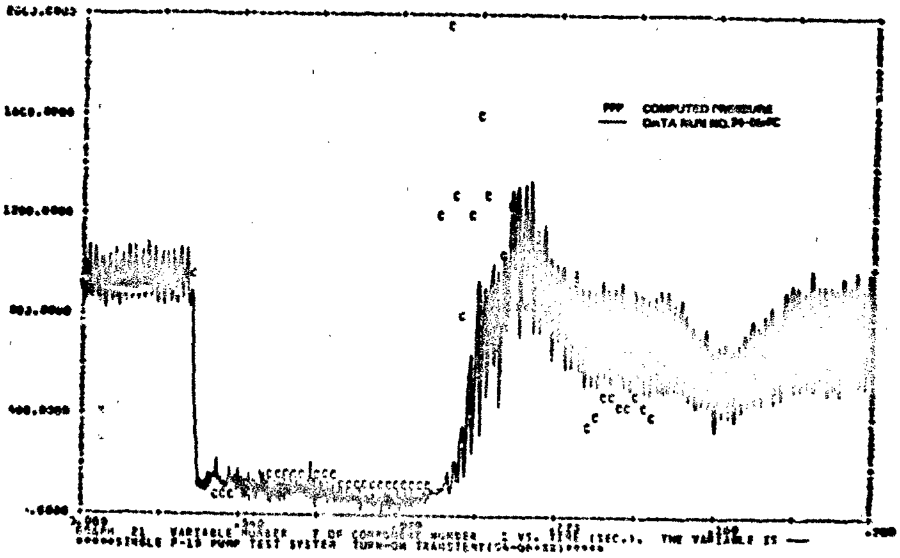


FIGURE 108. CONTROL PRESSURE 2-154 CIS TURN-ON TRANSIENT
130°F 4000 RPM

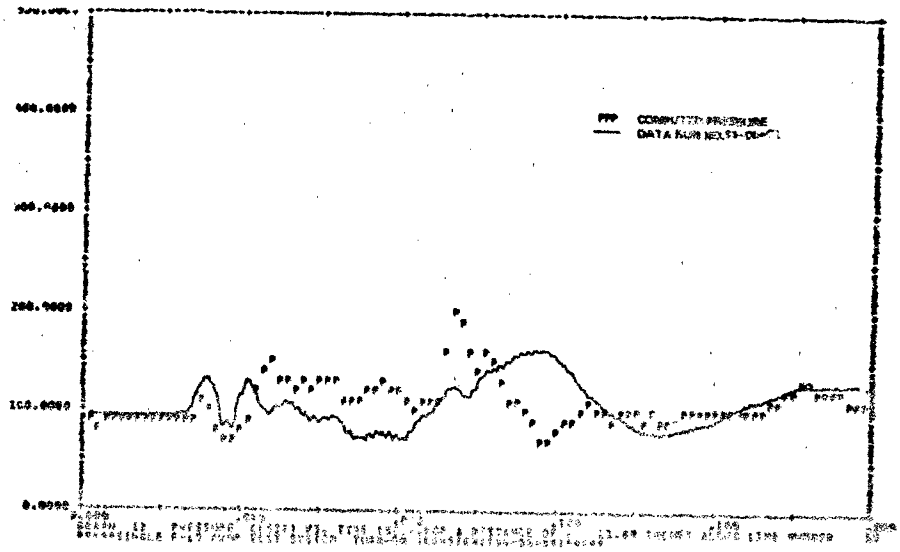


FIGURE 109. EXTERNAL CASE PRESSURE 2-154 CIS TURN-ON TRANSIENT
130°F 4000 RPM

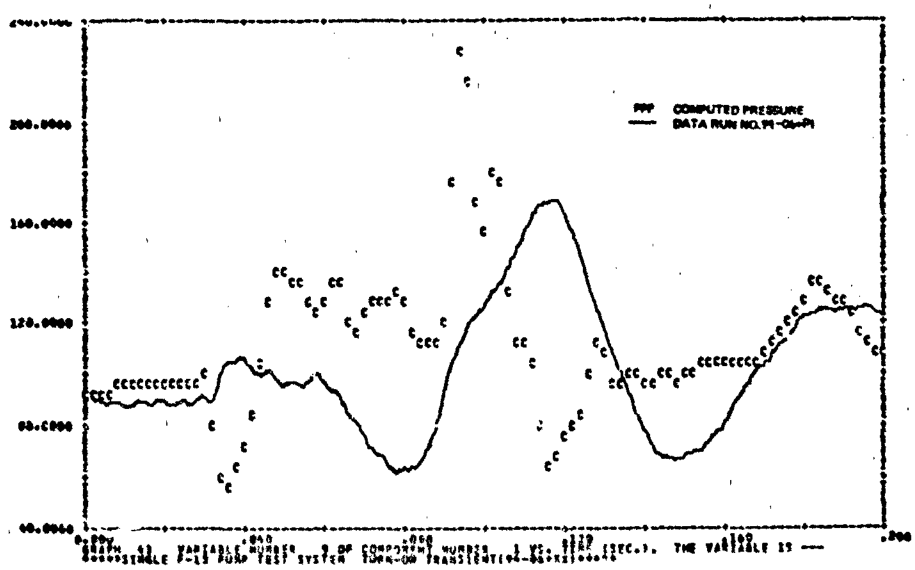


FIGURE 110. INTERNAL CASE PRESSURE 2-154 CIS TURN-ON TRANSIENT
130°F 4000 RPM

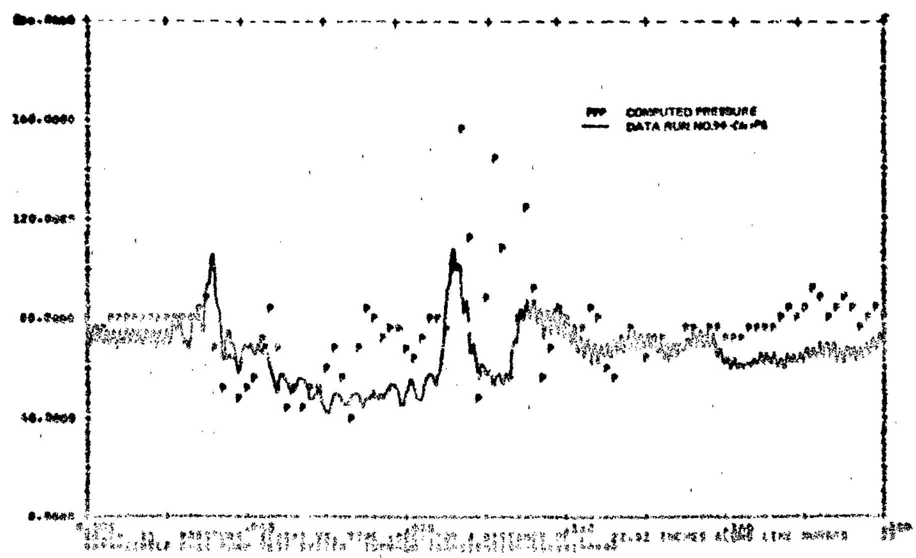


FIGURE 111. SUCTION PRESSURE 2-154 CIS TURN-ON TRANSIENT
130°F 4000 RPM

A turn-off transient with an initial pump outlet flow of 154 CIS was simulated. The pump outlet pressure measured at the P3 transducer location in Figure 95 is shown overplotted on the computer results in Figure 112. The transient valve on the simulation closed about 4 milliseconds too late, but the predicted peak pressure after turn-off is close to the measured value. The resultant phasing between the measured and computed data is incorrect. Several changes were made to the HYTRAN input data to try and correct the simulation. Altering the hanger damping term did not significantly improve the results. The test data in Figure 112 indicates that the pump response was damped. The pressure/flow energy was either absorbed by the pump to stroke the hanger to a low flow condition or the system had some unknown operating characteristics.

The transient valve used in the test was pressure opened and spring closed. Looking at the trace of valve position versus time it appeared that the poppet did bounce on closure. An attempt was made to try and simulate the poppet bounce. The HYTRAN results are shown in Figures 113, 114, 115 and 116. The computed pump outlet pressure in Figure 113 shows excellent correlation for the first 60 milliseconds of the simulation. Again the predicted pump undershoot does not correspond to the data. The transient valve does appear to cause the discrepancy. Unfortunately, on the transient valve, only the closed or open positions provide an accurate reading for the poppet location. The instrumentation was not able to measure intermediate poppet locations. However, the guessed poppet bounce characteristic did improve the simulation. The undershoot characteristics may be attributable to the pump model.

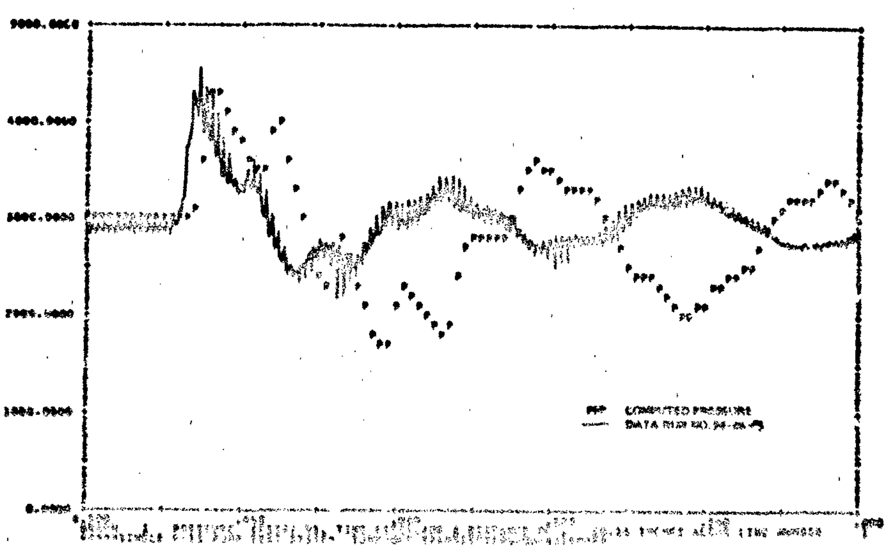

FIGURE 112. OUTLET PRESSURE 154-2 CIS TURN-OFF TRANSIENT 130°F 4000 RPM

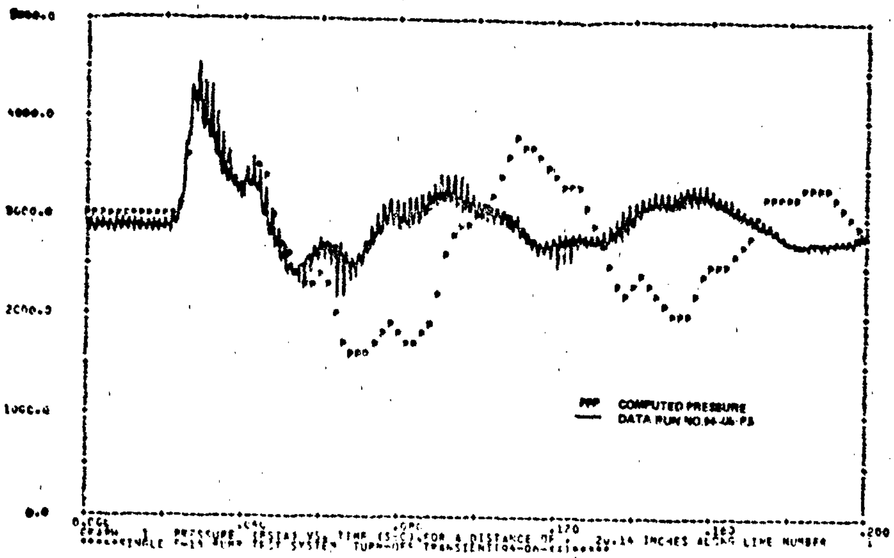


FIGURE 113. OUTLET PRESSURE 154-2 CIS TURN-OFF TRANSIENT
130°F 4000 RPM

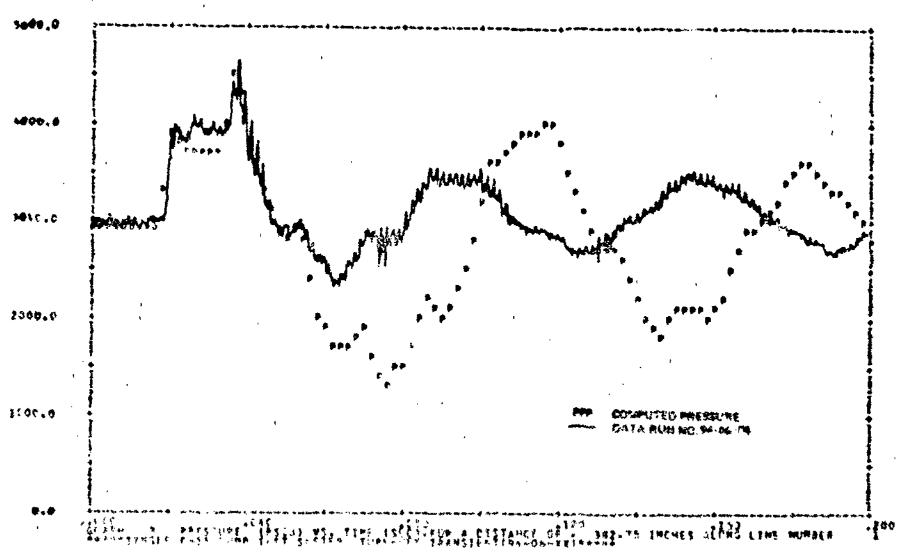


FIGURE 114. PRESSURE 378 INCHES FROM PUMP OUTLET 154-2
CIS TURN-OFF TRANSIENT
130°F 4000 RPM

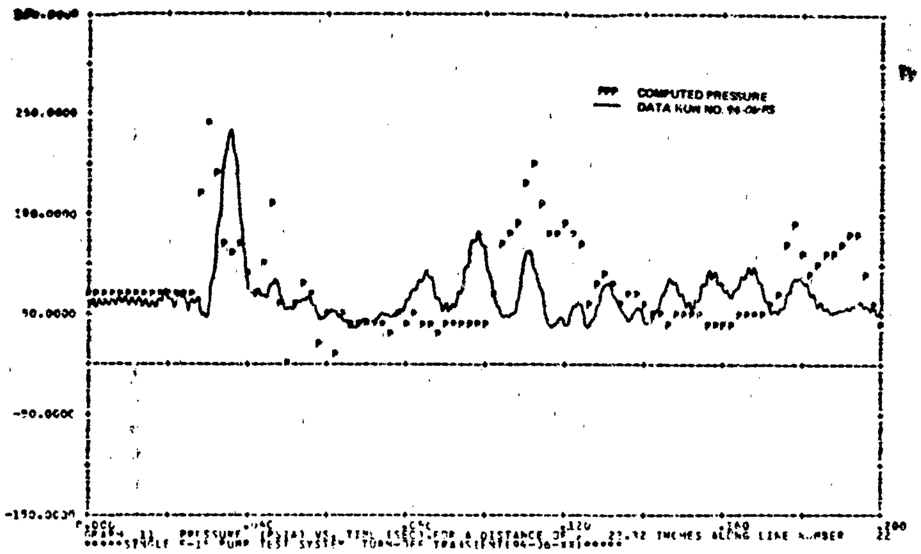


FIGURE 115. SUCTION PRESSURE 154-2 CIS TURN-OFF TRANSIENT
130°F 4000 RPM

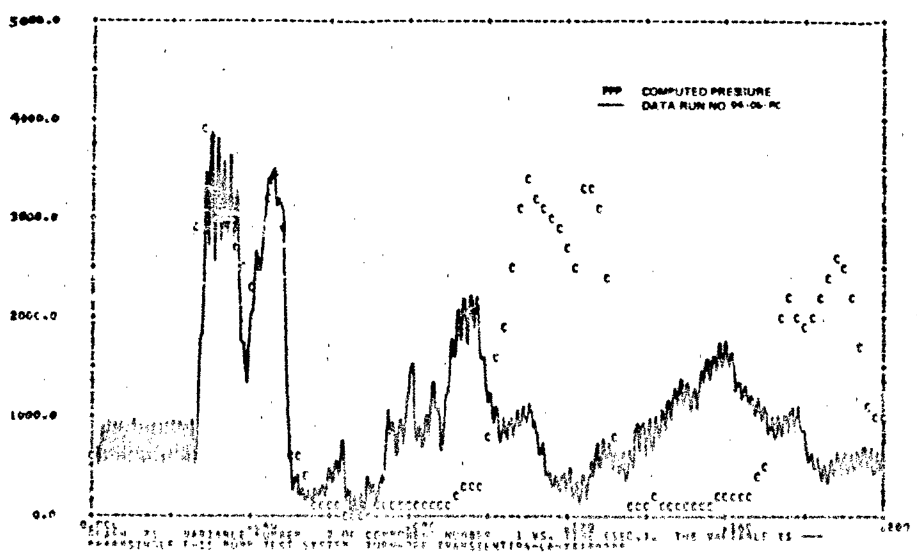


FIGURE 116. CONTROL PRESSURE 154-2 CIS TURN-OFF TRANSIENT
130°F 4000 RPM

## 4. F-15 INSTRUMENTED PUMP STEADY STATE TESTING

Steady state runs with MIL-H-5606B fluid were made of drive torque vs. drive speed, control (actuator) pressure vs. drive speed, and case drain pressure (internal and external) vs. case drain flow. The steady state test conditions are listed in Table 12. Testing was performed on the transient test bench (Figure 41.).

The drive torque vs. drive speed plots in Figures 117 thru 120 were used to compute the pump power loss (heat rejection). The ideal power was calculated as

$$\text{Power}_{\text{IDEAL}}\ (\text{PSI*CIS}) = (\text{Poutlet} - \text{Pinlet}) * Q_{\text{outlet}}$$

The torque is

$$\text{Torque (in-lbs)} = \frac{\text{Power}_{\text{IDEAL}}\ (\text{Psi * CIS})}{\text{RPM} * 2\pi/60}$$

TABLE 12

F-15 INSTRUMENTED PUMP STEADY STATE TESTING - 3000 PSI

| RUN # | TEST CONDITION | PUMP OUTLET FLOW (CIS) | PUMP INLET TEMP (°F) | RESERVOIR PRESSURE (PSIG) | COMPENSATOR SETTING (PSIG) |
|---|---|---|---|---|---|
| 1 | DT vs DS 1000 -5000 -1000 RPM SWEEP | 7.7 | 99-106-114 | 52 psig | 3040 |
| 2 | DT vs DS 1000 5000 1000 RPM SWEEP | u.0 | 99 105 115 | 48-52 | 3040 |
| 3 | DT vs DS 1000 5000 1000 RPM SWEEP | 7.7 | 209 209 211 | 48.5 | 3040 |
| 4 | DT vs DS 1000 5000 1000 RPM SWEEP | 0.0 | 208 200 203 | 47 | 3040 |
| 5 | PC vs DS 1000 5000 RPM SWEEP | 0.0 | 102 108 | 50 | 3040 |
| 6 | PC vs DS 1000 5000 1000 RPM SWEEP | 77.0 | 96 93 94 | 48 | 3040 |
| 7 | PC vs DS 1000 5000 1000 RPM SWEEP | 0.0 | 96 107 118 | 50 | 3040 |
| | | | | | 3040 |
| 8 | Pcd int. vs. Qcd @ 4000 RPM | 9.2 | 103 | 50 | 3040 |
| 9 | Pcd int. vs. Qcd @ 4000 RPM | 1.5 | 107 | 51 | 3060 |
| 10 | Pcd ext. vs Qcd @ 4000 RPM | 9.2 | 99 | 51 | 3060 |
| 11 | Pcd ext vs Qcd @ 4000 RPM | 1.5 | 106 | 51 | 3040 |
| 12 | Pcd int. and Pcd ext. vs. Qcd @ 4000 RPM | 9.2 | 97 | 51 | 3040 |
| 13 | Pcd int. and Pcd ext. vs. Qcd @ 4000 RPM | 1.5 | 103 | 51 | 3040 |
| 14 | Pcd int. and Pcd ext. vs. Qcd @ 4000 RPM | 77 | 97 | 51 | 3040 |
| 15 | Pcd int. and Pcd ext. vs. Qcd @ 4000 RPM | 7.7 | 100 | 48 | 3040 |
| 16 | Pcd int. and Pcd ext. vs. Qcd @ 4000 RPM | 1.0 | 99 | 50 | 3040 |
| 17 | Pcd int. and Pcd ext. vs. Qcd @ 4000 RPM | 77 | 204 | 52 | 3040 |
| 18 | Pcd int. and Pcd ext. vs. Qcd @ 3000 RPM | 7.7 | 195 | 50 | 30-0 |
| 19 | Pcd int and Pcd ext. vs. Qcd @ 3000 RPM | 1.0 | 195 | 49 | 3040 |
| 20 | Pcd int. and Pcd ext. vs. Qcd @ 4000 RPM | 1.0 | 202 | 48 | 3040 |
| 22 | Pcd int. and Pcd ext. vs. Qcd @ 4000 RPM | 7.7 | 203 | 51 | 3060 |
| 22 | Pcd int. and Pcd ext. vs. Qcd @ 4000 RPM | 7.7 | 98 | 51.5 | 3060 |
| 23 | Pcd int. and Pcd ext. vs. Qcd @ 4000 RPM | 1.0 | 112 | 50.5 | 2940 |
| 24 | Pcd int. and Pcd ext. vs. Qcd @ 4000 RPM | 7.7 | 200 | 57.0 | 2940 |
| 25 | Pcd int. and Pcd ext. vs. Qcd @ 4000 RPM | 1.0 | 197 | 56. | 2940 |
| | | | | | 2940 |

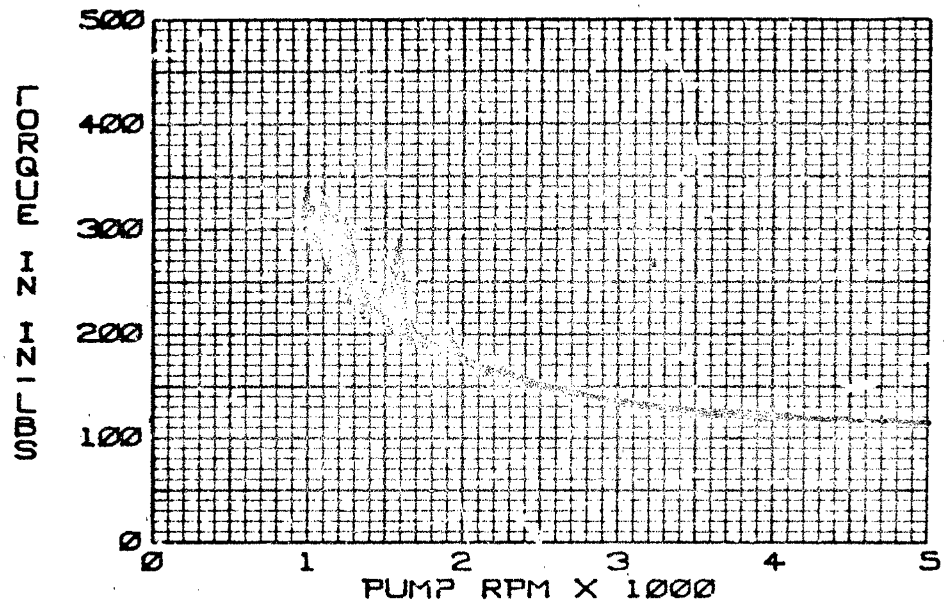


FIGURE 117. F-15 HYDRAULIC PUMP RUN #1 9 DEC 77
7.7 CIS 100°F

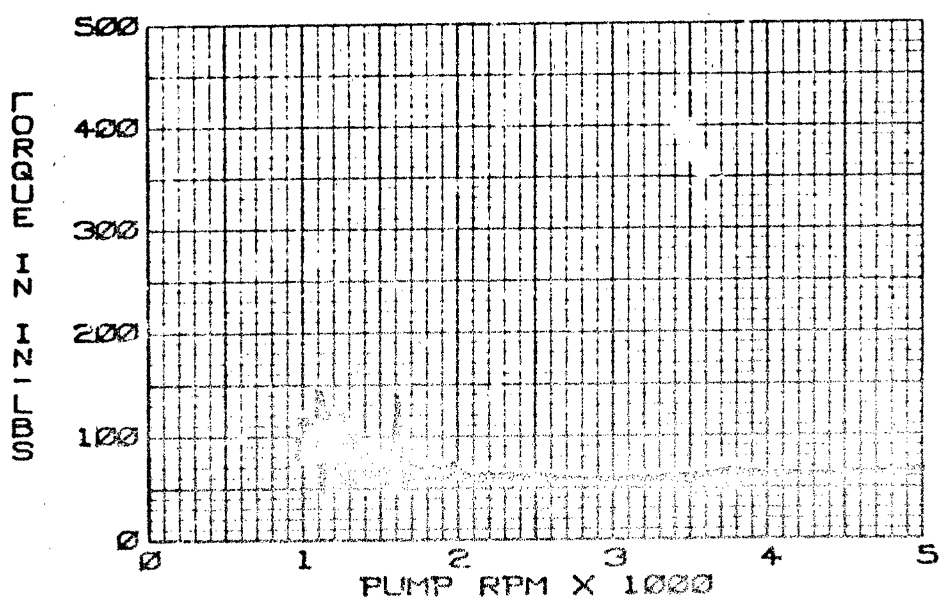


FIGURE 118. F-15 HYDRAULIC PUMP RUN #2 9 DEC 77
0 FLOW 100°F

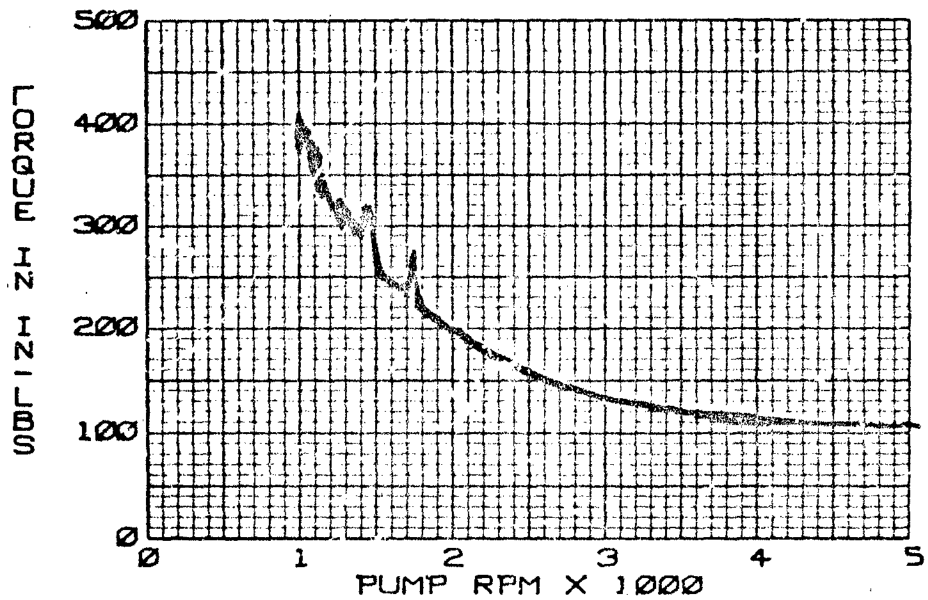


FIGURE 119. F-15 HYDRAULIC PUMP RUN #3 12 DEC 77
7.7 CIS 210°F

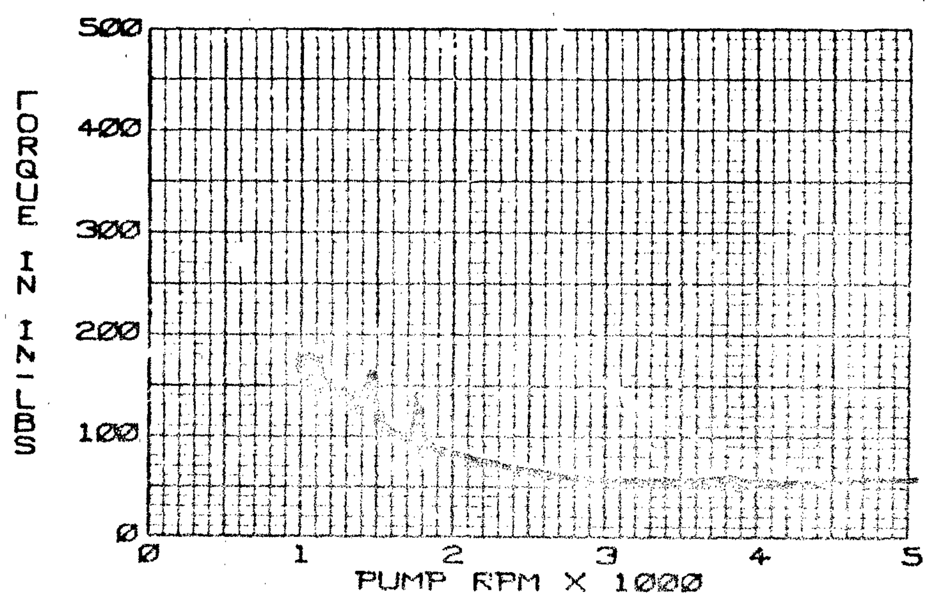


FIGURE 120. F-15 HYDRAULIC PUMP RUN #4 12 DEC 77
0 FLOW 200°F

The power loss is the difference between the ideal and measured values. The results are plotted in Figure 121. The heat rejection characteristics were similar to the original pump data. (3.8 HP @ 4560rpm ,200°F ,0 0 CIS outlet flow)

Figures 122, 123 and 124 show plots of pump actuator pressure versus drive RPM. The pressure spike at 1620 RPM in all three plots corresponds to a mechanical resonant condition of the compensator spool.

Plots of case drain pressure vs case flow were made for the conditions in Table 12. Some of the steady state plots are shown in Figures 125 thru 130.

The steady state pump tests still show an instability in the case drain pressure vs flow graphs at the low pump outlet flows. The instability occurs transiently as the flow control value in the case drain line is adjusted. Any looping effect results from the inability of the plotting device to adequately respond to the pressure signal. The origin of this anomaly in the pump is not known.

The 3000 psi steady state tests indicate a slight increase in the case drain flow from the previous testing. The increase may be attributable to the lack of a leakage path provided by the "wiped" port plate on the original pump.

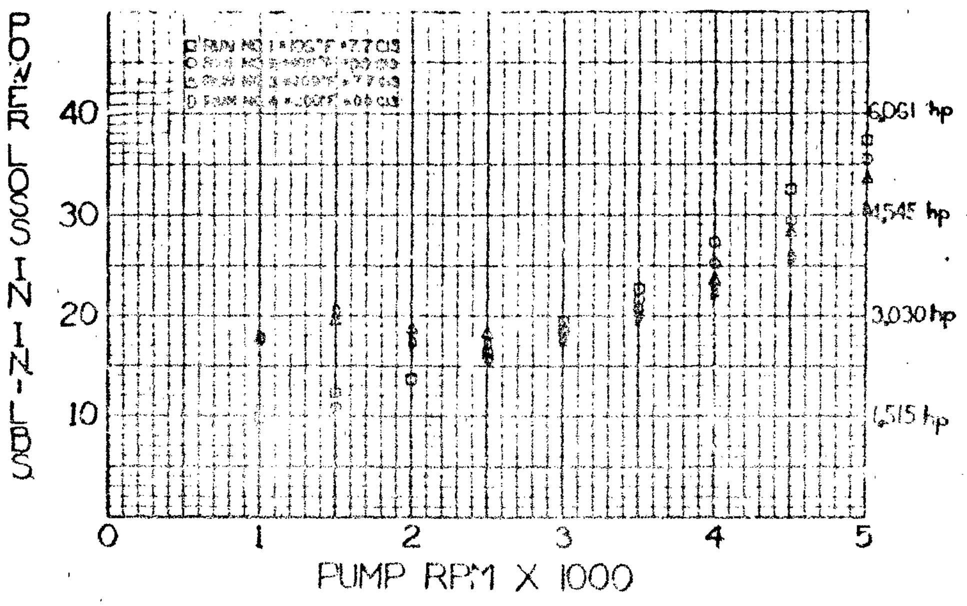


FIGURE 121. POWER LOSS FOR RUNS 1-4

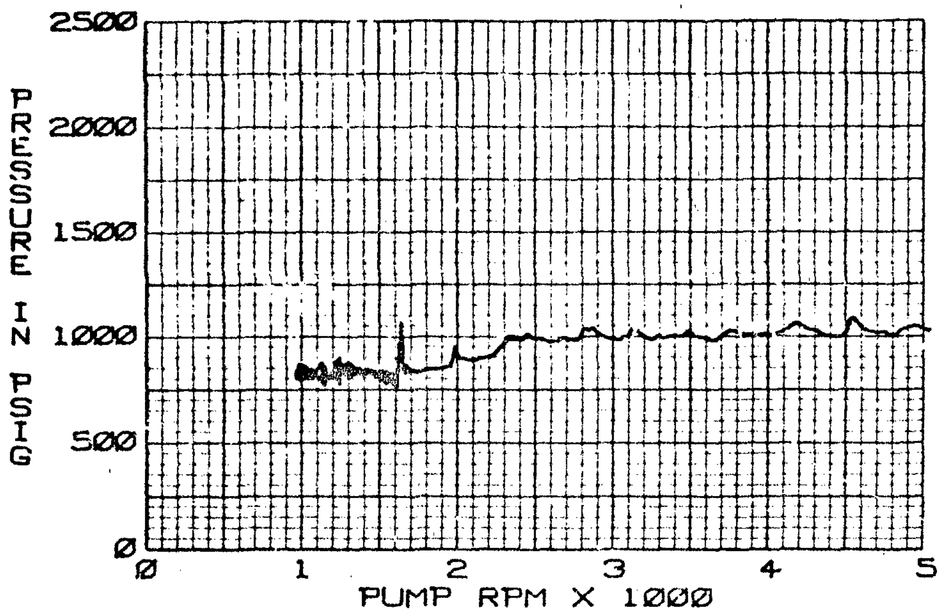


FIGURE 122. F-15 HYDRAULIC PUMP RUN #5 PC VS. PS 12 DEC 77
0 FLOW 100°F

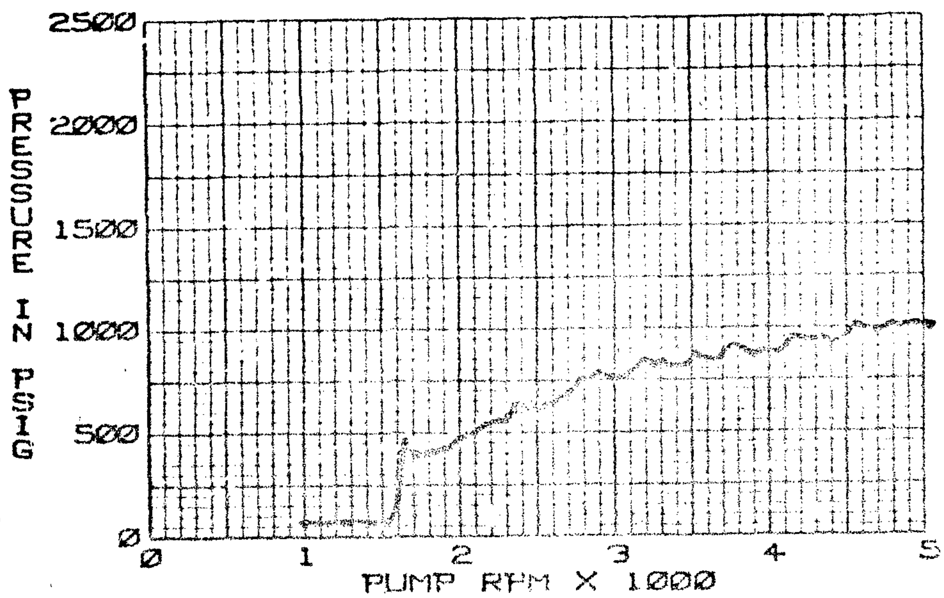


FIGURE 123. F-15 HYDRAULIC PUMP RUN #6 PC VS. PS 12 DEC 77
77 CIS 100°F

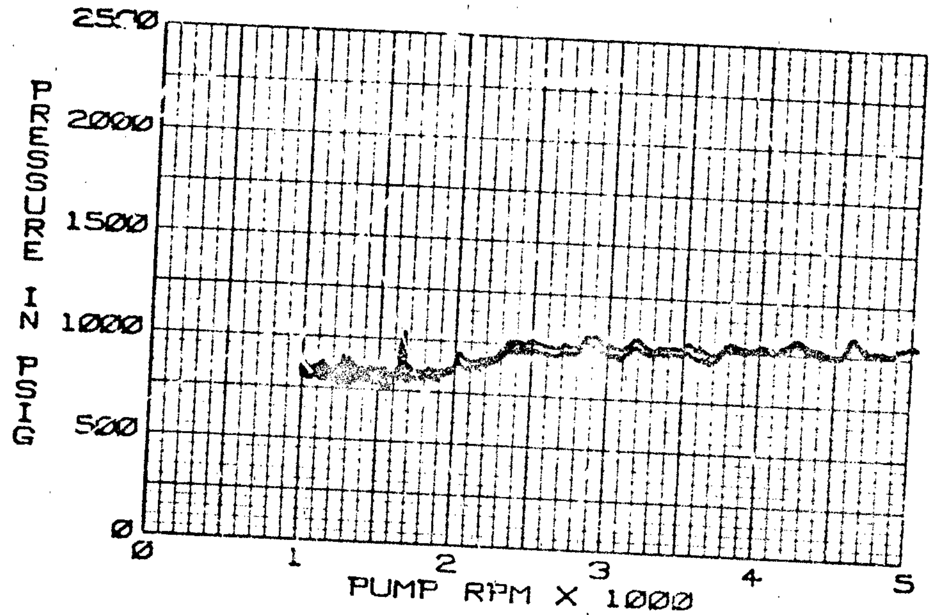


FIGURE 124. F-15 HYDRAULIC PUMP RUN #7 PC VS. PS 12 DEC 77
0 FLOW 100°F

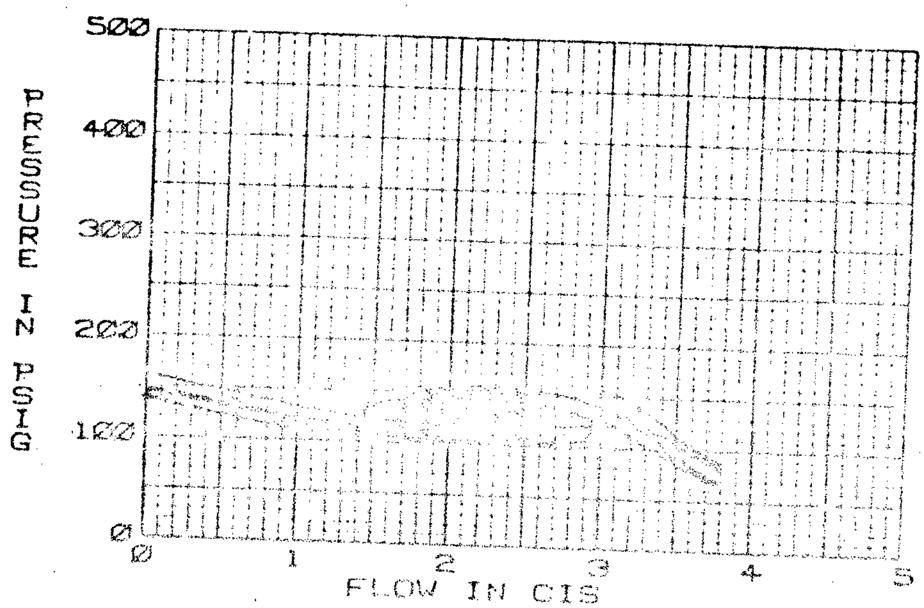


FIGURE 125. F-15 HYDRAULIC PUMP RUN #13 PCD INT. AND PCD EXT.
VS. QCD 1.5 CIS 100°F

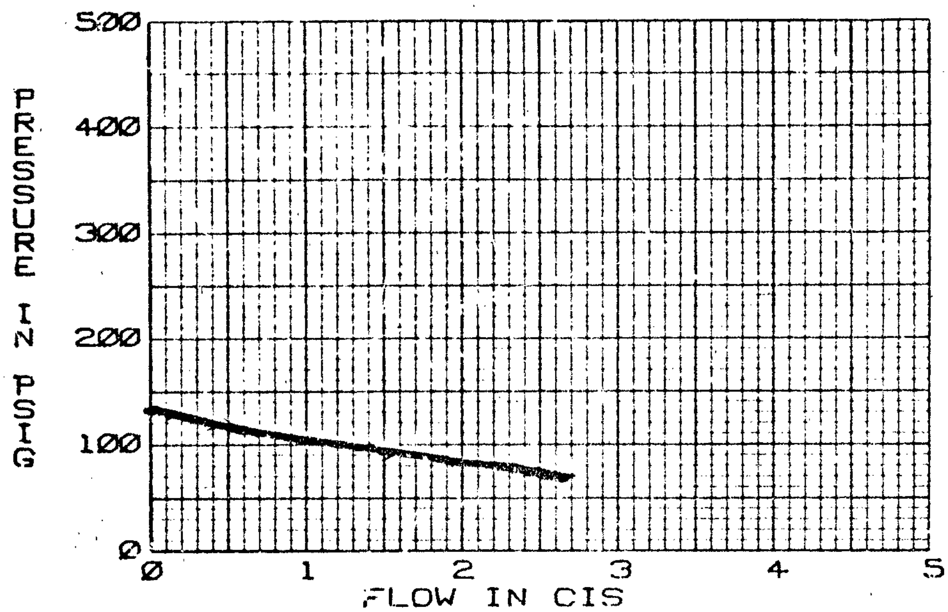


FIGURE 126. F-15 HYDRAULIC PUMP RUN #14 PCD INT. AND PCD EXT. VS. QCD 77 CIS 100°F

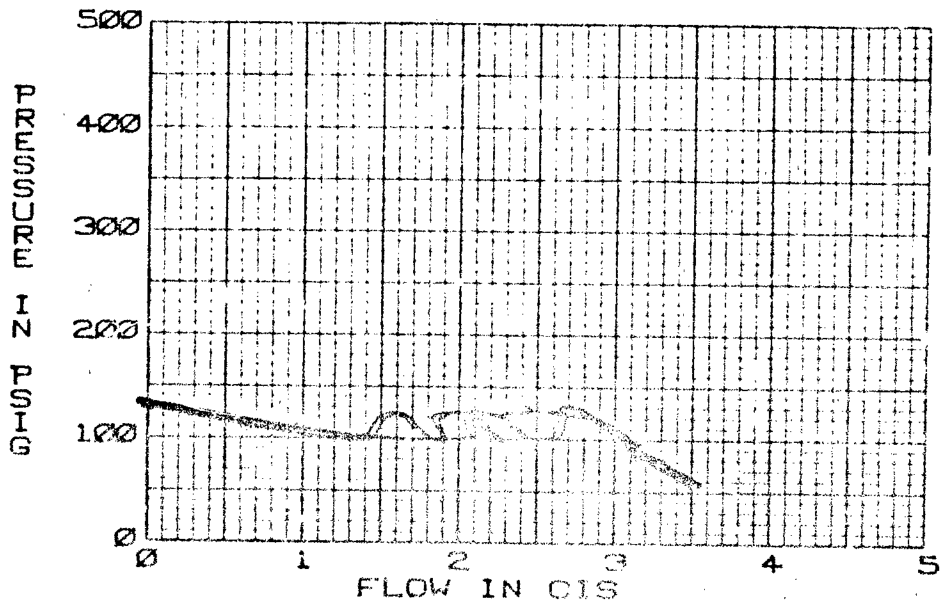


FIGURE 127. F-15 HYDRAULIC PUMP RUN #15 PCD INT. AND PCD EXT. VS. QCD 7.7 CIS 100°F

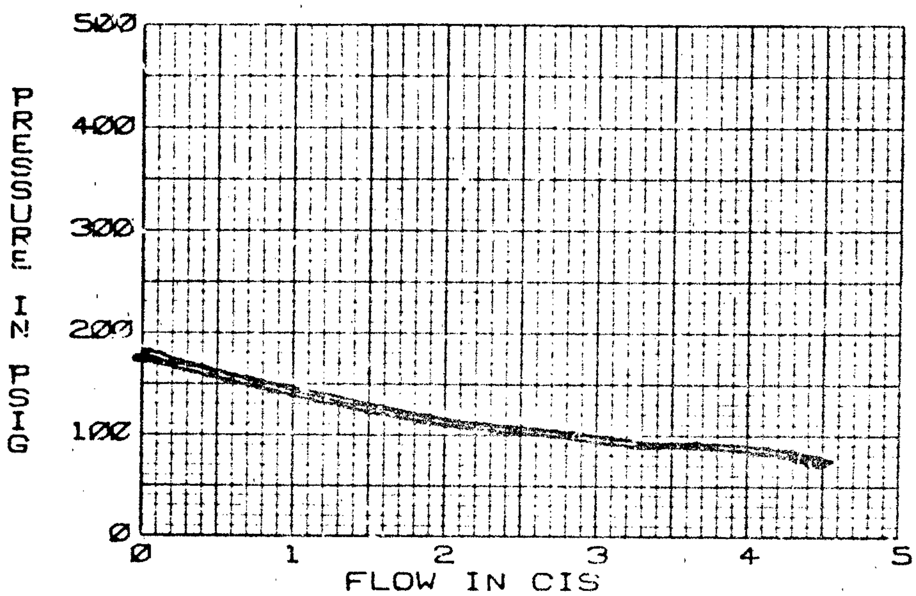


FIGURE 128. F-15 HYDRAULIC PUMP RUN #17 PCD INT. AND PCD EXT. VS. QCD 77 CIS 200°F

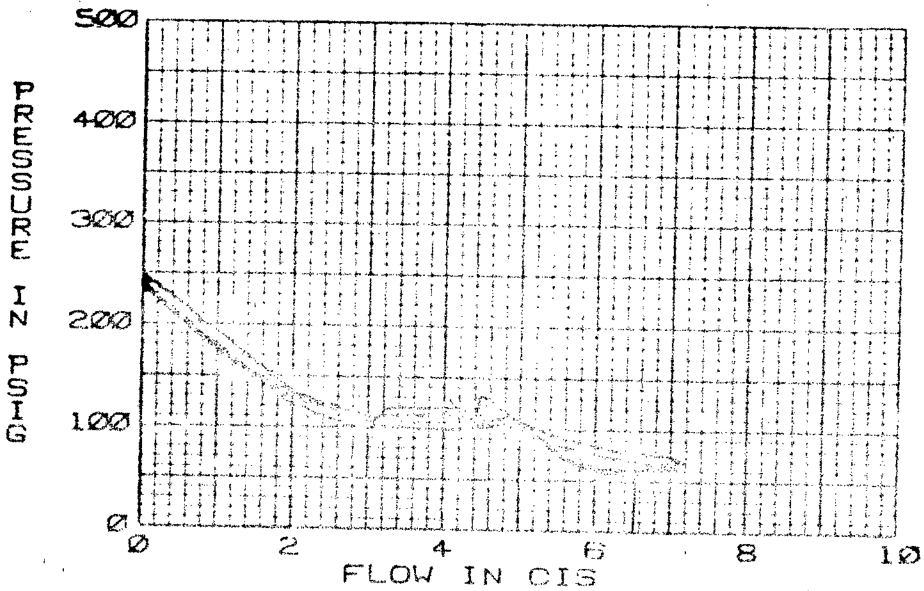


FIGURE 129. F-15 HYDRAULIC PUMP RUN #20 PCD INT. AND PCD EXT. VS. QCD 1 CIS 200°F

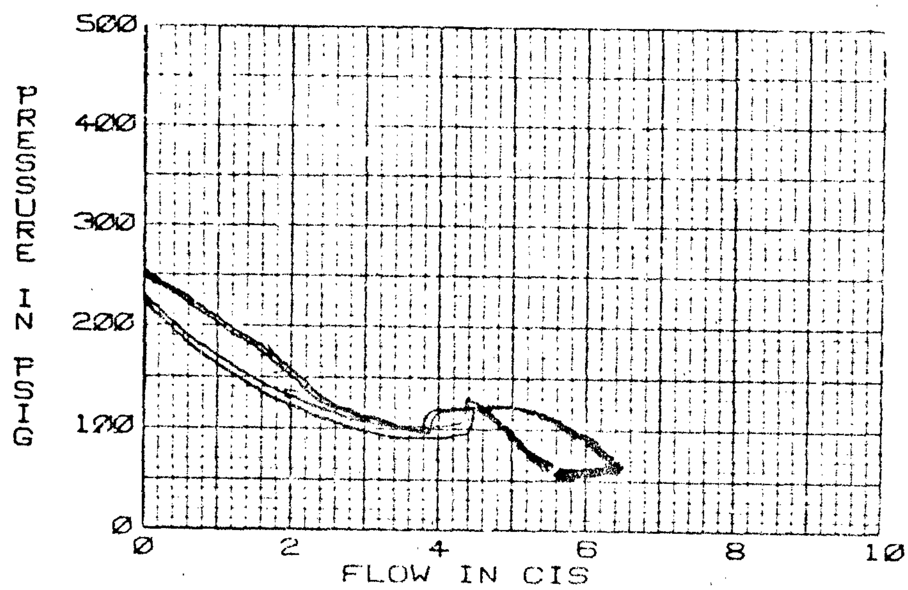


FIGURE 130. F-15 HYDRAULIC PUMP RUN #21 PCD INT. AND PCD EXT. VS. QCD 7.7 CIS 200°F

The steady state test series was repeated with the pump compensator set at 4435 psig. A listing of the test runs is shown in Table 13. Plots of drive torque vs. drive speed are shown in Figures 131, 132, 133 and 134. They show the instability of the pump through most of the sweep range. The plot of actuator pressure vs drive speed in Figure 135 shows that the compensator is fairly stable when the pump outlet flow of 77.0 CIS. Instabilities occur at 1900, 2350, 2700, and 3750 RPM. At a lower flow setting in Figure 136 the rattling is prevalent throughout the sweep range.

TABLE 13

F-15 INSTRUMENTED PUMP STEADY STATE TESTING - 4400 PSI

| RUN # | TEST CONDITION | PUMP OUTLET FLOW (CIS) | PUMP INLET TEMP (°F) | RESERVOIR PRESSURE (PSIG) | COMPENSATOR SETTING (PSIG) |
|---|---|---|---|---|---|
| 1 | DT vs DS 1000-5500 RPM | 0.0 | 100 133 | 53 | 4435 |
| 2 | DT vs DS 1000-4500 | 7.7 | 93 99 | 53 | 4435 |
| 3 | DT vs DS 1000-4500 | 0.0 | 196 21[illegible] | 53 | 4435 |
| 4 | DT vs DS 1000-3500 | 7.7 | 190 175 | 53 | 4435 |
| 5 | PC vs DS 1000-4500 | 77.0 | 100 97 | 52.5 | 4435 |
| 6 | PC vs DS 1000-4500 | 0.0 | 96 126 | 50 | 4435 |
| 7 | Pcd int. and Pcd ext. vs Qcd @ [illegible] RPM | 4.2 | [illegible] | 50 | 4435 |
| 8 | Pcd int. and Pcd ext. vs Qcd @ [illegible] RPM | 77 | 10[illegible] | 52 | 4435 |
| 9 | Pcd int. and Pcd ext. vs Qcd @ [illegible] RPM | 77 | 101 | 50.[illegible] | 4435 |
| 10 | Pcd int. and Pcd ext. vs Qcd @ [illegible] RPM | 4.2 | 93 102 | 52.5 | 4435 |
| 11 | Pcd int. and Pcd ext. vs Qcd @ [illegible] RPM | 77 | 19[illegible] 220 | 53 | 4435 |
| 12 | Pcd int. and Pcd ext. vs Qcd @ [illegible] RPM | 4.2 | 18[illegible] 183 | 50 | 4435 |
| 13 | Pcd int. and Pcd ext. vs Qcd @ [illegible] RPM | 77 | 199 [illegible] | 52 | 4435 |
| 14 | Pcd int. and Pcd ext. vs Qcd @ [illegible] RPM | 4.2 | [illegible] | - | 4435 |

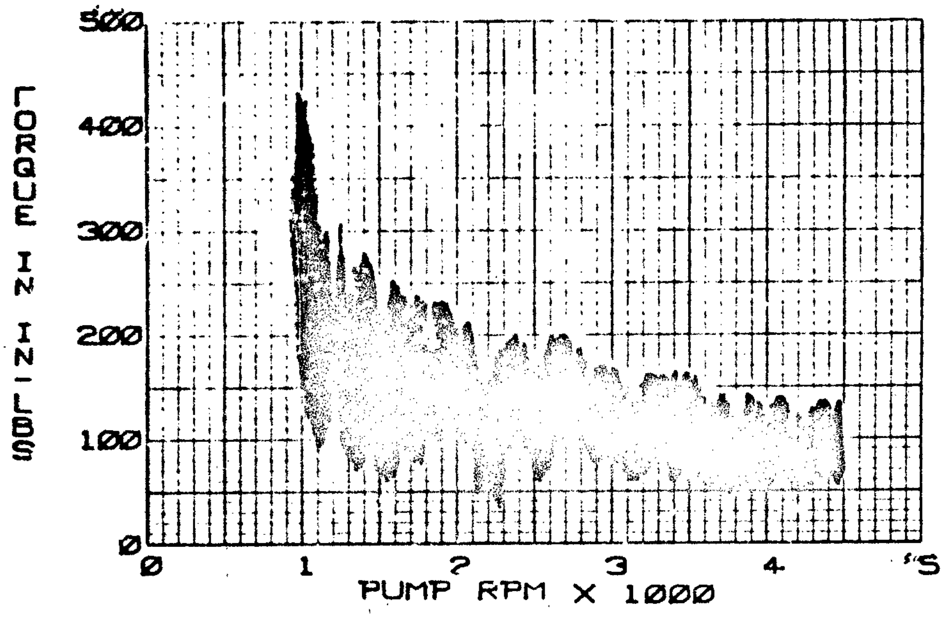


FIGURE 131. F-15 HYDRAULIC PUMP RUN #1 DT VS DS
5 CIS 100°-130°F

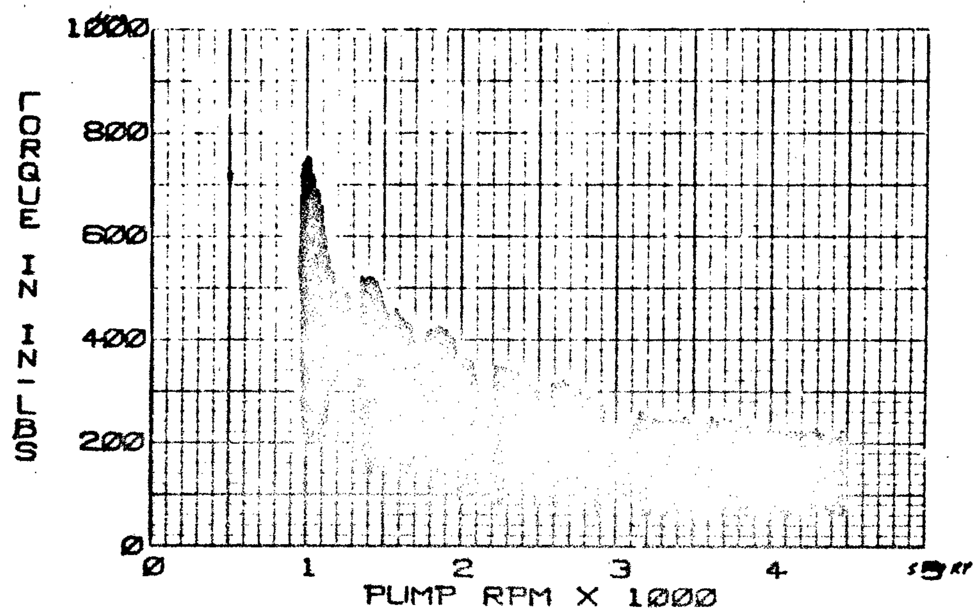


FIGURE 132. F-15 HYDRAULIC PUMP RUN #2 DT VS DS
7.7 CIS 93°-90°F

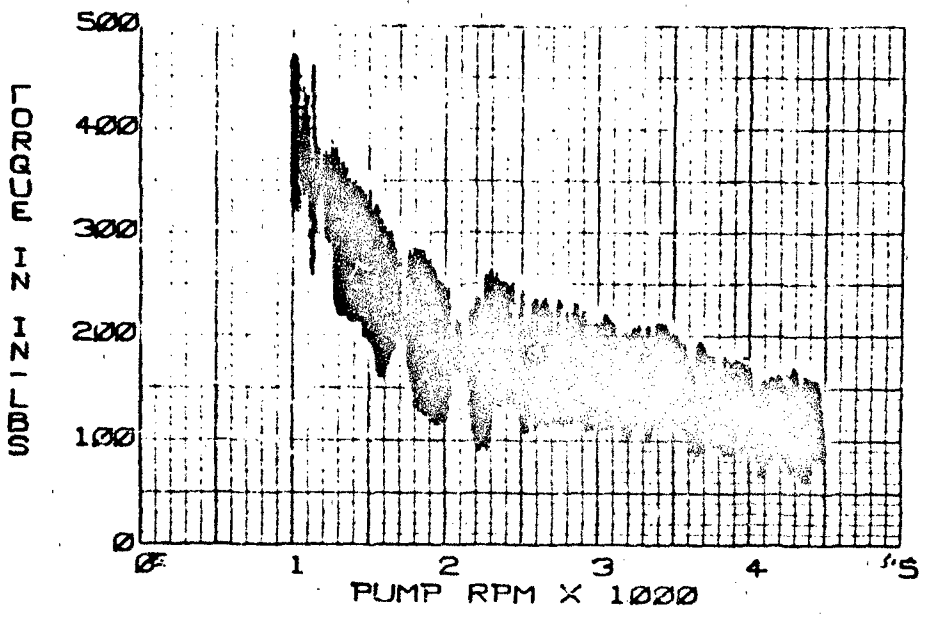


FIGURE 133. F-15 HYDRAULIC PUMP RUN #3 DT VS. DS
0.0 CIS 184-212°F

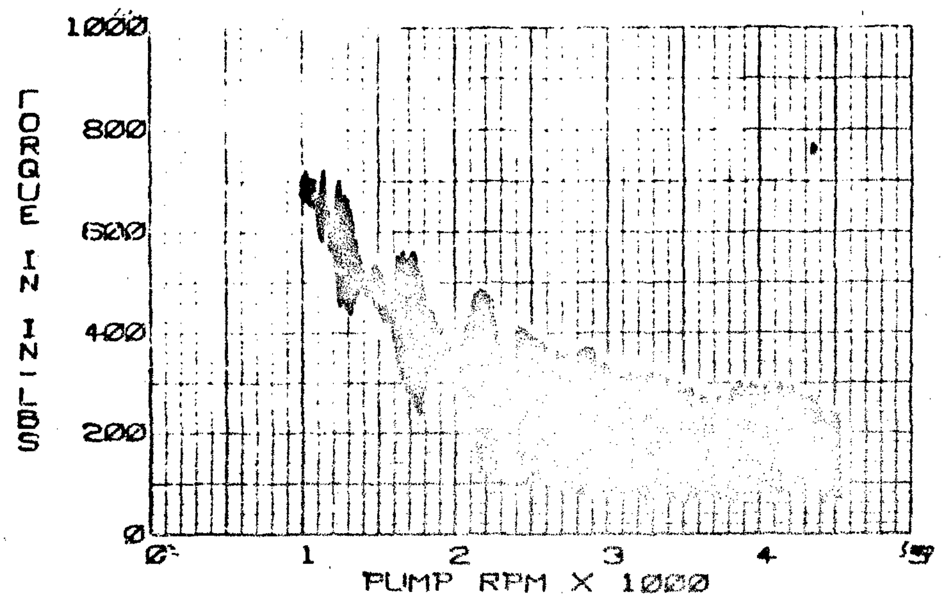


FIGURE 134. F-15 HYDRAULIC PUMP RUN #4 DT VS. DS
7.7 CIS 190°-[illegible]75°F

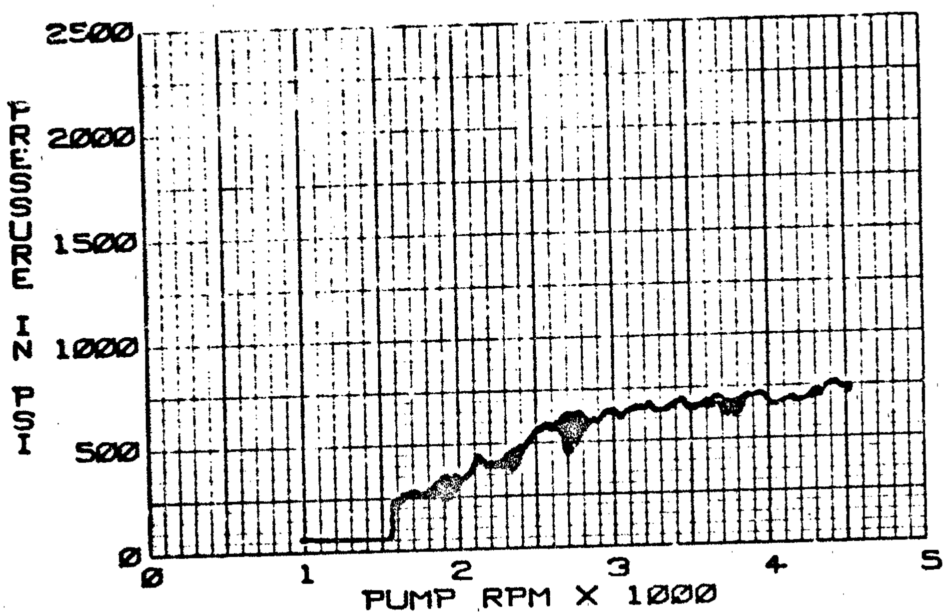


FIGURE 135. F-15 HYDRAULIC PUMP RUN #5 PC VS DS
77 CIS 100°-97°F

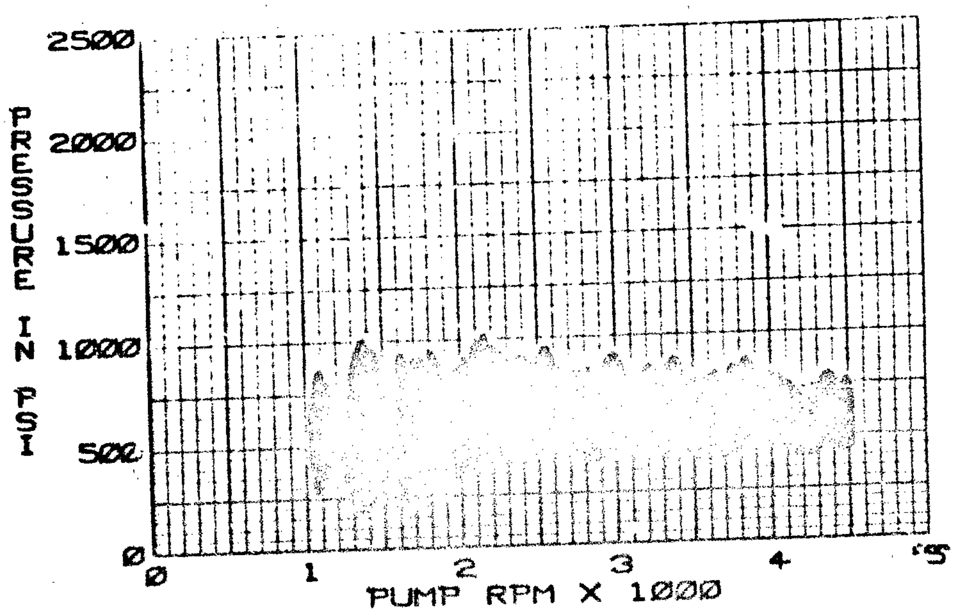


FIGURE 136. F-15 HYDRAULIC PUMP RUN #6 PC VS DS
0.0 CIS 96°-126°F

Plots of case drain pressure versus case flow are shown in Figures 137 thru 140 for the high compensator setting. As the case flow is changed the pressure instability still exists.

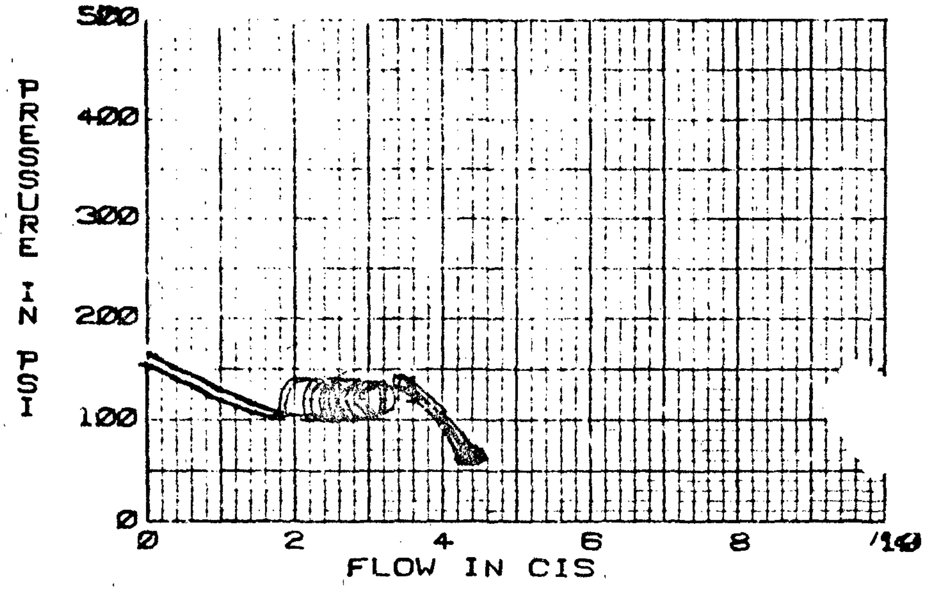


FIGURE 137. F-15 HYDRAULIC PUMP RUN #7 PCD VS QCD
4.2 CIS 105°F

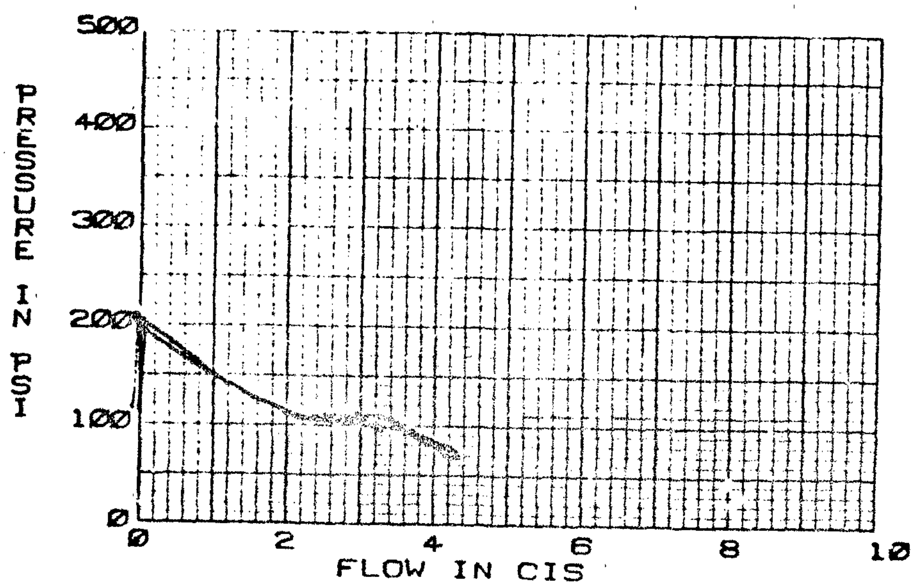


FIGURE 138. F-15 HYDRAULIC PUMP RUN #8 PCD INT. AND PCD EXT. VS QCD 77 CIS 102°F

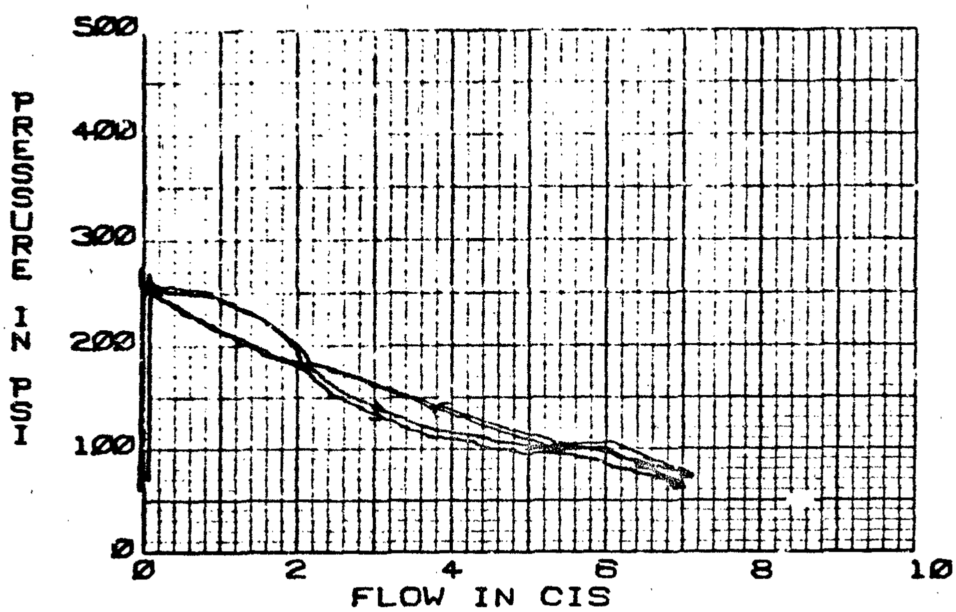


FIGURE 139. F-15 HYDRAULIC PUMP RUN #11 PCD INT. AND PCD EXT. VS QCD 77 CIS 193°-220°F

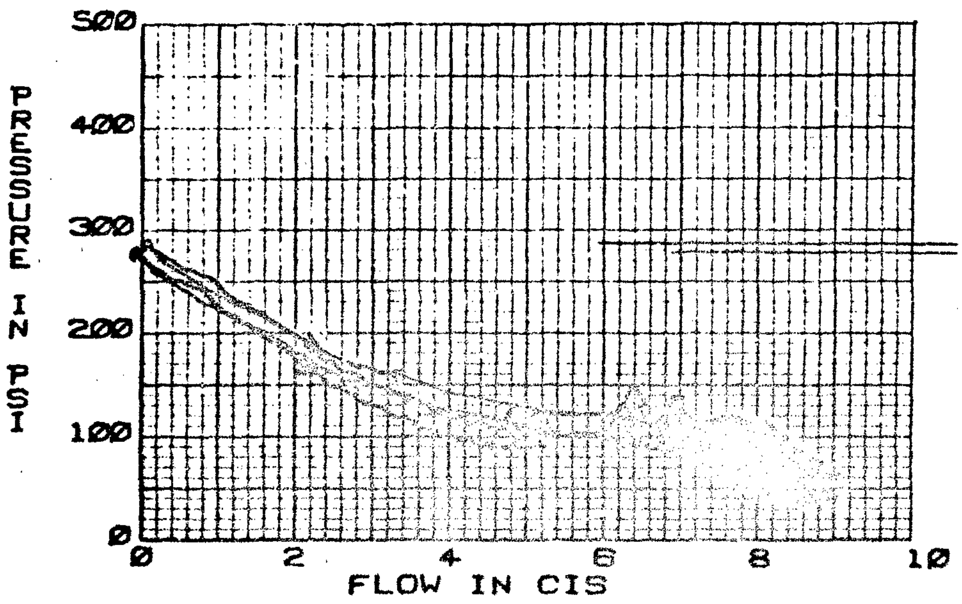


FIGURE 140. F-15 HYDRAULIC PUMP RUN #12 PCD INT. AND PCD EXT. VS QCD 4.2 CIS 183°-185°F

SECTION IV

VANE PUMP MODEL DEVELOPMENT AND VERIFICATION

Models of a variable volume vane pump were developed for the frequency (HSFR) and transient (HYTRAN) computer programs. The main fuel pump on the F-100 turbojet engine consists of a variable volume vane stage and a centrifugal boost stage. The pump was designed by Chandler Evans Inc., Controls Systems Division (CECO). A specially instrumented vane stage unit was supplied by CECO for computer model test verification. The boost stage was replaced with a plate which contained inlet and lubrication supply ports. The pump was tested with (MIL-H-5606B) hydraulic oil in order to make use of the existing verification test and test data processing facility at MCAIR. MIL-H-5606B is slightly more dense and viscous than the normal pump fluid media, JP-4 engine fuel.

1. VANE PUMP HSFR MODEL DEVELOPMENT AND VERIFICATION

a. HSFR Model

A frequency domain model of the vane pump was developed for use with the HSFR program. The model is similar to the existing piston pump model contained in References 2 and 3 HSFR program user and technical description manuals. User and technical description manual material for the vane pump model are contained in Appendix E.

b. HSFR Verification Test Set-Up and Procedure

Figure 141 is a schematic of the test set-up used for measurement of vane pump pressure pulsations. The test circuit plumbing size and length simulated the actual installation on the F-100 engine for the pump to metering valve flow and sensing lines. The throttle operated main fuel metering valve is an integral part of the engine unified controller unit. A ball valve was used to simulate the metering function. The pump control varies outlet flow to maintain a 60 psi drop across the metering valve. Downstream valves were used to create circuit back pressures (300-900 psig) similar to that of the actual system. Reservoir (F-4 hydraulic) bootstrap pressure was independently controllable so that pump suction pressure could be varied. The vane stage pump inlet pressure was maintained at the maximum reservoir capability (55-64 psig) during all tests except for runs made at 35 - 42 psig. Vane stage inlet pressure from the boost stage is normally about 120 psig.

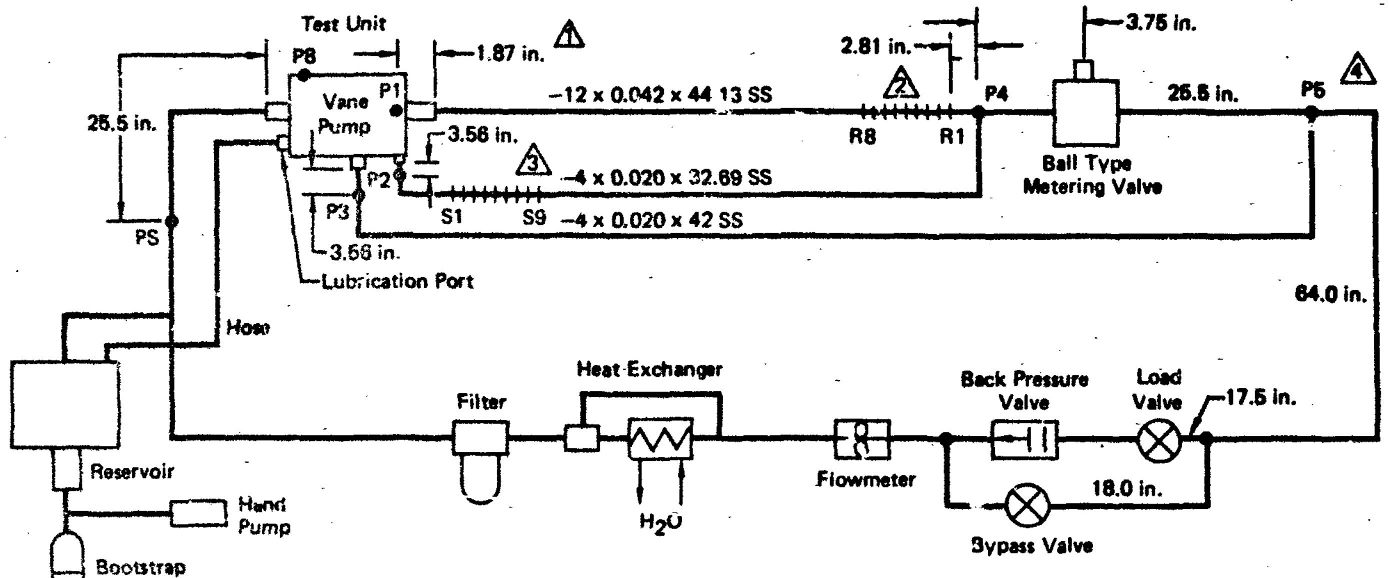


1. Length in inches (typical)
2. Roving transducer locations in 2 in. increments (R1 to R8)
3. Roving transducer locations in 2 in. increments (S1 to S9)
4. Fixed transducer locations (typical)

**FIGURE 141**
**CECO VANE PUMP**
HSFR Test Schematic

The vane pump was driven by a direct drive 200 hp AC electric motor with variable frequency speed control up to 7000 rpm. A 5/1 speed increaser loaned to MCAIR by CECO provided the proper drive interface to the vane pump whose rated speed is 15,000 rpm.

Pump pulsations were mapped in the outlet and upstream control lines with a roving Kistler transducer. Pump outlet maximum flow rates were set at 8, 20, and 30 gpm to vary the internal timing of the pump outlet flow porting. Pressure pulsation amplitudes were recorded for total and harmonic responses as the pump speed was swept from 5000 to 15000 rpm. The pump remained on full stroke until a speed was achieved where pump capacity exceeded the metering valve flow setting. Two levels of air content (2% and 17%) were tested to check the effect of dissolved air on pump outlet pulsations.

c. Test Run Summary

Table 14 presents a summary of test runs and test conditions for the vane pump frequency tests. Pump inlet oil temperatures were from 115° to 135°F during all tests.

d. Test Results and Discussion

Typical test results are presented herein. Test data for all runs are on file at MCAIR. Figure 142 compares total pressures at the pump outlet port (P1) for maximum outlet flows of 8, 20, and 30 gpm. Pulsations increase in amplitude with decreasing flow. This is as expected since the pump is apparently timed for minimum pulsations at higher flow rates. This accounts for the characteristic of increasing pulsation amplitudes as speed increases at a constant outlet flow rate. Total pulsations at the outlet port reach a maximum of 210 psi peak-peak (p-p) at 14,000-14,500 rpm. Figures 143, 144 and 145 show harmonic analysis of the outlet port pressure pulsations (P1) at 8 gpm. The fundamental pumping frequency (Figure 143 contains most of the pulsation energy, i.e. 98 psi peak or 196 psi p-p at 14,000 rpm. The fundamental pumping frequency is 4000 hz at 15000 rpm. Second and third harmonic pulsations (Figures 144 and 145) exhibit very low amplitudes, <20 psi p-p.

## TABLE 14. VANE PUMP TEST SUMMARY

| RUN NUMBER | OUTLET PRESSURE (PSIG) | RESERVOIR PRESSURE (PSIC) | OUTLET FLOW (GPM) | HARMONIC NUMBER | DISSOLVED AIR (% BY VOLUME) |
|---|---|---|---|---|---|
| 97-1A-P8 | 319 | 64 | 8 | 1 | 1 |
| -P5 | | | | | |
| -P1 | 343 | 43 | | 1-3 | 1 |
| -P4 | 358 | 62 | | 2 | 1 |
| -P2 | 360 | 63 | | 1-2 | [illegible] |
| -R6 | 360 | 63 | | 1 | 2 |
| -R8 | | | | | |
| -R7 | | | | | |
| -R5 | | | | | |
| -R4 | | | | | |
| -R3 | | 64 | | | |
| -R2 | | | | | |
| -R1 | | | | | |
| 97-1A-P1A | 361 | 62 | 8 | 1-3 | 17 |
| -P2A | | | | 1-2 | |
| -P4A | | | | 1 | |
| 97-1A-R1A | 362 | 62 | 8 | 1 | 17 |
| -R2A | | | | | |
| -R3A | | | | | |
| -R4A | | | | | |
| -R5A | | | | | |
| -R6A | | | | | |
| -R7A | | | | | |
| -R8A | | | | | |
| 97-1A-S1 | 361 | 62 | 8 | 1 | 2 |
| -S2 | | | | | |
| -S3 | | | | | |
| -S3 | | | 30(max.) | | |
| -S4 | | | | | |
| -S5 | | | | | |
| -S6 | | | | | |
| -S7 | | | | | |
| -S8 | | | | | |
| -S9 | | | | | |
| 97-1B-P8 | 297 | 44 | 8 | 1 | 1 |
| -P5 | | | | | |
| 97-2A-P4 | 460@15K | 56@15K | 20@15K | 1-5 | [illegible] |
| -P1 | 438@5K | 50@5K | 18@5K | | |
| -R8 | | | | 1 | 2 |
| -R7 | | | | | |
| -R6 | | | | | |
| -R5 | | | | | |
| -R4 | | | | | |
| -R3 | | | | | |
| -R2 | | | | | |
| -R1 | | | | | |
| 97-3A-P1 | 600@15K | 60@15K | 30@15K | 1-5 | 2 |
| -P2 | 440@5K | 55@5K | 18@5K | | |
| -P4 | | | | | |
| -P3 | | | | | 1.5 |
| -P5 | | | | | 1.5 |
| 97-3A-R1 | 615@15K | 60@15K | 30@15K | 1-2 | .5 |
| | 410@5K | 55@5K | 18@5K | | |
| -R2 | | | | 1 | .5 |
| -R3 | | | | | |
| -R4 | | | | | |
| -R5 | | | | | |
| -R6 | | | | | |
| -R7 | | | | 1-2 | |
| -R8 | | | | 1 | |
| 97-3B-P1 | 615@15K | 42@15K | 30@15K | 1 | .6 |
| -P2 | 393@5K | 35@5K | 19@5K | 1-4 | |
| -P4 | | | | 1-4 | |

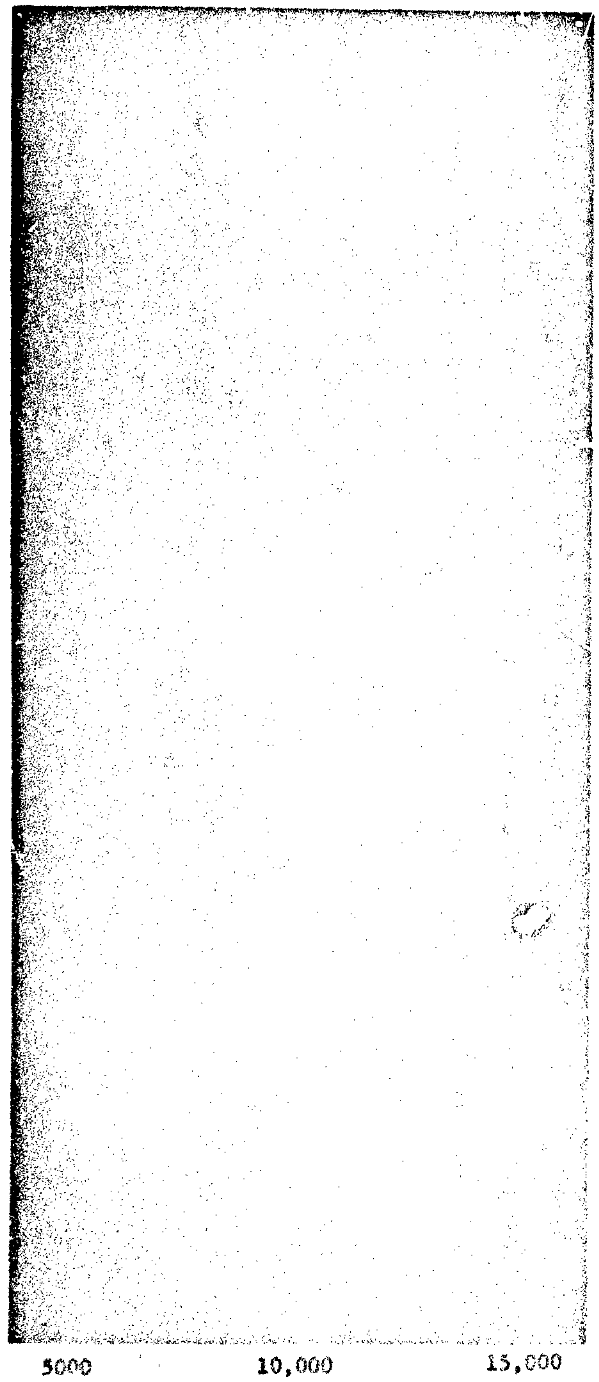


FIGURE 142.

TOTAL PRESSURE PULSATIONS AT PUMP OUTLET (P1)

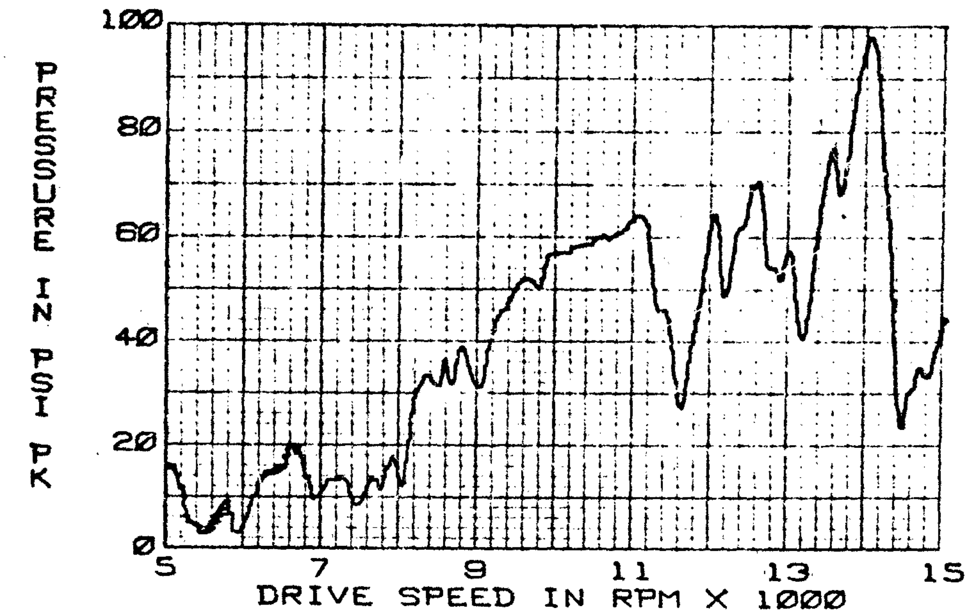


FIGURE 143. CECO MFP-330 VANE PUMP 97-1A-P1 FUNDAMENTAL
8 GPM 120°F

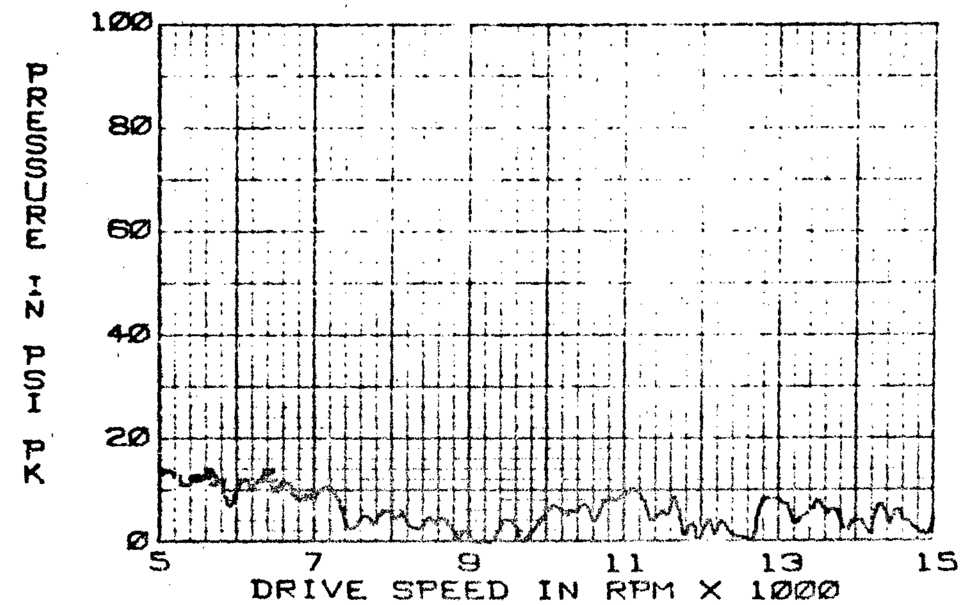


FIGURE 144. CECO MFP-330 VANE PUMP 97-1A-P1 2nd HARMONIC
8 GPM 120°F

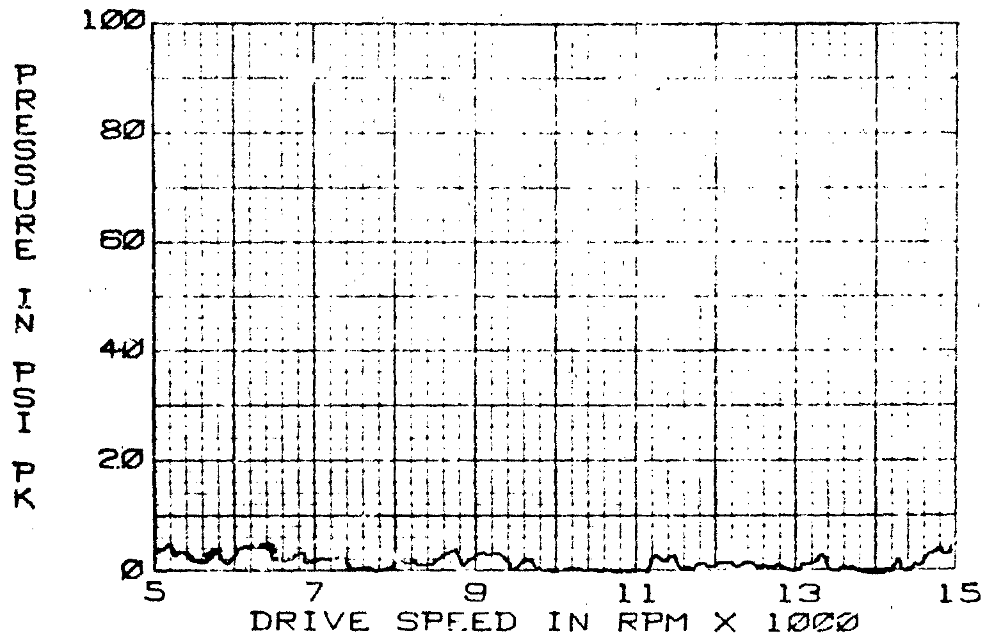


FIGURE 145. CECO MFP-330 VANE PUMP 97-1A-P1 3RD HARMONIC
8 GPM 120°F

Roving transducer data for total pulsations in the outlet line near the metering valve are shown in Figures 146, 147 and 148. Fundamental responses at these positions are shown in Figures 149 through 156. These also show the general trend of increasing pulsation amplitudes with increasing speed. Standing waves of the fundamental frequency pulsations for three system resonant pump speeds (11,300, 13,500, and 15,000 rpm) are shown in Figures 157, 158 and 159. These standing waves exist in the main line between the pump and metering valve, and are the result of acoustic energy reflected by the metering valve.

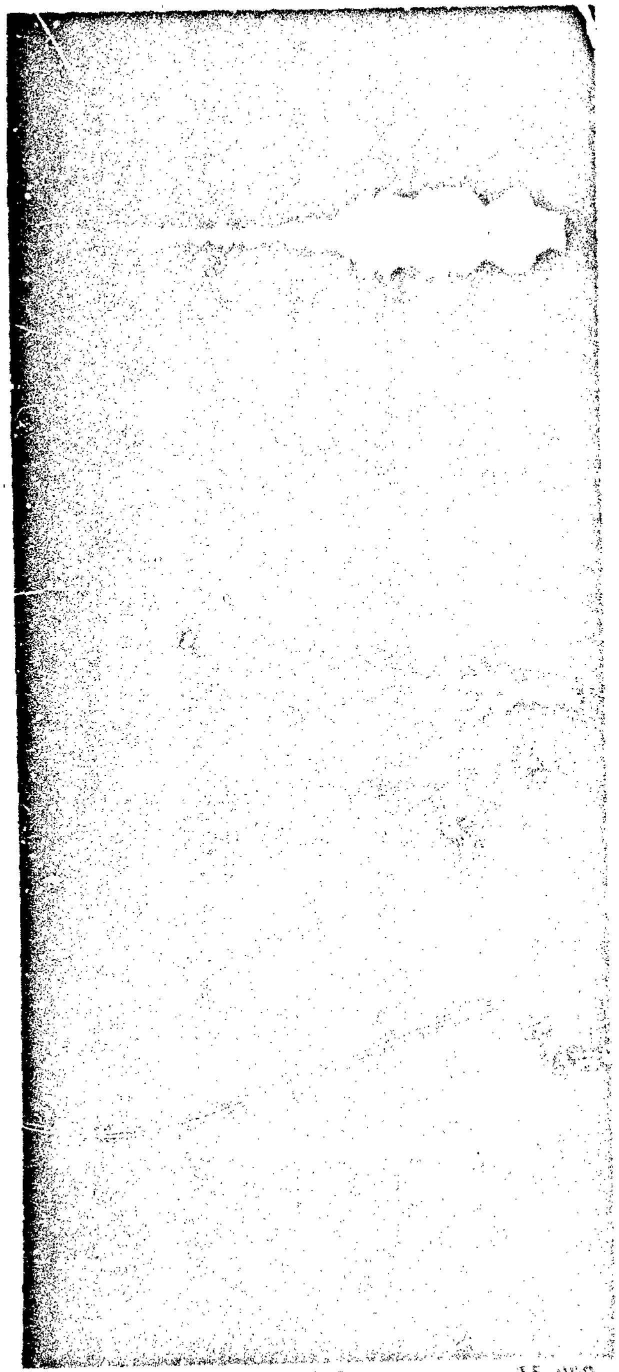


FIGURE 146.

OUTLET LINE TOTAL PRESSURE PULSATIONS -8 GPM

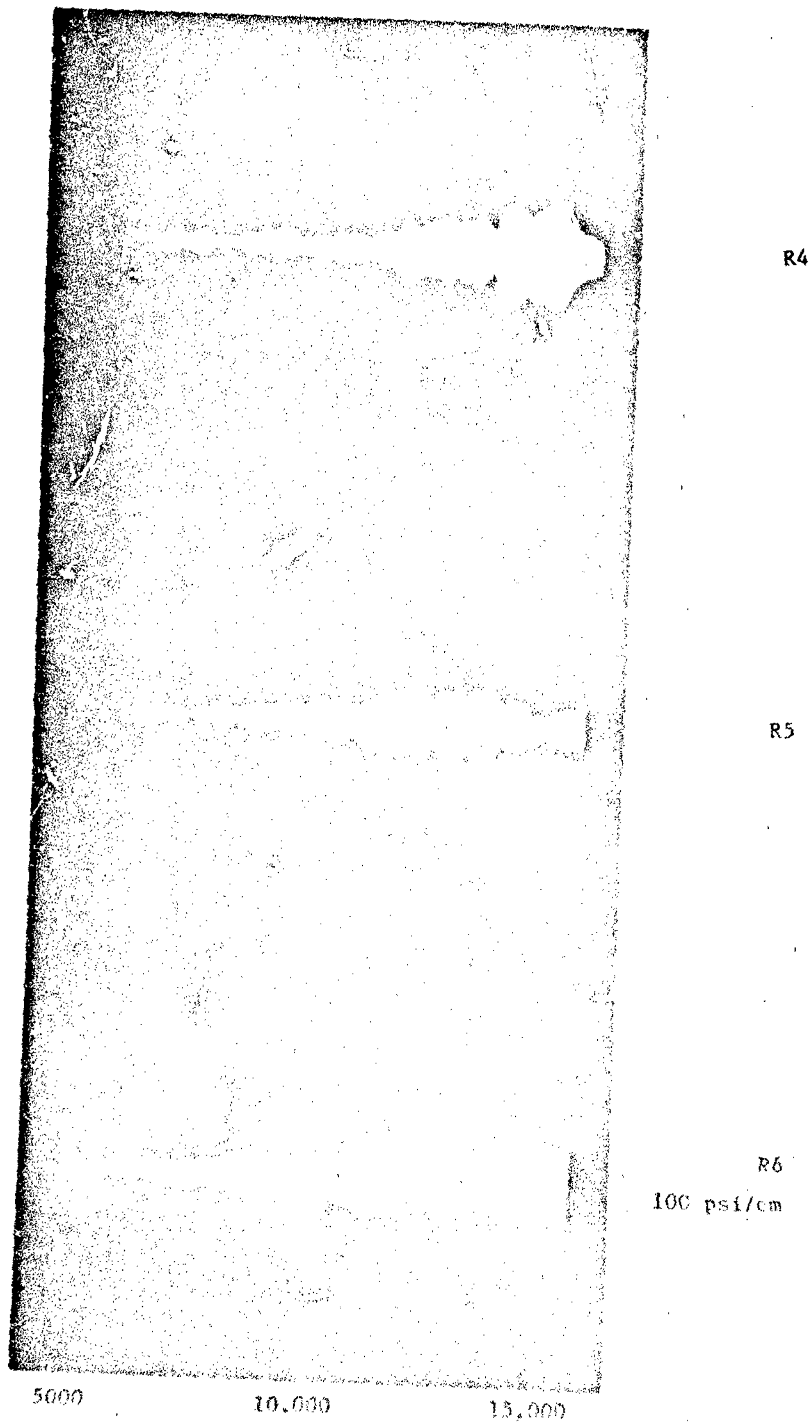


FIGURE 147.

OUTLET LINE TOTAL PRESSURE PULSATIONS -8 GPM

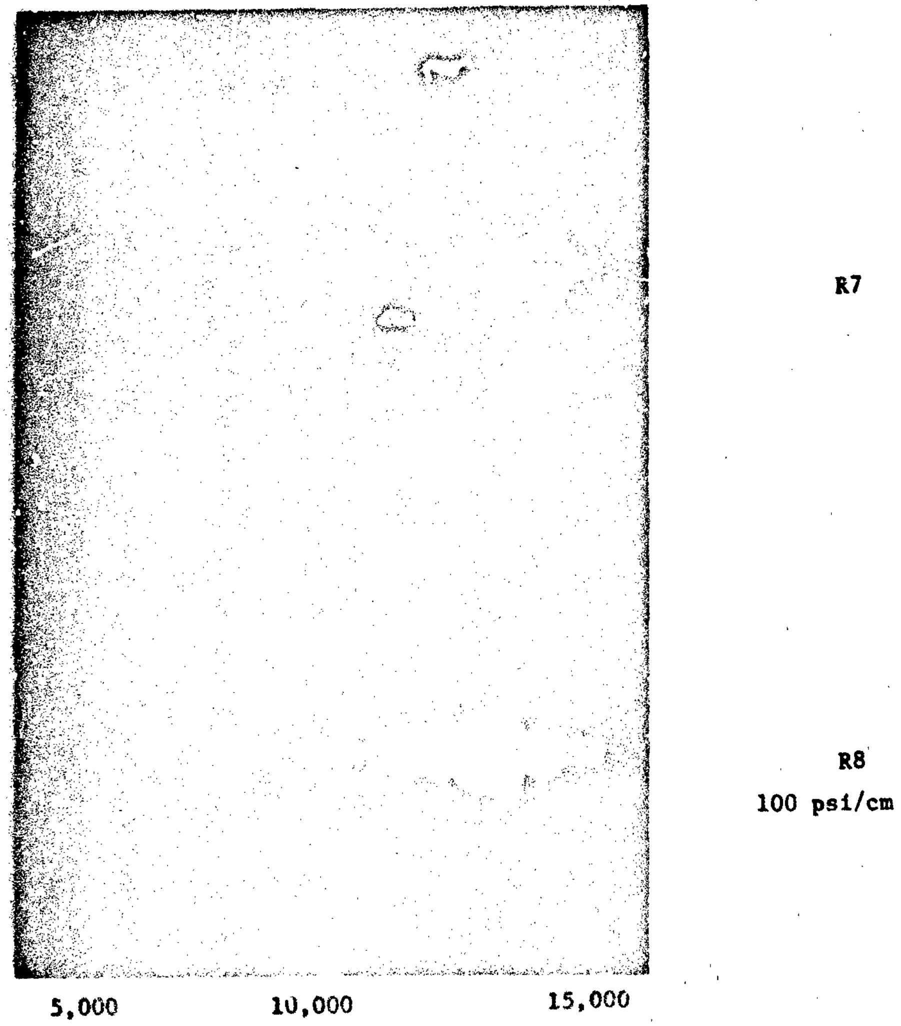


FIGURE 148.

OUTLET LINE TOTAL PRESSURE PULSATIONS - 8 GPM

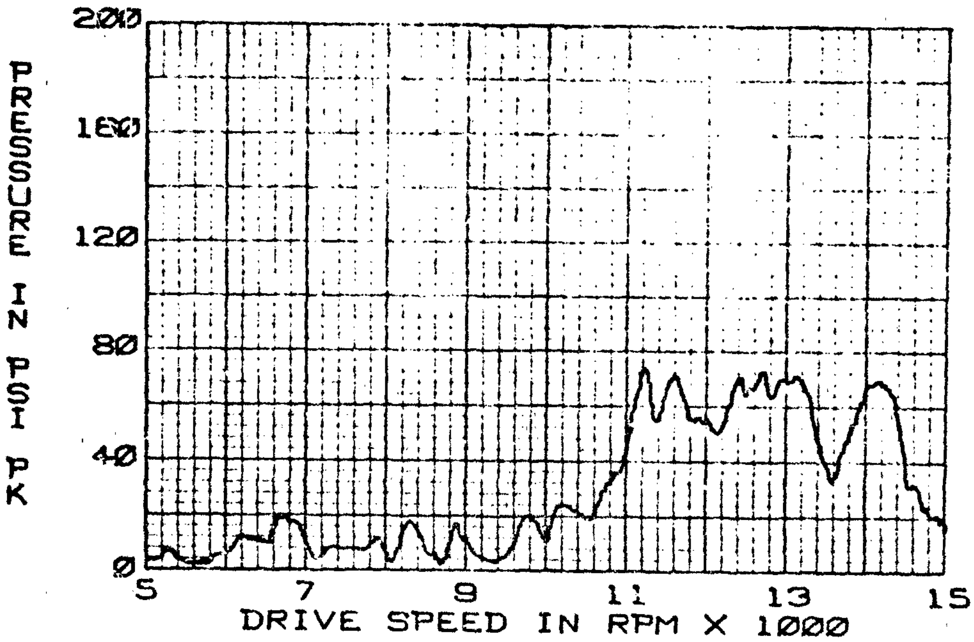


FIGURE 149. CECO MFP-330 VANE PUMP 97-1A-R1 FUNDAMENTAL
8 GPM 120°F

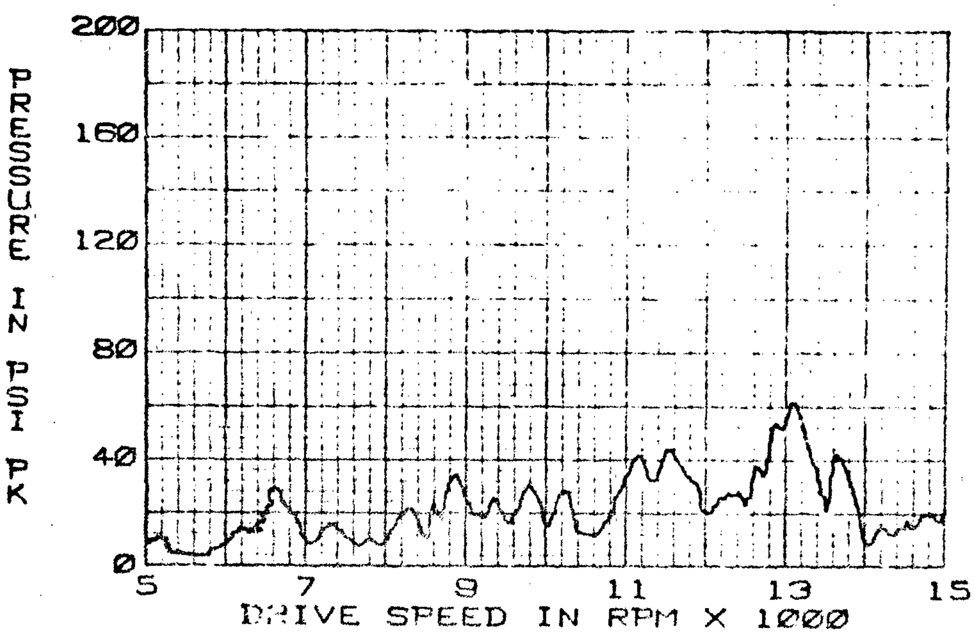


FIGURE 150. CECO MFP-330 VANE PUMP 97-1A-R2 FUNDAMENTAL
8 GPM 120°F

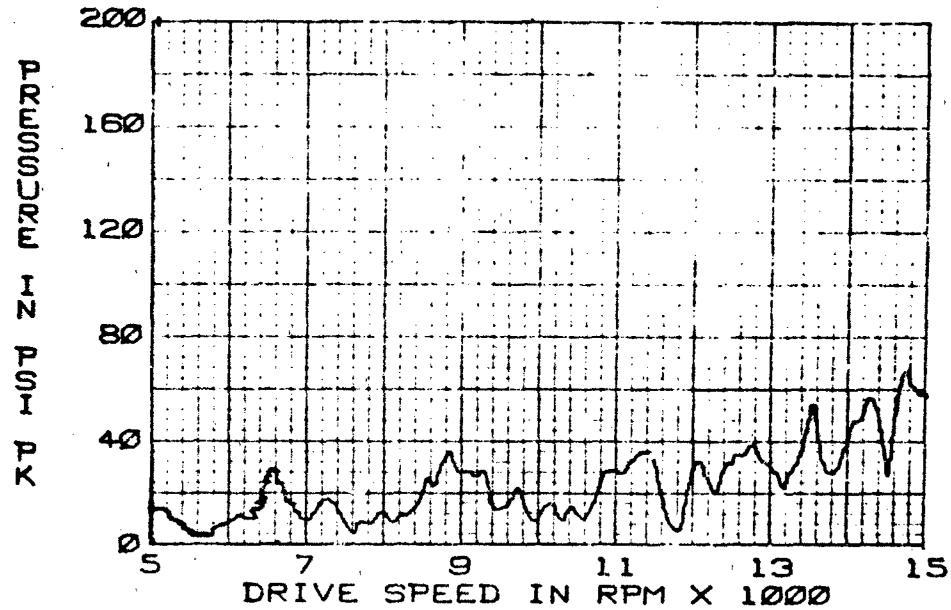


FIGURE 151. CECO MFP-330 VANE PUMP 97-1A-R3 FUNDAMENTAL

8 GPM 120°F

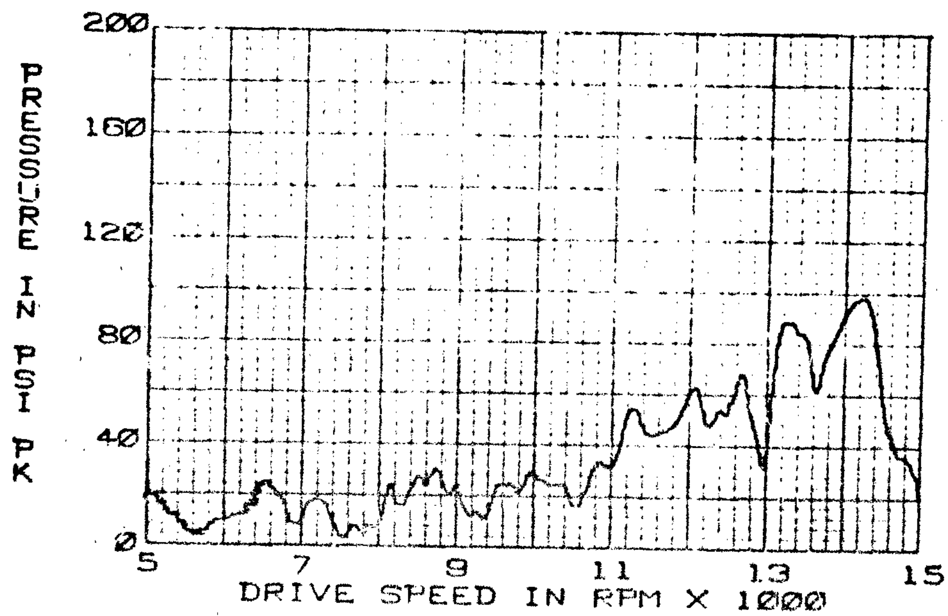


FIGURE 152. CECO MFP-330 VANE PUMP 97-1A-R4 FUNDAMENTAL

8 GPM 120°F

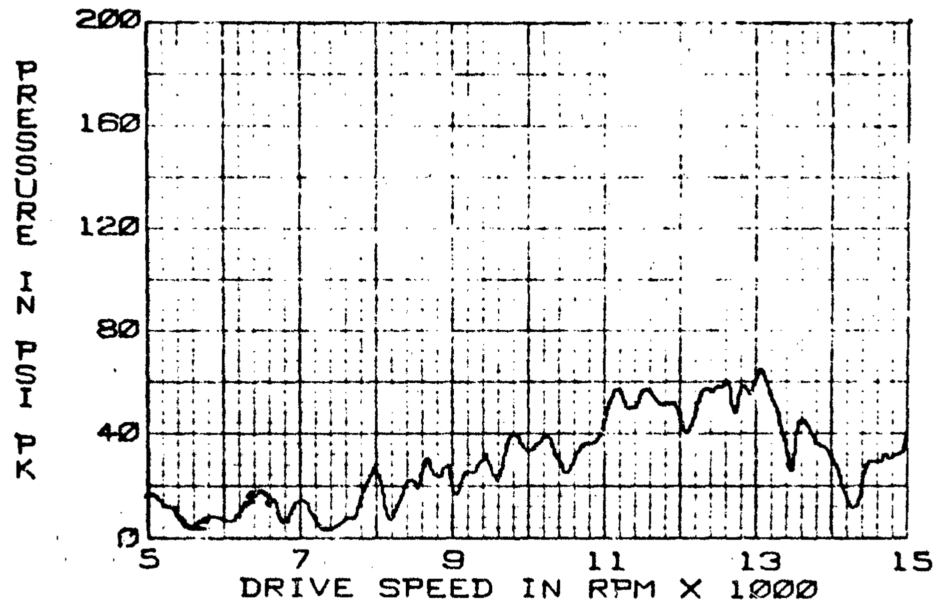


FIGURE 153. CECO MFP-330 VANE PUMP 97-1A-R5 FUNDAMENTAL
8 GPM 120°F

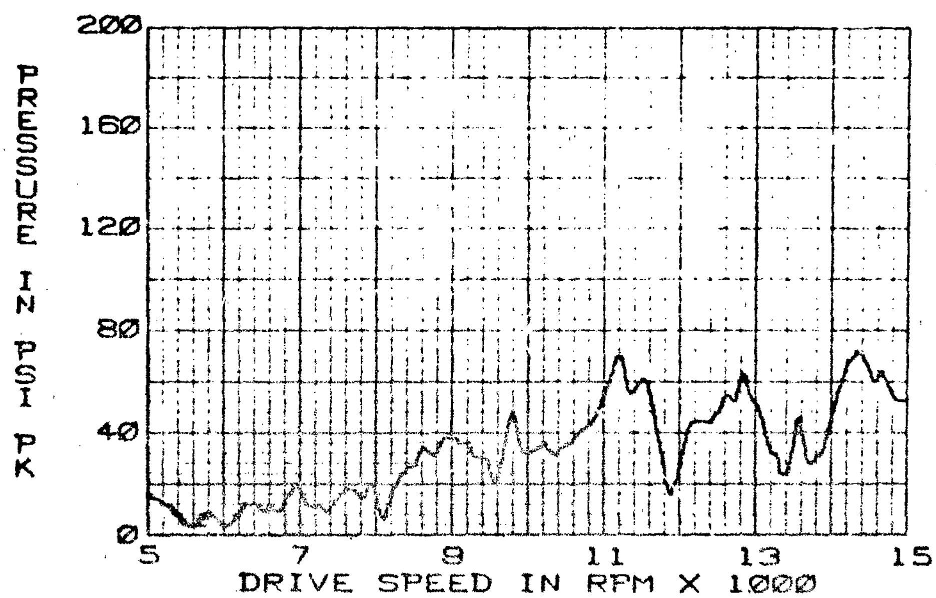


FIGURE 154. CECO MFP-330 VANE PUMP 97-1A-R6 FUNDAMENTAL
6 GPM 120°F

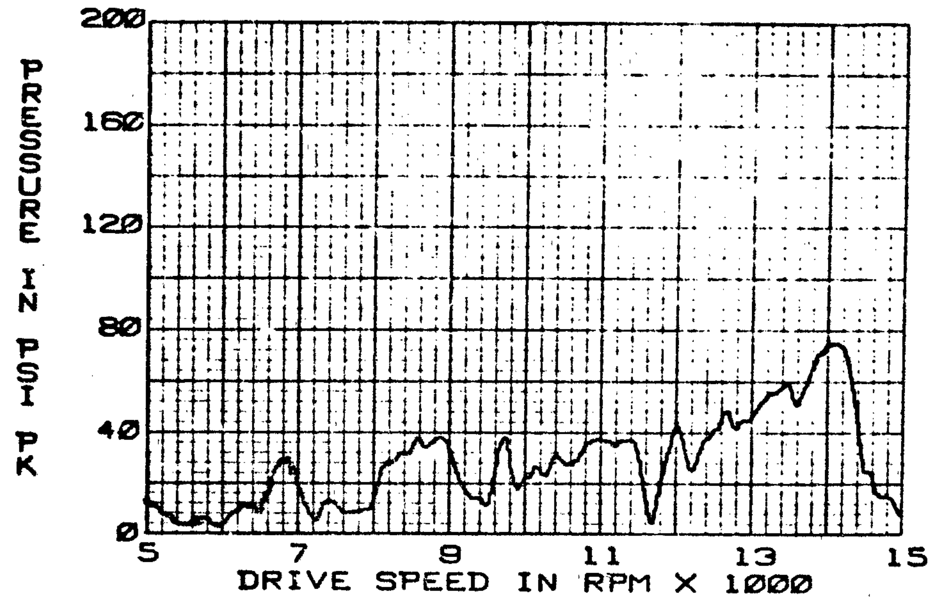


**FIGURE 155. CECO MFP-330 VANE PUMP 97-1A-R7 FUNDAMENTAL**
**8 GPM 120°F**

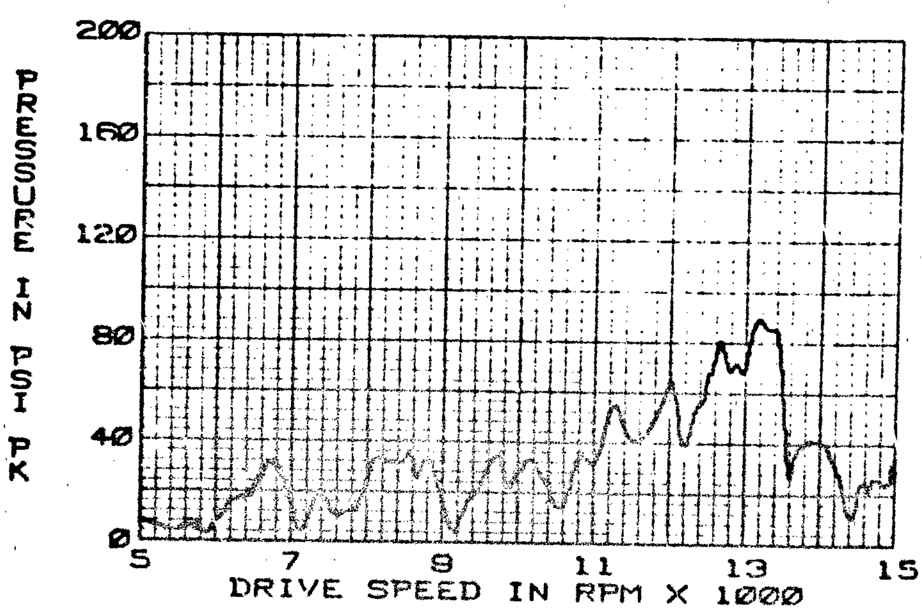


**FIGURE 156. CECO MFP-330 VANE PUMP 97-1A-R8 FUNDAMENTAL**
**8 GPM 120°F**

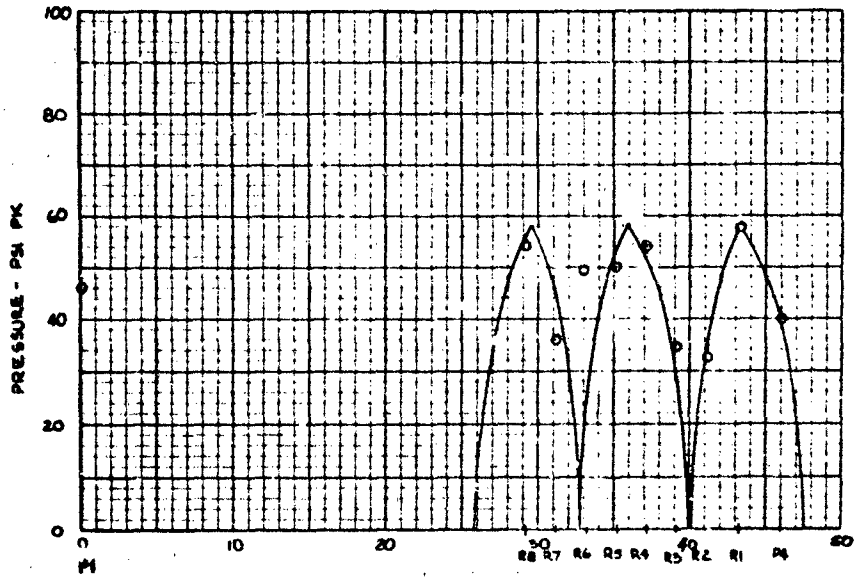


DISTANCE - INCHES FROM P1 X'DUCER
FIGURE 157. 11,300 RPM
8 GPM 120°F

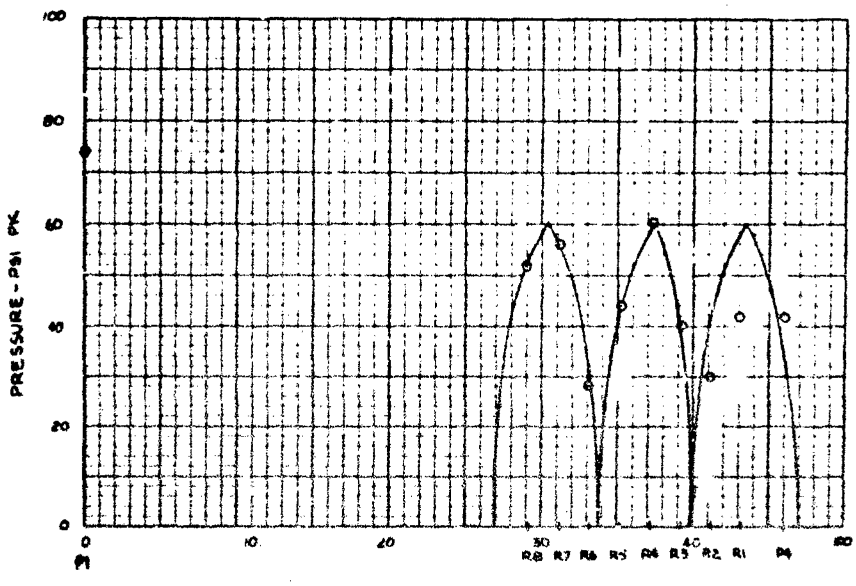


DISTANCE - INCHES FROM P1 X'DUCER
FIGURE 158. 13,500 RPM
8 GPM 120°F

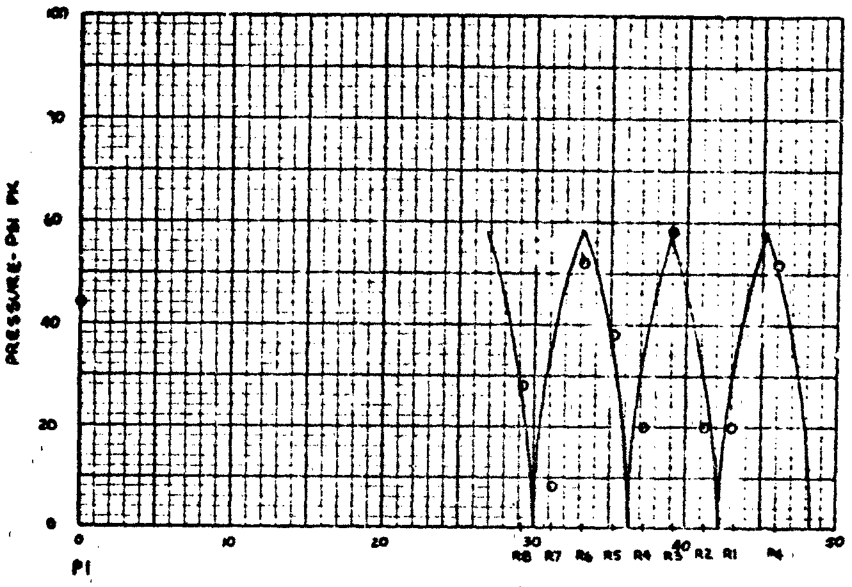


DISTANCE - INCHES FROM P1 X'DUCER
FIGURE 159. 15,000 RPM
8 GPM 120°F

Typical total pressure pulsations near the pump in the upstream control line are shown in Figure 160 for both fixed (P2) and roving transducers (S1,S2). Standing waves in the sensing line for the fundamental pulsations at 11,300 rpm and 15,000 rpm are shown in Figures 161. and 162. Total pulsations of up to 1000 psi p-p were recorded in the upstream sensing line. This is a small (1/4 OD), dead-ended line exposed to a strong acoustic source at the main fuel line. Such a line exhibits a 1/4 wavelength resonant frequency. Pulsating flow in the large main line (3/4 O.D.) is capable of generating very large pressure amplitudes in the small sensing line. Continuous pump operation at a resonant speed could cause adverse effects in the pump with such high pressure pulsations in the sensing line. The pulsation frequency is probably far above the control valve spring/mass natural frequency, therefore the valve does not respond to the high amplitude pulsations. However, early fatigue failure could result to parts exposed to the pump sensing port pressure pulsations.

Figure 163 shows total and fundamental case inlet pressure pulsations for an 8 gpm flow rate. Total case pressure pulsations reached a maximum of 130 psi p-p. Case pulsations are the result of vane inlet port timing and the test set-up inlet system. Case pulsations in the complete pump unit are also influenced by the output of the boost stage low flow impeller.

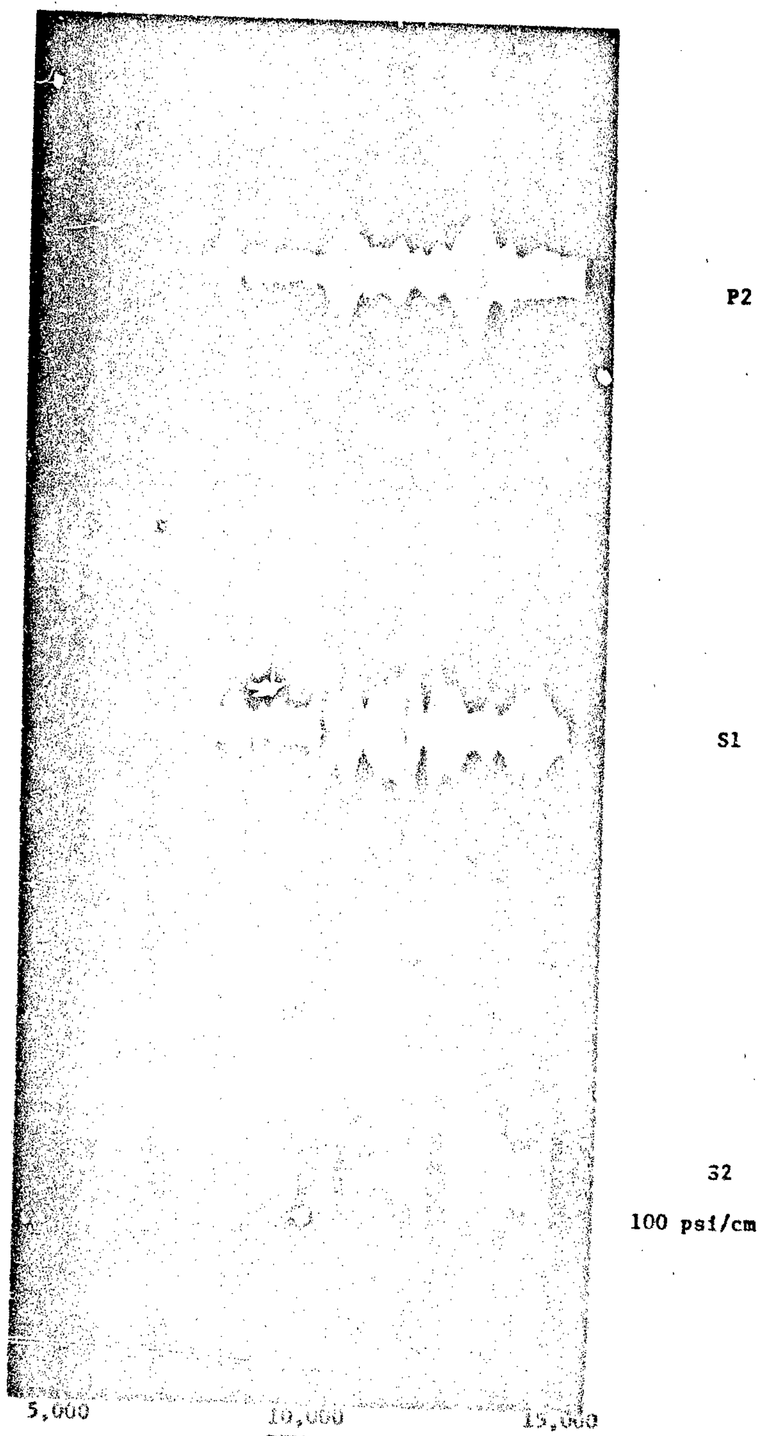


FIGURE 160.

UPSTREAM CONTROL LINE TOTAL PRESSURE PULSATIONS - 8 GPM

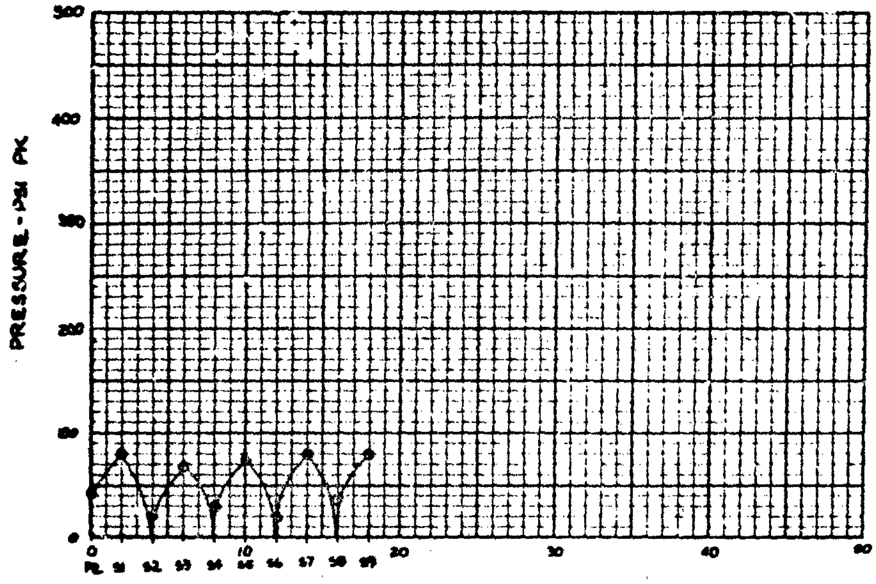


DISTANCE - INCHES FROM P2 X'DUCER
FIGURE 161. 11,300 RPM
8 GPM 120°F

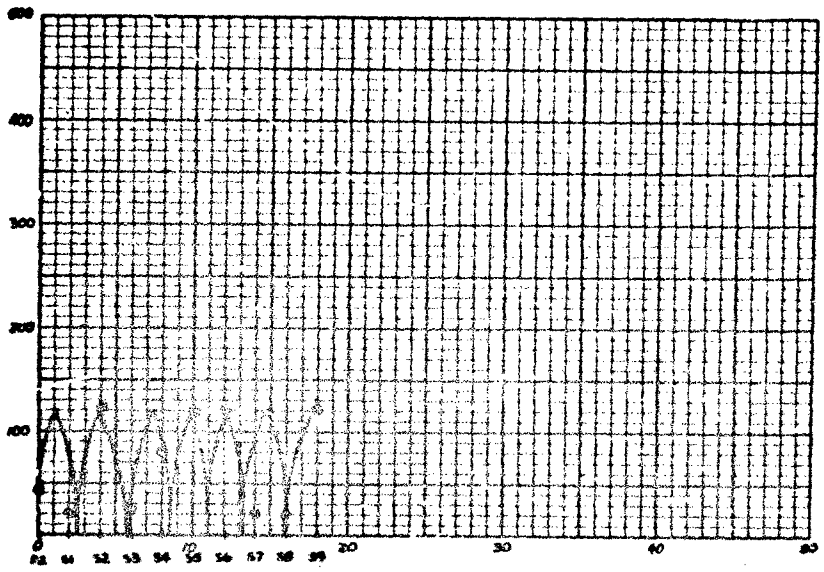


DISTANCE - INCHES FROM P2 X'DUCER
FIGURE 162. 15,000 RPM
8 GPM 120°F

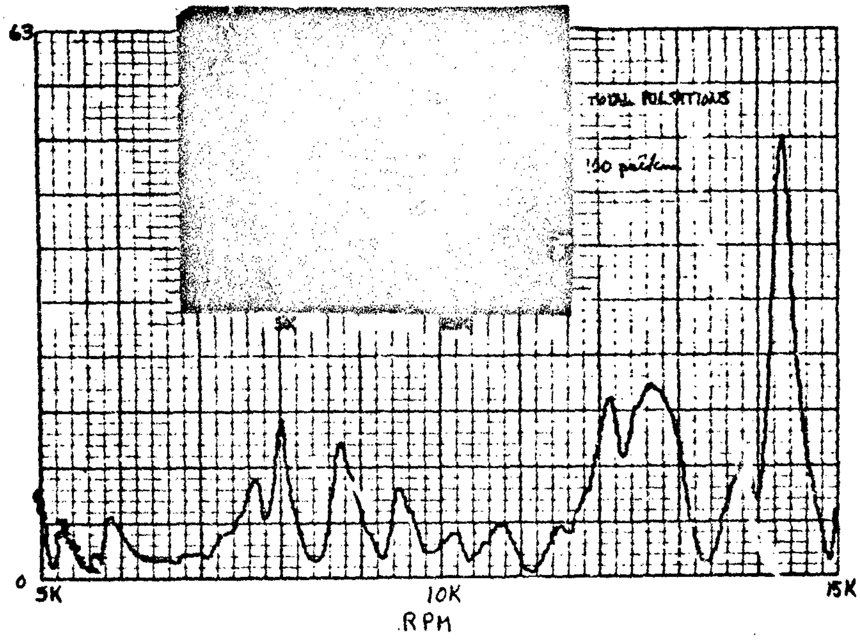


FIGURE 163. CECO MFP-330 VANE PUMP CASE INLET FUNDAMENTAL
8 GPM 120°F 50 PSIG

Figure 164 shows outlet (P1A) and upstream control port (P2A) pressure pulsations for a 17% dissolved air content at an 8 gpm flow rate. Inlet pressure was 62 psig. Outlet pulsations are slightly less than with 1% air and a 43 psig inlet pressure (Figure 147). Control line pulsations are slightly higher than with 2% air and the same inlet pressure (Figure 160). These limited tests suggest that the vane stage is not unduly sensitive to normal levels of dissolved air in the pumping fluid. Normal inlet pressure to the vane stage is boosted to about 120 psig, which makes the pump even less sensitive to air content. The tests were run at inlet pressures of 63 psig or less.

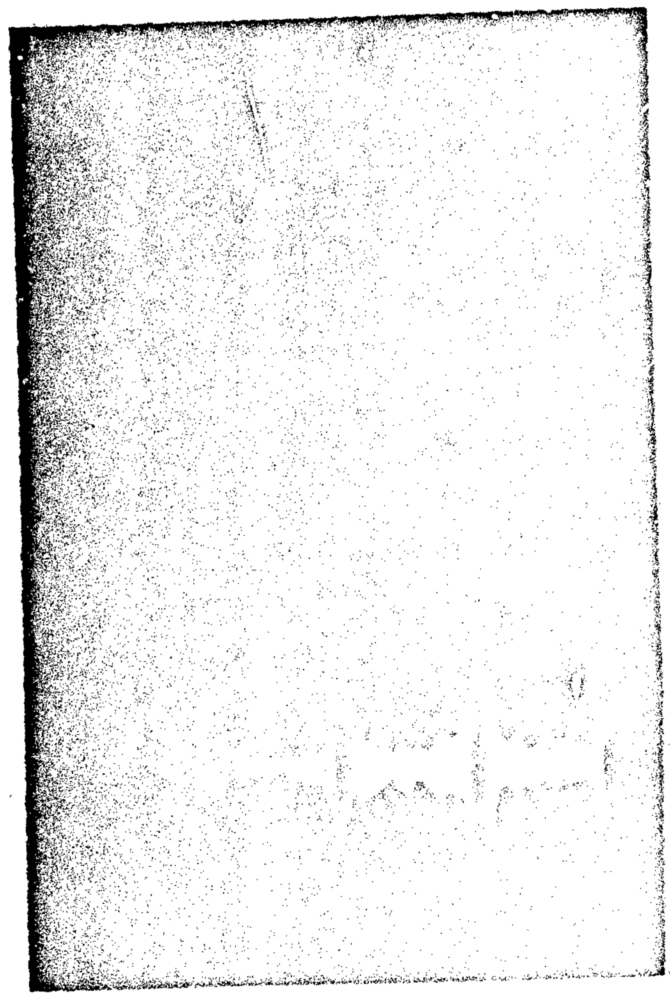

PUMP OUTLET PORT (P1A)

UPSTREAM CONTROL PORT (P2A)

100 psi/cm

5,000 10,000 15,000
RPM

FIGURE 164.

TOTAL PRESSURE PULSATIONS - 8 GPM, 17% AIR, 62 PSIG INLET

An HSFR computer simulation was made using the test conditions of run number 97-3A. The vane pump outlet flow was 30 gpm. The simulated test system included the components shown in Figure 141 from the vane pump to the load valve, including the high and low pressure sense lines terminating in the pump. A one cubic inch volume was assumed at these end points. The HSFR input data defining the system is listed in Table 15.

Figure 165 shows the computed fundamental peak pressure at the pump outlet and the measured fundamental response. The test data is quiet showing no major resonant frequencies through the rpm sweep. The system frequencies are close together because of the effects of long lines in the system. The load valve in the circuit did not provide a strong reflection point, so the measured data probably reflects system line resonant responses down to the reservoir. The HSFR circuit termination was the load valve and the lack of frequency correlation may be attributable to this. The comparison between the measured and computed fundamental responses and also shown at the load valve in Figure 166.

The control lines branching to the vane pump servo valve had well defined boundary conditions. Figure 167 compares the measured fundamental peak and total pressure pulsations with the HSFR predicted results at the high pressure sense line inlet. The program was able to predict the stong resonance points at 7800 and 10,100, although the computed higher point at 12,500 rpm was approximately 300 rpm in error from the data. The measured and predicted response for the low pressure sense line at the pump is shown in Figure 168. The program computed five major resonant peaks compared to the measured four. Amplitude correlation for all the plots is poor. This has been the general pattern for the HSFR runs. The vane pump model operation is very similar to the piston pump model. Therefore, this type of characteristic was not unexpected.

THIS PAGE IS BEST QUALITY PRACTICABLE
FROM COPY FURNISHED TO DDC

TABLE 15. HYDRAULIC SYSTEM FREQUENCY RESPONSE PROGRAM

**** FREQUENCY RESPONSE VANE PUMP MODEL ****(DVPFR1)

RESPONSE IS CALCULATED FROM 5000.00 TO 15000.00 R.P.M. IN INCREMENTS OF 100.00 R.P.M.
RESPONSE IS PLOTTED FOR THE -FIRST- HARMONIC FREQUENCY
NUMBER OF PUMPING ELEMENTS= 16.

FLUID DATA FOR MIL-H-5606C AT 700.0 PSIG AND 120.0 DEG F
VISCOSITY = .170E-01 IN**2/SEC
DENSITY = .808E-04 (LB-SEC**2)/IN**4
BULK MODULUS = .202E+06 PSI

ELEMENT NUMBER ****************************SYSTEM ELEMENT INPUT DATA****************************

| ELEMENT NUMBER | M TYPE | N TYPE | PHYSICAL DATA | | | | | | | |
|---|---|---|---|---|---|---|---|---|---|---|
| 1 | 9 | 15 | 1.000 | .260 | .035 | 38.000 | 9.806 | 12.000 | 15.000 | |
| | | | 95.00803 | 0.00000 | .12540 | 131.70000 | 238.54000 | .24030 | .06070 | .00350 |
| 2 | 1 | 0 | 15.274 | 1.000 | .100 | 30000000.000 | 0.000 | 0.000 | 0.000 | |
| 3 | 1 | 0 | 10.000 | .750 | .042 | 30000000.000 | 0.000 | 0.000 | 0.000 | |
| 4 | 1 | 0 | 10.000 | .750 | .042 | 30000000.000 | 0.000 | 0.000 | 0.000 | |
| 5 | 1 | 0 | 7.190 | .750 | .042 | 30000000.000 | 0.000 | 0.000 | 0.000 | |
| 6 | 1 | 0 | 2.000 | .750 | .042 | 30000000.000 | 0.000 | 0.000 | 0.000 | |
| 7 | 1 | 0 | 2.000 | .750 | .042 | 30000000.000 | 0.000 | 0.000 | 0.000 | |
| 8 | 1 | 0 | 2.000 | .750 | .042 | 30000000.000 | 0.000 | 0.000 | 0.000 | |
| 9 | 1 | 0 | 2.000 | .750 | .042 | 30000000.000 | 0.000 | 0.000 | 0.000 | |
| 10 | 1 | 0 | 2.000 | .750 | .042 | 30000000.000 | 0.000 | 0.000 | 0.000 | |
| 11 | 1 | 0 | 2.000 | .750 | .042 | 30000000.000 | 0.000 | 0.000 | 0.000 | |
| 12 | 1 | 0 | 2.000 | .750 | .042 | 30000000.000 | 0.000 | 0.000 | 0.000 | |
| 13 | 1 | 0 | 2.000 | .750 | .042 | 30000000.000 | 0.000 | 0.000 | 0.000 | |
| 14 | 1 | 0 | 2.010 | .750 | .042 | 30000000.000 | 0.000 | 0.000 | 0.000 | |
| 15 | 6 | 13 | 0.000 | 0.000 | 0.000 | 0.000 | 0.000 | 0.000 | 0.000 | |
| 16 | 1 | 0 | 10.000 | .250 | .020 | 30000000.000 | 0.000 | 0.000 | 0.000 | |
| 17 | 1 | 0 | 4.690 | .250 | .020 | 30000000.000 | 0.000 | 0.000 | 0.000 | |
| 18 | 1 | 0 | 2.000 | .250 | .020 | 30000000.000 | 0.000 | 0.000 | 0.000 | |
| 19 | 1 | 0 | 2.000 | .250 | .020 | 30000000.000 | 0.000 | 0.000 | 0.000 | |
| 20 | 1 | 0 | 2.000 | .250 | .020 | 30000000.000 | 0.000 | 0.000 | 0.000 | |
| 21 | 1 | 0 | 2.000 | .250 | .020 | 30000000.000 | 0.000 | 0.000 | 0.000 | |
| 22 | 1 | 0 | 2.000 | .250 | .020 | 30000000.000 | 0.000 | 0.000 | 0.000 | |
| 23 | 1 | 0 | 2.000 | .250 | .020 | 30000000.000 | 0.000 | 0.000 | 0.000 | |
| 24 | 1 | 0 | 2.000 | .250 | .020 | 30000000.000 | 0.000 | 0.000 | 0.000 | |
| 25 | 1 | 0 | 2.000 | .250 | .020 | 30000000.000 | 0.000 | 0.000 | 0.000 | |
| 26 | 1 | 0 | 2.000 | .250 | .020 | 30000000.000 | 0.000 | 0.000 | 0.000 | |
| 27 | 1 | 0 | 3.560 | .250 | .020 | 30000000.000 | 0.000 | 0.000 | 0.000 | |
| 28 | 13 | 0 | 1.000 | 0.000 | 0.000 | 0.000 | 0.000 | 0.000 | 0.000 | |
| 29 | 1 | 0 | 3.750 | .750 | .042 | 30000000.000 | 0.000 | 0.000 | 0.000 | |
| 30 | 4 | 0 | .911 | 0.000 | 0.000 | 0.036 | 0.000 | 0.000 | 0.000 | |
| 31 | 1 | 0 | 25.500 | .750 | .042 | 30000000.000 | 0.000 | 0.000 | 0.000 | |
| 32 | 6 | 3 | 0.000 | 0.000 | 0.000 | 0.000 | 0.000 | 0.000 | 0.000 | |
| 33 | 1 | 0 | 47.900 | .250 | .020 | 30000000.000 | 0.000 | 0.000 | 0.000 | |
| 34 | 1 | 0 | 3.560 | .250 | .020 | 30000000.000 | 0.000 | 0.000 | 0.000 | |
| 35 | 13 | 0 | 1.000 | 0.000 | 0.000 | 0.000 | 0.000 | 0.000 | 0.000 | |
| 36 | 1 | 0 | 82.000 | .750 | .042 | 30000000.000 | 0.000 | 0.000 | 0.000 | |
| 37 | 14 | 6 | 10.633 | 131.700 | 0.000 | 0.000 | 0.000 | 0.000 | 0.000 | |

19 Q PLOTS FOR INPUT TO ELEMENT NUMBERS 3 6 8 10 12 14 16 18 20 22 24 27 29 34 36
15 P PLOTS FOR INPUT TO ELEMENT NUMBERS 3 6 8 10 12 14 16 18 20 22 24 27 29 34 36
3 I PLOTS FOR INPUT TO ELEMENT NUMBERS 16 27 29
3 T PLOTS FOR INPUT TO ELEMENT NUMBERS 16 27 29
3 F PLOTS FOR INPUT TO ELEMENT NUMBERS 16 27 29

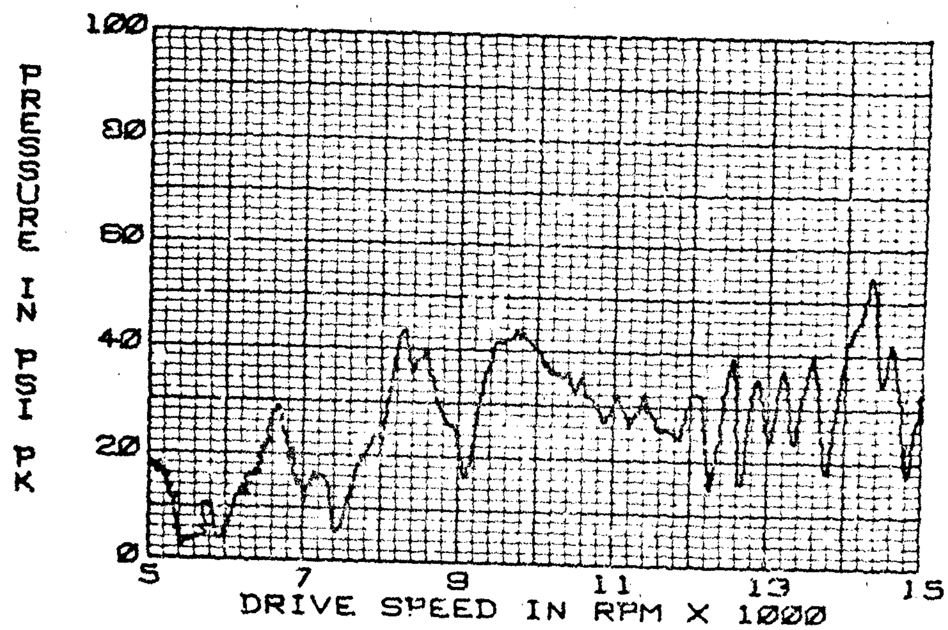


CECO MFP-330 VANE PUMP
97-3A-P1 FUNDAMENTAL
30 GPM 120 F

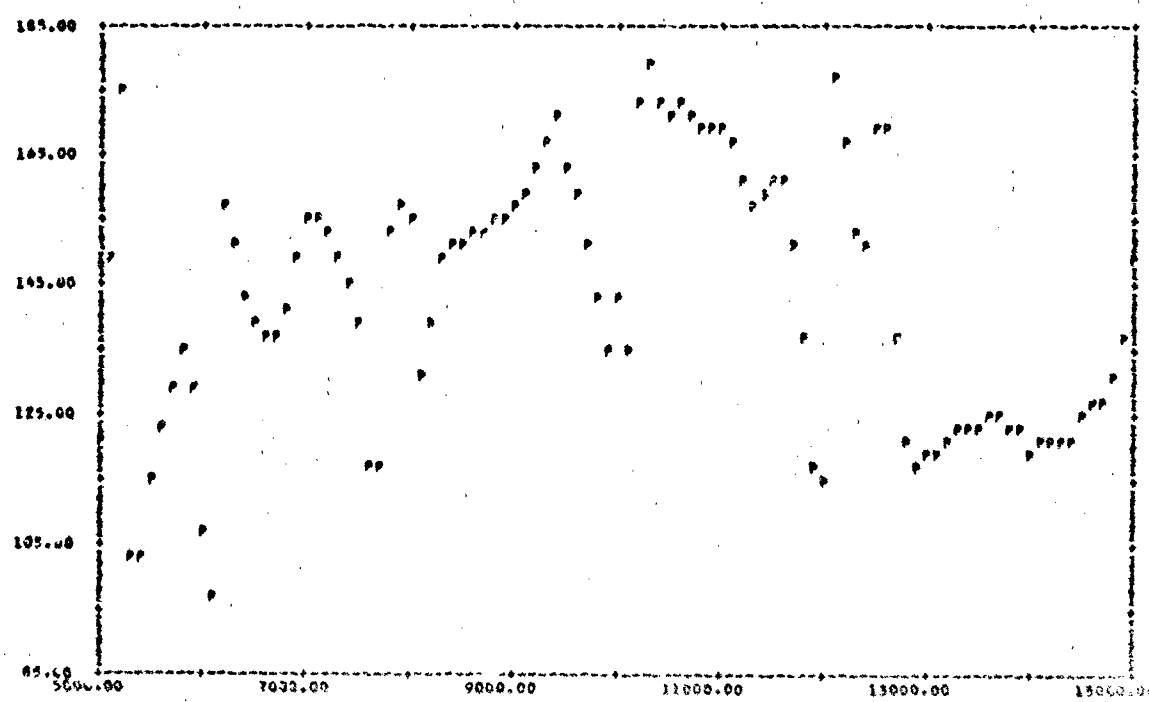


FIGURE 165. MEASURED AND COMPUTED PEAK PRESSURES PUMP OUTLET

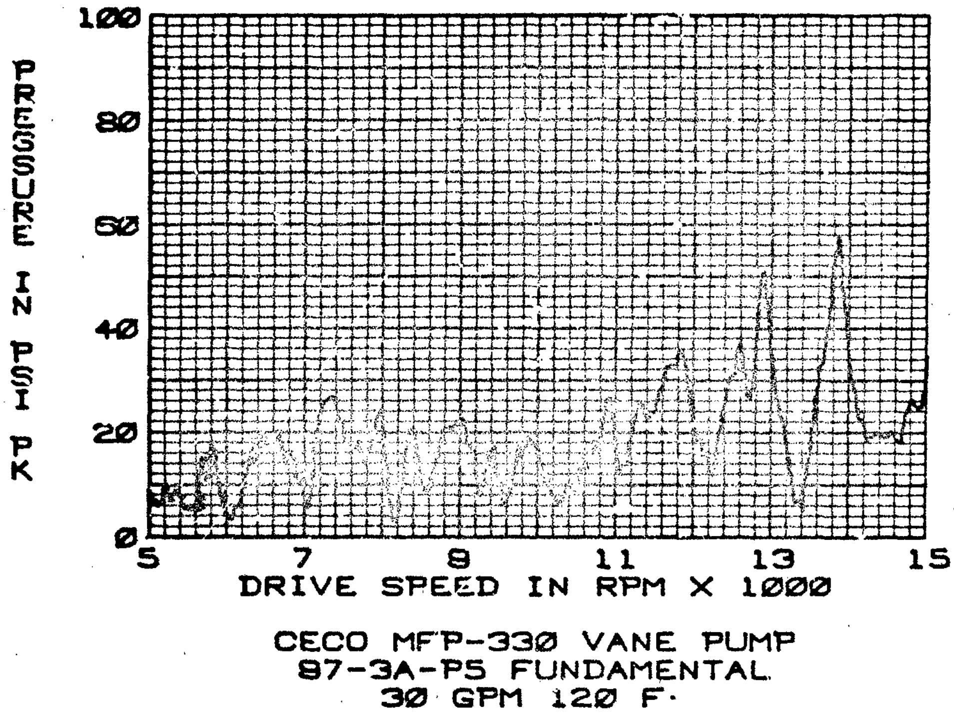


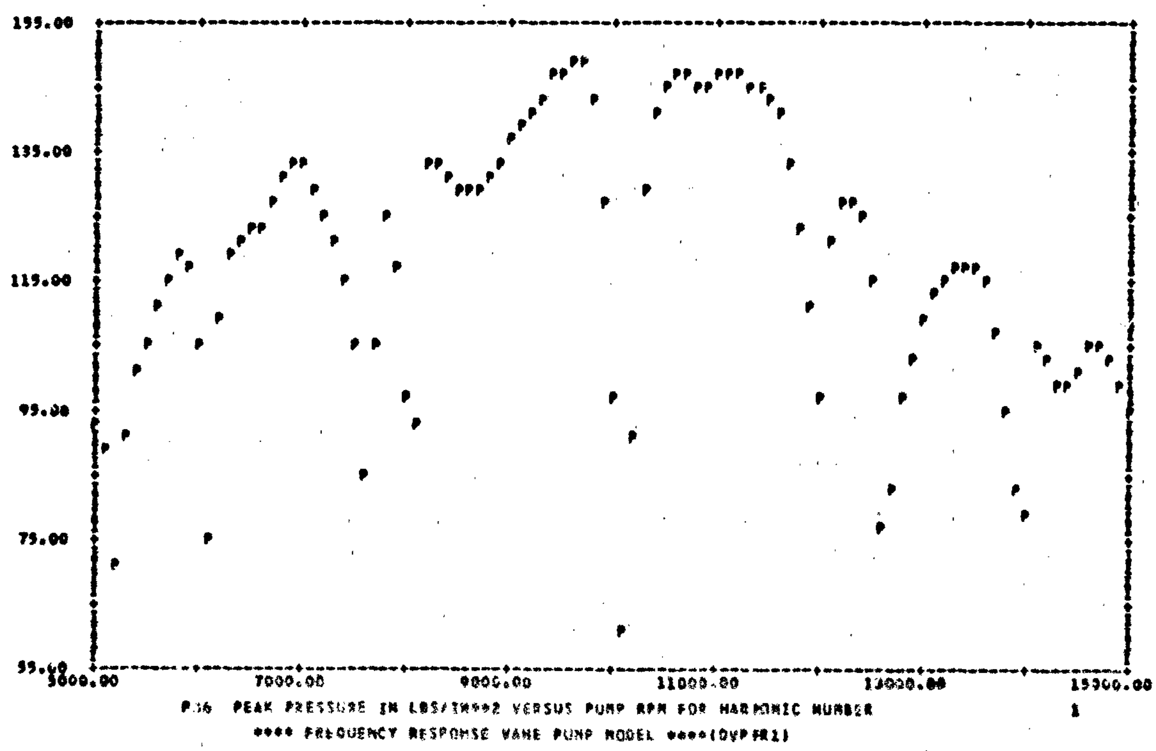


FIGURE 166. MEASURED AND COMPUTED PEAK PRESSURES LOAD VALVE INLET

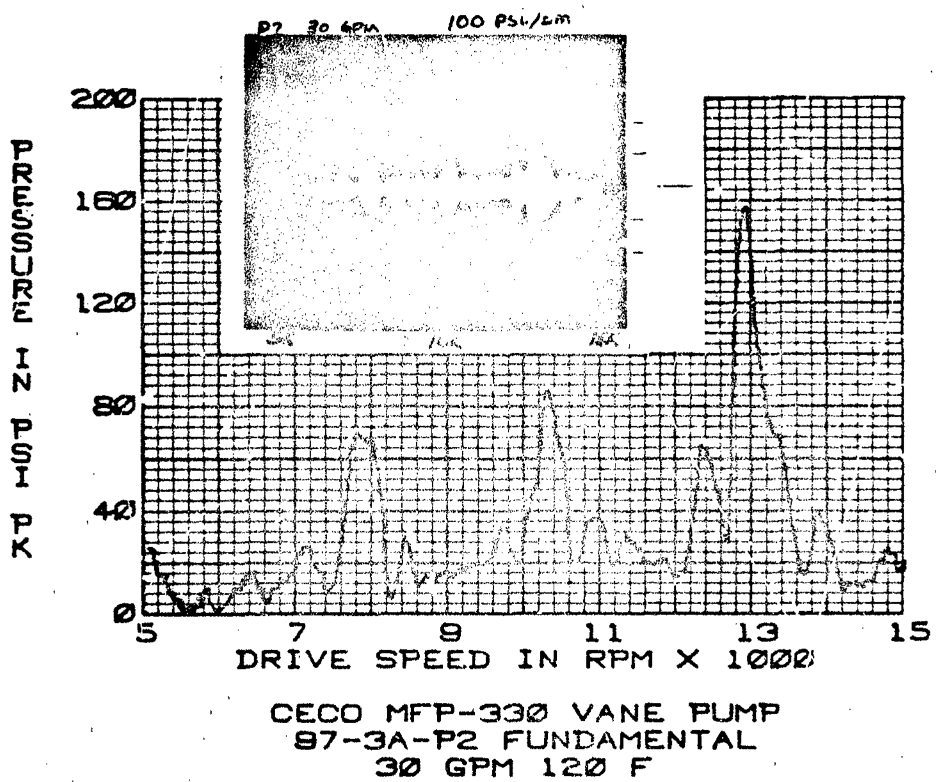


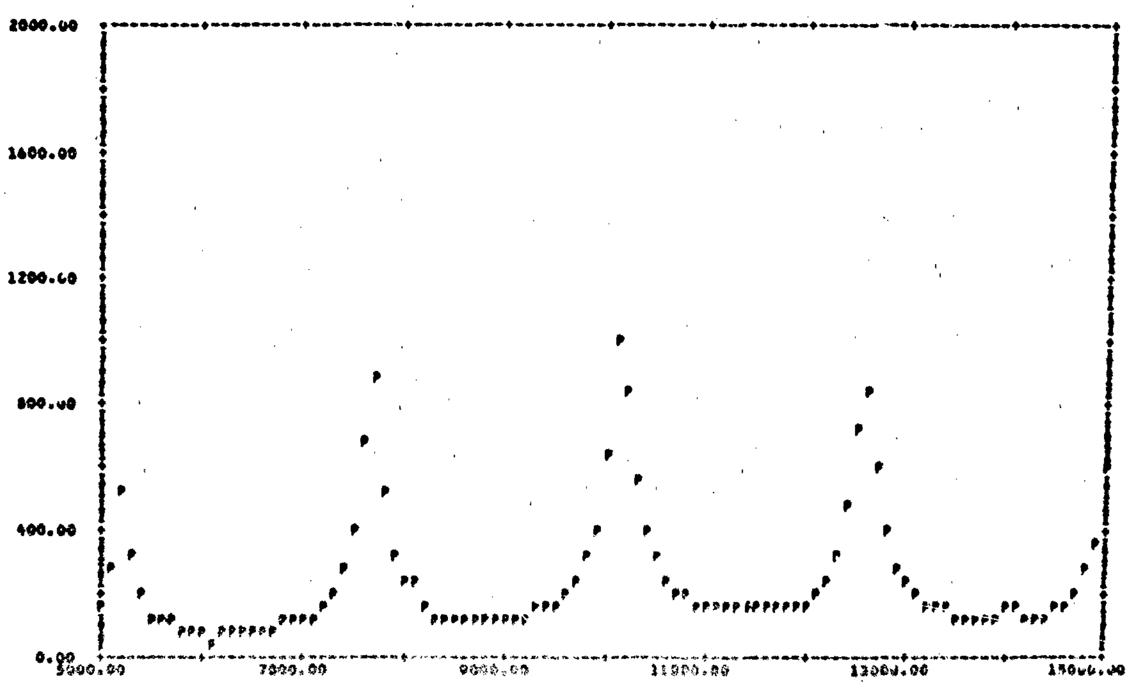


FIGURE 167. MEASURED AND COMPUTED PEAK PRESSURES TOTAL PRESSURE PULSATIONS HIGH PRESSURE SENSE LINE INLET

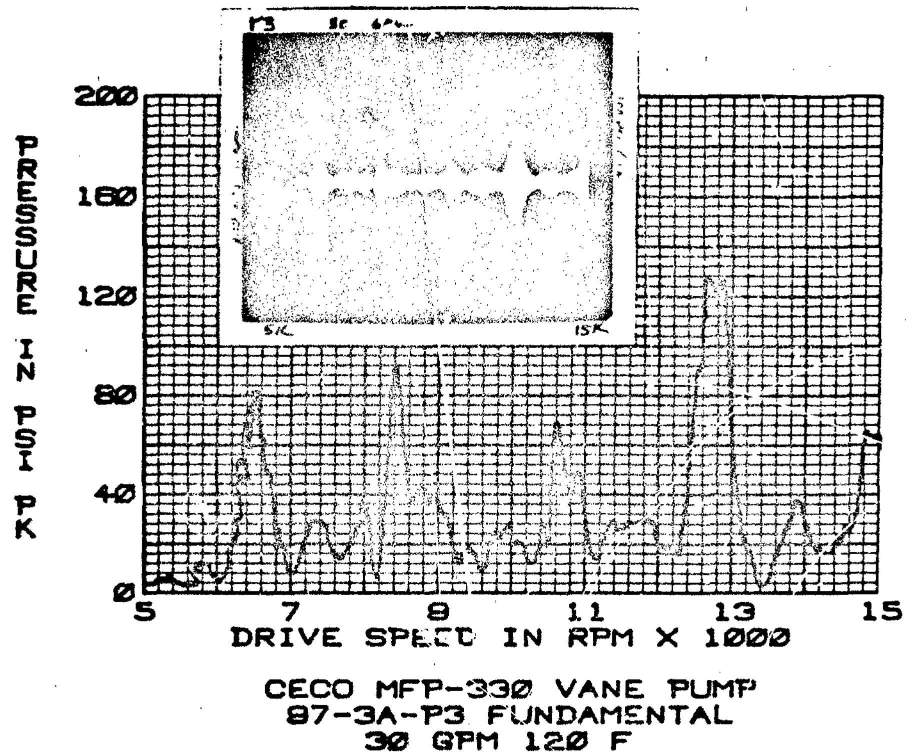


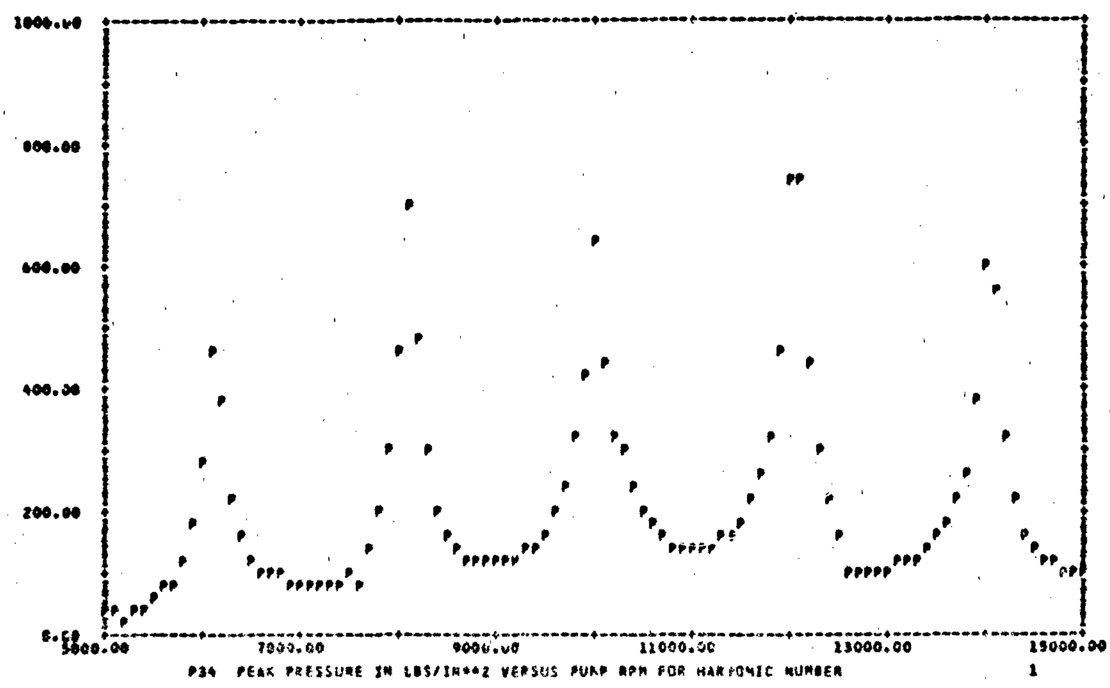


FIGURE 168. MEASURED AND COMPUTED PEAK PRESSURES WITH TOTAL PRESSURE PULSATIONS LOW PRESSURE SENSE LINE INLET

## 2. VANE PUMP HYTRAN MODEL DEVELOPMENT AND VERIFICATION

### a. HYTRAN Model

A transient model of the vane pump was developed for use with the HYTRAN Program. Specific design parameters such as servovalve flow area versus stroke, the relation between cam location and maximum pump flow, and the servo piston loading were provided by CECO and used in the HYTRAN model. User and technical description manual sections for the transient vane pump model are contained in Appendix E.

### b. HYTRAN Verification Tests and Test Set-up

The transient testing on the CECO vane pump was performed on the system illustrated in Figure 169. The transient test set-up is a close approximation of the fuel system installed on the F-100 engine. Extra lines were added upstream and downstream of the flow valve to provide at least one calculation interval for the HYTRAN program at the sampled data rate.

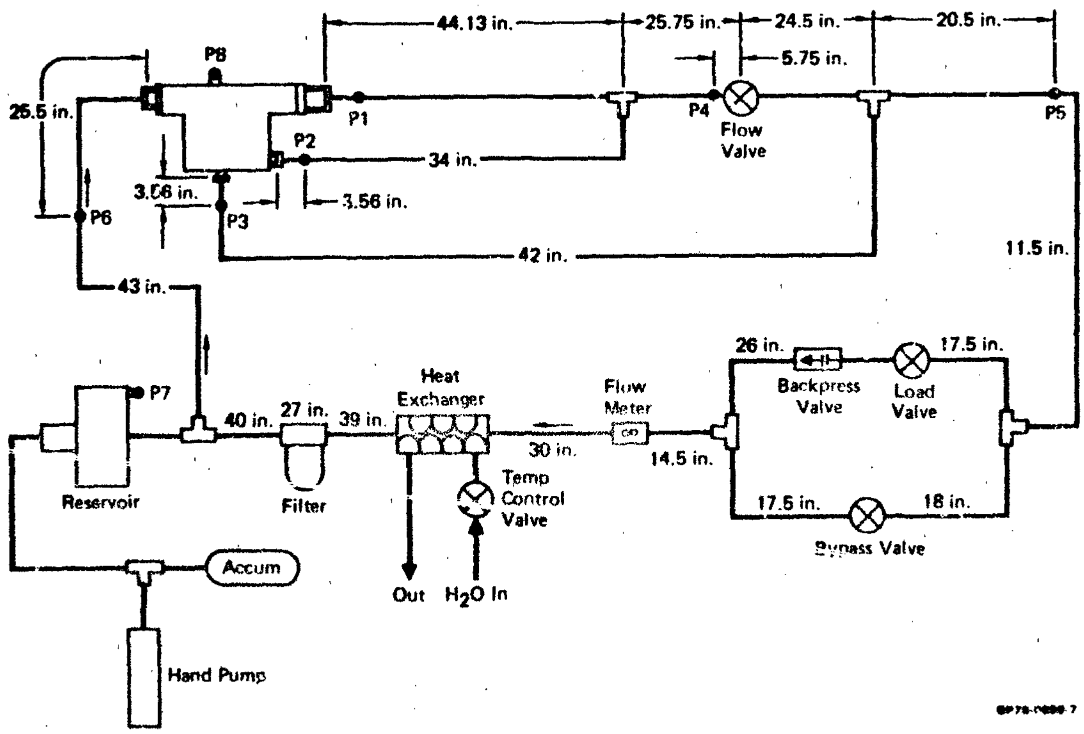


FIGURE 169
CECO VANE PUMP
Steady State and Transient Response Test Set-Up Schematic

Table 16 contains a listing of the system and pump parameters recorded during the transient testing. Figure 170 is a schematic showing the pump instrumentation and Figure 171 is a schematic cross section of the vane stage pump. A photograph of the instrumented pump, speed increaser, and drive is shown in Figure 172.

TABLE 16

CECO PUMP MODEL VERIFICATION TESTS

INSTRUMENTATION REQUIREMENTS

| | |
|---|---|
| EXTERNAL | CONTROL VALVE PRESSURE (P4) |
| | SYSTEM RETURN PRESSURE (P5, P7) |
| | SUCTION PRESSURE (P6) |
| | RETURN FLOW (Q1) |
| | TRANSIENT CONTROL VALVE POSITION (XCV) |
| | PUMP OUTLET PRESSURE (P1) |
| | PUMP INLET PRESSURE (P8) |
| | SERVOVALVE CONTROL PRESSURE HIGH SIDE (P2) |
| | SERVOVALVE CONTROL PRESSURE LOW SIDE (P3) |
| | SERVOVALVE CONTROL DIFFERENTIAL PRESSURE (P2-P3) |
| INTERNAL | SERVO PISTON PRESSURE (LARGE AREA, INCREASE FLOW SIDE) (PC1) |
| | SERVO PISTON PRESSURE (SMALL AREA, DECREASE FLOW SIDE) (PC2) |
| | SERVOVALVE POSITION (XCV) |
| | BALANCE PISTON POSITION TOP (XBP1) |
| | BALANCE PISTON POSITION BOTTOM (XBP2) |
| | SERVO PISTON POSITION (XP) |

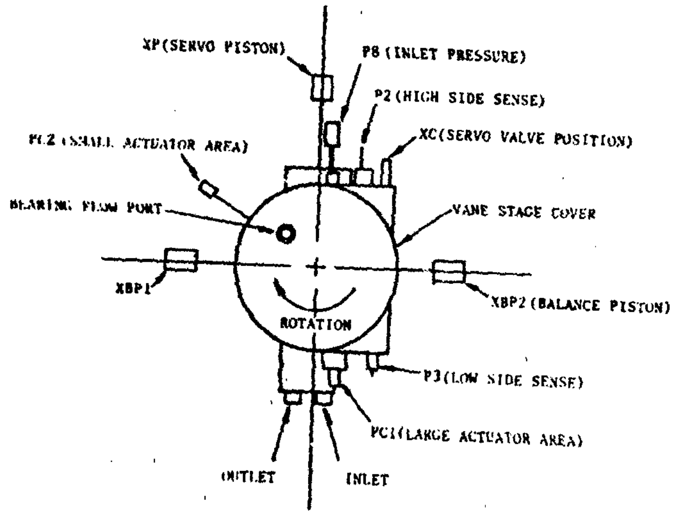


FIGURE 170. CECO MFP INSTRUMENTATION SCHEMATIC

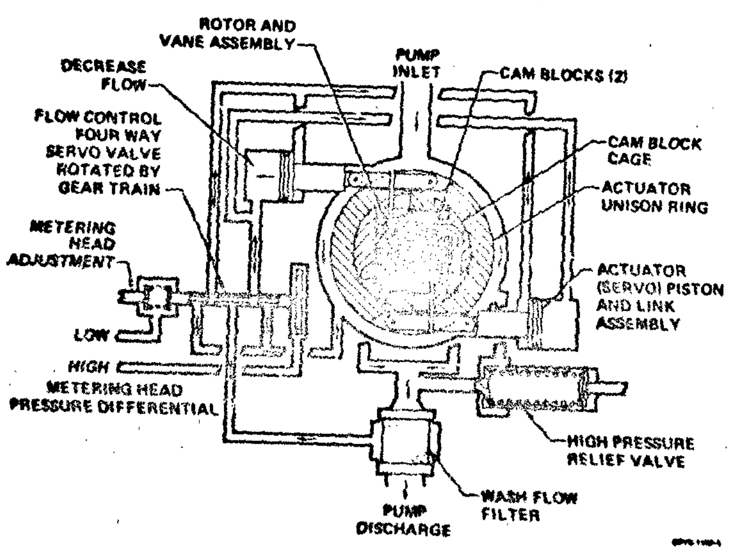


FIGURE 171. SCHEMATIC OF BALANCED VARIABLE DISPLACEMENT VANE PUMP AND CONTROLLER

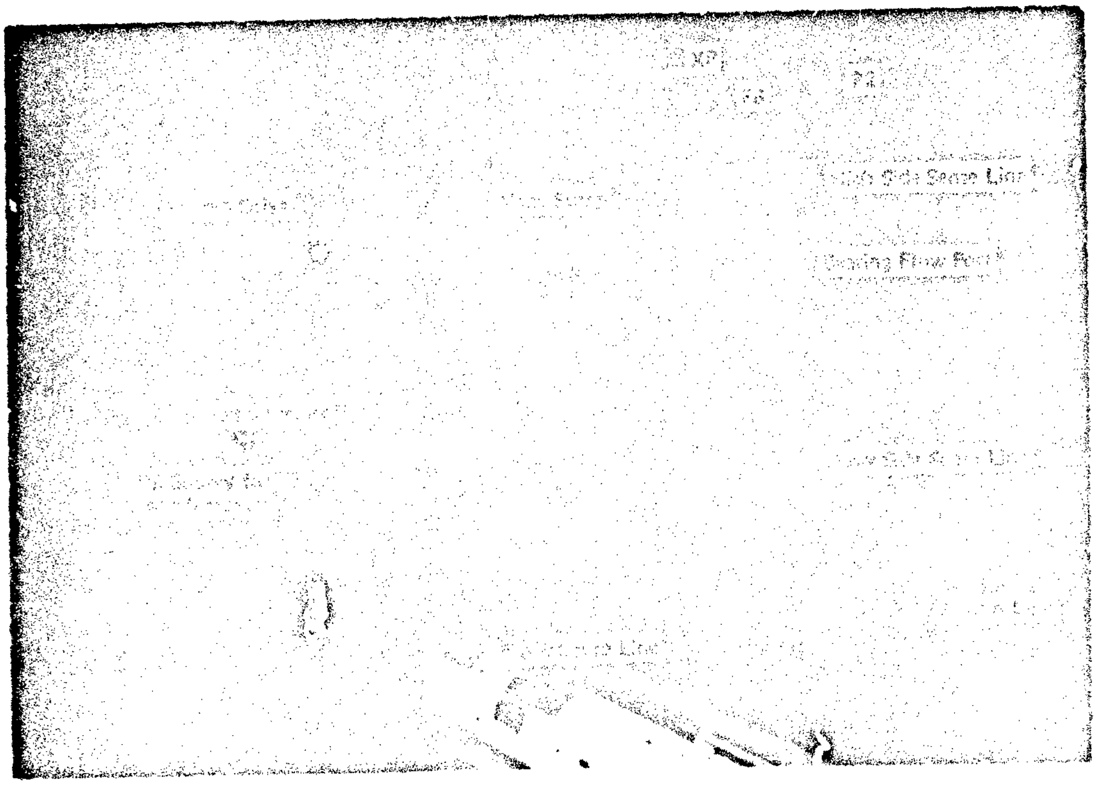

QP79-0899-4

FIGURE 172
**CECO VANE PUMP**

The transient flow control valve was a ball type hand valve located next to the P4 transducer in Figure 169. To obtain the desired transient flow changes in 20 and 40 milliseconds, the valve was powered by a hydraulic actuator attached to the valve lever arm. Figure 173 shows the control set-up for the transient flow valve. Flow rates at valve open and closed positions were regulated by adding spacers on the rod end of the actuator. The actuator was driven by an independent power supply. The accumulator was charged by system pressure then isolated from the system prior to the transient. An electrical signal to the servo valve provided the command to stroke the actuator.

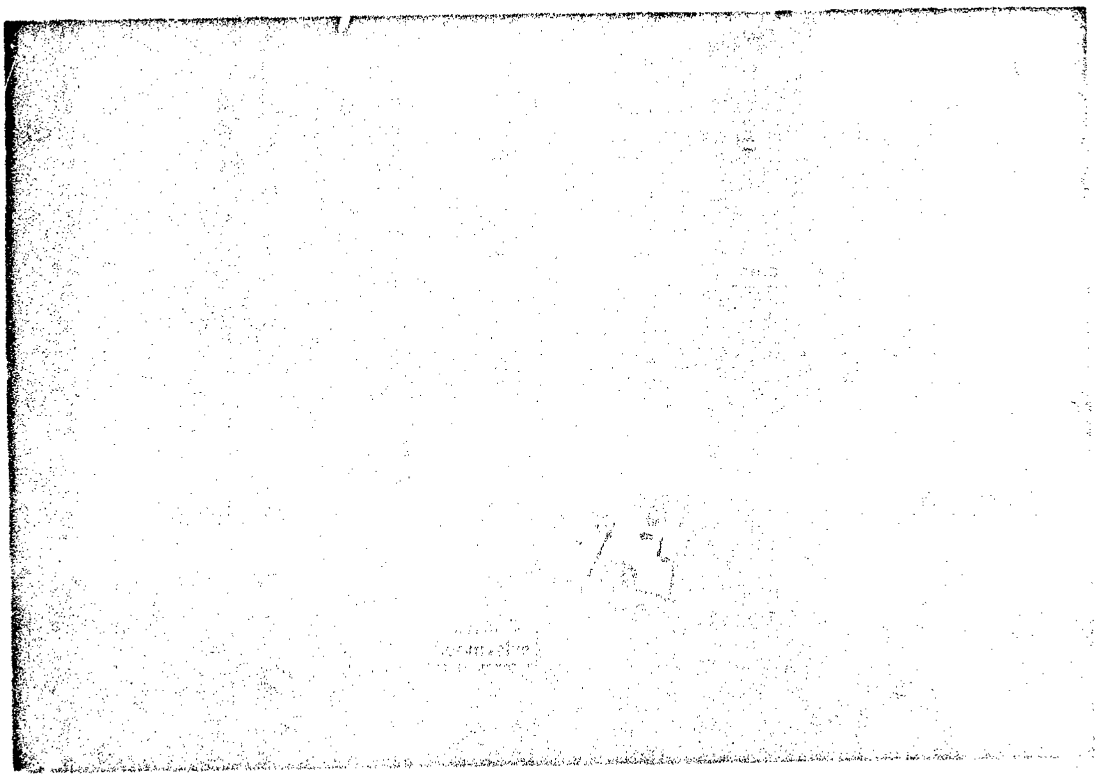

GP78-0899-2

**FIGURE 173**
**CONTROL SET-UP FOR METERING VALVE**

Transient tests in the lab were run to establish load level, loading rate, speed, temperature and inlet cavitation effects on the vane pump. Table 17 lists the tests that were made with the vane pump test set-up. When running the transient test steps were taken to assure that the pumps internal relief valve did not open. Also since the pump internal porting was timed for high flow conditions, the dwell time at low flow was minimized.

TABLE 17
CECO PUMP MODEL
TRANSIENT VERIFICATION TESTS

| Steady State Flow Rates (GPM) Hi | Lo | CTL Valve Operating Time (Sec) On | Off | Pump Speed (RPM) | Fluid Temp (°F) ±10°F | Reservoir Pressure (PSIG) | Run Number |
|---|---|---|---|---|---|---|---|
| 1. LOAD LEVEL EFFECTS | | | | | | | 97-10±XX |
| 35 | 8 | .020 | .020 | 15000 | 120 | 55 | 97-11±XX |
| 20 | 8 | .020 | .020 | 15000 | 120 | 56 | 97-12±XX |
| 2. LOADING RATE EFFECTS | | | | | | | |
| 35 | 8 | .040+ | .040+ | 15000 | 120 | 54 | 97-13±XX |
| 3. SPEED EFFECTS | | | | | | | |
| 35 | 8 | .020 | .020 | 11500 | 120 | 55 | 97-14±XX |
| 35 | 8 | .020 | .020 | 13500 | 120 | 55 | 97-15±XX |
| 4. TEMPERATURE EFFECTS | | | | | | | |
| 35 | 8 | .020 | .020 | 15000 | 210 | 54 | 97-16±XX |
| 5. INLET CAVITATION | | | | | | | |
| 35 | 8 | .020 | .020 | 15000 | 120 | 31 | 97-17±XX |
| 35 | 8 | .020 | .020 | 15000 | 120 | 21 | 97-18±XX |

NOTES: 1. ±XX denotes turn-on and turn-off transients

2. 97-10±XX same as run 97-11 except with ~700 psi back pressure

c. HYTRAN Simulation and Discussion

Test results for turn-on and turn-off transient runs were compared to the HYTRAN vane pump model. A computer simulation of the vane pump system was made with the HYTRAN program. The HYTRAN block diagram of the test system is shown in Figure 174. The elements which make up the system are divided into components and lines. The lines are numbered sequentially and have upstream and downstream ends. The components are also numbered in a separate sequence. Mode numbers are assigned to the points at which the flow divides or combines under steady state flow conditions and leg numbers are labeled between two nodes. The simulation consisted of running the HYTRAN program under lab test conditions. Initially, measured test data was used as boundary conditions in the simulation. The test data was too noisy and better results were achieved by modeling the entire test system. A turn-on transient was made with the test conditions similar to run number 97-13+XX. The turn-off transient was made with test conditions similar to run number 97-13-XX.

During the turn-on transient, flow through the metering valve was set at 30 CIS. Flow rate was initialized in the steady state portion of the program. Flow was then increased to 130 CIS by opening the flow control valve in approximately 40 milliseconds. The HYTRAN input data for the turn-on transient is listed in Table 18. The results of the computer simulation are presented in Figures 175 through 185.

The computed versus measured pump outlet pressure is plotted in Figure 175. Figures 176 and 177 show the comparison of the control pressures on the high and low side of the pumps internal servo valve. The pressure upstream of the transient flow valve is plotted in Figure 178, and Figure 179 is the pressure 34.0 inches along line number 7. The computed pressure data in these graphs indicate good transient correlation with the measured results. It appears that the final computed steady state pressure level is about 50 psi lower than the data even though Figure 180 indicates that the steady state flows are correct.

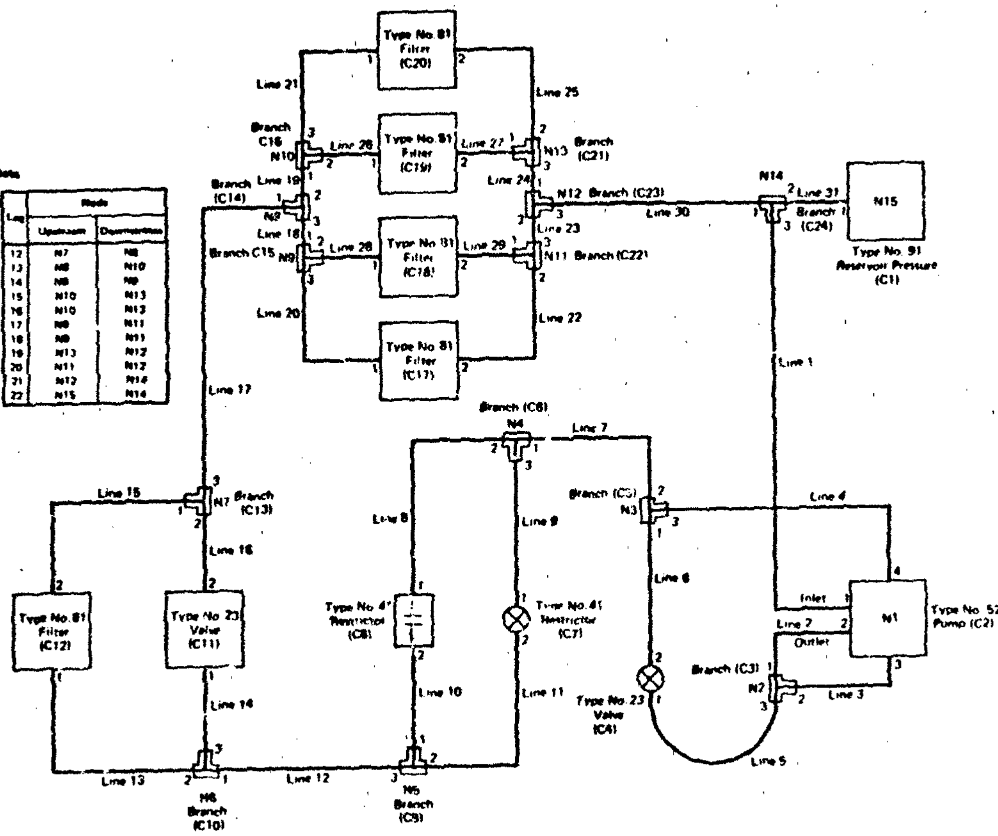


Leg Data

| Leg | Node Upstream | Node Downstream |
|---|---|---|
| 1 | N14 | N1 |
| 2 | N1 | N2 |
| 3 | N2 | N1 |
| 4 | N2 | N3 |
| 5 | N3 | N1 |
| 6 | N3 | N4 |
| 7 | N4 | N5 |
| 8 | N4 | N5 |
| 9 | N5 | N6 |
| 10 | N6 | N7 |
| 11 | N6 | N7 |
| 12 | N7 | N8 |
| 13 | N8 | N10 |
| 14 | N8 | N9 |
| 15 | N10 | N13 |
| 16 | N10 | N13 |
| 17 | N9 | N11 |
| 18 | N9 | N11 |
| 19 | N13 | N12 |
| 20 | N11 | N12 |
| 21 | N12 | N14 |
| 22 | N15 | N14 |

FIGURE 174. CECO VANE PUMP STEADY STATE AND TRANSIENT RESPONSE HYTRAN SCHEMATIC

# TABLE 18 HYTRAN INPUT DATA OF VANE FUMP TRANSIENT SIMULATION

```
****CECO VANE PUMP MODEL - 07-13-[illegible]****(DS/BON)

THE TRANSIENT RESPONSE IS FROM T=0.0 TO T= 1.030 SECONDS AT TIME INTERVALS OF DELT= .00050
WITH OUTPUT POINTS PLOTTED AT INTERVALS OF . .01000 SECONDS

FLUID DATA FOR MIL-H-5606 AT 400.0 PSIG, = 50.0 PSIG AND 120.0 DEG F IN 10.0 DEG F STEPS
                 VISCOSITY     = .174E-01     .169E-01IN**2/SEC
                 DENSITY       = .0075E-00    .800E-04(LB-SEC**2)/IN**4
                 BULK MODULUS  = .190E+06     .194E+06PSI
                 VAPOR PRESS.= .200E+01 AT 120.0 DEG F
FIX-UP TAKEN AT LINE 10,VEL OF SOUND IN LINE  8 IS   6.0PER CENT IN ERROR
FIX-UP TAKEN AT LINE 10,VEL OF SOUND IN LINE  9 IS  22.0PER CENT IN ERROR
FIX-UP TAKEN AT LINE 10,VEL OF SOUND IN LINE 10 IS  85.0PER CENT IN ERROR
FIX-UP TAKEN AT LINE 10,VEL OF SOUND IN LINE 11 IS  12.7PER CENT IN ERROR
FIX-UP TAKEN AT LINE 10,VEL OF SOUND IN LINE 31 IS  41.5PER CENT IN ERROR
```

| LINE DATA LINE NO. | LENGTH | INTERNAL DIA | WALL THICKNESS | MODULUS OF ELASTICITY | DELX | CHARACTERISTIC IMPEDANCE | VELOCITY OF SOUND |
|---|---|---|---|---|---|---|---|
| 1 | 85.0000 | .6000 | .0350 | .300E+08 | 32.5000 | 10.3751 | 46602.2281 |
| 2 | [illegible] | .6000 | .0350 | .300E+08 | 41.0000 | 10.3751 | 46602.2281 |
| 3 | 70.9000 | .2100 | .0200 | .300E+08 | 35.0000 | 111.4420 | 47022.3807 |
| 4 | 42.0000 | .2100 | .0249 | .300E+08 | 42.0000 | 111.4420 | 47022.3807 |
| 5 | 25.7250 | .6000 | .0350 | .300E+08 | 25.7500 | 10.3751 | 46602.2201 |
| 6 | 26.5000 | .6000 | .0350 | .300E+08 | 26.5000 | 10.3751 | 46602.2281 |
| 7 | 30.9000 | .6050 | .0350 | .300E+08 | 30.0000 | 10.3751 | 46602.2201 |
| 8 | 22.0000 | .9300 | .0350 | .300E+08 | 22.0000 | 5.4452 | 44000.0000 |
| 9 | 18.0000 | .6000 | .0350 | .300E+08 | 18.0002 | 10.3751 | 36000.0000 |
| 10 | 3.5000 | .6000 | .0350 | .300E+08 | 3.5000 | 10.3751 | 7600.0000 |
| 11 | 20.0000 | .9300 | .0350 | .300E+08 | [illegible] | 5.4452 | 48000.0000 |
| 12 | 33.5000 | .9300 | .0350 | .300E+08 | 33.5000 | 5.4452 | 45026.5741 |
| 13 | 26.0000 | .9300 | .0350 | .300E+08 | 26.0000 | 5.4452 | 45026.5741 |
| 14 | 33.0000 | .6600 | .0500 | .300E+08 | 33.0000 | 6.2081 | 47206.6609 |
| 15 | 26.0000 | .8040 | .0500 | .300E+08 | 26.0000 | 6.2081 | 47206.6609 |
| 16 | 26.0000 | .8030 | .0500 | .300E+08 | 26.0000 | 6.2081 | 47206.6609 |
| 17 | 33.5000 | .8040 | .0590 | .300E+08 | 33.5000 | 6.2081 | 47206.6609 |
| 18 | 25.0000 | .8040 | .0500 | .300E+08 | 25.0009 | 6.2081 | 47206.6609 |
| 19 | 25.0000 | .6340 | .0500 | .300E+08 | 25.0000 | 12.2122 | 47705.4155 |
| 20 | 25.0000 | .6940 | .0200 | .300E+08 | 25.0000 | 9.8229 | 46036.0701 |
| 21 | 50.0000 | .6940 | .0200 | .300E+08 | 25.0000 | 9.8229 | 46036.0701 |
| 22 | 25.0000 | .6940 | .0200 | .300E+08 | 25.0000 | 9.8229 | 46036.0701 |
| 23 | 25.0000 | .6940 | .0200 | .300E+08 | 25.0000 | 9.8229 | 46036.0701 |
| 24 | 25.0000 | .6940 | .0200 | .300E+08 | 25.0000 | 9.8229 | 46036.0701 |
| 25 | 25.0000 | .6940 | .0200 | .300E+08 | 25.0000 | 9.8229 | 46036.0701 |
| 26 | 25.0000 | .6940 | .0260 | .300E+08 | 25.0000 | 9.8229 | 46036.0701 |
| 27 | 25.0000 | .6940 | .0200 | .300E+08 | 25.0000 | 9.8229 | 46036.0701 |
| 28 | 25.0000 | .6940 | .0200 | .300E+08 | 25.0000 | 9.8229 | 46036.0701 |
| 29 | 25.0000 | .6940 | .0200 | .300E+08 | 25.0000 | 9.8229 | 46036.0701 |
| 30 | 40.3000 | .6940 | .0200 | .300E+08 | 40.3000 | 9.8227 | 46036.0701 |
| 31 | 13.0000 | .6940 | .0200 | .300E+08 | 13.0000 | 9.8229 | 26000.0030 |

```
COMP.   1 INTEGER DATA     1  61   1 -31   0   0   0   0   0   0   0   0   0   0   0   0
REAL DATA CARD #   1   .7700E+02 0.         0.         0.         0.         0.         0.         0.
COMP.   2 INTEGER DATA     2  52  15   1  -7   3   4  11  11   4   0   0   0   0   0   3
REAL DATA CARD #   1   .4900E-01 .5000E+02 .2940E+01 .9430E-03 .1960E+01 .6500E+00 -.1500E-01 .3500E-01
REAL DATA CARD #   2   .1112E+01 .7753E+00 .6500E+00 .1600E+00 .2000E-03 .1000E+01 .5045E+00 .1500E+05
REAL DATA CARD #   3   .5000E-01 .3900E+00 .3807E-11 .2000E+01 .3033E+02 .1563E+03 .3425E+02 0.
REAL DATA CARD #   4   0.         .6504E-01 .1300E+00 .1950E+04 .2600E+00 .3250E+00 .3966E+00 .6550E+00
REAL DATA CARD #   5   .5200E+00 .9450E+00 .6500E+00 .2520E+03 .5000E+03 .7500E+03 .1000E+04 .9200E+01
REAL DATA CARD #   6   .7000E+01 .4000E+01 .3900E+01 .2560E+01 .2000E+01 .1200E+01 .1400E+01 .5000E+00
REAL DATA CARD #   7   .1040E+01 .1203E+01 .5000E+02 .4705E+02 .3530E+02 .2360E+02 .1500E+02 .1000E+02
REAL DATA CARD #   8   .6000E+01 .3900E+01 .1700E+01 .3900E+01 .6800E+01 .1130E+03 .9728E+02 .6950E+02
REAL DATA CARD #   9   .4300E+02 .2900E+02 .1900E+02 .1210E+02 .7000E+01 .3003E+01 .7000E+01 .1210E+01
REAL DATA CARD #  10   .1720E+03 .1390E+03 .1050E+03 .6500E+02 .4400E+02 .2900E+02 .1045E+02 .1000E+02
REAL DATA CARD #  11   .4000E+01 .1890E+02 .1840E+02 .1000E+01 .0375E+00 .0087E+00 .0075E+00 .3375E+02
REAL DATA CARD #  12   .2257E+05 .1375E+00 .8130E+01 .3750E+01 .1870E-01 0.         0.         .3008E+02
REAL DATA CARD #  13   .6000E-02 .9900E-02 .1290E+01 .1500E-01 .1000E-01 .2100E-01 .2400E-01 .2770E-01
REAL DATA CARD #  14   .3000E-01 .1000E+00 .1400E-03 .2750E-03 .4200E-03 .5900E-03 .7400E-03 .1270E-02
```

TABLE 18 (CONTINUED)
HYTRAN INPUT DATA

THIS PAGE IS BEST QUALITY PRACTICABLE
FROM COPY FURNISHED TO DDC

```
REAL DATA CARD #   13   .1700E+02  .2550E+03  .3350E+02  .4470E+03 0.        0.        0.        0.
 COMPO,   3 INTEGER DATA   3  11   0   2  -3  -4   0   0   0   0   0   0   0   0   0   0
 COMPO,   4 INTEGER DATA   4  26   1   5  -6   0   0   0   0   0   0   0   0   0   0   0
REAL DATA CARD #    1   .5200E+06  .6504E+00 0.        0.        0.        0.        0.        0.
REAL DATA CARD #    2  0.          .1500E+00  .1900E+00  .1000E+01 0.        0.        0.        0.
REAL DATA CARD #    3   .3000E+01  .3000E 01  .1000E+00  .1000E+00 0.        0.        0.        0.
 COMPO,   5 INTEGER DATA   5  11   0   6  -6  -7   0   0   0   0   0   0   0   0   0   0
 COMPO,   6 INTEGER DATA   6  11   0   7  -8  -9   0   0   0   0   0   0   0   0   0   0
 COMPO,   7 INTEGER DATA   7  41   1   9 -11   0   0   0   0   0   0   0   0   0   0   0
REAL DATA CARD #    1   .1000E+00  .6500E+00 0.        0.        0.        0.        0.        0.
 COMPO,   8 INTEGER DATA   8  41   1   8 -10   0   0   0   0   0   0   0   0   0   0   0
REAL DATA CARD #    1   .5000E+00  .6500E+00 0.        0.        0.        0.        0.        0.
 COMPO,   9 INTEGER DATA   9  11   0  10  11 -12   0   0   0   0   0   0   0   0   0   0
 COMPO,  10 INTEGER DATA  10  11   0  12 -13 -14   0   0   0   0   0   0   0   0   0   0
 COMPO,  11 INTEGER DATA  11  21   3  14 -16   0   0   0   0   0   0   0   0   0   0   0
REAL DATA CARD #    1   .1000E+01  .6650E+06 0.        0.        0.        0.        0.        0.
REAL DATA CARD #    2  0.          .1000E+01  .2000E+01  .1000E+01 0.        0.        0.        0.
REAL DATA CARD #    3  0.         0.        0.        0.        0.        0.        0.        0.
 COMPO,  12 INTEGER DATA  12  41   1  13 -15   0   0   0   0   0   0   0   0   0   0   0
REAL DATA CARD #    1   .1000E+00  .1000E+00  .7421E+01  .1000E+01 0.        0.        0.        0.
 COMPO,  13 INTEGER DATA  13  11   0  15  16 -17   0   0   0   0   0   0   0   0   0   0
 COMPO,  14 INTEGER DATA  14  11   0  17 -18 -19   0   0   0   0   0   0   0   0   0   0
 COMPO,  15 INTEGER DATA  15  11   0  16 -20 -28   0   0   0   0   0   0   0   0   0   0
 COMPO,  16 INTEGER DATA  16  11   0  19 -21 -20   0   0   0   0   0   0   0   0   0   0
 COMPO,  17 INTEGER DATA  17  41   1  20 -22   0   0   0   0   0   0   0   0   0   0   0
REAL DATA CARD #    1   .4020E+01  .4020E+01  .4050E+02  .1055E+00 0.        0.        0.        0.
 COMPO,  18 INTEGER DATA  18  41   1  28 -24   0   0   0   0   0   0   0   0   0   0   0
REAL DATA CARD #    1   .4020E+01  .4020E+01  .4050E+02  .1055E+00 0.        0.        0.        0.
 COMPO,  19 INTEGER DATA  19  41   1  24 -27   0   0   0   0   0   0   0   0   0   0   0
REAL DATA CARD #    1   .4020E+01  .4020E+01  .4050E+02  .1055E+00 0.        0.        0.        0.
 COMPO,  20 INTEGER DATA  20  41   1  21 -25   0   0   0   0   0   0   0   0   0   0   0
REAL DATA CARD #    1   .4020E+01  .4020E+01  .4050E+02  .1055E+00 0.        0.        0.        0.
 COMPO,  21 INTEGER DATA  21  11   0  26  27 -28   0   0   0   0   0   0   0   0   0   0
 COMPO,  22 INTEGER DATA  22  11   0  22  29 -33   0   0   0   0   0   0   0   0   0   0
 COMPO,  23 INTEGER DATA  23  11   0  25  26 -30   0   0   0   0   0   0   0   0   0   0
 COMPO,  24 INTEGER DATA  24  11   0  30  31  -1   0   0   0   0   0   0   0   0   0   0
 CPU TIME IN SECONDS = [illegible]
                              STEADY STATE INPUT DATA
       NUMBER OF NODES = 13     NUMBER OF LEGS = 18     NUMBER OF CONSTANT PRESSURE NODES = 0

                              LEG CONNECTION INPUT DATA
 LEG NO      UPST NODE NO   DNST NODE NO   NO OF ELEMENTS   FLOW GUESS   UPST PRESS   DNST PRESS
 [illegible]

 LEG NO      ELEMENTS IN LEG
 [illegible]
```

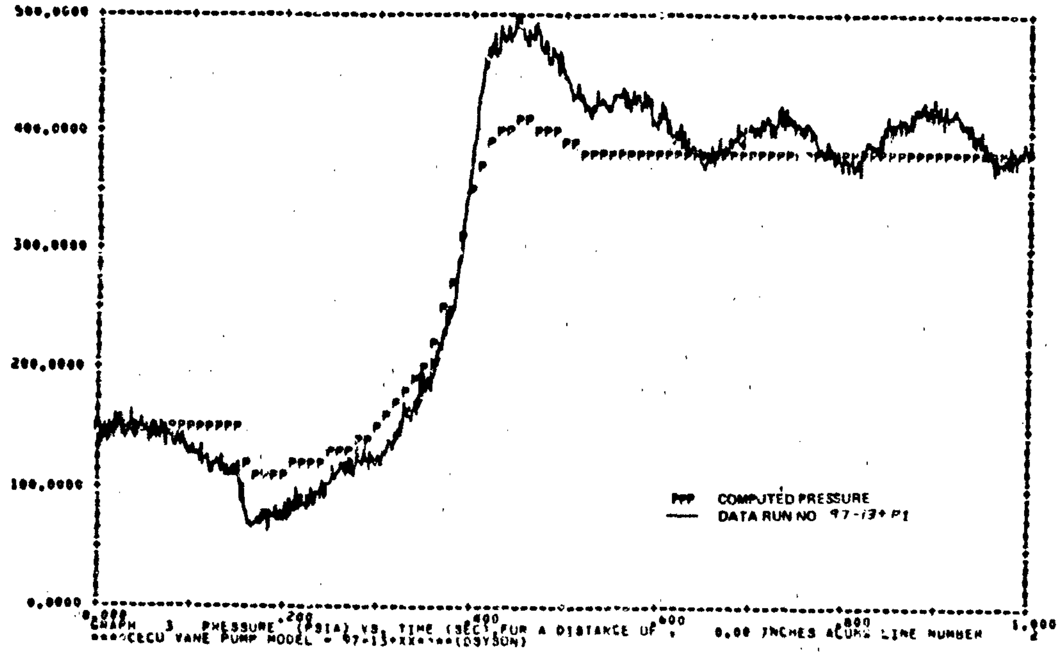


FIGURE 175. OUTLET PRESSURE 8-35 GPM TURN-ON TRANSIENT
120°F 15,000 RPM

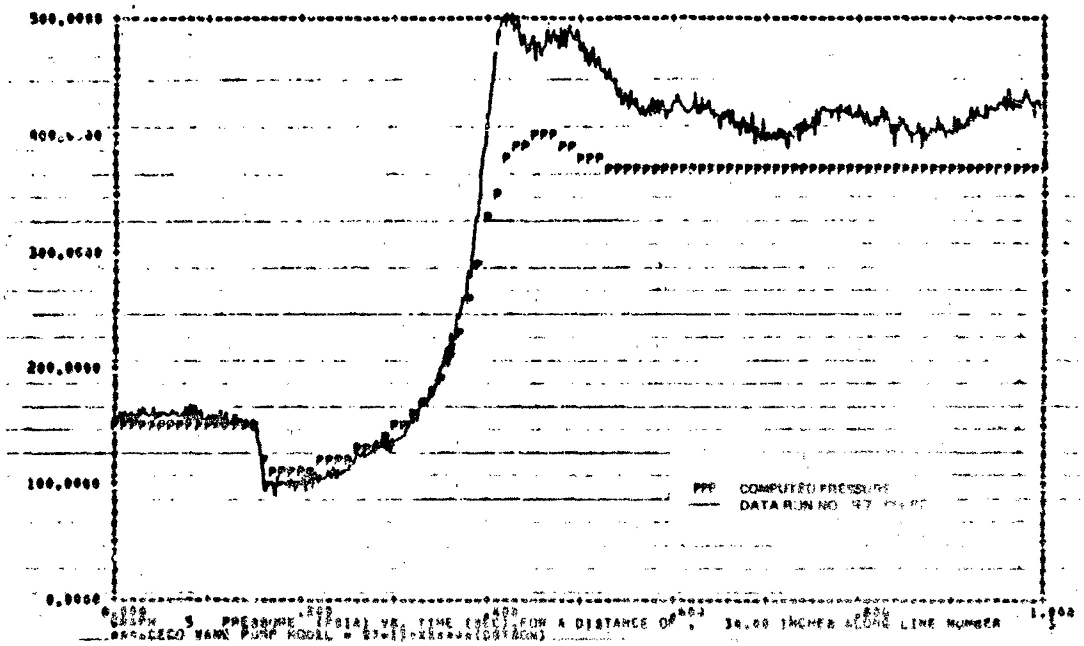


URE 176. CONTROL PRESSURE 8-36 GPM TURN-ON TRANSIENT
120°F 15,000 RPM

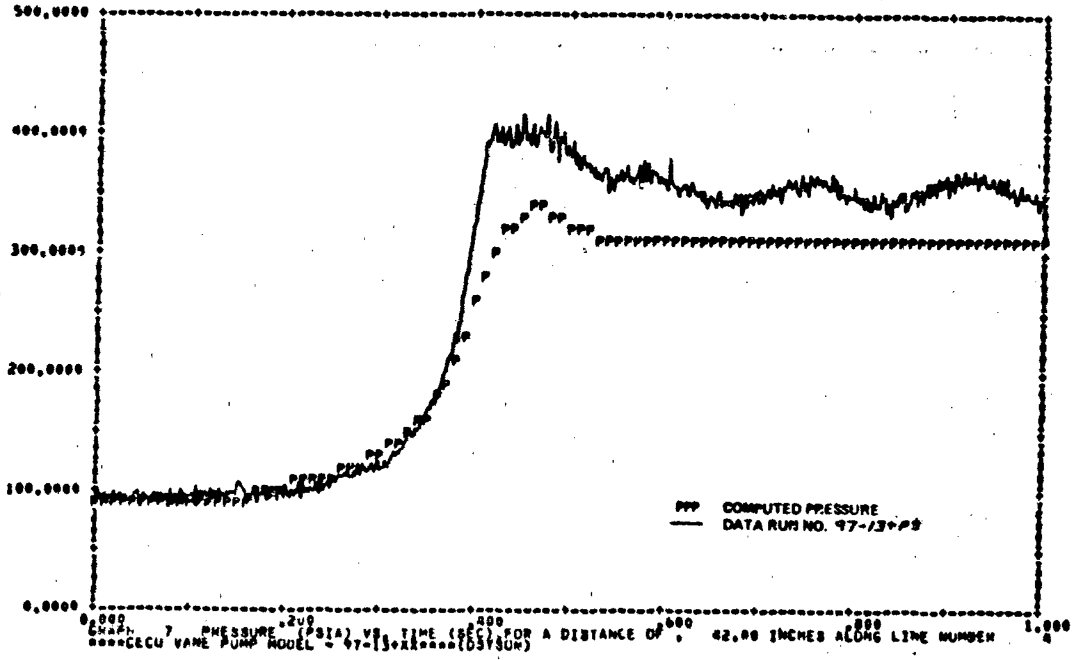


FIGURE 177. CONTROL PRESSURE 8-35 GPM TURN-ON TRANSIENT
120°F 15,000 RPM

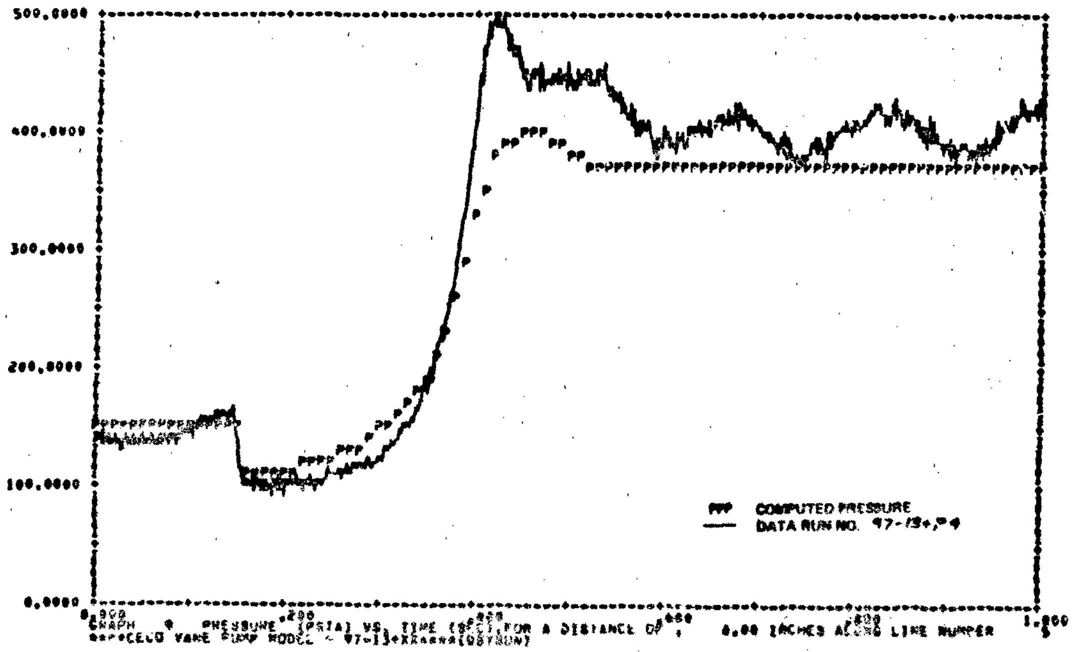


FIGURE 178. CONTROL VALVE PRESSURE 8-35 GPM TURN-ON TRANSIENT
120°F 15,000 RPM

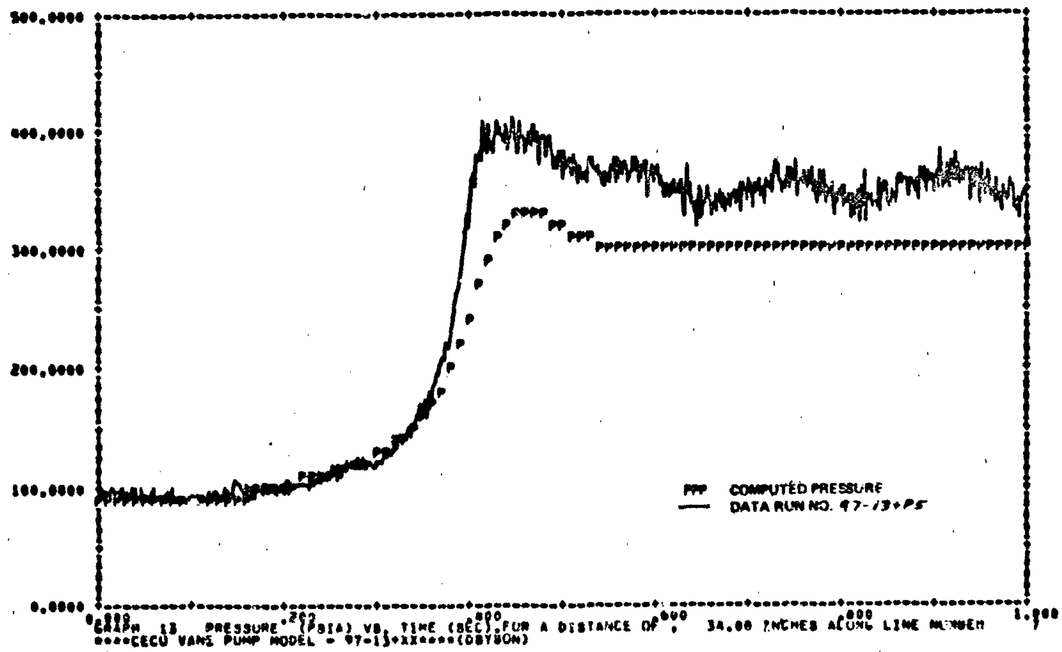


FIGURE 179. SYSTEM RETURN PRESSURE 8-35 GPM TURN-ON TRANSIENT
120°F 15.000 RPM

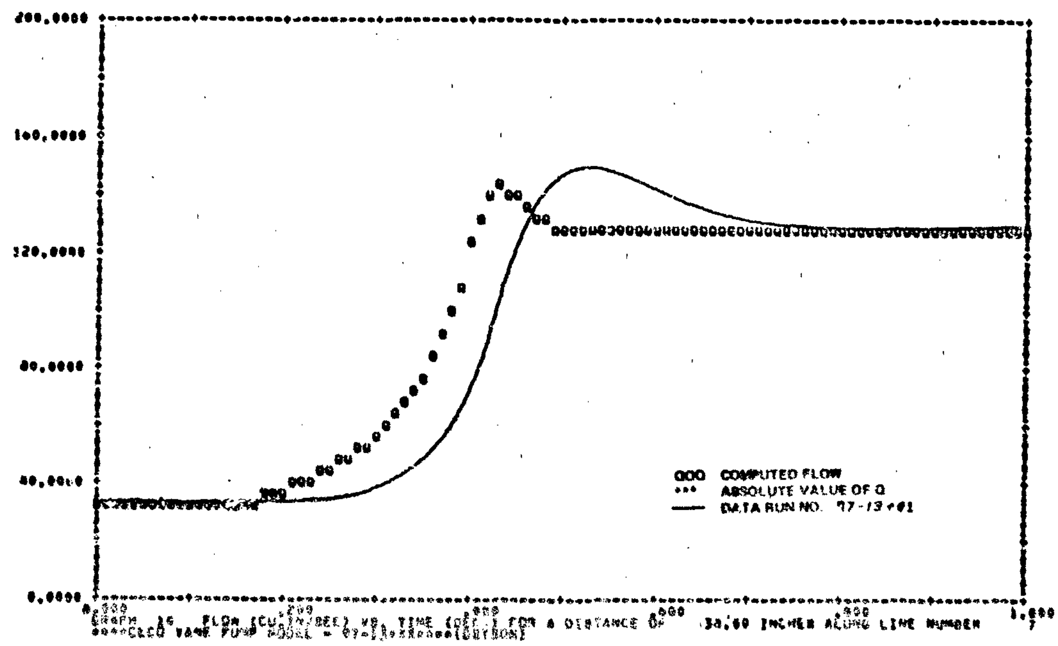


FIGURE 180. RETURN FLOW 8-35 GPM TURN-ON TRANSIENT
120°F 15,000 RPM

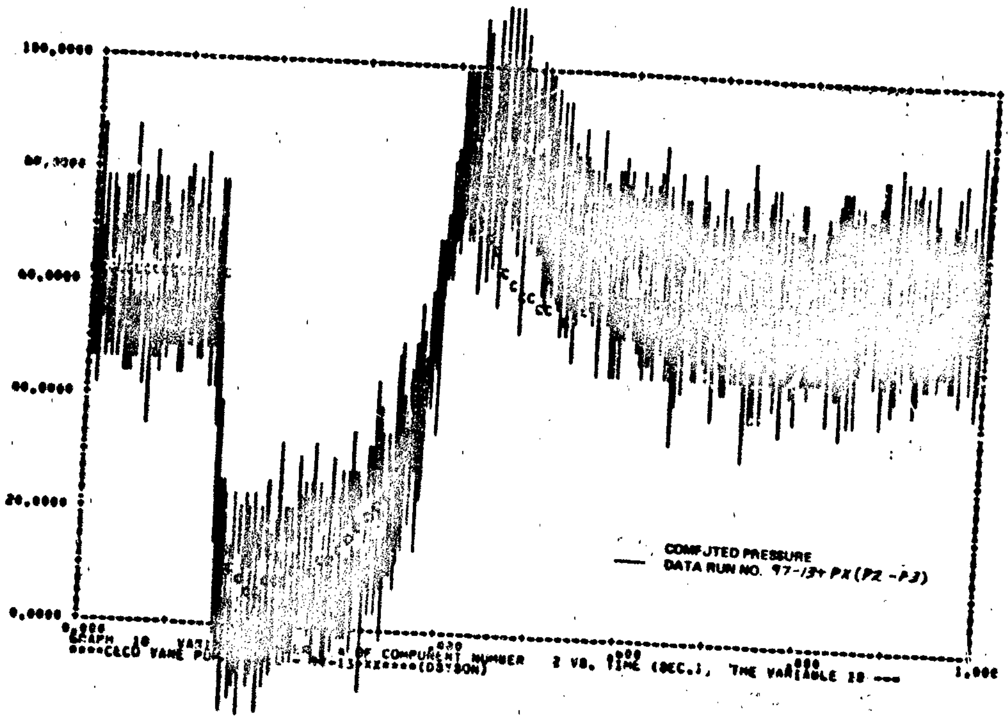


FIGURE 181. DIFFERENTIAL PRESSURE 8-35 GPM TURN-ON TRANSIENTS
120°F 15,000 RPM

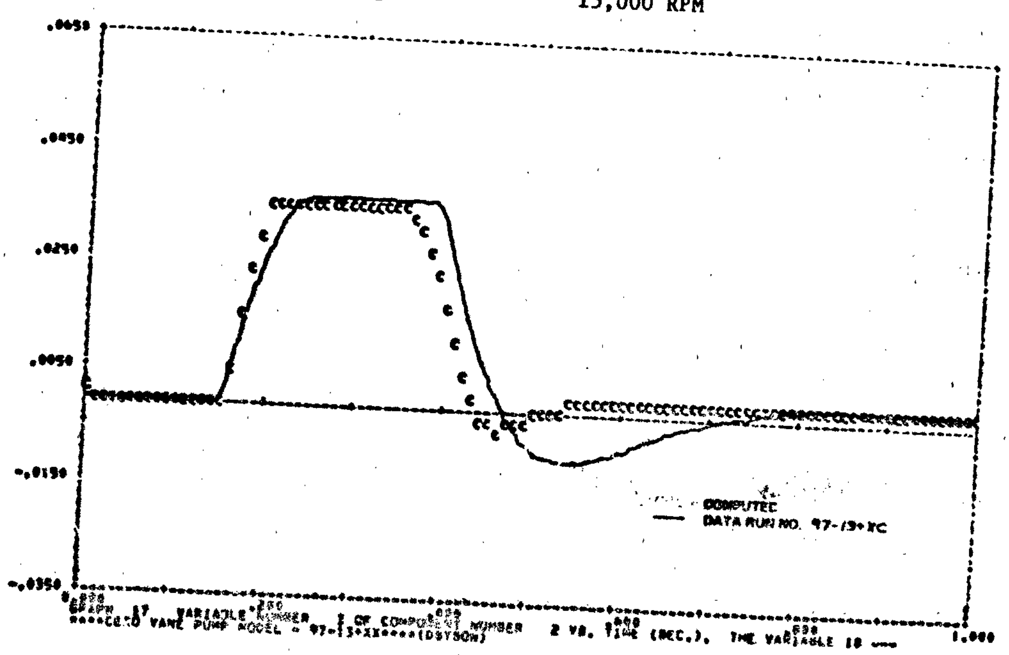


FIGURE 182. SERVOVALVE POSITION 8-35 GPM TURN-ON TRANSIENT
120°F 15,000 RPM

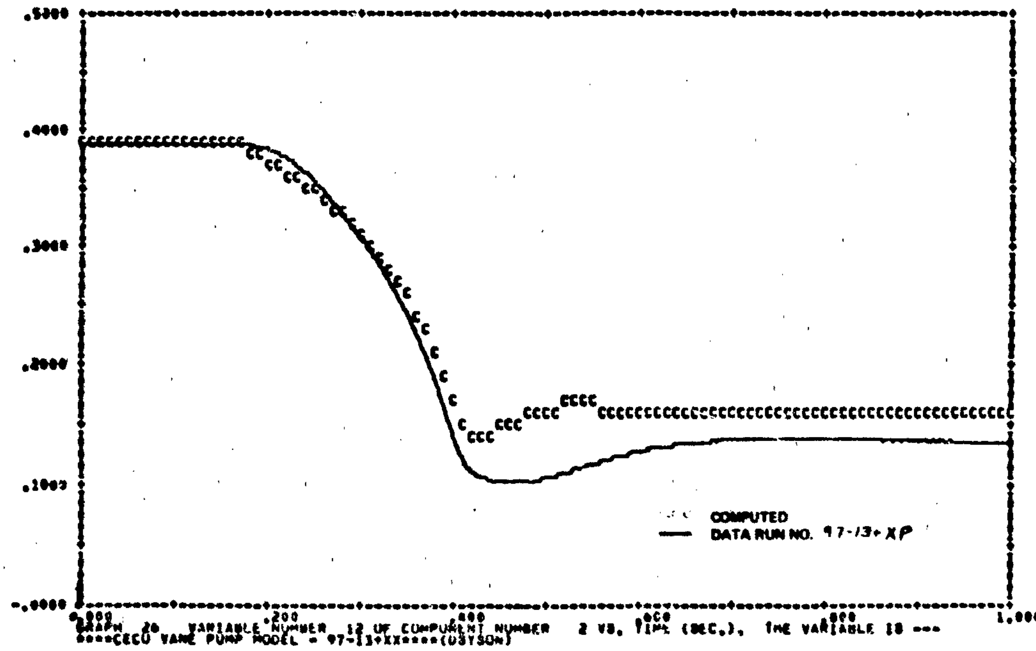


FIGURE 183. SERVO PISTON POSITION 8-35 GPM TURN-ON TRANSIENT
120°F 15,000 RPM

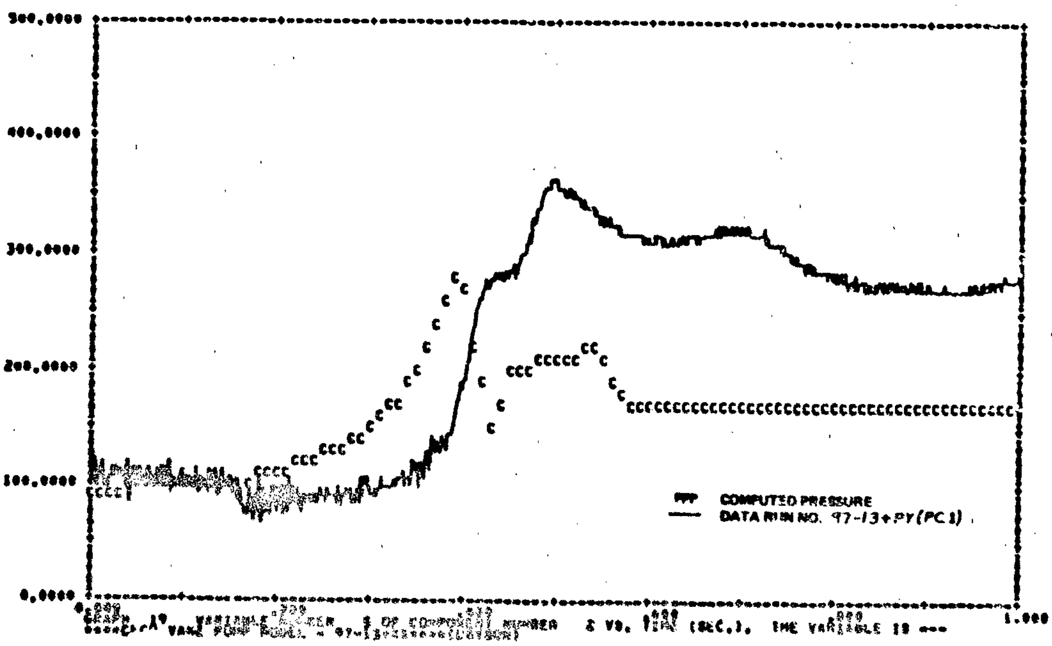


FIGURE 184. SERVO PISTON PRESSURE 8-35 GPM TURN-ON TRANSIENT
120°F 15,000 RPM

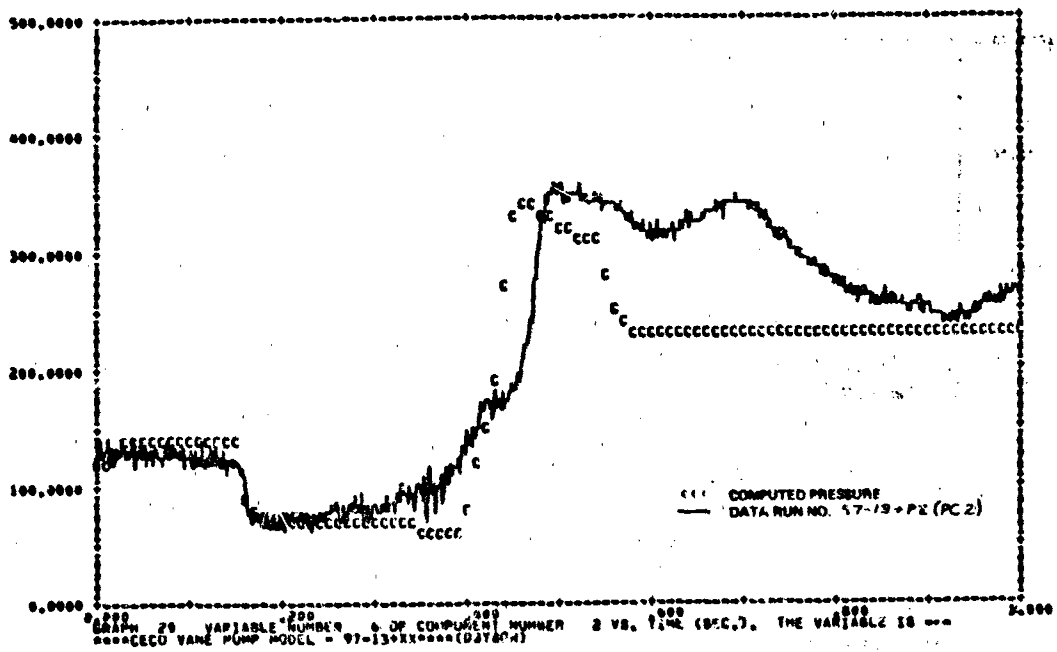


FIGURE 185. SERVO PISTON PRESSURE 8-35 GPM TURN-ON TRANSIENT
120°F 15,000 RPM

The computed metering head pressure differential in Figure 181 corresponds well to the measured data. The data noise results from instrumentation error in subtracting the two control signals (P2 and P3). The servo valve displacement in Figure 182 and the actuator position in Figure 183 correlate very well to test data. However, the slight delay in moving the servo valve back to the null position results in the computation of erroneous actuator pressures (Figures 184 and 185). Actuator friction and stiction are not taken into account in this model. Also the loading on the actuators under transient operating conditions is not well defined. These areas of the model can be improved with more thorough test data than the set-up in the hydraulics lab was to obtain.

Plots of the turn-off transient simulation at the same test conditions are shown in Figures 186 through 198. Again the slight delay in the computed servo valve position in Figure 195 causes the actuator pressures to be incorrect, although there is better correlation than for the turn-on case. The addition of an accurate pressure dependent load curve on the actuator would probably improve this simulation.

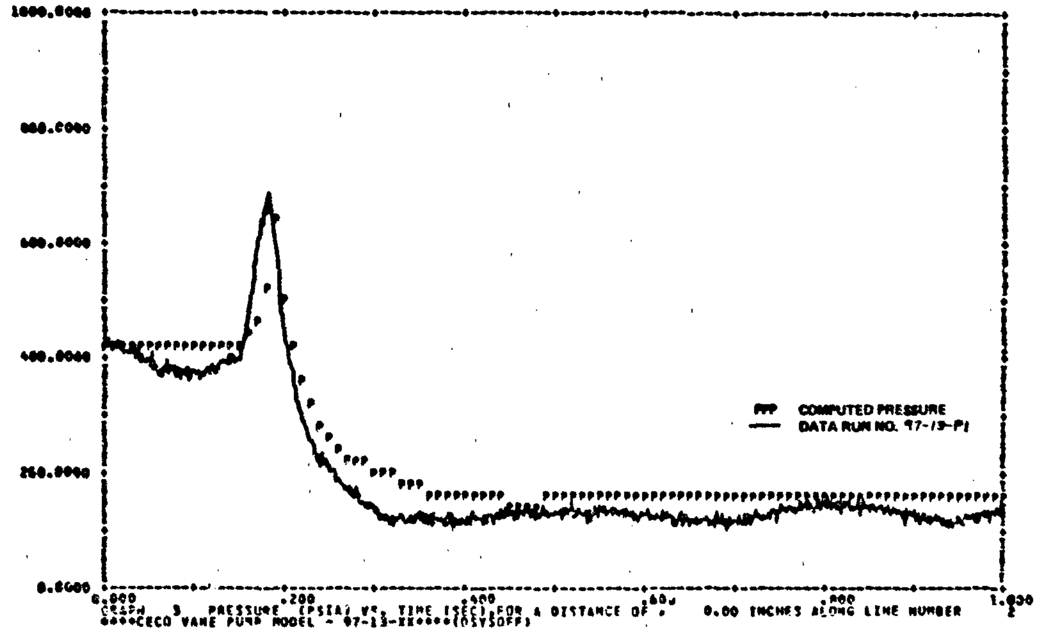


FIGURE 186. OUTLET PRESSURE 35-8 GPM TURN-OFF TRANSIENT
120°F 15,000 RPM

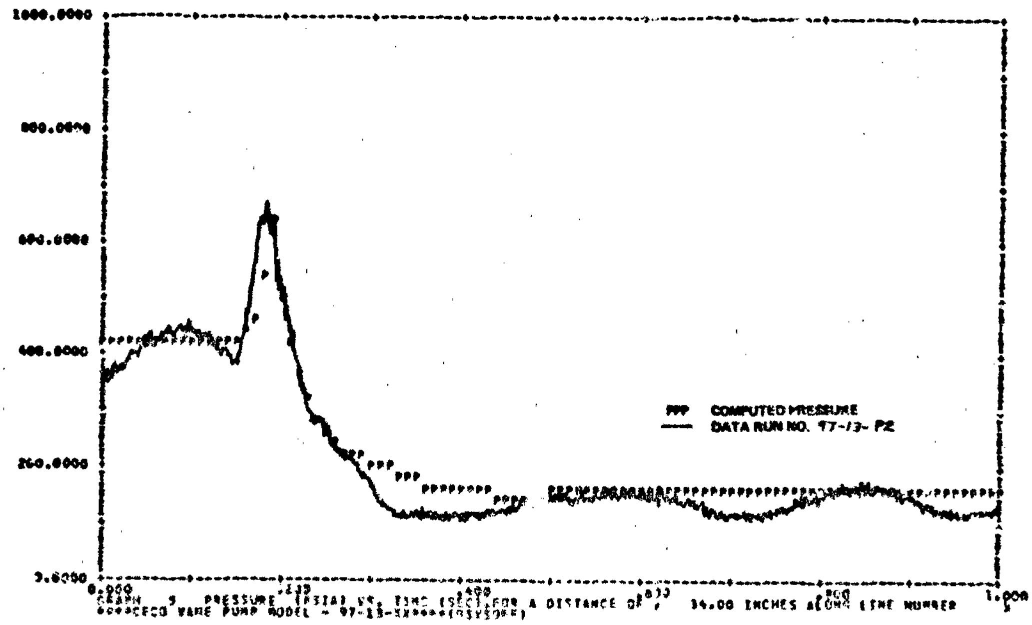


FIGURE 187. CONTROL PRESSURE 35-8 GPM TURN-OFF TRANSIENT
120°F 15,000 RPM

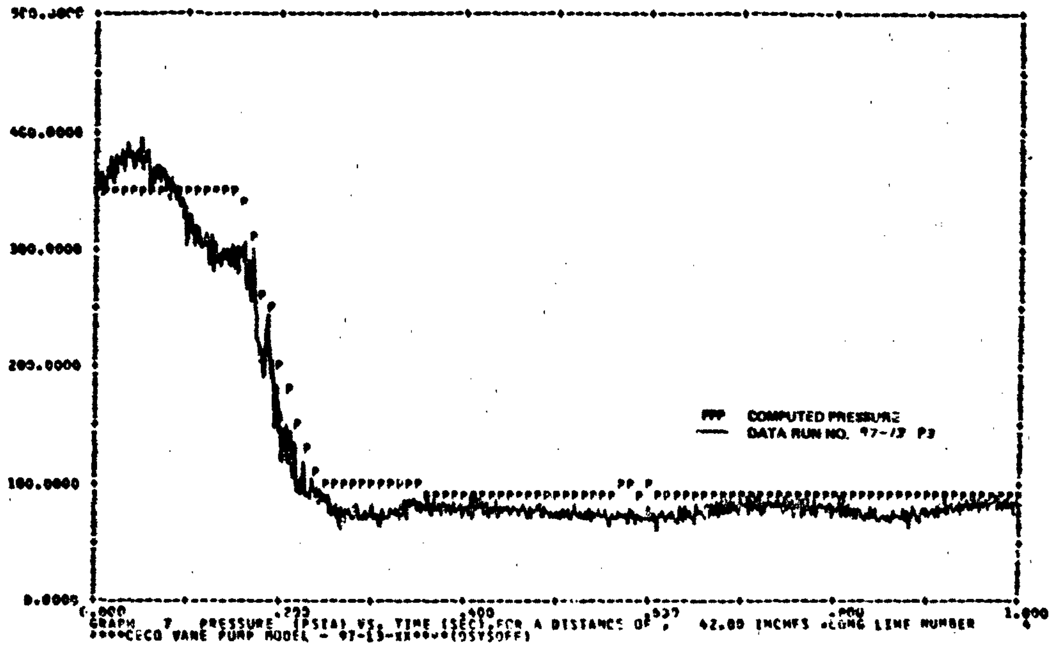

FIGURE 188. CONTROL PRESSURE 35-8 GPM TURN-OFF TRANSIENT
120°F 15,000 RPM

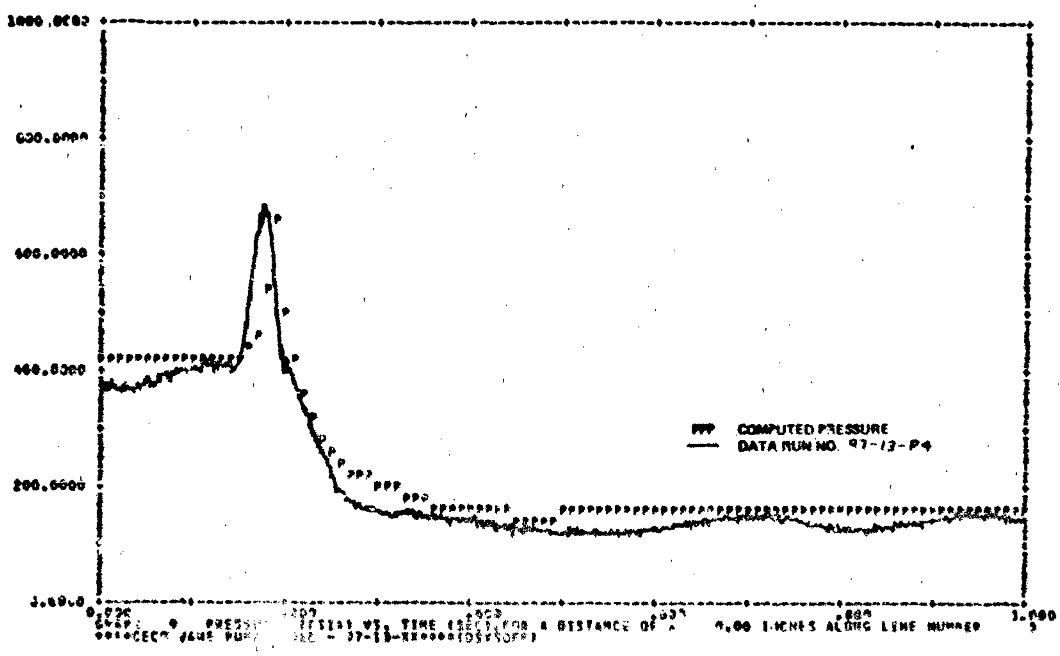

FIGURE 189. CONTROL PRESSURE 35-8 GPM TURN-OFF TRANSIENT
120°F 15,000 RPM

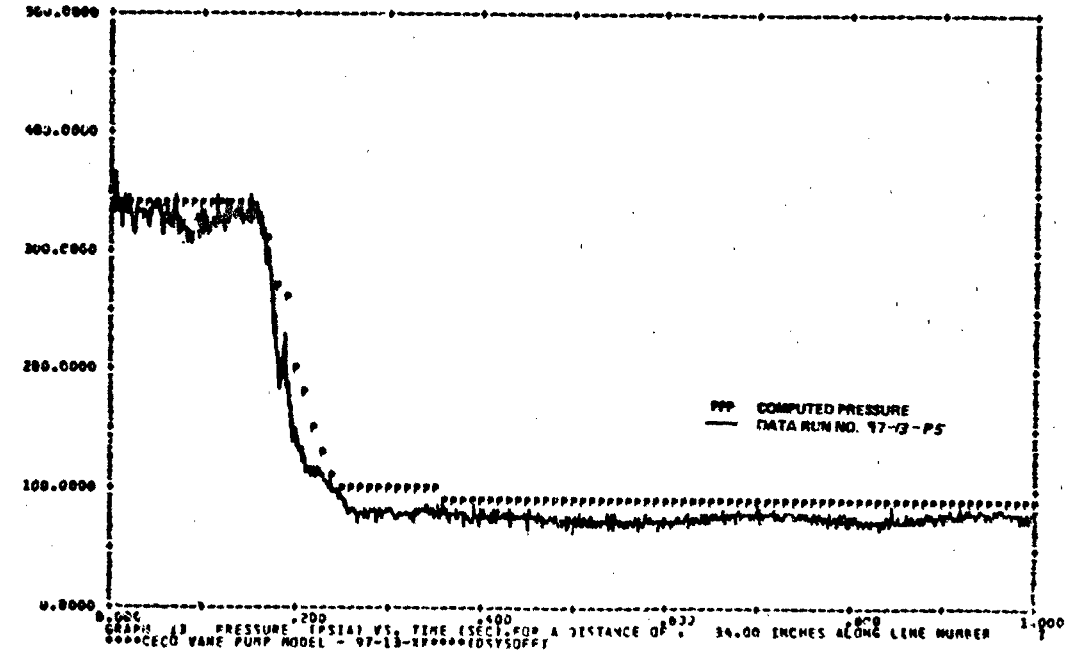


FIGURE 190. SYSTEM RETURN PRESSURE 35-8 GPM TURN-OFF TRANSIENT
120°F 15,000 RPM

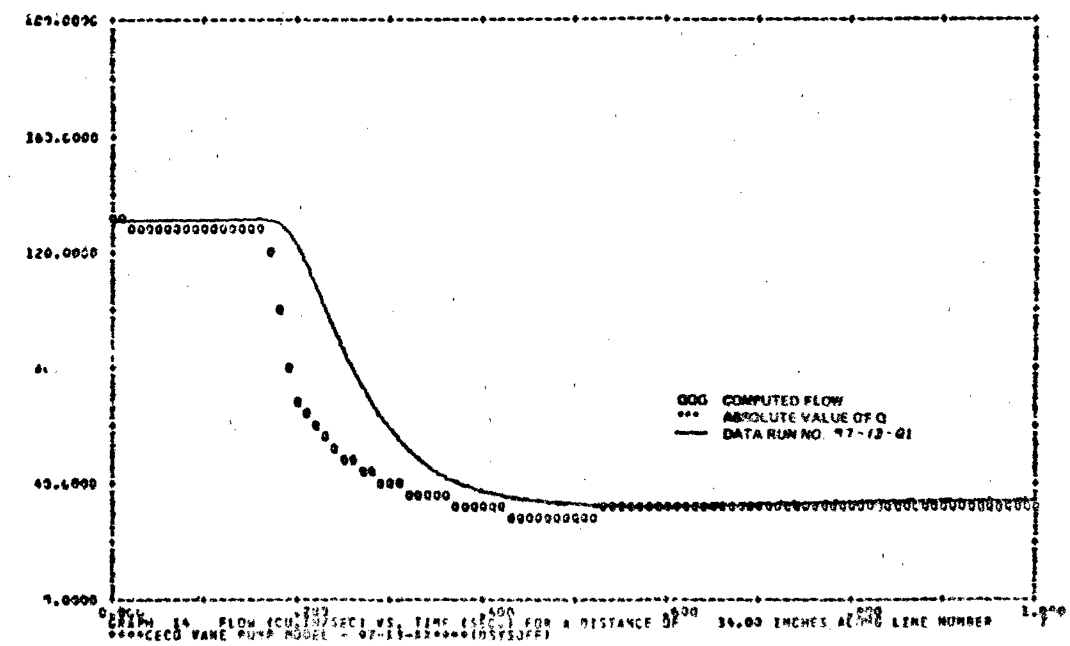


FIGURE 191. RETURN FLOW 35-8 GPM TURN-OFF TRANSIENT
120°F 15,000 RPM

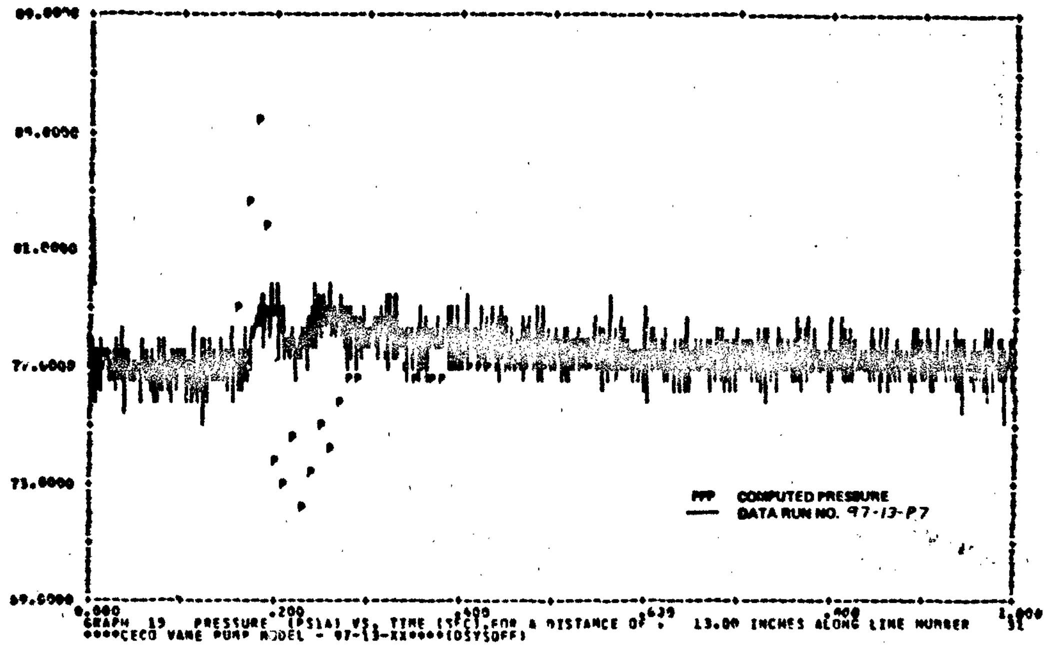


FIGURE 192. SYSTEM RETURN PRESSURE 35-8 GPM TURN-OFF TRANSIENT
120°F 15,000 RPM

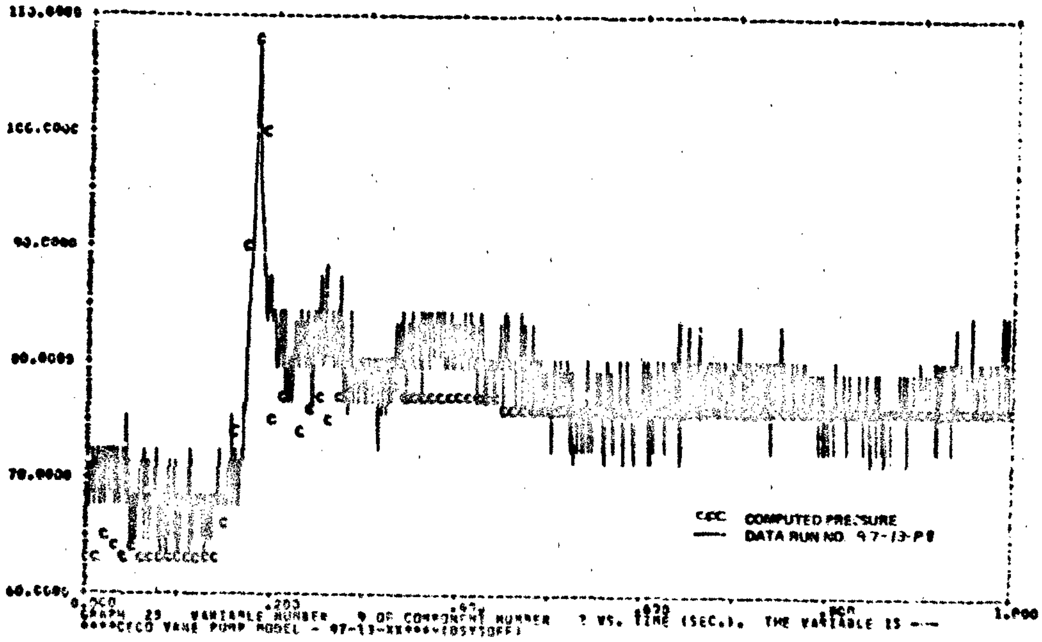


FIGURE 193. INLET PRESSURE 35-8 GPM TURN-OFF TRANSIENT
120°F 15,000 RPM

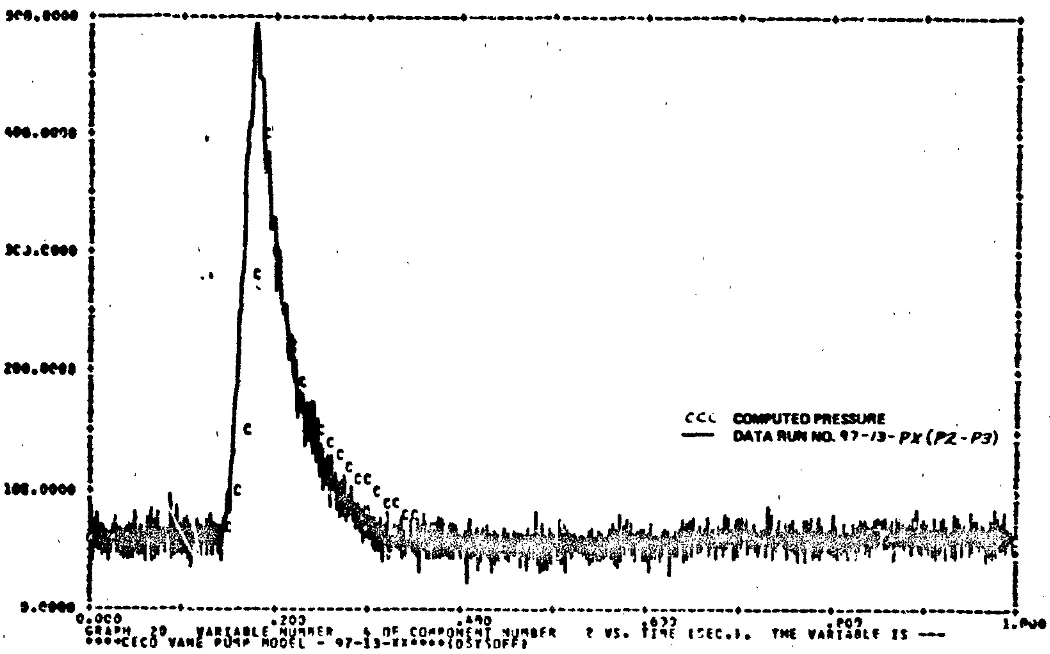


FIGURE 194. DIFFERENTIAL PRESSURE 35-8 GPM TURN-OFF TRANSIENT
120°F 15,000 RPM

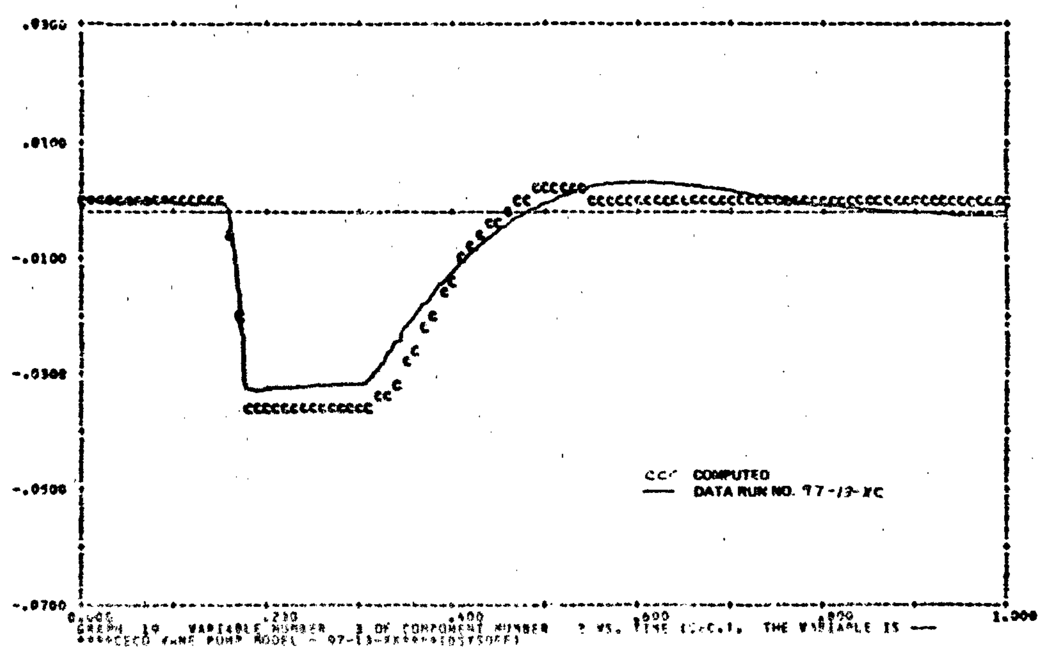


FIGURE 195. SERVOVALVE POSITION 35-8 GPM TURN-OFF TRANSIENT
120°F 15,000 RPM

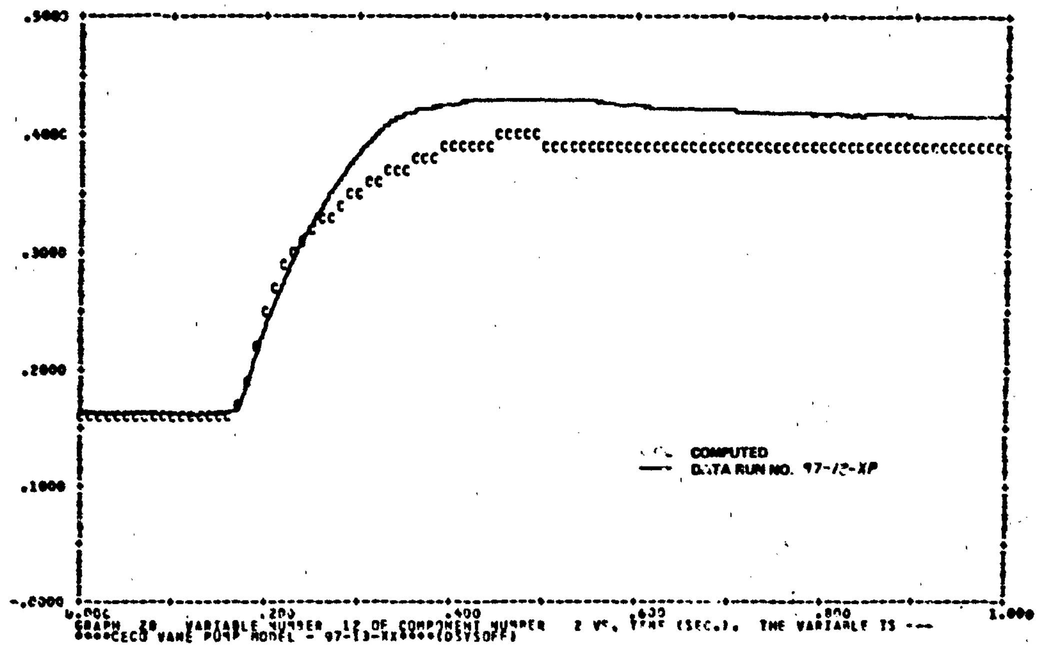


FIGURE 196. SERVO PISTON POSITION 35-8 GPM TURN-OFF TRANSIENT
120°F 15,000 RPM

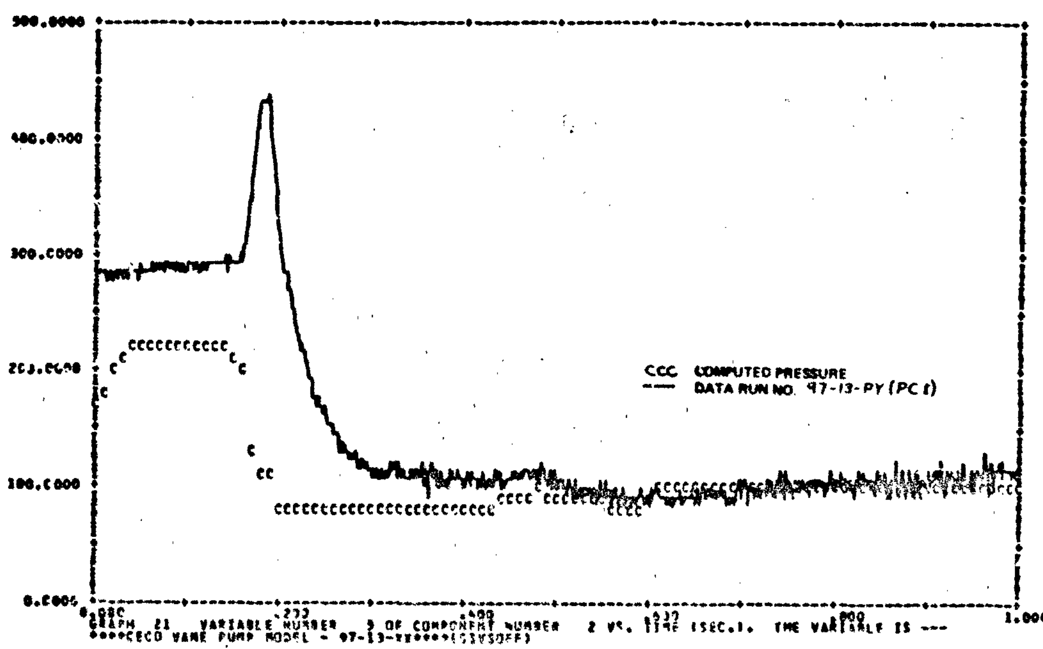


FIGURE 197. SERVO PISTON EXTEND PRESSURE 35-8 GPM TURN-OFF TRANSIENT
120°F 15,000 RPM

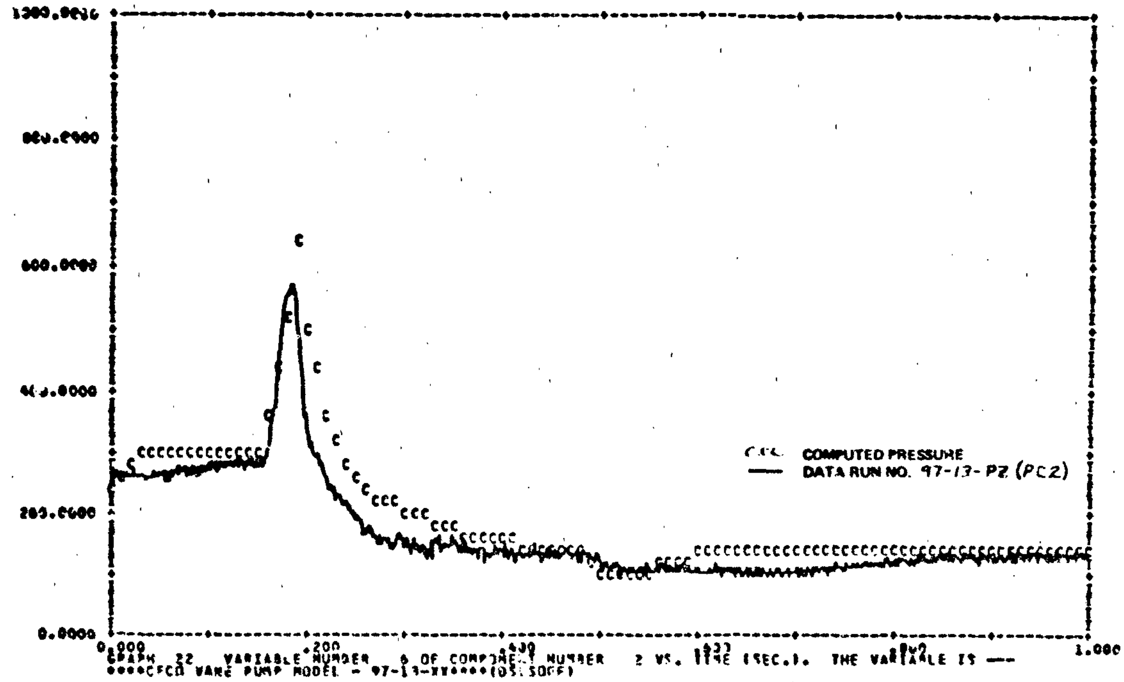


FIGURE 198. SERVO PISTON RETRACT PRESSURE 35-8 GPM TURN-OFF TRANSIENT
120°F 15,000 RPM

The turn-on transient simulation was repeated. The initial volumes of the actuator were decreased. This resulted in slightly better phase correlation with the actuator pressures and pump outlet flows as shown in Figures 199, 200 and 201. However, the computed outlet pressures is now leading the measured values. Knowing the accurate volumes of the retract and extend side of the actuator would provide the correct phasing between the model results and the data. The lack of a good actuator loading function during the transient probably prohibited the correlation of the actuator pressures.

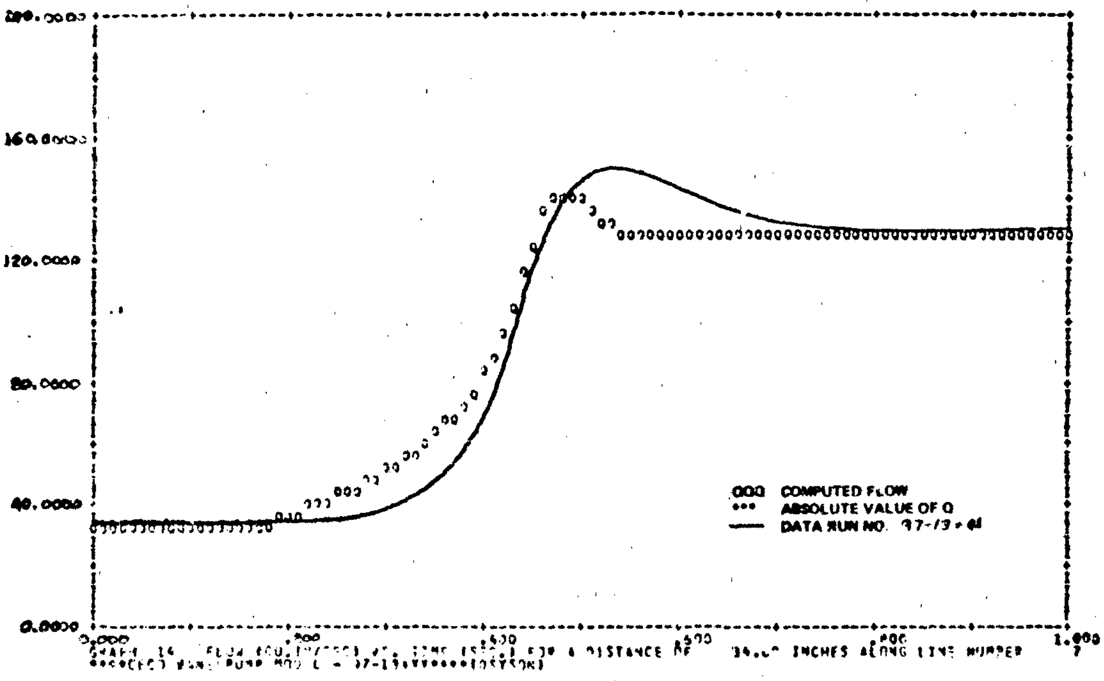


FIGURE 199. RETURN FLOW 8-35 GPM TURN-ON TRANSIENT
120°F 15,000 RPM

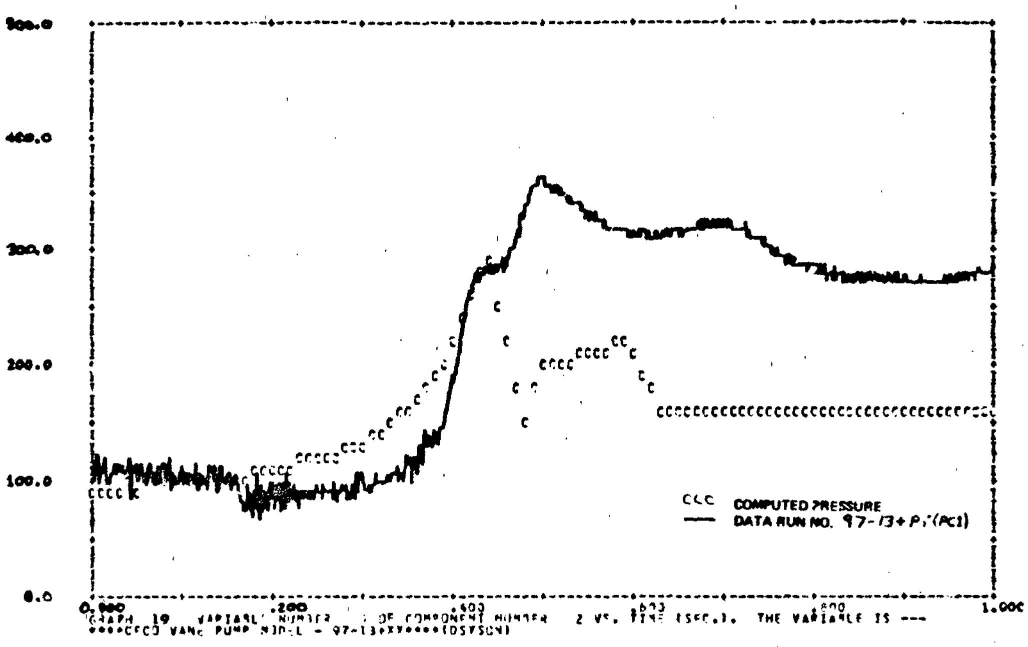


FIGURE 200. SERVO PISTON EXTEND PRESSURE 8-35 GPM TURN-ON TRANSIENT
120°F 15,000 RPM

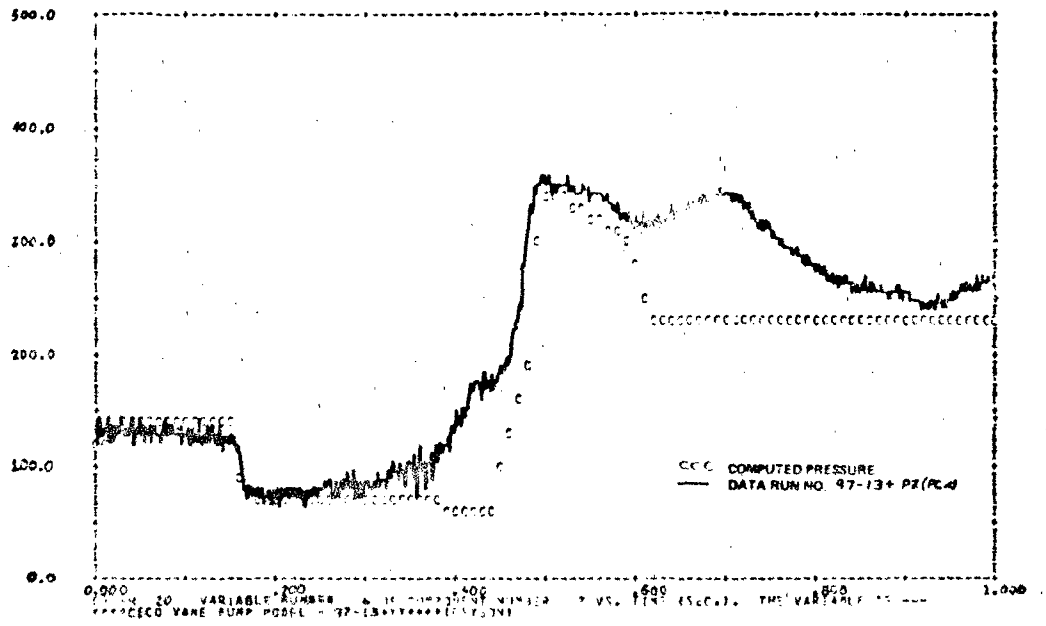


FIGURE 201. SERVO PISTON RETRACT PRESSURE 8-35 GPM TURN-ON TRANSIENT
120°F 15,000 RPM

## 3. STEADY STATE TESTS

Steady state tests were performed on the instrumented vane pump. The runs were made on the circuit shown in Figure 202. Test conditions involved flow and speed sweeps at 120°F and 210°F. Table 19 presents a listing of the completed steady state tests. The pump parameters recorded during the steady state testing were:

- Pump outlet pressure (P1)
- Pump outlet flow (Q1)
- Servo piston pressure (large area) (PC1)
- Servo piston pressure (small area) (PC2)
- Servo valve control differential pressure (P2-P3)
- Servo piston position (XP)
- Balance piston position top (XBP2)
- Balance piston position bottom (XBP1)

Figure 203 shows the pump outlet pressure for a flow sweep at 15000 RPM. The flow was varied by a hand operated metering valve. The outlet pressure is directly proportional to the flow and the curve represents the pressure/flow characteristics of the system. The piston position in Figure 204 is shown moving to the fully extended position, which corresponds to the minimum cam displacement and maximum pump outlet flow.

Sweeping the pump RPM from 4000 to 15000 RPM provided the vane pump operating characteristics. The metering valve was set to regulate the flow at 35 gpm. Figures 205 and 206 show how the pump outlet pressure and flow gradually attain the required values. In Figure 207 the control pressure signal is increasing until it reaches the required 60 psid across the metering valve. The balance piston in Figure 208 then starts moving at 9200 RPM as the cam adjusts to maintain a constant flow.

The servo piston position in Figure 209 shows that the piston is at a minimum position (corresponding to max flow) until the pump goes on control. Then the piston backs off the maintain the desired flow rate. A rough estimate of the internal leakage was made from these steady state plots. The leakage was assumed to be directly proportional to the vane stage pressure rise. A simplified formula for internal leakage was used.

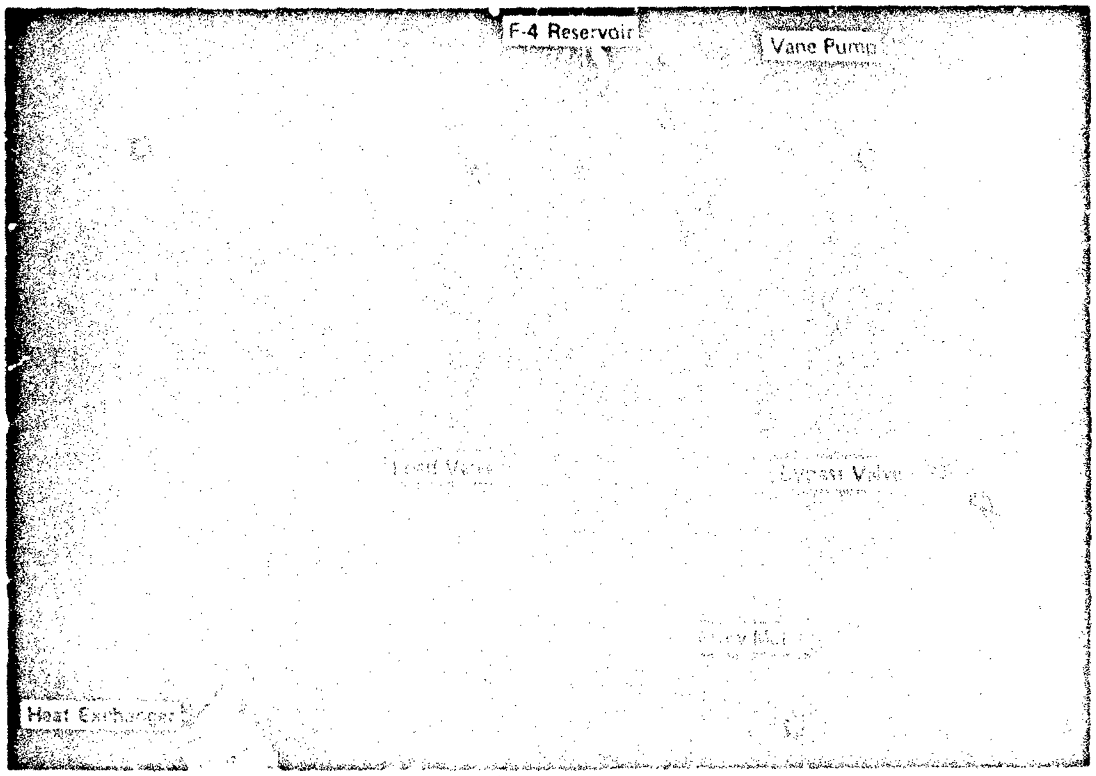


GP78-0899 3

**FIGURE 202**
**CECO VANE PUMP STEADY STATE AND TRANSIENT TEST SETUP**

TABLE 19 CECO VANE PUMP STEADY STATE TESTS

| SPEED (RPM) | FLOW (GPM) | FLUID TEMPERATURE (°F) |
|---|---|---|
| Sweep (4000-15000) | 8 | 120 |
| Sweep (4000-1500) | 25 | 120 |
| Sweep (4000-15000) | 35 | 120 |
| 11500 | 8-25 | 120&210 |
| 13500 | 8-30 | 120&210 |
| 15000 | 8-36 | 120 |

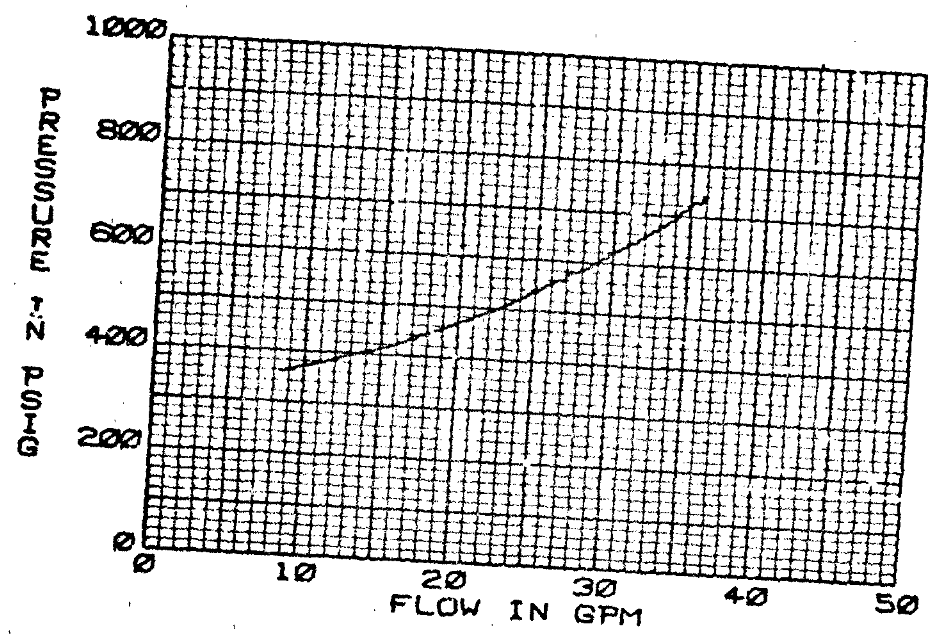


FIGURE 203. CECO MFP-330 VANE PUMP 97-03-P1 STEADY STATE TEST 15,000 RPM 120°F

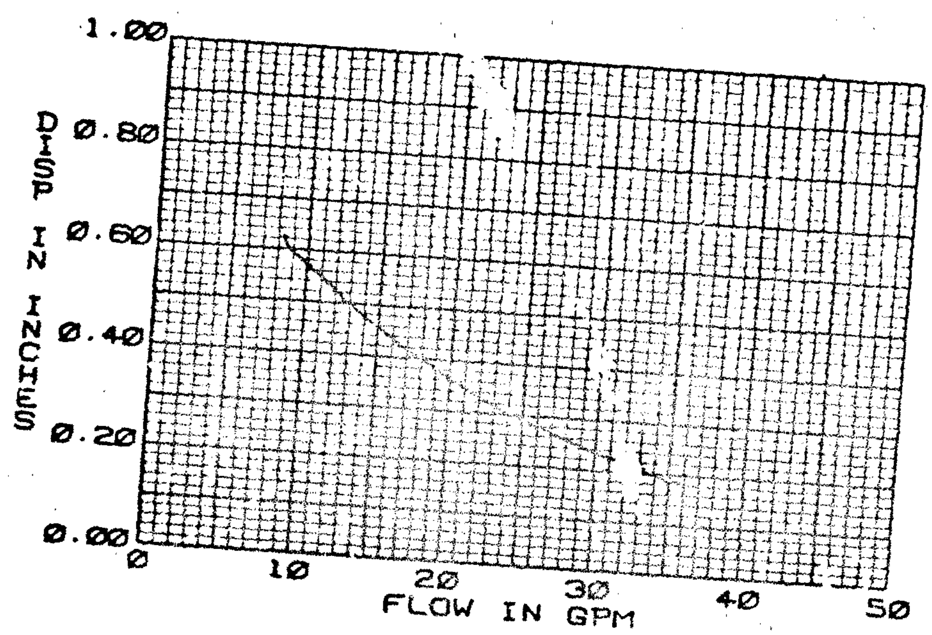


FIGURE 204. CECO MFP-330 VANE PUMP 97-03-XP STEADY STATE TEST 15,000 RPM 120°F

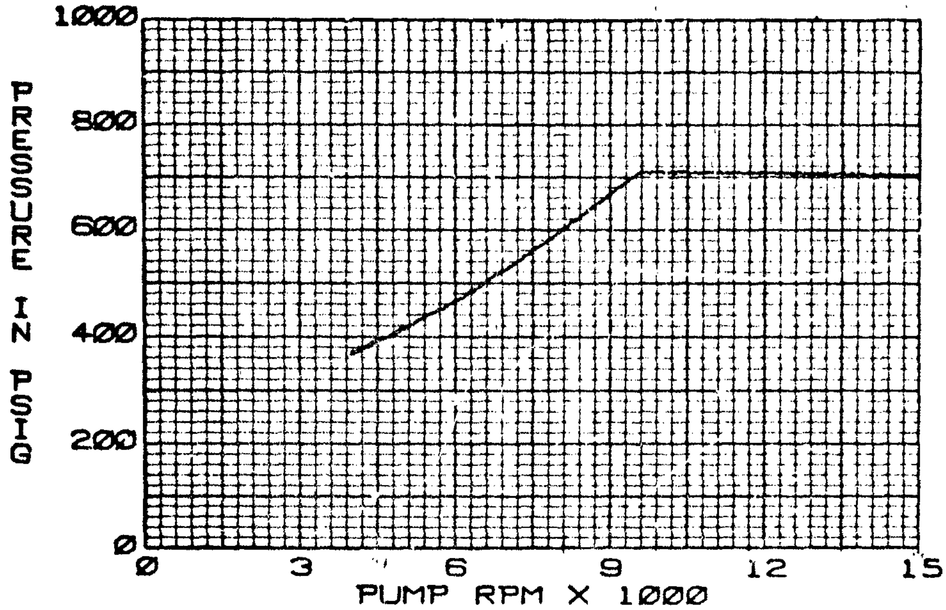


FIGURE 205. CECO MFP-330 VANE PUMP 97-07-P1 STEADY STATE TEST
35 GPM 120°F

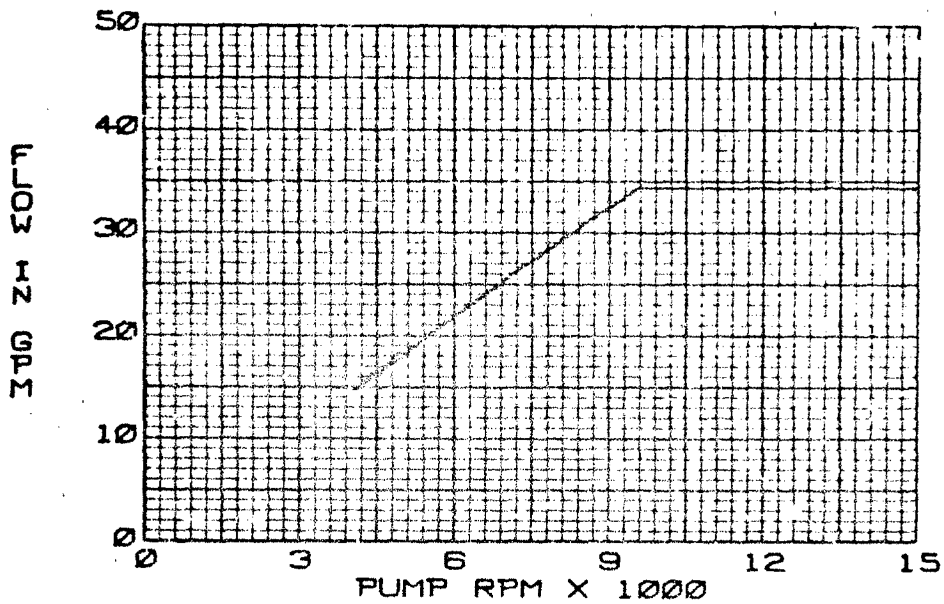


FIGURE 206. CECO MFP-330 VANE PUMP 97-07-Q1 STEADY STATE TEST
35 GPM 120°F

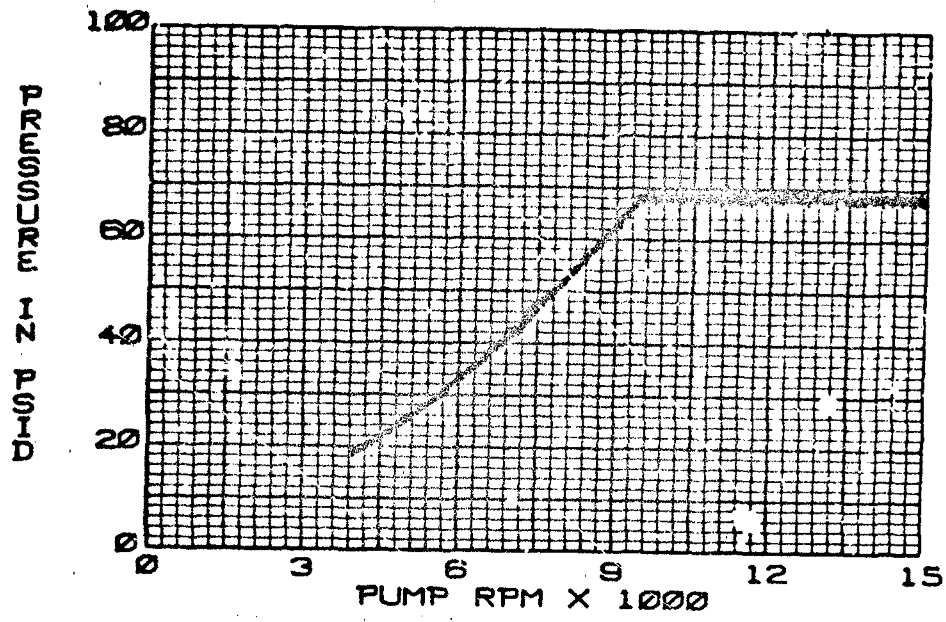


FIGURE 207. CECO MFP-330 VANE PUMP 97-07-(P2-P3) STEADY STATE TEST
35 GPM 120°F

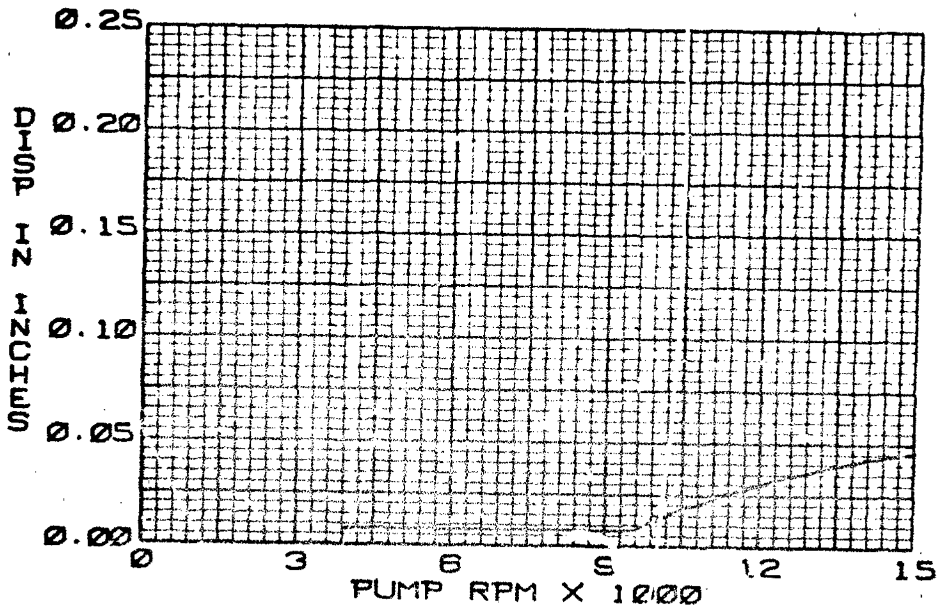


FIGURE 208. CECO MFP-330 VANE PUMP 97-07-MBP1 STEADY STATE TEST
35 GPM 120°F

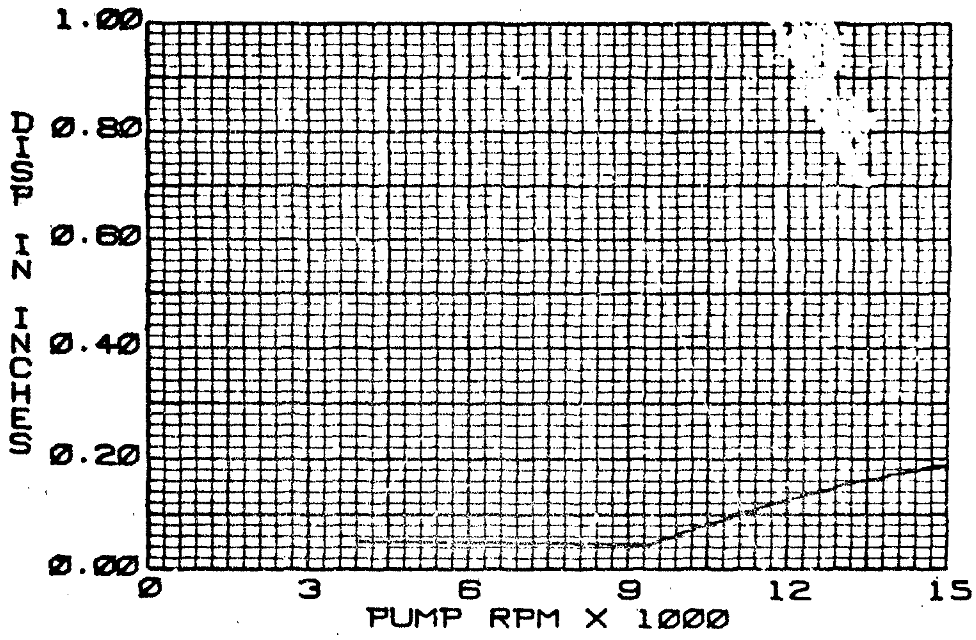


FIGURE 209. CECO MFP-330 VANE PUMP 97-07-XP STEADY STATE TEST
35 GPM 120°F

QLEAK = QMAX - QOVBD

where

QMAX = maximum pump flow at current RPM

QOVBD = pump outlet flow

from Figure 205 at 15000 RPM

QMAX = 250 CIS

QOVBD = 34.2*3.85 = 131.67 CIS

Therefore, QLEAK is about 118 CIS. The vane stage pressure rise was the difference between outlet and inlet pressure or about 650 psid. The leakage coefficient is then calculated as

$$\text{COEFLK} = \frac{\text{QLEAK}}{\Delta P_v} = \frac{118}{650} = .18 \text{ CIS/PSI}$$

for 15000 RPM. Unfortunately this term was not constant for throughout the on-control speed range. Also a different leakage term was computed for the non-controlled portion of the pump speed range. Leakage rates also varied for different flow test conditions. No reasonable value or expression for the vane internal leakage could be computed from the test data that was available.

The leakage flow calculation is dependent on the balance pistion position which gives a direct readout of the cam position. The cam position at any RPM was converted to a maximum flow rate through a table (supplied by CECO) relating cam position to maximum pump flow. The measured steady state cam position obviously were not the correct values. This was evident from the way the balance piston positions were calibrated. The zero cam position was set when the pump was off. This was a static calibration which was subject to offset errors once the pump was started. The balance piston positions are only capable of showing relative changes in cam position and not discrete cam locations. Leakage coefficients in the HYTRAN and HSTT pump models were assumed from data supplied by CECO.

## SECTION V

## HYDRAULIC MOTOR MODEL DEVELOPMENT AND VERIFICATION

A fixed displacement axial piston motor manufactured by Aero Hydraulics, Inc. was tested in the Hydraulic Performance Analysis Facility. The motor has a 0.62 CIR displacement and a rated operating speed of 8100 rpm. The maximum no-load flow through the unit at rated speed is 18.5 gpm with 415 psid across the motor ports. The motor used in the testing was controlled by a servo valve which together with the motor dropped about 2000 psid at the maximum no-load flow rate.

The objective of the test was to verify steady state, frequency, and transient math models of the motor unit. Tests were made with MIL-H-5606B hydraulic fluid. The test unit was an off-the-shelf item (Figure 210) with no special instrumentation requirements. Threaded ports were installed in lieu of the quill tubes normally used to couple the motor to the F-18 Leading Edge Flap servovalve package.

Figure 211 is a schematic of the test stand. The motor was powered by an F-15 pump and controlled by a servo valve unit. Pump noise and pressure ripple were isolated from the test unit by using a commercial Pulsco Hydraulic Acoustic Attenuator. The test specimen temperature was controlled by an industrial type heat exchanger in the return line. An independent pressure source was used to pressurize the F-4 reservoir. The test section consisted of the motor and the lines connecting it to the servo valve unit. Time and budget constraints precluded the inclusion of static and inertial loading in the test set-up. Internal motor inertia proved sufficient to verify transient effects, as expected, however the lack of a static load prevented the acquisition of meaningful frequency response data.

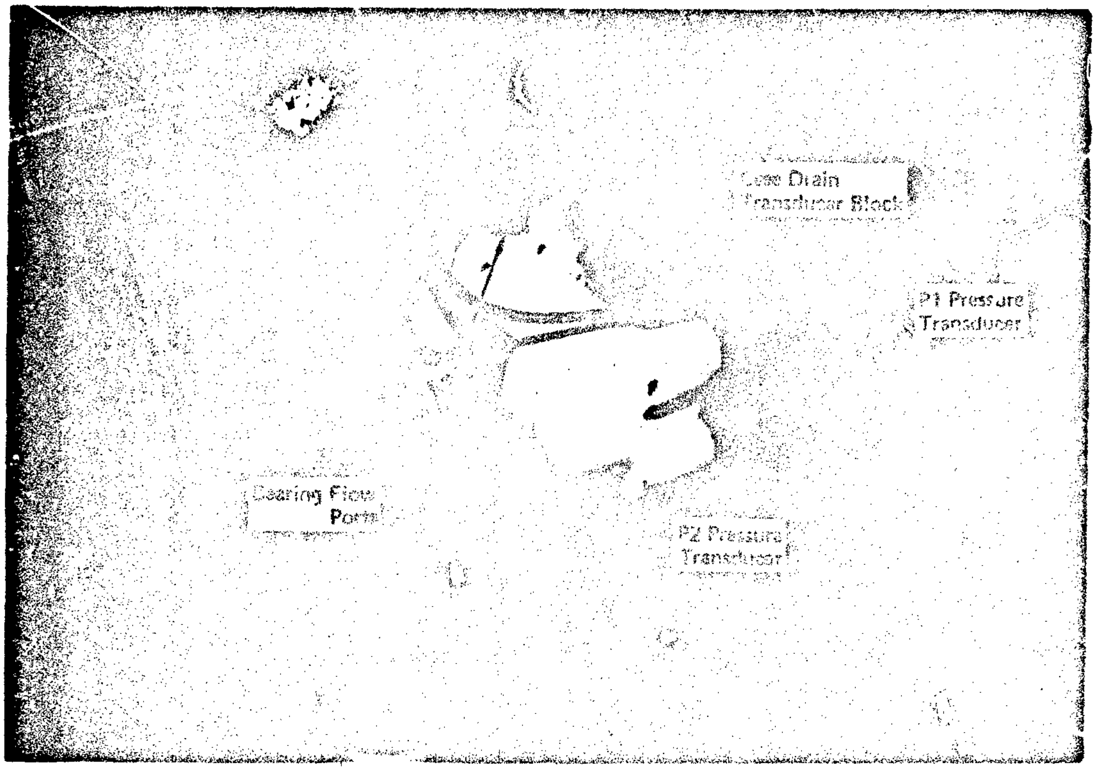


GP79-0689-1

**FIGURE 210**
**HYDRAULIC MOTOR**

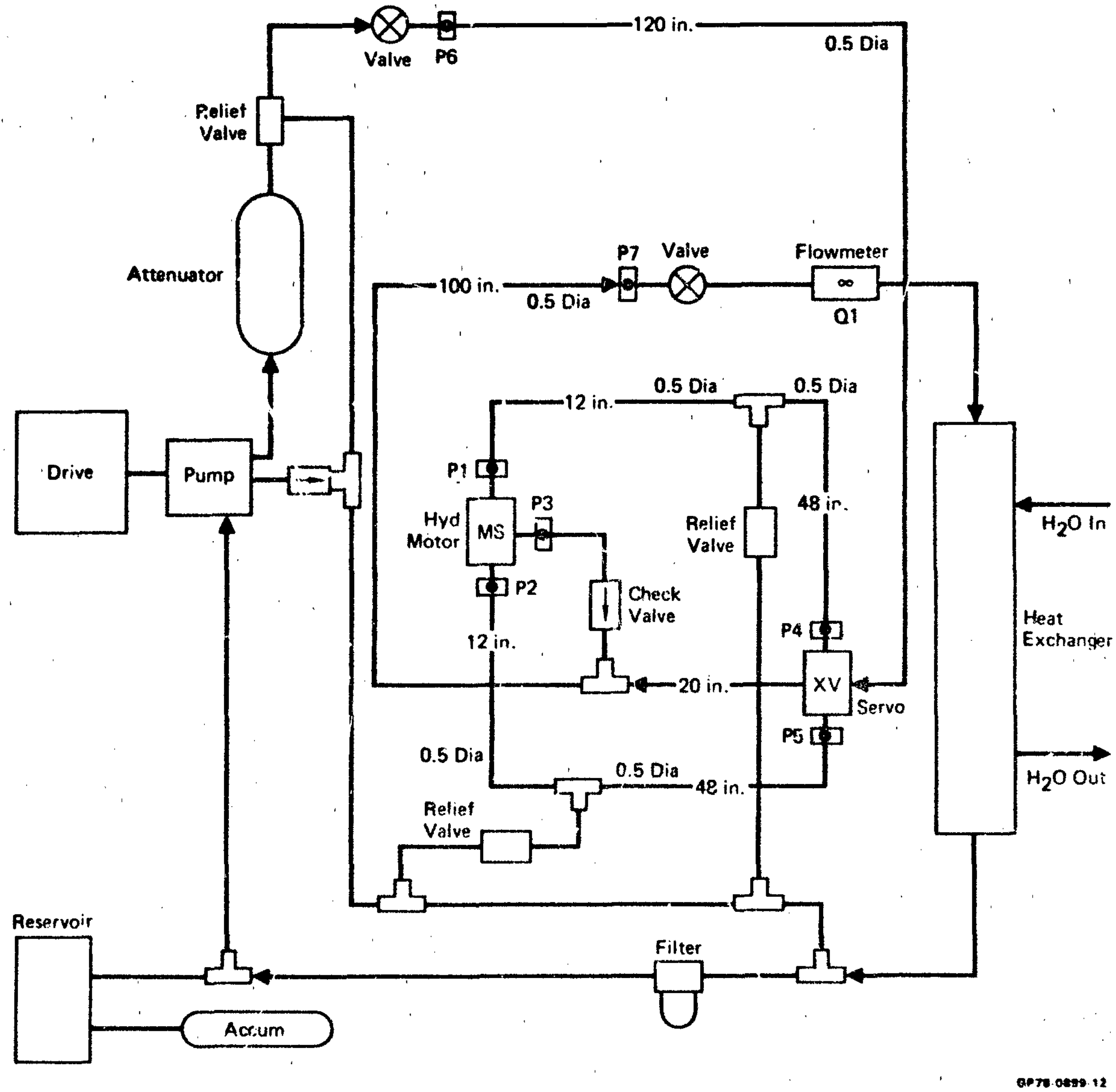


FIGURE 211
HYDRAULIC MOTOR TEST SCHEMATIC

## 1. FREQUENCY RESPONSE MODEL AND VERIFICATION

### a. Motor Model

The HSFR piston motor model uses the same calculations as the pump model. The input data requirements are also similar. The motor subroutine is programmed to perform both an inlet (pressure side) and outlet (return side) analysis. The motor ignores the overboard flow supplied by the load valve and computes its own flow during the AC portion of the program. The motor does not require an input steady state flow and there is no steady state balancing. Appendix F details the required input data for the HSFR motor model and gives a technical description of the subroutine.

### b. Verification Tests and Results

The inlet and outlet lines from the motor to the servo valve were to be mapped. Total pressure pulsations and fundamental frequency pulsations were to be plotted versus a motor speed sweep for fixed and roving pressure transducer locations. Motor speed was controlled by moving the servo valve control spool which varied the inlet flow and thus the motor's rpm. However, no reliable data could be produced from this arrangement. With no load on the motor, shaft rotation was very unstable causing the plotter to oscillate along the rpm axis. Without a good rpm signal the spectrum analyzer could not work properly. This is illustrated in Figures 212 and 213 which are the fundamental and second harmonic at the P1 pressure transducer location in Figure 211. No distinct fundamental or harmonics can be found on these plots with the motor set-up. Based on this information, the decision was made not to proceed with the frequency motor tests. The test stand however was modeled with the HSFR computer program. Table 20 presents a listing of the HSFR input data. The results of the simulation are shown in Figures 214 and 215.

Figure 214 shows the peak pressure pulsations at the inlet port plate of the motor and Figure 215 is the comparable location on the outlet. Predicted and measured pressure pulsations on either side of the motor were very low, less than 20 psi peak-peak. The computed resonant rpm's for the short line circuit were 2600, 5200 and 7800 rpm. No direct comparison of these results with test data could be made.

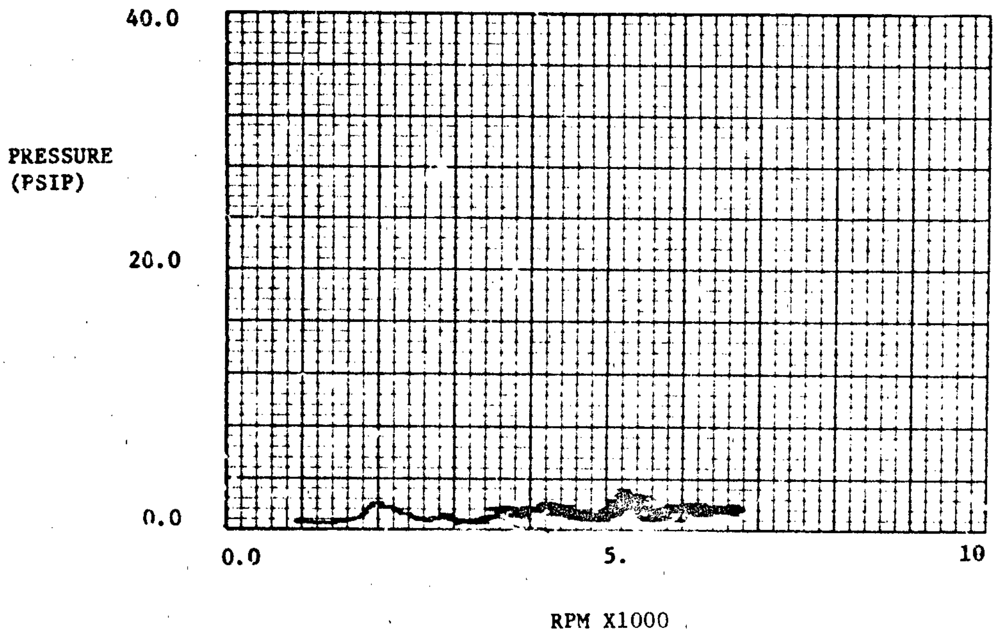


FIGURE 212. P1 FUNDAMENTAL PRESSURE

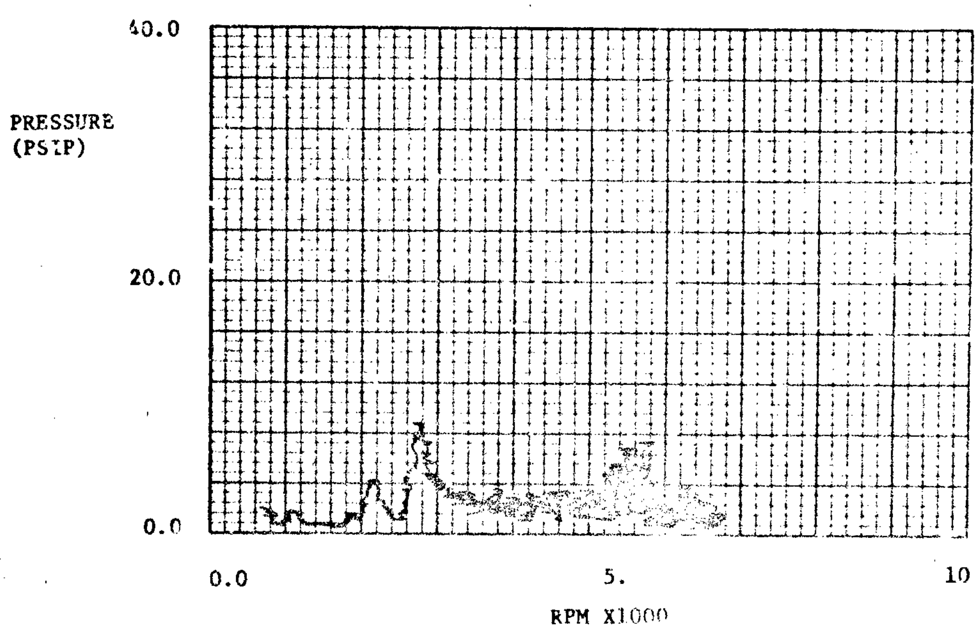


FIGURE 213. P1 2ND HARMONIC

## TABLE 20. HSFR INPUT DATA

```
DMOTOR      15:26 AUG 08,'78

       ***** HSFR MOTOR MODEL TEST CIRCUIT *****(DMOTOR)
  24    1      120.     1400.
   1000.     10000.      100.         1.          9.
   9   25      .219      .358       .694        .784        .400     .08736      .219
    .219       20.0      1.90       17.7        17.7        17.7      17.7     1800.0
    160.       200.
   1    0        6.      .500       .035      3.0E07
   1    0        6.      .500       .035      3.0E07
   1    0        6.      .500       .035      3.0E07
   1    0        6.      .500       .035      3.0E07
   1    0        6.      .500       .035      3.0E07
   1    0        6.      .500       .035      3.0E07
   1    0        6.      .500       .035      3.0E07
   1    0        6.      .500       .035      3.0E07
   1    0        6.      .500       .035      3.0E07
   1    0        6.      .500       .035      3.0E07
  14    0      50.0       7.7
   7    1
   1    0        6.      .500       .035      3.0E07
   1    0        6.      .560       .035      3.0E07
   1    0        6.      .500       .035      3.0E07
   1    0        6.      .500       .035      3.0E07
   1    0        6.      .500       .035      3.0E07
   1    0        6.      .500       .035      3.0E07
   1    0        6.      .500       .035      3.0E07
   1    0        6.      .500       .035      3.0E07
   1    0        6.      .500       .035      3.0E07
   1    0        6.      .500       .035      3.0E07
  14    0     50.00       7.7
  15    1    2    3    4    5    6    7    8   13   14   15   16   17   18   19
  15    1    2    3    4    5    6    7    8   13   14   15   16   17   18   19
   2    1   14
   2    1   14
   2    1   14
```

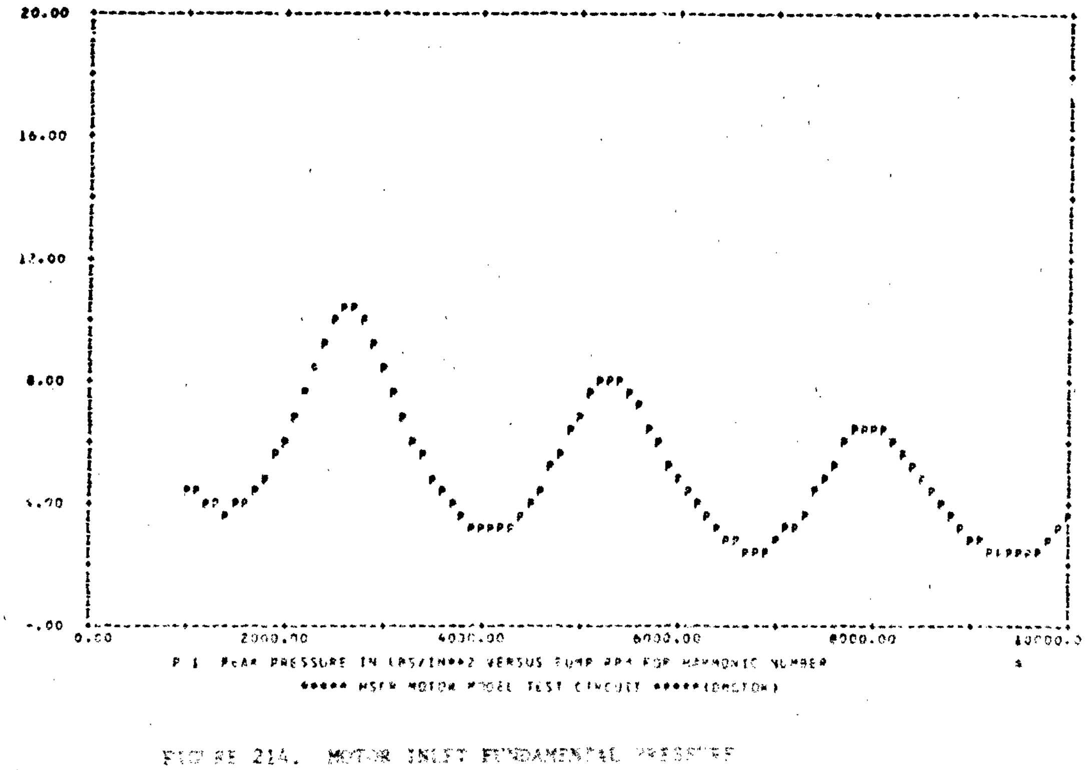


FIGURE 214. MOTOR INLET FUNDAMENTAL PRESSURE

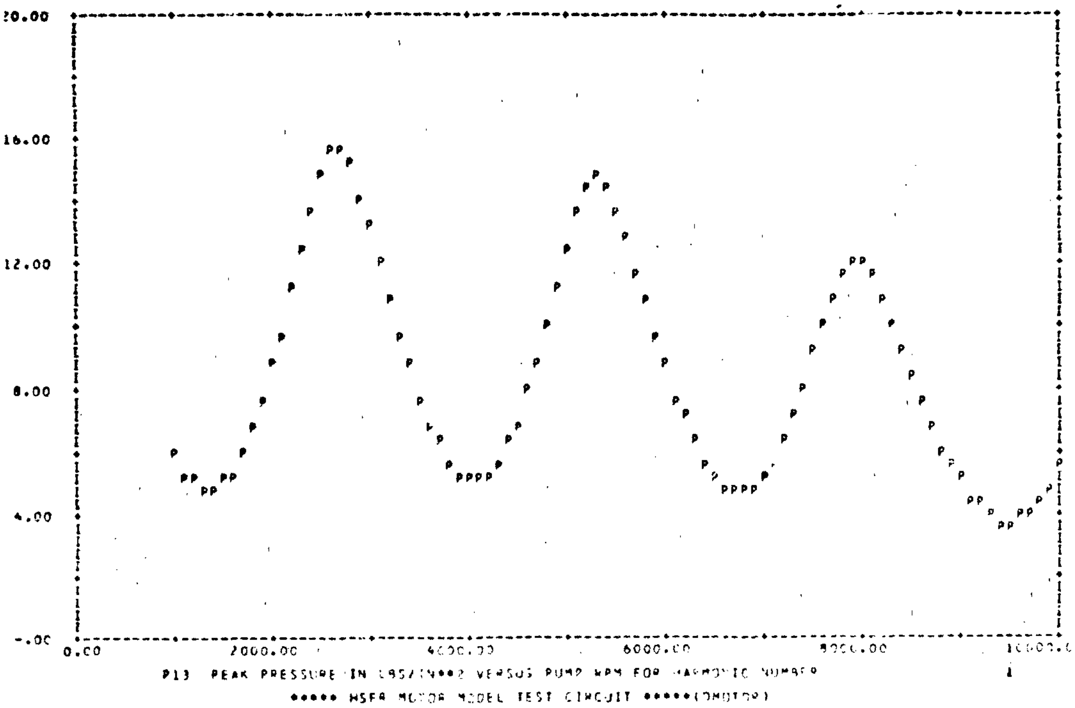


FIGURE 215. MOTOR OUTLET FUNDAMENTAL PRESSURE

2. TRANSIENT MODEL AND VERIFICATION

a. HYTRAN Motor Model - A HYTRAN motor model was written to simulate the operation of a constant displacement hydraulic motor. The MTR56 subroutine accounts for case drain and cross port leakages, in addition to the motor inertia, damping and breakout torque. Appendix F presents the HYTRAN user and technical sections of the MTR56 subroutine.

b. Verification Tests and Results - Test conditions were established to determine factors which would affect motor performance. The testing was done on a 1/2" line system (Figure 211) with MIL-H-5606B hydraulic fluid. A photograph of the system is shown in Figure 216. A summary of the transient test runs are shown in Table 21. For each test the following data was recorded.

Motor Port Pressures (P1 & P2)

Motor Case Drain Port Pressure (P3)

Servo Valve C1 Port Pressure (P4)

Servo Valve C2 Port Pressure (P5)

Servo Valve Position (XV)

Upstream Source Pressure (P6)

Return Pressure (P7)

Motor RPM (MS)

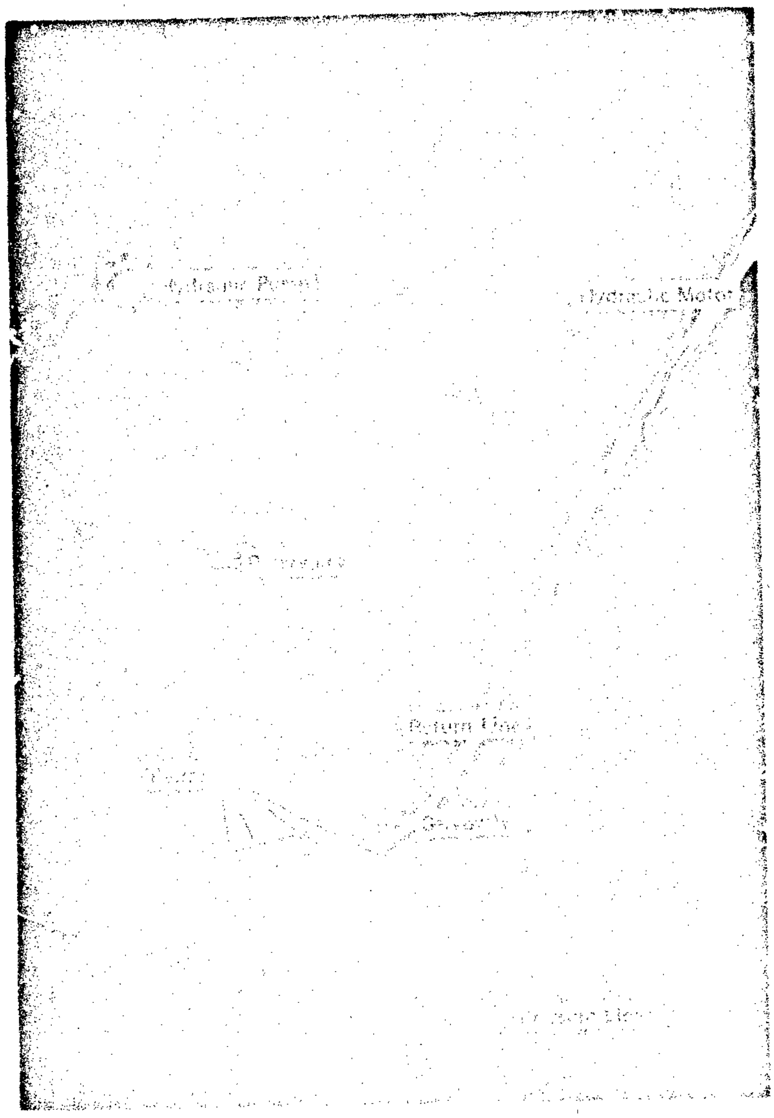


OP78-0899-5

**FIGURE 216**
**HYDRAULIC MOTOR TEST BENCH**

TABLE 21 HYDRAULIC MOTOR TRANSIENT TEST RUNS

| STEADY STATE FLOW (GPM) HIGH | LOW | MOTOR ROTATION | MOTOR INLET TEMPERATURE (°F) | RESERVOIR PRESSURE (PSIG) | RUN NUMBER |
|---|---|---|---|---|---|
| 2 | 0 | CCW | 119 | 62 | 98-03+ |
| +2 | -2 | CCW-CW | 120 | 62 | 98-03R |
| 5 | 0 | CCW | 123 | 62 | 98-04- |
| 5 | 0 | CCW | 122 | 62 | 98-04+ |
| +5 | -5 | CCW-CW | 122 | 62 | 98-04R |
| 10 | 0 | CCW | 120 | [illegible] | 98-05- |
| 10 | 0 | CCW | 120 | 63 | 98-05+ |
| +10 | -10 | CCW-CW | 120 | 63 | 98-05R |
| 15 | 0 | CCW | 121 | 59 | 98-06- |
| 15 | 0 | CCW | 122 | 62 | 98-06+ |
| +15 | -15 | CCW-CW | 122 | 62 | 98-06R |
| 18 | 0 | CCW | 120 | 62 | 98-07- |
| 18 | 0 | CCW | 121 | 61 | 98-07+ |
| +16.6 | -16.6 | CCW-CW | 123 | 63 | 98-07R |

Notes: 1. + indicates a turn-on transient
- indicates a turn-off transient
R indicates a motor reversal

The hydraulic motor was not loaded for the testing. The relief valves in the motor lines were set for a 4000 psig cracking pressure. Hydraulic pump speed was limited to 2000 rpm so as not to overspeed the motor beyond the design flowrate of 18 GPM. During the testing the transient pressures were monitored to assure that they did not exceed the cracking pressure of the relief valves.

The motor speed pick-up was an AC type unit. The signal was converted to a DC level to facilitate recording and playback. The conversion process introduced a lag in the signal. In addition because of the high frequency of the signal (23 tooth gear yields 2300 HZ at 6000 rpm) the electronics would roll off the peak values and smooth out the transient signal. Consequently, the measured motor rpm was only good for steady state values.

The turbine flowmeter (Q1) had the same problems, but had better response characteristics because of the lower operating frequencies (20 gpm = 175 HZ).

After completing the transient test series, the relief valves were rechecked for the proper setting. The relief valve in the line that contains the P1 and P4 pressure transducers had a cracking pressure around 1500 psig. The relief valve in the other line started leaking at 250 psig but did not fully open until 4300 psig. This introduced variables in the test runs that were not adequately measured. The leakage flows through the relief valves were not recorded. Also pressure histories downstream of the relief valves are not available. Without known boundary conditions a computer simulation of a test run is impractical. No meaningful correlation could be accomplished. However, a computer simulation of the test system was made to determine if the model was operating correctly.

c. HYTRAN SIMULATION AND DISCUSSION

A HYTRAN schematic of the motor test set-up is shown in Figure 217. A turn-off transient at 38.5 CIS flow was the first simulated run. The computer input data is presented in Table 22. Figures 218, 219 and 220 show the inlet and outlet port pressures and the motor RPM respectively. In Figure 219 the motor outlet pressure falls below the fluid vapor pressure because there is no cavitation model at the port. The initial steady state flow was 62.2 CIS. The steady flow after the valve closure was 3.85 CIS.

LEG DATA

| LEG | NODE UPSTREAM | NODE DOWNSTREAM |
|---|---|---|
| 1 | N1 | N2 |
| 2 | N3 | N6 |
| 3 | N6 | N4 |
| 4 | N5 | N7 |
| 5 | N6 | N7 |
| 6 | N7 | N8 |
| 7* | N2 | N3 |
| 8* | N4 | N5 |
| 9* | N2 | N4 |
| 10* | N3 | N5 |

* INTERNAL LEGS IN SERVOVALVE

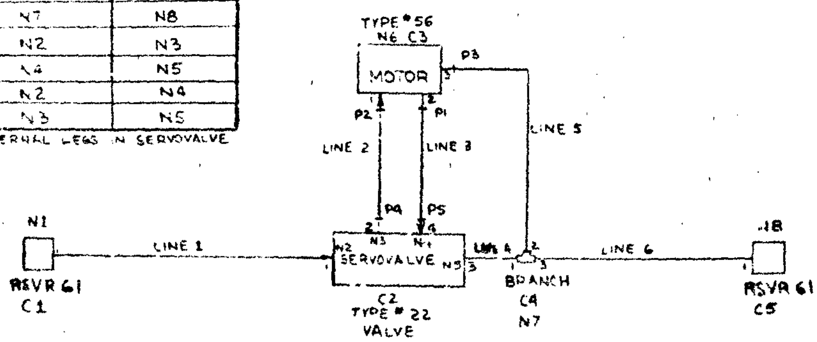


FIGURE 217. HYDRAULIC MOTOR TEST SCHEMATIC

TABLE 22. HYTRAN INPUT DATA FOR MOTOR

```
**** MOTOR MODEL  - MAX RATE TURN-ON TRANSIENT ****(ONTVERA)

      THE TRANSIENT RESPONSE IS FROM T=0.0  TO T=   .500 SECONDS AT TIME INTERVALS OF DELT= .00050
               WITH OUTPUT POINTS PLOTTED AT INTERVALS OF    ,    .00500  SECONDS

   FLUID DATA FOR  MIL-H-5606  AT  3100.0 PSIG, -     2.0 PSIG AND 120.0 DEG F  IN  10.0 DEG F STEPS
                          VISCOSITY     -  .214E-01        .169E-01IN**2/SEC
                          DENSITY       -  .816E-04        .806E-04(LB-SEC**2)/IN**4
                          BULK MODULUS  -  .231E+06        .194E+06PSI
                          VAPOUR PRESS.-   .200E+01 AT  120.0 DEG F
FIX-UP TAKEN AT LINE 16,VEL OF SOUND IN LINE   4  IS    21.2PER CENT IN ERROR
```

LINE DATA

| LINE NO. | LENGTH | INTERNAL DIA | WALL THICKNESS | MODULUS OF ELASTICITY | DELX | CHARACTERISTIC IMPEDANCE | VELOCITY OF SOUND |
|---|---|---|---|---|---|---|---|
| 1 | 170.0000 | .4300 | .0350 | .300E+08 | 30.0000 | 28.4999 | 50729.8433 |
| 2 | 60.0000 | .4300 | .0350 | .300E+08 | 30.0000 | 28.4999 | 50729.8433 |
| 3 | 60.0000 | .4300 | .0350 | .300E+08 | 30.0000 | 28.4999 | 50729.8433 |
| 4 | 20.0000 | .4300 | .0350 | .300E+08 | 20.0000 | 28.4999 | 40000.0000 |
| 5 | 32.7500 | .2100 | .0200 | .300E+08 | 32.7500 | 120.1706 | 51017.5728 |
| 6 | 100.0000 | .4300 | .0350 | .300E+08 | 33.3333 | 28.4999 | 50729.8433 |

```
COMP.,   1  INTEGER DATA      1  61   6  -1   0   0   0   0   0   0   0   0   0   0   0   0
REAL DATA CARD #    1    .3000E+04  0.          0.          0.          0.          0.          0.          0.
COMP.,   2  INTEGER DATA      2  22   4   1  -2  -4   3   0   0   0   0   0   0   4   0   0
REAL DATA CARD #    1    .5000E-03  .5000E-01  .1880E-01  .2000E+01  -.5000E-03  -.5000E-01  .1850E-01  .2000E+01
REAL DATA CARD #    2    .5000E-03  .5000E-01  .1880E-01  .2000E+01  -.5000E-03  -.5000E-01  .1850E-01  .2000E+01
REAL DATA CARD #    3    0.         .6000E-01  .7000E-01  .5000E+00  0.          0.          0.          0.
REAL DATA CARD #    4    .7475E-01  .7475E-01  .5000E-02  .5000E-02  0.          0.          0.          0.
COMP.,   3  INTEGER DATA      3  56   2   2  -3  -5   0   0   0   0   0   0   0   0   0   0
REAL DATA CARD #    1    .6200E+00  .1630E+04  .4260E+03  .5000E-01  .1230E-01  .1324E+02  .1600E+02  .4545E+01
REAL DATA CARD #    2    0.         0.          0.          0.          0.          0.          0.          0.
COMP.,   4  INTEGER DATA      4  11   0   4   5  -6   0   0   0   0   0   0   0   0   0   0
COMP.,   5  INTEGER DATA      5  61   1   6   0   0   0   0   0   0   0   0   0   0   0   0
REAL DATA CARD #    1    .1000E+03  0.          0.          0.          0.          0.          0.          0.
```

STEADY STATE INPUT DATA

NUMBER OF NODES = 8     NUMBER OF LEGS = 10     NUMBER OF CONSTANT PRESSURE NODES = 0

LEG CONNECTION INPUT DATA

| LEG NO | UPST NODE NO | DWST NODE NO | NO OF ELEMENTS | FLOW GUESS | UPST PRESS | DWST PRESS |
|---|---|---|---|---|---|---|
| 1 | 1 | 2 | 2 | .10000 | 0.00000 | 0.00000 |
| 2 | 1 | 6 | 2 | .10000 | 0.00000 | 0.00000 |
| 3 | 6 | 4 | 2 | .10000 | 0.00000 | 0.00000 |
| 4 | 5 | 7 | 2 | .10000 | 0.00000 | 0.00000 |
| 5 | 6 | 7 | 3 | .10000 | 0.00000 | 0.00000 |
| 6 | 7 | 8 | 3 | .10000 | 0.00000 | 0.00000 |
| 7 | 2 | 3 | 1 | .10000 | 0.00000 | 0.00000 |
| 8 | 4 | 3 | 1 | .10000 | 0.00000 | 0.00000 |
| 9 | 2 | 4 | 1 | .10000 | 0.00000 | 0.00000 |
| 10 | 3 | 5 | 1 | .10000 | 0.00000 | 0.00000 |

```
LEG NO      ELEMENTS IN LEG----
  1           1 --  3,  0 --  1,
  2           0 --  2,  3 --  1,
  3           1 --  2,  0 --  3,
  4           0 --  4,  4 --  1,
  5           3 --  3,  0 --  5,  4 --  2,
  6           4 --  3,  0 --  6,  5 --  1,
  7           2 --  1,
  8           2 --  1,
  9           2 --  6,
 10           2 --  2,
```

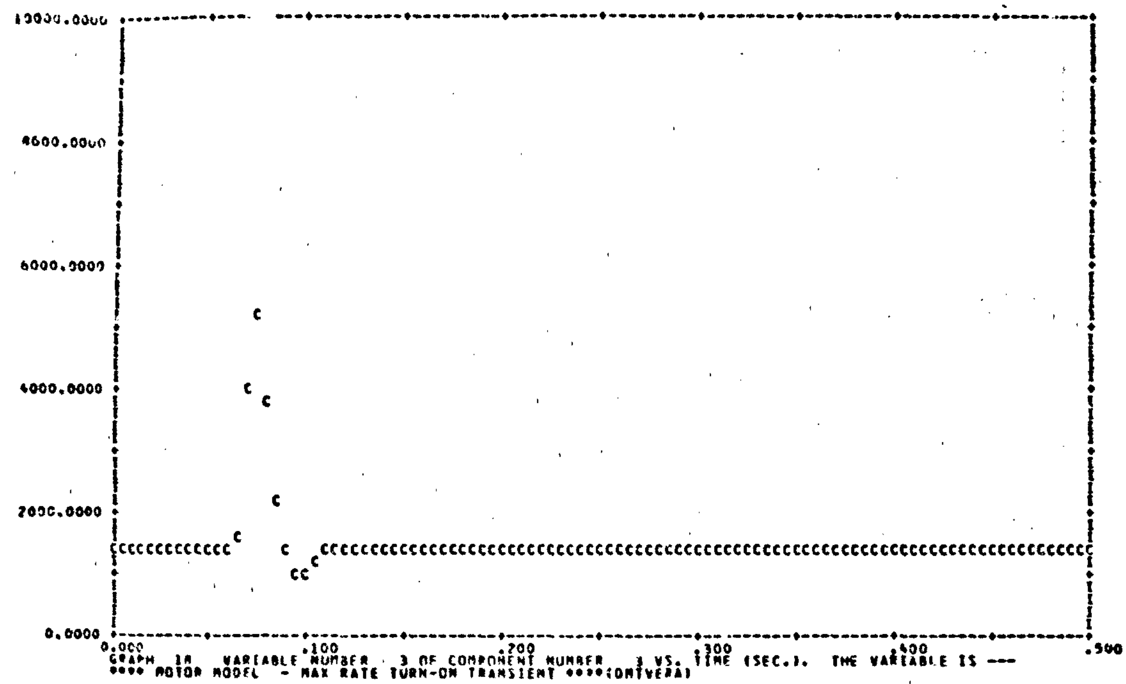


FIGURE 218. MOTOR INLET PRESSURE

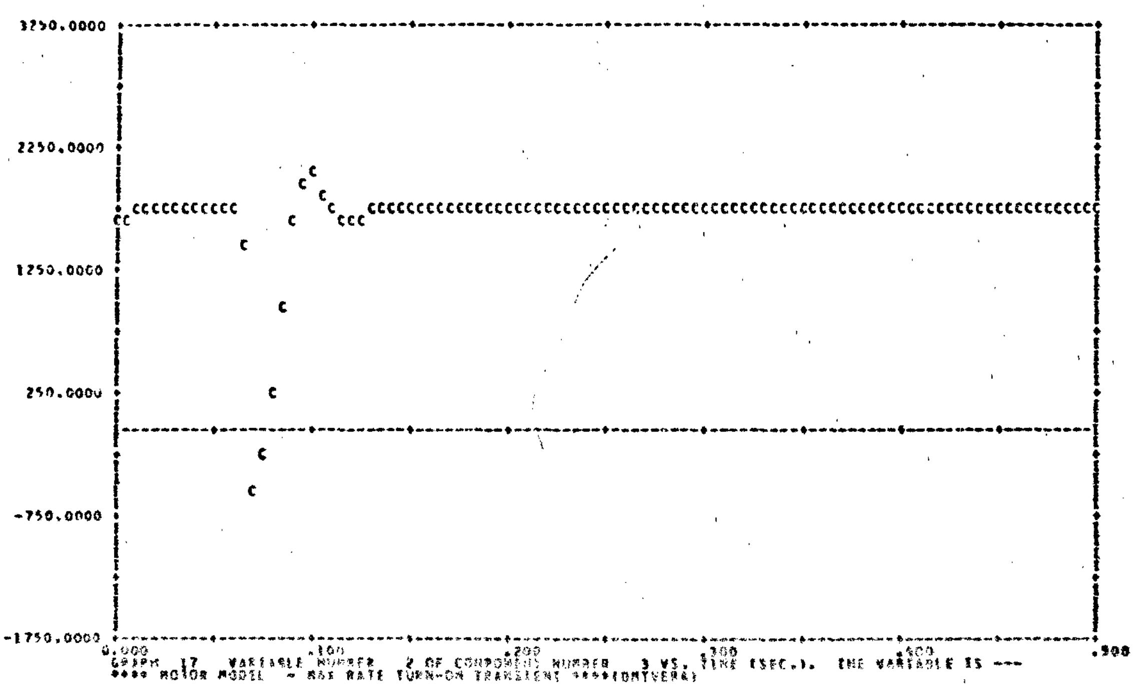


FIGURE 219. MOTOR OUTLET PRESSURE

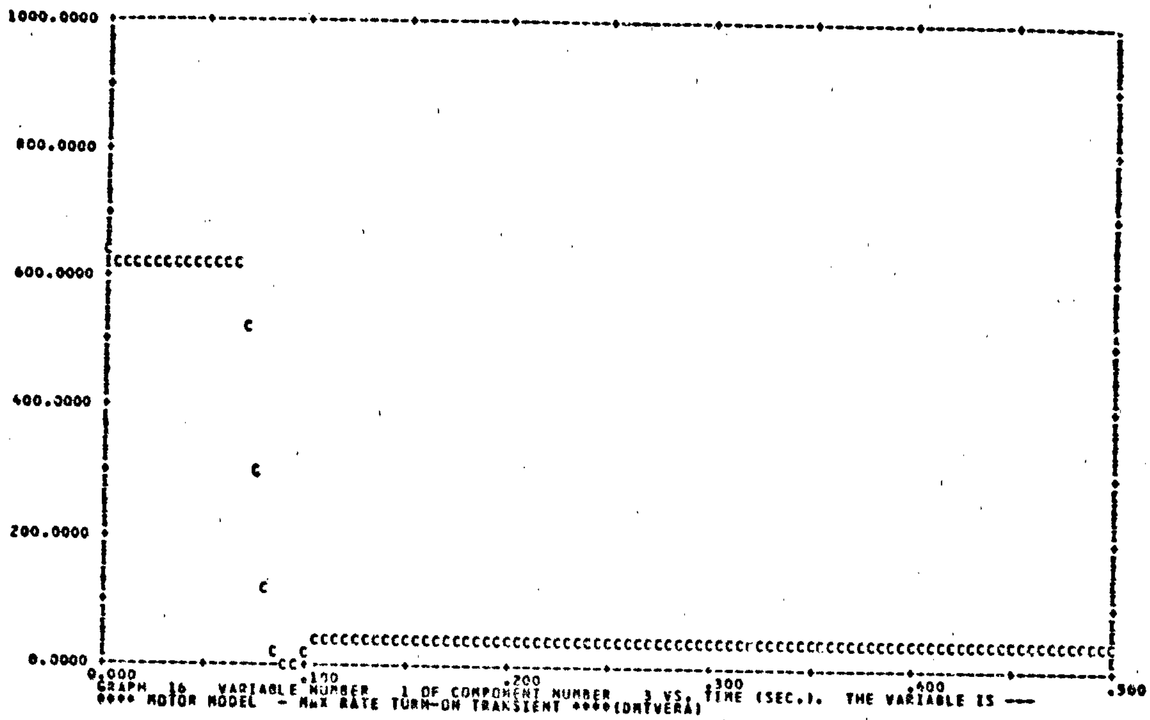


FIGURE 220. MOTOR RPM

3. STEADY STATE TESTS

Three Steady State Tests were performed on the motor in the Hydraulics Lab. The first test was to start with equal port pressures and by lowering one of the pressures, record the pressure at which the motor drive shaft begins to rotate at no load conditions. Table 23 presents the data for this test.

TABLE 23. HYDRAULIC MOTOR BREAKOUT PRESSURE TEST RESULTS

PRESSURE (PSIG)

| INLET | OUTLET |
|---|---|
| 100 | 20 |
| 200 | 60-65 |
| 250 | 85-90 |
| 300 | 110-115 |
| 500 | 210-220 |
| 740 | 325-350 |
| 930 | 425-450 |
| 1210 | 550-575 |
| 1610 | 760-790 |
| 1340 | 890-920 |
| 2010 | 975-1025 |

As the inlet pressures increased the pressure drop at which the shaft would begin to rotate also increased. The internal static friction coefficient for the motor may be determined by plotting the pressure differential versus the return pressure (Figure 221).

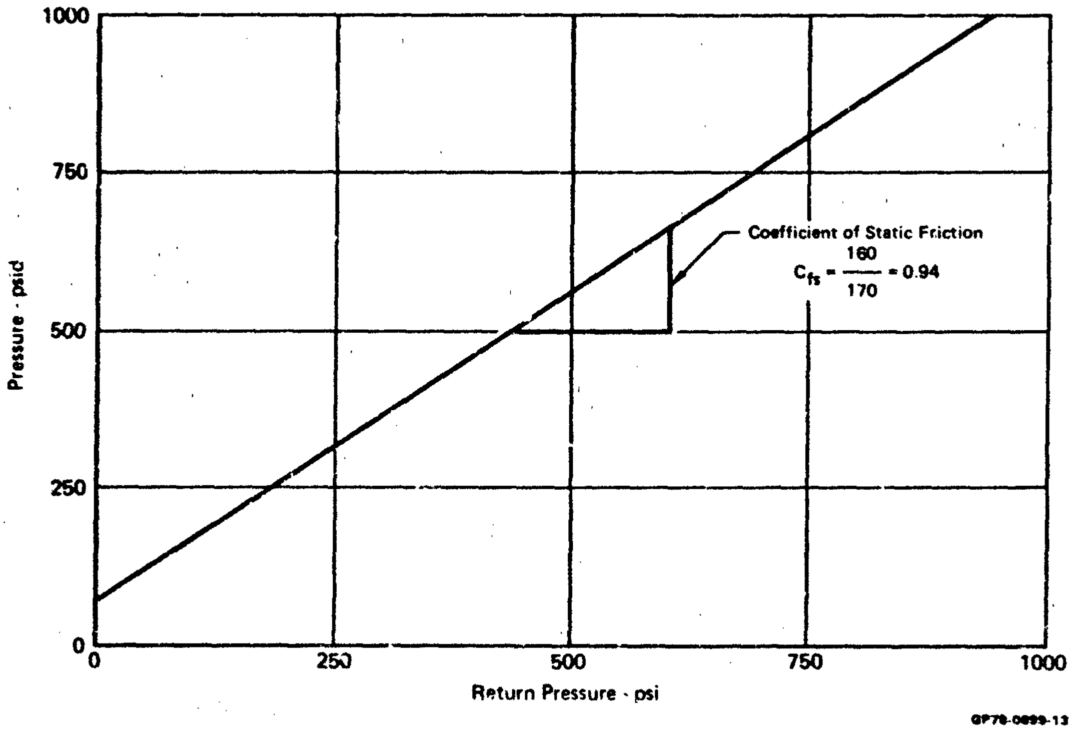


**FIGURE 221**
**MOTOR PRESSURE DROP vs RETURN PRESSURE**

Once rotation was achieved during the test the pressure difference gradually decreased until rotation ceased. Unfortunately this occurred transiently and the pressure difference across the motor when the shaft stopped rotating could not be read on the test bench gages. This value would have helped to determine the internal friction coefficient which the motor was running. Thus it was necessary to assume a value for use in the HYTRAN program.

The motor leakage characteristics were determined by locking the motor shaft and letting the return and case drain lines be vented to atmosphere. Pressure was then applied to the inlet and the flows in the return and case lines were measured. Figure 222 is a plot of the pressure drop versus flow for both port to port and port to case leakage. The leakage coefficients used in the HYTRAN motor model program were obtained from this data.

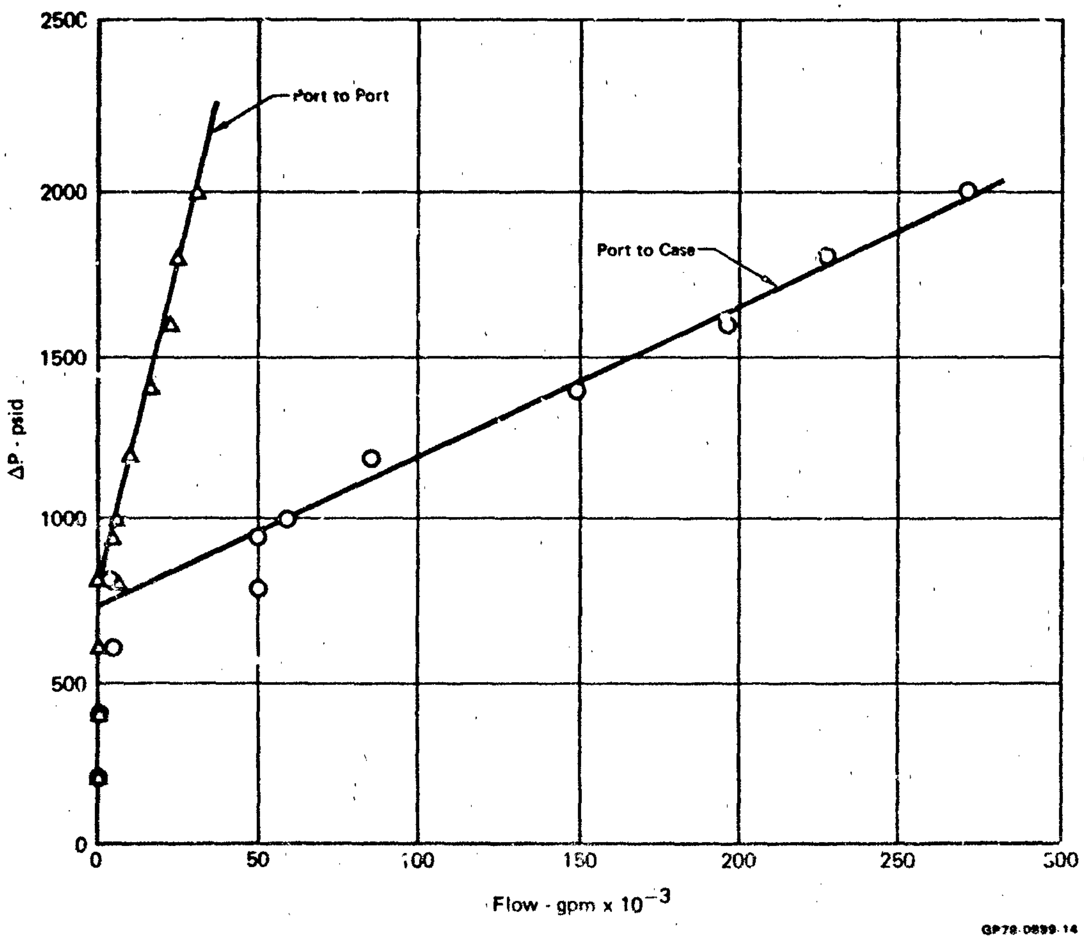


FIGURE 222
HYDRAULIC MOTOR LEAKAGE CHARACTERISTICS

The steady state pressure drop versus flow characteristics for the motor were recorded on the transient test stand (Figure 211) by slowly cycling the servo valve. Figure 223 shows a plot of the pressure differential across this motor versus flow for a clockwise motor rotation. The steady state case drain pressure versus system flow characteristics is shown in Figure 224.

A plot of motor speed versus motor flow is shown in Figure 225. This plot and Figure 223 were used to generate a graph of pressure drop across the motor versus motor speed (Figure 226). The slope of the resulting curve defines a dimensionless damping coefficient. The curve sweeps upward indicating that the pressure depends on higher powers of motor speed and is caused by the flow resistance of the motors internal passages.

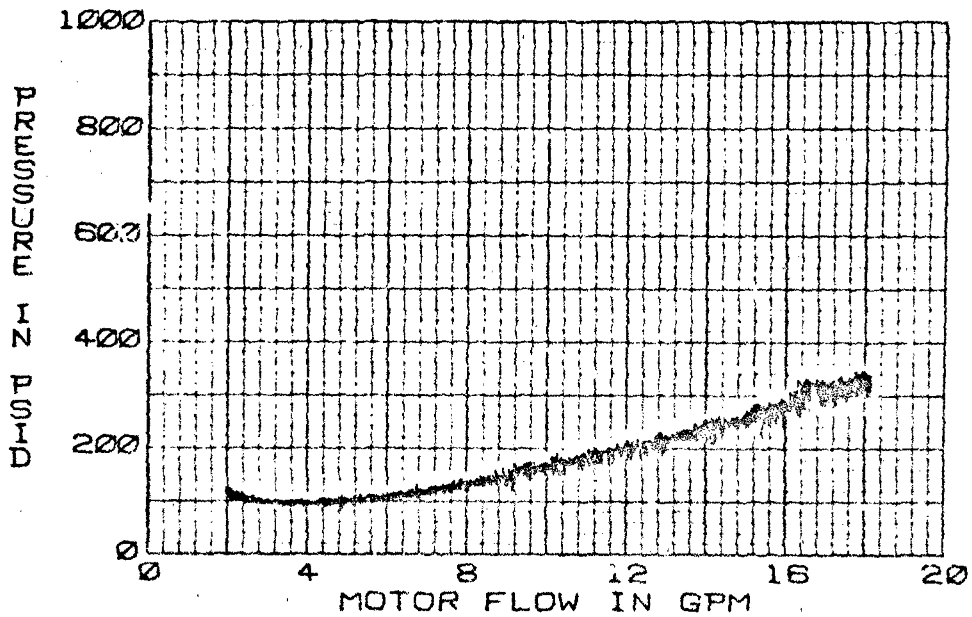


FIGURE 223. AERO HYDRAULIC MOTOR 98-02-(P1-P2) STEADY STATE TEST
CW SHAFT END 125°F

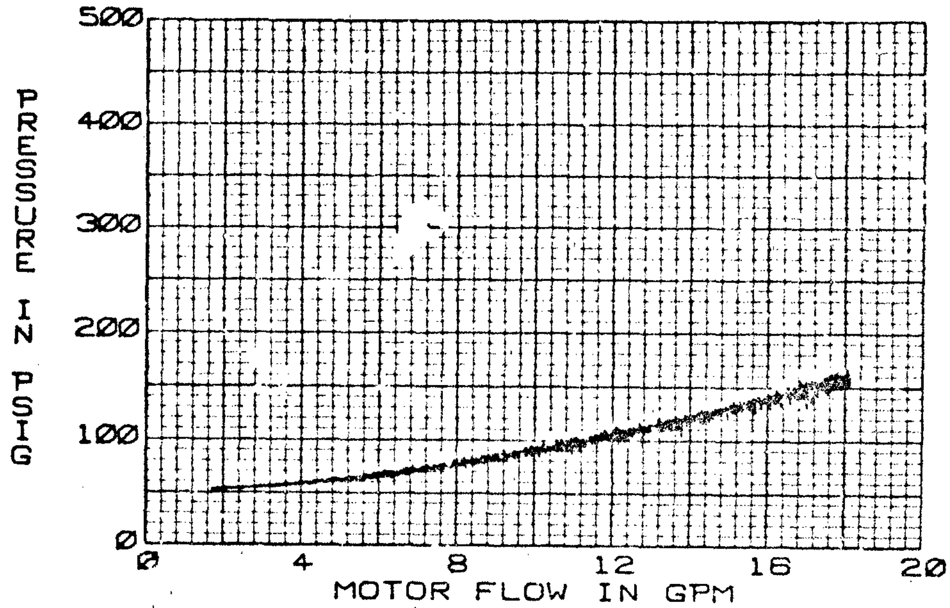


FIGURE 224. AERO HYDRAULIC MOTOR 98-02-P3 STEADY STATE TEST
CW SHAFT END 125°F

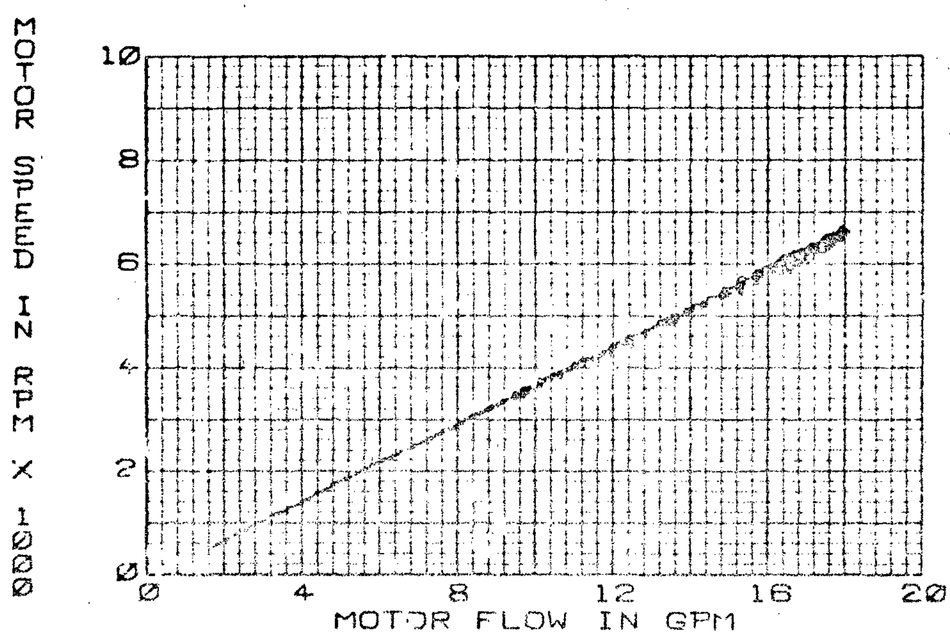


FIGURE 225. AERO HYDRAULIC MOTOR 98-02-MS STEADY STATE TEST
CW SHAFT END 125°F

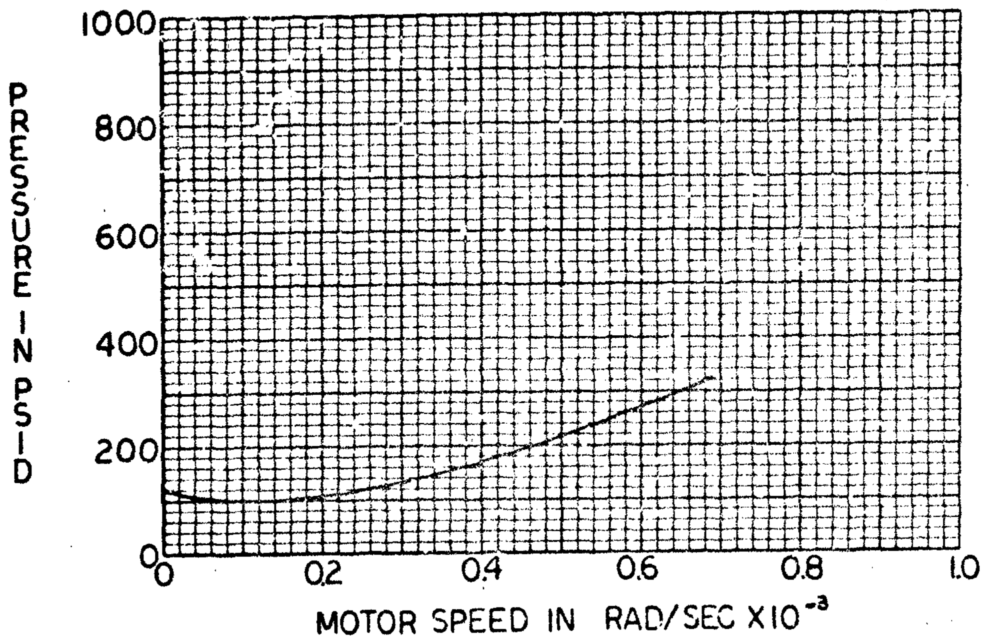


FIGURE 226. AERO HYDRAULIC MOTOR

# SECTION VI

## SUMMARY AND CONCLUSIONS

1. HYDRAULIC LINE MECHANICAL RESPONSE PROGRAM

a. Program Objectives

Development and verification of a computer program for predicting line mechanical response due to predicted pump pulsations was achieved, but to a limited degree. The computer program (Appendix B) developed was based on simplified beam analysis, but included coupling mode effects. Computer analysis of the straight pipe produced excellent correlation to test results. The one and two 90° bend configurations provided good correlation but required the use of simplifying assumptions.

The program can be used to determine the mode shape and frequency of fundamental line responses. Higher modes of line response, which were the predominant responses in the lines tested, are predicted accurately for certain configurations. However, these solutions could not be generalized, therefore a general purpose line response computer program was not achieved.

The present program, along with other analytical techniques and design aids developed, can be used to study the frequency response of a particular line installation. This capability can provide useful information in avoiding line resonance conditions in the hydraulic pump operating regime, particularly fundamental line responses which can lead to rapid fatigue failure of a line.

Ultimate usefulness of a line mechanical response computer program to the system designer will require prediction of line deflections and resulting line stress. This capability would allow the designer to avoid configurations which may result in early fatique failure of a line installation.

Wearout of line clamp cushion, clamps, and clamp mounting structure are long-range problems resulting from pulsation induced line motion. Prediction of line motion amplitude and direction is needed to allow more judicious placement of line clamps on the central system lines. This approach would place clamps at locations where axial line motion is low, thereby increasing clamp life.

A general purpose HLMR program will require considerably more test verification work and better mathmatical techniques. In recent years the finite element method has been developed. The basic idea is to divide a complex problem into a series of simpler interrelated problems. Thus, the whole is modeled as an assemblage of discrete parts of finite elements. Presently a number of disciplines are using this method to solve problems normally associated with stress analysis and solid mechanics, but also those connected to electromagnetics and fluid-flow networks.

b. Test Results

o Line specimens were excited by hydraulic resonances, and resulted in complex mechanical responses for which analytical tools are not presently available.

o No fundamental mechanical line responses were encountered in the pump operating regime.

o The elastomeric clamp produced only a minor effect by slightly lowering the peak "g" levels of the unclamped configuration. There was no significant change in mode shapes.

o Peak pressures and accelerations were out of phase for the straight pipe, near mid-span, and for the two-elbow pipe between the elbows. They were in-phase for the one-elbow pipe in the vicinity of the elbow.

c. Line Data Reduction

The use of single-axis accelerometers necessitated the re-run of the pump speed sweeps for each of the three orthogonal axes. Large amounts of data had to be coordinated and reduced for the multiple accelerometer locations and associated pump speeds. This was time consuming. The mode shapes were calculated and plotted for each significant pump speed to provide an overall view of the motion of the pipe and for mode identification. The large amount of time devoted to the testing, data reduction, and subsequent data presentation and correlation limited the time available to investigate better general mathmatical techniques.

d. Control of Line Mechanical Response

This effort and other MCAIR experience shows that destructive mechanical response of central hydraulic system lines is definitely the result of internal excitation by pump pulsations and the resultant resonant hydraulic response of the system. Reduction of pump pulsation energy produces a reduction in line motion. Unfortunately, pressure pulsation level cannot be accurately correlated to line mechanical response, which varies widely based on the specific line installation/configuration. Development and use of effective wide band pulsation attenuators offers an attractive and perhaps more cost effective alternative than development of a general purpose HLMR program. The use of an analytical definition for an optimum line configuration may be nullified by installation constraints which usually dictate routing, clamp locations, length, bends, etc.

Current design requirements for line clamp type and spacing address steady state loads and externally applied vibration loads from the airframe or engine. Cushioned line clamps do not significantly alter line response due to internal hydraulic excitation. They, therefore, must be designed to give good life with whatever line motion exists.

2. F-15 PISTON PUMP MODEL VERIFICATION

a. Objectives - The primary objective of this portion of the follow-on contract was to investigate means for improving and expanding the capabilities of the HSFR and HYTRAN pump computer models. This was accomplished by conducting frequency response and transient tests at 4400 psi pump outlet pressure to verify model simulation at higher operating pressure, installation of a case pressure transducer to improve the pump model calculation of case pressure at 3000 and 4400 psi pump outlet pressures, and model changes to improve the damping characteristics of the pump.

b. Test Article - The F-15 pump used in the original AFAPL contract was reworked by the supplier and used in this verification. The wiped port plate and cylinder barrel were replaced and, a case drain pressure tap was installed, and the pump was outfitted with new O' rings. Steady state tests were run to recheck the case pressure/flow and heat rejection characteristics.

c. Model Changes - The computation for pump hanger actuator leakage was updated using an equation for fully developed laminar steady flow between stationary flat plates. The computation for describing the flow forces on the compensator valve was investigated. A parametric study was performed to determine the sensitivity of input data in the computer simulation. The parameters investigated were hanger damping, actuator displacement, coefficient of pump leakage, and case volume.

d. Conclusions -

- When frequency response test data at 4400 psi was overplotted on HSFR computer output for comparison, the plots show excellent frequency correlation for the second and third system resonant frequency, however, much higher peak pressures were predicted by HSFR than were measured. The period of the standing pressure waves shows excellent correlation between computed and measured results, but again the measured amplitudes are much lower than the HSFR program predicts. Data is not available from the 3000 psi testing for direct comparison at the high flow rate required to keep the pump control stable at 4400 psi. The HSFR pump model is capable of accurately predicting system resonant frequency locations for system pressures up to 4400 psi. However, amplitude prediction is not accurate, the level of inaccuracy being about the same as that obtained at 3000 psi pressures.
- The computed and measured results during transient tests at 3000 and 4400 psi compare well in most cases. The general computed vs. measured data correlation is better for the turn-on transients. Both amplitude and period characteristics of the data fit much better than for the turn-off case. It is concluded the HYTRAN pump model can predict transients as accurately for system operating pressure up to 4400 psi as for 3000 psi system pressure.
- Of the pump model changes investigated, the hanger damping term has the most significant effect on yielding good correlation between computed and measured test results. Time did not permit determination of an algorithm for hanger damping that fits all cases. The installation of the case drain transducer enabled the study of case pressure/hanger dynamic relationships.

3. VANE PUMP MODEL DEVELOPMENT AND VERIFICATION

a. Vane Pump Pressure Pulsations

Total pulsations in the vane pump outlet line of a simulated system reached a maximum of 210 psi peak-peak at 14,000 - 14,500 rpm with an outlet flow and pressure of 8 gpm and 343 psig. Pressure pulsations at this speed in the upstream control line are very strong, reaching about 1000 psi peak-peak.

The relatively low impedance (low acoustic reflections) of the metering valve allows resonant responses from all the test circuit lines down to the load valves, and probably even to the reservoir, to be exhibited in the main flow line from the pump outlet. Therefore, measured resonant pulsations in the outlet line are numerous.

b. Vane Pump HSFR Model

The vane pump model is compatible with the HSFR program and can be used to predict flow and pressure pulsations in a vane pump system. The vane pump subroutine models the detailed motion and pumping action of the CECO vane pump. Although much of it is applicable to vane pumps in general, the complex variable geometry of the CECO design is hard modeled. Modeling of variable cam geometry and outlet port configuration and timing for other designs would require changes to the vane pump subroutine. Cam geometry and outlet porting are key factors in the prediction of pulsation amplitudes.

c. Vane Pump HSFR Model Verification

Resonant frequencies in the closed end sensing lines were predicted quite accurately. The best accuracy was obtained for resonant frequencies in the upstream sensing line. Simulation of the sensing line terminations inside the pump is a source of error. Predicted amplitudes were about twice measured values. Predictions of pressure pulsations in the outlet line are less conclusive. The test circuit was first modeled down to the metering valve and then to the load valves, and still does not seem to produce all the resonant responses present in the outlet line. Predicted amplitudes in the outlet line were generally about 2 times measured values.

d. Vane Pump HYTRAN Model Verification - The computer predicted values for turn-on and turn-off transients compare favorably with the measured test data. In setting up the simulation care must be taken in selecting the proper steady state operating characteristics, otherwise a transient will occur when the 3000 section of the HYTRAN program begins. The transient response predicted by the PUMP52 model is good. Lags between measured and computed data are dependent on the actuator extend and retract volumes. The cam loads on the actuators determine the extend and retract pressures which are not simulated well. A better definition of these loads might improve the calculated pressures.

## 4. HYDRAULIC MOTOR MODEL DEVELOPMENT AND VERIFICATION

### a. Motor HSFR Model & Verification

The motor model was readily adapted from the pump model. The lack of a static loading capability prevented the acquisition of extensive frequency test data. However, the limited test results and the pulsations predicted by the model showed very low amplitudes, less than 20 psi peak-peak. The motor model performs both inlet and outlet system acoustic analyses when used with the HSFR program.

### b. Motor HYTRAN Model & Verification

Some verification of a basic transient motor model was achieved within the limits of budget and schedule. The model is applicable to in-line axial piston motors. Computer results were good without simulating load inertia. Motor internal inertia is high compared to reflected load inertia in high gear reduction applications such as the F-18 leading edge manuevering flap system. However, load inertia is high in direct drive applications such as a gun drive.

The present model is adequate for transient analysis of motor driven utility functions controlled by separate selector valves. The motor model must be integrated with a servo control model to use it in simulations of servo controlled motor driven systems. MCAIR wrote a servo motor model for the Shuttle Orbiter rudder/speed brake and is working on a model for the F-18 leading edge flap drive. However, no direct verification of a servo controlled motor drive has been accomplished. This would require a specially instrumented servo motor drive package and static/inertial load simulation. Analysis of high response servo motor driven systems provides an excellent application for the HYTRAN program and should justify future modeling/verification effort.

Tests with high load inertia would enhance model verification for gun drive type applications. The present model includes internal leakage characteristics.

## SECTION VII

## RECOMMENDATIONS

### 1. HYDRAULIC LINE MECHANICAL RESPONSE PROGRAM

For long range activities it is recommended that the development of a digital computer program be initiated utilizing the matrix concept of the finite element method with a concurrent effort to further evaluate the ultimate usefulness of such a program to the design of hydraulic system installations. For short term activities a continuing program of test data accumulation and refinement of empirical solutions is recommended. The following are recommended for future efforts:

- o Investigate the feasibility of applying a finite element method (possibly the NASTRAN program) to predict mode shapes and frequencies.
- o Conduct tests on present tested specimens using strain gages to determine the relationship between stresses, hydraulic/mechanical resonances, and previously measured accelerations.
- o Determine the effect of increasing clamp flexibility by using F-15 type production clamps in the three previous test installations.

### 2. F-15 PISTON PUMP MODEL

Further investigation of the pump damping characteristics and its modeling is recommended. Tests should be conducted on another pump configuration, such as the F4 pump, to verify the adaptability of the pump model to pumps of other sizes and more conventional response characteristics.

### 3. CECO VANE PUMP

The pump and/or engine manufacturer should determine if the high pulsations in the upstream control line are contributing to pump or line failure modes. These pulsations could be reduced by the use of a larger control line e.g. 3/8 vs. 1/4 or an orifice in the control line at the main line junction. However, these techniques might adversely affect the control loop response.

a. HSFR MODEL - To improve the HSFR simulation a detailed knowledge of the pump's internal leakage characteristics is desirable. This would more accurately define the precompression characteristics and provide better correlation between outlet flow and cam position.

b. HYTRAN MODEL - The addition of an empirically derived actuator load versus stroke curve at various outlet pressures would improve the PUMP52 computation of actuator extend and retract pressures. More detailed testing is required to generate this data.

4. HYDRAULIC MOTOR MODELS

a. HSFR MODEL - Further tests on frequency hydraulic motors should include a static loading system for the motor. Tests with inertial load simulation should be conducted to further verify the HYTRAN motor model for direct drive applications.

b. HYTRAN MODEL - Modeling and verification of a complete servovalve motor package with simulated static and inertial loads is recommended to provide direct model capability of aerodynamic control surface applications.

## APPENDIX A

## BIBLIOGRAPHY OF FLUID-LINE COUPLING ANALYSES


1. Ashley, H., and Haviland, G., "Bending Vibrations of a Pipe Line Containing Flowing Fluid" Journal of Applied Mechanics, Vol. 17, No. 3, September 1950.

   Paper deals with vibrations caused by cross winds on large (30-inch) diameter steel pipe lines supported above ground at 66 ft intervals. The analytical investigation, based on simple beam theory, assumed that the pipe is simply supported (pinned-pinned) and calculations made for a number of flow rates. The fundamental frequency was determined to be 3.54 Hz and would be approximately constant for the practical limits of fluid flows. No relationship was made between winds and frequencies other than to state that any transient aerodynamically induced excitation could be handled by energy dissipation of the fluid motion.

2. Housner, G., "Bending Vibrations of a Pipe Line Containing Flowing Fluid" Journal of Applied Mechanics, June 1952, pp 205-208.

   Identical title as the Ashley-Haviland paper, with additional analytical study involving the coupling of vibration modes. It shows that little or no damping can result in large amplitudes, and that at a high critical velocity (380 ft/sec) the fluid flow can cause a dynamic instability. However, such a fluid speed is not realistic, being 25 times as large as the normal flow. Since amplitudes depend on the amount of damping in the system and the magnitude of the exciting force, a vibration problem can develop which is similar to the Tacoma Narrows Bridge case. The collapse of the bridge was caused by lack of built-in damping. A condition of no flow in the pipes would require a transverse, exciting force of 13 lb/ft to cause undesirable effects. Such a force rate was considered unreasonable and not attainable. No axial excitations were taken into consideration. Unanswered is the size of the aerodynamic force developed when air flows by a cylinder located near the ground.

3. Long, R. H., Jr., "Experimental and Theoretical Study of Tranverse Vibration of a Tube Containing Flowing Fluid" Journal of Applied Mechanics, March 1955, pp 65-68.

The equations of motion derived in Housner's paper are solved by means of a power-series approximation for specific boundary conditions. These conditions depend on the type of supports for the pipeline, i.e., fixed-fixed, pinned-pinned, or fixed-free.

The pinned-pinned experimental investigation was performed using a 120.03 in. long low-carbon-steel pipe, one-inch OD, and a wall thickness of 0.037 in. The natural frequency of the pipe containing water at zero velocity was determined to be 5.65 Hz. The frequency remained at this value as the water flow increased to 35 ft/sec. Independent unpublished experimental work on a similar tube was made at Cal Tech and reported in this paper which indicates that a ten-fold increase in fluid velocity reduced the natural frequency of the pipe by 3.2 percent.

Tests on fixed-fixed and fixed-free pipe end conditions using a one-inch OD, .073 in. wall thickness, 57.95-in long, SAE 4130 steel tubing filled with water produced reasonable agreement between the analytical and experimental results.

The significant results of the tests indicate that fluid flow has a small effect in reducing the frequency.

4. J. D. Regetz, Jr., "An Experimental Determination of the Dynamic Response of a Long Hydraulic Line," NASA TN D-576, December 1960.

   The primary objective of the tests was to determine the frequency response of small perturbations in pressure and fluid (JP-4 fuel) velocity in a long (68-ft) hydraulic line. The results indicated that the dynamic behavior of the line depended mainly on the elastic constants and inertia of the line and fluid, and on impedance. In addition, the longitudinal frequency of the pipe had a marked effect on the inlet impedance frequency response.

5. R. J. Blade, W. Lewis and J. H. Goodykoontz, "Study of a Sinusoidally Perturbed Flow in a Line Including a 90° Elbow with Flexible Supports" NASA TN D-1216, July 1962

   Tests were conducted on a 68-ft line, with a sharp bend at midpoint. The line was supported in a manner that allowed for longitudinal motion of the downstream half. Sinusoidal perturbations were imposed by oscillating a valve about a partially open position. The fluid used was JP-4 fuel. The method of analysis assumed the mechanical pipe vibrations as a spring-

mass system with viscous damping. The results of the analysis was considered to be in good agreement with the tests.

6. A. Bold, "Determination of Stresses in Fluid System Tubing Under Conditions of Pressure and Flexure" NAEC-AML-2263, 19 August 1965
The purpose of these tests were to determine the stresses developed in tubing while under pressure, or due to bending, or both. in order to establish a method to measure stresses in tube-fitting assemblies. The report concludes that the method outlined produced more accurate results than the procedure in MIL-F-18280B because it includes longitudinal as well as lateral changes in the tubing.

7. J. H. Ginsberg "The Dynamic Stability of a Pipe Conveying a Pulsatile Flow" International Journal of Engineering Science, Vol. 11, 1973, pp. 1013-1024.
The analysis deals with small displacements of a pipe conveying a pressurized fluid with a fluctuating harmonic velocity. Equations of motion are derived for the case of a pinned-pinned pipe. The pulsating flow causes the pipe to have regions of dynamic instability which increases proportionally to the amounts of fluctuation. The paper indicates that the results have great similarity to beams carrying pulsating end forces.

8. F. J. Shaker, "Effect of Axial Load on Mode Shapes and Frequencies of Beams" NASA TN D-8109, December 1975.
An investigation was conducted into the effects of axial load on the natural frequencies and mode shapes of uniform beams for various end conditions. The results are shown in a series of graphs so that frequency as a function of axial load can readily be determined. Another series of graphs shows the effect of axial load on mode shapes.

9. T. Iwatsubo, Y. Sugiyama, and S. Ogino, "Simple and Combination Resonances of Columns under Periodic Axial Loads" Journal of Sound and Vibration, 1974, 33(2), 211-221.
This paper is a theoretical study into resonances of columns under periodic axial loads for four boundary conditions. These were (a) a column pinned at both ends, (b) fixed at both ends, (c) fixed-pinned, and (d) fixed-free. It concluded the region for first mode resonance

may not necessarily be the most important region for columns under loading. Higher modes and combination resonances may be of equal or more importance.

10. M. P. Paidoussis, and C. Sundararajan, "Parametric and Combination Resonances of a Pipe Conveying Pulsating Fluid" ASME Paper 75-WA/APM-29, December 1975.

The authors studied the dynamics of a pipe conveying a pulsating fluid. The pipe hangs down vertically in a fixed-free configuration. Although much of the study was devoted to this case, a fixed-fixed condition was also analyzed. The conclusions were that for the fixed-fixed case, combination resonances are associated with the sum of the eigenfrequencies, while for the fixed-free case they are associated with the difference. It stated that the conclusions were in qualitative agreement with experiments. These experiments were to be reported at a later date.

11. D. B. Callaway, F. G. Tyzzer, and H. C. Hardy, "Resonant Vibrations in a Water-Filled Piping System" The Journal of the Acoustical Society of America, September 1951.

The study reported on experiments performed on a straight 52.8-foot long, 2.375-in. O.D, 0.067-in. wall thickness, copper nickel tube. The water-filled pipe was suspended horizontally by soft rubber loops and the ends were closed by membranes. It was determined that there was large coupling between water vibrations and pipe wall bending vibrations, so that longitudinal excitation of the water column resulted in wall motions of large amplitude. This is due to the large diameter-to-wall thickness ratio not encountered in aircraft applications. Bending modes were found to be more numerous than other modes and causing transmission of noise.

12. L. C. Davidson, and J. E. Smith, "Liquid-Structure Coupling in Curved Pipes" The Shock and Vibration Bulletin No. 40, Part 4, pp 197-207, December 1969.

A 78.28-in. long pipe, 4.5-in OD, copper-nickel pipe, with a 90-deg. elbow at midpoint, was filled with oil with a bulk modulus of 238,000 psi. The exciting force consisted of an external source driving a piston linked to the elbow. The results were reported graphically in terms of mobility (velocity/force) vs. frequency and showed good agreement

between computed and measured results over a frequency range between 20 Hz and 2000 Hz.

13. L. C. Davidson and D. R. Samsury, "Liquid-Structure Coupling in Curved Pipes-II" The Shock and Vibrations Bulletin, No. 42, Part 1, pp 123-135, January 1972.
A piping assembly consisting of straight sections and uniform bends in a non-planar arrangement containing a liquid was analyzed and tested. The analysis indicated coupling between compressional wave of the liquid and mechanical responses of the pipe. Tests generally confirmed existence of the coupling but not the frequency characteristics.

14. D. R. Samsury, "Liquid-Structure Coupling in Pipes," USN (NSRDC) Report 4191, April 1974.
A rigorous mathematical development of liquid-filled elbows and straight pipes is detailed. The analysis is based on the previous studies by the same Navy group as a continuing interest in the problem of noise transmission through liquid-filled piping systems. The study indicates that in straight pipes no liquid-to-structure coupling should occur which is contrary to the findings of other investigators. Experiments using four-in. diameter pipes, three to four feet in length, showed that the coupling phenomenon was suppressed.
Among the recommendations made were the following:
(a) The development of analytical models of other pipe components
(b) A design guide to analyze piping systems

15. Armed Services Investigating Subcommittee, "Crash of the F-14A", H. Res. 201, U.S. Government Printing Office, December 20, 1971
Allegations of defects and deficiencies in the F-14A aircraft design, manufacture, testing, and management, were made after a crash occurred on its second test flight.
Accident investigation revealed that the causes were fatigue fractures in the hydraulic control system tubing as a result of ripple vibrations of the hydraulic pumps.
The findings of the subcommittee indicated that the failure of all three control systems could be laid on faulty and inadequate design and possibly incomplete testing. In addition, the evidence did disclose basis for most of the allegations.

16. J. L. Sewall, D. A. Wineman, and R. W. Herr, "An Investigation of Hydraulic Line Resonance and Its Attenuation" NASA TM X-2787, December 1973.
The study mentions in its introduction "the crash of an advanced fighter-aircraft prototype", presumably the F-14 aircraft, and the failure of the hydraulic line due to pump pressure pulsations. The experimental investigation involved the use of two types of attenuators. One involved the use of a closed-end tube (standpipe) normal to the main pipe. The other, was a commercial damper with an intricate internal flow arrangement. The conclusions indicated that the commercial damper attenuated pressure pulsations over a wider frequency range than the standpipes.

17. J. A. Hutchinson, and R. N. Hancock, "Ground Vibration Survey as a Means of Eliminating Potential In-Flight Component Failures" Shock and Vibration Bulletin, No. 43, Part III, June 1973, pp 175-180.
This paper describes the ground vibrations tests and procedures that Vought Aeronautics Company performed on the XC-142A and A-7E aircraft. The company decided to resolve empirically the problems associated with complex installations which were considered not amenable to design analysis. Over a thousand surveys were made which resulted in 338 modifications to the aircraft components. The paper claims that the results of all these efforts virtually eliminated hydraulic leaks and intermittent connector failures.

# APPENDIX B

# HLMR COMPUTER PROGRAM

# AND

# SAMPLE RESULTS

B1. PROGRAM LISTING

B2. LIST OF SYMBOLS

A list of symbols with description and units used in the sample computer runs.

B3. SAMPLE COMPUTER RUNS

Tables B3 through B4 summarize the results of computer runs for the straight pipe, one-elbow pipe, and two-elbow pipe, respectively.

**TABLE B1**

**HLMR PROGRAM LISTING**

```
HLMR        10:24 MAY 03,'73

$PIKLD
      DIMENSION H(3),C0(10),C2(10),C3(10),C6(10),S7(3)
      DIMENSION U(3,3),V(3,3),S9(3),C9(3),C4(3),C8(3),C7(3)
      DIMENSION FIFTH(24),FOURTH(24),THIRD(24),SECOND(24),FIRST(24)
      DIMENSION RED(24),Y(50),CARDS(50),PEN(3),DOG(3)
      DATA FIFTH/12*0.0,-2.857E-10,11*0.0/
      DATA FOURTH/5*0.0,6.54695E-9,4*0.0,-4.06346E-9,0,
     Z1.19684E-7,10*0,3.76789E-9/
      DATA THIRD/0,4.11523E-8,0,4.23045E-8,7.20165E-8,-2.02768E-6,
     Z1.85185E-7,0,3.08642E-8,0,1.31033E-6,-1.13169E-7,-1.72737E-5,
     Z-1.64609E-7,-1.95473E-7,-2.26337E-7,-1.95473E-7,-1.64609E-7,
     Z-1.8518E-7,0,0,0,4.62963E-7,-5.50879E-7/
      DATA SECOND/0,-1.01852E-5,1.23016E-5,3.04233E-6,2.32804E-5,
     Z2.20118E-4,2.24869E-6,5.92593E-5,5.05291E-5,6.26984E-5,
     Z-4.4823E-5,1.23016E-4,1.09969E-3,1.44577E-4,1.64947E-4,
     Z1.8547E-4,1.95238E-4,2.0224E-4,2.2209E-4,2.07908E-4,
     Z2.13095E-4,2.34069E-4,1.36243E-4,2.2117E-4/
      DATA FIRST/0,1.3955E-3,6.7857E-4,1.17791E-3,1.41534E-4,
     Z-4.00156E-3,3.32143E-3,1.07143E-3,3.49603E-3,4.2619E-3,
     Z7.7298E-3,2.64153E-3,-1.21111E-2,6.54894E-3,5.81481E-3,
     Z5.00926E-3,3.969508E-3,3.38228E-3,2.08333E-3,3.58E-3,
     Z1.607144E-3,1.90476E-4,4.65476E-3,2.05279E-3/
      DATA RED/22.4,22.2393,21.8779,21.5023,21.201,20.9332,20.6463,
     Z20.2917,19.9517,19.6029,19.0952,18.6012,18.05,17.5005,17.1479,
     Z16.7964,16.5067,16.2064,15.9105,15.6,15.2079,14.79,14.4467,
     Z14.1003/
      DATA CARDS/.001,.099,.101,.149,.151,.199,.201,.249,.251,.274,.276,
     Z.299,.301,.332,.334,.3655,.3675,.399,.401,.449,.451,.499,.501,
     Z.549,.551,.599,.601,.6335,.6345,.666,.668,.699,.701,.724,.726,
     Z.749,.751,.799,.801,.849,.851,.899,.901,.949,.951,.999,2.,3.,4.,
     Z5./
   51 PRINT,'ENTER 1 FOR YES, AND 0 FOR NO!'
      PI=3.141592654
      PRINT,'IS THE PIPE STRAIGHT (0), ONE ELBOW (1), OR TWO ELBOW (2)'
      READ,ALR
      CALL INPTDA(D,T,R1,R2,E)
      IF(ALR.EQ.0)GO TO 1
      IF(ALR.EQ.1)GO TO 2
      IF(ALR.EQ.2)GO TO 3
      GO TO 51
    1 PRINT,'STRAIGHT PIPE: DO YOU WISH TO COMPUTE INPLANE AND OUT OF PLANEVIBR
     ZATIONS? Y OR N'
      READ,CIP
      PRINT,'DO YOU WISH TO COMPUTE MAGNIFICATION FACTORS? Y OR N'
      READ,GLW
      IF(CLR.EQ.0)GO TO 5
      PRINT,'ENTER THE PIPE LENGTH'
      READ,AL
      AL4=AL
```

```
      CALL BASCDA(BI,A1,A2,W1,W2,W3,G,R3,PI,D,T,R1,AL,R2)
      ADM=.5*SQRT(G*E/R1)
      F1=D-2*T
      D1=R2/R1
      D2=F1**2/(D**2-F1**2)
      F0=(22.4/(2*PI))*SQRT((E*BI*G)/(R3*AL**4))
      F2=(61.7/22.4)*F0
      F3=(121/22.4)*F0
      F4=(200/22.4)*F0
      F5=(ADM/AL)/SQRT(1+D1*D2)
    5 IF(BER.EQ.0)GO TO 6
      PRINT,'MAGNIFICATION FACTORS INPUT DATA'
      PRINT,'ENTER THE PIPE LENGTH'
      READ,AL
      PRINT,' ENTER THE NUMBER OF POINTS'
      READ,N1
      DO 55 N=1,N1
      WRITE(6,54)N
   54 FORMAT(8HINPUT X(,I1,1H))
      READ,C0(N)
   55 CONTINUE
      PRINT,'ENTER P1 & P2'
      READ,P1,P2
      PRINT,'ENTER Q1 & Q2'
      READ,Q1,Q2
      PRINT,'ENTER W0 & M'
      READ,W0,M
      PRINT,'ENTER THE SPRING RATE'
      T0=90
      R=3
      READ,S
      PRINT,'ENTER THE DISTANCE BETWEEN SUPPORTS'
      READ,B0
      CALL BASCDA(BI,A1,A2,W1,W2,W3,G,R3,PI,D,T,R1,AL,R2)
      S8=(E*BI*G)/(R2*A2+R1*A1)
      S6=SQRT(S8)
      DO 8 N=1,10
    8 C3(N)=((N*PI)**2)*S6/((B0/(M+1))**2)
      F6=A2*SQRT(P1**2+P2**2)
      F7=((R2/G)/A1)*(Q1**2+Q2**2)
      F8=SQRT(Q1**2+Q2**2)/A2
      R0=F6/F7
      IF(R0.LT.500)GO TO 9
      F7=0
    9 T1=T0/57.29578
      J0=F6*(1-COS(T1))
      J1=F7*(1-COS(T1))
      J2=F6*SIN(T1)
      J3=F7*SIN(T1)
      Q9=J2+J3
      Q8=J1+J0
```

```
      Y9=Q9/((W3/G)*C3(1)**2)
      W9=SQRT(S*A*G/W3)
      W4=W0*.3*PI
      A9=W4/C3(1)
      A8=W9/C3(1)
      D9=1-A9**2+A8**2
      IF(D9.EQ.0)GO TO 6
      C1=B0/2
      DO 11 N=1,N1
      C2(N)=0
      DO 10 J=1,10
      V8=2*(SIN(J*PI*C1/B0)*SIN(J*PI*C0(N)/B0))/ABS(J**4+D9-1)
   10 C2(N)=C2(N)+V8
   11 C6(N)=Y9*C2(N)
    6 CONTINUE
      DO 201 N=1,N1
      C2(N)=ABS(C2(N))
  201 CONTINUE
      IF(CER.EQ.1)GO TO 12
      IF(BER.EQ.1)GO TO 13
   12 CALL OUTPT1(E,D,T,AL,R1,R2)
      CALL OUTPT2(BI,AL4,A1,A2,W1,W2)
      CALL OUTPT3(W3)
      CALL OUTPT4(AL,F0,F2,F3,F4,F5)
      IF(BER.EQ.1)GO TO 13
      GO TO 14
   13 CALL OUTPT1(E,D,T,AL,R1,R2)
      CALL OUTPT5(F0,R,P1,P2,Q1,Q2,W0,C1,G,M)
      CALL OUTPT2(BI,AL4,A1,A2,W1,W2)
      CALL OUTPT6(W3,C3(1),F7,Q8,F8,W9,F6,Q9,Y9,A9,PI)
      CALL OUTPT7(C0(1),C2(1),C6(1),C3(1),PI,N1)
   14 GO TO 15
    2 Y(50)=0
      PRINT,'ENTER AL1 & AL2'
      READ,AL1,AL2
      R1=AL2/AL1
      AL=AL1+AL2
      CALL BASCDA(BI,A1,A2,W1,W2,W3,G,R3,PI,D,T,R1,AL,R2)
      PRINT,'ENTER THETA'
      READ,X1
      PRINT,'ENTER THE BEND RADIUS'
      READ,R
      DO 16 J=1,24
      Y(J)=FIFTH(J)*X1**5+FOURTH(J)*X1**4+THIRD(J)*X1**3+SECOND(J)*X1**2
      Y(J)=Y(J)+FIRST(J)*X1+RED(J)
   16 CONTINUE
      C=1
      A=1
      DO 17 J=1,47
      DELTA=C+1
      B=A+1
```

```
      IF(H1.GT.CARDS(A).AND.H1.LT.CARDS(B))Y(50)=(Y(C)+Y(DELTA))/2
      A=A+1
      B=B+1
      IF(H1.GT.CARDS(A).AND.H1.LT.CARDS(B))Y(50)=(Y(DELTA))
      IF(Y(50).NE.0)GO TO 57
      A=A+1
   17 C=C+1
   57 W5=Y(50)*((E*BI*G)/(W3*AL**3))**.5
      F9=W5/(2*PI)
      O2=F9/.15
      H(1)=15.4
      H(2)=50.0
      H(3)=104.0
      AL4=(AL1+AL2)-R*(2-PI/2)
      DO 18 N=1,3
      C0(N)=(H(N)/(2*PI*AL1**2))*SQRT(G*E*BI/(.4375*(R1*A1+.67*R2*A2)))
   18 C2(N)=(H(N)/(2*PI*AL2**2))*SQRT(G*E*BI/(.4375*(R1*A1+.67*R2*A2)))
      A3=1/(2*PI*AL1)*SQRT((G*E)/R1)*1/SQRT(1+(R2*A2)/(R1*A1))
      A6=1/(2*PI*AL2)*SQRT((G*E)/R1)*1/SQRT(1+(R2*A2)/(R1*A1))
      A31=1/(2*PI*AL1)*SQRT((G*E)/R1)*1/SQRT(1+(R2*.33*A2)/(R1*A1))
      A61=1/(2*PI*AL2)*SQRT((G*E)/R1)*1/SQRT(1+(R2*.33*A2)/(R1*A1))
      DO 19 N=1,3
      IF(AL1.EQ.0)GO TO 20
      C6(N)=C0(N)*A3/SQRT(C0(N)**2+A3**2)
   20 IF(AL2.EQ.0)GO TO 19
      C3(N)=C2(N)*A6/SQRT(C2(N)**2+A6**2)
   19 CONTINUE
      PRINT,'ONE ELBOW PIPE VIBRATIONS'
      CALL OUTPT1(E,D,T,AL,R1,R2)
      CALL OUTPT8(AL2,AL1,H1,R)
      CALL OUTPT2(BI,AL4,A1,A2,W1,W2)
      CALL OUTPT3(W3)
      CALL OUTPT9(A3,A6,C0(1),C2(1),C6(1),C3(1),X1,Y(1),O2,W5,F9,
     1A31,A61)
      GO TO 15
    3 PRINT,'TWO ELBOW PIPE INPLANE AND OUT OF PLANE VIBRATIONS'
      PRINT,'ENTER THE PIPE LENGTHS AL1,AL2,AL3'
      READ,AL1,AL2,AL3
      PRINT,'ENTER THE BEND RADIUS'
      READ,R
      CALL BASCDA(BI,A1,A2,W1,W2,W3,G,R3,PI,D,T,R1,AL,R2)
      AL4=(AL1+AL2+AL3)-R*(4-PI)
      LL=AL1*AL2
      IF(LL.EQ.0)GO TO 21
      X4=6*E*BI*(1+AL2/AL1)/(AL2*(2*AL1**2+3*AL3**2))
      GO TO 22
   21 X4=0
   22 X2=(R1*A1+R2*A2)*.25*(AL1+AL2+2*AL3)
      X3=(1/(2*PI)*SQRT(G*X4/X2))
      EM=SQRT(G*E/R1)
      G1=1/((2*PI)*(AL1+AL2))*EM*(1/SQRT(1+(R2*A2)/(R1*A1)))
```

```
      FM=.4375*((R1*A1)+(.67*R2*A2))
      H(1)=15.4
      H(2)=50.0
      H(3)=104.0
      DO 23 N=1,3
      IF(AL1.EQ.0)GO TO 24
      C0(N)=H(N)*EM*SQRT(R1)*SQRT(BI/FM)/(2*PI*AL1**2)
      GO TO 25
   24 C0(N)=0
   25 IF(AL2.EQ.0)GO TO 26
      C2(N)=H(N)*EM*SQRT(R1)*SQRT(BI/FM)/(2*PI*AL2**2)
      GO TO 27
   26 C2(N)=0
   27 C3(N)=G1*C0(N)/SQRT(G1**2+C0(N)**2)
   23 C6(N)=G1*C2(N)/SQRT(G1**2+C2(N)**2)
      GM=.25*(R1*A1+R2*A2)
      HM=1.5*GM
      OM=SQRT(G*E*BI)/(2*PI)
      B7(1)=22.4
      B7(2)=61.7
      B7(3)=121
      DO 28 N=1,3
      C7(N)=0.
      IF(AL1.NE.0.)C7(N)=(OM/SQRT(GM))*(H(N)/AL1**2)
      C8(N)=0.
      IF(AL2.NE.0.)C8(N)=(OM/SQRT(GM))*(H(N)/AL2**2)
      DM(N)=0.
      IF(AL3.NE.0.)DM(N)=(OM/SQRT(HM))*B7(N)/(AL3**2)
   28 CONTINUE
      DO 34 N=1,3
      DO 34 J=1,3
      U(N,J)=(C7(N)*DM(J))/SQRT(C7(N)**2+DM(J)**2)
      V(N,J)=(C8(N)*DM(J))/SQRT(C8(N)**2+DM(J)**2)
   34 CONTINUE
      IF(AL2.EQ.0)GO TO 35
      DL=(AL1/AL2)**3*AL3/(1+(AL1/AL2)**3)
      GO TO 36
   35 DL=0
   36 IF(LL.EQ.0)GO TO 37
      EL=DL/(AL1/AL2)**3
      GO TO 38
   37 EL=0
   38 LLL=AL1*AL2*AL3
      IF(LLL.EQ.0)GO TO 39
      FL=3*E*BI*LL/(AL2**3*DL)
      GL=3*E*BI/AL2**3
      TOAD=SQRT(GM)
      T2=1.73205081*OM/TOAD
      T3=T2/AL1**2
      T5=T2/AL2**2
      W6=4*GM*AL3
```

```
      B8=1.73205081*OM/SQRT(W6)*SQRT((AL1+AL2)**3/(AL1**3*AL2**3))
      GO TO 40
   39 FL=0
      GL=0
      T2=0
      T3=0
      T5=0
      B8=0
   40 DO 41 N=1,3
      B9(N)=OM/SQRT(HM)*(1/(AL1+AL2))**2*B7(N)
   41 C9(N)=B8*B9(N)/SQRT(B8**2+B9(N)**2)
      PRINT,'TWO ELBOW PIPE VIBRATIONS'
      CALL OUTPT1(E,D,T,AL,R1,R2)
      CALL OUTP10(R,AL1,AL2,AL3)
      CALL OUTPT2(BI,AL4,A1,A2,W1,W2)
      CALL OUTP11(W3,X4,FM,GM,HM,DL,EL,GL,W6,C0(1),C2(1),C3(1),C6(1),
     2C7(1),C8(1),X3,G1,DM(1),U(1,1),V(1,1),B8,T5,T3,B9(1),FL,C9(1))
      GO TO 15
   15 WRITE(5,52)
   52 FORMAT(31HDO YOU WISH TO CONTINUE? Y OR N)
      READ,DER
      IF(DER)53,53,51
   53 CONTINUE
      END
      SUBROUTINE INPTDA(D,T,R1,R2,E)
      PRINT,'GENERAL READ,DATA SECTION'
      PRINT,'INPUT THE MATERIAL CODE OF THE PIPE'
      PRINT,'  CODE #      MATERIAL'
      PRINT,'     1        TITANIUM'
      PRINT,'     2        ALUMINUM'
      PRINT,'     3           STEEL'
      PRINT,'     4           OTHER'
      READ,B
      GO TO(42,43,44,45),B
   42 E=16E6
      R1=.16
      GO TO 46
   43 E=10E6
      R1=.1
      GO TO 46
   44 E=30E6
      R1=.283
      GO TO 46
   45 PRINT,'ENTER THE MODULUS OF ELASTICITY'
      READ,E
      PRINT,'ENTER THE PIPE DENSITY'
      READ,R1
   46 PRINT,'INPUT THE SIZE CODE OF THE PIPE'
      PRINT,'  CODE #     PIPE DIMENSIONS'
      PRINT,'     1            1X.051'
      PRINT,'     2         .625X.032'
```

```
      PRINT,'    3              1.25X.065'
      PRINT,'    4                  OTHER'
      READ,AA
      GO TO(56,47,48,49),AA
   56 D=1
      T=.051
      GO TO 50
   47 D=.625
      T=.032
      GO TO 50
   48 D=1.25
      T=.065
      GO TO 50
   49 PRINT,'ENTER THE PIPE DIAMETER'
      READ,D
      PRINT,' ENTER THE WALL THICKNESS'
      READ,T
   50 PRINT,'ENTER THE FLUID DENSITY'
      READ,R2
      RETURN
      END
      SUBROUTINE BASCDA(BI,A1,A2,W1,W2,W3,G,R3,PI,D,T,R1,AL,R2)
      BI=(PI/64)*(D**4-(D-2*T)**4)
      A1=(PI/4)*(D**2-(D-2*T)**2)
      A2=(PI/4)*(D-2*T)**2
      W1=R1*A1*AL
      W2=R2*A2*AL
      W3=W1+W2
      G=386
      R3=R1*A1+.25*R2*A2
      RETURN
      END
      SUBROUTINE OUTPT1(E,D,T,AL,R1,R2)
      WRITE(6,100)
  100 FORMAT(/////,10HINPUT DATA,/,9X,1HE,11X,1HD,11X,1HT,11X,1HL,10X,
     Z3HRHO,9X,4HFRHO,/,8X,3HPSI,10X,2HIN,10X,2HIN,10X,2HIN,7X,7HLBS/IN3,
     Z6X,7HLBS/IN3)
      WRITE(6,101)E,D,T,AL,R1,R2
  101 FORMAT(2X,6E12.4)
      RETURN
      END
      SUBROUTINE OUTPT2(BI,AL4,A1,A2,W1,W2)
      WRITE(6,96)
   96 FORMAT(//,10HBASIC DATA)
      WRITE(6,102)
  102 FORMAT(9X,1HI,10X,3HCLL,8X,5HFAREA,7X,5HFAREA,8X,3HFWT,9X,3HFWT)
      WRITE(6,90)
   90 FORMAT(8X,3HIN4,10X,2HIN,9X,3HIN2,9X,3HIN2,9X,3HLBS,9X,3HLBS)
      WRITE(6,101)BI,AL4,A1,A2,W1,W2
  101 FORMAT(2X,6E12.4)
      RETURN
```

```
      END
      SUBROUTINE OUTPT3(W3)
      WRITE(6,103)W3
  103 FORMAT(/,8X,4HWTOT,/,8X,3HLBS,/,2X,1E12.4)
      RETURN
      END
      SUBROUTINE OUTPT4(AL,F0,F2,F3,F4,F5)
      WRITE(6,104)AL
  104 FORMAT(//,11HOUTPUT DATA,/,35HINPLANE AND OUT OF PLANE VIBRATIONS,
     Z//,11HPIPE LENGTH,1E12.4,2X,2HIN,//,
     Z33H N   TRANS FREQ(HZ)   LONG FREQ(HZ),/)
      J=1
      WRITE(6,124)J,F0,F5,F2,F5*2,F3,F5*3,F4,F5*4
  124 FORMAT(I2,3X,1E12.4,3X,1E12.4,/,2H 2,3X,1E12.4,3X,1E12.4,/,2H 3,3X,
     Z1E12.4,3X,1E12.4,/,2H 4,3X,1E12.4,3X,1E12.4)
      RETURN
      END
      SUBROUTINE OUTPT5(T0,R,P1,P2,Q1,Q2,W0,C1,S,M)
      WRITE(6,106)
  106 FORMAT(/,7X,5HTHETA,9X,1HR,10X,2HP1,10X,2HP2,10X,2HQ1,10X,2HQ2)
      WRITE(6,91)
   91 FORMAT(8X,3HDEG,10X,2HIN,9X,3HPSI,9X,3HPSI,9X,3HCIS,9X,3HCIS)
      WRITE(6,92)T0,R,P1,P2,Q1,Q2
   92 FORMAT(2X,6E12.4,/)
      WRITE(6,93)
   93 FORMAT(8X,2HW0,10X,3HCEE,9X,2HSK,11X,1HM)
      WRITE(6,94)
   94 FORMAT(8X,3HRPM,9X,2HIN,9X,5HLB/IN)
      WRITE(6,95)W0,C1,S,M
   95 FORMAT(2X,4E12.4)
      RETURN
      END
      SUBROUTINE OUTPT6(W3,C3,F7,Q8,F8,W9,F6,Q9,Y9,A9,PI)
      DIMENSION C3(1)
      BASE=C3(1)/(2*PI)
      BALL=W9/(2*PI)
      WRITE(6,97)
   97 FORMAT(/,8X,4HWTOT,8X,2H[illegible],10X,2HFQ,10X,2HFH,9X,4HFVEL,9X,2HWK)
      WRITE(6,107)
  107 FORMAT(8X,3HLBS,9X,2HHZ,10X,2HHZ,10X,2HHZ,10X,2HHZ,10X,2HHZ)
      WRITE(6,98)W3,BASE,F7,Q8,F8,BALL
   98 FORMAT(2X,6E12.4)
      WRITE(6,99)
   99 FORMAT(/,8X,2HFP,10X,2HFV,10X,3HYST,9X,2HA0)
      WRITE(6,64)
   64 FORMAT(8X,3HLBS,9X,3HLBS,9X,2HIN)
      WRITE(6,65)F6,Q9,Y9,A9
   65 FORMAT(2X,4E12.4)
      RETURN
      END
      SUBROUTINE OUTPT7(C0,C2,C6,C3,PI,W1)
```

```
      DIMENSION C0(1),C2(1),C6(1),C3(1)
      WRITE(6,108)
  108 FORMAT(//,11HOUTPUT DATA)
      WRITE(6,66)
   66 FORMAT(2X,5HX(IN),7X,4HSUMF,5X,5HY(IN),5X,1HN,5X,8HF(N)(HZ))
      DO 125 J=1,N1
      WRITE(6,109)C0(J),C2(J),C6(J),J,C3(J)/(2*PI)
  109 FORMAT(F8.4,2X,F9.4,2X,F8.4,3X,I2,1X,F11.4)
  125 CONTINUE
      L=N1+1
      DO 105 J=L,10
      WRITE(6,110)J,C3(J)/(2*PI)
  110 FORMAT(32X,I2,1X,F11.4)
  105 CONTINUE
      WRITE(6,71)
   71 FORMAT(////)
      RETURN
      END
      SUBROUTINE OUTPT8(AL2,AL1,H1,R)
      WRITE(6,111)AL2,AL1,H1,R
  111 FORMAT(/9X,2HL2,10X,2HL1,7X,7HAL2/AL1,8X,1HR,/,9X,2HIN,10X,2HIN,
     Z22X,2HIN,/,2X,4E12.4)
      RETURN
      END
      SUBROUTINE OUTPT9(A3,A6,C0,C2,C6,C3,T0,Y,O2,W5,F9,A31,A61)
      DIMENSION C0(3),Y(50),C2(3),C6(3),C3(3)
      J=1
      WRITE(6,112)
  112 FORMAT(//,11HOUTPUT DATA,/,18HINPLANE VIBRATIONS,/)
      WRITE(6,129)
  129 FORMAT(9X,6HL1:AXF,5X,6HL2:AXF,5X,1HJ,2X,7HL1:B(J),5X,7HL2:B(J),5X,
     $7HL1:F(J),5X,7HL2:F(J))
      WRITE(6,130)
  130 FORMAT(11X,2HHZ,10X,2HHZ,11X,2HHZ,10X,2HHZ,10X,2HHZ,10X,2HHZ)
      WRITE(6,131)A3,A6,J,C0(1),C2(1),C6(1),C3(1)
  131 FORMAT(4H 1.0,2E12.4,3X,I1,E10.4,3E12.4,
      J=2
      WRITE(6,200)A31,A61,J,C0(2),C2(2),C6(2),C3(2)
  200 FORMAT(4H .33,2E12.4,3X,I1,E10.4,3E12.4)
      L=3
      WRITE(6,113)L,C0(L),C2(L),C6(L),C3(L)
  113 FORMAT(31X,I1,E10.4,3E12.4)
      WRITE(6,114)
  114 FORMAT(//,23HOUT OF PLANE VIBRATIONS,/)
      WRITE(6,68)
   68 FORMAT(7X,5HTHETA,7X,5HALPHA,8X,3HNCF,8X,5HSPEED,7X,4HFREQ)
      WRITE(6,69)
   69 FORMAT(8X,3HDEG,19X,7HRAD/SEC,7X,3HRPM,9X,2HHZ)
      WRITE(6,70)T0,Y(50),W5,O2,F9
   70 FORMAT(2X,5E12.4)
      WRITE(6,72)
```

```
 72 FORMAT(////)
    RETURN
    END
    SUBROUTINE OUTP10(R,AL1,AL2,AL3)
    WRITE(6,115)R,AL1,AL2,AL3
115 FORMAT(/,9X,1HR,10X,2HL1,10X,2HL2,10X,2HL3,/,8X,2HIN,10X,2HIN,
   Z10X,2HIN,10X,2HIN,/,2X,4E12.4)
    RETURN
    END
    SUBROUTINE OUTP11(W3,X4,FM,GM,HM,DL,EL,GL,W6,C0,C2,C3,C6,C7,C8,X3,
   ZG1,DM,U,V,B8,T5,T3,B9,FL,C9)
    DIMENSION C0(1),C2(1),C3(1),C6(1),C7(1),C8(1),DM(3),U(3,3),V(3,3)
    DIMENSION B9(1),C9(1)
    WRITE(6,116)
116 FORMAT(/8X,4HWTOT,8X,3HXTK,9X,4HMUCP,8X,4HMUCF,8X,4HMUFF,8X,3HL3A)
    WRITE(6,132)
132 FORMAT(8X,3HLBS,8X,5HLB/IN,7X,5HLB/IN,7X,5HLB/IN,7X,5HLB/IN,8X,
   $2HIN)
    WRITE(6,58)W3,X4,FM,GM,HM,DL
 58 FORMAT(2X,6E12.4)
    WRITE(6,59)
 59 FORMAT(/,8X,3HL3B,9X,3HL1K,9X,3HL2K,9X,4HL3EW)
    WRITE(6,60)
 60 FORMAT(8X,2HIN,10X,2HIN,9X,5HLB/IN,8X,3HLBS)
    WRITE(6,61)EL,FL,GL,W6
 61 FORMAT(2X,4E12.4)
    WRITE(6,62)
 62 FORMAT(//,11HOUTPUT DATA,/,18HINPLANE VIBRATIONS,/)
    WRITE(6,119)X3,G1,DM(1),DM(2),DM(3)
119 FORMAT(7X,6HXTFREQ,6X,6HAXFREQ,4X,9HL3:FFF(1),3X,9HL3:FFF(2),3X,
   Z9HL3:FFF(3),/,9X,2HHZ,10X,2HHZ,10X,2HHZ,10X,2HHZ,10X,2HHZ,/,2X,
   Z5E12.4)
    WRITE(6,117)
117 FORMAT(/1X,1HJ,4X,9HL1:CPF(J),3X,9HL2:CPF(J),3X,9HL1:CPA(J),3X,
   Z9HL2:CPA(J),3X,9HL1:CFF(J),3X,9HL2:CFF(J),/,9X,2HHZ,10X,2HHZ,10X,
   Z2HHZ,10X,2HHZ,10X,2HHZ,10X,2HHZ)
    DO 127 J=1,3
    WRITE(6,118)J,C0(J),C2(J),C3(J),C6(J),C7(J),C8(J)
118 FORMAT(I2,6E12.4)
127 CONTINUE
    WRITE(6,120)
120 FORMAT(/,1X,1HJ,1X,14HL1:L3FREQ(1,J),2X,14HL1:L3FREQ(2,J),2X,
   $14HL1:L3FREQ(3,J),2X,14HL2:L3FREQ(1,J),2X,
   $14HL2:L3FREQ(2,J),2X,14HL2:L3FREQ(3,J))
    WRITE(6,63)
 63 FORMAT(9X,2HHZ,14X,2HHZ,14X,2HHZ,14X,2HHZ,14X,2HHZ,14X,2HHZ)
    DO 128 J=1,3
    WRITE(6,121)J,U(1,J),U(2,J),U(3,J),V(1,J),V(2,J),V(3,J)
121 FORMAT(1X,I1,1X,1E12.4,5E16.4)
128 CONTINUE
    WRITE(6,122)B8,T3,T5
```

```
 122 FORMAT(//,23HOUT OF PLANE VIBRATIONS,//,7X,5HL3:BF,7X,5HL1:TF,7X,
     Z5HL2:TF,/,8X,2HHZ,10X,2HHZ,10X,2HHZ,/,2X,3E12.4,//,1X,1HJ,4X,
     Z7H3NDF(J),4X,9HL1:CPA(J),3X,9HL2:CPA(J),2X,10HL1:L2BF(J))
      DO 67 J=1,3
      WRITE(6,123)J,C9(J),C3(J),C6(J),B9(J)
 123 FORMAT(1X,I1,4E12.4)
  67 CONTINUE
      WRITE(6,30)
  30 FORMAT(////)
      RETURN
      END
*BYE
```

TABLE B2

LIST OF SYMBOLS

| COMPUTER PROGRAM PRINT OUT | DESCRIPTIONS | UNITS |
|---|---|---|
| E | Pipe Modulus of Elasticity | $LB/IN.^2$ |
| RHO | Pipe Density | $LB/IN.^3$ |
| FRHO | Fluid Density | $LB/IN.^3$ |
| D | Pipe Outside Diameter | IN. |
| T | Pipe Wall Thickness | IN. |
| N | Mode Number | -- |
| THETA | Bend Angle | DEG. |
| $L_1, L_2\ L_3$ | Length of pipe segments | IN. |
| L | Total pipe length, $L_1 + L_2$ | IN. |
| I | Second Moment of Inertia | $IN.^4$ |
| PAREA | Pipe Cross-sectional area | $IN.^2$ |
| FAREA | Flow Area | $IN.^2$ |
| PWT | Pipe Weight | LB. |
| FWT | Fluid Weight | LB. |
| WTOT | Total Weight, pipe + fluid | LB. |
| ALPHA | Frequency Factor | -- |
| NCF | Natural Circular Frequency | RAD/SEC |
| FREQ | Natural Frequency | HZ |
| SPEED | Pump Speed | RPM |
| R | Bend Radius | IN. |
| CLL | Centerline length | IN. |
| L1:AXF,L2:AXF | Axial frequency, leg 1 and leg 2, respectively | HZ |
| L1:B(I),L2:B(I) | Bending frequency, fixed-pinned, mode(I), leg 1 and leg 2, respectively | HZ |
| L1:F(I),L2:F(I) | Coupled axial-bending frequency, mode(I), leg 1 and leg 2, respectively | HZ |
| G | Acceleration of gravity | $IN/SEC.^2$ |
| XTK | Translational spring rate | LB/IN. |
| MUCP | Weight per unit length, fixed-pinned end conditions | LB/IN. |
| MUCF | Weight per unit length, fixed-free | LB/IN. |
| MUFF | Weight per unit length, fixed-fixed | LB/IN. |

| COMPUTER PROGRAM PRINT OUT | DESCRIPTION | UNITS |
|---|---|---|
| L3A, L3B | Torsional moment arms | IN. |
| L1K, L2K | Torsional spring rate | LB/IN. |
| L3EW | Crosspipe effective weight | LB. |
| XTFREQ | Translational frequency | HZ |
| AXFREQ | Axial frequency | HZ |
| L1:CPF(I),L2:CPF(I) | Bending frequency, fixed-pinned mode (I), leg 1 and leg 2, respectively | HZ |
| L1:CPA(I),L2:CPA(I) | Coupled axial-bending frequency, mode(I), leg 1 and leg 2, respectively | HZ |
| L1:CFF(I),L2:CFF(I) | Bending frequency, fixed-fee, mode (I), leg 1 and leg 2, respectively | HZ |
| L3:FFF(J) | Bending frequency, fixed-fixed, mode (J), leg 3 | HZ |
| L1:L3FREQ(I,J) | Coupled frequency, leg 1 and leg 3 | HZ |
| L2:L3FREQ(I,J) | Coupled frequency, leg 2 and leg 3 | HZ |
| L1:TF,L2:TF | Torsional frequency | HZ |
| L3:BF | Bending frequency, leg 3 as a concentrated weight | HZ |
| L1:L2BF(J) | Bending frequency, leg 1 and leg 2 as distributed weights | HZ |
| BNDF(J) | Coupled frequency, leg 3 with legs 1 and 2 | HZ |

# STRAIGHT PIPE COMPUTER RUN

TABLE B3

INPUT DATA

| E | D | T | L | RHO | FRHO |
|---|---|---|---|---|---|
| PSI | IN | IN | IN | LBS/IN3 | LBS/IN3 |
| .1600E+08 | .1000E+01 | .5100E-01 | .5320E+02 | .1600E+00 | .3140E-01 |

BASIC DATA

| I | CLL | PAREA | FAREA | PWT | FWT |
|---|---|---|---|---|---|
| IN4 | IN | IN2 | IN2 | LBS | LBS |
| .1717E-01 | .5320E+02 | .1529E+00 | .6533E+00 | .1294E+01 | .1053E+01 |

| WTOF |
|---|
| LBS |
| .2352E+01 |

OUTPUT DATA
INPLANE AND OUT OF PLANE VIBRATIONS

PIPE LENGTH .5320E+02 IN

| N | TRANS FREQ(HZ) | LONG FREQ(HZ) |
|---|---|---|
| 1 | .7577E+02 | .1370E+04 |
| 2 | .2087E+03 | .2739E+04 |
| 3 | .4093E+03 | .4109E+04 |
| 4 | .6765E+03 | .5479E+04 |

# MAGNIFICATION FACTORS



TABLE B3 (CONTINUED)

INPUT DATA

| E | D | T | L | RHO | FRHO |
|---|---|---|---|---|---|
| PSI | IN | IN | IN | LBS/IN3 | LBS/IN3 |
| .1600E+08 | .1000E+01 | .5100E-01 | .5320E+02 | .1600E+00 | .3140E-01 |

| THETA | R | P1 | P2 | Q1 | Q2 |
|---|---|---|---|---|---|
| DEG | IN | PSI | PSI | CIS | CIS |
| .9000E+02 | .3000E+01 | .3000E+04 | 0. | .7700E+01 | 0. |

| W0 | CLE | SK | M |
|---|---|---|---|
| RPM | IN | LB/IN | |
| .1600E+04 | .2660E+02 | .1290E+04 | 0. |

BASIC DATA

| I | CLL | PAREA | FAREA | PWT | FWT |
|---|---|---|---|---|---|
| IN4 | IN | IN2 | IN2 | LBS | LBS |
| .1717E-01 | .5320E+02 | .1520E+00 | .6333E+00 | .1294E+01 | .1058E+01 |

| WTOT | WF | FO | FH | FVEL | WK |
|---|---|---|---|---|---|
| LBS | HZ | HZ | HZ | HS | HZ |
| .2352E+01 | .2713E+02 | 0. | .1900E+04 | .1216E+02 | 0. |

| FP | FV | YST | A0 |
|---|---|---|---|
| LBS | LBS | IN | |
| .1900E+04 | .1900E+04 | .1069E+02 | .8831E+01 |

OUTPUT DATA

| X(IN) | SUMF | Y(IN) | N | F(N)(HZ) |
|---|---|---|---|---|
| 0.0000 | 0.0000 | 0.0000 | 1 | 27.1772 |
| 13.3000 | .4525 | -4.8381 | 2 | 108.7090 |
| 26.6000 | .5942 | 7.4226 | 3 | 244.5952 |
| 39.9000 | .4525 | -4.8381 | 4 | 434.3359 |
| 53.2000 | .0000 | .0000 | 5 | 679.4311 |
| | | | 6 | 978.3808 |
| | | | 7 | 1331.5649 |
| | | | 8 | 1739.3436 |
| | | | 9 | 2201.3567 |
| | | | 10 | 2717.7244 |

THIS PAGE IS BEST QUALITY PRACTICABLE
FROM COPY FURNISHED TO DDC

# ONE ELBOW PIPE COMPUTER RUN

**TABLE B4**

INPUT DATA

| E | D | T | L | RHO | FRHO |
|---|---|---|---|---|---|
| PSI | IN | IN | IN | LBS/IN3 | LBS/IN3 |
| .1600E+08 | .1000E+01 | .5100E-01 | .5450E+02 | .1600E+00 | .3140E-01 |

| L2 | L1 | AL2/AL1 | R |
|---|---|---|---|
| IN | IN | | IN |
| .2725E+02 | .2725E+02 | .1000E+01 | .3000E+01 |

BASIC DATA

| I | CLL | PARLA | FARLA | PWT | FWT |
|---|---|---|---|---|---|
| IN4 | IN | IN2 | IN2 | LBS | LBS |
| .1717E-01 | .5321E+02 | .1520E+00 | .6333E+00 | .1326E+01 | .1984E+01 |

| [illegible] |
|---|
| LBS |
| .2410E+01 |

OUTPUT DATA
INPLANE VIBRATIONS

| | L1:AXF | L2:AXF | J | L1:W(J) | L2:W(J) | L1:F(J) | L2:F(J) |
|---|---|---|---|---|---|---|---|
| | HZ | HZ | | HZ | HZ | HZ | HZ |
| 1.0 | .8512E+03 | .8512E+03 | 1 | .2648E+03 | .2648E+03 | .2528E+03 | .2528E+03 |
| .33 | .1018E+04 | .1018E+04 | 2 | .8597E+03 | .8597E+03 | .6049E+03 | .6049E+03 |
| | | | 3 | .1788E+04 | .1788E+04 | .7685E+03 | .7685E+03 |

OUT OF PLANE VIBRATIONS

| THETA | ALPHA | NCF | SPEED | FREQ |
|---|---|---|---|---|
| DEG | | RAD/SEC | RPM | HZ |
| .9000E+02 | .1592E+02 | .2625E+03 | .2785E+03 | .4178E+02 |

# TWO ELBOW PIPE COMPUTER RUN

TABLE B5

INPUT DATA

| E | D | T | L | RHO | FRHO |
|---|---|---|---|---|---|
| PSI | IN | IN | IN | LBS/IN3 | LBS/IN3 |
| .1600E+08 | .1000E+01 | .5100E-01 | .5450E+02 | .1600E+00 | .3140E-01 |

| R | L1 | L2 | L3 |
|---|---|---|---|
| IN | IN | IN | IN |
| .3000E+01 | .1830E+02 | .1830E+02 | .1830E+02 |

BASIC DATA

| I | CLL | PAREA | FAREA | PWT | FWT |
|---|---|---|---|---|---|
| IN4 | IN | IN2 | IN2 | LBS | LBS |
| .1717E-01 | .5232E+02 | .1520E+00 | .6333E+00 | .1326E+01 | .1084E+01 |

| WTOT | XTK | HUCP | HUCF | HUFF | L3A |
|---|---|---|---|---|---|
| LBS | LB/IN | LB/IN | LB/IN | LB/IN | IN |
| .2410E+01 | .1076E+03 | .1647E-01 | .1105E-01 | .1658E-01 | .9150E+01 |

| L3B | L1K | L2K | L3EW |
|---|---|---|---|
| IN | IN | LB/IN | LBS |
| .9150E+01 | .1345E+03 | .1345E+03 | .8091E+00 |

TABLE B5 (CONTINUED)

OUTPUT DATA
IN-PLANE VIBRATIONS

| NTFREQ | NXFREQ | L3:CFF(1) | L3:CFF(2) | L3:FFF(3) |
|---|---|---|---|---|
| HZ | HZ | HZ | HZ | HZ |
| .3665E+02 | .6337E+03 | .8513E+03 | .2345E+04 | .4590E+04 |

| J | L1:CPF(J) | L2:CPF(J) | L1:CPA(J) | L2:CPA(J) | L1:CFF(J) | L2:CFF(J) |
|---|---|---|---|---|---|---|
| | HZ | HZ | HZ | HZ | HZ | HZ |
| 1 | .5871E+03 | .5871E+03 | .4307E+03 | .4307E+03 | .7168E+03 | .7168E+03 |
| 2 | .1906E+04 | .1906E+04 | .6014E+03 | .6014E+03 | .2327E+04 | .2327E+04 |
| 3 | .3965E+04 | .3965E+04 | .625[illegible]+03 | .6258E+03 | .4840E+04 | .4840E+04 |

| J | L1:L3FREQ(1,J) | L1:L3FREQ(2,J) | L1:L3FREQ(3,J) | L2:L3FREQ(1,J) | L2:L3FREQ(2,J) | L2:L3FREQ(3,J) |
|---|---|---|---|---|---|---|
| | HZ | HZ | HZ | HZ | HZ | HZ |
| 1 | .5493E+03 | .79[illegible]E+03 | .8334E+03 | .5403E+03 | .7991E+03 | .8334E+03 |
| 2 | .3055E+03 | .1652E+04 | .2110E+04 | .3055E+03 | .1652E+04 | .2110E+04 |
| 3 | .7[illegible]2E+03 | .2076E+04 | .3334E+04 | .7002E+03 | .2076E+04 | .3334E+04 |

OUT OF PLANE VIBRATIONS

| L3:BF | L1:TF | L2:TF |
|---|---|---|
| HZ | HZ | HZ |
| .1140E+03 | .2062E+02 | .2062E+02 |

| J | L3:BF(J) | L1:CPA(J) | L2:CPA(J) | L1:L23F(J) |
|---|---|---|---|---|
| 1 | .1005E+03 | .4307E+03 | .4307E+03 | .2128E+03 |
| 2 | .1119E+03 | .6014E+03 | .6014E+03 | .5862E+03 |
| 3 | .1135E+03 | .6258E+03 | .6258E+03 | .1150E+04 |

# APPENDIX C

## DERIVATION OF EQUATIONS

## HYDRAULIC LINE MECHANICAL RESPONSE COMPUTER PROGRAM

### C1. ONE-ELBOW PIPE, OUT-OF-PLANE, VIBRATIONS

Analysis determines the fundamental out-of-plane frequency of a one-elbow pipe with ends fixed. A force, F, is applied at the elbow normal to the plane defined by the centerlines of the pipes. The force then causes a downward deflection of the elbow. A free-body diagram in Figure C-1 shows that a single bend pipe can be split into two cantilever pipes with the appropriate forces and cancelling moments. These are depicted for leg 1 and the reverse would be applicable to leg 2 by use of different subscripts. There are three conditions to be considered:

- o torsional rotation due to a moment

$$\theta_T = \frac{TL}{GJ} \qquad \text{(C-1)}$$

where $\theta_T$ is the angle of rotation, radians

T is the torsional moment, in - lbs

L is the pipe length under torsion, in.

GJ is the pipe torsional rigidity, lb-in.$^2$

- o rotations due to a force and due to a moment applied at the free end

$$\theta_F = \frac{FL^2}{2EI} \qquad \text{(C-2)}$$

$$\theta_M = \frac{ML}{EI} \qquad \text{(C-3)}$$

where M is the bending moment, in-lbs

- o deflections due to a force and due to a moment applied at the free end

$$\delta_F = \frac{FL^3}{3EI} \qquad \text{(C-4)}$$

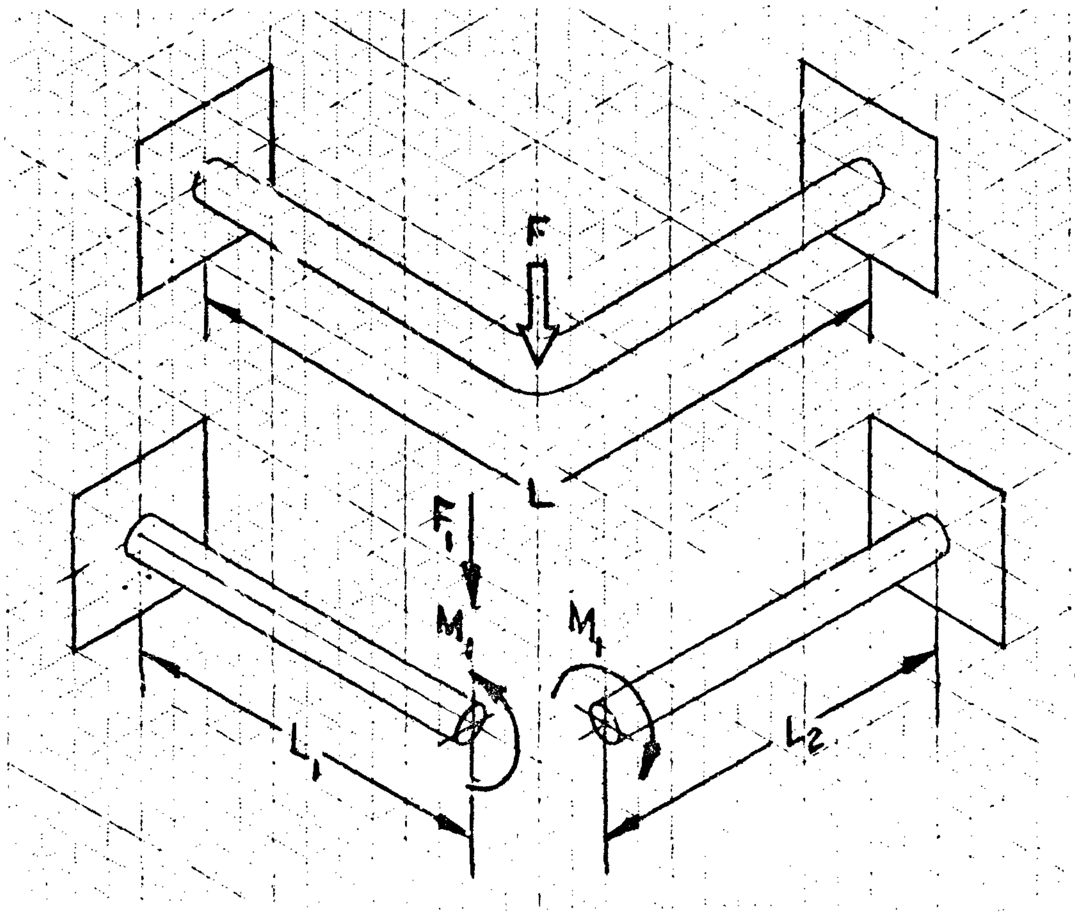


FIGURE C-1

ONE-ELBOW PIPE OUT-OF-PLANE LOADING

$$\delta_M = \frac{ML^2}{2EI} \quad \text{C-5}$$

where $\delta$ is the deflection, inches.

For compatibility of end rotations, the general relationship for the pipe legs defined by lengths $L_1$ and $L_2$ is

$$\theta_T + \theta_M = \theta_F \quad \text{C-6}$$

Consequently the expressions for each leg is obtained by substituting equations C-1 thru C-3 with appropriate subscripts.

For leg 1, $$\frac{M_1 L_2}{GJ_2} + \frac{M_1 L_1}{EI_1} = \frac{F_1 L_1^2}{2EI_1} \quad \text{C-7}$$

For leg 2, $$\frac{M_2 L_1}{GJ_1} + \frac{M_2 L_2}{EI_2} = \frac{F_2 L_2^2}{2EI_2} \quad \text{C-8}$$

Solving equations C-7 and C-8 for $M_1$ and $M_2$, respectively.

$$M_1 = \frac{F_1 L_1}{2}\left[\frac{1}{\left(\frac{EI_1}{GJ_2}\right)\left(\frac{L_2}{L_1}\right)+1}\right] \quad \text{C-9}$$

$$M_2 = \frac{F_2 L_2}{2}\left[\frac{1}{\left(\frac{EI_2}{GJ_1}\right)\left(\frac{L_1}{L_2}\right)+1}\right] \quad \text{C-10}$$

For compatibility of end deflections, the net deflection for leg 1 must equal that for leg 2.

Thus,

$$\delta = \delta_1 = \frac{F_1 L_1^3}{3EI_1} - \frac{M_1 L_1^2}{2EI_1} \quad \text{C-11}$$

$$\delta = \delta_2 = \frac{F_2 L_2^3}{3EI_2} - \frac{M_2 L_2^2}{2EI_2} \quad \text{C-12}$$

Considering that there is no change in physical characteristics from one leg to another, the second moment of inertia for both legs are the same, and the polar inertia for a circular cross-section pipe is twice that of the second moment of inertia. By substituting equations C-9 and C-10 into C-11 and C-12 respectively, the expression for the deflections are

$$\delta = \frac{F_1 L_1^3}{3EI}\left[1 - \frac{3/4}{1+\frac{E}{2G}\left(\frac{L_2}{L_1}\right)}\right] \quad \text{C-13}$$

$$\delta = \frac{F_2 L_2^3}{3EI}\left[1 - \frac{3/4}{1 + \left(\frac{E}{2G}\right)\left(\frac{L_1}{L_2}\right)}\right] \qquad \text{C-14}$$

Solving equations C-13 and C-14 for the components of the applied force results in

$$F_1 = \delta\left\{\frac{3EI}{L_1^3\left[1 - \frac{3/4}{1 + \frac{E}{2G}\left(\frac{L_2}{L_1}\right)}\right]}\right\} \qquad \text{C-15}$$

$$F_2 = \delta\left\{\frac{3EI}{L_2^3\left[1 - \frac{3/4}{1 + \frac{E}{2G}\left(\frac{L_1}{L_2}\right)}\right]}\right\} \qquad \text{C-16}$$

Noting that the applied force is defined as

$$F = F_1 + F_2 \qquad \text{C-17}$$

The deflection due to the applied force can be written as

$$\frac{\delta}{F} = \frac{1}{\frac{3EI}{L_1^3\left[1 - \frac{3/4}{1+\left(\frac{E}{2G}\right)\left(\frac{L_2}{L_1}\right)}\right]} + \frac{3EI}{L_2^3\left[1 - \frac{3/4}{1+\left(\frac{E}{2G}\right)\left(\frac{L_1}{L_2}\right)}\right]}} \qquad \text{C-18}$$

A simplification is made by setting the ratio of leg lengths to be unity which means that each leg length is equal to half of the total pipe centerline length. In addition, by assuming the bending rigidity to be approximately equal to the torsional rigidity, equation C-18 reduces to

$$\frac{\delta}{F} = \frac{1}{\frac{3EI}{\left(\frac{L}{2}\right)^3\left(1 - \frac{3/4}{2}\right)} + \frac{3EI}{\left(\frac{L}{2}\right)^3\left(1 - \frac{3/4}{2}\right)}} = \frac{5}{384}\left(\frac{L^3}{EI}\right) \qquad \text{C-19}$$

It is interesting to note that Reference (c) indicates that the maximum deflection of a pinned-pinned beam with uniform weight distribution is identical to equation C-19.

The spring rate of the single bend pipe is defined by the inverse of equation C-19 or

$$K = \frac{384}{5}\left(\frac{EI}{L^3}\right) \qquad \text{C-20}$$

The natural frequency of a system is given by:

$$f = \frac{1}{2\pi}\sqrt{\frac{Kg}{W_e}} \qquad \text{C-21}$$

where K is the spring rate, lb/in.

g is the acceleration of gravity, 386 in/sec$^2$

$W_e$ is the effective weight, lbs.

f is the natural frequency, Hz.

The next step is to determine the effective weight of a one-elbow pipe. It would be reasonable to assume that the effective weight is the average of the effective weights of a cantilever pipe ($W_{ec}$) and that of a pipe with fixed ends ($W_{ef}$).

To determine these effective weights the expressions for the respective deflection for the cantilever beam is given as a quarter sine wave

$$y_c = y_o\left(1 - \cos\frac{\pi x}{2L}\right) \qquad \text{C-22}$$

where $y_o$ is the maximum deflection

x is the distance measured along the beam from the fixed end

L is the length of the cantilever beam.

The effective weight is obtained by evaluating the following integral

$$W_e = \frac{W}{L}\int_0^L \left(\frac{y}{y_o}\right)^2 dx \qquad \text{C-23}$$

Applied to the cantilever beam results in

$$W_{ec} = \frac{W}{L}\int_0^L \left(1 - \cos\frac{\pi x}{2L}\right)^2 dx$$

$$= \frac{W}{L}\left[x - \frac{4L}{\pi}\sin\frac{\pi x}{2L} + \frac{x}{2} + \frac{L}{2\pi}\sin\frac{\pi x}{L}\right]_0^L$$

$$= W\left[\frac{3}{2} - \frac{4}{\pi}\right] = 0.23\,W \qquad \text{C-24}$$

Similarly, Reference C1 defines the deflection of a fixed-fixed beam as a cosine wave

$$y_F = \frac{y_o}{2}\left(1 - \cos\frac{2\pi}{L}x\right) \qquad \text{C-25}$$

and the effective weight is determined by substituting equation C-25 into C-23.

$$W_{eF} = \frac{W}{2L}\int_0^L \left(1 - \cos\frac{2\pi}{L}x\right)^2 dx$$

$$= \frac{W}{4L}\left[x - \frac{L}{\pi}\sin\frac{2\pi}{L}x + \frac{x}{2} + \frac{L}{8\pi}\sin\frac{4\pi}{L}x\right]_0^L$$

$$= \frac{W}{4L}\left[L + \frac{L}{2}\right] = \frac{3}{8}W \qquad \text{C-26}$$

Consequently the effective weight for the one-elbow pipe with equal length legs is

$$W_e = \frac{W_{eC} + W_{eF}}{2} = \frac{0.23\,W + 0.375\,W}{2} = 0.303\,W \qquad \text{C-27}$$

substituting equations C-20 and C-27 into C-21, the fundamental natural frequency is

$$f = \frac{1}{2\pi}\sqrt{\left(\frac{384}{5}\right)\left(\frac{EI}{L^3}\right)\left(\frac{g}{0.303\,W}\right)} = \frac{\alpha}{2\pi}\sqrt{\frac{EIg}{WL^3}} \qquad \text{C-28}$$

where the frequency factor $\alpha = \sqrt{\frac{384}{(5)(0.303)}} = 15.9$ (90-deg bend angle),

and the remaining parameters are identical to those used in beam theory.

To define the fundamental frequency variation as a function of the bend angle, the special case of equal leg lengths provides the lower boundary of the frequency factors and in turn similarly affect the natural frequency. Thus for the case of a zero bend angle, shown in Figure C-2, the natural frequency is obtained from Reference C1. for a dual cantilever pipe.

$$f = \frac{3.52}{2\pi}\sqrt{\frac{E(2I)g}{W\left(\frac{L}{2}\right)^3}} = \frac{\alpha}{2\pi}\sqrt{\frac{EIg}{WL^3}} \qquad \text{C-29}$$

where the frequency factor $\alpha$ = 14. 1 (zero-deg bend angle).

Similarly, for a 180-deg bend angle (a straight pipe with fixed ends) the frequency factor of 22.4 is obtained directly from Reference C1.

The upper frequency factor boundary is defined by having the ratio of $L_2/L_1$ = 0 which means again a straight pipe with a 22.4 frequency factor. Thus with the limits established the intermediate values can be estimated. The results are summarized in Figure C-3. The computer program based on the above analysis is shown in Appendix B.

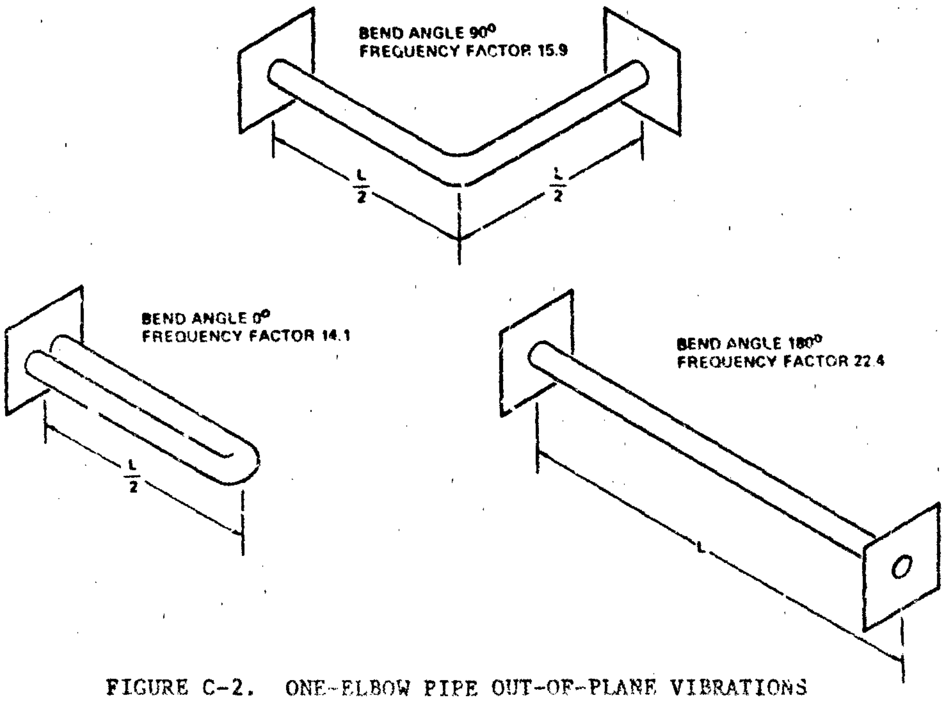


FIGURE C-2. ONE-ELBOW PIPE OUT-OF-PLANE VIBRATIONS EFFECT OF BEND ANGLE L2/L1 = 1.0

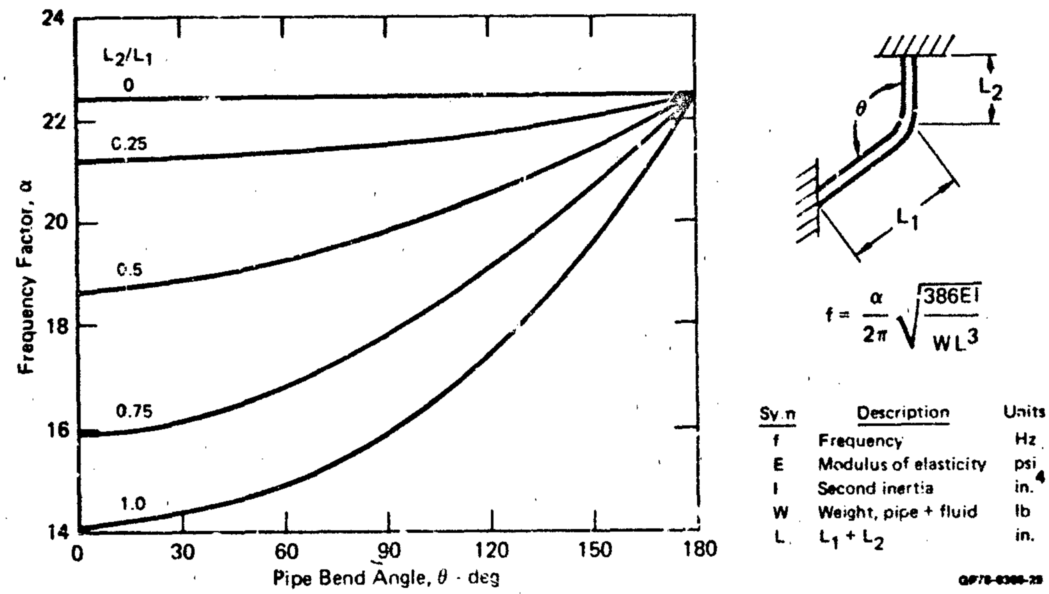


FIGURE C-3 **FUNDAMENTAL OUT-OF-PLANE FREQUENCY PIPE WITH A BEND**

## C2. TWO-ELBOW PIPE VIBRATIONS

Ca. Torsional Mode - This mode is an out-of-plane rocking motion of the crosspipe, Figure C-4, caused by the bending of the other two legs. Thus, the deflections $\delta_1$ and $\delta_2$ are defined as

$$\delta_1 = \delta_2\left(\frac{a}{b}\right) = \frac{FL_1^3}{3EI} \qquad \text{C-30}$$

The corresponding spring rates for each leg are as follows

$$L1K = \frac{3EI}{L_1^3} \qquad L2K = \frac{3EI}{L_2^3} \qquad \text{C-31, C-32}$$

considering the effective weight to be

$$MUCF = 0.25 * \left[ RHO * PAREA + FRHO * FAREA \right] \qquad \text{C-33}$$

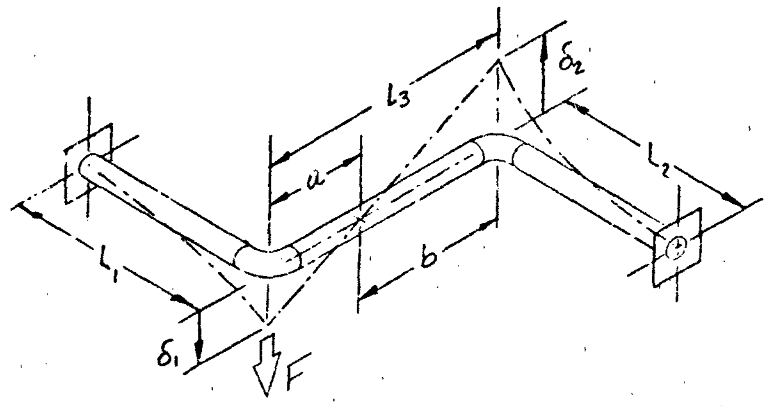


FIGURE C-4. HYDRAULIC LINE MECHANICAL RESPONSE
TWO-ELBOW PIPE TORSION MODE

The natural frequencies due to torsional mode are

$$L1{:}TK = \frac{1}{2\pi}\sqrt{\frac{386*L1K}{MUCF}} \qquad \text{C-34}$$

$$L2{:}TK = \frac{1}{2\pi}\sqrt{\frac{386*L2K}{MUCF}} \qquad \text{C-35}$$

Cb. <u>Crosspipe Translation</u> - This mode is an inplane motion of the crosspipe as depicted in Figure C-5. Neglecting deformations due to tension and compression in the members, and considering only bending, section $\overline{AB}$ is bent by two moments of equal magnitude but in opposite direction.

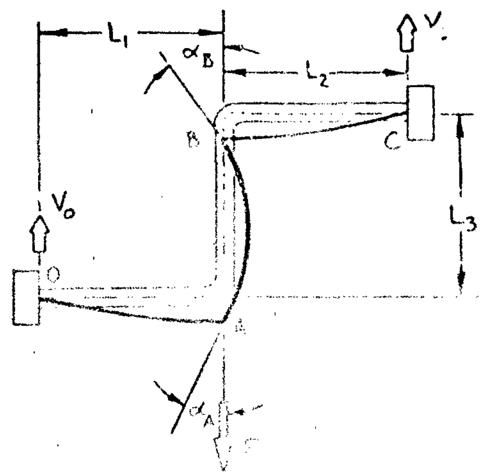


FIGURE C-5. HYDRAULIC LINE MECHANICAL RESPONSE
TWO ELBOW CROSSPIPE TRANSLATION

These moments are defined as

$$M_A = V_0 L_1 = \frac{F L_2}{1 + L_2/L_1} \qquad \text{C-36}$$

$$M_B = V_C L_2 = \frac{F L_2}{1 + L_2/L_1} \qquad \text{C-37}$$

which cause rotation angles about points A and B. These rotation angles are determined, from Reference [illegible] by the method of superposition, to be equal and opposite and of the form

$$\alpha = \alpha_A = -\alpha_B = \frac{F L_2 L_3}{2EI(1 + L_2/L_1)} \qquad \text{C-38}$$

The total deflection, $\delta$, is composed of the deflection due to bending of legs $L_1$ and $L_2$, and the deflection due to rotation at joints A and B. Thus,

$$\delta = \frac{V_0 L_1^3}{3EI} + \alpha L_3 = \frac{FL_2(2L_1^2 + 3L_3^2)}{6EI(1 + L_2/L_1)} \qquad \text{C-39}$$

The corresponding spring rate is given by

$$XTK = \frac{F}{\delta} = \frac{6EI(1 + L_2/L_1)}{L_2(2L_1^2 + 3L_3^2)} \qquad \text{C-40}$$

For the special case of equal leg lengths, $L = L_1 = L_2 = L_3$, the spring rate becomes

$$XTK = \frac{12EI}{5L^3} \qquad \text{C-41}$$

Considering the effective weight of the system to be defined by

$$XTWE = 0.25*\ (RHO*PAREA+FRHO*FAREA)*(L_1+L_2 + 2 * L_3) \qquad \text{C-42}$$

The natural frequency is determined by substituting C-40 or C-41, and C-42 into

$$XTFREQ = \frac{1}{2\pi}\sqrt{\frac{386*XTK}{XTWE}} \qquad \text{C-43}$$

C3. REFERENCES


C1. R. J. Roark, FORMULAS FOR STRESS AND STRAIN, McGraw-Hill, 1965.

## APPENDIX D

### F-15 PUMP MODEL CHANGES

### HYTRAN User Manual (AFAPL-TR-76-43, Vol. I)

CARD NUMBER 4

| COLUMN | FORMAT | DATA | DIMENSIONS |
|---|---|---|---|
| 1-10 | E10.0 | Theoretical Maximum Pump Displacement | IN**3/REV |
| 11-20 | E10.0 | Maximum Actuator Displacement @ Maximum Flow | IN |
| 21-30 | E10.0 | Minimum Actuator Displacement @ Minimum Pump Flow ( -ve) | IN |
| 31-40 | E10.0 | Flat Depth | IN |
| 41-50 | E10.0 | Minimum Actuator Engagement | IN |
| 51-60 | E10.0 | Coefficient of Pump Leakage | CIS/PSI |
| 61-70 | E10.0 | Coefficient of Leakage from Case to Inlet | CIS/PSI |
| 71-80 | E10.0 | Case Volume | IN**3 |

EXAMPLE CARD

```
      SUBROUTINE PUMP51 (D,DT,DD,L)
C **** REVISED MARCH 25, 1976 ****
C            X VERSION OF THE YPUMP54 SUBROUTINE  7 APR 76
      COMMON NTELPL,NTOLPL,IPT,IPOINT,NPTS,INEL,KNEL,NTOPL,NLPLT(61,3),
     1 POLEG(90,12),LCS(90,10),ILEG(1400),PN(90),QN(90)
      COMMON/SUB/PARM(150,9),PM(1500),QM(1500),P(300),Q(300),C(300)
     1,Z(300),RHO(20),S2ORHO(20),VISC(20),BULK(20),TEMP(20),PVAP(20)
     2,ATPRES,T,DELT,TFINAL,PLTDEL,PI,TITLE(20),LEGN,ICUN
     3,KTEMP(99),LSTART(150),NLCT(150),LTYPE(99),NC(9.),INX,INZ
     4,INV,ISTEP,NLINE,NEL,IND,IENTR,MNLINE,MNEL,MNLEG,MNNODE,MNPLOT
     5,MNLPTS,MOS
      DIMENSION D(37),DT(32),DD(1),L(10)
      INTEGER ARCOM,WIDTH,FLOFRC,COEVL1,COEVL2,ARACT,PSPRIZ,PSPRIM,
     1 PACCP,PZRPM,PSLRPM,PDISAC,PDAMP,DISP,DPVOA,DPVAC,
     2 DISAM,DISAMI,COEALK,COEALM,COEPLK,COECIN,VOLCAS,PINMIN,
     3 PSPEED,PRPM,PPOWER,FLAG,QACTU,QACTC,PACTU,POUTLT,
     4 PCASE,PINLET,COEV1,COEV2,BULKC,VFLACT,DISACT,DISVLV,
     5 COEALZ,COEALS,DELP13,DELP23,COECAS,POUTM,BULKO,COEOSO
     6 ,QINLET,QOUTLT,DISVM,VLVOL,VOLACT,BULKA,VOLOUT,PPCASE
C     D( ) ARRAY *****
      DATA DPVOA/1/,INPPSI/2/,ARCOM/3/,WIDTH/4/,FLOFRC/5/,VLVOL/6/,
     1 COEVL1/7/,COEVL2/8/,ARACT/9/,PSPRIZ/10/,PSPRIM/11/,
     2 PACCP/12/,PZRPM/13/,PDISAC/14/,PSLRPM/15/,PDAMP/16/,
     3 DISP/17/,DISAM/18/,DISAMI/19/,COEALK/20/,COEALM/21/,
     4 COEPLK/22/,COECIN/23/,VOLCAS/24/,PINMIN/25/,PSPEED/26/,
     5 COEOSO/27/,DISVM/28/,DPVAC/29/,INERT/30/,VOLACT/31/,VOLOUT/32/
C     DT( ) ARRAY *****
      DATA PRPM/1/,PPOWER/2/,FLAG/3/,QACTU/4/,QACTC/5/,
     1 PACTU/7/,POUTLT/8/,PCASE/9/,PINLET/10/,COEV1/11/,COEV2/12/,
     2 BULKC/13/,VFLACT/14/,DISACT/15/,DISVLV/16/,KO/17/,COEALZ/18/,
     3 COEALS/19/,COECAS/20/,POUTM/21/,DELP13/22/,DELP23/23/,BULKO/24/
     4 ,QINLET/25/,QOUTLT/26/,ITUP/27/,MITUP/28/,BULKA/29/,PPCASE/30/
C
C
      IF(IENTR) 1000,2000,3000
C *** 1000 SECTION
 1000 CONTINUE
      IF (INEL.NE.0) GO TO 1500
      DO 1001 I=1,43
 1001 DT(I)=0.0
      N=KTEMP(IND)
      IF(N.LT.11) N=N+10
C      .02443=VISC FOR MIL-H-83282 AT 100 F
      POWER=VISC(N)/.0243
      DT(BULKC)=BULK(N)*DELT/D(VOLCAS)
      DT(BULKA)=D(VOLACT)/(BULK(N)*DELT)
      D(VOLOUT)=D(VOLOUT)/(BULK(N)*DELT)
      DT(COEV1)=D(COEVL1)*S2ORHO(KTEMP(IND))*D(WIDTH)
      DT(COEV2)=D(COEVL2)*S2ORHO(N)*D(WIDTH)
      DT(COECAS)=1.4152339/((.028962*S2ORHO(KTEMP(IND)))**2)
      ACTRAD=SQRT(D(ARACT)*4./PI)/2.
      OPOUT=ACTRAD-D(COEALK)
      OPOUT=2*SQRT(ACTRAD**2-OPOUT**2)
      DT(COEALZ)=(OPOUT*2.*(D(COEALK)**3))/(12.*VISC(N)*RHO(N))
      D(INERT)=D(INERT)/(DELT*D(ARACT))
      IF(D(FLOFRC).NE.0.)GO TO 1290
      DT(COEALS)=(DT(COEALS)-DT(COEALZ))/D(DISAM)
      D(INPPSI)=D(ARCOM)/D(INPPSI)
      D(FLOFRC)=2.*D(WIDTH)*D(INPPSI)*(D(COEVL1)**2)*.358/D(ARCOM)
      D(DPVAC)=D(DPVOA)-D(VLVOL)/D(INPPSI)
      D(DISP)=D(DISP)/60./D(DISAM)
```

```
      D(PSPRIM)=(D(PSPRIM)-D(PSPRIZ))/D(DISAM)
      D(PACCP)=D(PACCP)/(D(DISAM)*3600.**2)
      D(PDISAC)=(D(PDISAC)-D(PZRPM))/D(DISAM)
      D(PZRPM)=D(PZRPM)-D(PSLRPM)*3600.
 1250 DT(PRPM)=D(PSPEED)
      DT(BULKO)=BULK(KTEMP(IND))*D(DPVJA)/232000.
C***  THIS SECTION CALCULATES THE STEADY STATE CHARCTERISTICS
C     OF THE PUMP OUTPUT PRESSURE VERSUS FLOW.
      COELKA=DT(COEALZ)/D(COEALM)
      DT(POUTLT)=D(DPVJA)+2.0
 1260 DT(QACTC)=DT(QACTU)
 1270 DT(PACTU)=D(PSPRIZ)+DT(DISACT)*D(PSPRIM)+DT(PCASE)
     1 +DT(DISACT)*(D(PACCP)*DT(PRPM)**2+D(PDISAC))
     2 +(D(PZRPM)+D(PSLRPM)*DT(PRPM))*DT(BULKO)/DT(POUTLT)
      IF(IENTR.EQ.2)RETURN
      DT(QACTU)=COELKA*DT(PACTU)
      DT(DISACT)=D(DISAM)
      COELKA=DT(COEALZ)/(2.1+DT(DISACT))
      IF(DT(QACTC).EQ.0.)GO TO 1250
      DT(POUTM)=DT(POUTLT)
      DT(QINLET)=D(DISP)*DT(PRPM)*D(DISAM)-DT(POUTM)*D(COEPLK)
     1 -DT(QACTU)
      DT(QOUTLT)=-(D(COEPLK))*DT(POUTLT)-DT(QACTC)
      DT(DELP23)=-DT(QOUTLT)/(DT(QINLET)-DT(QOUTLT))
      DT(DISVLV)=.5
      DT(DELP13)=10.
      GAIN=.7/(1.+20.*DT(COEV1)*D(INPPSI)*Z(L(2)))
      DT(ITUP)=GAIN
      DT(MITUP)=1.-GAIN
      RETURN
C
C      STEADY STATE CALCULATION SECTION
C     IND=COMPONENT #,KNEL=CONNECTION #,INEL=LEG #
C     CON #1=INLET,CON #2=OUTLET,CON #3=CASE DRAIN
C     THE INLET IS A NODAL POINT IN THE SYSTEM
C
 1500 IF(KNEL-2)1510,1530,1520
 1510 DT(PINLET)=POLEG(INEL,11)
      GO TO 1600
 1520 IF(INX.NE.1) GO TO 1700
      QCASDR=POLEG(INEL,1)*POLEG(INEL,2)
      DT(6)=QCASDR
      QACTLK=DT(DISVLV)*(DT(QACTC)-DT(QACTU))+DT(QACTU)
      DT(DELP13)=(DT(POUTM)*D(COEPLK)+QACTLK-QCASDR)/D(COECIN)
      POLEG(INEL,5)=POLEG(INEL,5)+DT(DELP13)+QCASDR/D(COECIN)
      POLEG(INEL,6)=POLEG(INEL,6)+1.0/D(COECIN)
      LCS(INEL,7)=5
      POLEG(INEL,11)=POLEG(INEL,11)+DT(DELP13)
      DT(PCASE)=POLEG(INEL,11)
      POLEG(INEL,8)=POLEG(INEL,8)+DT(COECAS)
      POLEG(INEL,11)=POLEG(INEL,11)-DT(COECAS)*(QCASDR**2)
      GO TO [illegible]
 1530 IF(INX.NE.1) GO TO 1700
      DT(DISVLV)=POLEG(INEL,1)*POLEG(INEL,2)-DT(QOUTLT)
      DT(DISVLV)=DT(DISVLV)/(DT(QINLET)-DT(QOUTLT))
      IF(DT(DISVLV).LT.0.0) DT(DISVLV)=0.0
      IF(DT(DISVLV).GT.1.0) DT(DISVLV)=1.0
      POLEG(INEL,5)=POLEG(INEL,5)+DT([illegible])*DT(DELP13)
      POLEG(INEL,6)=POLEG(INEL,6)+0.0001
      POLEG(INEL,11)=POLEG(INEL,11)+DT(POUTM)+DT(DFLP13)
      DT(POUTLT)=POLEG(INEL,11)
```

```
      LCS(INEL,7)=5
 1600 RETURN
 1700 WRITE(6,1800) IND,KNEL,INEL
 1800 FORMAT(5X,46H CALL SEQUENCE ERROR DETECTED IN COMPONENT NO    ,
     1 I5,14H CONNECTION NO   ,I5,7H LEG NO   ,I5)
      WRITE(6,943)
  943 FORMAT(10X,33HPROGRAM STOP IN SUBROUTINE PUMP51)
      STOP 6054
C *** 2000 SECTION
 2000 CONTINUE
      DT(31)=0.0
      DT(DISACT)=DT(DISVLV)*D(DISAM)
      DT(QACTU)=DT(DISVLV)*(DT(QACTC)-DT(QACTU))+DT(QACTU)
      DT(QACTC)=0.0
      DT(DISVLV)=0.0
      DT(PPCASE)=DT(PCASE)
      GO TO 1270
C
C *** 3000 SECTION
 3000 CONTINUE
      ICOUNT=0
C
C     CALCULATE TRANSIENT RESPONSE OF PUMP
C
      POWER=0.0
      L1=L(1)
      L2=L(2)
      L3=L(3)
      C1=C(L1)
      C2=C(L2)
      C3=C(L3)
      VOLD=DT(VELACT)
      DPDAMP=D(PDAMP)
      DPDAMP=D(ARACT)/(DPDAMP+D(INERT))
      DT(QACTU)=0.0
      DT(QACTC)=0.0
      PACTUO=DT(PACTU)
      PDISA=DT(DISACT)+DT(VELACT)*DELT
      PACTUR=D(PSPRIZ)+PDISA*D(PSPRIM)+VOLD*D(INERT)
     1 +PDISA*(D(PACCP)*DT(PRPM)**2+D(PDISAC))+DT(PPCASE)
     2 +(D(PZRPM)+D(PSLRPM)*DT(PRPM))*DT(BULKO)/DT(POUTLT)
      QOSIN=-VOLD*D(COEQSO)
      QPUMP=PDISA*D(DISP)*DT(PRPM)+QOSIN
      DT(PINLET)=(C1/Z(L1)+DT(PPCASE)*D(COECIN)-QPUMP)
     1  /(1./Z(L1)+D(COECIN))
      IF(DT(PINLET).LT.D(PINMIN)) DT(PINLET)=D(PINMIN)
      DT(QINLET)=(C1-DT(PINLET))/Z(L1)
      QCASIN=(DT(PPCASE)-DT(PINLET))*D(COECIN)
      QPUMP=DT(QINLET)+QCASIN+QOSIN
      COELKA=DT(COEELZ)/(D(COEACR)+PDISA)
      DT(COEELA)=COELKA
      ZOUT=Z(L2)/(1.+Z(L2)*D(COEPLK)+Z(L2)*D(VOLOUT))
      QPOUT=DT(POUTLT)
      B=1./(DPDAMP+DT(BULKA)+COELKA)
      DP1=(DT(PPCASE)*COELKA+PACTUO*DT(BULKA)+PACTUR*DPDAMP)*B
      DP2=B*(PACTUR*DPDAMP+PACTUO*DT(BULKA)+DT(PPCASE)*(COELKA-1./B))
 3200 POUTMX=(C2/Z(L2)+QPUMP+DT(PPCASE)*D(COEPLK)+D(VOLOUT)*QPOUT)*ZOUT
      POUTMI=D(PVOA)+DT(PPCASE)
      IF(POUTMX.LE.POUTMI) GO TO 3220
      DT(POUTLT)=POUTMX*DT(ITUP)+POUTMI*DT(MITUP)
```

```
 3210 DIS=(DT(POUTLT)-POUTMI)*D(INPPSI)
      DIS=DIS/(D(FLOFRC)*(DT(POUTLT)-DT(PACTU))+1.0)
      IF(DIS.GT.D(DISVM))DIS=D(DISVM)
 3215 IF(POWER.EQ.0.0) GO TO 3216
      CONA=(DIS*DT(COEV1))**2/(2.*COELKA)
      CONB=2.*ABS(DT(POUTLT)-DT(PPCASE))*COELKA/CONA
      DT(QACTU)=CONA*(SQRT(1.0+CONB)-1.0)
      WRITE(6,997)CONA,CONB,COELKA,DT(PPCASE),DT(COEV1),DT(POUTLT)
  997 FORMAT(3X,8E12.5)
      GO TO 3217
 3216 CONTINUE
      A=DIS*DT(COEV1)
      DT(QACTU)=-B*A**2/2.+A/2.*SQRT((A*B)**2+4*(DT(POUTLT)-DP1))
      DT(PACTU)=DT(POUTLT)-(DT(QACTU)/A)**2
 3217 TPOUT=POUTMX-DT(QACTU)*ZOUT
      IF(ABS(TPOUT-DT(POUTLT)).LT.0.05) GO TO 3230
      DT(POUTLT)=DT(POUTLT)*DT(MITUP)+TPOUT*DT(ITUP)
      ICOUNT=ICOUNT+1
      IF(ICOUNT.EQ.25)WRITE(6,999)ICOUNT
      IF(ICOUNT.EQ.25)WRITE(6,998)DT(POUTLT),TPOUT,POUTMX,POUTMI
  998 FORMAT(10X,4F20.5)
      IF(ICOUNT.EQ.25)GO TO 3230
  999 FORMAT(10X,13HEXCEEDED ITER,I10)
      GO TO 3210
C
C     FLOW FROM ACTUATOR PISTON TO CASE
C
 3220 POUTMI=D(DPVAC)+DT(PPCASE)
      IF(POUTMX.GE.POUTMI) GO TO 3230
      DIS=(POUTMI-POUTMX)*D(INPPSI)
      DIS=DIS/((DT(PACTU)-DT(PPCASE))*D(FLOFRC)+1.0)
      IF(DIS.GT.D(DISVM))DIS=D(DISVM)
 3226 CONTINUE
      A=DIS*DT(COEV2)
      DT(QACTC)=-B*A**2/2.+A/2.*SQRT((A*B)**2+4*DP2)
      DT(PACTU)=DT(PPCASE)+(DT(QACTC)/A)**2
 3230 IF(POWER.NE.0.0) GO TO 3250
C
C     TEST PISTON DISPLACEMENT AGAINST MAXIMUM STROKE
C
      QACTLK=(DT(PACTU)-DT(PPCASE))*COELKA
      QNET=DT(QACTU)-QACTLK-DT(QACTC)-(DT(PACTU)-PACTUO)*DT(BULKA)
      DT(VELACT)=-QNET/D(ARACT)
      DT(DISACT)=DT(DISACT)+(VOLD+DT(VELACT))/2.*DELT
      CALL XLIMIT(DT(DISACT),DT(VELACT),POWER,D(DISAMI),D(DISAM))
      IF(POWER.EQ.0.0) GO TO 3300
      IF(DT(PINLET).LE.D(PINMIN)) GO TO 3240
      QPUMP=D(DISP)*DT(PRPM)*DT(DISACT)
      QDSIN=0.0
 3240 IF(POWER.EQ.-1.0) GO TO 3200
      DT(QACTC)=0.0
      DT(PACTU)=DT(PPCASE)
      QACTLK=0.0
      GO TO 3300
 3250 DT(PACTU)=DT(PPCASE)+DT(QACTU)/COELKA
      QACTLK=DT(QACTU)
 3300 P(L1)=DT(PINLET)
      Q(L1)=DT(QINLET)
      QPLEAK=(DT(POUTLT)-DT(PPCASE))*D(COEPLK)
      Q(L2)=-(QPUMP-QPLEAK-DT(QACTU)-(DT(POUTLT)-OPOUT)*D(VOLOUT))
      DT(DISVLV)=(DT(POUTLT)-DT(PPCASE)-D(DPVDA))*D(INPPSI)
```

PUMP 51 SUBROUTINE LISTING (Cont.)

```
      DT(POUTLT)=C(L2)-Q(L2)*Z(L2)
      P(L2)=DT(POUTLT)
      QCASDR=QPLEAK+QACTLK+DT(QACTC)-D(ARACT)*DT(VELACT)-QCASIN-QDSIN*2.
      DT(6)=QCASDR
      ALPHA=DT(COECAS)
      BETA=Z(L3)+DT(BULKC)
      CHI=DT(PCASE)+QCASDR*DT(BULKC)-C(L3)
      Q(L3)=(-BETA+SQRT(BETA**2+4.*ALPHA*ABS(CHI)))/(2.*ALPHA)
      Q(L3)=SIGN(Q(L3),-CHI)
      DT(PPCASE)=DT(PCASE)
      DT(PCASE)=DT(PCASE)+(QCASDR+Q(L3))*DT(BULKC)
      P(L3)=C(L3)-Q(L3)*Z(L3)
      DT(PPCASE)=2.*DT(PCASE)-DT(PPCASE)
C
      POWER=-Q(L2)*(P(L2)-P(L1))/6600.0
      DT(PPOWER)=POWER+DT(PPOWER)
      IF(DT(PINLET).LE.D(PINMIN)) WRITE(6,3310)T,IND
      DT(31)=DIS
      RETURN
 3310 FORMAT(2X,36H******** PUMP CAVITATION ONSET AT T= ,E12.5,
     +10X,8HCOMP NO.,I5)
      END
```

## APPENDIX E

## VANE PUMP MODELS

## HSFR USER MANUAL (AFAPL-TR-76-43, VOL. III)

### 2.3.10 Pumps (Variable Displacement, Vane)

When a pump model is used, it should always be the first element in the system and identified as an NTYPE "9" element. This number is the general pump element designator. To specify the vane pump model a KTYPE "15" must be entered in columns 6-10 of the first pump data card.

The complete vane pump model (SUBROUTINE VPUMP) is based on actual physical dimensional data of the pump. Physical data for a given pump is read into the element data list in the same manner as for the other system elements.

Input data for the complete vane pump model requires two data cards. In addition, a BLOCK DATA section must be loaded after the "END" statement of the main SFR program to provide other vane pump parameters. Required card input data is described in the following tables.

Input data for the vane pump model must include a description of the system pressure drop characteristics. The following generalized equation for system flow and pressure is used in the model:

ΔP = CK1 + CKL * Q + CKT * Q ** 1.75 + CKV * Q**2

Where

ΔP = Vane stage pressure rise + reservoir pressure

Q = Pump overboard flow (CIS)

CK1, CKL, CKT, CKV = System coefficients described on input data cards

The data cards are supplemented by the use of a BLOCK DATA attached to the end of the main HSFR program. The BLOCK DATA initializes arrays providing cam position versus pump flow and the rate of change in vane bucket volume versus rotation angle. A listing of BLOCK DATA is shown in Figure 2-6. The arrays in BLOCK DATA are:

CAMP( ) = Cam position (IN)

CQMAX( ) = Max flow at cam position (CIR)

ANGLE( ) = Vane angle rotation (DEG)

DVOL( ) = $\frac{d\ Volume}{dt}$ at vane angle (IN**3/SEC)

NA(1) = Number of input DVOL at each cam setting

NA(2) = Number of different cam settings (The cam settings are stored at the end of the ANGLE( ) array)

CAMPI( )= Inverse of CAMP( ) array

CQMAXI( ) = Inverse of CQMAX( ) array

VANE PUMP MODEL INPUT DATA

CARD NUMBER 1

| COLUMN | FORMAT | DATA | DIMENSIONS |
|---|---|---|---|
| 1-5 | I5 | NTYPE = 9 | - |
| 6-10 | I5 | KTYPE = 15 (VANE PUMP) | - |
| 11-20 | E10.0 | BLANK | - |
| 21-30 | E10.0 | SLOTWO (CAM SLOT WIDTH-OUTLET) | IN |
| 31-40 | E10.0 | COEPLK (COEFFICIENT OF PUMP LEAKAGE) | CIS/PSI |
| 41-50 | E10.0 | THPRS (VANE PRESSURE SLOT START ANGLE) | DEG |
| 51-60 | E10.0 | THPRE (VANE PRESSURE SLOT END ANGLE) SEE | DEG |
| 61-70 | E10.0 | THSUCS (VANE SUCTION SLOT START ANGLE) FIGURE 2-7 | DEG |
| 71-80 | E10.0 | THSUCE (VANE SUCTION END ANGLE) | DEG |

EXAMPLE CARD

VANE PUMP MODEL INPUT DATA

CARD NUMBER 2

| COLUMN | FORMAT | DATA | DIMENSIONS |
|---|---|---|---|
| 1-10 | E10.0 | LPRESS (INLET PRESSURE) | PSI |
| 11-20 | E10.0 | SZCAM (INITIAL ZCAM POSITION) | IN |
| 21-30 | E10.0 | VVOL (MAXIMUM VANE VOLUME) | $IN^3$ |
| 31-40 | E10.0 | PQOVBD (OVERBOARD FLOW) | CIS |
| 41-50 | E10.0 | CK1 (SYSTEM CONSTANT PRESSURE RISE) | PSI |
| 51-60 | E10.0 | CKL (SYSTEM LAMINAR TERM) | PSI/CIS |
| 61-70 | E10.0 | CKT (SYSTEM TURBULENT TERM) | PSI/CIS**1.75 |
| 71-80 | E10.0 | CKV (METERING VALVE TERM) | PSI/CIS**2 |

EXAMPLE CARD

```
      BLOCK DATA
C     *****   MAY 10,1978   *****
      COMMON /VANE/CAMP(11),COMAX(11),ANGLE(30),DVOL(81),NA(2)
     + ,CAMPI(11),COMAXI(11)
      DATA CAMP/.08,.0785,.0765,.073,.069,.062,.053,.0415,.027,
     + .014,0.0/
      DATA COMAX/0.,.0187,.0375,.0813,.1375,.225,.3375,.4875,.6687,
     + .8375,1./
      DATA CAMPI/0.,.014,.027,.0415,.053,.062,.069,.073,.0765,
     + .0785,.08/
      DATA COMAXI/1.,.8375,.6587,.4875,.3375,.225,.1375,.0913,.0375,
     + .0187,0.0/
      DATA ANGLE/0.,5.,10.,15.,20.,22.,30.,40.,50.,60.,63.,70.,80.,90.,
     1,100.,110.,120.,130.,135.,138.,140.,145.,150.,160.,170.,175.,180.,
     2,0.,.05,.07/
      DATA DVOL/9.0,3.5,-1.0,-6.25,-12.0,-15.0
     M,-30.0,-50.0,-60.0,-58.0,-55.0,-42.0
     M,-21.0,-8.0,0.0,10.0,27.0,45.0,53.0,56.0
     M,58.0,60.0,58.0,45.0,25.0,14.0,9.0,-28.0
     M,-13.0,3.0,23.0,29.0,28.0,14.0,-12.0,-34.0
     M,-41.0,-40.0,-34.0,-17.0,-4.0,0.0
     M,5.0,21.0,37.0,40.5,41.0,40.5,37.0,29.0
     M,5.0,-20.0,-31.0,-28.0,-41.0,-21.0
     M,7.0,33.0,45.0,46.0,33.0,5.0,-20.0,-32.0
     M,-34.0,-29.0,-14.0,-1.0,0.0,4.0,18.0
     M,30.0,32.0,31.0,32.0,24.0,15.0,-14.0
     M,-40.0,-45.0,-41.0/
      DATA NA/27,3/
      END
```

FIGURE 2-6

VANE PUMP BLOCK DATA INITIALIZATION

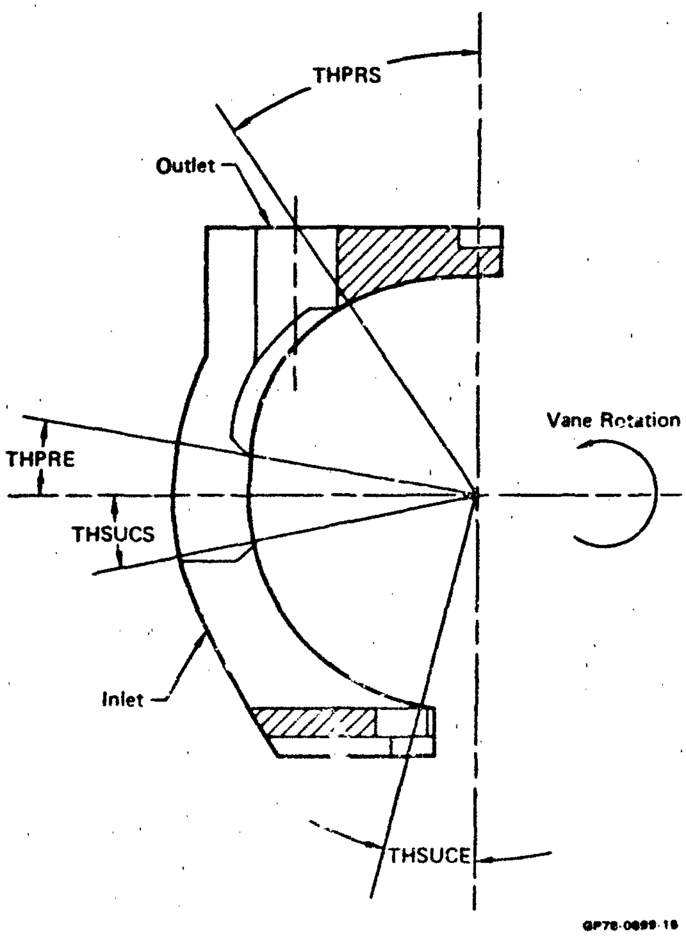


**FIGURE 2-7**
**VANE PUMP CAM BLOCK PARAMETERS**

3.8 BLOCK DATA - MAIN PROGRAM

BLOCK DATA is used to initialize values in labeled COMMON/VANE/. The labeled COMMON is used to pass the initialized data to the VANE PUMP SUBROUTINE.

The arrays in COMMON/VANE/are:

CAMP( ) = Cam position (IN)

CQMAX( ) = Max flow at cam position (CIP)

ANGLE( ) = Vane angle rotation (DEG)

DVOL( ) = $\frac{dVolume}{dt}$ at vane angle (IN**3/SEC)

NA(1) = Number of input DVOL at each cam setting

NA(2) = Number of different cam settings (The cam settings are stored at the end of the ANGLE( ) array)

CAMPI( ) = Inverse of CAMP( ) array

CQMAXI( ) = Inverse of CQMAX( ) array

3.8.1 BLOCK DATA - LISTING

```
      BLOCK DATA
C     *****   MAY 10,1978    *****
      COMMON /VANE/CAMP(11),COMAX(11),ANGLE(30),DVOL(81),NA(2)
     + ,CAMPI(11),COMAXI(11)
      DATA CAMP/.08,.0785,.0765,.073,.069,.062,.053,.0415,.027,
     ( .014,0.0/
      DATA COMAX/0.,.0187,.0375,.0813,.1375,.225,.3375,.4875,.6687,
     + .8375,1./
      DATA CAMPI/0.0,.014,.027,.0415,.053,.062,.069,.073,.0765,
     + .0785,.08/
      DATA COMAXI/1.,.8375,.6687,.4875,.3375,.225,.1375,.0813,.0375,
     + .0187,0.0/
      DATA ANGLE/0.,5.,10.,15.,20.,22.,30.,40.,50.,60.,63.,70.,80.,90.
     1,100.,110.,120.,130.,135.,138.,140.,145.,150.,160.,170.,175.,180.
     2,0.,.05,.07/
      DATA DVOL/9.0,3.5,-1.0,-6.25,-12.0,-15.0
     M,-30.0,-50.0,-60.0,-58.0,-55.0,-42.0
     M,-21.0,-8.0,0.0,10.0,27.0,46.0,53.0,56.0
     M,58.0,60.0,53.0,45.0,25.0,14.0,8.0,-28.0
     M,-13.0,3.0,23.0,29.0,28.0,14.0,-12.0,-34.0
     M,-41.0,-40.0,-34.0,-17.0,-4.0,0.0
     M,5.0,21.0,37.0,40.5,41.0,40.5,37.0,29.0
     M,5.0,-20.0,-31.0,-28.0,-41.0,-21.0
     M,7.0,33.0,45.0,45.0,33.0,5.0,-20.0,-32.0
     M,-34.0,-29.0,-14.0,-1.0,0.0,4.0,18.0
     M,30.0,32.0,31.0,30.0,24.0,15.0,-14.0
     M,-40.0,-46.0,-41.0/
      DATA NA/27,3/
      END
```

## 4.15 VANE PUMP SUBROUTINE

### 4.15.1 Introduction and Flow Diagram

SUBROUTINE VPUMP is a general, detailed model of a balanced variable displacement vane pump. The model computes the ability of the pump to deliver flow against an output pressure by modeling the nonlinear relationship between pump output flow and pressure in the time domain. The main program calculates the harmonic load impedance of the circuit, and this provides the linear phase and gain relationship between the harmonic flows into the load and the corresponding pressures across the load, in the frequency domain. The balance is obtained in the time domain, although a check is performed in the frequency domain.

The vane pump model accounts for valving areas, precompression, steady state cam position, fluid bulk modulus, pump internal leakage, circuit termination flow and vane motion. Steady state cam position is calculated as a function of pump internal leakage, circuit overboard flow, and pump speed. If the cam position is a minimum corresponding to maximum pump flow, the steady state pressure is calculated at each RPM. The dynamics of the cam controlling circuit are not included in the model.

Vane bucket pressure at the beginning of precompression is assumed constant and equal to one plus the input steady state inlet pressure. Piston pressure is then computed continuously until the end of the compression stage.

Figure 4-6 is a general flow chart of the VPUMP subroutine. The specification section includes initialization of variables from input data, and the calculation of several constants. Specification statements are followed by the initialization of pump variables from the input data and calculates the vane indexing positions for 180° of vane revolution. These operations are performed only once, when VPUMP is called on the first pump speed. Steady state pump outlet pressure and overboard flow for a cam position are then calculated. The subroutine will next determine if the pump is on control at the given RPM and assign a value to the control indicator - ICTL. After this is accomplished the precompression pressures are computed. Pump outlet flow is calculated for each incremental bucket volume and then a Fourier Analysis is done of the resulting computed forms. If the pump is on control, the corrected cam position is determined. The Fourier Analysis is completed to calculate harmonic flows up through the user input harmonic. Harmonic pressure and flow are then balanced dynamically by reconstructing the time dependent output pressure and recomputing flow from Section 4. Pump outlet flow and pressure for the harmonic of interest are then returned to the main program.

The VPUMP subroutine is divided into seven sections. Each section is discussed and a listing provided in subsequent paragraphs.

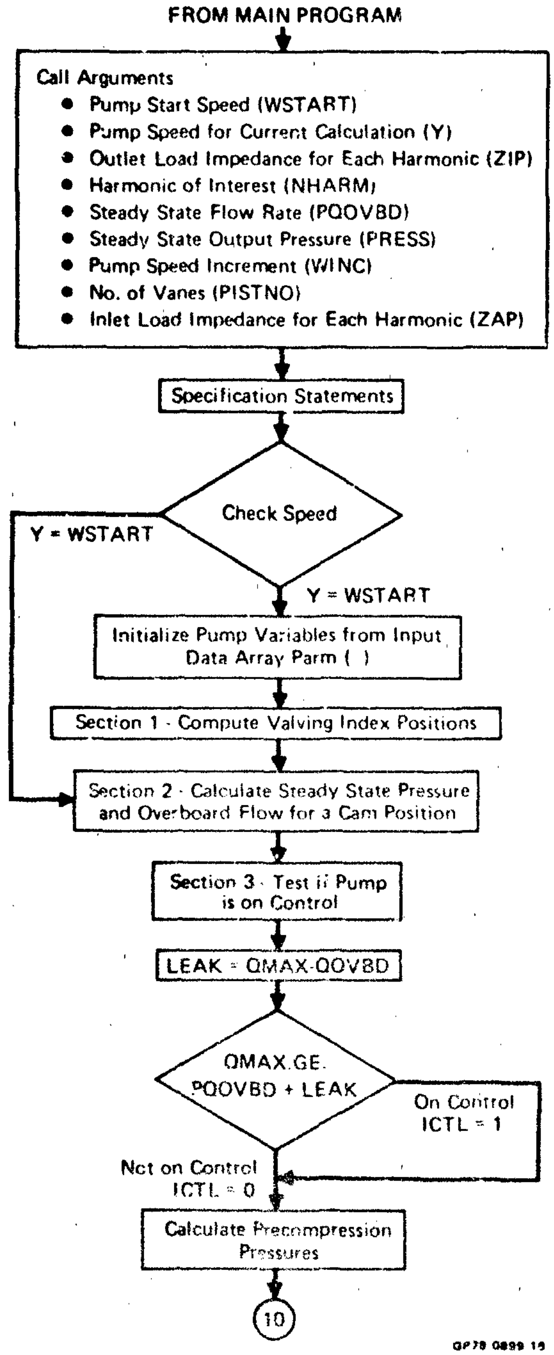


**FIGURE 4-8**
**HSFR VANE PUMP**
Subroutine Flow Chart

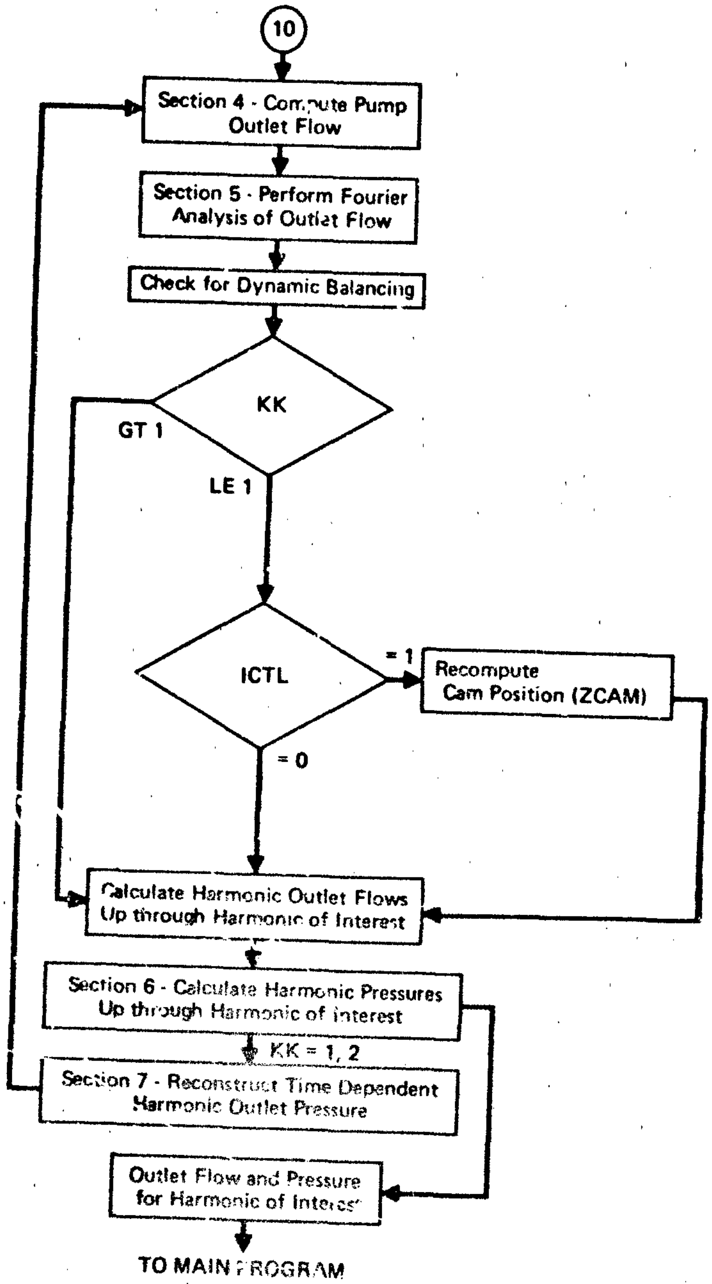


FIGURE 4-6 (Continued)
HSFR VANE PUMP
Subroutine Flow Chart

4.15.1.1 Variable Names - Variable names unique to the PUMP subroutine are listed below. Common variables are discussed in the main program paragraph 3.1.6.1

| SYMBOL | DESCRIPTION | UNITS |
|---|---|---|
| AINC | Incremental shaft rotation angle | DEGREES |
| AN | Temporary variable | - |
| BULKP | Bulk modulus during precompression | PSI |
| C | Temporary variable used in Fourier calculation | - |
| CAVOL | Piston cavitation volume | IN**3 |
| CKL | System laminar coefficient | PSI/CIS |
| CKT | System turbulent coefficient | PSI/CIS**1.75 |
| CKV | Metering valve coefficient | PSI/CIS**2. |
| CK1 | System constant pressure rise | PSI |
| COEF | Temporary variable used in Fourier calculation | - |
| COEPLK | Coefficient of pump leakage | CIS/PSI |
| CORR | Dummy variable | - |
| C1 | Temporary variable used in Fourier calculation | - |
| DANG | Incremental shaft rotation angle used in precompression calculation | RAD |
| DELVOL | Change in vane bucket volume for rotation through DANG | IN**3 |
| DLEAK | Leakage from one vane during rotation through incremental angle (DANG) | IN**3 |
| DPRESP | Pressure change in cylinder during precompression | PSI |
| DT | Incremental time for rotation through incremental angle (DANG) | SEC |
| DTERM | Temporary variable | - |
| DTHETA | Temporary variable | - |
| DV | Incremental vane volumes for rotation through (DANG) | IN |

| SYMBOL | DESCRIPTION | UNITS |
|---|---|---|
| DVDT | Change in vane volume per unit time | CIS |
| DδCAM | Delta cam position | IN |
| ETA(J) | Percentage error between predicted and resulting $J^{th}$ harmonic pressure | % |
| FNTZ | Temporary variable used in Fourier analysis | - |
| FQ1(I,KK) | Complex output flow of the $I^{th}$ harmonic, for the $KK^{th}$ test, from Fourier analysis | CIS |
| FQ1(KK,1) | Complex flow for the next harmonic, KKN, equals the last Fourier flow for the next harmonic, calculated from the final KK=3 test balanced flow from the last harmonic-FQ1(KKN,1) = FQ1(KKN,3) | CIS |
| FQ1I(-,-) | Complex inlet flow | CIS |
| HPRESS | Pump outlet steady state pressure | PSI |
| I | Integer counter | - |
| ICTL | Pump control indicator (1 = on control, 0 = off control) | - |
| IERR | Error indicator | - |
| IFL | Integer counter for number of steady state balance loop iterations | |
| ITEM | Integer indicator | - |
| ITER, I1, I3, J | Integer counters | - |
| KK | Integer counter for dynamic balancing test | - |
| KKN | Order of harmonic (1, 2, 3, ---) | - |
| LEAK | Constant for piston lap leakage | CIS/PSI |
| LK1 - LK8 | Temporary variables used in flow calculations | - |
| LPRESS | Input data-steady state inlet pressure | PSI |
| LPRESP | Piston pressure in precompression calculation | PSI |
| LVOL | Piston volume in precompression calculation | IN**3 |
| M, N | Integer counters | - |
| NAPP | Number of active pistons pumping | - |
| NAPS | Number of active pistons sucking | - |

| SYMBOLL | DESCRIPTION | UNITS |
|---|---|---|
| NDEG I | Integer counter for stepping cylinder rotation 1/4 degree increments, beginning with NDEG=1 | - |
| NHARM | Integer form of WHARM | |
| NKM | Index position of vane bucket during flow calculation | - |
| NPRSOP | Index position when vane slot starts to open to pressure slot | - |
| NPROP | Index position when vane slot is fully open to pressure slot | - |
| NPRSCL | Index position when vane slot starts to close to pressure slot | - |
| NPRCL | Index position when vane slot is fully closed to pressure slot | - |
| NSUSOP | Index position when vane slot starts to open to suction slot | - |
| NSUOP | Index position when vane slot is fully open to suction slot | - |
| NSUSCL | Index position when vane slot starts to close to suction slot | - |
| NSUCL | Index position when vane slot is fully closed to suction slot | - |
| NSTEPP | Number of steps in precompression calculation | - |
| NVANG | Number of steps in one bucket | - |
| ORF | Orifice coefficient of valve | IN**2/SEC/LB**.5 |
| PISTNO | Number of pumping vanes | - |
| PP( ), PPI( ) | Internal pressure in pistons 1, 2, 3, or 4 at a given index position | PSI |
| PISPR | Bucket pressure | PSI |
| PPM(I) | Magnitude of the $I^{th}$ harmonic peak pressure | PSI |
| PLEAK | Leakage out of bucket | CIS/PSI |
| PP(I) | Phase angle of the $I^{th}$ harmonic peak pressure | RAD |
| PPT( ) | Time dependent amplitude of pump output pressure for each rotation index position during output cycle | PSI |
| PQOVBD | Total overboard state leakage from main program | CIS |
| PQ1(I,KK) | Complex output test pressure of the $I^{th}$ harmonic, for the $KK^{th}$ test in dynamic balancing | PSI |

| SYMBOL | DESCRIPTION | UNITS |
|---|---|---|
| PQ1I(I,KK) | Complex inlet test pressure of the $I^{th}$ harmonic | PSI |
| PRESS | Input data for steady state pump output pressure | PSI |
| QERR | Steady state flow error | CIS |
| QMAX | Maximum flow capability at cam position | CIS |
| QOUT | Flow out of bucket | CIS |
| QOVBD | Overboard flow for steady state | CIS |
| QQFC(I) | COSINE peak amplitude of pump output (inlet) flow from Fourier analysis for $I^{th}$ harmonic | CIS |
| QQFS(I) | SINE amplitude of pump output (inlet) flow from Fourier analysis for $I^{th}$ harmonic | CIS |
| QQT(N) | Time dependent output flow from pump | CIS |
| Q1, Q2 | Temporary variables | - |
| RTHETA | Temporary variable in area calculation | - |
| S | Temporary variable in Fourier analysis | - |
| SLEAK | Leakage into bucket | CIS/PSI |
| SLOTWO | Slot width of outlet | IN |
| SZCAM | Input cam position | IN |
| TERM | Temporary variable | - |
| THPRS | Input data cam pressure slot start angle | DEG |
| THPRE | Input data cam pressure slot end angle | DEG |
| THSUCS | Input data cam suction slot start angle | DEG |
| THSUCE | Input data cam suction slot end angle | DEG |
| THETA | Angular position of vane centerline | DEG |
| THEOLD | Last Angular position of vane centerline | DEG |
| TQMAX | Temporary variable | - |
| UO,U1,U2, U3 | Temporary variables used in Fourier analysis | - |

| SYMBOL | DESCRIPTION | UNITS |
|---|---|---|
| VA | Bucket volume at a given index position | IN**3 |
| VAREA | Cylinder slot flow area at each index position, 0-360° in 1/2° increments | IN**2 |
| VVOL | Maximum vane volume | IN**3 |
| WINC | Input data pump speed increment | RPM |
| W | Harmonic frequency (same as A in main program) | RAD/SEC |
| WSTART | Input data first pump speed calculation point | RPM |
| XA( ) | XA(1) = vane angle<br>XA(2) = cam position | DEG<br>IN |
| Y | Current calculation pump speed (same as W in main program) | RPM |
| ZO | Pump shunt impedance for I$^{th}$ harmonic | PSI/CIS |
| ZIP( ) | Complex impedance of load on pump outlet for each harmonic | PSI/CIS |
| ZAP( ) | Complex impedance of load on pump inlet for each harmonic | PSI/CIS |
| ZCAM | Cam position | IN |

4.15.1.2 <u>Specifications and Initialization - Listing</u>

```
      SUBROUTINE VPUMP(WSTART,Y,ZIP,NHARM,POOVBD,PRESS,WINC,PISTNO,
     +ZAP)
C
C     ***** CECO VANE PUMP MODEL *****        MAY 8,1978
C
C         *VARIABLE TYPES, DIMENSIONS, COMMONALITY*
C
      REAL LPRESS,LPRESP,LVOL,LEAK,LK1,LK2,LK3,LK4,LK5,LK6,LK7,LK8
      COMPLEX BETA,G,P,Q,Z,ZO,ZIP,ZAP,P3,FQ1,PQ1
      COMMON BETA,G,P,Q,Z, XBE,BER,BEI,BERP,BEIP,RHO,BULK,VOL,W,VISC,PAR
     1M,PI, IEL,NEL,KTYPE(40)
      COMMON /VANE/CAMP(11),COMAX(11),ANGLE(30),DVOL(81),NA(2)
     + ,CAMPI(11),COMAXI(11)
      DIMENSION G(2,2,40),PARM(8,40),P(40),Q(40),Z(40),XA(2),DV(91)
      DIMENSION QQT(91),PPT(91),QQFC(11),QQFS(11),PPM(11) ,PPP(11)
      DIMENSION ZIP(10),ZAP(10),PISPR(1400)
      DIMENSION FQ1(10,3),PQ1(10,3),ETA(10)
      DATA PISPR/1400*0.0/
C
C *INITIALIZE VARIABLES FROM INPUT DATA OR MAIN PROGRAM*
C
      IF(Y.NE.WSTART) GO TO 140
      TERM=PARM(1,1)
      SLOTWO=PARM(2,1)
      COEPLK=PARM(3,1)
      THPRS=PARM(4,1)
      THPRE=PARM(5,1)
      THSUCS=PARM(6,1)
      THSUCE=PARM(7,1)
      LPRESS=PARM(1,NEL+1)
      SZCAM=PARM(2,NEL+1)
      VVOL=PARM(3,NEL+1)
      POOVBD=PARM(4,NEL+1)
      CKJ=PARM(5,NEL+1)
      CKL=PARM(6,NEL+1)
      CKT=PARM(7,NEL+1)
      CKV=PARM(8,NEL+1)
      ZCAM=0.0
      IF(SZCAM.GT.0.0)ZCAM=SZCAM
      NAPP=(90-THPRE-THPRS)/PISTNO+1
      NAPS=(90-THSUCE-THSUCS)/PISTNO+1
      Q1=10.
```

### 4.15.2 Section 1 - Compute Valve Index Positions

Figure 4-7 illustrates modeling parameters for a vane pump. Section 1 calculates the angular increment based on the number of vanes to produce 720 divisions per 180 degrees of revolution. In addition, the index positions for the beginning and end of the CAM pressure and Sultan slots are computed.

#### 4.15.2.1 Section 1 - Listing

```
C
C      SECTION 1
C      COMPUTE VALVING INDEX POSITIONS
C
       VANG=360./PISTNO
       AINC=4./PISTNO
       NDEGI=180/AINC+.001
       NVANG=VANG/AINC+.001
       NVANG1=NVANG+1
       NPRSOP=THPRS/AINC+1.
       NPROP=NPRSOP+NVANG+1.
       NPRSCL=(90.-THPRE)/AINC+1.
       NPRCL=NPRSCL+NVANG+1.
       NSUSOP=(90.+THSUCS)/AINC+1.
       NSUOP=NSUSOP+NVANG+1.
       NSUSCL=(180.-THSUCE)/AINC+1.
       NSUCL=NSUSCL+NVANG-NDEGI
       NSTOR=NDEGI+1
       WRITE(6,840) NPRSOP,NPROP,NPRSCL,NPRCL,NSUSOP,NSUOP,NSUSCL,NSUCL
  840  FORMAT(8(5X,I5))
C
```

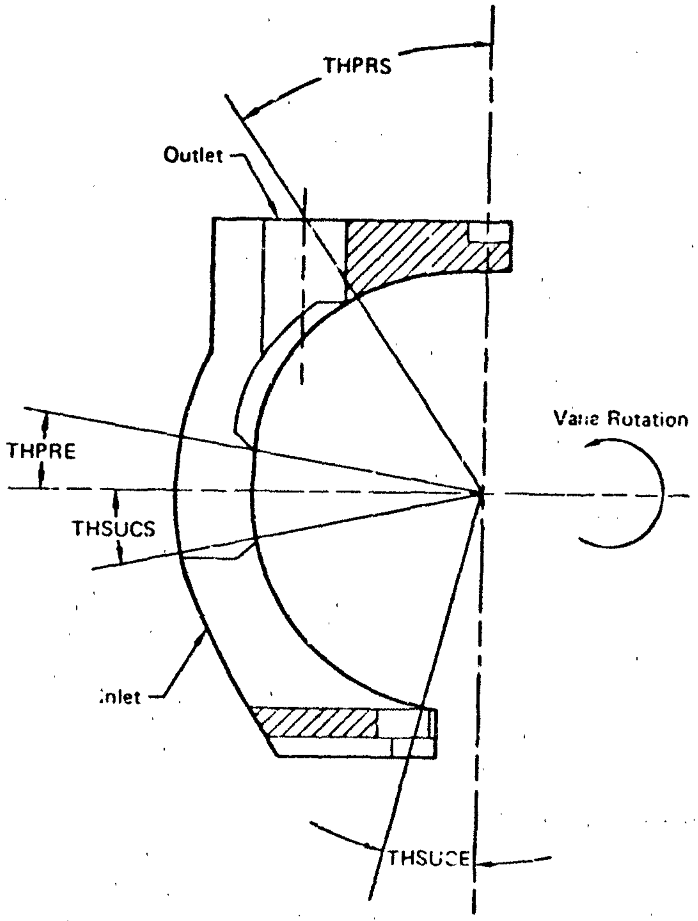


FIGURE 4-7

**VANE PUMP CAM BLOCK PARAMETERS**

### 4.15.3 Section 2 - Steady State Output Pressure Calculation

Section 2 calculates the steady state outlet pressure and flow as a function of cam position, pump speed, and pump internal leakage rate.

On the first call to VPUMP the orifice flow coefficient (ORF) is calculated, the first incremental bucket volume is initialized to pump inlet pressure and the bucket cavitation volume is set to zero. These calculations are bypassed on all subsequent calls of VPUMP. Each time VPUMP is called for a new pump speed and the cam position (ZCAM) is estimated as a function of incremental and maximum pump RPM.

#### 4.15.3.1 Math Model

Two equations are solved to obtain pump overboard flow and outlet pressure. Equation (1) describes the system pressure drop characterics input by the user:

```
    HPRESS = CKI + CKL * Q1 + CKT * Q1 ** 1.75 + CKV ** 2    (1)
Where
     PRESS = Pump outlet pressure (PSI)
        Q1 = Pump overboard flow (CIS)
```

The second equation describes the pump outlet flow in terms of max flow rate at the current RPM (QMAX) minus a leakage flow. Leakage is assumed to be directly proportional to the vane stage pressure rise as shown in Equation (2).

```
    Q1 = QMAX - (HPRESS - LPRESS) * COEPLK                    (2)
```

Equation (2) is solved for HPRESS and substituted into Equation (1). Newton's method of finding successive approximations to a real root (Q1) of the resulting equation is used. When the error between successive iterations is less than 0.001 CIS the value of overboard flow is used in Equation (2) to find HPRESS.

4.15.3.2 Section 2 - Listing

```
C
C       SECTION 2  ZCAM POSITION AND STEADY STATE OUTPUT PRESSURE CALCULATION
        PISPR(NSUCL)=LPRESS
        CAVCL=0.00
        ORF=.65*SQRT(2.0/RHO)
  140   CONTINUE
        ITER=0
        CALL INTERP(ZCAM,CAMPI(1),COMAXI(1),10,11,QMAX,IERR)
        QMAX=QMAX*Y/60.
  145   ITER=ITER+1
        TERM=CK1+CKL*Q1+CKT*Q1**1.75+CKV*Q1*Q1-LPRESS+(Q1-QMAX)/COEPLK
        DTERM=CKL+1.75*Q1**.75+2.*CKV+1./COEPLK
        Q2=Q1-TERM/DTERM
        QERR=Q2-Q1
        IF(ABS(QERR).LT.0.001)GO TO 150
        Q1=ABS(Q2)
        IF(ITER.GT.50)WRITE(6,9000)
 9000   FORMAT(10X,'EXCEEDED 50 ITERATIONS IN PUMP SS FLOW BALANCE')
        IF(ITER.GT.50)STOP
        GO TO 145
  150   CONTINUE
        QOVBD=Q2
        IF(QOVBD.GT.PQOVBD)QOVBD=PQOVBD
        HPRESS=(QMAX-QOVBD)/COEPLK+LPRESS
        IF(HPRESS.GT.PRESS)HPRESS=PRESS
        QMAX=QOVBD+(HPRESS-LPRESS)*COEPLK
        TQMAX=QMAX*60./Y
        CALL INTERP(TQMAX,COMAX(1),CAMP(1),10,11,ZCAM,IERR)
        IF(ZCAM.LT.0.0)ZCAM=0.0
        IF(ZCAM.GT.0.08)ZCAM=0.08
        WRITE(6,926)LPRESS,COEPLK,PQOVBD,QOVBD,HPRESS,PRESS,ZCAM,QMAX
  926   FORMAT(20X,8E12.5)
```

### 4.15.4 Section 3 - Bucket Precompression Calculation and Control Test

Section 3 determines if the computed flow capacity for a given cam position and RPM is sufficient to provide the demanded flow with a given pump leakage flow. If the pump can supply this flow, the control indicator is set to one (ICTL = 1).

Prior to the precompression pressure calculation, the maximum bucket volume is adjusted. The change in volume is added to the total volume as the vane increments NVANG times starting from the point where the leading edge of a vane is just closed to the inlet.

The remainder of Section 3 calculates the bucket pressure which exists before the vane starts to open the bucket to the pressure slot. This pressure is the result of precompression in the bucket during that portion of rotor rotation when the bucket is blocked by the cam block between the suction and pressure slots.

4.15.4.1 Math Model - The change in bucket volume is a function of the cam position and angular displacement of the rotor as shown in Figure 4-8. Total bucket volume is the sum of the volume changes for increasing bucket volume and minus the changes for decreasing volume. A pressure dependent factor for leakage from each vane to inlet is estimated for bucket pressures above input suction pressure as

PLEAK = COEPLK/(2.*NAPP)

Leakage from inlet to each bucket is

SLEAK = -PLEAK

Any cavitation volume in the bucket is calculated and tracked throughout the bucket revolution. Bucket pressures are stored for each position throughout the calculation. Time dependent oscillatory outlet pressure is initialized to zero PSI.

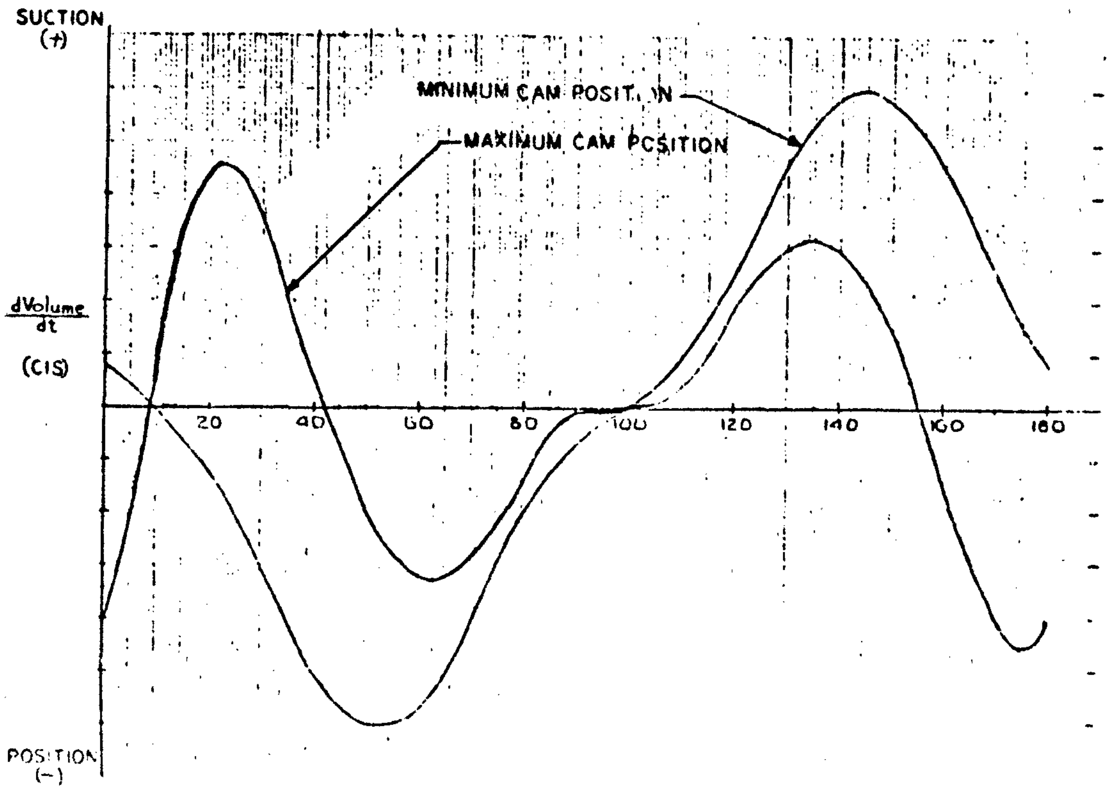


LEAD VANE ANGULAR POSITION THETA (DEG)

FIGURE 4-8

$\frac{dVolume}{dt}$ VERSUS VANE ANGLE

4.15.4.2 Assumptions - The bucket is assumed to be completely filled on the suction stroke and the initial cylincer is assumed to be one plus the input steady state value. Pressure dependent leakage is assumed, bulk modul s is recalculated at each step based on the last step incremental bucket pressure, and the bulk modulus formula used in fluid.

4.15.4.3 Computation Method - The calculation is performed in DANG increments with the initial vane centerline angle computed from the suction slot end angle (THSUCE) and the bucket angle (VANG). The number of calculation steps (NSTEPP) is calculated based on index positions defining the end of the suction slot plus NVANG and the beginning of the pressure slot in the cam block.

### 4.15.4.4 Section 3 - Listing



```
C
C     SECTION 3- PISTON PRECOMPRESSION CALCULATION
C
C     TEST IF ON CONTROL
  155 CONTINUE
      LEAK=QMAX-QOVBD
      ICTL=0
      IF(QMAX.GE.POOVBD+LEAK)ICTL=1
      NSTEPP=NPRSOP-NSUCL
      NP=(VANG-THSUCE)/AINC+1
      DPRESP=0.0
      LPRESP=PISPR(NSUCL)
      PLEAK=COEPLK/(2.*NAPP)
      SLEAK=-PLEAK
      DANG=AINC
      THETA=VANG-THSUCE
      DT=AINC/(6.*Y)
      XA(1)=THSUCE
      XA(2)=ZCAM
      I1=NSUSCL
      I2=NDEGI
      ITEM=0
      LVOL=VVOL
      I3=0
C      CALCULATE VOLUME FOR ONE BUCKET
  166 DO 168 I=I1,I2
      I3=I3+1
      XA(1)=XA(1)+DANG
      CALL LUCUP(ND,MA(1),ANGLE(1),DVOL(1),XA(1),DVDT,K,IE,NEXTR)
      DV(I3)=(DVDT)*DT
      LVOL=LVOL+DV(I3)
      DV(I3)=-DV(I3)
  168 CONTINUE
      IF(ITEM.EQ.1)GO TO 169
      ITEM=1
      I1=1
      I2=NP
      XA(1)=-DANG
      GO TO 166
  169 I1=0
      I3=90
      LPRESP=LPRESS+1.0
C     COMPUTE PRECOMPRESSION TO PRESSURE SLOT
      DO 160 I=1,NSTEPP
      IF(LPRESP.LT.LPRESS) GO TO 162
      DLEAK=(LPRESP-LPRESS)*PLEAK*DT
      GO TO 164
  162 DLEAK=(LPRESS-LPRESP)*SLEAK*DT
  164 BULKP=BULK+12.*(LPRESP-PRESS)
      XA(1)=THETA+DANG
      THETA=XA(1)
      CALL LUCUP(ND,MA(1),ANGLE(1),DVOL(1),XA(1),DVDT,K,IE,NEXTR)
      I3=I3+1
      IF(I3.GT.91)I3=1
      DV(I3)=(DVDT)*DT
      LVOL=LVOL+DV(I3)
      DELVOL=-DV(I3)
      DPRESP=(DELVOL-DLEAK-CAVOL)/LVOL*BULKP
      LPRESP=LPRESP+DPRESP
      NP=NP+1
      IF(LPRESP.GT.0.01) GO TO 165
      CAVOL=CAVOL-DELVOL+DLEAK
      IF(CAVOL.LT.0.0)CAVOL=0.0
      LPRESP=0.01
      DPRESP=0.0
      GO TO 167
  165 CAVOL=0.0
  167 PISPR(NP)=LPRESP
C     IF(Y.EQ.5000.)WRITE(6,931)CAVOL,NP,LPRESP,DV(I3),I3,DELVOL,I,
C    + LVOL,DLEAK,BULKP,THETA
  931 FORMAT(5X,1E12.5,I10,2E12.5,I5,1E12.5,I5,4E12.5)
  160 CONTINUE
      CAVOLD=CAVOL
      THEOLD=THETA
      DO 151 N=1,NVANG7
  151 PPT(N)=0.0
      KKN = 1
      KK = 1
  170 CONTINUE
```

### 4.15.5 Section 4 - Pump Outlet Flow Calculation

Section 4 calculates the total output flow from the pump for one cycle. Each of the active pumping buckets (NAPP) is sequentially incremented through steps. The outlet flow is determined from summing the flow from each bucket per side. The total flow is then multiplied by two since each side of the pump supplies approximately one half of the flow. The calculation is started one index step after the precompression ends. Pressure in the first bucket is initially the final precompression value. Pressure in the other open buckets is equal to the sum of the previously calculated steady state output pressure (HPRESS) and time dependent oscillating pressure (PPT). Bucket pressure and outlet flow computed at each step account for bucket leakage, pressure drop across the cam block, vane motion and fluid compressibility. QOT(1) is set equal to QOT(NVANG1) to reduce the effects of calculation start-up discontinuity, caused by the assumed initial cylinder pressures.

4.15.5.1 Math Model - The math model derivation is almost identical to that for the piston pump discussed in Section 4.5.1. The only significant change occurs in equation (22). The pressure loss due to fluid flow over a time DT is estimated as four times the flow rate, because there is one equation for each slot in the cam block. Equation (22) now becomes

$$\Delta P_f = ((DT*BULK)/(VA*LK1))*4*Q=4*LK3*Q$$

Following through on the substitution into equations (23) and (24), equation 25 is

$$Q**2+2*LK5*Q-LK6 \qquad (25)$$

Where

$$LK5 = LK4 * LK3 *2 \qquad (26)$$

The solution for Q in Equation (25) remains the same.

Before computing the vane outlet flow, the outlet flow area is calculated. As the leading edge vane of the bucket rotates through the outlet slot on the cam block, the arc length of the bucket exposed to the outlet is computed as

VAREA = .60935 * DTHETA / 57.3

This value is then multiplied by the cam block slot width to obtain the vane outlet flow area for one slot.

VAREA = VAREA * SLOTWO

The outlet flow calculation also tracks a cavitation volume if it should occur on the outlet. Outlet flow is computed for one output cycle of NVANG increments regardless of the increment size.

## 4.15.5.2 Section 4 - Listing

```
C
C     SECTION 4- PUMP OUTPUT FLOW CALCULATION
C
      CAVOL=CAVOLD
      VA=LVOL
      THETA=THEOLD
      XA(2)=ZCAM
      RTHETA=VANG
      DO 180 N=1,NVANG1
  180 QOT(N)=0.0
      WRITE(6,925)NP,CAVOL,LPRESP,VA,THETA
  925 FORMAT(10X,I10,4E12.5)
      NKM=NPRSOP
      DO 200 M=1,NAPP
      DO 190 N=1,NVANG
      NKM=NKM+1
      IF(NKM.GE.NPRCL) GO TO 190
      XA(1)=THETA+DANG
      THETA=XA(1)
      CALL LUCUP(ND,NA(1),ANGLE(1),CVOL(1),XA(1),DVDT,K,IE,NEXTR)
      I3=I3+1
      IF(I3.GT.91)I3=1
      DV(I3)=(DVDT)*DT
      VA=VA+DV(I3)
      DELVOL=-DV(I3)
C     COMPUTE VANE OUTLET FLOW AREA
      DTHETA=THETA-THPRS
      IF(DTHETA.GE.VANG)DTHETA=VANG
      IF(THETA.GT.(90.-THPRE))RTHETA=RTHETA-DANG
      IF(THETA.GT.(90.-THPRE))DTHETA=RTHETA
      VAREA=.60935*DTHETA/57.3
      VAREA=VAREA*SLOTWC
      IF(CAVOL.GT.0.00) GO TO 187
      BULKP=BULK+12.*(PISPR(NKM-1)-PRESS)
      IF(PISPR(NKM-1).GE.LPRESS) GO TO 186
      LEAK=SLEAK/(2.*NAPS)
      LK1=1.+SQRT(BULKP)*LEAK*DT/VA
      GO TO 185
  186 LEAK=PLEAK
C     LEAK=LEAK*(WSTART/Y)**1.25
      LK1=1.+BULKP*LEAK*DT/VA
  185 LK2=(PISPR(NKM-1)+BULKP/VA*(DELVOL))/LK1
      LK3=BULKP*DT/VA/LK1
      LK4= (ORF*VAREA)**2
      LK5 =LK3*LK4 *2.0
      LK6 = LK4 *(LK2 -HPRESS-PPT(N))
      LK7 =LK5*LK5 +ABS(LK6)
      LK8 = -LK5 +SQRT(LK7)
      QOUT= SIGN(LK8,LK6)
      PISPR(NKM)=LK2-QOUT*LK3
      IF(PISPR(NKM).GT..01) GO TO 188
  187 CONTINUE
      LEAK=SLEAK
      QOUT=-(0.65*VAREA*SQRT(2.*(HPRESS+PPT(N))/RHO))
      PISPR(NKM)=.01
      CAVOL=CAVOL-DELVOL+SLEAK*DT*LPRESS+QOUT*DT
      IF(CAVOL.LE.0.00) CAVOL=0.00
  188 QOT(N)=QOUT+QOT(N)
      CAVOL=0.0
C     IF(Y.EQ.5000..AND.KK.EQ.1)WRITE(6,932)CAVOL,N,NKM,PISPR(NKM),
C    + DELVOL,LK1,VA,LEAK,BULKP,THETA,QOT(N)
  932 FORMAT(5X,1E12.5,2I5,8E12.5)
  190 CONTINUE
  200 CONTINUE
      QOT(NVANG1)=QOT(1)
      DO 201 M=1,NVANG1
  201 QOT(M)=2.*QOT(M)
  927 FORMAT(5X,10E12.5)
```

### 4.15.6 Section 5 - Fourier Analysis of Pump Outlet Flow

Section 5 performs a harmonic analysis of the time dependent pump total output flow calculated in Section 4. Flow is computed over the cycle period for each harmonic from the fundamental up to and including the input harmonic.

If the pump is on control, the overboard flow is used to adjust the cam position (ZCAM). Harmonic flows (FQ1(I,KK)) are then calculated from the steady state conditions.

The steady state cam position calculation is bypassed during subsequent dynamic balancing in Section 6.

#### 4.15.6.1 Section 5 - Listing

```
C
C
C      SECTION 5- FOURIER ANALYSIS OF PUMP OUTPUT FLOW
       AN=VANS/AINC/2.
       N=AN+.001
       COEF=2./(2.*AN+1.)
       C1=3.141593*COEF
       S1 =SIN(C1)
       C1 =COS(C1)
       S  =0.0
       C  =1.0
       FNTZ=QOT(1)
       J  =1
  210  U2=0.0
       U1=0.0
       I=2*N+1
C      FORM FOURIER COEFFICIENTS RECURSIVELY
  220  U0=QOT(I)+2.0*C*U1-U2
       U2=U1
       U1=U0
       I=I-1
       IF(I-1) 230,230,220
  230  QCFC(J)=COEF*(FNTZ+C*U1-U2)
       [illegible]
       [illegible] 240,250,250
  240  U3=[illegible]
       S  =[illegible]
       C  =U3
       J  =J+1
       GO TO 210
  250  QQFC(1)=QCFC(1)*0.5
       IF([illegible].LE.0.01) QCFC(1)=0.01
C      CHECK STEADY STATE FLOW ERROR
       IF(KK.GT.1)GO TO 255
       IF([illegible]) GO TO 255
C      COMPUTE ZCAM POSITION
       [illegible]*COEFLK
       [illegible]
       CALL [illegible](CONV(1),CAMF(1),10,11,ZCAM,IERR)
       [illegible]
       [illegible]
C      [illegible] FLOWS FROM FOURIER ANALYSIS
  255  DO 260 I=1,N
       FQ1(I,KK) = CMPLX(QCFC(I+1), QSFC(I+1))
  260  CONTINUE
```

## 4.15.7 Section 6 - Outlet Pressure - Flow Balance Calculation and Listing

Section 6 of the vane pump model is identical to Section 6 of the axial piston pump model described in Paragraph 4.7.

```
C
C     SE[illegible]ION 6- OUTLET PRESSURE-FLOW BALANCE CALCULATION
C
 270 CO[illegible]NUE
     I = [illegible]
     IF ([illegible] - 2) 280,290,300
 280 CON[illegible]NUE
     W=Y*PISTNO*PI*KKN/30.
     ZO=1.0[illegible]/W*(.2,-1.)
     PQ1(I,[illegible]) = FQ1(I,KK )*ZO*ZIP(I)/(ZO +ZIP(I)) / 5.0
     P6=CA[illegible](PQ1(I,KK))*5.0
     P3=[illegible]Q1(I,KK)
     PPM([illegible]) = CABS(PQ1(I,KK))
     GO TO 320
 290 CONTINUE
     ZO = PQ1(I,KK-1) /(FQ1(I,KK-1)-FQ1(I,KK))
     PQ1(I,KK) = FQ1(I,KK-1)*ZO*ZIP(I)/(ZO +ZIP(I))
     P6=CABS(PQ1(I,KK))
     P3=PQ1(I,KK)-PQ1(I,KK-1)
     PQ1(I,KK+1) = PQ1(I,KK) - PQ1(I,KK-1)
     PPP(I) = ATAN2(AIMAG(PQ1(I,KK+1)),REAL(PQ1(I,KK+1)))
     PPM(I) = CABS(PQ1(I,KK+1))
     GO TO 320
 300 CONTINUE
     J=KKN
     PQ1(J,KK) = ZIP(J) * FQ1(J,KK)
     P6=CABS(PQ1(I,KK))
     ETA(J) = CABS(100 * (PQ1(J,KK) - PQ1(J,KK-1)) / PQ1(J,KK))
     KKN = KKN + 1
     IF(KKN.GT.NHARM) GO TO 335
     KK = 1
     FQ1(KKN,1) = FQ1(KKN,3)
     GO TO 270
 320 CONTINUE
```

### 4.15.8 Section 7 - Reconstruction of Time Dependent Pressures and Listing

Section 7 computes the time dependent outlet pressure (PPT) from each estimate of complex dynamic output pressure (P3) in Section 6. This section is identical to Section 7 in the axial pump model described in Paragraph 4.8.

```
C
C      SECTION 7- RECONSTRUCTION OF TIME DEPENDENT OUTLET PRESSURE
C
       TERM=(2.*PI)/NVANG
       DO 330 J=1,NVANG1
       THETA= (J-1)*I*TERM
       PPT(J) =PPT(J) + REAL(P3)* SIN(THETA) +AIMAG(P3)* COS(THETA)
       IF (PPT(J).LT.-HPRESS) PPT(J)=-HPRESS
   330 CONTINUE
       KK = KK + 1
       GO TO 170
   335 CONTINUE
       WRITE(6,901)ZCAM,QMAX,HPRESS,PRESS,QQFC(1),QOVRD,Y,ICTL
   901 FORMAT(/,7F12.4,3X,I5,/)
C      WRITE(6,927)(PISPR(I),I=31,416)
       Q(1)=FQ1(NHARM,3)
       P(1)=PQ1(NHARM,3)
       RETURN
       END
```

## 8.6 SUBROUTINE LUCUP

Subroutine LUCUP provide linear interpolation of data points for a three dimensional table. Two coordinate points are input and LUCUP returns the third value.

8.6.1 SUBROUTINE LUCUP-LISTING

```
      SUBROUTINE LUCUP(ND,NA,X,Z,XA,ZR,K,IE,NEXTR)
      DIMENSION X(1),Z(1),NA(1),XA(1)
      NT=NA(1)
      L2=NA(1)
      T=XA(1)
      P=XA(2)
      IT=1
      IF(T-X(1))80,90,50
   50 DO 60 I=2,L2
      IF(T-X(I))70,90,60
   60 CONTINUE
      IT=L2
      KODE=1
      GO TO 100
   70 IT=I
      KODE=1
      GO TO 100
   80 IT=2
      KODE=1
      GO TO 100
   90 IT=I
      KODE=2
      GO TO 110
  100 CONTINUE
      RATIOT=(T-X(IT-1))/(X(IT)-X(IT-1))
  110 CONTINUE
      L1=L2+2
      L2=L2+NA(2)
      I=L1-1
      IF(P-X(L1-1))180,190,150
  150 DO 160 I=L1,L2
      IF(P-X(I))170,190,160
  160 CONTINUE
      IP=L2
      KODEP=1
      GO TO 200
  170 IP=I
      KODEP=1
      GO TO 200
  180 IP=L1
      KODEP=1
      GO TO 200
  190 IP=I
      KODEP=2
      GO TO 210
  200 CONTINUE
      RATIOP=(P-X(IP-1))/(X(IP)-X(IP-1))
  210 CONTINUE
      IP=IP-NT
      IF(KODE.EQ.1.AND.KODEP.EQ.2)GO TO 400
      IF(KODE.EQ.2.AND.KODEP.EQ.1)GO TO 600
      IF(KODE.EQ.2.AND.KODEP.EQ.2)GO TO 800
      IZ=NT*(IP-2)+(IT-1)
      T1=Z(IZ)+RATIOT*(Z(IZ+1)-Z(IZ))
      IZ=IZ+NT
      T2=Z(IZ)+RATIOT*(Z(IZ+1)-Z(IZ))
      ZR=T1+RATIOP*(T2-T1)
      GO TO 1000
  400 CONTINUE
      IZ=NT*(IP-1)+(IT-1)
      ZR=Z(IZ)+RATIOT*(Z(IZ+1)-Z(IZ))
      GO TO 1000
  600 CONTINUE
      IZ=NT*(IP-2)+IT
      IZT=IZ+NT
      ZR=Z(IZ)+RATIOP*(Z(IZT)-Z(IZ))
      GO TO 1000
  800 CONTINUE
      IZ=NT*(IP-1)+IT
      ZR=Z(IZ)
 1000 CONTINUE
      RETURN
      END
```

## 6.52 TYPE #52 VANE PUMP

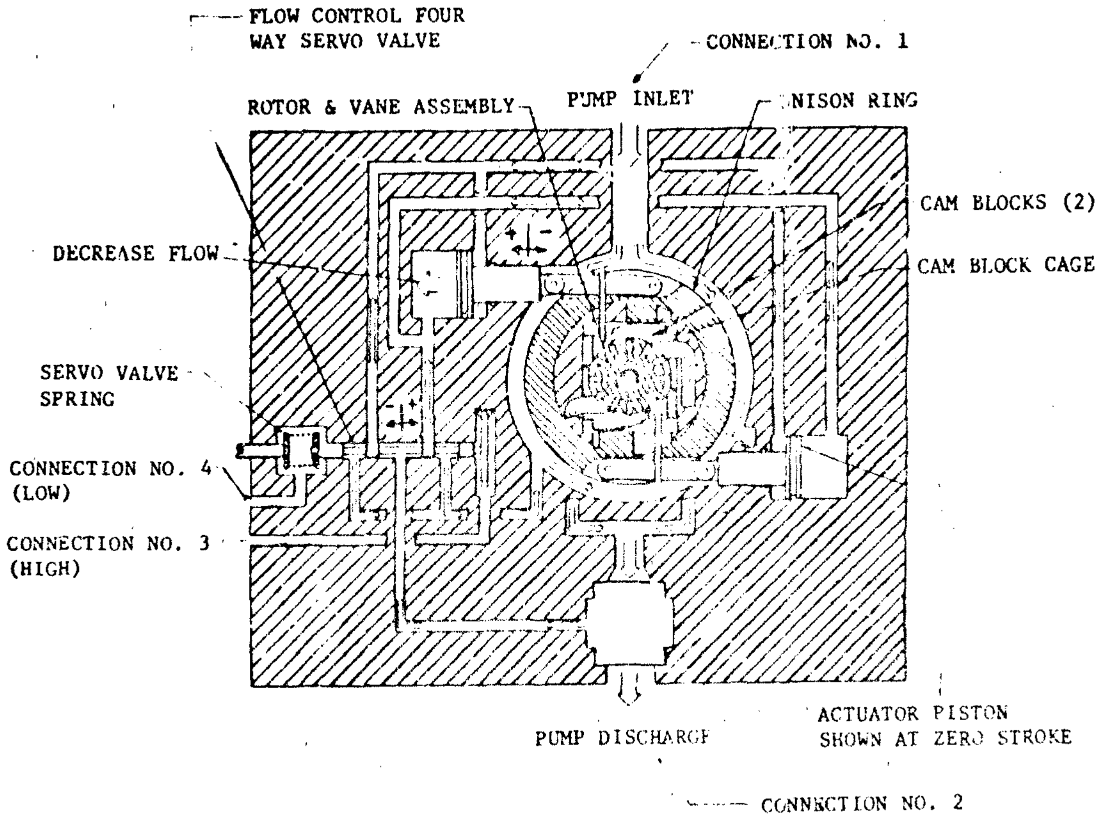


FIGURE 6.52-1
TYPE NO. 52 VANE PUMP

The CECO main fuel pump (MFP) is simulated by the PUMP52 subroutine. The variable displacement sliding vane pump is double acting with radial pressure balance. The pump is controlled by coupling an external metering valve to a single stage spool valve within the pump housing. The valve regulates pump displacement as required to meet metering valve area changes and speed changes.

The PUMP52 subroutine is written to work with an external metering valve (subroutine VALV24) supplying the control signals to the four way servo valve, which functions essentially as a null-type differential pressure sensor. The MFP

model will sense the signal pressures and adjust the outlet flow and pressure accordingly.

The transient pump model must be initialized at reasonable steady state values. Otherwise the resulting discontinuity between the steady state and transient sections of pump subroutine will cause a transient before the user selected time.

The MFP model requires the input of actuator stroke versus pump outlet flow and actuator load. The valve stroke versus flow area is also input.

Though the vane pump model was specifically written to model the CECO MFP, other variable displacement vane pumps may be modeled with this subroutine.

CARD NUMBER 1

| COLUMN | FORMAT | DATA |
|---|---|---|
| 1-5 | I5 | Component Number |
| 6-10 | I5 | Type Number = 52 |
| 11-15 | I5 | Number of Real Data Cards = |
| 16-20 | I5 | Line Number (with sign) attached to Connection 1 (Inlet) |
| 21-25 | I5 | Line Number (with sign) attached to Connection 2 (Outlet) |
| 26-30 | I5 | Line Number (with sign) attached to Connection 3 (High Control Pressure) |
| 31-35 | I5 | Line Number (with sign) attached to Connection 4 (Low Control Pressure) |
| 36-40 | I5 | Number of Servo Valve Positions |
| 41-45 | I5 | Number of Actuator Positions |
| 46-50 | I5 | Number of Outlet Pressures |
| 51-55 | I5 | |
| 56-60 | I5 | |
| 61-65 | I5 | |
| 66-70 | I5 | |
| 71-75 | I5 | |
| 76-80 | I5 | Temperature/Pressure Code (See Page 4.0-2) |

EXAMPLE CARD

CARD NUMBER 2

| COLUMN | FORMAT | DATA | DIMENSIONS |
|---|---|---|---|
| 1-10 | E10.0 | Servo Valve Area | $In^2$ |
| 11-20 | E10.0 | Servo Valve Spring Rate | Lb/In |
| 21-30 | E10.0 | Servo Valve Spring Preload | Lb |
| 31-40 | E10.0 | Servo Valve Mass | Lb-sec/In |
| 41-50 | E10.0 | Servo Valve Damping | Lb-sec/In |
| 51-60 | E10.0 | Servo Valve Discharge Coefficient | -- |
| 61-70 | E10.0 | Minimum Valve Displacement | In |
| 71-80 | E10.0 | Maximum Valve Displacement | In |

EXAMPLE CARD

CARD NUMBER 3

| COLUMN | FORMAT | DATA | DIMENSIONS |
|---|---|---|---|
| 1-10 | E10.0 | Actuator Extend Area | $In^2$ |
| 11-20 | E10.0 | Actuator Retract Area | $In^2$ |
| 21-30 | E10.0 | Maximum Actuator Stroke | In |
| 31-40 | E10.0 | Unison Ring Damping Factor | $\frac{\text{Lb-Sec}}{\text{In}}$ |
| 41-50 | E10.0 | Servo Valve Overlap | In |
| 51-60 | E10.0 | Extend Actuator Volume @ Zero Stroke | $In^3$ |
| 61-70 | E10.0 | Retract Actuator Volume @ Zero Stroke | $In^3$ |
| 71-80 | E10.0 | Pump RPM | RPM |

EXAMPLE CARD

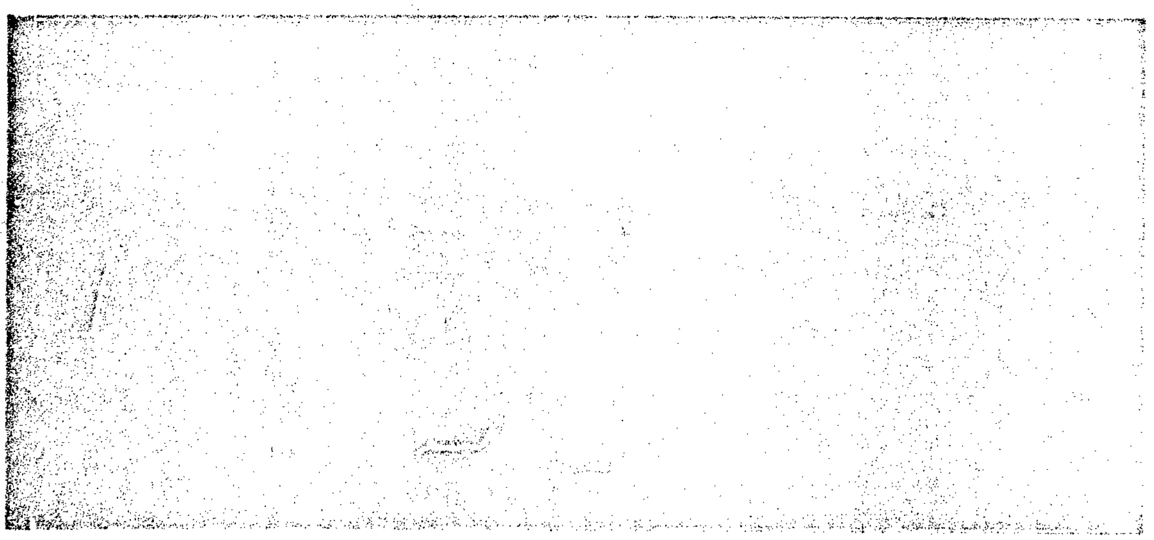

CARD NUMBER 4

| COLUMN | FORMAT | DATA | DIMENSIONS |
|---|---|---|---|
| 1-10 | E10.0 | Coefficient of Pump Leakage | $\frac{CIS}{PSI}$ |
| 11-20 | E10.0 | Initial Actuator Position | In |
| 21-30 | E10.0 | Coefficient of Servovalve Leakage @ Null Position and 100°F | - |
| 31-40 | E10.0 | Outlet Volume | $In^3$ |
| 41-50 | E10.0 | Initial Steady State Outlet Flow | CIS |
| 51-60 | E10.0 | Initial Steady State Pressure | PSI |
| 61-70 | E10.0 | Maximum Pump Flow @ Operating RPM | CIS |
| 71-80 | E10.0 | | |

EXAMPLE CARD

CARD NUMBER 5

| COLUMN | FORMAT | DATA | DIMENSIONS |
|---|---|---|---|
| 1-10 | E10.0 | First Actuator Position | In |
| 11-20 | E10.0 | Enter as Many Values As | " |
| 21-30 | E10.0 | Listed in Columns 41-45 of | " |
| 31-40 | E10.0 | Card No. 1) | " |
| 41-50 | E10.0 | Last Actuator Position | " |
| 51-60 | E10.0 | Outlet Pressure for Cam Load | PSI |
| 61-70 | E10.0 | (Enter as Many Values as | " |
| 71-80 | E10.0 | Listed in Columns 46-50 of Card No. 1) | " |

EXAMPLE CARD

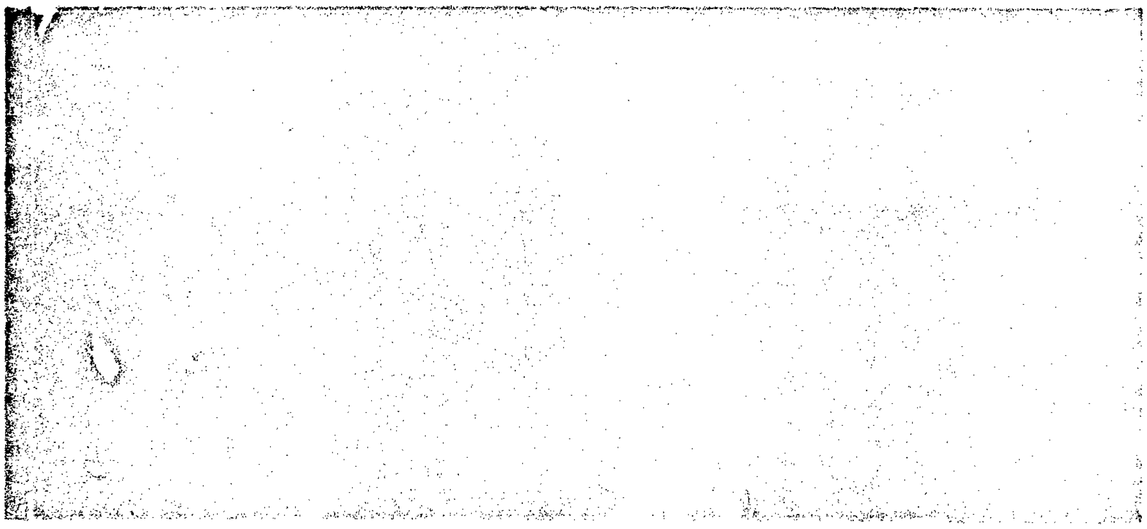

CARD NUMBER 6

| COLUMN | FORMAT | DATA | DIMENSIONS |
|---|---|---|---|
| 1-10 | E10.0 | Cam Load On Actuator at First Outlet Pressure | Lb |
| 11-20 | E10.0 | (Enter Number of Actuator | " |
| 21-30 | E10.0 | Positions Times Number of | " |
| 31-40 | E10.0 | Outlet Pressure Values) | " |
| 41-50 | E10.0 | Last Cam Load On Actuator | " |
| 51-60 | E10.0 | Ideal Pump Flow for First Actuator Position | CIR |
| 61-70 | E10.0 | (Enter as Many Values as Listed in Columns | " |
| 71-80 | E10.0 | 41-45 of Card No. 1) | " |

EXAMPLE CARD

CARD NUMBER 7

| COLUMN | FORMAT | DATA | DIMENSIONS |
|---|---|---|---|
| 1-10 | E10.0 | First Servovalve Position (Positive Direction Only) | In |
| 11-20 | E10.0 | (Enter As Many Values as Listed in | " |
| 21-30 | E10.0 | Columns 36-40 of Card No. 1) | " |
| 31-40 | E10.0 | " | " |
| 41-50 | E10.0 | Last Servovalve Position | " |
| 51-60 | E10.0 | Servovalve Flow Area Correspond To First Position | $IN^2$ |
| 61-70 | E10.0 | (Enter as Many Values As | " |
| 71-80 | E10.0 | Servovalve Positions) | " |

EXAMPLE CARD

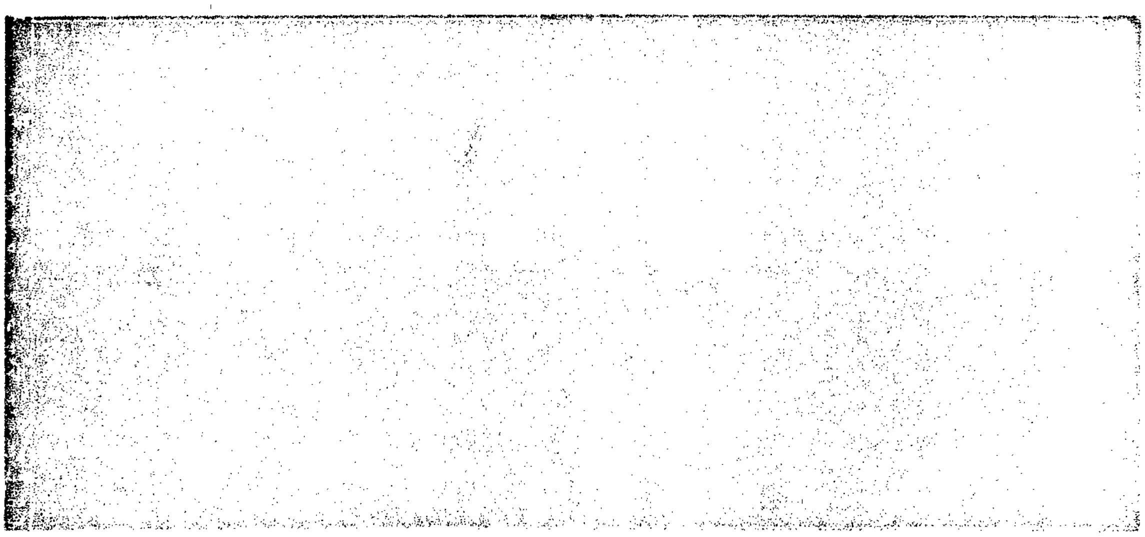

6.24 TYPE #24 TWO-WAY CONTROL VALVE TO BE USED WITH TYPE #52 VANE PUMP

TYPE #24 is a specially modified TYPE21 valve that is used with the PUMP52 subroutine. The valve uses an externally controlled time history input. The valve opening area is derived from the tabulated data input on the third and fourth cards. The total number input on both the time and area tables must be equal to the number input in column 70 of the first data card.

Care must be taken in choosing the proper metering valve areas for the initial steady state pressure and flow conditions input with the PUMP52 subroutine.

CARD NUMBER 1

| COLUMN | FORMAT | DATA |
|---|---|---|
| 1-5 | I5 | Component Number |
| 6-10 | I5 | Type Number = 24 |
| 11-15 | I5 | Number of Real Data Cards = 3 or more |
| 16-20 | I5 | Line Number (with sign) attached to Connection 1 |
| 21-25 | I5 | Line Number (with sign) attached to Connection 2 |
| 26-30 | I5 | |
| 31-35 | I5 | |
| 36-40 | I5 | |
| 41-45 | I5 | |
| 46-50 | I5 | |
| 51-55 | I5 | |
| 56-60 | I5 | |
| 61-65 | I5 | |
| 66-70 | I5 | Number of data points in table. |
| 71-75 | I5 | |
| 76-80 | I5 | Temperature/Pressure Code (See Page 4.0-2) |

EXAMPLE CARD

CARD NUMBER 2

| COLUMN | FORMAT | DATA | DIMENSIONS |
|---|---|---|---|
| 1-10 | E10.0 | | |
| 11-20 | E10.0 | Valve Discharge Coefficient | -- |
| 21-30 | E10.0 | | |
| 31-40 | E10.0 | | |
| 41-50 | E10.0 | | |
| 51-60 | E10.0 | | |
| 61-70 | E10.0 | | |
| 71-80 | E10.0 | | |

EXAMPLE CARD

CARD NUMBER 3

| COLUMN | FORMAT | DATA | DIMENSIONS |
|---|---|---|---|
| 1-10 | E10.0 | First Time Value (Must be 0.0) | SEC |
| 11-20 | E10.0 | (Enter as many time values as | |
| 21-30 | E10.0 | required using as many columns and | |
| 31-40 | E10.0 | cards as necessary. Final time must | |
| 41-50 | E10.0 | be greater than or equal to final | |
| 51-60 | E10.0 | calculation time.) | |
| 61-70 | E10.0 | | |
| 71-80 | E10.0 | | |

EXAMPLE CARD

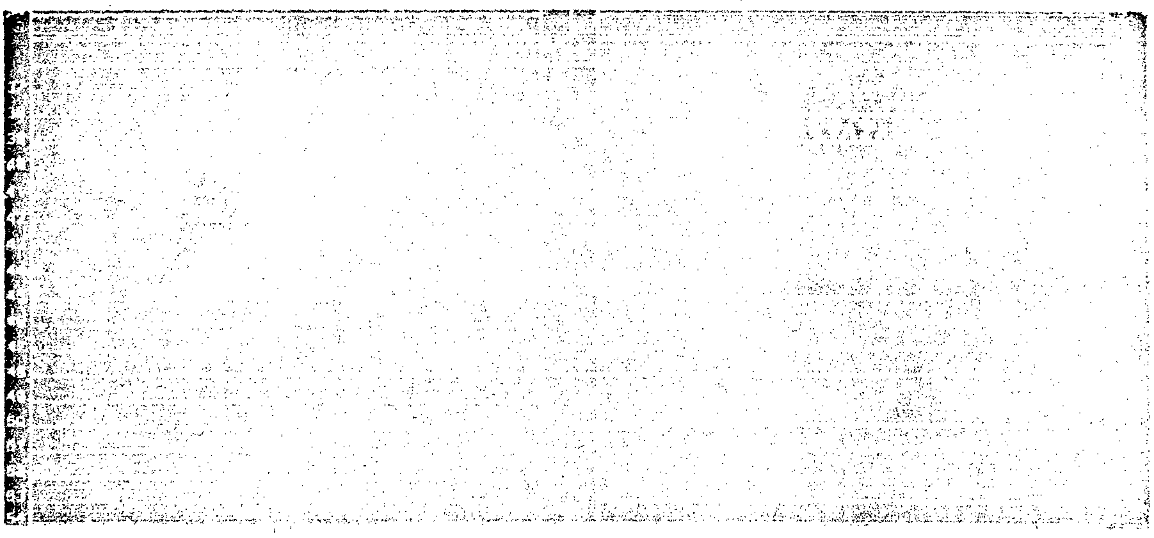

CARD NUMBER 4

| COLUMN | FORMAT | DATA | DIMENSIONS |
|---|---|---|---|
| 1-10 | E10.0 | Initial Metering Valve Area @ T=0.0 | $In^2$ |
| 11-20 | E10.0 | (Enter as many valve areas as | |
| 21-30 | E10.0 | time values). | |
| 31-40 | E10.0 | | |
| 41-50 | E10.0 | | |
| 51-60 | E10.0 | | |
| 61-70 | E10.0 | | |
| 71-80 | E10.0 | | |

EXAMPLE CARD

6.52 SUBROUTINE PUMP52

Subroutine PUMP52 was set up to model a variable displacement vane pump of the type used as the main fuel pump on the F-15.

The vane pump is a double-acting pump with 100 percent radial pressure balance. The internal vane track contour provides for two inlet and discharge ports per revolution. Pump flow control is achieved by hydraulically coupling an external metering valve to an internal single stage hydraulic servovalve.

The servovalve regulates pump displacement as required to meet valve area changes and speed changes. A schematic of the variable displacement vane pump is shown in Figure 6.51-1. The pump is shown in a maximum flow condition. The pumping element consists of a rotor, vane and shaft assembly and two vane track cam blocks. Two side plates at each end (not shown) are required to complete the seal of the pump volume. A cage and unison ring assembly is used to support the cam blocks and control their position.

The cage restrains the cam blocks vertically while allowing horizontal motion. The horizontal motion is controlled by the angular position of the unison ring and the relationship between the two inwardly protruding surfaces on it and the external cam surface that contacts it. The volumetric displacement of the pump is determined by the allowable vane accelerations that will insure continuous vane contact with the vane track.

6.52.1 Math Model

To compute the transient response of the pump, the control characteristics are modeled using simplified calculation techniques. The pump supplies fluid flow in response to metering head pressure differential. Summing forces on the flow control servo valve in Figure 6.52-1 yields equation (1).

DT(ACCEL) = (PMH*D(ARVAL) - D(BVAL) * VLST - D(KSPG) * XLST)/D(MVAL) (1)

where

DT(ACCEL) = VALVE ACCELERATION

PMH * D(ARVAL) = CONTROLLING FORCE INPUT

D(BVAL) = VALVE DAMPING COEFFICIENT

VLST = PREVIOUS VALVE VELOCITY

D(KSPG) = VALVE SPRING CONSTANT

XLST = PREVIOUS VALVE POSITION

D(MVAL) = VALVE MASS

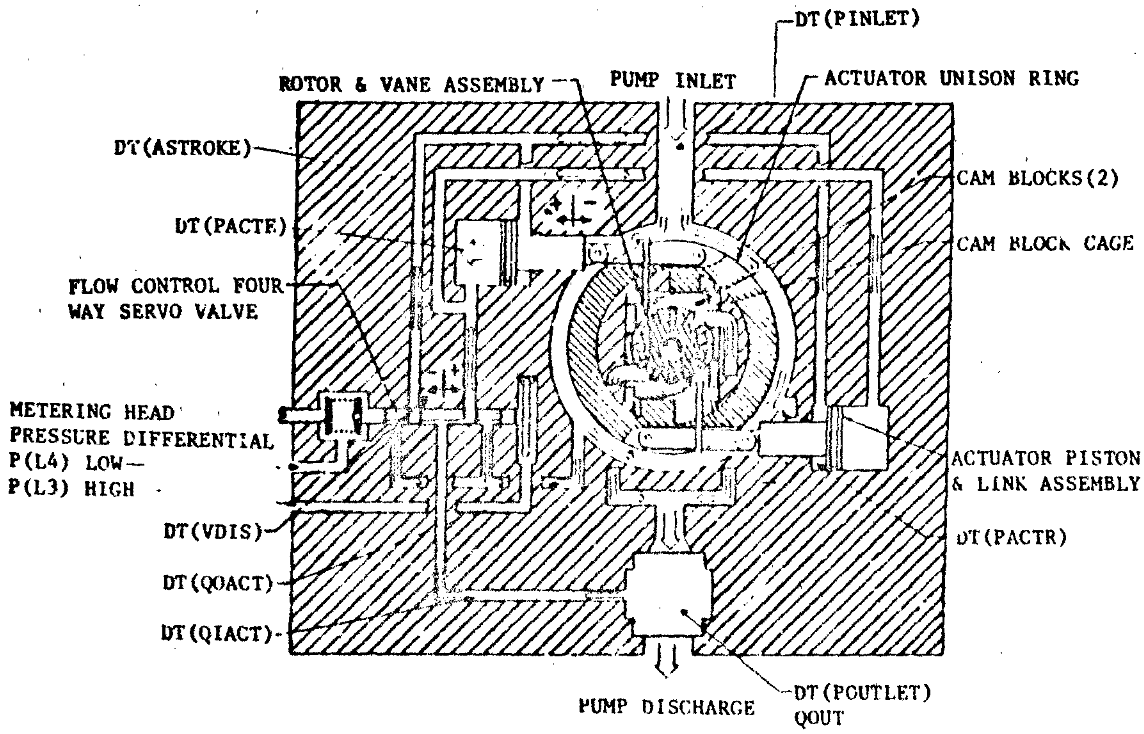


FIGURE 6.52-1

SCHEMATIC OF BALANCED VARIABLE DISPLACEMENT VANE PUMP AND CONTROLLER

The servovalve displacement for the current time step is computed using a corrected Euler method. The calculation of actuator flows is based on a combination of the servovalve orifice equations and the volumetric impedance. The exact formulation of equations changes depending on whether the actuator is retracting - decreasing pump outlet flow, or the actuator is extending - increasing the pump outlet flow.

An equivalent diagram for the flows entering and leaving an extending actuator is shown in Figure 6.52-2. The pressure drop for the Q1 flow is written as

$$DT(POUTLT) - DT(PACTE) = Q1 * \frac{1}{DT(BULKE)} + Q1^2 * \frac{1}{COEV1^2} \quad (2)$$

A similar expression can be written for the Q2 flow. The subsequent quadratic equations are then solved to obtain Q1 and Q2, the flows entering and leaving the actuator as it is extending. The flow values are doubled because there are two actuators controlling the cams in the pump.

The actuator velocity is then calculated using the equivalent network given in Figure 6.52-2. The network is solved for the piston velocity DT(VELACT). A damping term and actuator load are included in the calculation. The load is based on the previous or last time step value of the actuator velocity.

The network accounts for the volumetric effects of the two actuator cavities, under the assumption that a portion of the flow is lost to or obtained from these volumes due to changes in pressure within the cavities. The basic network equations are:

$$DT(VELACT) * D(AEXT) = -Q1 - DT(BULKE) * (OPACTE - DT(PACTE)) \quad (3)$$

$$DT(VELACT) * D(ARET) = +Q2 + DT(BULKR) * (OPACTR - DT(PACTR)) \quad (4)$$

$$DT(VELACT) * D(DAMP) = -DT(PACTE) * D(AEXT) + DT(PACTR) * D(ARET) + ALOAD \quad (5)$$

Solving EQNS (3) and (4) for DT(PACTE) and DT(PACTR) and substituting into Equation (5) yields

$$DT(VELACT) = FDRIVE / ZN \quad (6)$$

where

$$FDRIVE = \frac{Q2}{G2} + OPACTR* D(ARET) - \frac{Q1}{G1} - OPACTE* D(AEXT) + ALOAD$$

$$ZN = D(DAMP) + \frac{D(AEXT)}{G1} + \frac{D(ARET)}{G2}$$

G1 = DT(BULKE) / D(AEXT)

G2 = DT(BULKR) / D(ARET)

Once the actuator velocity is obtained the stroke is computed as:

DT(ASTROKE) = DT(ASTROKE) + (AVELO + DT(VELACT))*DELT/2. (7)

where

AVELO = the previous time step value of actuator velocity

The actuator stroke is directly related to pump flow. The actuator pressures may be computed for the current time step.

DT(PACTE) = DT(PACTE) + (Q1 + AVELO * D(AEXT))/DT(BULKE)

DT(PACTR) = DT(PACTR) + (Q2 - AVELO * D(ARET))/DT(BULKR)

Equivalent circuit schematics of the pump's inlet and outlet are shown in Figure 3.5-3. Solving for DT(PINLET) yields

DT(PINLET) = (C(L1)/Z(L1) + DT(PPOUT) * D(COEPLK) (8)

+ DT(QOACT) - DT(QMAX))/(1/lZ(L1) + D(COEPLK))

The pump outlet flow is

QOUT = -(DT(QMAX)-D(COEPLK) *(DT(PPOUT)-DT(PINLET))

-DT(QIACT)-DT(BULKO) *(DT(PPOUT)-OPOUTLT)) (9)

and the outlet pressure is then

DT(POUTLT) = C(L2) - QOUT * Z(L2) (10)

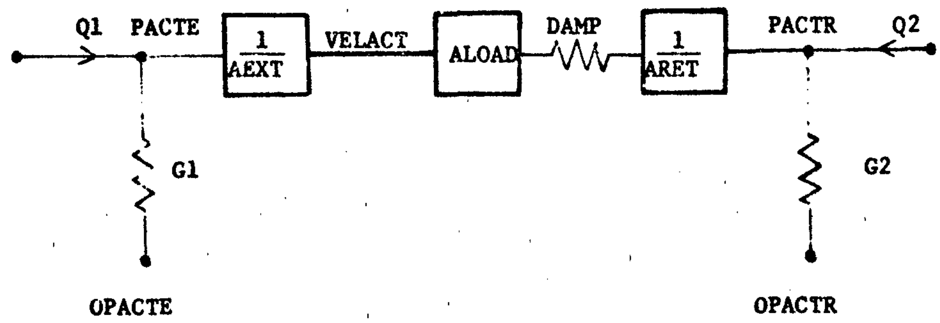


FIGURE 6.52-2

ACTUATOR PRESSURE AND FLOW CIRCUIT DIAGRAM

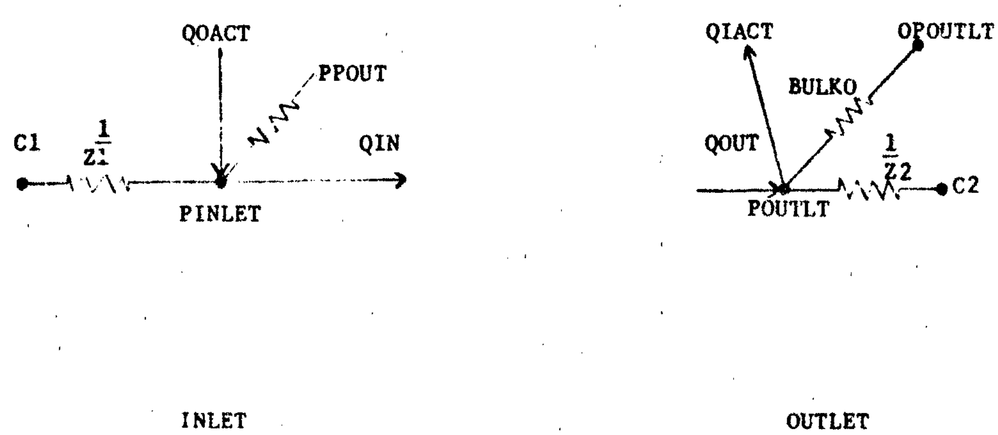


FIGURE 6.52-3

INLET AND OUTLET CIRCUIT DIAGRAMS

6.52-2 ASSUMPTIONS

The vane pump is a symmetrical unit, thus actuator loads were assumed identical. Once the actuator flows were calculated they were simply doubled to obtain the total flows that were recycling through the unit. Friction and stiction in the actuators were ignored.

The pump internal leakage is assumed to be directly proportional to the pump pressure rise. The model also does not incorporate the high pressure relief valve or the wash flow filter shown in Figure 6.52-1. The dynamic effects of these elements are negligible during normal pump operation.

6.52-3 COMPUTATIONS

1000 SECTION

In this section pump constants are initialized for use in the subroutine.

1500 SECTION

Steady State Calculations

The pump has four connections. The two metering pressure connections are handled as zero flow legs and they are not part of the steady state flow pressure balance. Only the inlet and outlet connections are used.

The user inputs the initial steady state pump outlet flow, pressure, and actuator position for the given flow. The pump vane stage pressure rise is derived from an equation incorporating maximum and overboard flow and the coefficient of pump leakage.

DT(PPOUT) = (DT(QMAX) - D(QOVBD))/ D(COEPLK)

To initialize the actuator pressures an iterative procedure is used. The pressures are dependent on the actuator load at the initial stroke and the leakage through the servovalve.

2000 SECTION

Actuator stroke and velocity, predicted outlet pressure, valve acceleration, velocity and displacement, and valve set spring pressure are initialized in the 2000 section.

3000 SECTION

In the 3000 section, the pump transient response is calculated. A flow chart for this section is shown in Figure 6.52-4. First control servovalve flows and pressures are computed. The valve acceleration is determined using a force balance on the spool. Integrating the acceleration equation yields the following equation for control valve velocity:

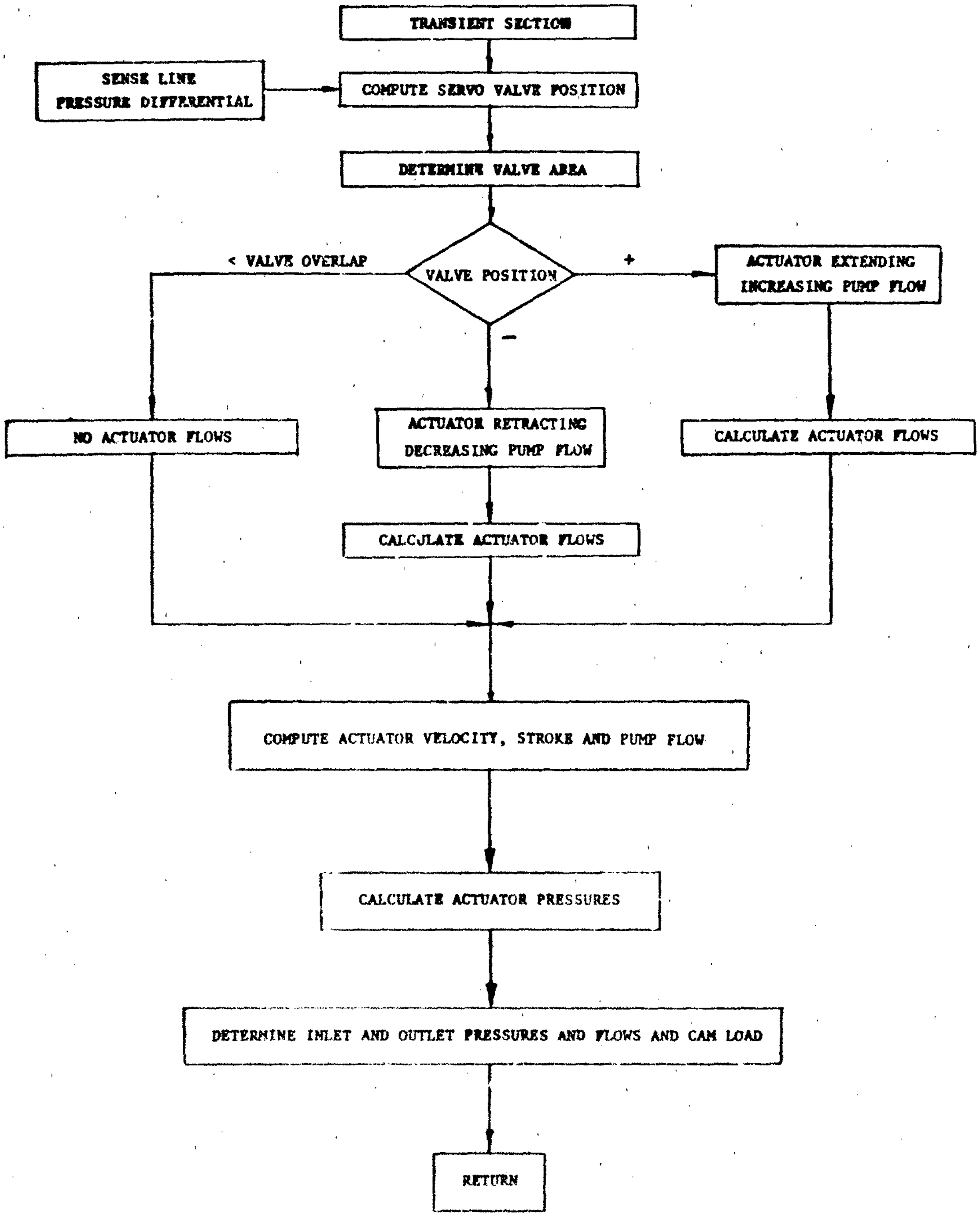


FIGURE 6.52-4 CECO MFP MATH MODEL FLOW DIAGRAM

DT(VAVEL) = VLST + (DT(ACCEL) + ALST)*DELT/2.

The integration of the velocity equation results in an equation for valve displacement:

DT(VDIS) = XLST + (DT(VAVEL) + VLST) * DELT/2.

If the absolute value of the valve displacement is less than the valve overlap, the leakage flow through the valve is set to zero. If the valve displacement is greater than the valve overlap, the program will compute orifice characteristics of the valve from subroutine INTERP.

For decreasing flow, (actuator retracting), the program will compute pressures and flows for pump inlet and outlet. If the flow is increasing, (actuator extending), another set of equations is used to calculate the pressures and flow rates. Actuator piston position is determined by integrating the actuator velocity equation. Pump flow can then be computed using the INTERP subroutine. Equations relating leakage coefficients and pump flows yield pump inlet and outlet pressures. A predicted pump outlet pressure is computed for the next time step. The cam load is computed in subroutine LUCUP and is a function of actuator stroke and outlet pressure. The final step in this section defines the pressures and flows at the inlet and outlet lines of the pump.

6.52-4 Variable Names

| Name | Description | Dimension |
|---|---|---|
| A | Temporary Variable | -- |
| DT(ACCEL) | Valve Acceleration | IN/SEC**2 |
| D(AEXT) | Actuator Extend Area | IN**2 |
| ALOAD | Last Actuator Load | LBS |
| ALST | Last Valve Acceleration | IN/SEC**2 |
| D(ARET) | Actuator Retract Area | IN**2 |
| D(ARVAL) | Control Servovalve Area | IN**2 |
| ASIGN | Sign of Valve Velocity | -- |
| ASTRO | Last Actuator Stroke | IN |
| DT(ASTROKE) | Actuator Stroke | IN |
| AVDIS | Absolute Value of Valve Displacement | IN |
| AVELO | Last Actuator Velocity | IN/SEC |
| B | Temporary Variable | -- |
| DT(BULKE) | Actuator Extend Compressibility | PSI |
| DT(BULKO) | Pump Outlet Compressibility | PSI |
| D(BVAL) | Servovalve Damping | -- |
| D(COEPLK) | Coefficient of Pump Leakage | -- |
| D(COEVL1) | Coefficient of Valve Leakage (Open Valve) | CIS/PSI |
| D(COEVL2) | Coefficient of Valve Leakage (Laminar) | CIS/PSI |
| COEV1 | Temporary Variable | -- |
| CCN | Temporary Variable | -- |
| D(DAMP) | Unison Ring Damping Factor | LBS/IN/SEC |
| DELTAP | Temporary Variable | -- |
| DELTP | Temporary Variable | -- |
| FDRIVE | Temporary Variable | -- |
| FF | Temporary Variable | -- |
| FRIC | Actuator Friction | LBS |
| G1 | Temporary Variable | -- |
| G2 | Temporary Variable | -- |
| I | Counter | -- |
| IE | Error Indicator | -- |
| IERR | Error Indicator | -- |

| Name | Description | Dimension |
|---|---|---|
| IFAIL | Iteration Fail Indicator | -- |
| ILOC | Array Location Indicator | -- |
| ILOC1 | Array Location Indicator | -- |
| D(ISTR) | Initial Actuator Position | IN |
| ITER | Iteration Counter | -- |
| K | Counter | -- |
| KSPG | Spring Rate | LBS/IN |
| DT(LOAD) | Actuator Load | LBS |
| LOC | Array Location Indicator | -- |
| L1 | Dummy Variable | -- |
| L2 | Dummy Variable | -- |
| L3 | Dummy Variable | -- |
| L4 | Dummy Variable | -- |
| D(MAVDIS) | Maximum Valve Displacement | IN |
| DT(MHSET) | Servovalve Set Spring Pressure | PSI |
| D(MIVDIS) | Minimum Valve Displacement | IN |
| D(MSTROKE) | Maximum Actuator Stroke | IN |
| D(MVAL) | Servovalve Mass | (LBS-SEC**2)/IN |
| N | Counter | -- |
| L(NAST) | Number of Tabulated Actuator Strokes | -- |
| L(NPR) | Number of Reference Load Pressures | -- |
| L(NVDIS) | Number of Tabulated Valve Displacements | -- |
| OPACTE | Last Actuator Extend Pressure | PSI |
| OPACTR | Last Actuater Retract Pressure | PSI |
| OPOUTLT | Last Outlet Pressure | PSI |
| OQ1 | Temporary Variable | -- |
| OQ2 | Temporary Variable | -- |
| DT(PACTE) | Extend Actuator Pressure | PSI |
| DT(PACTR) | Retract Actuator Pressure | PSI |
| DT(PINLET) | Inlet Pressure | PSI |
| PMH | Sense Line Pressure Differential | PSID |
| DT(POUTLT) | Outlet Pressure | PSI |
| DT(PPOUT) | Predicted Outlet Pressure | PSI |
| D(PRESS) | Pump Outlet Pressure | PSI |

| Name | Description | Dimension |
| --- | --- | --- |
| D(PRPM) | Pump RPM | REV/MIN |
| QAREA | Servovalve Opening Area | IN**2 |
| DT(QAREA1) | Valve Orifice Constant | -- |
| DT(QIACT) | Flow to Actuator | CIS |
| QLOSS | Temporary Variable | -- |
| DT(QMAX) | Maximum Pump Flow | CIS |
| DT(QOACT) | Flow from Actuator | CIS |
| QOUT | Flow Out of Pump | CIS |
| D(QOVRD) | Initial Pump Outlet Flow | CIS |
| QPUMP | Temporary Variable | -- |
| Q1 | Temporary Variable | -- |
| Q2 | Temporary Variable | -- |
| D(SPLOAD) | Spring Preload | LBS |
| DT(VDIS) | Valve Displacement | IN |
| DT(VELACT) | Actuator Velocity | IN/SEC |
| VLST | Last Valve Velocity | IN/SEC |
| D(VOLAP) | Servovalve Overlap | IN |
| D(VOLE) | Extend Actuator Volume at Zero Stroke | IN**3 |
| D(VOLOUT) | Outlet Volume | IN**3 |
| D(VOLR) | Retract Actuator Volume at Zero Stroke | IN**3 |
| XDD | Temporary Variable | -- |
| XDDS | Temporary Variable | -- |
| XLST | Last Valve Displacement | IN |
| ZN | Temporary Variable | -- |

```
      SUBROUTINE PUMP52 (D,DT,DD,L)
      DOUBLE PRECISION DD
C ***       DECEMBER 12,1977        ***
C        CECO VARIABLE DISPLACEMENT VANE PUMP MODEL(RPUMP52)
      COMMON NTELPL,NTOLPL,IPT,IPOINT,NPTS,INEL,KNEL,NTOPL,NLPLT(61,3),
     1 POLEG(90,12),LCS(90,10),ILEG(1400),PN(90),QN(90)
      COMMON/SUE/PARM(150,9),PM(1500),QM(1500),P(300),Q(300),C(300)
     1,Z(300),RHO(20),S2ORHO(20),VISC(20),BULK(20),TEMP(20),PVAP(20)
     2,ATPRES,T,DELT,TFINAL,PLTDEL,PI,TITLE(20),LEGN,ICON
     3,KTEMP(99),LSTART(150),NLPT(150),LTYPE(99),NC(99),INX,IN7
     4,INV,ISTEP,NLINE,NEL,IND,IENTR,MNLINE,MNEL,MNLEG,MNNODE,MNPLOT
     5,MNLPTS,MOS
      DIMENSION D(124),DT(24),DD(1),L(10)
      DIMENSION XA(2)
C       D VARIABLE INTEGERS
      INTEGER ARVAL,SPLOAD,BVAL,COEVL1,COEVL2,AEXT,ARET,DAMP,VOLAP,
     1 VOLF,VOLP,VOLOUT,PRPM,COEPLK,QOVBD,PRESS,QCMAX
C       DT VARIABLE INTEGERS
      INTEGER ACCEL,VAVEL,VDIS,PACTE,PACTR,BULKE,BULKR,VELACT,
     1 POUTLT,PINLET,ASTROKE,BULKO,QMAX,PPOUT,CIACT,OPACT,QAREA1
C       D( ) ARRAY *****
      DATA ARVAL/1/,KSPG/2/,SPLOAD/3/,MVAL/4/,BVAL/5/,COEVL1/6/,
     1 MIVDIS/7/,MAVDIS/8/,AEXT/9/,ARET/10/,MSTROKE/11/,DAMP/12/,
     2 VOLAP/13/,VOLF/14/,VOLP/15/,PRPM/16/,COEPLK/17/,ISTR/18/,
     3 COEVL2/19/,VOLOUT/20/,QOVBD/21/,PRESS/22/,QQMAX/23/
C       DT( ) ARRAY *****
      DATA ACCEL/1/,VAVEL/2/,VDIS/3/,MHSET/4/,PACTE/5/,PACTR/6/,
     1 BULKE/7/,BULKR/8/,PINLET/9/,POUTLT/10/,VELACT/11/,ASTROKE/12/,
     2 PPOUT/13/,LOAD/14/,BULKO/15/,QMAX/16/,CIACT/17/,OPACT/18/
     3 ,QAREA1/19/
C       L( ) ARRAY
      DATA NVDIS/5/,NAST/6/,NPR/7/
C
C
      IF(IENTR) 1000,2000,3000
C
C *** 1000 SECTION
C
 1000 CONTINUE
      IF (INEL.NE.0) GO TO 1500
      DO 1001 I=1,24
 1001 DT(I)=0.0
      N=KTEMP(IND)
      IF(N.LT.11) N=N+10
      D(SPLOAD)=D(SPLOAD)/D(ARVAL)
      D(COEVL1)=D(COEVL1)*S2ORHO(N)
      D(PRPM)=D(PRPM)/60.
      D(COEVL2)=D(COEVL2)/(12.*RHO(N)*VISC(N))
      DT(BULKO)=D(VOLOUT)/(BULK(N)*DELT)
C     LOC=L(NAST)+25+L(NPR)+L(NAST)*L(NPR)
C     CALL INTERP(D(ISTR),D(25),D(LOC),10,L(NAST),QPUMP,IERR)
C     DT(QMAX)=QPUMP*D(PRPM)
C     DT(PPOUT)=DT(QMAX)*.25/D(COEPLK)
C     QPUMP=D(QOVBD)+(D(PRESS)-65.)*D(COEPLK)
      DT(QMAX)=D(QQMAX)
      DT(PPOUT)=D(PRESS)
      RETURN
C
C ***   STEADY STATE CALCULATION SECTION
C ***  IND=COMPONENT #,KNEL=CONNECTION #,INEL=LEG #
C ***  THE INLET IS A NODAL POINT IN THE SYSTEM
C
 1500 IF(KNEL-2)1510,1520,1530
```

```
 1510 DT(PINLET)=POLEG(INEL,11)
      IF(DT(PINLET).LT.30.)DT(PINLET)=30.
      GO TO 1600
C
C *** DETERMINE PUMP OUTLET PRESSURE
C
 1520 IF(INX.NE.1) GO TO 1700
C     QIN=POLEG(INEL,1)*POLEG(INEL,2)
C     SPOUT=DT(PPOUT)
C     IF(QIN.GT.DT(QMAX))QIN=DT(QMAX)
C     DT(PPOUT)=(DT(QMAX)-QIN)/D(COEPLK)
C     DT(PPOUT)=.5*(DT(PPOUT)+SPOUT)
      DT(PPOUT)=(DT(QMAX)-D(QDVBO))/D(COEPLK)
      POLEG(INEL,5)=POLEG(INEL,5)+DT(PPOUT)
      LCS(INEL,7)=5
      POLEG(INEL,11)=POLEG(INEL,11)+DT(PPOUT)
      DT(POUTLT)=POLEG(INEL,11)
      GO TO 1600
C
C *** INITIALIZE SERVOVALVE PRESSURES
C
 1530 CONTINUE
      IF(KNEL.EQ.3)RETURN
      LOC=L(NAST)+L(NPR)+25+L(NAST)*L(NPR)
      QPUMP=DT(QMAX)/D(PRPM)
C     CALL INTER2(QPUMP,D(LOC),D(25),10,L(NAST),DT(ASTROKE),IERR)
      XA(1)=D(ISTR)
      XA(2)=DT(POUTLT)
C
C *** CAM LOAD FUNCTION
C
      ILOC=L(NAST)+25+L(NPR)
      CALL LUCUP(NO,L(NAST),D(25),D(ILOC),XA(1),DT(LOAD),K,IF,NEXTR)
      IF(DT(LOAD).LT.0.0)DT(LOAD)=0.0
      DT(LOAD)=DT(LOAD)/2.
C
C *** ACTUATOR PRESSURES
C
      ITER=1
      DT(PACTE)=400.
      G1=D(COEVL2)/D(VOLAP)
      Q1=1.
      QQ1=1.
      QQ2=1.
 1540 CONTINUE
      DT(PACTR)=(DT(PACTE)*D(AEXT)-DT(LOAD))/D(ARET)
      DELTAP=DT(PACTR)-DT(PACTE)
      QLOSS=Q1*(D(ARET)/D(AEXT)-1.)
      DT(PACTE)=(G1*(DT(PINLET)+DT(POUTLT))+QLOSS-DELTAP*G1)/(2.*G1)
      Q1=(DT(POUTLT)-DT(PACTE))*G1
      Q2=(DT(PACTE)-DT(PINLET)+DELTAP)*G1
      IFAIL=0
      IF(ABS(Q1-QQ1)/(1.+Q1).GT.0.001)IFAIL=1
      IF(ABS(Q2-QQ2)/(1.+Q2).GT.0.001)IFAIL=1
      IF(IFAIL.EQ.0)GO TO 1600
      Q1=(QQ1+Q1)/2.
      Q2=(QQ2+Q2)/2.
      QQ1=Q1
      QQ2=Q2
      ITER=ITER+1
      IF(ITER.GT.25)GO TO 1590
      GO TO 1540
 1590 WRITE(6,950)ITER,DT(PACTE),DT(PACTR),Q1,Q2
  950 FORMAT(5X,I10,4E12.5)
 1600 RETURN
```

```
 1700 WRITE(6,1800) IND,KNEL,INEL
 1800 FORMAT(5X,46H CALL SEQUENCE ERROR DETECTED IN COMPONENT NO    ,
     1 I5,14H CONNECTION NO   ,I5,7H LEG NO   ,I5)
      WRITE(6,943)
  943 FORMAT(10X,33HPROGRAM STOP IN SUBROUTINE PUMP52)
      STOP 6052
C
C *** 2000 SECTION
C
 2000 CONTINUE
      DT(ASTROKE)=D(ISTR)
      DT(PPOUT)=DT(POUTLT)
      DT(VELACT)=0.0
      DT(VDIS)=0.0
      DT(ACCEL)=0.0
      DT(VAVEL)=0.0
      DT(MHSET)=P(L(3))-P(L(4))
      WRITE(6,9000)(DT(I),I=1,19)
 9000 FORMAT(5X,10E12.5)
      RETURN
C
C *** 3000 SECTION
C
 3000 CONTINUE
C
C     CALCULATE TRANSIENT RESPONSE OF PUMP
C
      L1=L(1)
      L2=L(2)
      L3=L(3)
      L4=L(4)
C     WRITE(6,900)P(L1),P(L2),P(L3),P(L4),Q(L1),Q(L2),Q(L3),Q(L4)
C    + ,C(L1),C(L2),C(L3),C(L4)
      FRIC=0.0
      ALST=DT(ACCEL)
      VLST=DT(VAVEL)
      XLST=DT(VDIS)
      AVELO=DT(VELACT)
      ASTRO=DT(ASTROKE)
      OPOUTLT=DT(POUTLT)
      ALOAD=DT(LOAD)
      LOC=L(NAST)+L(NPR)+25+L(NAST)*L(NPR)
C
C *** ACTUATOR COMPRESSIBILITY EFFECTS
C
      DT(BULKE)=(D(VOLE)-ASTRO*D(AEXT))/(BULK(KTEMP(IND))*DELT)
      DT(BULKR)=(D(VOLR)+ASTRO*D(ARET))/(BULK(KTEMP(IND))*DELT)
      OPACTE=DT(PACTE)+DT(VELACT)*D(AEXT)/DT(BULKE)
      OPACTR=DT(PACTR)-DT(VELACT)*D(ARET)/DT(BULKR)
      Q(L3)=-VLST*D(ARVAL)
      Q(L4)=-Q(L3)
      IF(Q(L3).EQ.0.0)Q(L4)=0.0
      P(L3)=C(L3)-Z(L3)*Q(L3)
      P(L4)=C(L4)-Z(L4)*Q(L4)
      DT(MHSET)=P(L3)-P(L4)
      PMH=D(SPLOAD)-(P(L3)-P(L4))
      IF(ABS(PMH).LT.2.0)PMH=0.0
      DT(ACCEL)=(PMH*D(ARVAL)-D(BVAL)*VLST-D(KSPG)*XLST)/D(MVAL)
      IF(ABS(DT(ACCEL)).LE.0.00001)DT(ACCEL)=0.0
      DT(VAVEL)=VLST+(DT(ACCEL)+ALST)*DELT/2.
      IF(ABS(DT(VAVEL)).LE.0.00001)DT(VAVEL)=0.0
      DT(VDIS)=XLST+(DT(VAVEL)+VLST)*DELT/2.
      CALL XLIMIT(DT(VDIS),DT(VAVEL),ASIGN,D(MIVDIS),D(MAVDIS))
      IF(DT(VAVEL).EQ.0.0)DT(ACCEL)=0.0
      IF(DT(VDIS).LE.D(VOLAP).AND.DT(VDIS).GE.-D(VOLAP))GO TO 3010
```

6.52-5 LISTING (CONTINUED)



```
C
C *** VALVE AREA FUNCTION
C
      ILOC=LOC+L(NAST)
      ILOC1=ILOC+L(NVDIS)
      AVDIS=ABS(DT(VDIS))
      CALL INTERP(AVDIS,D(ILOC),D(ILOC1),10,L(NVDIS),OAREA,IERR)
      COEV1=D(COEVL1)*OAREA
      DT(OAREA1)=COEV1
      IF(DT(VDIS).GT.D(VOLAP))GO TO 3020
C
C *** DECREASING FLOW - ACTUATOR RETRACTING(+ DIR)
C
      A=(1./COEV1)**2
      B=1./DT(BULKE)
      CON=OPACTE-DT(PINLET)
      IF(CON.LT.0.) CON=0.
C
  991 Q1=(-B+SQRT(B**2+4.*A*CON))/(2.*A)
      DT(OEACT)=2.*Q1
      Q1=-Q1
      B=1/DT(BULKR)
      CON=DT(POUTLT)-OPACTR
      IF(CON.LT.0.) CON=0.
C
  992 Q2=(-B+SQRT(B**2+4.*A*CON))/(2.*A)
      DT(QIACT)=2.*Q2
      GO TO 3030
C
C *** INCREASING FLOW - ACTUATOR EXTENDING(- DIR)
C
 3020 CONTINUE
      A=(1./COEV1)**2
      B=1./DT(BULKE)
      CON=DT(POUTLT)-OPACTE
      IF(CON.LT.0.) CON=0.
C
  993 Q1=(-B+SQRT(B**2+4.*A*CON))/(2.*A)
      DT(QIACT)=2.*Q1
      B=1./DT(BULKR)
      CON=OPACTR-DT(PINLET)
      IF(CON.LT.0.) CON=0.
C
  994 Q2=(-B+SQRT(B**2+4.*A*CON))/(2.*A)
      DT(OOACT)=2.*Q2
      Q2=-Q2
      GO TO 3030
C
C *** COMPUTE VALVE LEAKAGE FLOWS
C
 3010 CONTINUE
      DT(QIACT)=0.0
      DT(OOACT)=0.0
      Q1=0.0
      Q2=0.0
 3030 CONTINUE
      G1=DT(BULKE)/D(AEXT)
      G2=DT(BULKR)/D(ARET)
      ZN=D(DAMP)+D(AEXT)/G1+D(ARET)/G2
      DELTP=Q2/G2+OPACTR*D(ARET)-Q1/G1-OPACTE*D(AEXT)
      FDRIVE=DELTP+SLOAD
      DT(VELACT)=FDRIVE/ZN
C     CALL CFRIC(FDRIVE,FF,DT(VELACT),AVELO,XDD,XDDS,FRIC,1.,1.)
      IF(ABS(DT(VELACT)).LT.0.01)DT(VELACT)=0.0
C
C *** ACTUATOR PISTON POSITION
C
      DT(ASTROKE)=DT(ASTROKE)+(AVELO+DT(VELACT))*DELT/2.
      CALL XLIMIT(DT(ASTROKE),DT(VELACT),ASIGN,0.0,D(MSTROKE))
```

```
      DT(PACTE)=DT(PACTE)+(Q1+AVELO*D(AEXT))/DT(BULKE)
      DT(PACTR)=DT(PACTR)+(Q2-AVELO*D(ARET))/DT(BULKR)
C
C *** PUMP FLOW
C
      CALL INTERP(DT(ASTROKE),D(25),D(LOC),10,L(NAST),QPUMP,IERR)
      DT(QMAX)=D(PRPM)*QPUMP
      DT(ASTROKE)=2.*DT(ASTROKE)-ASTRO
C
C *** PUMP INLET PRESSURE
C
      DT(PINLET)=(C(L1)/Z(L1)+DT(PPOUT)*D(COEPLK)+DT(QIACT)
     + -DT(QMAX))/(1./Z(L1)+D(COEPLK))
C
C *** PUMP OUTLET PRESSURE
C
      QOUT=-(DT(QMAX)-D(COEPLK)*(DT(PPOUT)-DT(PINLET))-DT(QIACT)
     + -DT(BULKO)*(DT(PPOUT)-OPOUTLT))
      DT(POUTLT)=C(L2)-QOUT*Z(L2)
      DT(PPOUT)=(DT(POUTLT)+OPOUTLT)/2.
C
C *** CAM LOAD FUNCTION
C
      XA(1)=DT(ASTROKE)
      XA(2)=DT(POUTLT)
      ILOC=L(NAST)+25+L(NPR)
      CALL LUCUP(ND,L(NAST),D(25),D(ILOC),XA(1),DT(LOAD),K,IE,NEXTR)
      IF(DT(LOAD).LT.0.0)DT(LOAD)=0.0
      DT(LOAD)=DT(LOAD)/2.
C
C *** DEFINE PUMP EXTERNAL PARAMETERS
C
      P(L1)=DT(PINLET)
      Q(L1)=(C(L1)-P(L1))/Z(L1)
      P(L2)=DT(POUTLT)
      Q(L2)=QOUT
C     IF(T.LT.0.05)WRITE(6,9000)(DT(I),I=1,19)
C     WRITE(6,900)C(L1),C(L2),C(L3),C(L4),Q1,Q2,QPUMP,P(L1),P(L2)
C    + ,P(L3),P(L4),Q(L1),Q(L2),Q(L3),Q(L4)
  900 FORMAT(5X,10E12.5)
      RETURN
      END
```

## APPENDIX F

## HYDRAULIC MOTOR MODELS

## HSFR USER MANUAL (AFAPL-TR-76-43, VOL. III)

### 2.3.11 MOTOR (Piston, Constant Displacement)

The motor is identified as an NTYPE "9" element, with a KTYPE designator of "25". The motor model should always be the first element in the system.

The piston motor model is based on the axial piston pump model and it requires similar input data. Three data cards are required in the sequence described in the following pages. Figures 2-8 and 2-9 should be referred to for the physical description data. Physical data for a given motor is read into the element data list in the same manner as for the other system elements. Motor outlet pressure is input on the second general control data record (para. 2.2). Motor inlet pressure is input on the second motor data record.

CARD NUMBER 1

| COLUMN | FORMAT | DATA | DIMENSIONS |
|---|---|---|---|
| 1-5 | I5 | NTYPE = 9 | -- |
| 6-10 | I5 | KTYPE = 25 Hydraulic Motor | -- |
| 11-20 | E10.0 | R1 = Cylinder Slot Radius | IN |
| 21-30 | E10.0 | SLOTW = Cylinder Slot Width | IN |
| 31-40 | E10.0 | RV = Cylinder and Valve Plate Slot Centerline Radius | IN |
| 41-50 | E10.0 | RBORC = Cylinder Centerline Radius | IN |
| 51-60 | E10.0 | DIAPIS = Piston Diameter | IN |
| 61-70 | E10.0 | POVOL = Oil Volume Between Piston at Mid-stroke and Port Face | IN**3 |
| 71-80 | E10.0 | R2 = Valve Plate Outlet Slot Radius | IN |

EXAMPLE CARD

CARD NUMBER 2

| COLUMN | FORMAT | DATA | DIMENSIONS |
|---|---|---|---|
| 1-10 | E10.0 | R4 = Valve Plate Inlet Slot Radius | IN |
| 11-20 | E10.0 | SWASH = SWASH Angle | DEG |
| 21-30 | E10.0 | TLEAK = Motor Internal Leakage to Case at Steady State Pressure | CIS |
| 31-40 | E10.0 | THPRS = Valve Plate Outlet Slot Start Angle | DEG |
| 41-50 | E10.0 | THPRE = Valve Plate Outlet Slot End Angle | DEG |
| 51-60 | E10.0 | THSUCS = Valve Plate Inlet Slot Start Angle | DEG |
| 61-70 | E10.0 | THSUCE = Valve Plate Inlet Slot End Angle | DEG |
| 71-80 | E10.0 | LPRESS = Motor Inlet Steady State Pressure | PSIG |

EXAMPLE CARD

CARD NUMBER 3

| COLUMN | FORMAT | DATA | DIMENSIONS |
|---|---|---|---|
| 1-10 | E10.0 | CPRESS = Steady State Case Pressure | PSI |
| 11-20 | E10.0 | CSPRESS = Case to outlet Pressure Difference at Zero Case Drain Flow | PSI |
| 21-30 | E10.0 | | |
| 31-40 | E10.0 | | |
| 41-50 | E10.0 | | |
| 51-60 | E10.0 | | |
| 61-70 | E10.0 | | |
| 71-80 | E10.0 | | |

EXAMPLE CARD

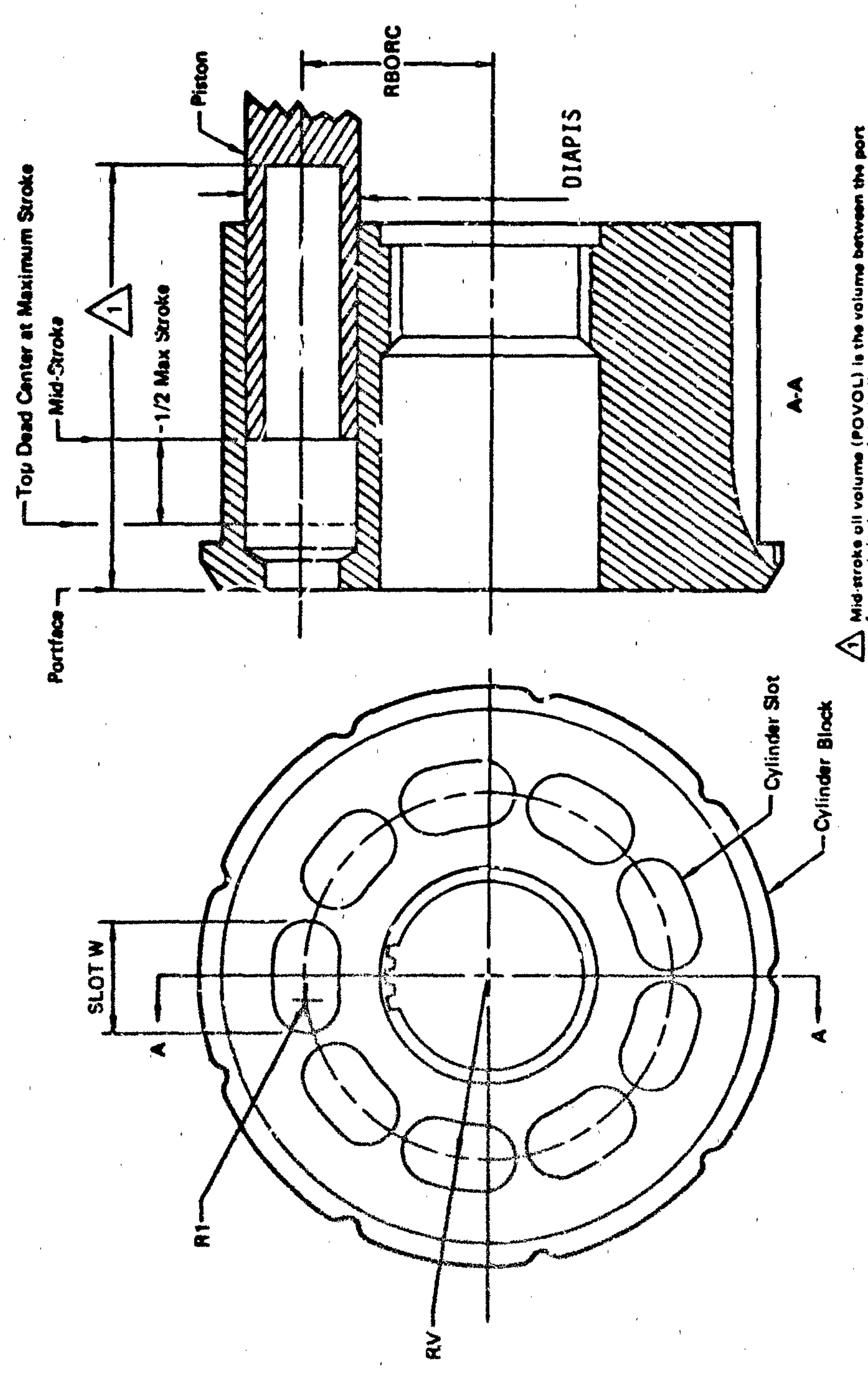


FIGURE 2-8

MOTOR CYLINDER BLOCK PARAMETERS

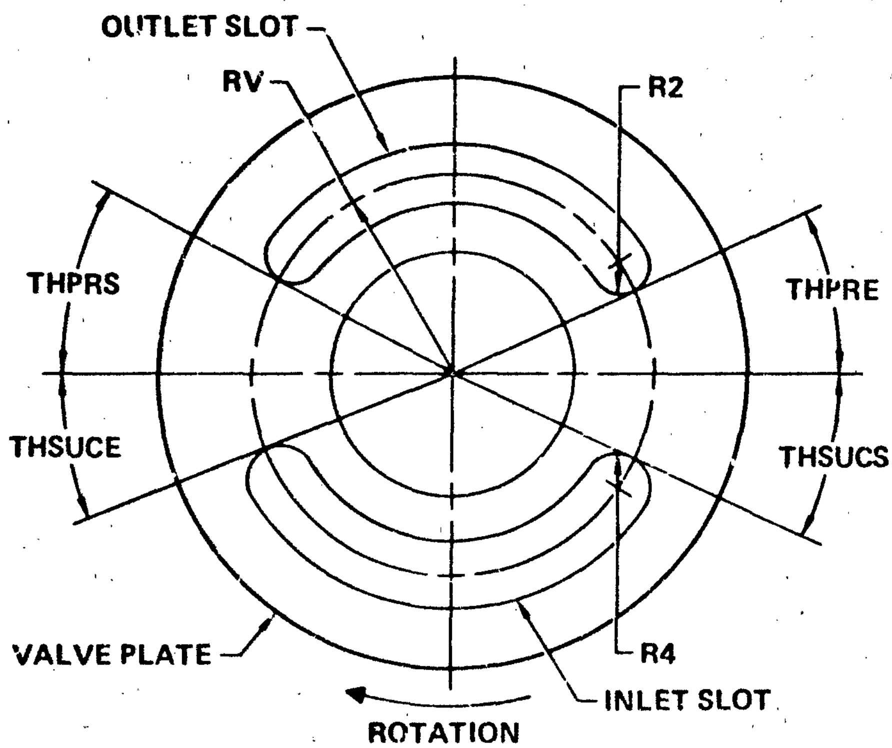


FIGURE 2-9
MOTOR VALVE PLATE PARAMETERS

## 4.16 MOTOR SUBROUTINE

### 4.16.1 Introduction and Flow Diagram

SUBROUTINE MOTOR is a general, detailed model of a rotating, axial, nine piston, constant displacement hydraulic motor. The model computes dynamic inlet and outlet pressures and flows. The main program calculates the harmonic load impedances of the rest of the circuit, and this provides the linear phase and gain relationship between the harmonic flows into and from the loads and the corresponding pressures across the loads in the frequency domain. A pressure and flow balance is performed in the time domain between the motor and system. A check of the balance is performed in the frequency domain.

The motor model considers valving areas, precompression, decompression, fluid bulk modulus, and piston motion. Piston pressure at the beginning of precompression is assumed constant and equal to the input steady state inlet pressure. Piston pressure is then calculated continuously for the full motor revolution.

Figure 4-9 is a general flow chart of the MOTOR subroutine. The specification section includes initialization of variables from input data and the calculation of several constants. At the start RPM the motor indexing variables are calculated for the plate porting and the valve port areas are computed for a full 360° revolution. In Section 2, the precompression pressures are computed followed by the calculation of motor outlet flow. A Fourier analysis is performed to calculate harmonic flows up through the harmonic of interest. Harmonic pressure and flow are then balanced dynamically by reconstructing the time dependent outlet pressure and recomputing flow from Section 3.

For the inlet side, piston decompression and inlet flow are calculated. A Fourier analysis of inlet flow is performed, followed by dynamic balancing of inlet flow with the supply system load. Inlet and outlet flow and pressure for the harmonic of interest are returned to the main program.

The MOTOR subroutine is divided into eleven sections. Each section is discussed and a listing of that section is presented individually in subsequent paragraphs.

4.16.1.1 Variable Names - The variable names used in the MOTOR subroutine are the same and have the identical meaning as those used in the PUMP subroutine. Some of the PUMP variables have been deleted. The variables are discussed in the PUMP subroutine paragraph 4.1.6.

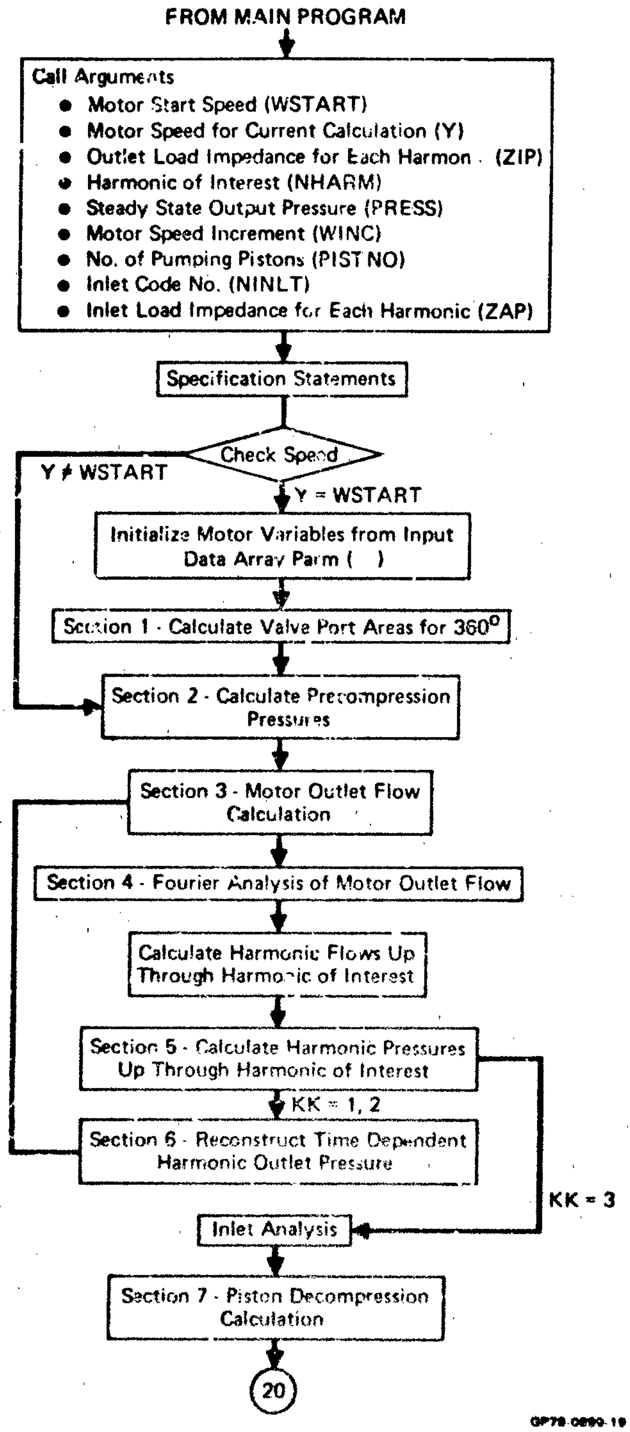


FIGURE 4-9
**HSFR COMPUTER PROGRAM**
Motor Subroutine Flow Chart

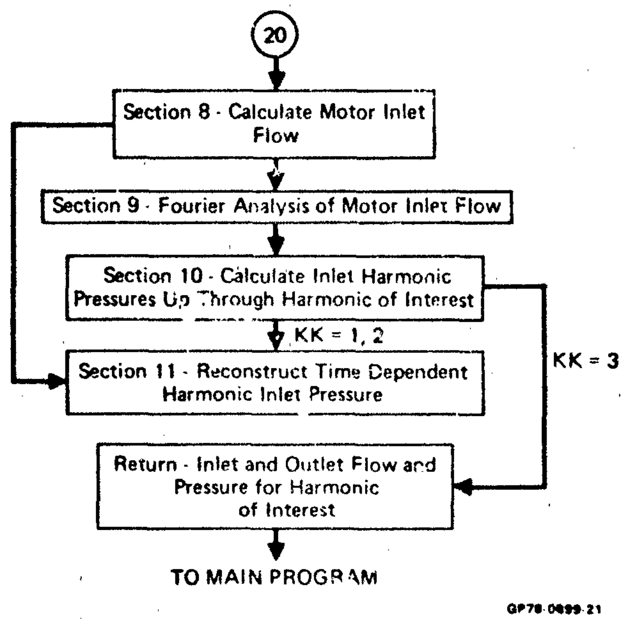


**FIGURE 4-9 (Continued)**
**HSFR COMPUTER PROGRAM**
Motor Subroutine Flow Chart

### 4.16.1.2 Specifications and Initialization - Listing

```
      SUBROUTINE MOTOR (WSTART,Y,ZIP,NHARM,PRESS,WINC,PISTNO,
     +NINLT,ZAP)
C
C
C         *VARIABLE TYPES, DIMENSIONS, COMMONALITY*
C
      REAL LPRESS,LVOL,LEAK,LK1,LK2,LK3,LK4,LK5,LK6,LK7,LK8
      REAL LPRESP,LPRESO
      COMPLEX BETA,G,P,Q,Z,ZV2,ZV
      COMPLEX QC,ZO,ZIP,P3,ZAP
      COMPLEX FQ1,PQ1,ZEQ,PQ1I,FQ1I
      COMMON BETA,G,P,Q,Z, XBE,BER,BEI,BERP,BEIP,RHO,BULK,VOL,W,VISC,PAR
     1M,PI, IEL,NEL,KTYPE(40)
      DIMENSION G(2,2,40),PARM(8,40),P(40),Q(40),Z(40)
      DIMENSION QQT(81),PPT(81),QQFC(11),QQFS(11),PPM(11) ,PPP(11)
      DIMENSION PP(6),CQ(6),PTP(81)
      DIMENSION ZIP(10),ZAP(10)
      DIMENSION XL(6),VAREA(1400)
      DIMENSION FQ1(10,3),PQ1(10,3),ZEQ(10),ETA(10)
      DIMENSION PISPR(1400),QQI(81),PPI(81)
      DIMENSION QIFC(11),QIFS(11),FQ1I(10,3),PQ1I(10,3)
      DATA VAREA/1400*0.0/,PISPR/1400*0.0/
C
C                         *SOLUTION METHOD*
C
C *INITIALIZE VARIABLES FROM INPUT DATA OR MAIN PROGRAM*
C
      IF(Y.NE.WSTART) GO TO 140
      R1=PARM(1,1)
      SLOTW=PARM(2,1)
      RV=PARM(3,1)
      PBORC=PARM(4,1)
      DIAPIS=PARM(5,1)
      POVOL=PARM(6,1)
      R2=PARM(7,1)
      P4=PARM(1,NEL+1)
      SWASH=PARM(2,NEL+1)
      TLEAK=PARM(3,NEL+1)
      THPRS=PARM(4,NEL+1)
      THPRE=PARM(5,NEL+1)
      THSUCS=PARM(6,NEL+1)
      THSUCE=PARM(7,NEL+1)
      LPRESS=PARM(8,NEL+1)
      CPRESS=PARM(1,NEL+2)
      CSPRES=PARM(2,NEL+2)
      ASWASH=SWASH/57.3
      NOPIST=PISTNO
      SLTHAG=(ASIN(SLOTW/(2.*RV)))*57.3
      NAPP=(180.+2.*SLTHAG-THPRS-THPRE)/360.*PISTNO+1.
      NAPS=(180.+2.*SLTHAG-THSUCS-THSUCE)/360.*PISTNO+1.
```

### 4.16.2 Section 1 - Valve Area Calculation

Figures 4-10 and 4-11 illustrate the modeling parameters for a typical aircraft rotating piston hydraulic motor, including those required for area calculations.

Section 1 of the motor model is identical to Section 1 of the pump model. Consult paragraph 4.2 for a description of this section.

#### 4.16.2.1 Section 1 - Listing

```
C
C       SECTION 1 VALVE AREA CALCULATION FOR FULL 360 DEGREES REVOLUTION
C
C
C
C       COMPUTE VALVING INDEX POSITIONS FOR EIGHTY FLOW INCREMENTS
C
        AINC=4.5/PISTNO
        NPRSOP=(THPRS-SLTHAG)/AINC+1.
        NPROP=(THPRS+SLTHAG)/AINC+1.
        NPRSCL=(180.-THPRE-SLTHAG)/AINC+1.
        NPRCL=(180.-THPR +SLTHAG)/AINC+1.
        NSUSOP=(180.+THSUCS-SLTHAG)/AINC+1.
        NSUOP=(180.+THSUCS+SLTHAG)/AINC+1.
        NSUSCL=(360.-THSUCE-SLTHAG)/AINC+1.
        NSUCL=(360.-THSUCE+SLTHAG)/AINC
        DO 400 NDEG=1,NPRSOP
        VAREA(NDEG)=0.0
  400   CONTINUE
        R3=R1
        IF(R1.GT.R2) R3=R2
        ND1=NPRSOP+1
        ND2=NPROP-1
        DO 500 NDEG=ND1,ND2
        ANG=(NDEG-NPRSOP)*AINC/57.3
        RVX =ANG * RV
        IF(RVX.GT.SLOTW) RVX=SLOTW
        RO=R1+R2 -RVX
        IF(RO.LE.0.01) GO TO 410
        ALPHA=(RO**2-R1**2+R2**2)/(2.0*RO*R2)
        ABETA=(RO**2+R1**2-R2**2)/(2.0*RO*R1)
        IF(ALPHA.GT..9999.OR.ABETA.GT..9999) GO TO 420
        ABETA =ACOS (ABETA)
C360    ABETA=ARCOS(ABETA)
        ALPHA=ACOS (ALPHA)
C360    ALPHA=ARCOS(ALPHA)
        AVAREA=R1*R1*(ABETA-SIN(ABETA)*COS(ABETA))
        VAREA(NDEG)=R2*R2*(ALPHA-SIN(ALPHA)*COS(ALPHA))+AVAREA
        GO TO 500
  410   CONTINUE
        VAREA(NDEG)= 0.5*PI*(R1*R1+R2*R2)-2.0*RO*R3
        GO TO 500
  420   VAREA(NDEG)=0.0
  500   CONTINUE
        DO 550 NDEG=NPROP,NPRSCL
        VAREA(NDEG)=PI*(R3**2)+(SLOTW-2.*R3)*2.*R3
  550   CONTINUE
        ND3=NPRSCL+1
        ND4=NPRCL-1
        I=1
        DO 600 NDEG=ND3,ND4
        VAREA(NDEG)=VAREA(NPROP-I)
        I=I+1
  600   CONTINUE
```

```
      DO 650 NDEG=NPRCL,NSUSOP
      VAREA(NDEG)=0.0
  650 CONTINUE
      IF(R1.GT.R4) R3=R4
      ND5=NSUSOP+1
      ND6=NSUOP-1
      DO 700 NDEG=ND5,ND6
      ANG=(NDEG-NSUSOP)*AINC/57.3
      RVX=ANG*RV
      IF(RVX.GT.SLOTW) RVX=SLOTW
      RO=R1+R2-RVX
      IF(RO.LE.0.01) GO TO 660
      ALPHA=(RO**2-R1**2+R2**2)/(2.0*RO*R2)
      ABETA=(RO**2+R1**2-R2**2)/(2.0*RO*R1)
      IF(ALPHA.GT..9999.OR.ABETA.GT..9999) GO TO 670
      ABETA=ACOS(ABETA)
C360  ABETA=ARCOS(ABETA)
      ALPHA=ACOS(ALPHA)
C360  ALPHA=ARCOS(ALPHA)
      AVAREA= R1*R1*(ABETA-SIN(ABETA)*COS(ABETA))
      VAREA(NDEG)= R2*R2*(ALPHA-SIN(ALPHA)*COS(ALPHA))+AVAREA
      GO TO 700
  660 CONTINUE
      VAREA(NDEG)=0.5*PI*(R1*R1+R2*R2)-2.0*RO*R3
      GO TO 700
  670 VAREA(NDEG)=0.0
  700 CONTINUE
      DO 750 NDEG=NSUOP,NSUSCL
      VAREA(NDEG)=PI*(R3**2)+(SLOTW-2.*R3)*2.*R3
  750 CONTINUE
      ND7=NSUSCL+1
      ND8=NSUCL-1
      I=1
      DO 800 NDEG=ND7,ND8
      VAREA(NDEG)=VAREA(NSUOP-I)
      I=I+1
  800 CONTINUE
      ND9=360./AINC
      DO 850 NDEG=NSUCL,ND9
      VAREA(NDEG)=0.0
  850 CONTINUE
      WRITE(6,840) NPRSOP,NPROP,NPRSCL,NPRCL,NSUSOP,NSUOP,NSUSCL,NSUCL
  840 FORMAT(8(5X,I5))
      NJ=ND9/6
      DO 860 J=1,NJ
      N2=J+NJ
      N3=J+2*NJ
      N4=J+3*NJ
      N5=J+4*NJ
      N6=J+5*NJ
      WRITE(6,855)VAREA(J),J,VAREA(N2),N2,VAREA(N3),N3
     1,VAREA(N4),N4,VAREA(N5),N5,VAREA(N6),N6
  855 FORMAT(5X,6(F10.4,7X,I3))
  860 CONTINUE
      HPRESS=PRESS
```

THIS PAGE IS BEST QUALITY PRACTICABLE
FROM COPY FURNISHED TO DDC

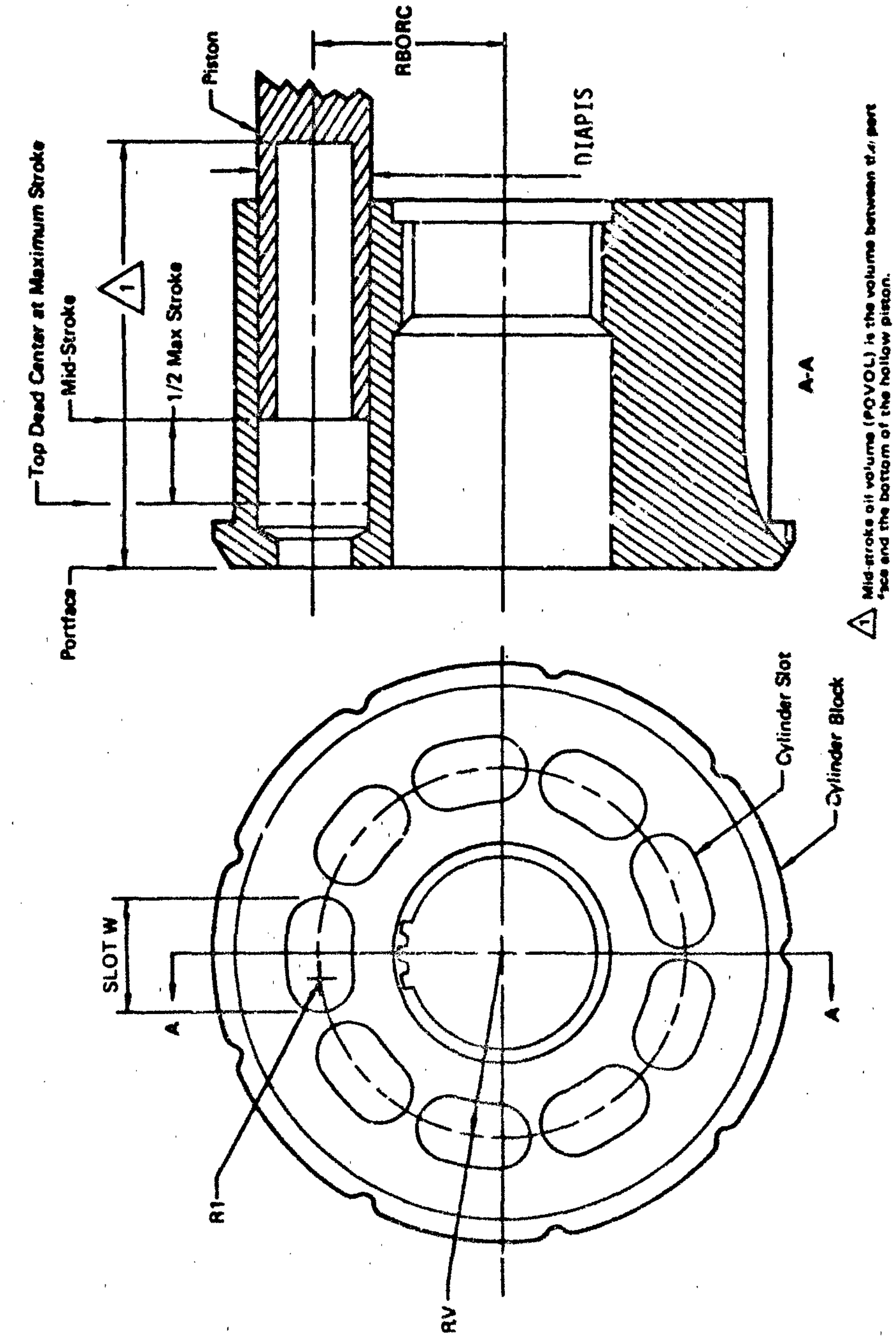


FIGURE 4-10
MOTOR CYLINDER BLOCK PARAMETERS

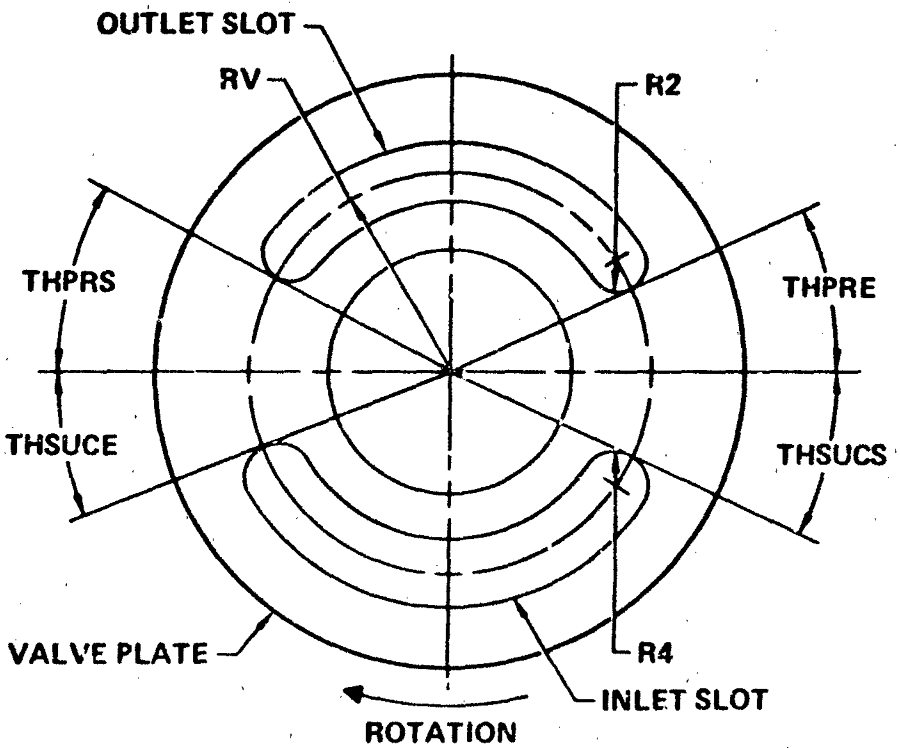


FIGURE 4-11

MOTOR VALVE PLATE PARAMETERS

## 4.16.3 Section 2 - Calculation of Piston Precompression Pressure

Section 2 calculates the cylinder pressure which exists just before the cylinder slot starts to open to the valve plate outlet (pressure) slot. This pressure is the result of piston motion during that portion of cylinder block rotation when the cylinder slot is blocked by the valve plate, between the inlet and outlet slots.

### 4.16.3.1 Math Model

Piston motion is sinusodial and due to the fixed swash (SWASH) angle of the hanger. A pressure dependent factor for leakage from each cylinder to case is estimated for cylinder pressure above the input case pressure as

PLEAK = TLEAK/(PRESS*NAPP)

Leakage from the case to each cylinder for cylinder pressures below case pressure is estimated from

SLEAK = -(TLEAK/NAPS/SQRT(CSPRESS))

Cavitation volume in the cylinder, if any, is calculated and tracked throughout the cylinder block revolution. Piston pressures are stored for each position throughout the 360° calculation. Time dependent oscillatory outlet pressure is initialized to zero PSI.

4.16.3.2 Assumptions - For the first calculation rpm, the piston is assumed to be completely filled on the inlet stroke and the initial cylinder pressure is assumed to be the input steady state value. The remainder of the simulation uses the initial cylinder pressure of the last speed calculation. Pressure dependent leakage, and sinusoidal piston motion are assumed. Bulk modulus is recalculated at each step based on the last step cylinder pressure, and the bulk modulus formula used in FLUID.

4.16.3.3 Computation Method - The calculation is performed in 1/2 degree increments (DANG) with the initial cylinder slot centerline angle (THETA) computed from the inlet slot end angle (THSUCE) and the cylinder slot half-angle (SLTHAG). The number of calculation steps (NSTEPP) is computed based on index positions defining the end of the inlet slot and the beginning of the outlet slot in the valve plate.

### 4.16.3.4 Section 2 - Listing

```
C
C     SECTION 2- PISTON PRECOMPRESSION CALCULATION
C
      PIA=DIAPIS**2*PI/4.0
      PISPR(NSUCL)=LPRESS
      CAVOL=0.0C
      SAM=RBORC*TAN(SWASH/57.3)
      QMAX=0.3*SAM*PIA
      ORF=2.0/RHO
      ORF=.65*SQRT(ORF)
  140 CONTINUE
      SFLOW=QMAX*Y
  179 NSTEPP=ND1+ND9-ND8-2
      DPRESP=C.0
      LPRESP=PISPR(NSUCL)
      THETA=(SLTHAG-THSUCE)/57.3
      PLEAK=TLEAK/(PRESS*NAPP)
      SLEAK=-(TLEAK/NAPS/SQRT(CSPRES))
      DANG=AINC/57.3
      DT=AINC/(Y*6.)
      SA=RBORC*TAN(ASWASH)
      XLAST=-SA*COS(THETA)
      WRITE(6,925) CAVOL,NSUCL,LPRESP,XLAST,THETA
      DO 160 I=1,NSTEPP
      IF(LPRESP.LT.CPRESS) GO TO 162
      DLEAK=(LPRESP+DPRESP/2.-CPRESS)*PLEAK*DT
      GO TO 164
  162 DLEAK=SQRT(CPRESS-LPRESP)*SLEAK*DT
  164 BULKP=BULK+12.*(LPRESP-PRESS)
      THETA=THETA +DANG
      XNEW=-SA*COS(THETA)
      DX= XNEW -XLAST
      DVOL=DX*PIA
      LVOL=PDVOL-XNEW*PIA
      DPRESP=(DVOL-DLEAK-CAVOL)/LVOL*BULKP
      XLAST=XNEW
      LPRESP=LPRESP+DPRESP
      NP=NSUCL+I
      IF(NP.GE.ND9+1) NP=NP-ND9
      IF(LPRESP.GT.C.01) GO TO 166
      CAVOL=CAVOL-DVOL+DLEAK
      LPRESP=0.01
      DPRESP=0.0
      GO TO 169
  166 CAVOL=C.0
  169 PISPR(NP)=LPRESP
      IF(Y.EQ.50.) GO TO 161
      IF(Y.EQ.1000.) GO TO 161
      IF(Y.EQ.3000.) GO TO 161
      GO TO 160
  161 WRITE(6,930) CAVOL,NP,LPRESP,
     +XLAST,DX,LVOL,DLEAK,BULKP,THETA
  160 CONTINUE
      CAVOLD=CAVOL
      XOLD=XLAST
      THEOLD=THETA
      DO 150 N=1,81
  150 PPT(N)=0.0
      KKN = 1
      KK = 1
  170 CONTINUE
```

### 4.16.4 Section 3 - Motor Outlet Flow Calculation

The calculation of motor outlet flow is identical to that described in Section 4 of the pump model, paragraph 4.5. The initial calculation is based on the input steady state outlet pressure.

### 4.16.4.1 Section 3 - Listing

```
C
C     SECTIPN 3- MOTPP PUTLET FLPW CALCULATION
C
      CAVPL=CAVPLD
      XLAST=XPLD
      THETA=THEPLD
      DO 18C N=1,81
  180 QQT(N)=0.C
      WRITE(6,925) CAVPL,NP,LPRESP,XLAST,THETA
      DO 200 M=1,NAPP
      DO 190 N=1,80
      NKM=NPRSCP+N+(M-1)*80
      IF(NKM.GE.NPRCL+1) GO TO 190
      THETA=THETA+DANG
      XNEW=-SA*COS(THETA)
      DX=XNEW-XLAST
      VA=POVPL-XNEW*PIA
      XLAST=XNEW
      IF(CAVPL.GT.0.00) GO TO 187
      BULKP=BULK+12.*(PISPR(NKM-1)-PRESS)
      IF(PISPR(NKM-1).GE.CPRESS) GO TO 186
      LEAK=SLEAK
      LK1=1.+SQRT(BULKP)*LEAK*DT/VA
      GO TO 185
  186 LEAK=PLEAK
      LK1=1.+BULKP*LEAK*DT/VA
  185 LK2=(PISPR(NKM-1)+BULKP/VA*DX*PIA)/LK1
      LK3=BULKP*DT/VA/LK1
      LK4= (ORF*VAREA(NKM))**2
      LK5 =LK3*LK4 *0.5
      LK6 = LK4 *(LK2 -HPRESS-PPT(N))
      LK7 =LK5*LK5 +ABS(LK6)
      LK8 = -LK5 +SQRT(LK7)
      QOUT= SIGN(LK8,LK6)
      PISPR(NKM)=LK2-QOUT*LK3
      IF(PISPR(NKM).GT..01) GO TO 188
  187 CONTINUE
      LEAK=SLEAK
      QOUT=-(0.65*VAREA(NKM)*SQRT(2.*(HPRESS+PPT(N))/RHO))
      PISPR(NKM)=.01
      CAVPL=CAVPL-DX*PIA+SLEAK*DT*CPRESS+QOUT*DT
      IF(CAVOL.LE.0.00) CAVPL=0.00
  188 QQT(N)=QOUT+QQT(N)
      IF(Y.NE.5000.) GO TO 190
      WRITE(6,930) CAVPL,NKM,PISPR(NKM),XLAST,DX,VA,
     +LEAK,BULKP,THETA,QQT(N)
  190 CONTINUE
  200 CONTINUE
      QQT(81)=QQT(1)
```

4.16.5 Section 4 - Fourier Analysis of Motor Outlet Flow

The motor outlet flow is mathematically analyzed as described in Section 5 of the hydraulic pump model, paragraph 4.6. The steady state balancing in the pump model is not done for the motor.

4.16.5.1 Section 4 - Listing

```
C
C     SECTION 4- FOURIER ANALYSIS OF MOTOR OUTLET FLOW
C
      COEF=.02469
      C1=.07753
      S1 =SIN(C1)
      C1 =COS(C1)
      S =0.0
      C =1.0
      FNTZ=QOT(1)
      J =1
  210 U2=0.0
      U1=0.0
      I= 81
C       FORM FOURIER COEFFICIENTS RECURSIVELY
  220 U0=QOT(I)+2.0*C*U1-U2
      U2=U1
      U1=U0
      I=I-1
      IF(I-1) 230,230,220
  230 QOFC(J)=COEF*(FNTZ+C*U1-U2)
      QOFS(J)=COEF*S*U1
      IF(J-NHARM-1) 240,250,250
  240 U3=C1*C-S1*S
      S =C1*S+S1*C
      C =U3
      J = J+1
      GO TO 210
  250 QOFC(1)=QOFC(1)*0.5
      IF(QOFC(1).LE.0.01) QOFC(1)=0.01
C
C      COMPUTE HARMONIC FLOWS FROM FOURIER ANALYSIS
C
  255 DO 260 I=1,NHARM
      FO1(I,KK) = CMPLX(QOFS(I+1), QOFC(I+1))
  260 CONTINUE
```

### 4.16.6 Section 5 - Outlet Pressure - Flow Balance Calculation

The motor outlet flow is dynamically balanced as described for the pump outlet flow in Section 6 of the pump model, paragraph 4.7.

#### 4.16.6.1 Section 5 - Listing

```
C
C     SECTION 5- OUTLET PRESSURE-FLOW BALANCE CALCULATION
C
  270 CONTINUE
      I = KKN
      IF (KK - 2) 280,290,300
  280 CONTINUE
      W=Y*PISTNO*PI*KKN/30.
      ZO=1.0E5/W*(.2,-1.)
      PQ1(I,KK) = FQ1(I,KK )*ZO*ZIP(I)/(ZO +ZIP(I)) / 5.0
      P6=CABS(PQ1(I,KK))*5.0
      IF(Y.NE.5000.) GO TO 281
      WRITE(6,1682) P6,QQFC(1)
  281 P3=PQ1(I,KK)
      JK=0
      TO= -45
      MNO= 10
      PPM(I) = CABS(PQ1(I,KK))
      GO TO 320
  290 CONTINUE
      ZO = PQ1(I,KK-1) /(FQ1(I,KK-1)-FQ1(I,KK))
      PQ1(I,KK) = FQ1(I,KK-1)*ZO*ZIP(I)/(ZO +ZIP(I))
      P6=CABS(PQ1(I,KK))
      IF(Y.NE.5000.) GO TO 291
      WRITE(6,1682) P6,QQFC(1)
  291 P3=PQ1(I,KK)-PQ1(I,KK-1)
      PQ1(I,KK+1) = PQ1(I,KK) - PQ1(I,KK-1)
      PPP(I) = ATAN2(AIMAG(PQ1(I,KK+1)),REAL(PQ1(I,KK+1)))
      PPM(I) = CABS(PQ1(I,KK+1))
      GO TO 320
  300 CONTINUE
      J=KKN
      PQ1(J,KK) = ZIP(J) * FQ1(J,KK)
      P6=CABS(PQ1(I,KK))
      IF(Y.NE.5000.) GO TO 301
      WRITE(6,1682) P6,QQFC(1)
  301 CONTINUE
      ETA(J) = CABS(100 * (PQ1(J,KK) - PQ1(J,KK-1)) / PQ1(J,KK))
      KKN = KKN + 1
      IF(KKN.GT.NHARM) GO TO 335
      KK = 1
      FQ1(KKN,1) = FQ1(KKN,3)
      GO TO 270
  320 CONTINUE
```

### 4.16.7 Section 6 - Reconstruction of Time Dependent Outlet Pressure

Motor outlet dynamic pressures are reconstructed as described for the pump outlet pressure in Section 7, paragraph 4.8. Balanced outlet flow (Q(1)) and pressure (P(1)) are stored and control is passed to the piston decompression section.

#### 4.16.7.1 Section 6 - Listing

```
C
C     SECTION 6- RECONSTRUCTION OF TIME DEPENDENT OUTLET PRESSURE
C
      DO 330 J=1,81
      THETA= (J-1)*I*0.07854
      PPT(J) =PPT(J) + REAL(P3)* SIN(THETA) +AIMAG(P3)* COS(THETA)
      IF (PPT(J).LT.-HPRESS) PPT(J)=-HPRESS
  330 CONTINUE
      KK = KK + 1
      GO TO 170
  335 CONTINUE
      ASWAST=ASWASH*57.3
      WRITE(6,900) ASWAST,SWASH,HPRESS,PRESS,QOFC(1),
     +SFLOW,TLEAK,Y
  900 FORMAT(/,7(F10.4,3X),F10.0,/)
      Q(1)=FQ1(NHARM,3)
      P(1)=PQ1(NHARM,3)
```

### 4.16.8 Section 7 - Piston Decompression Calculation

The calculation of piston pressure during decompression is identical to the precompression calculation described in Section 4.16.3. Index numbers for the decompression portion of the block revolution are used. Cylinder cavitation volume is tracked continuously. Piston pressure is limited to .01 psi if the cylinder cavitates.

#### 4.16.8.1 Section 7 - Listing

```
C
C     SECTION 7- PISTON DECOMPRESSION CALCULATION
C
      LPRESD=PISPR(NPRCL)
      NSTEPD=NSUSOP-NPRCL
      DPRESD=0.0
      WRITE(6,925) CAVOL,NPRCL,LPRESD,XLAST,THETA
      DO 1000 I=1,NSTEPD
      IF(LPRESD.LT.CPRESS) GO TO 360
      DLEAK=(LPRESD+DPRESD/2.-CPRESS)*PLEAK*DT
      GO TO 365
  360 DLEAK=SQRT(CPRESS-LPRESD)*SLEAK*DT
  365 BULKP=BULK+12.*(LPRESD-PRESS)
      THETA=THETA +DANG
      XNEW=-SA*COS(THETA)
      DX= XNEW -XLAST
      DVOL = DX * PIA
      LVOL= POVOL-XNEW *PIA
      DPRESD=(DVOL-DLEAK-CAVOL)/LVOL*BULKP
      XLAST=XNEW
      LPRESD=LPRESD+DPRESD
      NP=NPRCL+I
      IF(LPRESD.GT.0.01) GO TO 918
      CAVOL=CAVOL-DVOL+DLEAK
      LPRESD=0.01
      DPRESD=0.0
      GO TO 920
  918 CAVOL=0.0
  920 PISPR(NP)=LPRESD
      IF(Y.EQ.50.) GO TO 922
      IF(Y.EQ.1000.) GO TO 922
      IF(Y.EQ.5000.) GO TO 922
      GO TO 1000
  922 WRITE(6,930) CAVOL,NP,LPRESD,
     +XLAST,DX,LVOL,DLEAK,BULKP,THETA
  930 FORMAT(F10.7,5X,I3,5X,F8.2,2X,4(F10.6,2X),F10.0,5X,2(F10.3,5X))
  925 FORMAT(F10.7,5X,I3,5X,F8.2,2X,F10.6,53X,F10.3)
 1000 CONTINUE
      CAVOLD=CAVOL
      XOLD=XLAST
      THEOLD=THETA
      KKN = 1
      KK = 1
      DO 1050 N=1,81
 1050 PPI(N)=0.0
 1100 CONTINUE
```

#### 4.16.9 Section 8 - Motor Inlet Flow Calculation

Section 8 calculates the total inlet motor flow for one cycle (40° of cylinder block rotation for a nine piston motor). Each of the active pistons sucking (NAPS) is sequentially incremented through 80 steps. The total outlet flow is determined by summing that from each piston. The calculation is started on the index step after the decompression ends. Pressure in the first cylinder is initially the final decompression value. Pressure in the other open cylinders is equal to the sum of the previously calculated steady state inlet pressure (LPRESS) and time dependent oscillating pressure (PPT). Cylinder pressure and flow calculated at each step account for piston and valve plate leakage, pressure drop across the valve, piston motion, and fluid compressibility. The math model of this section is identical to the pump inlet flow calculation. See Section 9, paragraph 4.10 for details of the equation derivation.

## 4.16.9.1 Section 8 - Listing

```
C
C      SECTION 8- MOTOR INLET FLOW CALCULATION
C
       CAVOL=CAVOLD
       XLAST=XOLD
       THETA=THEOLD
       DO 1150 N=1,81
 1150  QOI(N)=0.0
C
       WRITE(6,925) CAVOL,NP,LPRESD,XLAST,THETA
       DO 1500 M=1,NAPS
       DO 1400 N=1,80
       NKM=NSUSOP+N+(M-1)*80
       IF(NKM.GE.NSUCL+1) GO TO 1400
       THETA=THETA+DANG
       XNEW=-SA*COS(THETA)
       DX=XNEW-XLAST
       VA=POVOL-XNEW*PIA
       XLAST=XNEW
       IF(CAVOL.GT.0.00) GO TO 1370
       BULKP=BULK+12.*(PISPR(NKM-1)-PRESS)
       IF(PISPR(NKM-1).GE.CPRESS) GO TO 1360
       LEAK=SLEAK
       LK1=1.+SQRT(BULKP)*LEAK*DT/VA
       GO TO 1365
 1360  LEAK=PLEAK
       LK1=1.+BULKP*LEAK*DT/VA
 1365  LK2=(PISPR(NKM-1)+BULKP/VA*DX*PIA)/LK1
       LK3 = BULKP*DT/VA/LK1
       LK4= (ORF*VAREA(NKM))**2
       LK5 =LK3*LK4 *0.5
       LK6=LK4*(LK2-LPRESS-PPI(N))
       LK7 =LK5*LK5 +ABS(LK6)
       LK8 = -LK5 +SQRT(LK7)
       QIN=SIGN(LK8,LK6)
       PISPR(NKM)=LK2-QIN*LK3
       IF(PISPR(NKM).GT..01) GO TO 1380
 1370  CONTINUE
       LEAK=SLEAK
       QIN=-(0.65*VAREA(NKM)*SQRT(2.*(LPRESS+PPI(N))/RHO))
       PISPR(NKM)=.01
       CAVOL=CAVOL-DX*PIA+SLEAK*DT*CPRESS+QIN*DT
       IF(CAVOL.LE.0.00) CAVOL=0.00
 1380  QOI(N)=QIN+QOI(N)
       IF(Y.NE.5000.) GO TO 1400
       WRITE(6,930) CAVOL,NKM,PISPR(NKM),XLAST,DX,VA,
      +LEAK,BULKP,THETA,QOI(N)
 1400  CONTINUE
 1500  CONTINUE
       QOI(81)=QOI(1)
```

### 4.16.10 Section 9 - Fourier Analysis of the Motor Inlet Flow

Section 9 performs a mathematical harmonic analysis of the time dependent motor total inlet flow calculated in Section 8 of the motor model. Flow is calculated over the cycle period for each harmonic from the fundamental up to and including the input harmonic of interest. See Section 10, paragraph 4.11 of the pump model for details of the calculations.

#### 4.16.10.1 Section 9 - Listing

```
C
C      SECTION 9- FOURIER ANALYSIS OF MOTOR INLET FLOW
C
       COFF=.02469
       C1=.07753
       S1 =SIN(C1)
       C1 =COS(C1)
       S =0.0
       C =1.0
       FNTZ=QOI(1)
       J =1
 1610  U2=0.0
       U1=0.0
       I= 81
C        FORM FOURIER COEFFICIENTS RECURSIVELY
 1620  U0=QOI(I)+2.0*C*U1-U2
       U2=U1
       U1=U0
       I=I-1
       IF(I-1) 1630,1630,1620
 1630  QIFC(J)=COEF*(FNTZ+C*U1-U2)
       QIFS(J)=COEF*S*U1
       IF(J-NHARM-1) 1640,1650,1650
 1640  U3=C1*C-S1*S
       S =C1*S+S1*C
       C =U3
       J = J+1
       GO TO 1610
 1650  QIFC(1)=QIFC(1)*.5
C
C        COMPUTE HARMONIC FLOWS FROM FOURIER ANALYSIS
C
 1655  DO 1660 I=1,NHARM
       FQ1I(I,KK) = CMPLX(QIFS(I+1), QIFC(I+1))
 1660  CONTINUE
```

4.16.11 Section 10 - Inlet Pressure - Flow Balance Calculation

After the calculation of pump inlet flow and its Fourier analysis in Sections 8 and 9, Section 10 estimates the shunt impedance (ZO). Shunt impedance is then combined with the system supply load impedance (ZIP) to give the total impedance seen by the pump. This value is then used in the dynamic pressure-flow balance calculation. The math model is identical to Section 6, paragraph 4.7 of the PUMP subroutine.

4.16.11.1 Section 10 - Listing

```
C
C     SECTION 10- INLET PRESSURE-FLOW BALANCE CALCULATION
C
 1670 CONTINUE
      I = KKN
      IF (KK - 2) 1680,1690,1700
 1680 CONTINUE
      W=Y*PISTNO*PI*KKN/30.
      ZO=1.0E5/W*(.2,-1.)
      PQ1I(I,KK) = FQ1I(I,KK )*ZO*ZAP(I)/(ZO +ZAP(I)) / 5.0
      P5=CABS(PQ1I(I,KK))
      P6=LPRESS/P5
      IF(Y.NE.5000.) GO TO 1681
      P7=P5*5.0
      WRITE(6,1682) P7,QIFC(1)
 1682 FORMAT(10X,2(F10.4),//)
 1681 P3=PQ1I(I,KK)
      GO TO 1720
 1690 CONTINUE
      ZO = PQ1I(I,KK-1) /(FQ1I(I,KK-1)-FQ1I(I,KK))
      PQ1I(I,KK) = FQ1I(I,KK-1)*ZO*ZAP(I)/(ZO +ZAP(I))
      P5=CABS(PQ1I(I,KK))
      P6=LPRESS/P5
      IF(Y.NE.5000.) GO TO 1691
      WRITE(6,1682) P5,QIFC(1)
 1691 P3=PQ1I(I,KK)-PQ1I(I,KK-1)
      PQ1I(I,KK+1) = PQ1I(I,KK) - PQ1I(I,KK-1)
      PPP(I) = ATAN2(AIMAG(PQ1I(I,KK+1)),REAL(PQ1I(I,KK+1)))
      GO TO 1720
 1700 CONTINUE
      J=KKN
      PQ1I(J,KK) = ZAP(J) * FQ1I(J,KK)
      P5=CABS(PQ1I(J,KK))
      P6=LPRESS/P5
 1713 IF(Y.NE.5000.) GO TO 1715
      WRITE(6,1682) P5,QIFC(1)
 1715 ETA(J)=CABS(100*(PQ1I(J,KK)-PQ1I(J,KK-1))/PQ1I(J,KK))
      KKN = KKN + 1
      IF(KKN.GT.NHARM) GO TO 340
      KK = 1
      FQ1I(KKN,1) = FQ1I(KKN,2)
      GO TO 1670
 1720 CONTINUE
```

### 4.16.12 Section 11 - Reconstruction of Time Dependent Inlet Pressure

Section 11 computes the time dependent inlet pressures (PFT) from each estimate of complex dynamic inlet pressure (P3) from Section 10. The dynamic balance counter (KK) is incremented and control is returned to Section 8 until dynamic balancing is completed. Complex pump inlet flow Q (NINLT) and pressure P (NINLT) for the harmonic of interest are then stored for returning to the main program.

The math model for Section 11 is identical to that for Section 12, paragraph 4.13 in the pump model.

#### 4.16.12.1 Section 11 - Listing

```
C
C     SECTION 11- RECONSTRUCTION OF TIME DEPENDENT INLET PRESSURE
C
      DO 1730 J=1,81
      THETA= (J-1)*1*0.07854
      PPI(J) =PPI(J) + REAL(P3)* SIN(THETA) +AIMAG(P3)* COS(THETA)
      IF(PPI(J).LT.-LPRESS) PPI(J)=-LPRESS
 1730 CONTINUE
      KK = KK + 1
      GO TO 1100
  340 CONTINUE
      Q(NINLT)=FQ1I(NHARM,3)
      P(NINLT)=PQ1I(NHARM,3)
      RETURN
      END
```

## 6.56 TYPE #56 - HYDRAULIC MOTOR

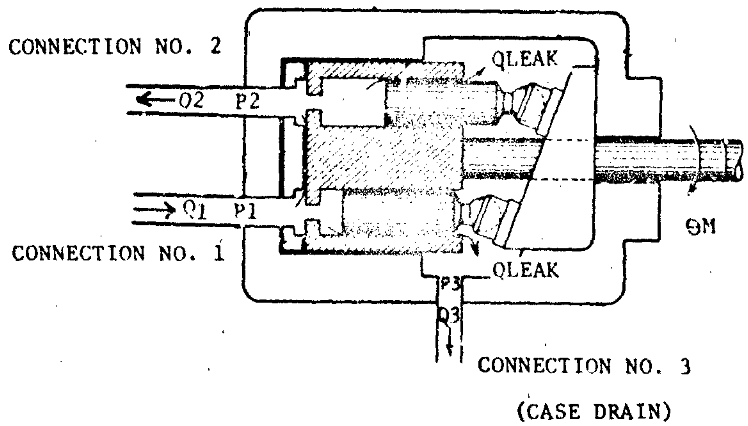


FIGURE 6.56-1

TYPE NO. 56 HYDRAULIC MOTOR

Type #56 motor is used to simulate a constant displacement hydraulic motor. In developing the model it has been necessary to estimate certain leakage characteristics and assume a viscous damping coefficient.

CARD NUMBER 1

| COLUMN | FORMAT | DATA |
|---|---|---|
| 1-5 | I5 | Component Number |
| 6-10 | I5 | Type Number = 56 |
| 11-15 | I5 | Number of Real Data Cards = 2 |
| 16-20 | I5 | Line Number (with sign) attached to Connection 1 (Inlet) |
| 21-25 | I5 | Line Number (with sign) attached to Connection 2 (Outlet) |
| 26-30 | I5 | Line Number (with sign) attached to Connection 3 (Case Drain) |
| 31-35 | I5 | |
| 36-40 | I5 | |
| 41-45 | I5 | |
| 46-50 | I5 | |
| 51-55 | I5 | |
| 56-60 | I5 | |
| 61-65 | I5 | |
| 66-70 | I5 | |
| 71-75 | I5 | |
| 76-80 | I5 | Temperature/Pressure Code (See Page 4.0-2) |

EXAMPLE CARD

CARD NUMBER 2

| COLUMN | FORMAT | DATA | DIMENSIONS |
|---|---|---|---|
| 1-10 | E10.0 | Motor Displacement | $IN^3$/REV |
| 11-20 | E10.0 | Case Drain Leakage Coefficient | PSI/CIS |
| 21-30 | E10.0 | Case Drain Constant Pressure Drop | PSI |
| 31-40 | E10.0 | Viscous Damping Coefficient | -- |
| 41-50 | E10.0 | Motor Inertia | IN-LB-$SEC^2$ |
| 51-60 | E10.0 | Breakout Torque | IN-LBS |
| 61-70 | E10.0 | Motor Constant Pressure Drop | PSI |
| 71-80 | E10.0 | Motor Leakage Coefficient | PSI/CIS |

EXAMPLE CARD

CARD NUMBER 3

| COLUMN | FORMAT | DATA | DIMENSIONS |
|---|---|---|---|
| 1-10 | E10.0 | LOAD TORQUE | IN-LBS |
| 11-20 | E10.0 | | |
| 21-30 | E10.0 | | |
| 31-40 | E10.0 | | |
| 41-50 | E10.0 | | |
| 51-60 | E10.0 | | |
| 61-70 | E10.0 | | |
| 71-80 | E10.0 | | |

EXAMPLE CARD

## 6.56 SUBROUTINE MTR 56

MTR 56 simulates a fixed displacement piston motor. Figure 6.56-1 shows an axial piston motor having a stationary hanger and using valve plate porting. The valve plate ports inlet fluid to half of the cylinder barrel, and the pistons receiving the fluid are forced against the inclined fixed hanger. This causes the cylinder, which is connected to the output shaft, to rotate.

The HYTRAN motor model accounts for internal leakage to case which is directly proportional to motor pressure. The dynamic analysis of the load and case flows and port pressures are functions of motor inertia, volumetric displacement, viscous damping, friction, and shaft rotation.

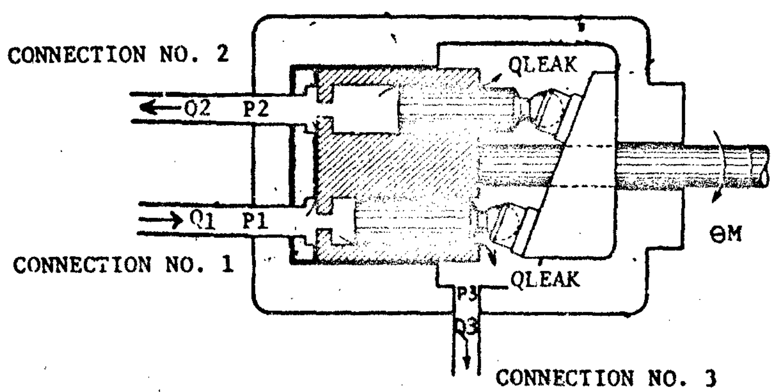


FIGURE 6.56-1

### 6.56.1 MATH MODEL

MTR56 simulates a simple hydraulic motor. Figure 6.56-2 shows the various torques acting on the motor.

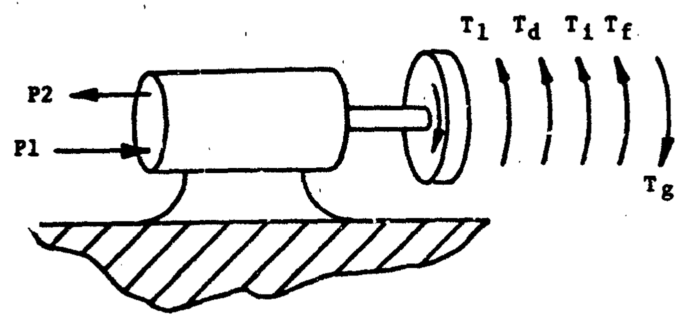


Figure 6.56-2

Summing the torques yields:

$T_l = T_g - T_i - T_d - T_f$

where $T_l$ = resisting load torque on the motor (in.lb)

$T_g$ = generated motor torque

$T_i$ = resisting torque due to motor inertia

$T_d$ = resisting torque due to damping

$T_f$ = resisting torque due to friction

The load torque ($T_l$) is set to zero. The other torques are defined as:

$T_g$ = DM*(P1-P2)

$T_i$ = ALPHA*I = (RPS-RPS$_{last}$)*I/ t

$T_d$ = CD*DM*$\mu$*RPS

$T_f$ = $\frac{RPS}{|RPS|}$*CF*DM*(P1+P2)

where,

$DM$ = motor displacement ($IN^3/RAD$)

$P1$ = inlet pressure (PSIA)

$P2$ = outlet pressure (PSIA)

$RPS$ = motor speed (RAD/SEC)

$RPS_{last}$ = last time step calculation of motor speed (RAD/SEC)

$CD$ = damping coefficient

$\mu$ = fluid viscosity ($IN^2/SEC$)

$CF$ = coefficient of dynamic friction

$t$ = calculation time step (SEC)

$I$ = motor inertia ($LB*IN*SEC^2$)

Using the last time step's calculation of P1, P2 and RPS, a value for the friction torque may be calculated.

$$T_f = \frac{RPS_{last}}{|RPS_{last}|} *CF*DM*(P1+P2) = DFRIC$$

Grouping of the inertia and damping components of the torque equation allows further simplification.

$$T_d + T_i = CD*DM*\mu*RPS + (RPS-RPS_{last})*I/\Delta t$$

$$= RPS(\mu*DM*CD+I/\Delta t) - RPS_{last}*I/\Delta t$$

By defining the variables:

$DAMP = CD*\mu*DM+I/\Delta T$

$CINERT = RPS_{last}*I/\Delta t$

The torque balance becomes

$T_1 = DM*(P1-P2)-RPS*DAMP-DFRIC+CINERT$

with P1, P2 and RPS being the unknowns

The flow diagram for the motor, Figure 6.56-3 gives the following flow relationships:

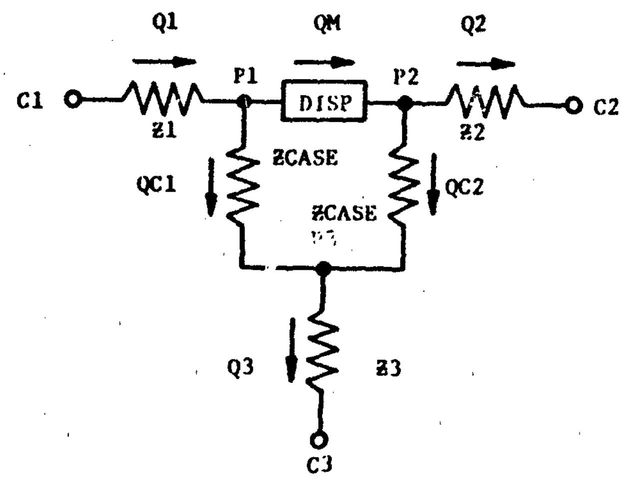


Figure 6.56-3

$$Q1 = (C1-P1)/Z1 \qquad (1)$$

$$Q2 = (C2-P2)/Z2 \qquad (2)$$

$$Q3 = QC1+QC2 = (C3-P3)/Z3 \qquad (3)$$

$$QM = RPS*DM$$

$$QC1 = (P1-P3)/ZCASE$$

$$QC2 = (P2-P3)/ZCASE$$

where

ZCASE = case leakage coefficient (PSI/CIS)

P3 = case drain pressure (PSIA)

Initially assuming QC1 and QC2 are zero one can write

$$P1 = C1 - DM * RPS * Z1$$

$$P2 = C2 + DM * RPS * Z2$$

having found P1 and P2 in terms of RPS, the torque balance becomes

$$T_L = DM\ (P1-P2) + CINERT - DPRIC - RPS * DAMP$$

the solution of which is:

$$RPS = (DM\ (P1-P2) + CINERT - DPRIC - FRPS * T_L)/DAMP$$

where

$T_L$ = Load Torque

All the motor flows may now be calculated and P3 determined using the values of P1, P2 and C3.

6.56.2 ASSUMPTIONS

Breakout pressure drop is assumed to follow the relationship

delta $P_{brk} = .5*P_{inlet} + 30$, which was derived from the test results.

The coefficient of dynamic friction is assumed to be .106.

### 6.56.3 COMPUTATIONAL METHOD

1000 SECTION

In the 1000 section, all DT variables are initialized to zero and the leakage terms are corrected for viscosity.

1500 SECTION

A check is made for the leg under calculation (pressure, return, case drain), by which control is routed to one of three areas.

If the motor connection in the leg is number one (pressure), DT(P1) is set equal to the upstream node pressure and control is returned to the program.

If the motor connection is number 2 (return), new values of the upstream pressure and laminar flow coefficient are calculated using the leg flow and cross port leakage term. DT(P2) is set equal to the upstream pressure.

If the leg under calculation is connected to the case drain port, the leg flow and case drain leakage term are used to calculate new values of upstream pressure and laminar flow coefficient. DT(P3) is set equal to the upstream pressure.

2000 SECTION

The 2000 section corrects cross port and case drain impedances for viscosity and calculates the constant DT(DAMP).

3000 SECTION

Predicted values of P1, P2, and P3 are made based on the line equations. These values are used to calculate the dynamic friction force, the motor delta P for a breakout check, and case drain parameters.

From the predicted pressures, values of the temporary variables are calculated.

A check is then made, using the predicted values of P1 and P2, to see if the pressure drop across the motor is sufficient for breakout.

If the last calculation of RPS is zero and the predicted value of the pressure drop is less than that required for breakout, flows and pressures are calculated using the leakage characteristics of the motor.

If breakout conditions are met, a new value of RPS is calculated, from which flows and pressures are calculated.

### 6.56.4 APPROXIMATIONS

Case drain flow is calculated based on a predicted value of case pressure from the previous time step. Since cross port leakage is negligible, it is neglected when the motor is moving.

### 6.56.5 LIMITATIONS

The sign of the dynamic friction term is determined from the last time steps calculation of RPS. This will cause a slight inaccuracy when the model passes through zero RPS during a reversal.

### 6.56.6 VARIABLE NAMES

| VARIABLE | DESCRIPTION | UNITS |
|---|---|---|
| ARPS | Absolute Value of Motor Speed | RAD/SEC |
| BRAKEP | Breakout Pressure Drop | PSI |
| D(BRAKET) | Breakout Torque | IN-LB |
| D(CASE) | Case Drain Leakage Coefficient | PSI/CIS |
| CIN/COUT | Temporary Variables | - |
| CINERT | Torque Due to Inertia | IN-LB-RAD |
| D(CDROP) | Motor Pressure Drop Coefficient | PSI/CIS |
| DT(DAMP) | Inertia Damping | IN-LB-SEC$^2$ |
| DELT | Calculation Time Interval | SEC |
| DELTP | Motor Pressure Drop | PSI |
| DFRIC | Torque Due to Dynamic Friction | IN-LB/RAD |
| D(DM) | Motor Displacement | IN$^3$/RAD |
| D(INERT) | Inertia of Motor | IN-LB-SEC |
| L1, L2, L3 | Dummy Variables | --- |
| D(LTORQ) | Load Torque | IN-LB |
| DT(P1) | Inlet Pressure | PSI |
| DT(P2) | Outlet Pressure | PSI |
| DT(P3) | Case Drain Pressure | PSI |
| QA | Flow | CIS |
| QS | Flow Sign | --- |
| QC1 | Inlet to Case Flow | CIS |
| QC2 | Outlet to Case Flow | CIS |
| DT(RPS) | Motor Speed | RAD/SEC |
| D(VIDAMP) | Viscous Damping Coefficient | --- |
| DT(ZCASE) | Case Drain Impedance | PSI/CIS |
| Z1 | Temporary Variable | --- |
| Z2 | Temporary Variable | --- |
| Z3 | Temporary Variable | --- |

## 6.56.7 MTR56 SUBROUTINE LISTING



```
      SUBROUTINE MTR56(D,DT,DD,L)
C *** REVISED JULY 1978 ****
      DIMENSION D(10),DT(10),DD(1),L(5)
      COMMON NTFLPL,NTOLPL,IPT,IPOINT,NPTS,INEL,KNEL,NTOPL,NLPLT(61,3),
     1PQLEG(90,12),LCS(90,10),ILEG(1400),PN(90),QN(90)
      COMMON/SLB/PARM(150,9),PM(1500),QM(1500),P(300),C(300),C(300)
     1,Z(300),RHO(20),S2RHO(20),VISC(20),BULK(20),TEMP(20),PVAP(20)
     2,ATPRES,T,DELT,TFINAL,PLTDEL,PI,TITLE(20),LEGN,ICON
     3,KTEMP(99),LSTART(150),NLPT(150),LTYPE(99),NC(99),INX,INZ
     4,INV,ISTEP,NLINE,NFL,IND,IENTR,MNLINE,MNFL,MNLEG,MNODE,MNPLOT
     5,MNLPTS,MDS
      INTEGER DM,CASE,CPORT,VIDAMP,DAMP,ZCASE,ZLEAK,P1,P2,P3,RPS,
     1BREAKT,PDROP,ONET,PDCASE,CPDROP
C *** D ARRAY VARIABLES ***
      DATA DM/1/,CASE/2/,PDCASE/3/,VIDAMP/4/,INERT/5/,BREAKT/6/
     + ,PDROP/7/,CPDROP/8/,LTORQ/9/
C *** DT ARRAY VARIABLES
      DATA RPS/1/,P1/2/,P2/3/,P3/4/,DAMP/5/,ZCASE/6/,ZLEAK/7/
     +,ONET/8/
      IF(IENTR)1000,2000,3000
C
C *** 1000 SECTION
 1000 CONTINUE
      IF(INEL.NE.0)GO TO 1500
      DO 1001 I=1,10
 1001 DT(I)=0.0
C *** LEAKAGE COEFFICIENT VISCOSITY CORRECTION ***
C *** VISCOSITY OF MIL-H-5606B AT 125 F=.0213 ***
      D(DM)=D(DM)/(2.*PI)
      RETURN
C
C     STEADY STATE SECTION
 1500 CONTINUE
      IF(KNEL-2)1501,1502,1503
 1501 DT(P1)=PQLEG(INEL,11)
      RETURN
 1502 CONTINUE
      QA=PQLEG(INEL,1)
      QS=PQLEG(INEL,2)
      PQLEG(INEL,6)=PQLEG(INEL,6)+D(CPDROP)
      PQLEG(INEL,5)=PQLEG(INEL,5)-D(PDROP)
      PQLEG(INEL,11)=PQLEG(INEL,11)-D(PDROP)-D(CPDROP)*QA*QS
      DT(P2)=PQLEG(INEL,11)
      RETURN
 1503 QA=PQLEG(INEL,1)
      QS=PQLEG(INEL,2)
      PQLEG(INEL,5)=PQLEG(INEL,5)-D(PDCASE)
      PQLEG(INEL,6)=PQLEG(INEL,6)+D(CASE)
      PQLEG(INEL,11)=PQLEG(INEL,11)-QA*QS*D(CASE)-D(PDCASE)
      DT(P3)=PQLEG(INEL,11)
      RETURN
C
C *** 2000 SECTION
 2000 CONTINUE
      DT(RPS)=Q(L(1))/D(DM)
      N=KTEMP(IND)
      DT(DAMP)=D(VIDAMP)*RHO(N)*VISC(N)*D(DM)+D(INERT)/DELT
      DT(ZCASE)=Z(L(3))*(DT(P1)+DT(P2))-2.*Z(L(3))*DT(P3)
      DT(ZCASE)=DT(ZCASE)/(DT(P3)-C(L(3)))
      WRITE(6,900)(DT(I),I=1,6)
  900 FORMAT(5X,8E12.5)
      RETURN
C
```

## 6.56.7 MTR56 SUBROUTINE LISTING (CONTINUED)



```
C *** 3000 SECTION
 3000 CONTINUE
      L1=L(1)
      L2=L(2)
      L3=L(3)
      PCAV=PVAP(KTEMP(IND))
      ARPS=ABS(DT(RPS))
      SRPS=SIGN(1.0,DT(RPS))
      CINERT=DT(RPS)*D(INERT)/DELT
      DFRIC=.106*D(DM)*(DT(P1)+DT(P2))*SRPS
      DELTP=DT(P1)-DT(P2)
      POUT=DT(P2)
      IF(DELTP.LT.0.0)POUT=DT(P1)
      BRAKEP=.05*POUT+75.
      IF(ABS(DELTP).LT.BRAKEP.AND.ARPS.LE.10.) GO TO 3010
      CIN=C(L1)
      COUT=C(L2)
      ZIN=Z(L1)
      ZOUT=Z(L2)
      PIN=CIN-D(DM)*DT(RPS)*ZIN
      POUT=COUT+D(DM)*DT(RPS)*ZOUT
      DT(RPS)=(D(DM)*(PIN-POUT)+CINERT-DFRIC-SRPS*D(LTORQ))/DT(DAMP)
      GO TO 3040
 3010 DT(RPS)=0.0
      DT(P1)=C(L1)/Z(L1)+DT(P3)/DT(ZCASE)
      DT(P1)=DT(P1)/(1./Z(L1)+1./DT(ZCASE))
      DT(P2)=C(L2)/Z(L2)+DT(P3)/DT(ZCASE)
      DT(P2)=DT(P2)/(1./Z(L2)+1./DT(ZCASE))
      P(L1)=DT(P1)
      P(L2)=DT(P2)
      Q(L1)=(C(L1)-DT(P1))/Z(L1)
      Q(L2)=(C(L2)-DT(P2))/Z(L2)
      Q(L3)=Q(L1)+Q(L2)
 3070 Q(L3)=-Q(L3)
      DT(P3)=C(L3)-Q(L3)*Z(L3)
      P(L3)=DT(P3)
      WRITE(6,900)C(L1),C(L2),C(L3),Q(L1),Q(L2),Q(L3)
      RETURN
 3040 CONTINUE
      P(L1)=PIN
      P(L2)=POUT
      DT(P1)=PIN
      DT(P2)=POUT
      Q(L1)=D(DM)*DT(RPS)
      Q(L2)=-Q(L1)
      DT(P3)=Z(L3)*(DT(P1)+DT(P2))+DT(ZCASE)*C(L3)
      DT(P3)=DT(P3)/(2.*Z(L3)+DT(ZCASE))
      IF(DT(P3).LT.PCAV)DT(P3)=PCAV
      IF(DT(QNET).GT.0.0)DT(P3)=PCAV
      QC1=(DT(P1)-DT(P3))/DT(ZCASE)
      QC2=(DT(P2)-DT(P3))/DT(ZCASE)
      IF(DT(P3).EQ.PCAV)GO TO 3100
      Q(L3)=QC1+QC2
      GO TO 3070
 3100 Q(L3)=(C(L3)-DT(P3))/Z(L3)
      DT(QNET)=DT(QNET)-Q(L3)-QC1-QC2
      IF(DT(QNET).LE.0.0)DT(QNET)=0.0
      P(L3)=PCAV
      WRITE(6,900)C(L1),C(L2),C(L3),Q(L1),Q(L2),Q(L3)
      RETURN
      END
```

## REFERENCES


1. Amies, G. E., Greene, J. B., Levek, R. J., Pierce, N. J., AIRCRAFT HYDRAULIC SYSTEM DYNAMIC ANALYSIS-FINAL REPORT, AFAPL-TR-77-63, October 1977.
2. Amies, G., and Greene, J. B., HYDRAULIC SYSTEM DYNAMIC ANALYSIS-FREQUENCY RESPONSE (HSFR) COMPUTER PROGRAM USER MANUAL, AFAPL-TR-76-43 VOL. III, February 1977.
3. Amies, G. and Greene, J. B., HYDRAULIC SYSTEM DYNAMIC ANALYSIS-FREQUENCY RESPONSE (HSFR) COMPUTER PROGRAM TECHNICAL DESCRIPTION, AFAPL-TR-76-43 VOL. IV, February 1977.
4. Amies, G., Levek, R., and Struessel, D., HYDRAULIC SYSTEM DYNAMIC ANALYSIS-TRANSIENT ANALYSIS (HYTRAN) COMPUTER PROGRAM USER MANUAL, AFAPL-TR-76-43 VOL. I, February 1977.
5. Amies, G., Levek, R., and Struessel, D., HYDRAULIC SYSTEM DYNAMIC ANALYSIS-TRANSIENT ANALYSIS (HYTRAN) COMPUTER PROGRAM TECHNICAL DESCRIPTION, AFAPL-TR-76-43 VOL. II, February 1977.
6. deGarcia, H., HYDRAULIC LINE RESPONSE TO PUMP PULSATION EXCITATION, MDC Report A4163, 10 January 1977.
7. Timoshenko, S., Young, D. H., VIBRATION PROBLEMS IN ENGINEERING, D. Van Nostrand, 1956.
8. Den Hartog, J. P., MECHANICAL VIBRATIONS, McGraw-Hill, 1947.




*U.S.Government Printing Office: 1979 — 657-002/465